II-96-01
II-A-864

Diesel Engine Noise Conference

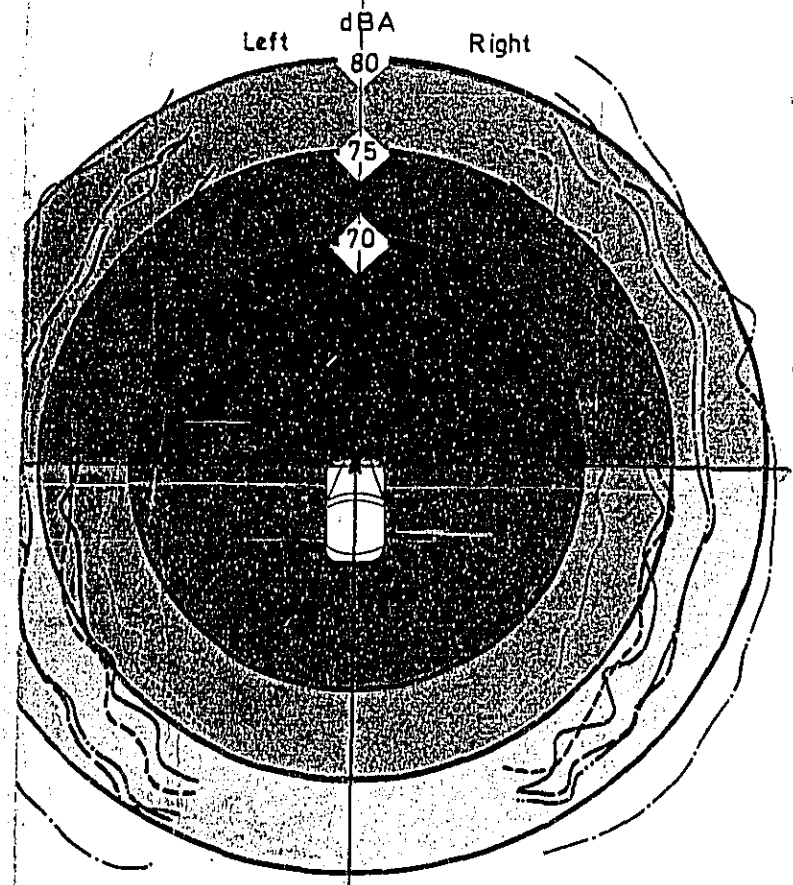

PROPERTY OF
EPA/ONAC
NOISE INFORMATION SYSTEM
TECHNICAL REFERENCE CENTER

SAE FREEDOM THROUGH MOBILITY 1905-1980 75th anniversary

Proceedings P-80

Congress and Exposition
Cobo Hall, Detroit
February 26-March 2, 1979

334619 A-Z
334620 A-F
c.2

Diesel Engine Noise Conference

Proceedings
P-80

Published by:
Society of Automotive Engineers, Inc.
400 Commonwealth Drive
Warrendale, PA 15096
February 1979

The appearance of the code at the bottom of the first page of each article in this volume indicates SAE's consent that copies of an article may be made for personal or internal use, or for the personal or internal use of specific clients. This consent is given on the condition, however, that the copier pay the stated per article copy fee through the Copyright Clearance Center, Inc., Operations Center, P.O. Box 765, Schenectady, NY 12301 for copying beyond that permitted by Sections 107 or 108 of the U.S. Copyright Law. This consent does not extend to other kinds of copying such as copying for general distribution, for advertising or promotional purposes, for creating new collective works, or for resale.

Articles published prior to 1978 in similar SAE collective works may also be copied at a per article fee of $2.50 under the above stated conditions.

To obtain quantity reprint rates, permission to reprint an article, or permission to use copyrighted SAE publications in other works, contact the SAE Publications Division.

SAE/P-79/80
Library of Congress Catalog Card Number: 79-83912
Copyright © 1979 Society of Automotive Engineers, Inc.

TABLE OF CONTENTS

790205

PROBLEMS AND DEVELOPMENTS IN AUTOMOTIVE ENGINE NOISE RESEARCH

by

T.Priede

Automotive Group
Institute of Sound and Vibration Research
University of Southampton
U.K.

ABSTRACT

The paper critically reviews the requirements for internal combustion reciprocating engines to meet present and future noise legislations according to their specific road vehicle applications.

It reviews the significance of the vibration characteristics of structure elements in relation to the combustion systems employed and attempts to identify the importance of the balance between mechanical and combustion induced noise in engines falling into specific categories.

IN ENGINEERING EVOLUTION only those products which show a marked superiority in all aspects tend to obtain a wide use in practice. It is for such reasons that the internal combustion reciprocating engine, based on Otto and Diesel cycles, almost exclusively power road vehicles. These engines, built in a wide range of size and power satisfy all the road transportation requirements, namely for private cars which are mainly fitted with high speed gasoline engines providing a high power to vehicle weight ratio of 60 to 80 HP per ton while for public service and commercial vehicles larger and slower speed diesel engines are fitted where power to vehicle weight ratio of only 6 to 8 HP per ton is required.

There are many reasons for the success of the internal combustion engine. One of the most important is the availability of the oil, which apart from water remains the second most plentiful fluid on earth. The oil has all the essential properties required for road transportation, namely the high energy content for its volume and mass; therefore the fuel tends to be only a small fraction of the total vehicle weight even for radii of operation up to 500 miles. The rate of fuelling of road vehicles at the service station is also very fast - the energy filling process being equivalent to an output of a small power station.

In comparison, electric battery vehicles where the energy source, i.e. the battery unit, is about 50% of the vehicle weight its fuelling process, i.e. charging, is extremely slow. If at any time electric vehicles are envisaged for private use the load capacity of the electric wiring system to all private dwellings would have to be increased ten-fold and even then it would never equal the convenience of oil.

Regarding the internal combustion engine itself, it can be stated that it has one of the highest specific power outputs for its size and weight; the design is extremely simple and cheap and the overall economy is good. In comparison with gas turbines which may be considered as a competitor, the reciprocating engine is also superior in transient response characteristics which are essential in road transportation.

The main reasons why environmental considerations regarding noise and emissions are so essential at present is that road vehicles have multiplied to such enormous numbers, so that the total quantity of emissions are threatening life on earth while noise has become unbearable to the community.

The engineers, therefore, are faced again with an almost impossible demand and thus over the last decade challenging research and development has been initiated to evolve engines which would be environmentally acceptable. As will be shown by the papers presented in this conference the studies of the diesel engine noise are made from every conceivable aspect and include advanced analytical and experimental techniques in vibration, acoustics and even the application of advanced optical methods in vibration studies. In considering such a wide range of efforts there is no reason to doubt that the required aims will be readily achieved.

In this paper no single solution is put forward to achieve these aims, but some of the more problematic areas are highlighted and discussed with the general intention of contributing to their better understanding.

VEHICLE NOISE LEGISLATION AND ENGINE NOISE

During the fifties there were great advances made in automotive diesel engine development. It was found that automotive diesel engines could be satisfactorily run at higher speeds and higher specific loads, thus considerably improving the specific power output. Although Daimler Benz successfully introduced a high speed diesel engine in a car before the war, it was not until the fifties that a widespread development of the high

SAE/P-79/80/$02.50
Copyright © 1979 Society of Automotive Engineers, Inc.

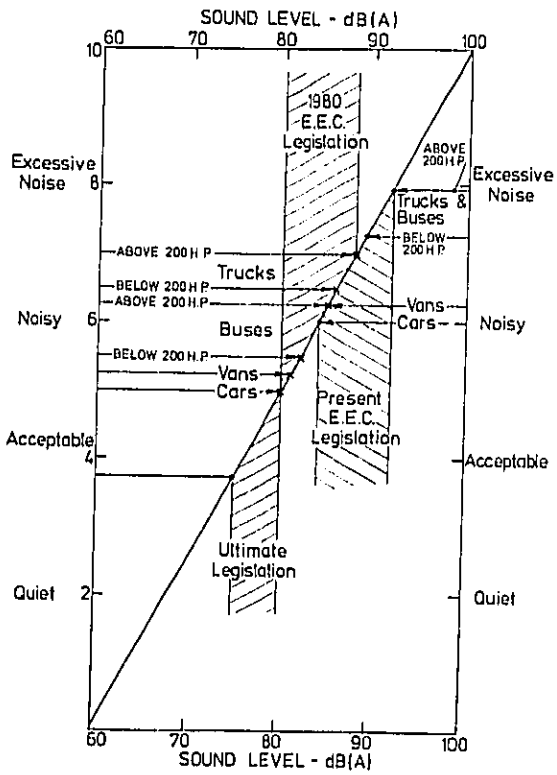

Fig. 1 - Legislation and subjective assessments

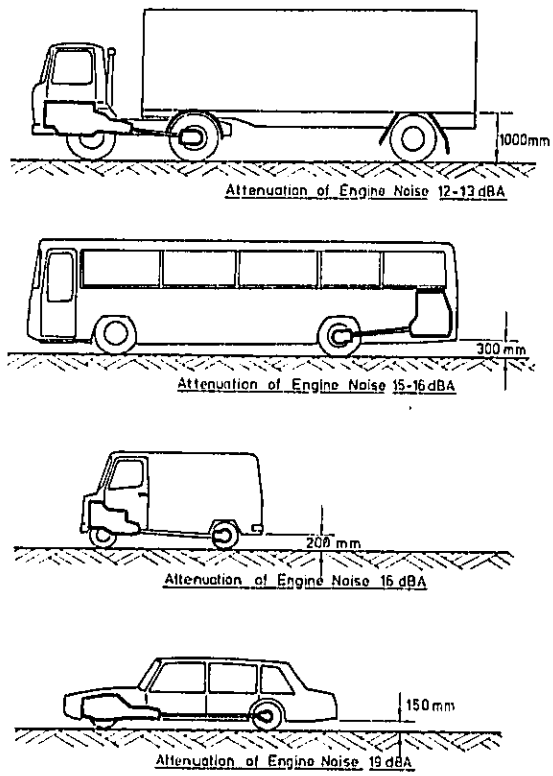

Fig. 3- Typical vehicle layouts

speed diesel engine for vans and light industrial applications also took place. The noise of the automotive truck diesel engines produced before 1950, running at moderate speeds was around 98 to 100 dBA measured at a distance of 1 metre. By 1960 the engines were running much faster with often large bore to stroke ratios and the noise levels reached 103 to 107 dBA. The result was an appreciable increase of vehicle noise. Similar trends could be noted also in gasoline car engine developments. It is for these reasons that in the mid-sixties the first noise legislations were introduced which up to date have remained virtually the same. The present European Economic Community noise legislation for road vehicles is illustrated in Figure 1 together with subjective assessments of vehicle noise (1)*. The ISO vehicle test procedure (i.e. the vehicle noise quoted) ensures the maximum engine noise (usually at full speed, full load) under accelerating conditions. As can be seen the legislated noise depend on the vehicle type and from the graph it can be deduced that trucks and buses would be rated by the community as 'extremely noisy' while cars and vans rated 'noisy'. The legislation is usually based on practically observed data - trucks have been found noisier than cars and therefore they have been permitted higher levels of noise

* Numbers in parentheses designate References at end of paper.

The detailed investigations on the origins of road vehicle noise (2) have shown that noise radiated by the engine surfaces in various vehicles is the main contributor. Since there are significant differences in the legislated levels the question is, is the individual vehicle in a particular group quieter because of a quieter engine, or is it due to basic principles of vehicle design?

Figure 2 shows the test bed overall noise at 1 metre distance from the side of the engine, of a large number of engines running at rated conditions (maximum speed and load) and classified in the various vehicle categories. The data presented are from the engines measured at ISVR and AVL Laboratories.

The mean values of noise are as follows:

Group 1. - Truck diesel engines above 200 HP - 102.4 dBA
Group 2. - Truck diesel engines below 200 HP - 101.8 dBA
Group 3. - Van high speed diesel engines - 101 dBA
Group 4. - Car gasoline engines 99 dB

As can be seen the mean levels between various diesel engine groups only differ by 1.4 dBA. Also the mean noise level of the gasoline engines is only 2 dBA quieter than the diesel engines.

It may be concluded that differences of the noise vehicle groups is mainly due to principles of vehicle design. The relevant features of various vehicles are illustrated schematically in Figure 3.

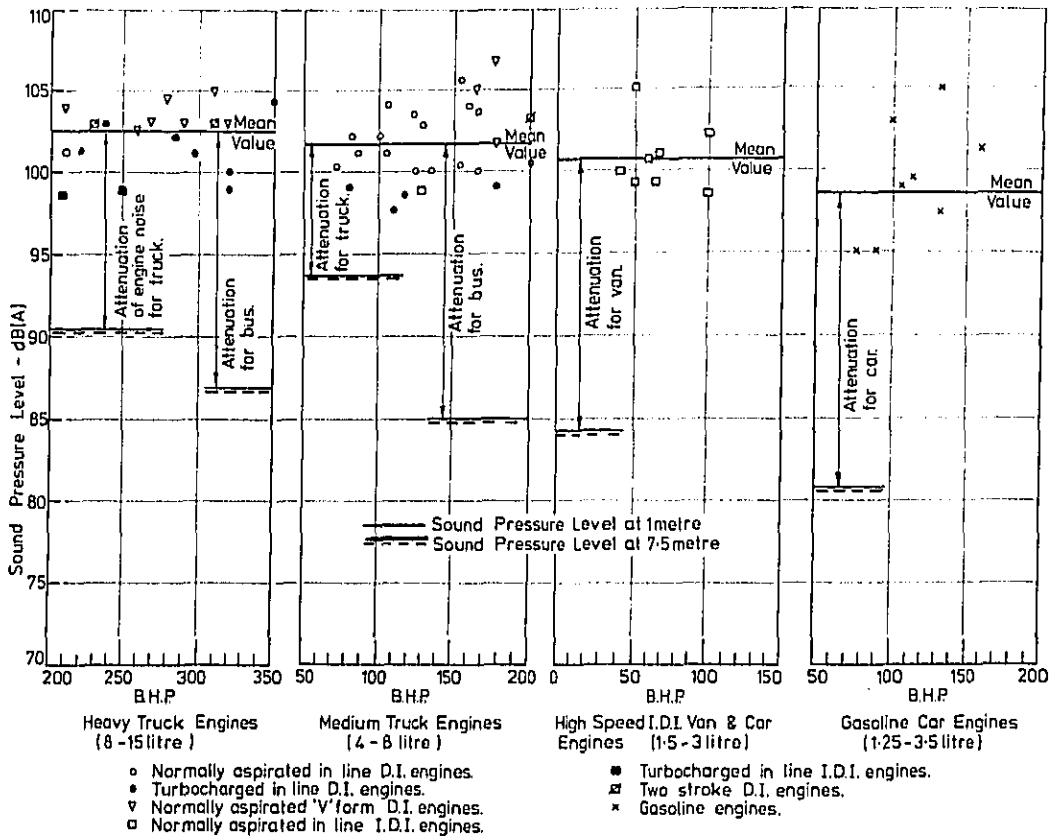

Fig. 2 - Attenuation of engine noise by vehicle structure and distance

As can be seen trucks have a high ground clearance, the engine is more exposed and the vehicle also provides little attenuation of noise. In buses vans and cars the vehicle body provides considerable shielding of engine noise and also the ground clearance is considerably smaller.

Investigations on the ISVR open air pad have shown that attenuation with distance from 1 metre to 7.5 metres also depends on engine size. For large engines attenuation of noise is about 12 dBA, for medium size engines 13 dBA, while for small high speed diesel and gasoline engines about 14 to 15 dBA.

The general attenuation of engine noise measured as the noise on the test bed at 1 metre distance less the noise from the vehicle, with no specific acoustic treatment, at 7.5 metres is as follows :

Large truck engines above 200 HP	- 12 dBA
Medium truck engines below 200 HP	- 13 dBA
Large truck engine in a bus or coach	- 15 dBA
Medium size truck engine in a bus or coach	- 16 dBA
Vans	- 16 dBA
Cars	- 19 dBA

These values of attenuation are shown in Figure 2 and correspond to values which are imposed by present noise legislation.

Figure 2 shows that there is a considerable variation in the noise levels of the various engines in the various groups and this variation is not only due to particular engine design features but also to a great extent to the manufacturer's choice of rated engine conditions.

It has also been found that in vehicles where noisier engines are installed the vehicle manufacturer had to incorporate in the vehicle design some noise reducing features, e.g. partial shielding.

Figure 1 also shows the details of E.E.C. Directive No. 77/212/EEC regarding the legislated levels for 1980. Trucks, vans and cars have to obtain a further 3 to 4 dBA reduction of noise. This requirement does not present vans and cars with any formidable problem, but for trucks, if present engines are used, significant shielding techniques will be required. Buses require the greatest reductions, namely 7 - 8 dBA, but this is possible to achieve since bus designs lead more readily to complete engine enclosure schemes.

The ultimate legislation envisaged is expected to be from 80 dBA for trucks down to about 75 dBA for cars and vans. In order to achieve an elegant solution to this problem it can be easily estimated from the data given in Figure 2 that future engine noise should not exceed 93 dBA at its rated conditions. This figure can be considered as a target at which present engine designers must aim.

AUTOMOTIVE ENGINE STRUCTURE

The predominant noise of the automotive engine lies in the frequency band from 900 to 2000 Hz which is determined by the vibration of various structure elements of the engine which thus determine the characteristics of radiated noise.

Figure 4 illustrates schematically the four major elements of the automotive engine system. These are :-

(a) combustion chamber,
(b) the moving parts, mechanically separated from the main structure by running clearances, namely - crankshaft, connecting rods, pistons, timing system and valve gear.
(c) load carrying structure, cylinder block, crankcase and cylinder head (either integral or separate, gasketed or plain machined mating surfaces) and
(d) covers and accessories (sump, valve cover, timing cover, bellhousing, injection pump, water pump, etc).

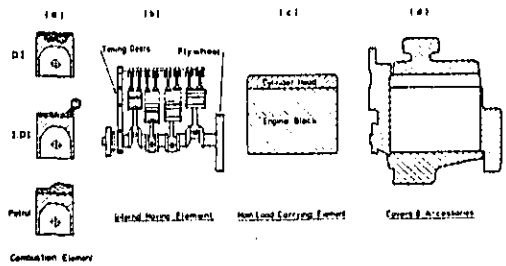

Fig. 4 - Elements of reciprocating engine

Each of the elements is capable of vibration at its natural frequency if an impulsive force is applied to it and thus contributes to the characteristics of resultant noise.

In practice the effect of the gas oscillations (element (a)) which are induced by rapid pressure rise resulting from combustion in the engine cylinder can be incorporated in the force time history of the exciting force and can therefore be considered as part of the basic exciting force. The covers (element (d)) are attached to basic load carrying structure (element (c)) and thus are excited by vibratory forces of the main load carrying structure. The covers mainly respond to the characteristics of the load carrying structure although their own natural frequency, to some extent, amplifies vibration in particular frequency regions.

Based on these considerations it is possible to simplify the engine system and to describe it by only two basic structure elements as illustrated in Figure 5. These are:-

(A) The internal load carrying structure, i.e. piston connecting rod-crankshaft system, and
(B) Outer load carrying cylinder block structure.

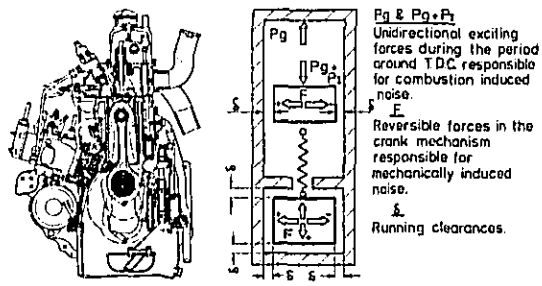

Fig. 5 - Engine structure and equivalent system

The internal load carrying structure is mechanically separated from the main outer load carrying structure by running clearances. A simple equivalent system of the engine thus can be developed as shown in Figure 5(b) illustrating the principle exciting forces which are responsible for the generation of vibration and noise. The outer elastic load carrying structure provides location for the piston and crankshaft represented as two masses joined together by a spring.

In the engine system as shown in Figure 5(b) there are two major forces which are responsible for the engine structure vibration and the emitted noise, namely unidirectional forces, (P) and reversible forces, (F).

COMBUSTION INDUCED NOISE - UNIDIRECTIONAL FORCE EXCITATION - Unidirectional forces, (P) illustrated in Figure 6, are only important in the vicinity of TDC on the compression stroke and are produced from compression and the subsequent pressure rise resulting from combustion. The clearances in the vertical direction for the equivalent mass of piston, connecting rod and crankshaft are taken up by these forces and a linear vibratory system results. Since during this period the force does not change its direction, any appreciable vibration can only be produced if there is a rapid change in the magnitude of the force.

As shown by the typical diagrams the rapid change in the magnitude is produced by the onset of combustion in the engine cylinder and thus can be defined as combustion induced noise. The gas force (Pg) excites the top part of the engine structure (i.e. cylinder head) while the lower part of the structure is excited by the combined gas force and inertia force, i.e. Pg + Pi. Investigations have shown (3) that in this period engine structure excitation is similar to a simple linear spring mass

system and its vibration can be represented by the equation :-

$$M\ddot{x} + C\dot{x} + Kx = P(t)$$

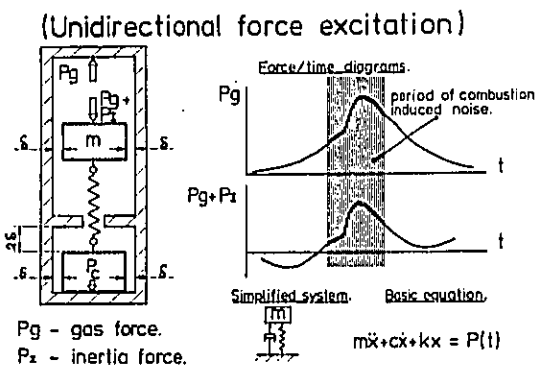

Fig. 6 - Schematic representation of combustion induced noise

This is illustrated in Figure 7, which shows the cylinder pressure diagram of a six cylinder diesel engine at 1000 rev/min and the corresponding cylinder head displacement and resultant noise emitted by the cylinder head.

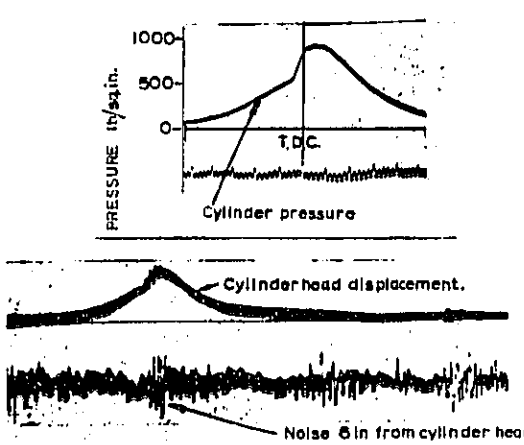

Fig. 7 - Combustion induced cylinder head excitation

The cylinder head deflects according to the shape of the exciting gas force (Pg). Superimposed on this deflection are vibrations of the cylinder head at its natural frequency (complementary function $m\ddot{x} + c\dot{x} + kx = o$) coinciding with the onset of the rapid pressure rise resulting from combustion. This vibration of the cylinder head reflects clearly in the emitted noise.

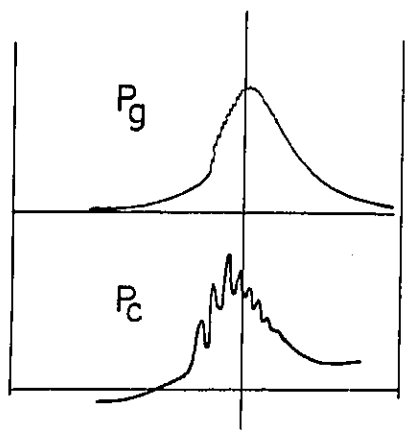

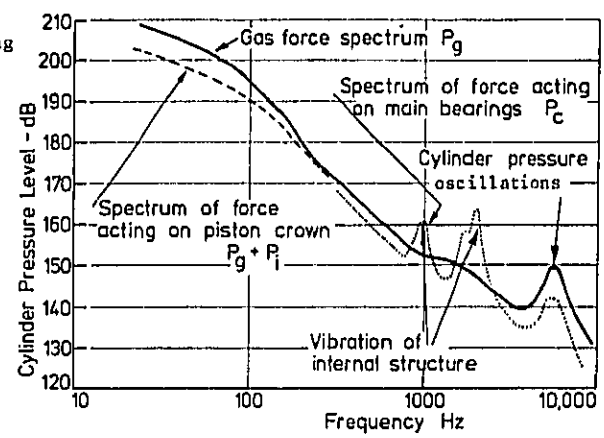

Fig. 8 - Force spectra acting on structure

Assessment of exciting propensities by spectral analysis of cylinder pressure development was proposed by Austen and Priede in 1958 (4) which enabled the amount of combustion noise and its characteristics to be determined independent of engine structure. It also led to explanations of the basic reasons for the increase of noise with engine speed, load and other operating parameters. This technique is now widely adopted to assess the noise making potential of various combustion systems and has led to the prediction of engine noise from basic design parameters (5).

A typical analysis of a direct injection diesel engine cylinder pressure development is shown in Figure 8. This spectrum represents the exciting

propensities of the force Pg (shown in Figure 6) which is applied to the top part of the engine st structure.

The cylinder pressure spectrum shows a distinct peak at around 5000 Hz which is due to cylinder pressure oscillations induced by the rapid pressure rise resulting from ignition of the premixed part of the fuel/air mixture. The frequency of pressure oscillations for direct injection engines is determined by the bore diameter and the temperature in the combustion chamber (6) as shown in Figure 9.

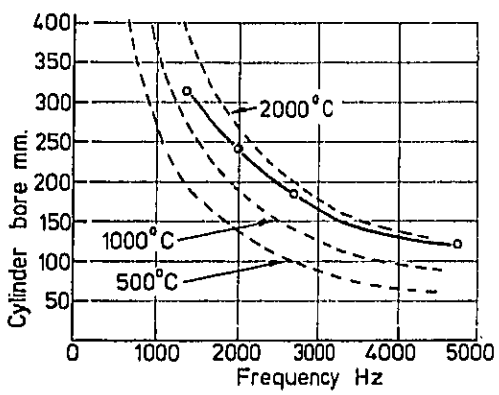

Fig. 9 - Relation between bore, gas temperature and cylinder pressure oscillations

For automotive size engines of up to 140 mm bore diameter cylinder pressure oscillations contribute very little to the total engine noise and its characteristics since the frequency (3500 to 5000 Hz) is too high in comparison with the predominant frequency response region of the structure. On larger engines from about 7 litres per cylinder capacity the noise due to pressure oscillations forms a significant part of the engine noise.

On some automotive size IDI engines, where communicating passage between the prechamber and the space above piston offers little restriction Helmholz type gas oscillations can occur in the frequency range between 1500 to 3000 Hz. On such engines this combustion noise is clearly audible and may even constitute the predominant noise at that frequency.

The peak amplitude of the force acting on the piston ($P_g + P_I$), which subsequently acts on the lower part of the structure, has lower peak amplitude than the gas force P_g since the inertia force acts in the opposite direction to the gas force. The inertia force mainly contains the low frequency harmonics so the spectrum of the $P_g + P_I$ (expressed per unit piston area) only differs from the gas force spectrum in the low frequency range as shown in Figure 8. Since the force $P_g + P_I$ is transmitted via piston connecting rod and crankshaft to the main load carrying structure of the engine at its main bearings it is modified by the resultant complex vibration of this internal structure. There is some evidence that this actually takes place from investigations carried out on impulsive gas force. This technique was originally conceived by Alcock of Ricardo (7) and has since been developed by ISVR where it is being frequently used for the study of characteristics of automotive engine structures and it represents one of the most realistic forms of rig test.

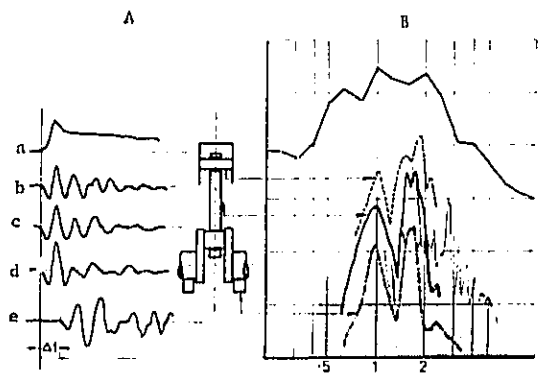

Fig. 10 - Structure vibration resulting from combustion pulse

Figure 10A illustrates typical results. The top oscillogram (a) indicates the cylinder pressure time history which also acts as a time datum. Below it are shown the resulting vibration of the piston (b), connecting rod (c), main bearing caps (d) and outer surface of the crankcase (e). It can be seen that the crank mechanism completes approximately one cycle of oscillation before the crankcase starts to move showing that the piston, connecting rod and crankshaft are vibrating at their own natural frequencies and thus are contributing to a great extent to the characteristics of the emitted engine noise. The vibration spectra of the internal structure shown in Figure 10B consists of two predominant frequencies; 1000 and 1800 Hz. The same two frequencies are noticeable in the crankcase vibration except that the spectrum is generally broader with a considerably larger number of peaks (number of natural frequencies is substantially increased by various modes of crankcase cylinder block vibration).

From these experiments it can be concluded that the force spectrum (P_c) acting on the crankcase at its main bearings should contain the oscillating characteristics of the internal structure as illustrated in Figure 8.

Figure 11 shows a computer plot of the time domain development of the engine block vibration resulting from the impulsive gas load. The vibration of the crankcase is considerably delayed and and only after about 1.2 m/sec from the time of the initiation of the load does vibration of any significance develop throughout the block structure.

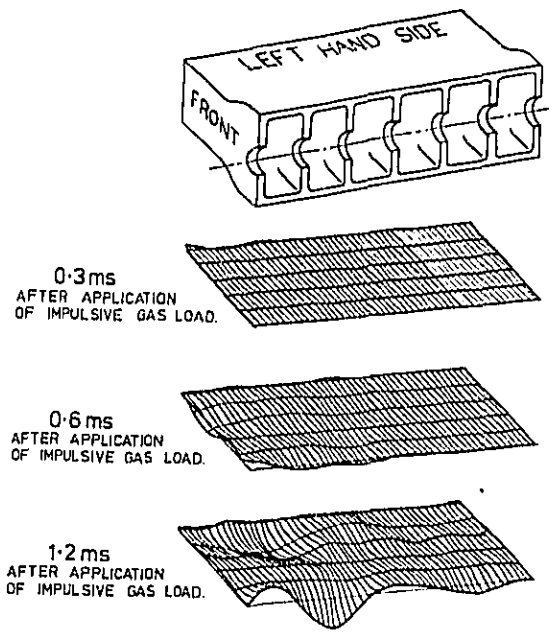

Fig. 11 - Propagation of transient excitation

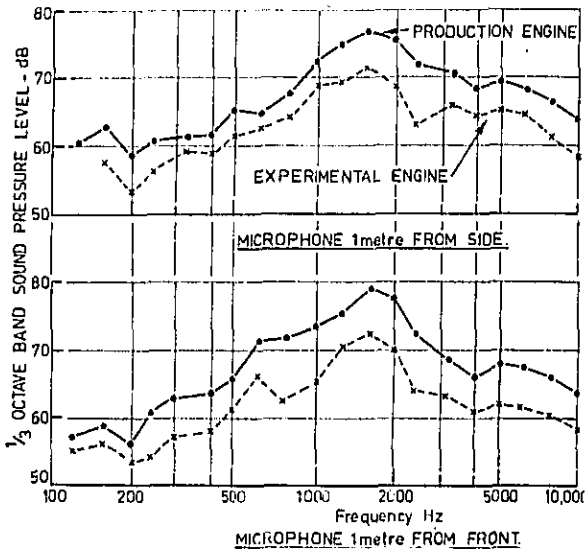

Fig. 12 - Characteristics of noise of production and experimental 2-litre IDI engines

There is further practical evidence that the internal structure vibration (i.e. piston connecting rod and crankshaft) is the main factor which controls the predominant frequency region of the noise of the engine. Presently, attempts to reduce engine noise are made mainly by improvements to the design of the stationary outer load carrying structure (element c in Figure 4) while using the same internal running parts. So far ten different experimental engines have been designed and built at ISVR on this principle and it generally provided worthwhile reductions of overall engine noise. None of the engines, however, showed a significant change in the noise characteristics, as in all cases the predominant frequency range of the engine noise remained the same.

This is illustrated by two examples. Figure 12 compares one-third octave band noise spectra of two 2-litre high speed IDI diesel engines (a) the production engine with a conventional cast iron engine block and (b) the experimental engine where the engine block was made from thick walled (20 mm) aluminium casting. The natural frequencies of the crankcase thus should be significantly increased. The bearing caps supporting the crankshaft were the same as in the production engine. Although worthwhile reductions of noise have been obtained, the predominant component of the noise remains the same at around 1600 Hz. This component is more marked from the front of the engine (2 dB higher) suggesting the radiation of noise from the front pulley which is rigidly attached to the crankshaft.

Figure 13 compares one-third octave band noise spectra of two 8-litre direct injection truck engines: a production engine and an experimental engine, where substantial changes have been made to the design of load carrying structure. In this instance a split crankcase design was employed in the experimental engine forming an integral bearing bedplate and thus crankshaft support replacing the conventional bearing caps was considerably stiffer. Crankcase and cylinder block walls were lined with 3-ply steel sandwich sheets bonded together by synthetic rubber. Again, the predominant noise at 1250 Hz is the same in both engines despite the large reduction of noise (of 8 dBA) which had been achieved with this design.

Figure 14 shows a typical comparison of noise spectra from an engine at different microphone positions, namely side, front and top. At all positions the predominant noise is the same, i.e. 1000 to 1250 Hz. The shape of the noise spectra from the front and top is peakier where the noise energy is concentrated in much narrower bands around these predominant frequencies. From the

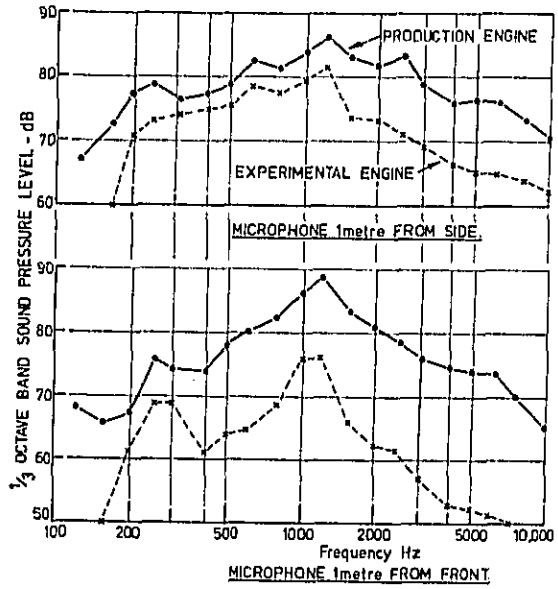

Fig. 13 - Characteristics of noise of production and experimental 8-litre DI engines

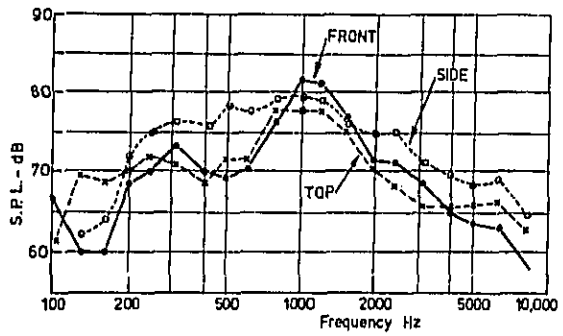

Fig. 14 - Characteristics of noise of 6-litre DI engine at various microphone positions

side the noise in this predominant range is of about the same level but on either side of the peak it is higher; thus the noise spectrum has broader characteristics. This may be due to the side of the engine having a larger area than the front and top. The crankcase block would contribute to the noise by its own natural modes of vibration. However, the fact remains that vibration of some characteristic frequency is radiated from all parts of the engine structure, strongly suggesting forced vibration of the outer structure by vibratory forces developed in the internal structure.

Regarding low frequency noise of the engine due to bending in its fundamental mode, Ochiai (8) has clearly demonstrated from theoretical and experimental analysis that the engine fundamental bending mode is closely associated with the torsional vibrations of the crankshaft (internal structure). By relevant changes to the crankshaft system he has demonstrated a large reduction of low frequency engine noise. Grover (9) on the other hand has demonstrated on a high speed diesel engine that fundamental engine bending noise can be reduced by 8 dB by stiffening the engine structure.

These findings clearly illustrate the importance of optimum matching of the internal engine structure with its outer structure. This view has been held by many engineers with long experience in engine design and development, but as yet no quantitative experimental evidence has been produced.

MECHANICALLY INDUCED NOISE - REVERSIBLE FORCE EXCITATION

Reversible forces (F) which change direction are produced by the engine crank mechanism and associated inertia forces as illustrated in Figure 15.

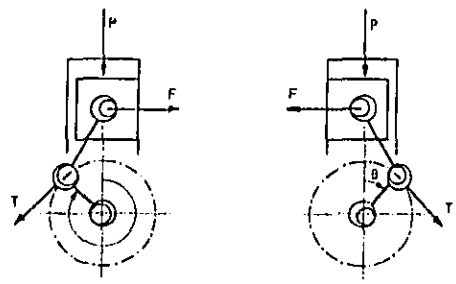

Fig. 15 - Schematic showing forces producing mechanical noise

Although these forces change in magnitude, the rate of change is too low to induce any appreciable vibration amplitudes in the comparatively stiff (high natural frequency) engine structure. These forces, however, accelerate the various elements of the internal load carrying structure across the clearances and thus cause impacts which effectively induce engine structure vibration.

Figure 16 illustrates the basic principles of mechanically induced noise. The equation in

this instance is based on the fact that transverse motion is governed by the rate of change of acceleration -

$$\dddot{Mx} = \frac{dF}{dt} = \text{const}$$

$\frac{dF}{dt}$ is approximately constant while the actual component moves across the clearance. For rotational parts the equation is similar except it is presented in terms of angular acceleration (θ) and the moment of inertia (J)

$$J\dddot{\theta} = \frac{dT}{dt} = \text{const}$$

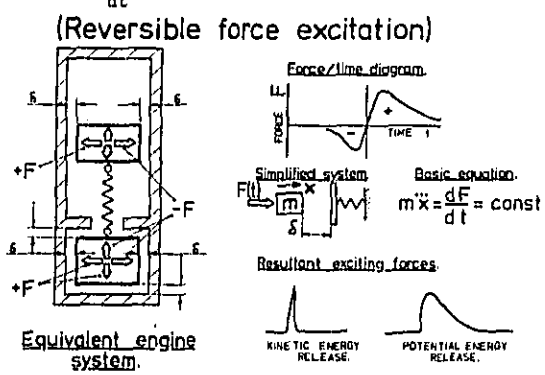

Fig. 16 - Mechanically induced noise - Reversible force excitation

The result of the acceleration of the moving components across the clearances is to impart on contact, as shown in Figure 15, kinetic energy to the structure in the form of an instantaneous step load which depends on the time taken for the component to move across the clearances. Once impacted the continuing application of the changing force produces further excitation of the structure. Since there is lubricating oil in the clearances the movement of components in this manner produces impulsive hydraulic loads (10).

Exact classification of the mechanically induced noise presents enormous problems and it is unlikely to be achieved in the near future. In an engine the various exciting forces occur within a very short time interval (for example combustion impulse and subsequent piston impact around TDC on the working cycle). Oscillographic studies to identify these events can on some engines at certain conditions lead to a reasonable understanding but even then, particularly if the study is made on a multicylinder engine the whole picture can be still very confused. For example it was shown for the impulsive gas excitation test (combustion noise) that any appreciable onset of vibration on the engine block is substantially delayed due to transmission paths through the internal structure while impact by the piston, acting directly on the block, would be almost instantaneous. This means that vibration and noise oscillograms which are actually observed can contain at the same instant effects from both sources of excitation.

Rig tests, where a single source of mechanical noise is induced in the absence of all the other sources normally present in an engine, can help in understanding many aspects of the generation and propagation of that particular source.

Haddad at ISVR (11) developed a method for the simulation of piston slap in a non-running engine. The method is illustrated in Figure 17 which employs a powerful hydraulic force generator which can reproduce the actual magnitude of the sideways piston force diagram.

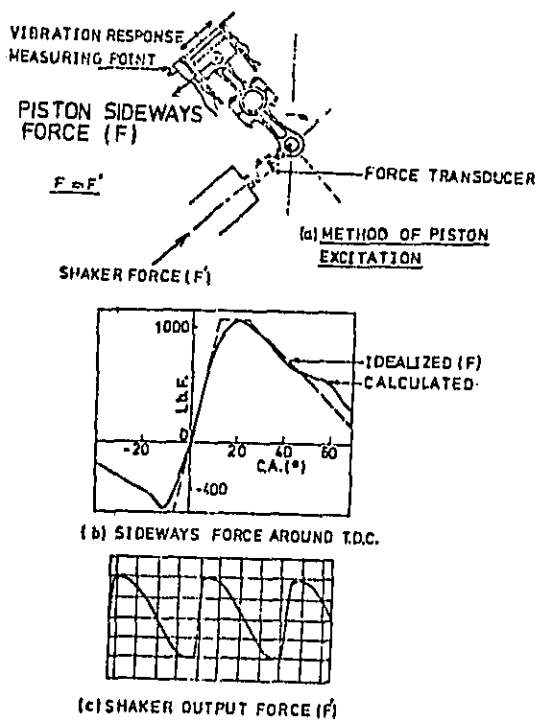

Fig. 17 - Piston slap simulation rig

The force is applied through a monitoring force transducer to the piston via two back-to-back connecting rods using the crankshaft as a pivot. The crankshaft bearings are packed with grease to eliminate friction and bearing impacts. Even then some errors are introduced because of the inertia forces of the back-to-back connecting rod system and the uncertainty of the hot piston shape. The piston can be excited at operating frequencies and force characteristics corresponding to any engine speed. Subjectively the noise in these tests often is indistinguishable from the running engine.

Figure 18 shows the one-third octave band

spectra of the vibration of the crankcase on the running engine on a test bed. Compared with this spectrum are averaged spectra from all the cylinders slapped on a rig with the non-running engine. An average spectrum is also shown from impulsive gas load tests (combustion noise). As can be seen on this this particular engine, in the frequency range between 800 and 1800 Hz, the resultant vibration is of equal magnitude whether resulting from piston slap predominates over the combustion induced vibration. The results illustrate that on this particular engine both sources are of equal importance which is commonly the case of DI engines. Elimination of piston slap would only give a marginal reduction of noise (2 to 2.5 dBA) which is also commonly observed in practice.

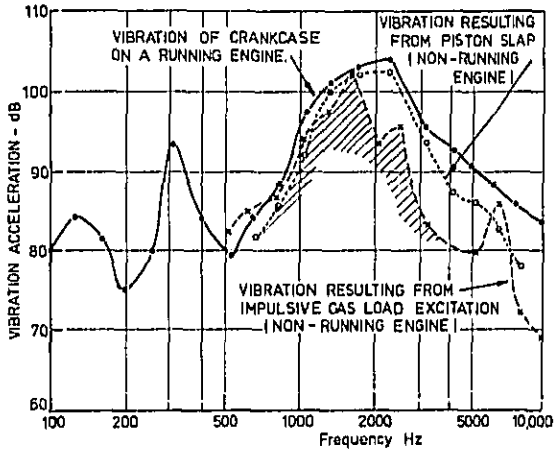

Fig. 18 - Comparison of vibration spectra from running engine, and test rig excitation

The value of the rig tests is that they enable the establishment of the effects of important parameters which control the noise. For example, the increase of noise with piston clearance has been found at high engine speeds to be: $I \sim \delta^{1.5 \text{ to } 2}$, while at low engine speeds: $I \sim \delta^3$. Emitted noise, as already predicted by theoretical considerations, depends on the rate of side force, i.e. $(\frac{dF}{df})$ (see Figure 16) and at constant maximum amplitude of F: $I \sim (\frac{dF}{df})^2$. The value of $\frac{dF}{df}$ can be readily calculated from the known cylinder pressure development and the magnitude of inertia forces, and it can be seen that piston slap noise can follow the same rate of increase of noise with speed as combustion induced noise. The rig tests also enable the study of effect of piston shape (hot or cold shape) to be carried out and thus gradually provide the essential in formation in quiet piston design.

Regarding the noise generation in the main bearings, a test rig at ISVR was jointly developed with Glacier Metal Company. The rig is so designed that the engine pistons can be removed, yet the crankshaft is subjected to realistic inertia loads. The rig has been used for the study of the gasoline engine noise phenomena where a very high rate of increase of noise with speed at the top of the engine speed range is commonly observed. (15)

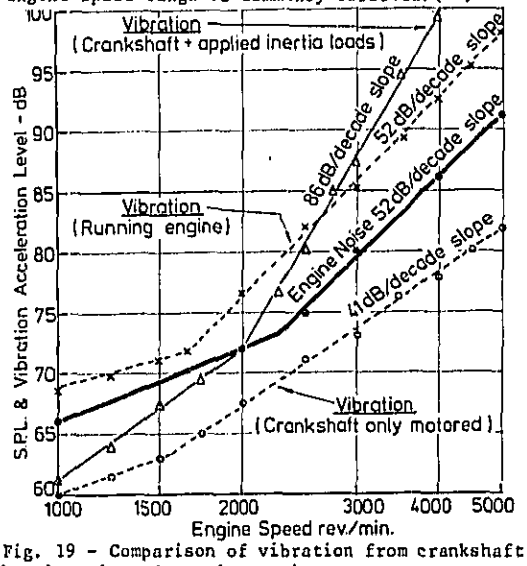

Fig. 19 - Comparison of vibration from crankshaft bearing rig and running engine

Figure 19 illustrates that vibration measurements on the rig closely represent the vibration measured on the running engine thus confirming that exciting forces develop in the main bearing due to some irregular movement of the shaft, i.e. similar impacts to the piston which are cushioned by an oil film. Impulsive oil pressures, however, have been observed which correlate, to a reasonable accuracy, with the observed vibration and noise. High speed diesel engines exhibit similar characteristics and similar trends have been observed on some DI truck engines at the top end of the speed range.

RELATION BETWEEN COMBUSTION SYSTEM ENGINE DESIGN AND EMITTED NOISE

Until recently the majority of engines were of the normally aspirated direct injection combustion type and the noise of the engine was predominantly controlled by the rapid pressure rise resulting from combustion. The form of the pressure diagram and its magnitude, to a first approximation, remain the same on a degree basis over the whole engine speed range. The characteristics of the gas pressure therefore (shape and form of cylinder pressure diagram) control the rate of increase of force with speed and the resultant noise (12). Based also on extensive studies of the effect of bore diameter and bore to stroke ratio on DI engine noise (3) the engine noise can be expressed in very simple terms by the following equation.

Engine noise intensity $I \sim C_f \cdot C_s (N^n \times B^5)$

where C_f defines the level of gas force
C_s defines the engine structure characteristic
B is bore diameter

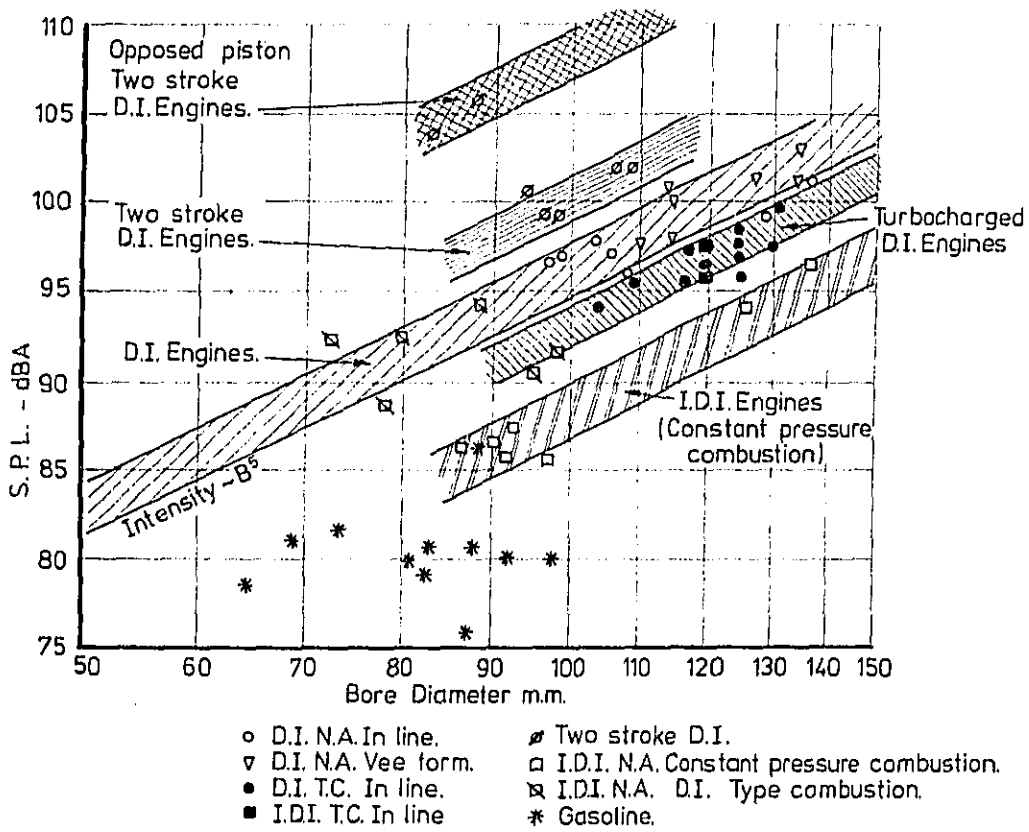

Fig. 20 - Relation between overall noise and bore size at 2000 rev/min full load

N is engine speed
n is the combustion index

Using this formula engine noise could be predicted with reasonable accuracy.

Recently, however, considerable progress has been been made in reducing combustion induced noise by matching of fuel injection characteristics (speed and load advance or injection timing), by turbo-charging and development of low noise high swirl DI combustion systems and IDI engines with constant pressure combustion. Thus in many engines now in production the shape and form of the pressure diagram changes significantly over its speed and load range and therefore the combustion index, n, and the level of gas force C_f are no longer valid for predicting total engine noise. This was apparent when a noise survey of a large number of engines was carried out (3). The constant C_s which defines the engine structure characteristics also is rapidly changing by the introduction of improved engine structure.

The last parameter, the bore diameter, however, tends to remain an important criterion as illustrated in Figure 20 where the overall noise, dBA, at full load conditions of some 60 different engines is plotted versus bore diameter at 2000 rev/min. The data were obtained from tests carried out at ISVR and A V L.

The various engine types fall in distinct classified groups according to the combustion system and the fundamental design principles.

Apart from gasoline engines which show a considerable scatter, the noise of engines with different combustion characteristics fall within specific 3 dB bands of slope of $(\text{bore})^5$. There is, however, no difference between engines of different structural configuration whether Vee form or inline or from 4 to 10 cylinders.

The clearly defined bands starting from the noisiest are :

1. Opposed piston two-stroke engines
2. Two-stroke DI engines
3. Direct injection normally aspirated and DI type IDI engines
4. Turbocharged engines
5. IDI engines with constant pressure combustion

Based on investigations by Anderton (12) on normally aspirated DI engine noise the level of combustion induced noise for each of the engine groups could be predicted; but only the normally aspirated DI engine and the two-stroke cycle DI engines give reasonable prediction of overall noise.

Turbocharged engines, which in practice are only some 3 to 4 dBA quieter, should in theory be about 10 dBA quieter, and IDI engines about 5 dBA

quieter if their noise were combustion controlled and therefore mechanically induced noise plays an important part. It is, however, of interest that also for mechanically induced noise, as shown by Lalor (3) by simple first order calculations that an increase proportional to (bore)^5 can be expected.

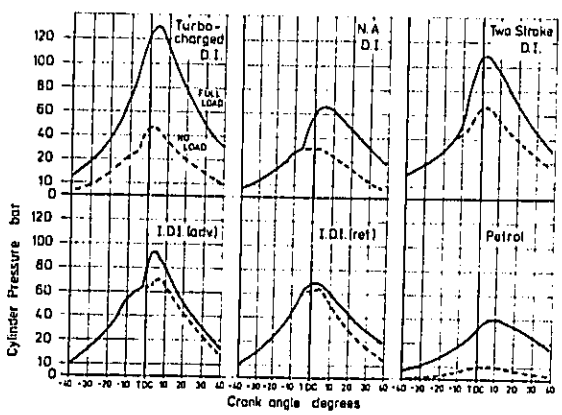

Fig. 21 - Typical pressure diagrams of various combustion systems

Many of the differences between these various groups can be explained by the salient features of cylinder pressure development. Typical pressure diagrams are shown in Figure 21 for a normally aspirated DI engine, a turbocharged engine, both DI type combustion and constant pressure combustion IDI engines and a gasoline engine.

The diagram of the turbocharged engine is extremely smooth but with a high peak pressure of 100-135 bar. The DI engine pressure diagram is abrupt but the peak pressure is considerably lower at 65-80 bar. The DI type combustion IDI diagram is similar to that of the DI while the constant pressure IDI or smooth double hump peaking at 65-75 bar. The petrol engine diagram is smooth and the peak pressure low at 35-50 bar.

Comparisons of the exciting propensities of various combustion systems in terms of normalised cylinder pressure level (12) and peak pressure are broadly illustrated in Figure 22. As can be seen the various systems occupy distinct bands. Swirl in normally aspirated engines has a very marked effect on reducing the cylinder pressure level (combustion noise). High swirl DI engines, as M.A.N. 'M' system (13), A.V.L. system (14), achieve equivalent smoothness of pressure development to the turbocharged and IDI constant pressure combustion engines. This smoothness is achieved with some increase in peak cylinder pressures. In the turbocharged engines, however, the smoothness of cylinder pressure development is obtained at thee expense of very high peak pressures. It is of interest to note the two turbocharged IDI engines

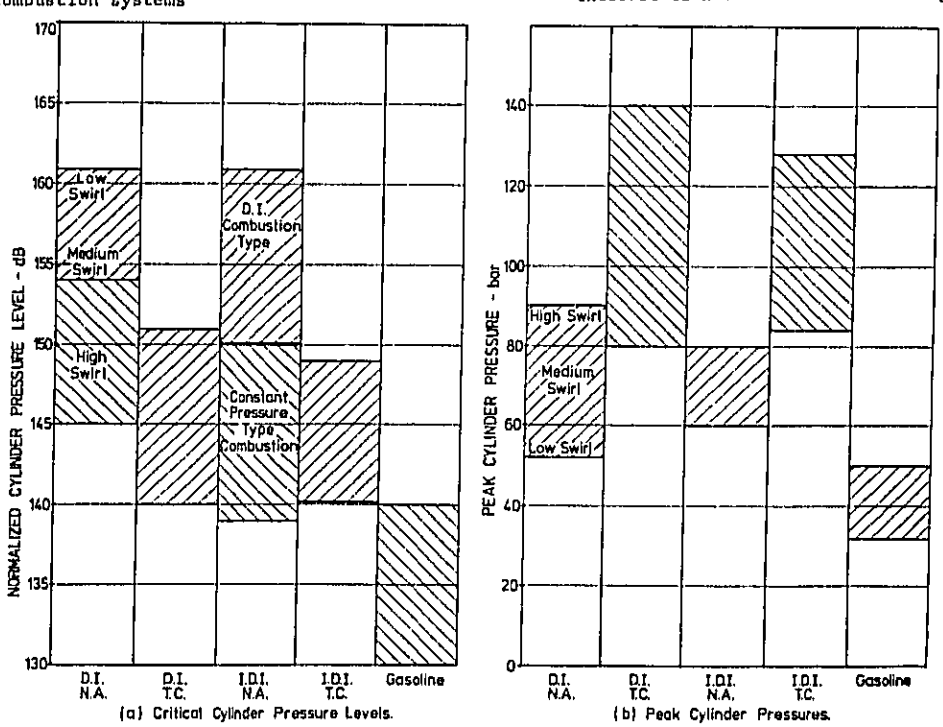

Fig. 22 - General ranking of normalised cylinder pressure levels and peak pressures for various combustion systems (Full load conditions)

shown in Figure 20 (AVL results) fall in the same band as DI turbocharged engines. In both types of engine the peak cylinder pressures are high. The peak cylinder pressure and inertia forces control the rates of reversible forces. Table I summarises the average values for the various engine groups.

Table I

	Parameters controlling combustion induced noise		Parameters controlling mechanically induced noise	
	Cylinder pressure level $CPL_N(1.0)$dB	Cylinder pressure spectrum slope, n,	Peak cylinder pressure (bar)	Piston side force at 1000 rev/min dF/dt N/sec
Two-stroke DI engine	160.5	4.15	110	4.7×10^6
DI engine	156	3.4	70	2.2×10^6
Turbocharged DI engine	144	5.1	130	5×10^6
IDI engine	145	4.45	70	1.8×10^6
Gasoline engine	130	5.0	40	0.9×10^6

In the turbocharged engine the very low cylinder pressure level (combustion induced noise) is achieved at the expense of very high peak pressure and consequently the rate of reversible force is increased. (Normally by a factor of two or more).

In gasoline engines there are low cylinder pressure levels, which are also associated with low peak pressures, (one-third of the turbocharged diesel engine) and thus also the rate of reversible forces is only about one-fifth of those of the turbocharged diesel engine. The low gas pressures permit the engine to be designed considerably lighter (weaker structure) which also permits the design of much lower reciprocating mass (piston, gudgeon pin and the connecting rods) thus also reducing noise.

These considerations also require the effect of the bore to stroke ratio on engine noise to be reconsidered. The investigations which have been made on gasoline engines reveal that by increasing the bore to stroke ratio a quieter engine is obtained, thus contradicting the findings on the direct injection diesel engines, where increase of bore to stroke ratio for a given cylinder capacity, increased the noise.

It can be concluded that bore to stroke ratio only affects the engine noise above a certain "critical value" of cylinder pressure level. It is suggested that above a cylinder pressure level $CPL_N(1.0) \approx 140$ dB the bore to stroke ratio for a *given capacity* increases the noise, while below this value there is some evidence that noise decreases with increasing bore/stroke ratio.

EFFECT OF SPEED OF ENGINES WITH VARIOUS COMBUSTION SYSTEMS

From the engines investigated which are illustrated in Figure 20 four engines of approximately 100 mm bore are chosen to illustrate the effect of speed. For the same bore diameter at 2000 rev/min there is about 17 dBA difference in the level of noise between the gasoline and the direct injection normally aspirated engine. The IDI engine is 10 dBA noisier while the turbocharged engine is 14 dBA noisier than the gasoline engine. (Fig. 23).

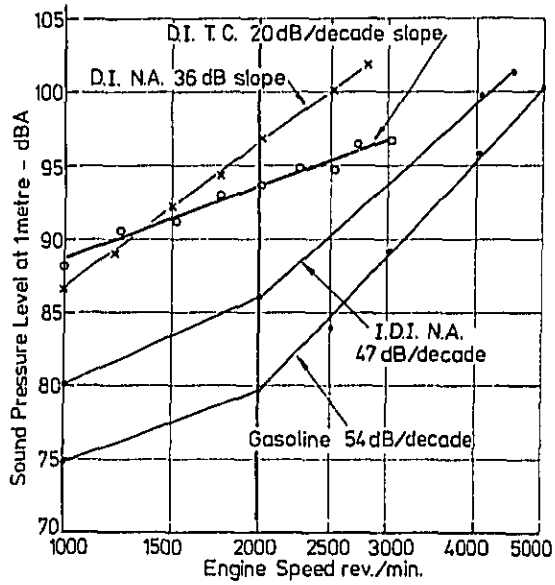

Fig. 23 – Typical noise versus speed curves for engines of 100 mm bore with different combustion systems

Comparing these results with the combustion indexes given in Table I it can be seen that only the direct injection engine follows the principle of the combustion model with the noise increasing in proportion to the increase of cylinder pressure level. On the turbocharged engine the rate of increase of noise is only around 20 dB/decade whereas the combustion index predicts about 50 dB/dec.

Tests at ISVR of some eight different turbocharged DI engines have shown slopes ranging from only 21 to 24 dB/decade. AVL also have found this generally to be the case, though in some instances slopes as high as 33 dB/decade have been found on both IDI and DI turbocharged engines. The high speed engines, namely the gasoline and high speed IDI, have two distinct slopes and neither of them can be correlated to the combustion mechanism.

THE PROBLEM OF THE NOISE OF A TURBOCHARGED ENGINE

The main problem of a turbocharged engine lies in the fact that the smoothness of the cylinder pressure diagram is obtained only around the maximum speed and load. At low speeds full load, and high speeds light load, the cylinder pressure diagrams become abrupt resembling those of the original direct injection engine as shown in Figure 24.

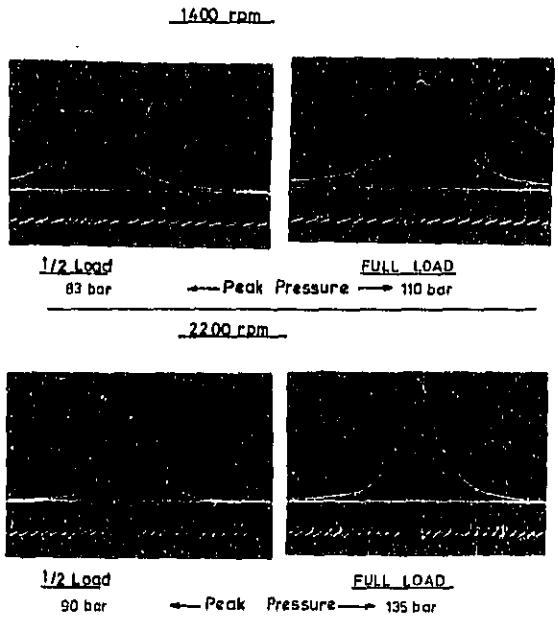

Fig. 24 - Cylinder pressure diagrams of a turbocharged diesel engine

Thus it can be expected that the predominant noise in the turbocharged engine will change from "combustion controlled" to "mechanically controlled" over its operating range. This is illustrated in Figure 25 for a 300 HP turbocharged engine.

At full load the engine noise increases by 25 dB/decade, while at the same time the cylinder pressure levels decrease, i.e. they have a negative slope of 33 dB/decade. At no load, however, (noise level is somewhat lower) the noise increases by 32 dB/decade which approximately corresponds with an increase of cylinder pressure level. Thus it may be assumed that at no load the engine is combustion controlled since the peak pressures (around 50 bar) are almost half of that of full load. Calculations of piston rate of side force values over the speed range show about 25 dB/decade if $\frac{dF}{dt}$ is expressed as 20 $\log_{10} \frac{dF}{dt}$ corresponding

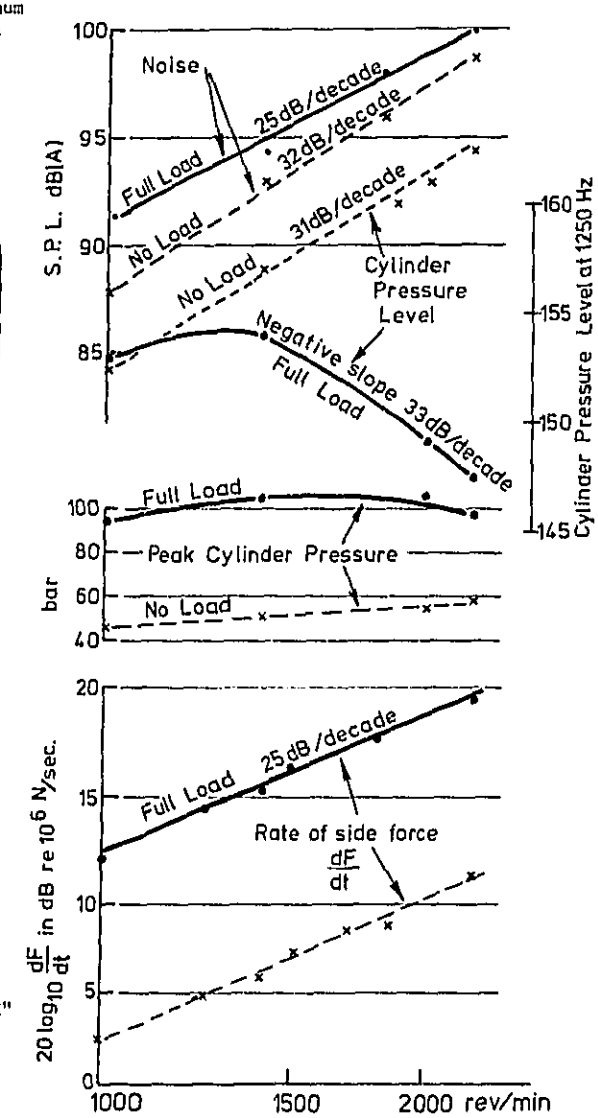

Fig. 25 - Correlation between noise, cylinder pressure and inertia characteristics of a turbocharged DI engine

with the rate of increase of noise. At no load, the values or $\frac{dF}{dt}$ are low. Previous work (6) by the writer suggests that mechanically induced noise,

either in the bore or bearings should have some 20 to 25 dBA/decade characteristic.

Some experiments have been made on two turbocharged engines where attempts were made to maintain the same cylinder pressure levels as far as possible in the frequency region of the predominant engine noise, but only changing the peak pressure. Figure 26 shows the relationships between noise and peak pressures obtained.

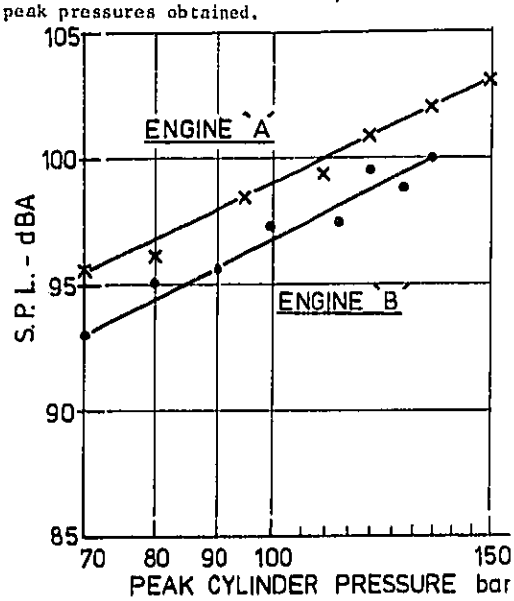

Fig. 26 - Effect of peak cylinder pressure on noise of two turbocharged engines

On both engines, the noise-peak cylinder pressure relation (peak pressure plotted on a logarithmic scale) are linear and therefore can be expressed in the form

Engine A $I \sim P^{2.16}$

Engine B $I \sim P^{2.3}$

where P is peak cylinder pressure

These observations indicate the great potential in reducing the turbocharged engine noise provided the reduction of peak pressure is acceptable from performance considerations.

CONCLUSIONS

In the paper an attempt has been made to elucidate the many problems associated with diesel and gasoline engine noise. It is clear that the chosen combustion system to a great extent predetermines the basic engine design and is largely responsible also for determining whether the engine will be combustion or mechanical noise controlled. The exact relationship between these two sources, despite the enormous quantity of theoretical and analytical work that has been carried out, remains unresolved.

Control of engine noise by external structural redesign holds some promise but the influence of the internal structure is at present a limitation.

ACKNOWLEDGEMENTS

The author is deeply indebted to all his colleagues at ISVR for all their help and to many engine companies throughout the world which have supplied engines for research, thus making this wide spectrum study possible and to Dr. Gerhard Thien for most valuable discussions and for additional noise data of engines of varying type. In particular thanks are due to Mrs. G.Pullen, Mr. P. Prust and Mr. Grover, who have given great help in the preparation of the manuscript.

REFERENCES

1. C.H.G. Mills and D.W. Robinson, "The subjective rating of motor vehicle noise", Noise Final Report, H.M.S.O, 1966.

2. P.E. Waters and T. Priede, "Origins of diesel truck noise and its control", Society of Automotive Engineers (SAE) paper 720636, 1972.

3. D. Anderton, E.C. Grover, N. Lalor and T. Priede, "Automotive diesel engine noise - its combustion and design", Land Transport Engine Symposium, Institution of Mechanical Engineers, 1976.

4. A.E.W. Austen and T. Priede, "Origins of diesel engine noise", Engine Noise and Noise Suppression Symposium, Institution of Mechanical Engineers, October 1958.

5. D. Anderton, E.C. Grover, N. Lalor and T. Priede, "Origins of reciprocating engine noise - its characteristics, prediction and control", A.S.M.E. paper 70-WA/DGP-3, 1970.

6. T. Priede and E.C. Grover, "Noise of industrial engines", Noise from Power Plant Equipment Symposium, Institution of Mechanical Engineers Proceedings, Vol. 181, 1966-67.

7. -. Alcock. Contribution to discussion, Institution of Mechanical Engineers Symposium, Engine Noise and Noise Suppression, London, Oct. 1958.

8. K. Ochiai, "Relationsbetween crankshaft torsional vibrations and engine noise", Society of Automotive Engineers, February 1979.

9. E.C. Grover, "Engine Structures and Noise", M.Phil Thesis, University of Southampton, 1966.

10. J.A. Raff and E.C. Grover, "A primary noise generation mechanism in petrol engines", Institution of Mechanical Engineers Conference on passenger car engines, Paper C320/73, 1973.

11. S.D. Haddad, H.L. Pullen and T. Priede, "Relation between combustion and mechanically induced noise in automotive diesel engines", F.I.S.I.T.A. Conference, paper A-2-4, 1974.

12. D. Anderton, "Combustion as a source of diesel engine noise", Ph.D. Thesis, University of Southampton, 1974.

13. J.S. Meurer and A.C. Urlands, "Development and operational results of the M A N FM combustion system", Society of Automotive Engineers, (SAE) paper 690255, 1969.

14. W.P.S. Cartellieri and B. Shukoff, "Die Direkte Einspritzung fur Leichte Dieselmotoren", 17 F.I.S.I.T.A. Congress, Budapest, 1978.

15. Baker, J.H. Private Communication

790506

A REVIEW OF BASIC DESIGN PRINCIPLES FOR LOW-NOISE DIESEL ENGINES

Gerhard E. Thien

AVL Prof. List Ges.m.b.H.
Graz, Austria

ABSTRACT

In accordance with the main efforts of research and development in noise control of diesel engines measures which are essential for a noise reduction of more than 10 dB(A) and results achieved with an advanced direct injection combustion system are described. In general the noise of external engine parts can be reduced to a large extent only by vibration isolation or sound reducing shells. Considering economic aspects the attenuation of the total engine noise by more than 10 dB(A) requires a complete encapsulation of the engine which can with newly designed engines at least be partly integrated into the engine structure. Outgoing from some fundamentals about sound reducing shells the different approaches for low noise engines based on these principles and developed in the last decade are discussed. Specific measures applied with the advanced D.I. combustion system are discussed resulting, in comparison with optimized I.D.I. combustion systems, in equivalent exhaust emission, acceptable combustion noise and, regarding small diesel engines, in the same power output and speed maintaining the big advantage in fuel consumption.

THE REDUCTION OF DIESEL ENGINE NOISE has been considered as an important task by AVL, a private engine design and development center, already twenty years ago (1)*. Research and development work for noise control of diesel engines concentrated for the last twelve years on the elaboration of practical and easily applicable solutions for production (2-14). The goal of this research was, right from the beginning, to achieve a significant noise reduction. The loudness ought to be reduced at least by half, in other words the target of noise control was a reduction of the noise level by more than 10 dB(A). The essential result of these investigations is that such a high noise reduction can only be achieved with all components, constituting the engine surface, being vibration isolated against the vibrations of the inner engine structure. The major part of this paper represents a review of different engine design approaches corresponding to the target concept resulting from investigations at AVL. The fundamentals leading to these approaches and the theoretical basis are discussed in detail.

Beside measures necessary for a significant noise reduction, a reduction of the excitations caused by the combustion and mechanical processes and an acoustical improvement of the engine structure are always being attempted. This is particularly the case if no increase in the cost of production and operation of the engine is involved. But also more extensive measures are applied to conventionally designed engines if they are economically justified from the point of view of requirement. Experience proved that this is true for noise reductions up to 5 dB(A). Newly developed analyzes and computational methods which are described in the contribution of ISVR enable in the design and development stage a quicker and better detection of possibilities for acoustically improved engine structures. To keep the mechanical excitations as low as possible is a goal that is generally aimed at, but limited by economic considerations. Be it that a better arrangement of components, where the mechanical noise is excited, proves too expensive compared with the acoustical advantage achieved or be it that the material and machining quality required as well as the tolerance limit cause unreasonably high additional costs.

An essential task in the course of any diesel engine development consists in the search for an optimum combustion system. The predominant importance with regard to fuel consumption initiated AVL years ago to concentrate on the development of the direct injection (D.I.) combustion system (15-24). Maintaining the high fuel economy AVL succeeded in reducing exhaust emission and combustion noise. With this advanced D.I. system equivalent exhaust emission, power output and speed as with I.D.I. systems can be achieved. Also with regard to noise, this system represents an interesting alternative for today's I.D.I. high-speed light-duty diesel engines. The specific measures applied and results achieved will be discussed later.

STATE OF DEVELOPMENT OF MODIFICATIONS OF THE ENGINE DESIGN TO ACHIEVE SIGNIFICANT NOISE REDUCTIONS

The results of investigations carried out on different conventionally designed diesel engines show that vibrations starting from the vibration excited inner engine structure are transmitted, due to the stiff connection to all parts of the engine structure. These vibrations cause emission of air

*Numbers in parentheses designate References at end of paper.

SAE/P-79/80/$02.50
Copyright © 1979 Society of Automotive Engineers, Inc.

borne sound so that practically all individual engine components contribute to the total engine noise (5,6,8,12). The air borne sound measurements, as shown in Fig. 1, were taken on two different engines at one microphone position each and demonstrate that there are certain engine components which contribute to the total engine noise with a higher percentage than others. With the inline engine, upper part of the figure, these are the crankcase side wall with 20 %, the air intake duct with 18 % and the oil pan with 10 %. With the V-engine, lower part of the figure, the oil pan is contributing with 22.5 %, the crankcase side wall with 20 % and intake and outlet manifolds with 12.5 % and 10 % respectively. The elimination of the noise of these single engine components contributing approximately half of the total sound intensity would, however, only result in a noise reduction of 3 dB(A). To achieve a noise reduction of 10 dB(A) and more the sound intensity must be reduced to under 10 %. This requires a noise reduction of practically all individual engine components of the outer engine structure. Also with one or the other engine component contributing only insignificantly to the sound intensity at one of the microphone positions, experience shows that at other microphone positions a contribution of several percent is seen (12).

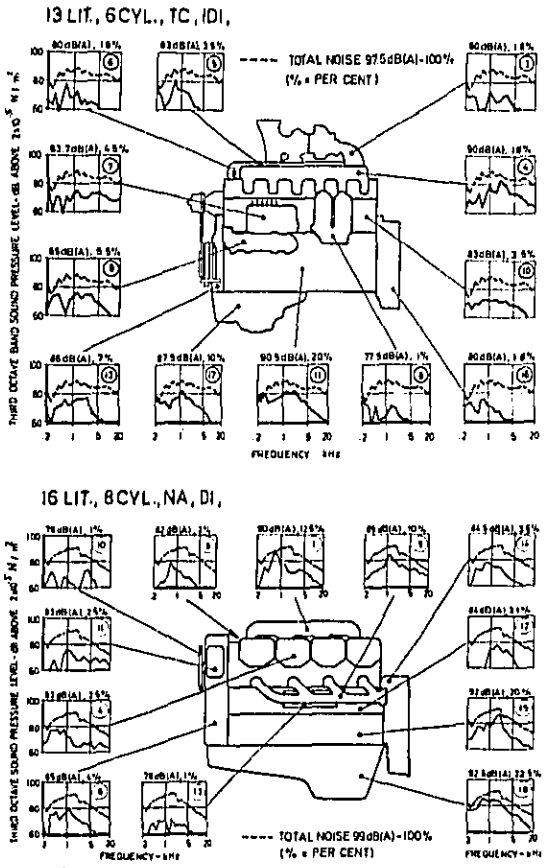

Fig. 1 - Water-cooled diesel engines, noise radiated by the engine surfaces (6,8)

The outer engine structure consists on the one hand of components subjected to the operating forces, such as cylinder block, cylinder head, crankcase, gear box and flywheel housing and on the other hand of parts which do not carry any load, but are attached to the load carrying engine structure. A noise reduction of the individual engine components requires the reduction of their structural vibrations or else a reduction of the air borne sound emission caused by the structural vibrations. Various measures such as damping, stiffening or vibration isolation result in a reduction of the structural vibrations. However, the effect and applicability of such measures varies considerably.

The loss factor of components of assembled engines is already relatively high so that only insignificant or sometimes no improvements can be achieved by the application of an additional damping layer. More effective is the use of composite material, but also here noise reductions of the individual component of 10 dB(A) or more cannot be achieved (12). The stiffening causes essentially a shifting of the natural bending frequencies. On the one hand an unfavorable coincidence of natural frequencies can thus be avoided in the path of vibration transmission. On the other hand by raising the natural frequencies the range of lower excitations

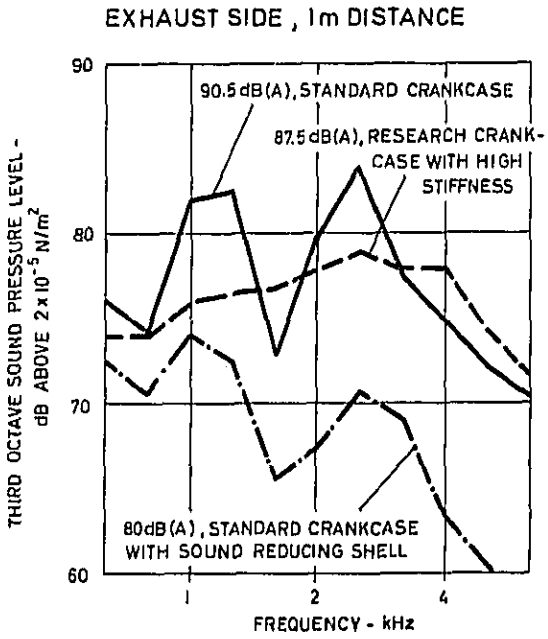

Fig. 2 - Water-cooled 4-cylinder diesel engine, noise of the side wall with various crankcase versions (8)

is reached as the frequency spectra of the exciting forces show a decreasing tendency in line with the frequency. This measure, however, only allows improvements by a few dB(A) (7,8,13). Fig. 2 shows as an example the effect of the extreme cross-ribbing of a crankcase side wall. The sound level is reduced at some third octave bands up to 7 dB, the total noise of the wall, however, is only 3 dB(A) lower.

Whereas damping and stiffening can be applied to load carrying engine parts as well as other components, the vibration isolation can only be achieved with detachable parts. It is, however, a highly effective measure, as can be seen in Fig. 3 demonstrating the noise emission of an intake manifold. Contrary to the stiffening and damping, improvements of 10 dB(A) and more can generally be achieved and this measure therefore meets the requirement for an essential noise reduction (3,4,6, 12). In this connection it has to be noted that the sealing element of an attached part cannot easily perform the function of a vibration isolating element. The contact pressure, which in this case has to be reduced considerably, will hardly guarantee sufficient sealing, e.g. against oil. Solutions already used in production prove, however, that by varying the shape or separating the sealing function from the vibration isolating function satisfactory design approaches are possible.

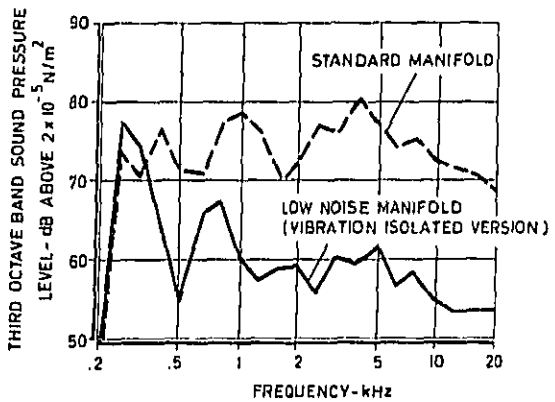

Fig. 3 - Water-cooled 4-cylinder diesel engine, intake manifold noise (8)

For load carrying engine components, as described above, the only possibility for an essential noise reduction consists of obstructing the sound emission. This can be achieved most effectively by so-called sound reducing shells, these are flexible panels which are mounted at a certain distance from the component surface (3,5,6,12). They are either connected to the engine component itself by intermediate vibration isolating elements or to other adjacent components. A sound emission from the space between engine component and sound reducing shell has to be avoided. The easiest way to meet this requirement is by an elastic sealing along the complete circumference. An example for the noise reducing effect of such a shell, mounted on the crankcase side wall of a diesel engine, can be seen in Fig. 2. As these shells represent an important factor in the highly effective noise reduction efforts with diesel engines they will be discussed separately in the following section.

SOUND REDUCING SHELLS - Theoretical Background - The effect of sound reducing shells mainly depends on three processes, namely the transmission loss of the covering plates, the trapped air between covering plates and engine surface and the transmission of structural vibrations via the connecting elements. It is difficult to determine mathematically the noise reducing effect of the entire shells. In the following the effect of these parameters will be described by the aid of simplifying models.

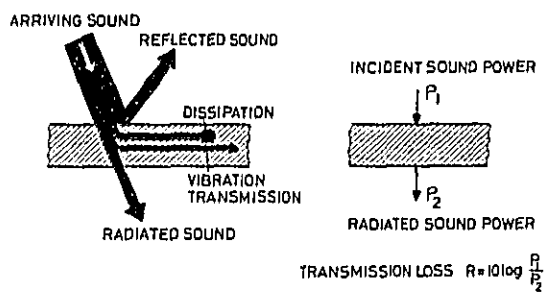

Fig. 4 - Interaction of sound with solid structure

Fig. 4 shows schematically the process occuring when the air borne sound propagation is obstructed by a solid structure e.g. a wall. One part of the incident sound energy is reflected from the wall, the other part stimulates a structural vibration excitation of the wall. Part of the structural vibration energy is dissipated into heat by the damping effect of the wall, part of it is transmitted to adjacent components by the propagation of structural vibration and part of it is emitted as air borne sound energy from the other side of the wall. On the right side of Fig. 4 the transmission loss R, describing the acoustical effect of the wall is defined. In the case of a periodic plane sound wave incident on an elastic wall at any angle ϑ deviating from the normal of the wall, bending frequencies are usually generated. This process is shown schematically in Fig. 5 by taking a plane, thin wall as an example (12,25). The wave length λ_{Bc} of these forced bending waves depends, as can be seen in Fig. 5, on the air borne sound wave length λ and the angle of incidence. Contrary to the forced bending waves, the free bending waves (wave-length λ_B, wave number k_B) are determined by the wall material (bending stiffness B, wall mass m) and the frequency, see Fig. 5. Free bending waves occur at the edges of finite plates due to the reflection of the forced bending waves. The difference between the forced and

free bending waves has in general a considerable effect on the transmission loss.

As can be seen in Fig. 5, the transfer impedance Z_T, a decisive factor for the transmission loss, depends not only on the bending stiffness B of the wall and the circular frequency ω, but also on the difference between the wave number of the

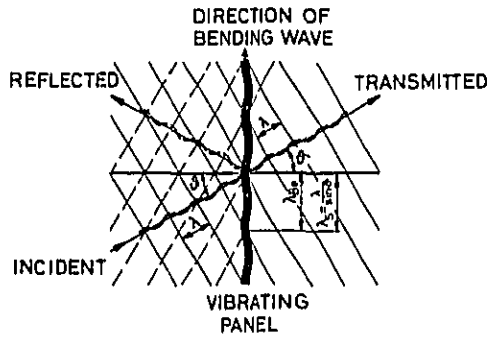

TRANSMISSION LOSS	$R = 20\log\left\|1 + \frac{Z_T}{2\varrho c}\cos\vartheta\right\|$
TRANSFER IMPEDANCE	$Z_T = \frac{p_1 - p_2}{v_W} = \frac{B}{j\omega}(k^4\sin^4\vartheta - k_B^4) = j\omega m(1 - \frac{\omega^2 B}{c^4 m}\sin^4\vartheta)$
COINCIDENCE	$\lambda_{Be} = \lambda_s = \lambda_B = \frac{\lambda}{\sin\vartheta} \longrightarrow Z_T = 0,\ R = 0$
CRITICAL FREQUENCY	$f = \frac{\omega}{2\pi} = f_c = \frac{c^2}{2\pi}\sqrt{m/B} \qquad \lambda = \lambda_B,\ \sin\vartheta = 1$
MASS LAW	$\frac{\omega^2 B}{c^4 m} \ll 1 \longrightarrow Z_T = j\omega m$

p_1... SOUND PRESSURE ON SIDE OF INCIDENCE (SUM OF SOUND PRESSURE OF INCIDENT AND REFLECTED SOUND WAVE)
p_2... SOUND PRESSURE ON THE OTHER SIDE
v_W... VELOCITY OF PANEL — ω... CIRCULAR FREQUENCY — $j = \sqrt{-1}$
ϱ... DENSITY OF AIR — c... SPEED OF SOUND IN AIR
B... BENDING STIFFNESS OF PANEL PER UNIT WIDTH
$k = \frac{2\pi}{\lambda} = \frac{\omega}{c}$ $\quad k_B = \frac{2\pi}{\lambda_B} = \sqrt{\omega}\sqrt[4]{m/B}$
λ_B... WAVE LENGTH OF FREE BENDING WAVES — m... PANEL SURFACE DENSITY
λ_{Be}... WAVE LENGTH OF FORCED BENDING WAVES — λ_s... TRACE WAVE LENGTH

Fig. 5 - Plane sound wave incident on an infinite homogenous panel (12,25)

forced ($k_{Be} = k.\sin\vartheta$) and free bending waves (k_B) to the power of four. From the consequently occurring so-called critical frequency f_c (angle of incidence $\vartheta = 90^\circ$) on, it is possible that the wave-lengths of the forced and unforced bending waves coincide ($0 < \vartheta < 90^\circ$), and at this frequency the transmission loss R decreases to theoretically zero. The critical frequency of materials that are suitable for sound reducing shells is above the frequency range considered with engine noise reductions, this is 12-6 kHz for sheet steel of 1-2 mm and 6-3 kHz for aluminium-sheet of 2-3 mm respectively. A break in the sound reduction caused by coincidence is therefore of no importance with regard to the sound reducing shells. As the sound incident is in general far from uniform, i.e. the angle of incidence ϑ is random with all frequencies (diffused incidence of sound), no complete breaks in the sound reduction occur in the real case but only a diminished sound reduction is given above the critical frequency. The relations plotted in Fig. 5 demonstrate furthermore that below the critical frequency f_c the transfer impedance Z_T reduces to the mass impedance $j\omega m$. In this range the transmission loss takes the form of the generally known mass law.

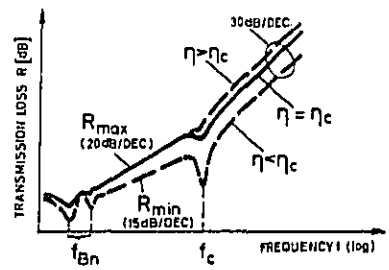

I) BELOW CRITICAL FREQUENCY f_c

$k < k_B$, $\omega^2 B/c^4 m \ll 1 \longrightarrow Z_T = j\omega m$

a) $\eta \geq \eta_c = 1000\,(h/a)^2$ — LARGE PANELS RESP HIGH DAMPING (MAIN INFLUENCE FROM FORCED BENDING WAVES)

$R = 10\log\left[1 + \left(\frac{\omega m}{2\varrho c}\cdot\cos\vartheta\right)^2\right]$

IN GENERAL $\omega m/2\varrho c \gg 1$ AND IN THE AVERAGE $\vartheta = 45^\circ$

$R_{RANDOM} = R_{max} = 20\log\frac{\omega m}{2\varrho c} - 3$

b) $\eta < \eta_c$ — SMALL PANELS RESP LOW DAMPING (MAIN INFLUENCE FROM REFLECTED FREE BENDING WAVES)

$R_{RANDOM} = R_{min} = 10\log\frac{\omega m}{2\varrho c} + 10\log K_B\, a - 3$

II) ABOVE CRITICAL FREQUENCY f_c

$R_{RANDOM} = 20\log\frac{\omega m}{2\varrho c} + 10\log\frac{f}{f_c} + 10\log\frac{f}{\eta}\eta$

η ... LOSS FACTOR OF THE STRUCTURE — COMPLEX BENDING STIFFNESS $\underline{B} = B(1 + j\eta)$
h ... THICKNESS OF PANEL
2a ... SMALLEST SIZE OF PANEL BETWEEN EDGES OR STIFFENING RIBS
f_{Bn} ... FREQUENCIES OF FUNDAMENTAL NATURAL PANEL VIBRATIONS FOR SIMPLY SUPPORTED PANEL $f_{Bn_x n_y} = \frac{1}{2\pi}\sqrt{\frac{B}{m}}\left[\left(\frac{n_x\pi}{2a_x}\right)^2 + \left(\frac{n_y\pi}{2a_y}\right)^2\right]$

Fig. 6 - Transmission loss of a finite panel (12,25)

Fig. 6 shows (schematically) the transmission loss curve of a finite panel over the whole frequency range, taking into consideration the damping of the panel (12,25). The three ranges are separated by dips. The first dip occurs at the frequencies of fundamental natural panel bending vibrations f_{Bn} and the second dip at the critical frequency f_c. The lowest frequency range is influenced by the stiffness of the panel. In the range between the fundamental natural frequencies and the critical frequency the mass law, as mentioned earlier, applies above a critical loss factor η_c determined by the dimensions of the panel. The mass law is taken in Fig. 6 for an average angle of incidence of $\vartheta = 45^\circ$ according to a random incidence of sound and describes the maximum possible transmission loss in this range (R_{max}). Below this critical loss factor the influence of the free bending waves reflected from the edges of the panel is gaining increased influence. This is the case with small panels respectively panels with low damping. In this case it is

possible to describe the transmission loss by an equation, as illustrated in Fig. 6, representing a lower limit (R_{min}). The increase of this curve is 15 dB/decade instead of 20 dB/decade (R_{max}). (It has to be noted that R_{min} only applies to values below R_{max}). Fig. 6 furthermore demonstrates that the increase of the transmission loss is 30 dB/decade in the range above the critical frequency. Here the damping of the panel has a greater effect and causes a higher transmission loss also for values above the critical loss factor. Fig. 7 outlines the possible magnitude of the transmission loss for the range below the critical frequency of panels made of 1 mm, 2 mm and 4 mm sheet steel and with a dimension (R_{min}) of 2a ≈ 200 mm. It can be seen that, already with a 1 mm sheet steel at 1 kHz and with sufficient damping for the size of panel, a transmission loss of 32 dB (R_{max}) can be achieved. It is therefore possible to achieve sufficient noise reductions, i.e. more than 10 dB(A), with 1 mm sheet steel.

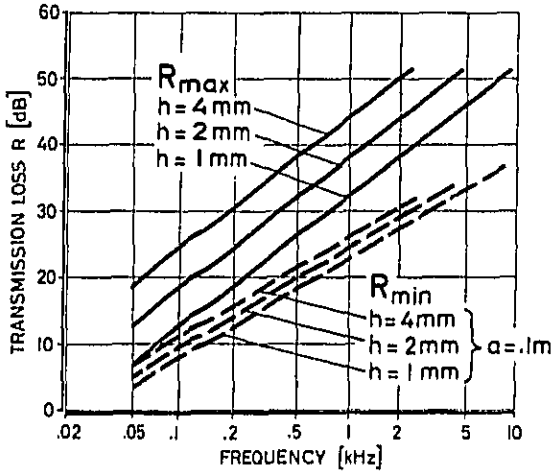

Fig. 7 – Random incidence transmission loss below critical frequency of finite panels of sheet steel

The effect of a sound reducing shell can, of course, not solely be described by the transmission loss of a panel representing the sound reducing shell. There is an interaction between the sound reducing shell, the vibrating engine surface, the trapped air and the air outside the shell, and a vibration transmission via the supporting and the sealing elements between the sound reducing shell and the engine surface. A plane wave model of such a system has been investigated by Jackson (12,26). The result is given in Fig. 8 in terms of the insertion loss at the microphone due to fitting the shell. The sound reducing shell is not spring supported at the vibrating surface but on a sub-system which is however of minor importance for principal conclusions. Very informative is the example of a 2 mm panel of sheet steel mounted at a distance of 190 mm

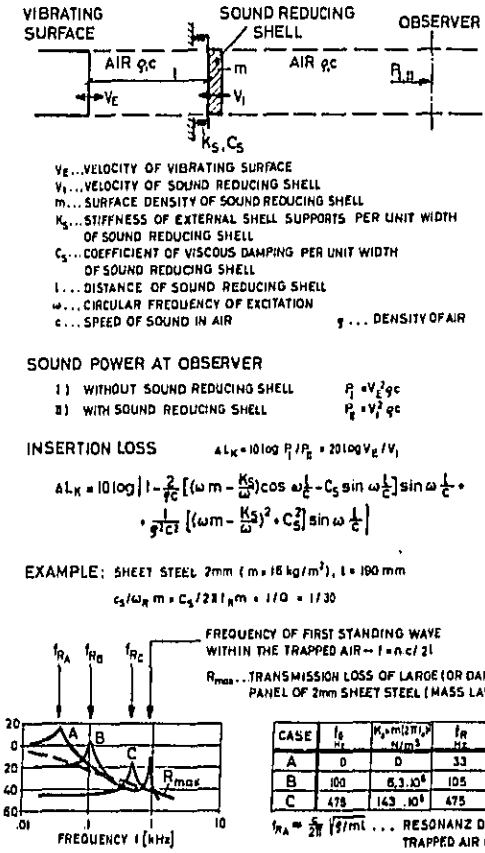

Fig. 8 – Plane wave model of a sound reducing shell (12,26)

which has been calculated with three different stiffnesses of the spring supports, Fig. 8. The insertion loss ΔL_K (that is the difference between the sound level taken at an observation point first with and then without sound reducing shell) shows a distinctive dip (first peak of curves A, B, and C), at a resonance frequency which is given by the oscillatory system consisting of the sound reducing shell, acting as mass, as well as the trapped air and the supports as a parallel spring system. Above this frequency the insertion loss approximately agrees with the transmission loss R_{max}, but at frequencies at which the half wave-length of the air borne sound and its multiples correspond to the distance of the sound reducing shell from the engine surface further dips appear. It is worth noting that

with increasing stiffness of the support the insertion loss considerably improves in the low frequency range. Sufficient damping has to be ensured, however, to avoid an exaggerated transmission loss dip at the air cushion-spring resonance f_R.

A substantial disadvantage inherent in the plane wave model, described in Fig. 8, is that the sound propagation parallel to the wall in the space between engine surface and sound reducing shell cannot be considered. The bending vibrations are neglected as well. Fig. 9 shows the concept of a model considering these conditions. In this model

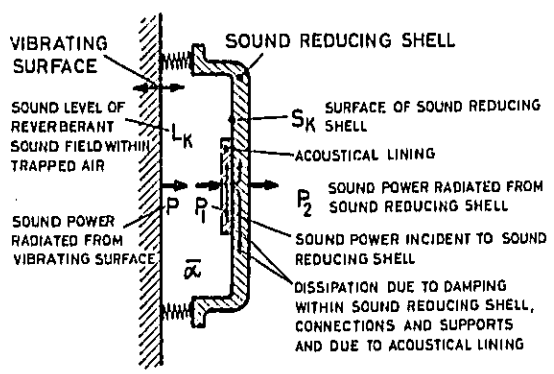

$$L_K = 10\log \frac{P}{\bar{\alpha}.S_R P_0} \quad , P_1 = S_K . 10^{-\frac{L_K}{10}}, \frac{p_0^2}{\varrho c}, \quad P_2 = P_1 . 10^{-\frac{R}{10}}$$

INSERTION LOSS

$$\Delta L_K = R - 10\log \frac{S_K}{\bar{\alpha}.S_R}$$

S_R ... TOTAL SURFACE OF SPACE BETWEEN VIBRATING SURFACE AND SOUND REDUCING SHELL

$\bar{\alpha}$ ... MEAN VALUE OF SOUND ABSORPTION COEFFICIENT RELATED TO TOTAL SURFACE S_R, COVERING SOUND RADIATION AND DISSIPATION

$P_0 = \frac{p_0^2}{\varrho c} = 10^{-12}$ W ... REFERENCE SOUND POWER

$p_0 = 2.10^{-5}$ N/m² ... REFERENCE SOUND PRESSURE

ϱ ... DENSITY OF AIR c ... SPEED OF SOUND IN AIR

R ... TRANSMISSION LOSS OF SOUND REDUCING SHELL

Fig. 9 - Model of sound reducing shell with reverberant sound field within the trapped air (12,27)

the space between the engine surface and the sound reducing shell is assumed to be a reverberant sound field. This is certainly justified if the distance of the sound reducing shell from the engine surface is larger than the wave length of the air borne sound. Experience has shown, however, that under this assumption the results agree well with theory, even if the distance is smaller than the wave length of the air borne sound and that up to a distance of approximately 30 mm (27). Because of the sound reducing shell there is a built-up of the sound level in the space between the engine surface resulting from the sound power P radiated from the engine surface and the reflections of the sound reducing shell. The sound level of the reverberant sound field within the trapped air depends on the overall sound absorbing capacity of the surfaces S_R surrounding the space. The mean value of the sound absorption coefficient related to the total surface is not only the result of the effect of an acoustical lining, but also of the damping within the sound reducing shell, its connections and supports and the sound power P_2 radiated from the surface of the sound reducing shell. The equation for the insertion loss, Fig. 9, demonstrates that no sound reduction can be achieved without some sound absorption. Depending on the design of the sound reducing shell, this can however be achieved without sound absorbing lining by the damping of the shell, particularly at its connections and supports (3,5,6,12).

Examples - The insertion loss of some typical designs, obtained as a result of investigations carried out on a large number of sound reducing shells (3,5,6,12), is given in Fig. 10. The investigation of these sound reducing shells was performed

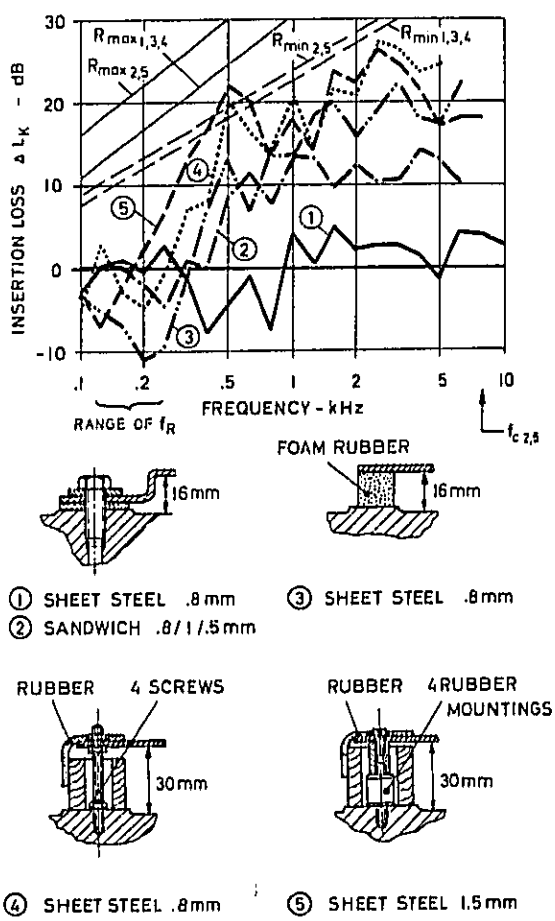

Fig. 10 - Insertion loss of different sound reducing shells 200 x 800 mm attached to the crankcase wall of a 5 liter water-cooled inline 6-cylinder diesel engine

at the crankcase side wall of a water-cooled 6-cylinder inline engine. The examples chosen allow an assessment of the effect of different methods of attaching the shell and the effect of the distance, wall thickness and damping. They also show to which extent the simplified mathematical models, as discussed in the above section, sufficiently describe the effect obtained. The sound reducing shell 1, which is made of sheet metal of 0.8 mm thickness and bolted to the engine wall along its circumference brings about – as could be expected – practically no improvement. In this case the influence of the vibration transmission at the connections is a most important parameter. The first modes of the bending vibrations are very distinct causing a negative insertion loss at low frequencies. The bending vibrations are hardly dampened as the bending waves are reflected already at the bend of the deep drawn shell so that there is hardly any damping effect from the sealing. The sound reducing shell 2 of the same shape made of damped sandwich material should therefore be more effective. With this type of shell it is possible to achieve a considerable insertion loss despite the stiff connections. At frequencies above 630 Hz values of more than 10 dB are obtained. Also the dip of the insertion loss curve at the fundamental bending mode of the sound reducing shell is relatively low, namely -5 dB, due to the damping.

An even increased insertion loss is achieved with the other sound reducing shells which are attached to the crankcase side wall in a more or less vibration isolated manner. With these shells the transmission loss described in the theoretical part of the paper is the dominating parameter. Another important parameter is the built-up of sound power between the shell and the crankcase wall, which is radiated from the crankcase wall. Its effect can be seen in the middle frequency range from the difference between the transmission loss R_{max} and R_{min}, drawn in Fig. 10, and the insertion loss of the sound reducing shells. This difference is in the range of 10 dB to 15 dB. The slope of the insertion loss curves of the three sound reducing shells 3, 4 and 5 without damping rather correspond to R_{min} in the middle frequency range. This shows that with additional damping slight improvements could be achieved. It has to be said that the insertion losses achieved with sound reducing shells attached in a vibration isolated manner are very good. They amount to 13 dB to 27 dB above 1 kHz. As can be seen it is an enchanced solution to use a larger distance to the crankcase wall as well as to attach the shell with a limited number of rubber elements or screws instead of attaching the shell elastically around its outer edges. In the latter case the fundamental frequency f_R of the vibration system, consisting of rubber fillet and trapped air acting as a spring and the sound reducing shell acting as a mass, results in an increased dip of the insertion loss at low frequencies.

The importance of careful sealing of the space between sound reducing shell and crankcase wall in the case of shells without acoustical lining on the inner surface can be seen in Fig. 11. The comparison of curve 2 with curve 1 shows that four holes with a diameter of 8 mm, representing approximately 2/1000 of the shell area, result in a considerable reduction of the insertion loss over the whole middle and upper frequency range, approximately 6 dB on the average. Curve 3 in Fig. 11 demonstrates how the insertion loss is affected by cutting off approximately half the area of the crankcase wall located underneath the sound reducing shell. Doing this, the

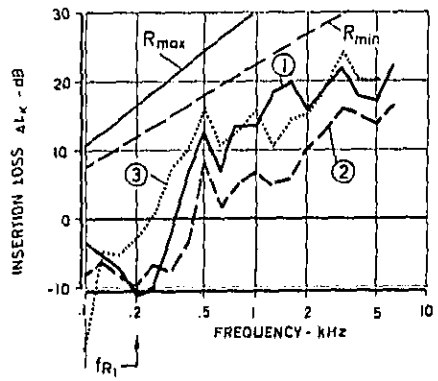

① SHELL CAREFULLY SEALED
② 4 HOLES 8mm DIA IN THE SHELL (ABOUT 2/1000 OF SHELL AREA)
③ PARTS OF CRANKCASE WALL CUT OUT (ABOUT ONE HALF)

SOUND REDUCING SHELL 200 x 700 mm OF SHEET STEEL .8mm BONDED WITH FILLET OF FOAM RUBBER 15 x 15 mm ALONG ENTIRE EDGE AT 16mm DISTANCE ON THE CRANKCASE WALL OF A 5l WATERCOOLED 6 CYL INLINE DIESEL ENGINE

Fig. 11 – Effect of holes in shell or crankcase wall on insertion loss of a sound reducing shell

sound reducing shell forms a cover of the crankcase which retains the oil and which is connected in a vibration isolating manner. Therefore, the pronounced dip of the insertion loss at 200 Hz corresponding to the resonance frequency of the system, consisting of trapped air and rubber mountings acting as a spring and the sound reducing shell acting as a mass, disappears. Instead, another dip of the insertion loss at or below 100 Hz arises which corresponds to the pressure fluctuations in the crankcase due to the piston movement. Both have, however, very little influence on the A-weighted sound level. As there is little difference in the insertion loss at middle and higher frequencies the cutting out of parts of the crankcase wall below the sound reducing shells does not have any effect on the noise reduction of the crankcase wall. Also the increased potential for the occurrence of standing air borne sound waves below the sound reducing shell due to the considerably larger distance to the opposite crankcase wall remains negligable on the whole. Only the fluctuations of the insertion loss are shifted, e.g. an additional dip occurs at 1-2 kHz which might be caused by standing air borne sound waves.

On one example of an air-cooled 4-cylinder diesel engine, Fig. 12, it was attempted to achieve the greatest possible noise reduction by improving individual components of the engine surface. This has been done by the installation of a low-noise

cooling fan, vibration isolation of the oil pan as well as the use of sound reducing shells attached to the crankcase, the gear box, the crankshaft pulley and the manifolds and by acoustical lining of the cooling air distribution chamber and the cooling air outlet duct. Although the measures cover

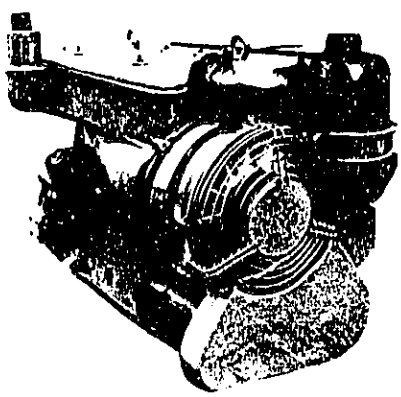

Fig. 12 - Air-cooled 4-cylinder diesel engine, noise reduced by the acoustic treatment of individual engine parts (8)

the major part of the engine surface, the noise of this engine is only about 5 dB(A) lower than the average noise level of existing engines of the output and speed. This example demonstrates very clearly that it is not possible to reduce the noise radiated from all engine surfaces by improving individual engine components at a reasonable cost. There still remain a noise emission of marginal areas along the sound reducing shells or along vibration isolated components and also of other components contributing to a lesser extent to the total noise which by this means can only be silenced at unreasonably high costs. Therefore, it is much better to completely enclose the engine. In principle, several sound reducing shells are stiffly joined together forming a closed, sound reducing casing which is supported in a vibration isolated manner on the engine or outside of the engine. It was expected and is confirmed that the insertion loss obtained with individual sound reducing shells can also be achieved with a sound reducing enclosure covering the whole engine. Therefore, with such an enclosure a reduction of the total engine noise of 10 dB(A) to 20 dB(A) is possible. The development work carried out at AVL in the past years has resulted in designs featuring high acoustical efficiency with only a slight increase in bulk volume and weight and still giving good access for maintenance work. These enclosures will be described in the following sections.

SOUND REDUCING ENCLOSURES FOR ALREADY EXISTING ENGINES - Design Principles - As an example for water-cooled turbocharged engines Fig. 13 schematically shows in longitudinal sections the design and the essential characteristics of the sound reducing enclosure when applied to already existing engines (8). With respect to material thin sheet steel, i.e. of 1 mm thickness for truck engines, or other materials with the same transmission loss such as aluminium with 3 mm wall thickness or synthetic resin materials are of interest. For smaller engines less wall thickness is suitable, e.g. sheet steel of 0.7 mm or 0.5 mm. For larger engines an increased

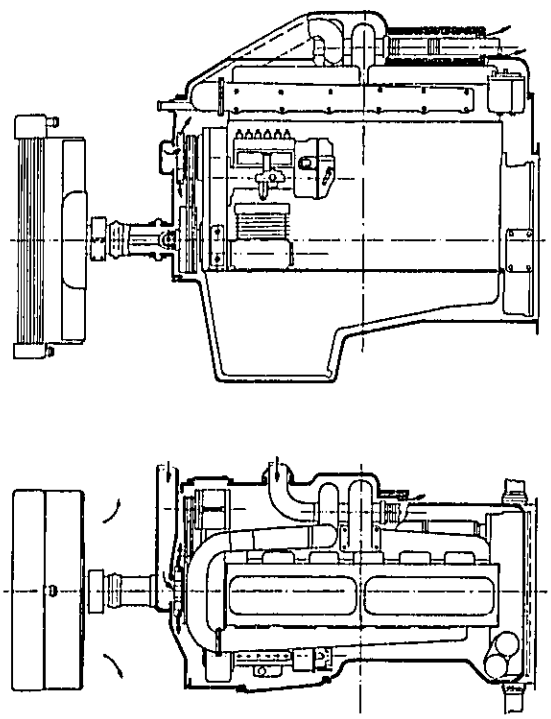

Fig. 13 - Concept of a low-noise, water-cooled production diesel engine featuring an additional sound reducing enclosure (8)

wall thickness is necessary. This depends on the frequency range dominating the noise emission which is slightly shifted with engine size. On the other hand a certain wall thickness is required for stability reasons. The enclosure is made of ordinary sheet steel, i.e. no damping layers nor acoustical linings are used. The individual enclosure parts are joined together in a rigid and sound tight manner. The enclosure is either supported on the engine with intermediate vibration isolating elements or is rigidly connected to the chassis, engine compartment or base which can form parts of the enclosure. In the latter case the vibration isolation is obtained by the engine mountings.

Due to the hot parts of the exhaust system located underneath the enclosure, and to provide unrestricted dissipation of the engine heat, the space between the engine and the enclosure is ventilated by a fan which is, in this particular case, attached to the water pump shaft. The cooling air intake and exhaust ducts must be designed like absorption muff-

lers. The air which is conducted through the enclosure is separated into two streams in order to provide optimum cooling as well as protection against fire hazards, for instance in the case of a fuel line breakage: One stream flows along the hot parts of the exhaust system, the other one is directed along the remaining engine surfaces and also provides the cooling of the fuel system. Both streams are exhausted through separate ducts. Fig. 13 furthermore shows a proven design for the penetration of the exhaust pipe through the enclosure to the outside. The sound reducing cooling air outlet duct is installed around the exhaust pipe in order to avoid an excessive heat transfer to the enclosure itself.

Since any load carrying part or parts which are rigidly connected to the engine would radiate noise (if they protrude to the outside of the enclosure) a special connecting link is used on the exhaust pipe inside the enclosure in order to prevent the transmission of structural vibrations to the outer part of the exhaust pipe. The same technique is used on all the other lines and tubing leading to the outside. Structural vibrations are transmitted from the engine into the transmission gear box which is in the case of vehicles rigidly connected to the flywheel housing. This necessitates not only a sound reducing enclosure for the engine but also for the transmission. The best solution is to connect the transmission enclosure with the engine enclosure which can then be ventilated as a unit.

Fig. 14 shows sectional views of a sound reducing enclosure for an air-cooled 6-cylinder inline engine (8). In principle this enclosure does not differ from the one of the water-cooled inline engine as far as the support on the engine, the material, the pipes and the possibility to connect a transmission enclosure are concerned. Since the cooling system is already a part of the engine the

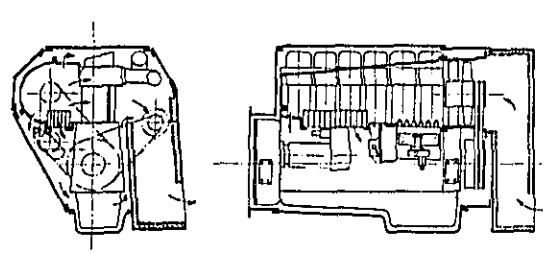

Fig. 14 - Concept of a low-noise air-cooled production diesel engine featuring an additional sound reducing enclosure (8)

cooling air is conducted through the enclosure. It is therefore not necessary to install an additional blower for ventilating the space inside the enclosure. The relatively large cooling air openings require effective mufflers which are, as in this case, integrated into the enclosure in form of ducts provided with an air borne sound absorbing lining. From the cooling air distribution chamber located downstream of the blower the cooling air is separated into one major stream flowing towards the ribs of the cylinder heads and the cylinder liners and into partial streams which are directed towards the oil cooler and other hot engine surfaces.

Examples - Fig. 15 shows a water-cooled 5-liter 6-cylinder diesel engine featuring the first enclosure of this kind which was designed about ten years ago (3,6,12). The enclosure was made of sheet steel of 0.7 mm thickness and its total mass amounted to 40 kg. The enclosure essentially consists of

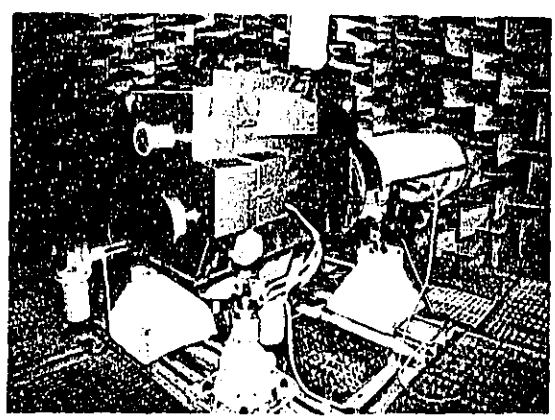

Fig. 15 - Water-cooled 5 liter inline 6-cylinder diesel engine fitted with an additional sound reducing enclosure of first design (3)

individual covers which are connected with eachother. As some pipes or tubing protrude through these covers the servicability at some parts of the engine is rendered more difficult. These considerations, however, were of secondary importance with this first experimental research enclosure. The stress was laid on acoustic and operational efficiency.

The acoustical efficiency can be seen in Fig. 16. The noise reduction amounts to 16 dB(A) with an enclosure made of ordinary sheet steel. If a damping layer, such as a commercial damping material of double the sheet thickness, i.e. approxi-

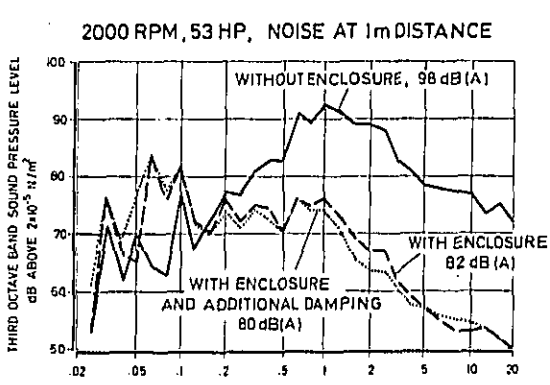

Fig. 16 - Noise of a water-cooled 5 liter inline 6-cylinder diesel engine with and without sound reducing enclosure

mately 1.5 mm thickness, is applied to the enclosure walls the sound reducing effect is further increased by 2 dB(A), resulting in a noise reduction of 18 dB(A). The sound reducing effect starts at 160 Hz, and increases sharply with increasing frequency. The predominant frequency range of the noise is therefore shifted to lower frequencies. Apart from the significant reduction of the total noise level the impulsive characteristic of diesel engine noise that is most irritating to the human ear is considerably reduced as well. With this enclosure - and also with sound reducing shells, in particular by those which are elastically connected along their edges - the sound level increases considerably in the lower frequency range below 160 Hz. This fact which is not decisive for the dB(A) level can have a negative effect on the durability if the displacement is too large. However, as will be shown later, this increase in the sound level can be completely eliminated by an appropriate enclosure design and the careful choice of enclosure support.

Fig. 17 demonstrates the insertion loss of this first example of a sound reducing enclosure. It can be seen that the insertion loss curve is parallel to R_{max} between 160 Hz and 630 Hz and then up to 2 kHz, without additional damping of the enclosure sheet steel, parallel to R_{min}. Therefore, additional damping shows its effect in the latter range,

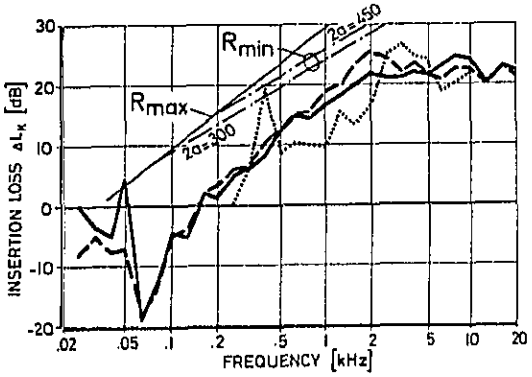

INSERTION LOSS ΔL_K:

——— ENGINE WITH ENCLOSURE OF SHEET STEEL .7mm

— — ENGINE WITH ENCLOSURE AND ADDITIONAL DAMPING LAYER

····· NOISE REDUCING ENCLOSURE OF SHEET STEEL .8mm ON CRANKCASE OF ENGINE 3, SIZE 300x300mm, DISTANCE 30mm, SUPPORTED WITH FILLET 15 x 30mm OF FOAM RUBBER ALONG THE EDGES

CALCULATED TRANSMISSION LOSSES OF SHEET STEEL .7mm:

——— R_{max}

—·— R_{min} WITH DIFFERENT PANEL SIZE 2a

Fig. 17 - Insertion loss of sound reducing enclosure of water-cooled 5 liter inline 6-cylinder diesel engine (12)

according to the theoretical considerations illustrated in Fig. 6. Taking the size and wall thickness of the enclosure parts into consideration it can be shown from this result that the loss factor of the assembled enclosure parts without additional damping lies in the range of 0.02. The sound radiation in the lower of the two mentioned frequency ranges is determined by panels which have, due to their large dimensions, a critical loss factor which is below 0.02, whereas above 800 Hz obviously smaller panels, the critical loss factor of which is correspondingly higher, are important for the noise emission. The difference between the transmission loss R of the sheet metal and the insertion loss ΔL_K, caused by the increase of the sound level in the space between engine surface and enclosure amounts to 10 dB to 12 dB. This is very good compared with the results obtained with sound reducing shells of the same material, as can be seen in Fig. 17 and Fig. 10. Consequently an insertion loss of 17 dB to 19 dB is achieved at 1 kHz despite a wall thickness of 0.7 mm.

The significant dip of the transmission loss curve at low frequencies, particularly pronounced at 63 Hz in this case, is in the range of the fundamental bending frequencies of the panels, as can be checked very easily with the equation in Fig. 6. The excitation is mainly caused by the vibration transmission via the elastic supports. A resonance of the panels acting as mass and of the trapped air acting as a spring, as it is clearly the case with the sound reducing shells, is less likely as the decisive distance between the panels and the engine surfaces varies largely. In the upper frequency range, that is above 2 kHz, the insertion loss does not increase any more. There it is in the range of 20 dB to 25 dB. The transmission loss of the panels increasing with a steady rate of 15 to 20 dB/decade is obviously not the dominating parameter at higher frequencies. Depending on the practicability and the design approach the sound reducing effect of the sealings as well as the vibration isolation between engine structure and parts connected to the engine and passing through the enclosure is limited. Therefore, the sound power radiated from these surface areas above a certain frequency exceed the sound power radiated from the panels, limiting the insertion loss of such sound reducing enclosures.

Fig. 18 shows the sketch of an enclosed water-cooled 6-cylinder diesel engine with bolted on transmission considering advanced developments in this field (8). The enclosure is designed for mass production using deep-drawn sheet steel. An essential characteristic of recent enclosure developments is that the sound reducing enclosure consists of two groups of parts. The parts of the first group form a supporting frame. The enclosure is elastically supported in the area of this supporting frame by carefully choosing the connection points. The parts of the second group consist of covers with largest possible dimensions which are rigidly connected to the supporting frame in a sound tight manner mainly using quick fasteners. All pipes, tubing, engine supporting elements, etc. penetrate through the supporting frame and do not obstruct the maintenance covers. The covers can be dimensioned considerably larger than shown in Fig. 18 so that there is free access to all the upper area of the engine or the oil pan when removing one of these covers. As the

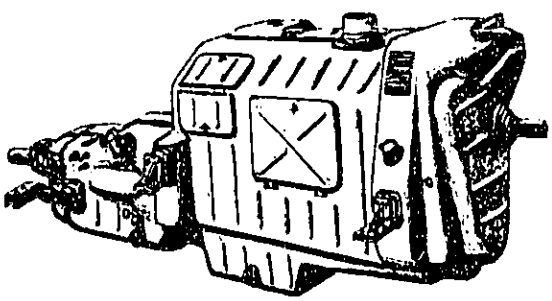

Fig. 18 - Low-noise water-cooled 6-cylinder production diesel engine with transmission gear featuring an additional sound reducing enclosure (8)

development work on various prototypes demonstrated an over-heating of engine or enclosure parts, which are ventilated by a cooling fan with the running engine, can be avoided when shuting the engine down. It is important in this connection to consider the chimney effect which means that the air entering the enclosure through the ventilating openings located at the lower part of the enclosure flows to the openings in the upper part of the enclosure after a hot engine stop and therefore the fan stops.

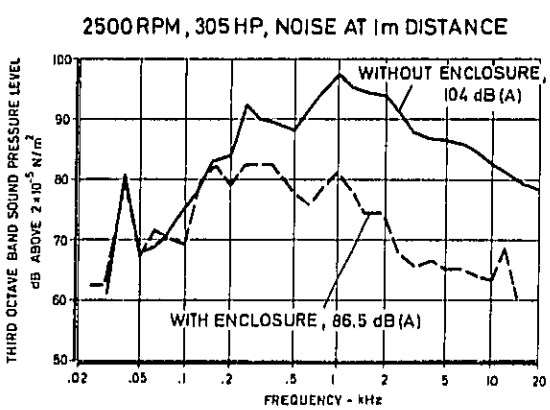

Fig. 19 - Noise of a low-noise water-cooled V8 diesel engine with transmission gear featuring an additional sound reducing enclosure

Fig. 19 shows the acoustical effect of a recently developed sound reducing enclosure for a V8 truck diesel engine with bolted on transmission. The enclosure is, also in this case, made of ordinary sheet steel without damping layers or acoustical lining with a wall thickness of 1 mm appropriate for this engine size. The noise is reduced by 17.5 dB(A). The noise reduction is again starting at 160 Hz, see also Fig. 16. It is worth noting that at low frequencies the dip of the transmission loss curve is suppressed as a result of the newly developed enclosure design and enclosure support. The sound level in this frequency range is practically the same as without sound reducing enclosure.

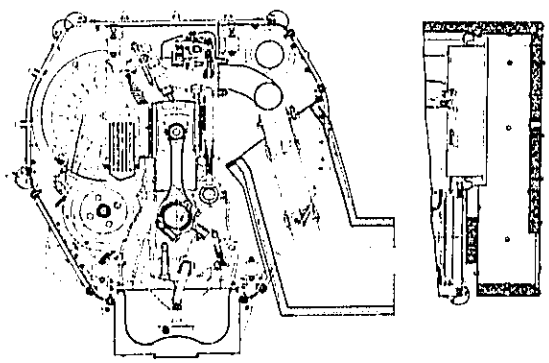

Fig. 20 - Sectional drawings of a low-noise air-cooled 6-cylinder inline diesel engine featuring an additional sound reducing enclosure (9)

Fig. 20 shows sectional drawings of the prototype of such a low-noise, air-cooled 6-cylinder diesel engine of 100 mm x 120 mm bore and stroke (9,12). A view of this engine is given in Fig. 21.

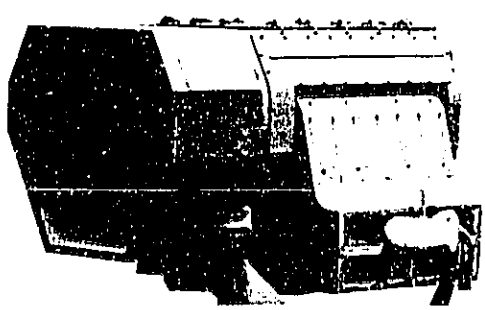

Fig. 21 - Low-noise air-cooled 6-cylinder inline diesel engine 100 mm x 120 mm bore and stroke featuring an additional sound reducing enclosure (9)

The prototype was developed by slightly modifying an existing inline engine. In the course of these modifications the starter was removed from the cooling air outlet side of the engine to the other side of the engine in order to gain space for the arrangement of the cooling air outlet duct of the enclosure. This prototype engine is characterized by the arrangement of a sound reducing enclosure which has been designed under consideration of the principles described before. It is based on two frame systems; one above the cylinder heads and the other in the area of the oil pan, each made of 1.5 mm thick sectional steel. The frames are supported in a vibration isolated manner on the cylinder heads

respectively the crankcase housing by means of rubber elements. Both frames are bolted on to the front and rear wall of the enclosure each made of 1 mm thick sheet steel. Together with these walls they form the supporting frame-work of the enclosure. The upper, side and lower parts of the wall, made of 1 mm steel, are attached to this supporting frame-work; in the area which has to be accessible for servicing this is accomplished by quick fasteners, otherwise with screws. The cooling air ducts are directly connected with the enclosure. However, the design of the enclosure is such that the ducts can be arranged separated from the engine under certain installation conditions for the sake of accessability. In this case the engine ducts would have to be connected with the cooling outlet ducts by means of elastic sound reducing ducts.

The total mass of the sound reducing enclosure amounts to 127 kg, that is 28 % of the mass of the original engine. This is a fairly high percentage, but it has however to be considered that the cooling air ducts which may be used separately from the engine are included. In the case of the cooling air ducts completely integrated in the enclosure the mass will furthermore be reduced by omitting double walls. In comparison, the mass of the latest sound reducing enclosures of water-cooled engines is in the range of 9-14 % of the engine mass. The noise emitted by the radiator-fan-system remains, however, the same, whereas with air-cooled engines the noise emitted by the cooling system is reduced together with the noise emitted by the engine surface.

The noise reduction achieved with the air-cooled prototype engine can be seen in Fig. 22. It amounts to 19 dB(A). The noise level measured at rated speed and full load at 1 m distance in the anechoic chamber is reduced from 102 dB(A) to 83 dB(A). The difference between the two spectra shows that the insertion loss reaches values up to 25 dB and amounts to almost 20 dB at 1 kHz. Here too the chosen enclosure design made it possible to avoid a dip of the transmission loss curve at low frequencies. The average sound level measured with the sound reducing enclosure is therefore lower than

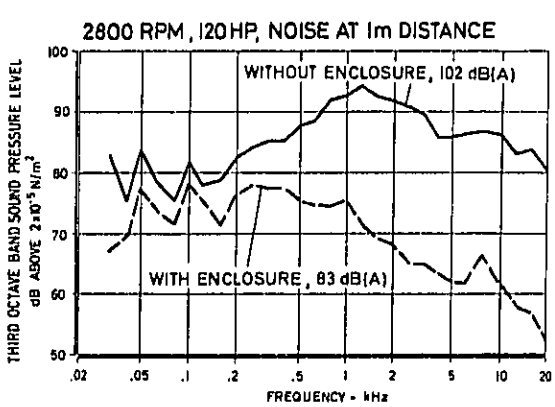

Fig. 22 – Noise of an air-cooled 6-cylinder inline diesel engine 100 mm x 120 mm bore and stroke with and without sound reducing enclosure (9)

the sound level of the original engine over the whole frequency range.

In the course of recent developments prototype solutions for sound reducing enclosures which are combined with the chassis were also realized. Such a solution is reported elsewhere at this conference. In principle the enclosure does not differ from the ones described above which are attached to the engine in a vibration isolated manner and are practically part of the engine. The sound reducing enclosure therefore consists also in this case of two groups of enclosure parts – the supporting frame comprising the passing through of pipes, lines and shafts and the quickly removable covers. In the case of the enclosure supported on the chassis of a vehicle the enclosure parts are rigidly connected with the chassis. Parts of the chassis, for instance the main frames can replace parts of the supporting frame of the enclosure. That means a simplification of the enclosure, in particular it is not necessary to arrange an additional enclosure part, obstructing the accessability of the engine, between the chassis and the engine. With cab-over-engine trucks, covers, as for instance the large upper cover, can be connected elastically with the cab so that the upper engine area is dismantled when tilting the cab.

A disadvantage of the enclosure connected with the chassis is among others that the enclosure parts are subjected to the distortions of the chassis. This problem needs careful consideration. Furthermore, the fundamental natural frequencies of the main frames of the vehicle are around some 100 Hz which could impair the acoustic efficiency of the enclosure. Finally, an enclosure connected to the chassis is part of the vehicle so that for any other type of application of the same engine a new enclosure has to be developed. It can be established in principle that both types of supports for an enclosure – on the engine and on the vehicle – give good results if carefully designed and developed. This can also be seen from the earlier mentioned paper about a truck diesel engine enclosure connected to the frame.

FUTURE LOW-NOISE DIESEL ENGINES – With newly designed engines the principle which has been recognized as being of primary importance for an essential noise reduction in the range of more than 10 dB(A) can be realized in a different way. This principle finds its implementation in different kinds of vibration isolation of all components forming the outer surface towards the load carrying inner engine structure. One possibility consists in further optimizing the engine and enclosure parts of the additional dry enclosure as described in the previous sections. A number of possibilities arises if the vibration isolated external casing is substantially integrated into the engine structure and provides both the attenuation of the noise as well as the sealing of the oil chamber.

Optimized Additional Dry Enclosures – Here the enclosure is added to a fully sealed engine structure which is designed right away to consider the special requirements which arise in connection with the enclosure. Furthermore, it is important with water-cooled engines, especially in the case of vehicle installations, to provide unrestricted flow conditions for the cooling air at the outlet of the radiator-fan-system in order to ensure the shortest

possible overall length of the power unit. Fig. 23 shows the longitudinal section of a turbocharged water-cooled 6-cylinder inline engine with an additional dry enclosure featuring such an optimized design (8). In order to keep the front side of the engine and the enclosure as small as possible the gear drive is located at the flywheel end. This arrangement is also advantageous from the point of

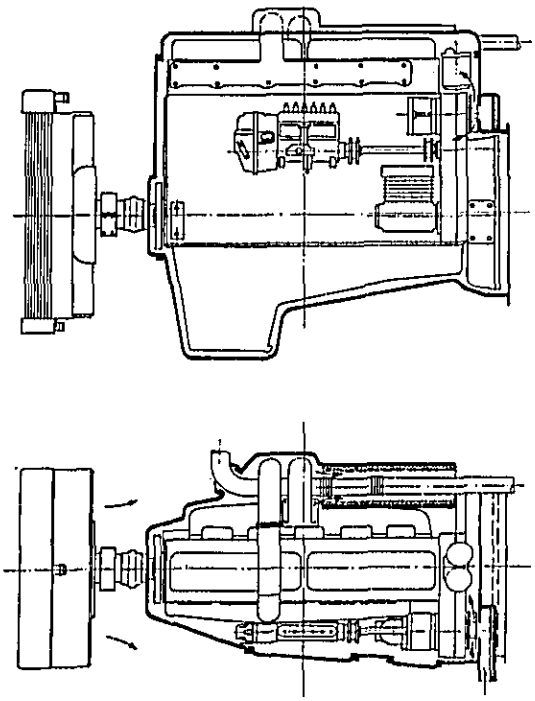

Fig. 23 - Concept of a low-noise water-cooled diesel engine especially designed to fit an enclosure (8)

view of noise, if the engine is used without sound reducing enclosure. As many accessories as possible were installed at the rear of the engine. The air intake duct for the enclosure ventilation does not restrict the air flow downstream of the cooling fan, as it would be the case with a blower arranged at the front side of the engine. With the compact design of the total engine it is possible to have a smooth and simply shaped enclosure, thus keeping the weight and manufacturing costs as low as possible. The extremely small front surface of the enclosure provides good flow conditions for the cooling air despite the fact that the fan, which is driven by a universal shaft, is mounted quite close to the engine. It is advantageous, as also demonstrated in the figure, to eliminate all belts within the enclosure. Belt drives would require maintenance and need considerable space, making it more difficult to design an optimized enclosure.

Acoustic Enclosures Integrated into the Engine Structure of Water-Cooled Inline Engines - Fig. 24 shows on a water-cooled 6-cylinder inline engine the realization of the principle of a vibration isolated external enclosure which is to a large extent integrated into the engine structure (8). The usual crankcase of the engine is replaced by a so-called central support which has no side walls in the area of the crankshaft and which therefore has a low weight. The external enclosure which is attached to the central support with elastic elements

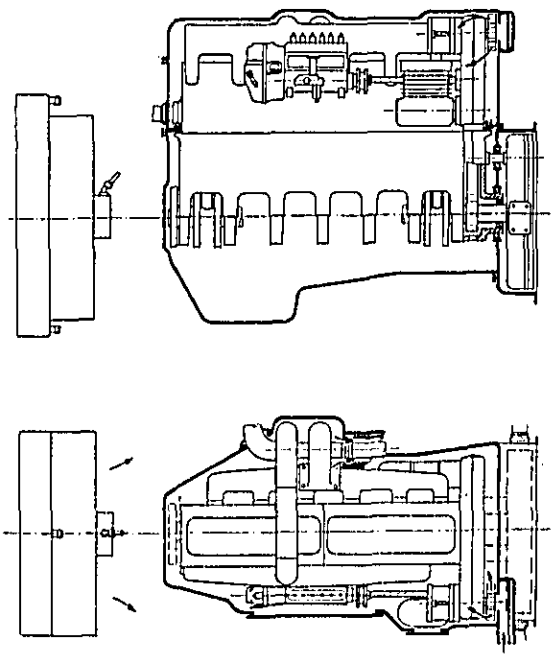

Fig. 24 - Concept of a low-noise water-cooled diesel engine featuring a modified engine structure with an oil sealing acoustic enclosure (8)

provides the sound attenuation as well as the oil sealing. The upper part of the engine where all the accessories are arranged is surrounded by a sound reducing ventilated enclosure of the conventional dry design. The sealing between both parts of the enclosure, the upper dry section and the lower wet part is effected by an elastic gasket. At the flywheel end the oil chamber is sealed by means of elastic, ring-shaped elements which are inserted into the rear wall of the enclosure at the connections between the central support and the flywheel housing and at the opening for the crankshaft. With regard to the arrangement of the gear drive on the flywheel end and the ventilation of the upper enclosure space as well as to the shaping of the front part of the enclosure the same aspects as mentioned above were considered. The described concept has the advantage of a considerable weight saving over the concept of an additional dry enclosure.

Fig. 25 shows in sectional drawings a prototype of the above concept of a low-noise, water-cooled

6-cylinder diesel engine 118 mm x 125 mm bore and stroke (9,13). The engine is a conversion of an existing diesel engine without modifying the crank-drive, injection system, combustion system, valve timing and cylinder heads. This enables a direct comparison of the effect of the modified engine structure and reduced the design, manufacturing and development cost as well. This prevented however a number of optimizations. Therefore, the gear drive illustrated in Fig. 24 had to remain on the engine front side, thus the auxiliaries are also driven from this side. The central support replaces the

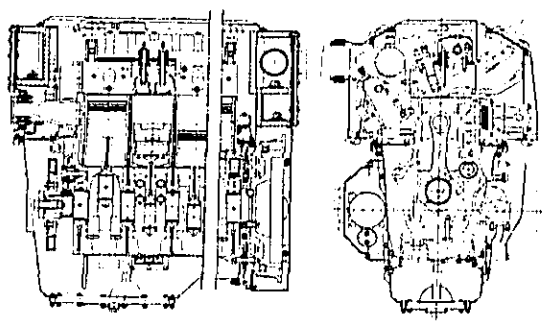

Fig. 25 - Sectional drawings of the prototype model of a low-noise water-cooled 6-cylinder inline diesel engine featuring an integrated oil sealing acoustic enclosure (9)

crankcase. To ensure sufficient stiffness the lower main bearing caps are connected with eachother by a supporting beam forming a bearing cap bridge. The upper and lower part of the external enclosure are connected by a frame of sectional steel horizontally surrounding the engine. This frame is attached to the central support in a vibration isolated manner using rubber elements located in the dry enclosure space. To restrict the movements between enclosure and central support additional rubber elements are located between the bearing cap bridge and the oil pan. The oil chamber is sealed on the top with a rubber diaphragm surrounding the engine. The inner edge of this diaphragm is pressed onto the central support and its outer edge on the lower wet part of the enclosure. Elastic, ring-shaped elements, as already described in Fig. 24, are inserted into the rear wall of the lower part of the enclosure at the openings for the crankshaft and at the connections between the central support and the flywheel housing.

An additional blower arranged at the front side of the gear drive provides the ventilation of the upper enclosure space. The cooling air intake duct on the front side of the engine and two separate cooling air outlet ducts on the rear side of the engine are designed as sound reducing ducts. The cooling air which comes in contact with the hot parts of the exhaust manifold is directed through separate ducts in order to ensure optimum cooling and protection against fire hazard. All auxiliaries and pipe penetrations are located in the dry enclosure space. Therefore, it is impossible that cooling water or fuel come into contact with lubricating oil in the case of a line breakage. Quickly removable covers arranged on the upper part of the dry enclosure enable easy access for maintenance. The engine is supported in the area of the dry enclosure on the front side and on both sides of the flywheel housing. Transmission gears can be rigidly bolted on the flywheel housing as with conventionally designed engines. In this case a sound reducing enclosure for the transmission is necessary because of the vibration transmission from the central support. This enclosure can be connected with the engine enclosure. Fig. 26 shows the water-cooled engine dur-

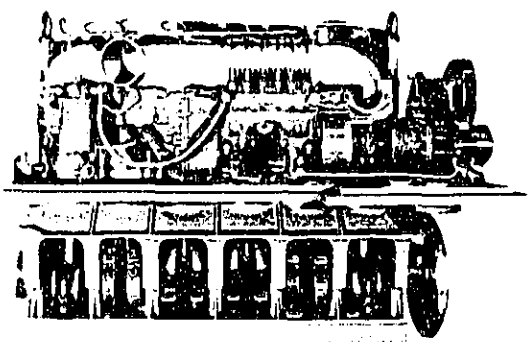

Fig. 26 - Internal structure of the prototype model of a low-noise water-cooled 6-cylinder inline diesel engine featuring an integrated,oil sealing, acoustic enclosure (9)

ing assembling. The frame horizontally surrounding the engine as well as the diaphragm sealing, which provides the sealing of the upper part of the oil chamber, is already mounted, whereas flywheel and external enclosure are not attached yet. Fig. 27

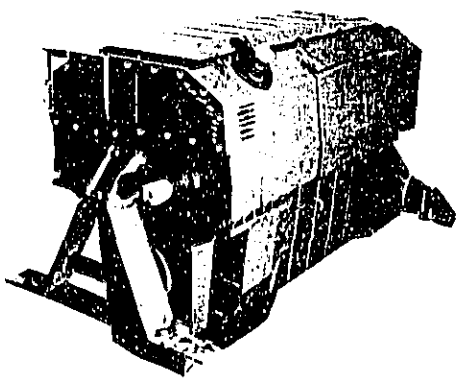

Fig. 27 - Fully assembled prototype model of a low-noise water-cooled 6-cylinder inline diesel engine featuring an integrated oil sealing acoustic enclosure (9)

is a view of the completely assembled engine on a transport frame.

The acoustical effect of the engine design chosen for this prototype engine can be seen in Fig. 28. Compared with the original design of the engine a noise reduction of 19.5 dB(A) could be achieved. Relatively good results could also be achieved in the lower frequency range in spite of the fact that the fundamental bending modes of the walls of the lower part of the enclosure, which are exposed to the pressure fluctuations caused by the piston movements in the lubrication oil chamber, are within the frequency range of these pressure fluctuations. If the lower part of the enclosure is made of 3 mm aluminium the fundamental natural bending frequencies are tripled, causing a distinct decrease of the structural vibrations in the low frequency range, which also affect the air borne sound, without significantly influencing the total noise reduction.

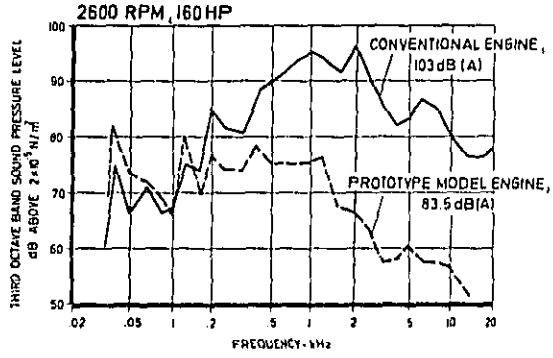

Fig. 28 - Water-cooled 6-cylinder inline diesel engine - noise of production engine and of low-noise prototype model featuring an integrated oil sealing acoustic enclosure (9)

The low-noise prototype engine has only a 3 % mass increase compared to the original engine. That is a considerable advantage compared to the additional sound reducing enclosure of a conventionally designed engine, which increases the mass, as already mentioned, by 9-14 %. This involves, however, extensive development work, and this concept cannot be applied to any cylinder number, type of engine or any application. The described prototype engine has already been installed in a truck some time ago for the purpose of further investigations and comparisons. The results achieved in the course of these investigations are discussed in a separate paper also presented at this conference.

Water-Cooled Engine with a Vibration Isolated Engine Housing - Fig. 29 shows a water-cooled 4-cylinder inline engine featuring another solution for an integrated acoustic enclosure (8,10). The concept essentially consists in the reduction of the number of those engine components which are subject to structural vibrations to a bare minimum, namely to the crankdrive, the central support, the cylinder block and the cylinder head. Contrary to the concept described above where the flywheel housing is rigidly connected with the central support and where the attached transmission has to be enclosed due to the transmission of structural vibrations, the flywheel housing is attached to the lower part of the sound attenuating enclosure which is designed as a rigid housing. This housing supports the

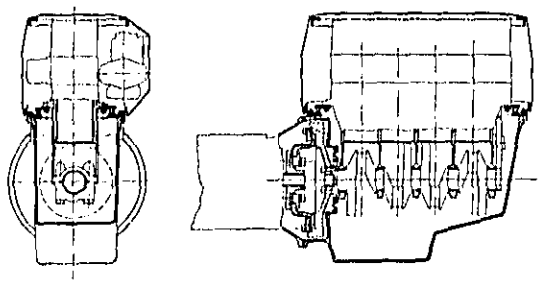

Fig. 29 - Concept of a low-noise water-cooled diesel engine featuring a modified engine structure with a vibration isolated housing (8)

central engine structure by means of an elastic, frame-like element. The upper part of the engine is again fitted with a dry, sound attenuating enclosure. The transmission has not to be enclosed since it is bolted-on to the flywheel housing which is already vibration isolated against the central support. The transmission of power from the flywheel to the transmission is effected by a flexible coupling because of the possible relative movement between these parts. Contrary to the engine described earlier which is supported on the flywheel housing and on the central support, this engine may be supported directly on the engine housing.

A development program of a 2.1 liter prototype engine corresponding to this design concept is in progress (14). Fig. 30 shows a view of the fully assembled engine. The total mass of the naturally aspirated version amounts to 155 kg resulting in a very low specific weight, namely 2.6 kg/HP, at a rated output of 60 HP at 4000 RPM. For this design the vibration isolating connection between central support and external housing is subject to the crankshaft torque. Therefore, the design has to be such that resonances with low harmonics of the crankshaft torque have to be avoided in the operating range. The same applies to excitations due to unbalanced inertia forces, e.g. the second order inertia force with the 4-cylinder engine. A natural frequency above these excitation frequencies proves to be far better, as in this case the connection is relatively stiff and the relative movements between flywheel and flywheel housing remain small. However, to ensure sufficient vibration isolation careful development work is required. Following this compromise the noise reduction cannot be expected to be as high as with other concepts. The noise of this prototype is therefore about 12 dB(A) lower than that of an average existing engine, and about 7 dB(A) lower than a conventionally designed engine optimized with regard to noise.

A separate paper about this prototype engine is being presented at the conference.

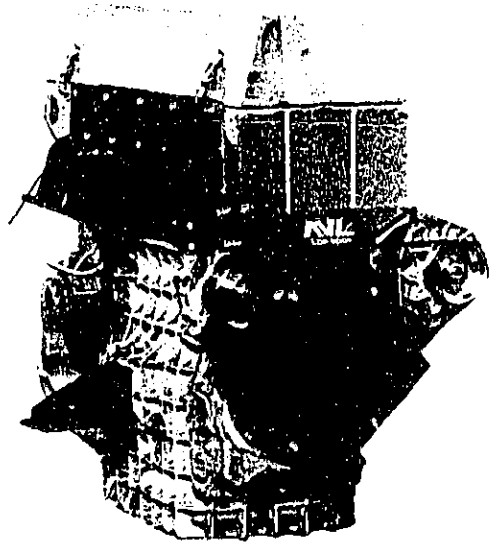

Fig. 30 - Fully assembled prototype model of a low-noise low-weight water-cooled 4-cylinder inline engine featuring a modified engine structure and a vibration isolated housing (14)

STATE OF DEVELOPMENT OF AN ADVANCED DIRECT INJECTION COMBUSTION SYSTEM

HIGH SPEED HEAVY DUTY DIESEL ENGINES - Diesel engines using direct injection (D.I.) combustion systems are characterized by a fuel consumption which is at least 15 % lower than with equivalent pre-chamber or swirl chamber (I.D.I.) engines. This advantage in fuel consumption is the reason why diesel engines in trucks and busses are almost exclusively equipped with this combustion system. However, with regard to the combustion noise, problems arise with the application of the D.I. system. The entire combustion process takes place in the space between piston and bottom of cylinder head and the resulting cylinder pressure is acting as noise exciting force on the engine structure. Contrary to spark-ignition engines, where a fuel-air mixture is ignited from one point entailing a smooth start of the combustion, with diesel engines the fuel is injected into the combustion chamber filled with compressed, hot air under ignition conditions. Depending on the type of injection one part of the injected fuel mixes directly with the air so that a certain amount of fuel burns instantaneously due to the ignition delay.

The frequency spectrum of a pressure diagram featuring an instantaneous pressure rise, although very small, differs from the spectrum of a continuous process as it occurs with the cylinder pressure of normal spark ignition engines, that is without knocking. The frequency spectrum of such a pressure diagram is up to the middle frequency range more and more decreasing with increasing frequency as without instantaneous pressure rise, but is limited at higher frequencies to values above a curve with a steady rate of decrease of 20 dB/decade, the level of which is determined by the amount of fuel burnt instantaneously (28,29). This disadvantage does not occur with the divided chamber systems, especially in the case of a narrow throat. The combustion starts in the separated chamber, its pressure development insignificantly influences the vibration excitation of the engine structure. One possibility to improve the D.I. system in this respect consisted in the practically complete accumulation of the fuel on the cavity wall, as it was done with the M.A.N-M-system. Due to evaporation the fuel then gradually mixes with the air. In order to create satisfying ignition conditions one part of the fuel, even if it is of insignificant quantity, has to be mixed directly with the air. Therefore, the combustion also starts with a jump which is hardly visible but can be noticed in the spectrum.

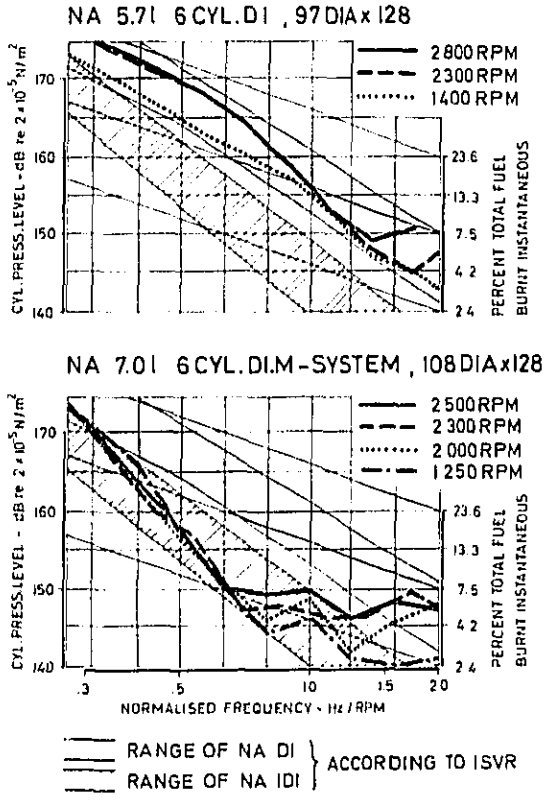

Fig. 31 - Cylinder pressure spectra at full load of naturally aspirated D.I. diesel engines of previous development

Fig. 31 shows as an example the normalised cylinder pressure spectra of naturally aspirated D.I. engines, on top a 5.7 liter 6-cylinder diesel engine with a normal D.I. system, i.e. central multi-

hole nozzle and air swirl, below a 7-liter 6-cylinder D.I. diesel engine with M-system, i.e. high rate of air swirl and accumulation of the fuel on the cavity wall (30). Both engines originate from a previous development aiming at optimum performance and optimum fuel consumption. Compromises were only taken into consideration in view of a lowest possible combustion noise. At the time of development there were no special requirements with regard to the exhaust emission. The spectra of the normal D.I. system, determined at full load and different engine speeds, fall within the range of existing low-noise D.I. engines established by the ISVR (31). The noise optimization becomes apparent in very low values of 3.5 % for the amount of total injected fuel burnt instantaneously. Naturally, in this respect, the values for the M-system are even lower, namely below 2 %. Particularly striking is the spectrum of the M-engine in the middle frequency range as it transverses the very low range of noise optimized I.D.I. engines, stated by the ISVR (31). For comparison Fig. 32 gives the cylinder pressure spectra of a 5.7 liter I.D.I. 6-cylinder diesel engine with a pre-chamber combustion system (30). As one can see, the curves confirm the range plotted for I.D.I. engines. The curves homogenously decreasing up to high frequencies also show that the sudden initiation of the combustion does not become effective in the main combustion chamber between piston and bottom of cylinder head.

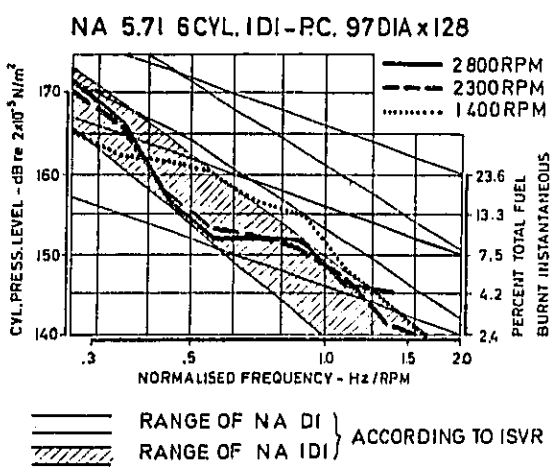

Fig. 32 - Cylinder pressure spectra at full load of a naturally aspirated pre-chamber diesel engine

Fig. 33 exhibits the cylinder pressure spectra of a naturally aspirated 15.9 liter D.I. V8 diesel engine which has been developed at AVL during the past years (23). This concept is aimed at optimum performance and low consumption considering at the same time the limiting values for the exhaust emission as well as a low combustion noise. As one can see the cylinder pressure spectra of the V8 diesel engine are very smooth. At full load they are mainly below the range of previous low-noise D.I. systems. From the position of the spectra a maximum pressure rise of 4 bar/°CA can be derived. With 3 % of the total fuel injected the amount of fuel burnt instantaneously is also very low. To enable an assessment of the effect of the combustion on the overall engine noise the spreading range of the critical

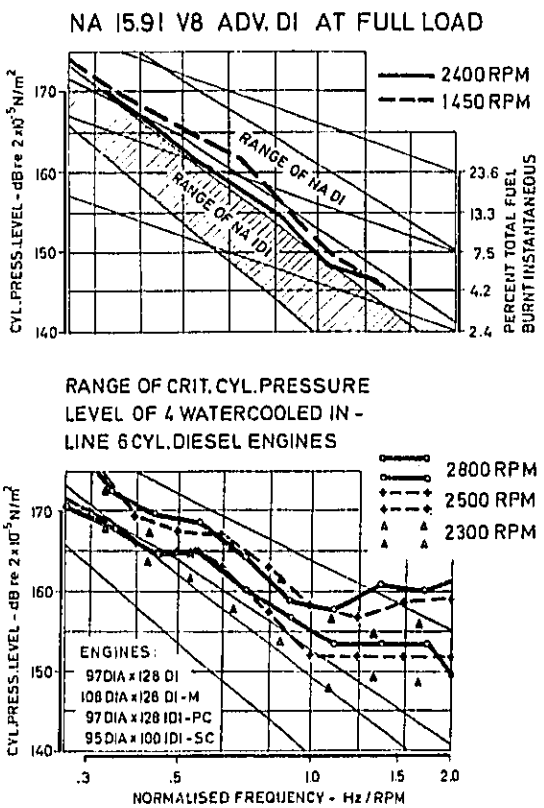

Fig. 33 - Cylinder pressure spectra of a 15.9 liter diesel engine with advanced D.I. system and critical cylinder pressure spectra of four water-cooled 6-cylinder inline diesel engines

cylinder pressure spectra of four typical water-cooled 6-cylinder diesel engines of conventional design and similar size are shown in the lower part of this figure (30). Comparing the cylinder pressure spectra of the 15.9 liter V8 D.I. engine with the spreading range of the critical cylinder pressure spectra, as shown in the lower diagram in Fig. 33, one can see that they are mostly below this spreading range especially at rated speed (full load). Since the combustion induced and the mechanically induced noise are of the same magnitude at the critical cylinder pressure level the contribution of combustion to the total engine noise is smaller with this combustion system than the contribution due to mechanical processes. Therefore, the combustion does not represent the dominating noise source any more. On the average it can be estimated that with an en-

gine using such an advanced D.I. system the contribution of the combustion to the total engine noise amounts to approximately 2 dB(A). Taking an engine equipped with a low-noise I.D.I. system, the cylinder pressure spectrum of which falls within the spreading range, as plotted in the diagrams, the total noise emission of this engine would be about 1 dB(A) to 2 dB(A) lower.

Comparing the total noise of the V8 engine with 137 mm bore to the statistics and predictions with regard to the noise emission of different diesel engine groups at full load and 2000 RPM, published by ISVR (31), one can see that this engine with a mean value of 101 dB(A) measured at 1 m distance does not fall within the spreading range of the naturally aspirated D.I. engines. It is about 3 dB(A) lower than the mean value of this engine group being approximately in the middle of the spreading range of turbocharged D.I. engines. This result confirms the evidence already given by the cylinder pressure spectrum of this engine. Nevertheless, the combustion induced noise of this engine is even higher than with I.D.I. or D.I.-M-system engines. However, the slight difference justifies its application in view of the noise emission regarding the considerably lower fuel consumption in comparison with the I.D.I. engine. This difference in fuel consumption does not exist with the M-system, whereas, however, problems arise in connection with the reduction of the HC emission.

HIGH SPEED LIGHT DUTY DIESEL ENGINES - Contrary to the heavy duty diesel engines the prechamber and swirl chamber systems are today mainly used for high-speed light-duty diesel engines. With these light-duty engines of less than 3 liter total swept volume the D.I. system could not compete with the I.D.I. system despite of its lower fuel consumption, for the following reasons:

The speed range is too small for an acceptable operation - 4000 RPM to 5000 RPM are aimed at - and the performance is unsatisfying with the required engine speed.

The high exhaust emission of HC and NO_x. With a D.I. engine HC emission is approximately eight times and NO_x emission approximately two to three times as high as with I.D.I. engines. It has to be considered in this context that well developed I.D.I. engines of today's market already meet the most stringent U.S. exhaust emission standards.

More exhaust odor and irritants.

Higher combustion noise.

Higher engine weight due to higher firing pressure.

The advantage of a 15 % lower fuel consumption stimulated AVL to develop a D.I. system over the past years which eliminates the afore-mentioned disadvantages to a large extent. Such a concept has in the meantime been realized on several naturally aspirated engines and recently also on a turbocharged engine. Basically, it makes use of an accelerated combustion and increased utilization of air. Both targets have to be realized with delayed ignition for diminishing NO_x and with increased compression ratio for diminishing HC exhaust emission (23,24). Fig. 34 shows in detail what measures were taken to solve the mentioned problems. Some results which can be achieved with the advanced D.I. system are shown in Fig. 35. It also includes a comparison of the values obtained with I.D.I. systems. In detail

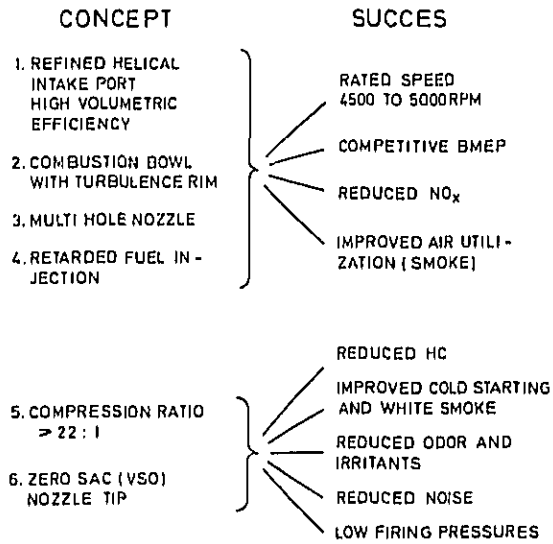

Fig. 34 - Development of advanced D.I. combustion system

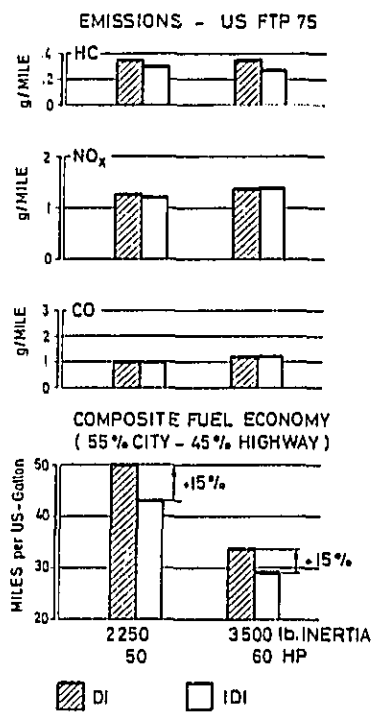

Fig. 35 - Gaseous emission and fuel economy - D.I. versus I.D.I. diesels

results are given for HC, NO_x, CO and composite fuel economy (all measured in line with the U.S. Exhaust Emissions and Fuel Economy Regulations according to the Federal Register) with a vehicle of 1020 kg (2250 lb) inertia and 50 HP D.I. engine and a vehicle of 1588 kg (3500 lb) inertia and 60 HP D.I. engine, both naturally aspirated. It can be seen that the D.I. system discussed is equal to today's I.D.I. systems as far as exhaust emissions are concerned, but maintains a 15 % advantage in fuel economy.

Figs. 36, 37 and 38 give information about the noise of this combustion system. Fig. 36 shows in the upper part of the diagram the cylinder pressure spectra of a 1.6 liter engine with an advanced D.I. system. At middle frequencies the curves are at the lower limit of the spreading range of previous noise-optimized D.I. engines. At higher frequencies they are moving towards the middle of the spreading range. In comparison with the critical cylinder pressure spectra, Fig. 33, this constitutes an acceptable result. The spreading range of these critical cylinder pressure spectra is also shifted with increasing frequency to the middle of the

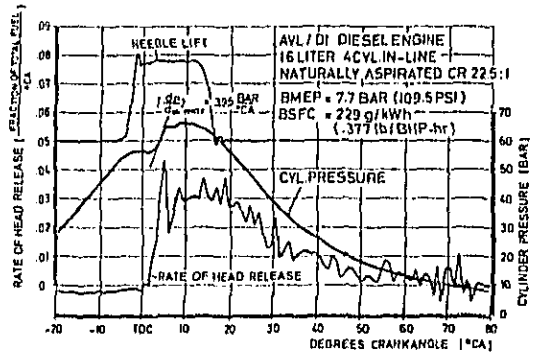

Fig. 37 - Cylinder pressure, rate of heat release and needle lift of 1.6 liter diesel engine with advanced D.I. system

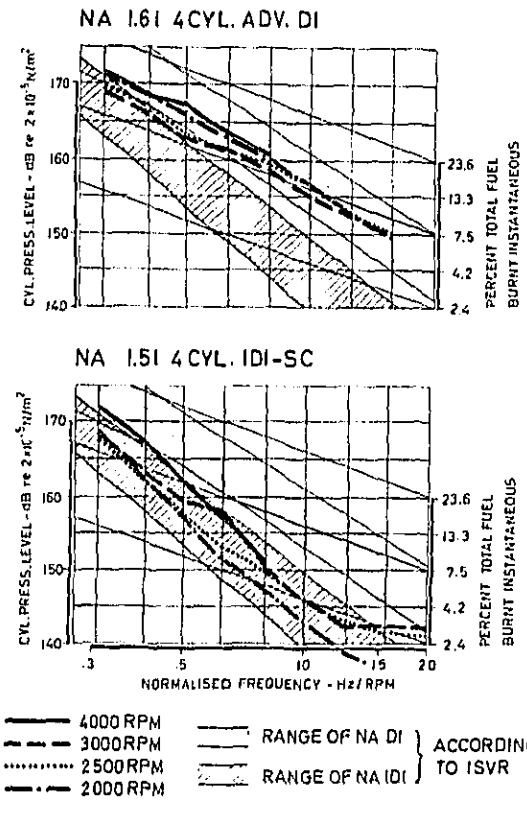

Fig. 36 - Cylinder pressure spectra at full load of a 1.6 liter diesel engine with advanced D.I. system and 1.5 liter diesel engine with up to date swirl chamber system

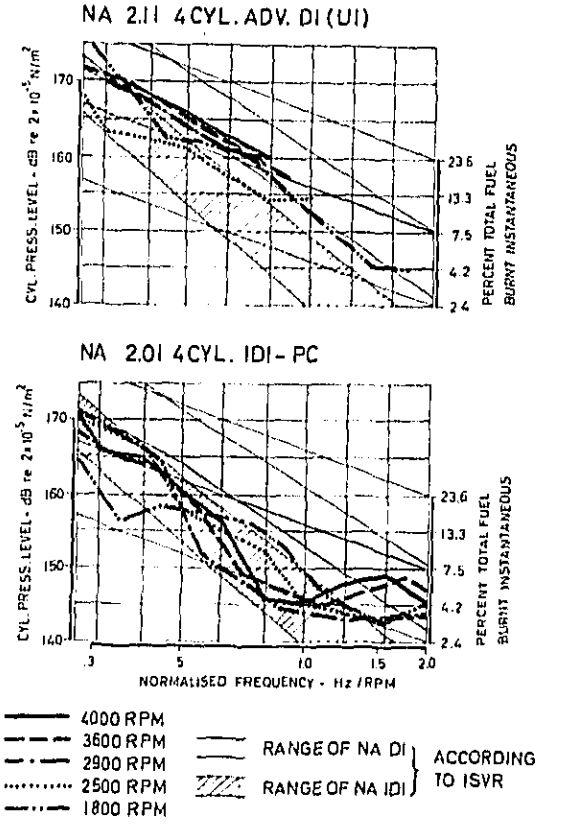

Fig. 38 - Cylinder pressure spectra at full load of a 2.1 liter diesel engine with advanced D.I. system and 2.0 liter diesel engine with up-to-date prechamber system

spreading range of the cylinder pressure spectra of previous noise-optimized D.I. engines so that all the cylinder pressure spectra of the 1.6 liter engine are at the lower limit of the spreading range of the critical cylinder pressure levels. As for the 15.9 liter engine discussed in the previous section, the contribution of the combustion to the total engine noise also with this high-speed light-duty D.I. engine is approximately 2 dB(A). From the comparison with I.D.I. engines - the lower diagram in Fig. 36 shows cylinder pressure spectra of a modern and well-developed 1.5 liter swirl chamber engine - it can be seen that the application of advanced D.I. or I.D.I. combustion system results in a difference of about 1 dB(A) to 2 dB(A) of the total engine noise with engines of the same size. Fig. 37 illustrates the cylinder pressure development, rate of heat release and needle lift of the 1.6 liter D.I. engine at full load and 2500 RPM. The very low quantity of premixed combustion and the maximum value of the pressure rise $dp/d\alpha$ being below 4 bar/°CA can be seen. The high compression ratio of 22.5:1 results in a compression pressure of approximately 57 bar. Due to the retarded injection, the firing pressure is slightly higher amounting to 66 bar.

Fig. 38 finally demonstrates the cylinder pressure spectra of the 2.1 liter diesel engine with the advanced D.I. system. In this case the position of these spectra is even more favorable than with the 1.6 liter engine, they are at the lower limit of the spreading range of previous noise optimized D.I. systems respectively partly even in the middle of the spreading range of noise optimized I.D.I. systems in the medium speed range of 2500 RPM. This exceeds the already very successful results obtained with the 1.6 liter engine and can be ascribed to the use of unit injectors, making it easier to obtain optimum conditions over the wide speed range of high-speed light-duty diesel engines. For comparison cylinder pressure spectra of a modern well-developed 2.0 liter pre-chamber engine are given in the lower diagram. Considering the entire speed range, the spectra cover the whole spreading range of I.D.I. engines and therefore partly coincide with the values obtained with the advanced D.I. system using unit injectors.

CONCLUSIONS

1. According to experience a significant improvement of the environmental conditions requires the lowering of the loudness at least by half. This corresponds to a noise reduction of more than 10 dB(A).

2. In general noise reductions of more than 10 dB(A) can only be achieved by vibration isolation between the excited and the sound radiating parts of the engine or by the attachment of sound reducing shields.

3. Due to the stiff connection of all parts of the engine structure with existing engines all outer engine parts contribute to the total noise. Therefore, in general a reduction of more than 5 dB(A) of the total noise needs the treatment of all external engine parts, although some of these parts contribute to the total noise to a larger extent.

4. Completely enclosing the engine is the most economic way of reducing the total noise to the required extent of more than 10 dB(A).

5. Such additional noise reducing enclosures have been designed and developed in the last decade for several existing diesel engines. In general, they are supported elastically by the engine representing a part of it. Under installation conditions, however, a stiff connection with parts of the vehicle or with the base is also possible. Bulk volume and weight of the engine are only slightly increased, the latter by approximately 10 %. Using simple sheet metal without damping layer and acoustical lining noise reductions of 10 dB(A) to 20 dB(A) are achieved. Over-heating of the engine and enclosure is prevented by a ventilation system. Large covers attached to the frame system of the enclosure enable easy access for the maintenance of the engine.

6. In the case that a future engine is designed initially with consideration of the special requirements of the enclosure technique, an enclosure of a simpler design and a lower weight than with existing engines can be conceived.

7. With newly designed engines it is possible to integrate the sound reducing enclosure into the engine structure in order to minimize the additional weight and bulk volume. With this concept, one part of the engine housing is replaced by the sound attenuating casing which then also provides the sealing of the oil chamber. The feasability of this concept which is applicable to some types of engines, is already demonstrated successfully with a water-cooled 6-cylinder inline engine. Prototypes of a low-noise high-speed light-weight water-cooled 4-cylinder inline engine, featuring a vibration isolated engine and flywheel housing supporting the inner engine structure are in the stage of development.

8. As a result of extensive development applying specific measures an advanced D.I. combustion system is available which in comparison with optimized I.D.I. systems is still maintaining a 15 % lower fuel consumption, featuring acceptable combustion noise and equal exhaust emission levels, complying with the severe U.S. emission limits. Also with light-duty diesel engines the same power output and speed as with optimized I.D.I. systems can be achieved. With the advanced D.I. combustion system the cylinder pressure spectrum is located between previously optimized D.I. and I.D.I. systems as well as close below the average spreading range of the critical cylinder pressure spectra of existing engines. Applying such an advanced D.I. system results in a contribution of approximately 2 dB(A) of combustion to the total engine noise. Using an I.D.I. system would decrease the total engine noise by hardly more than 1 dB(A) to 2 dB(A).

REFERENCES

1.K.S.Shah, "Geräuschuntersuchungen an Dieselmotoren." ("Noise Investigations of Diesel Engines.") Graz, Dissertation Techn. University, 1960.

2.G.E.Thien, "Methods and Problems in Noise Reduction of High Speed Diesel Engines." SAE Transactions, Vol 77 (1968), Paper 680407.

3.G.E.Thien and H.A.Fachbach, "Geräuschverminderung an Dieselmotoren durch Änderung äußerer Bauteile und schalldämmendes Verkleiden." ("Noise Reduction on Diesel Engines by Modification of External Engine Parts and Sound Reducing Enclosures.") MTZ, 32. Jg., No. 5 (May 1971), pp. 145-152.

4.G.E.Thien and B.Nowotny, "Untersuchungen über den Einfluß von Körperschallvorgängen auf das Geräusch von Dieselmotoren." ("Investigations into the Influence of Structure Vibrations on Noise of Diesel Engines.") MTZ, 32. Jg., No. 6 (1971), pp. 186-193.

5.G.E.Thien, "Ein Beitrag zur Geräuschverminderung bei schnellaufenden Dieselmotoren." ("A Contribution to the Noise Reduction of High Speed Diesel Engines.") FISITA, London 1972, Paper 1/10.

6.G.E.Thien, "The Use of Specially Designed Covers and Shields to Reduce Diesel Engine Noise." SAE Paper 730244, Detroit, Jan. 1973.

7.G.E.Thien and H.A.Fachbach, "Geräuscharme Dieselmotoren in neuartiger Bauweise." ("A New Design Concept of Low Noise Diesel Engines.") MTZ, 35. Jg., No. 8 (1974).

8.G.E.Thien and H.A.Fachbach, "Design Concepts of Diesel Engines with Low Noise Emission." SAE Paper 750838, Milwaukee, Sept. 1975, SP-397.

9.H.A.Fachbach and G.E.Thien, "Musterausführungen geräuscharmer Dieselmotoren." ("Prototype Models of Quiet Diesel Engines.") MTZ, 36. Jg., No. 10 (1975).

10.G.E.Thien and H.A.Fachbach, "Quiet Automobiles - A Realistic Objective." FISITA, Tokyo 1976, Paper 3-1.

11.H.A.Fachbach and G.E.Thien, "Körperschallausbreitung bei Dieselmotoren." ("Structure Vibration with Diesel Engines.") MTZ, 37. Jg., No. 7/8 (1976).

12.G.E.Thien, "Elemente zur Abminderung der Schallemission von Verbrennungsmotoren heute üblicher Bauart." ("Elements Reducing the Sound Emission of I.C. Engines of Conventional Design.") Dissertation Technical University Graz, Sept. 1977.

13.H.A.Fachbach, "Entwicklung von neuartigen geräuscharmen Dieselmotoren." ("Development of Newly Designed Diesel Engines with Low Noise.") Dissertation Technical University Graz, Sept. 1977.

14.H.A.Fachbach and G.E.Thien, "Ein neuer Weg zum geräuscharmen Dieselmotor." ("A New Approach for a Low Noise Diesel Engine.") FISITA, Budapest, 1978, pp. 11-23.

15.G.E.Thien, "Beurteilung der geräuscherregenden Eigenschaften der Verbrennung an Diesel- und Ottomotoren mittels Frequenzanalyse des Brennraumdruckes." ("Assessment of Noise Inducing Characteristics of Combustion with Diesel and Gasoline Engines by Frequency Analysis of Cylinder Pressure.") MTZ, 25.Jg., No. 7 (1964).

16.H.List and S.Pachernegg, "Developing High Speed Direct Injection Diesel Engines." SAE Paper 978 B, Detroit, Jan. 1965.

17.G.E.Thien, "Entwicklungsarbeiten an Ventilkanälen von Viertakt-Dieselmotoren." ("Development of Intake and Exhaust Parts of 4 Stroke Diesel Engines.") Österr. Ingenieur-Zeitschrift, Jg. 8, Heft 9, (1965).

18.R.Pischinger and W.Cartellieri, "Combustion System Parameters and their Effect upon Diesel Engine Exhaust Emissions." SAE Paper 720756.

19.E.Schreiber and R.Cichocki, "Der Entwicklungsstand schadstoffarmer Fahrzeug-Dieselmotoren." ("State of Development of Automotive Diesel Engines with Low Exhaust Emissions.") ATZ, Jg. 77, No. 3, (1975).

20.S.J.Pachernegg, "Efficient and Clean Combustion." SAE Paper 750787, Milwaukee, Sept. 1975.

21.F.Freyn, "Verbrennungsmotoren der AVL - Ein Rückblick auf 25 Jahre Entwicklung." ("I.C. Engines of AVL - a Retrospect of 25 Year Development.") MTZ, Jg. 36, No. 6 and 7/8 (1975).

22.P.Tritthart and W.P. Cartellieri, "Ein Beitrag zur zuverlässigen Messung der aliphalischen Aldehyde - Teil 1 und Teil 2." ("A Contribution to Reliable Measurement of Aliphatic Aldehydes - Part 1 and Part 2.") MTZ, 38. Jg., No. 2 and 3 (1977).

23.W.P.Cartellieri, R.Cichocki, G.E.Thien and H.A.Fachbach, "The Swirl Supported Direct Injection Diesel Combustion System - Its Potential of Meeting Economical and Environmental Requirements." Conf. on Land Transp. Engines, Instn. Mech. Engrs, Paper C11/77, 1977.

24.W.P.Cartellieri and B.Schukoff, "Die direkte Einspritzung als Verbrennungsverfahren für leichte Dieselmotoren." ("The Direct Injection as a Combustion System for Light Diesel Engines.") FISITA, Budapest 1978, pp. 1-10.

25.E.Lotze, "Schalldämmung." ("Interaction of Sound with Solids." in W. Schirmer, Lärmbekämpfung, Verlag Tribüne, Berlin 1971, Chapter 9, pp. 329-372.

26.R.S.Jackson, "The Performance of Acoustic Hoods at Low Frequencies." Acustica, Vol 12 (1966), pp. 139-152.

27.E.Lotze, "Kapseln." ("Acoustic Hoods." in W. Schirmer, Lärmbekämpfung, Verlag Tribüne, Berlin 1971, Chapter 11, pp. 411-435.

28.T.Priede, "Relation between Form of Cylinder Pressure Diagram and Noise in Diesel Engines." Proc. Instn. Mech. Engrs. (A.D.), No. 1, 1960-61, pp. 63-77.

29.D.Föller, "Geräuscharme Maschinenteile." ("Noise Reduced Machine Members.") Forschungsbericht des Forschungskuratoriums Maschinenbau, Frankfurt/M, Heft 15, 1972.

30.E.Wodiczka, "Verbrennungsgeräusch bei Dieselmotoren." ("Combustion Noise with Diesel Engines.") Forschungsbericht der Forschungsvereinigung Verbrennungskraftmaschinen, Frankfurt/M, Heft 123, 1972

31.D.Anderton and T.Priede, "The Influence of Automotive Diesel Engine Design on Combustion, Noise and Performance." Paper pres. to DOT Conference, Sept. 7-9, 1977.

790267

A NEW MEASURING METHOD FOR THE DIRECT DETERMINATION OF DIESEL ENGINE COMBUSTION NOISE

F.F. Pischinger
K.P. Schmillen
F.W. Leipold

Institute of Applied Thermodynamics, Technical University Aachen
Daimler-Benz AG, Stuttgart

ABSTRACT

Previously indirect test methods were used to investigate Diesel engine combustion noise. Now digital signal analysis gives the possibility of determining it and its narrow band spectra directly. Such a method for direct evaluation of the combustion noise is described and the possibilities offered by it are shown. A single-cylinder direct-injection Diesel serves as a test engine. Steady-state as well as transient conditions of the engine are evaluated by the procedure.

THE DIESEL ENGINE, widely used as a power unit because of its excellent fuel economy, represents a very complex noise source from an acoustic point of view.

Investigations carried out separately on the individual noise sources of a Diesel engine have shown that after elimination of the intake and exhaust noises by means of suitably designed silencers, the noise radiated from the surfaces of the engine becomes the main irritant. This sound is a combination of mechanical and combustion noises.

Series investigations on many Diesel engines of widely varying types and designs (1)* indicated that combustion noise represents a considerable part of the overall noise emitted. In order to achieve noticeable reductions in noise level, it is therefore necessary to reduce the combustion noise.

Effective development efforts with the aim of reducing combustion noise require a method of noise signal evaluation, which enables isolation of the combustion noise from the overall engine noise. Several methods of determination of the combustion noise have been used already. Before describing a new method a comprehensive review of the procedures used so far is given in the following chapter.

PREVIOUS METHODS OF DETERMINING THE COMBUSTION NOISE

Because of the dominance of combustion noise in Diesel engines, a great deal of research work was devoted to this subject and a series of excellent methods were developed for the measurement and assessment of this noise factor. Exclusively indirect measuring methods are involved here. For example, the combustion noise is established by comparing the noise levels of a motored and a fired engine (2), or it is assessed from the spectrum of the cylinder pressure curve (3), by the 2nd differential quotients of the cylinder pressure in terms of time (4) or from the solid-borne noise signal at a measuring point near the cylinder head (5).

The individual methods for the determination or assessment of the combustion noise are briefly explained below by examples from the references listed.

COMPARISON BETWEEN A FIRED ENGINE AND A MOTORED ENGINE - Mechanical noise can be understood in the first approximation as the noise produced by a motored engine; consequently the two components combustion noise and mechanical noise overlap during engine operation.

As representative of a series of researchers who have accepted this theory, one should mention Leipold and Hardenberg (2) who have studied the acoustic features of a combustion process on the same power unit. One result of this work is shown in Fig. 1a. The increase in the sound pressure level is a result of the combustion process for both DI and IDI systems.

Separation of the noise components can be achieved by this method only if the combustion noise is predominant.

METHOD OF CRITICAL CYLINDER PRESSURE LEVEL - The cylinder pressure signal can be interpreted as a sound pressure signal and analysed in the same way. Priede (3) used as a basis the model theory that the engine components represent a linear transmission system for the cylinder pressure excitation. By varying the combustion process (for instance by altering the start of injection) he determined for the frequency bands concerned the relationship between the sound pressure level and the relevant cylinder pressure level.

As Fig. 1b shows, two areas can be clearly distinguished: at relative low cylinder pressure

*Numbers in parentheses designate References at end of paper

SAE/P-79/80/$02.50
Copyright © 1979 Society of Automotive Engineers, Inc.

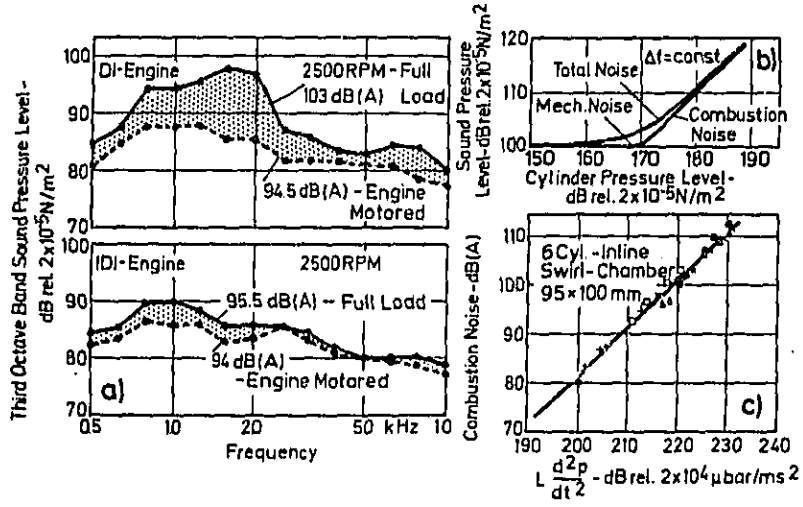

Fig. 1 - Methods for indirect determination of combustion noise
a) Comparison fired and motored engine
b) Critical cylinder pressure level
c) Pressure rise acceleration

levels the dependency of the sound pressure level on these is low. If a so-called critical cylinder pressure level is exceeded, the noise level increases at about the same rate as the excitation level.

Mechanical noise predominates below the critical cylinder pressure level, and combustion noise predominates above it. A characteristic dependency of the sound pressure level on the excitation level results in an addition curve. Knowledge of this relationship for a given engine enables the combustion noise to be calculated from the cylinder pressure spectrum.

PRESSURE RISE ACCELERATION AND COMBUSTION NOISE - The method of the critical cylinder pressure level for the assessment of the combustion noise was also used by Huber and Wodiczka (4) in their noise tests on several water and air-cooled Diesel engines which were representative of the latest technical standards. For all engines there was a relatively narrow scatter band for the frequency response of the transmission factor of the engine components (difference between cylinder pressure level and level of combustion noise). By suitable choice of the upper limiting frequency of a differentiating amplifier to form the 2nd differential quotient of the cylinder pressure in terms of time it was possible to simulate the frequency response of the transmission factor. Measurement of the engines showed that there was a very good correlation between the combustion noise level and the 2nd differential quotient of the cylinder pressure in terms of time. This relationship is shown in Fig. 1c for one of the engines examined.

SOLID-BORNE SOUND MEASUREMENT - As a signal for the assessment of the combustion noise, Hauser (5) suggests the impulse of surface acceleration (which occurs synchronously with the combustion process) at a measuring point near the cylinder head. The frequency spectra of this signal period are determined both for engine operation and for the subsequent motoring process (fuel injection cut off for a short time). The level differences between the spectra represent a qualitative measure for the assessment of the combustion noise.

DIRECT DETERMINATION OF COMBUSTION NOISE

As is shown by the short list of reference works, there are as yet no direct measuring methods for the combustion noise. Such possibilities will be discussed below.

QUANTITATIVE TIME-FREQUENCY ANALYSIS - The sound radiated by a Diesel engine is very impulsive, and with an oscillogram it is relatively easy to evaluate the instants at which the individual impulses occur. Correlation of these in terms of time to the process within the engine (e.g. closing and opening of the valves, combustion process) provides indications as to the possible cause of the sound impulses.

In order to enable conclusions to be drawn regarding the frequency content of the impulses an analogous band-pass filter can be inserted in the measuring chain and the filter response displayed on a screen (time-frequency analysis). As regards the intensity, such a time-frequency analysis is only a qualitative examination method because it supplies no level values.

On the other hand, one can achieve a quantitative time-frequency analysis with the aid of equipment used for digital signal processing, as the effective values of the impulses can be calculated. Fig. 2 will help to explain by means of the sound pressure characteristics of a single-cylinder four-stroke engine the quantitative time-frequency analysis in more detail.

In order to enable a correlation of the impulses in terms of time, Fig. 2 shows the characteristics of the cylinder pressure p versus the crank angle, with the dead centres

marked. The speed of the engine is $n = 1200\,min^{-1}$, the time required for one work cycle (2 revolutions) being T_o = 100 ms.

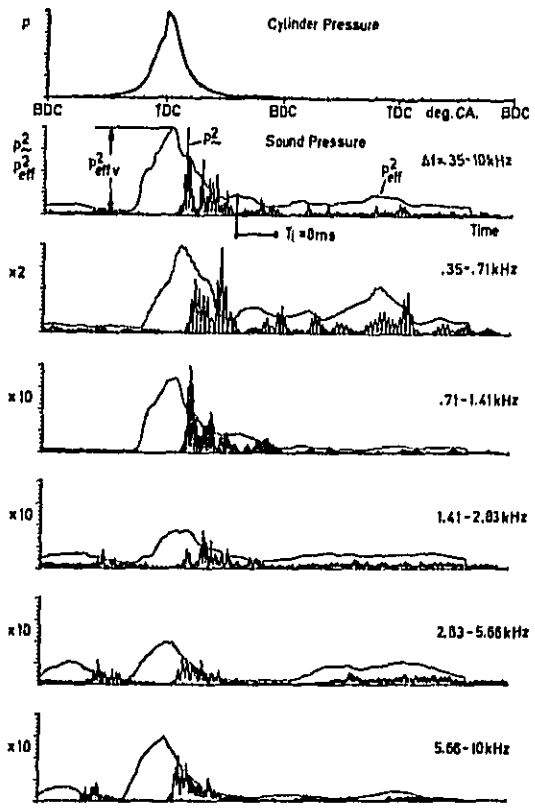

Fig. 2 – Quantitative time-frequency analysis (the numbers 2 and 10 are scale factors of the ordinate)

Below the curve for the cylinder pressures, the squares of the alternating sound pressure ($p_\sim^2$) are plotted synchronously for different frequency bands. Because of the travelling time of the airborne sound from the engine surface to the microphone, there is a time lag of about 3 ms. For each frequency band there is shown a second curve indicated with p_{eff}^2. It is obtained by summing up the $p_\sim^2$ values within a sliding time window which, in the example shown, has a length of T_i = 8 ms. p_{eff}^2 is proportional to the intensity of sound within the time window. If T_i exceeds the period of the lowest frequency component in the signal p_{eff}^2 can be interpreted as the square effective value of $p_\sim$ and the following is valid:

$$p_{eff}^2 = \frac{1}{T_i} \int^{T_i} p_\sim^2 \, dt \qquad (1)$$

As the sound pressure characteristics were traced by an ADC at discrete time intervals Δt, the integral becomes a sum

$$p_{eff}^2 = \frac{1}{n\,\Delta t} \sum_1^n p_\sim^2 \,\Delta t = \frac{1}{n} \sum_1^n p_\sim^2 \qquad (2)$$

The maximum value of p_{eff}^2 near the TDC can be used as a measure for combustion noise. It is designated p_{effV}^2 in Fig. 2. Correspondingly the level of the combustion noise is

$$L_V = 10 \log \frac{p_{effV}^2}{p_o^2} \qquad (3)$$

L_V is an objectively measured value for the combustion noise obtained by a direct method. Because of the relative short integration time, L_V is largely unaffected by noise excited by other sources than combustion when investigating a single cylinder engine.

The remaining noise from the engine at this time is negligibly low compared with the combustion noise. This is evident from Fig. 2 for all frequency ranges because during the compression phase shortly before TDC $p_\sim^2$ is very low.

The method of quantitative time-frequency analysis is very time-consuming as each frequency range investigated must be individually re-analysed. It is therefore only practicable for relatively wide frequency bands (e.g. octave band width). Furthermore a frequency error occurs because of the limited attenuation slope of analogous frequency band filters.

TIME-FREQUENCY-WINDOWS METHOD – Based on the experience gained with the quantitative time-frequency analysis, another measuring method for the combustion noise was developed which avoids the disadvantages mentioned, such as frequency error and high expenditure in terms of time.

In order to determine the combustion noise it is sufficient to consider only the sound pressure impulse which is produced by the cylinder pressure characteristics during combustion. Considering and analysing only parts of a noise in more detail is not a new method of acoustic measurements. When investigating the acoustic behaviour of an one-cylinder Diesel engine, Hauser (5) used a special tape recorder (rotating heads) to play back repeatedly parts of interest of the recorded noise signal for further evaluation by a hybrid analyser. This method is time consuming and difficult. Measurement results of greater scope are therefore lacking.

To avoid the disadvantages of analogous filtering or of an intricate tape play back technique for determining the combustion noise the following procedure was established.

As it is shown in Fig. 3, a sound pressure-time signal picked up by a microphone, is used without applying a frequency filter. A part of this noise signal is cut out for further treatment by a time window of 20 ms which covers the

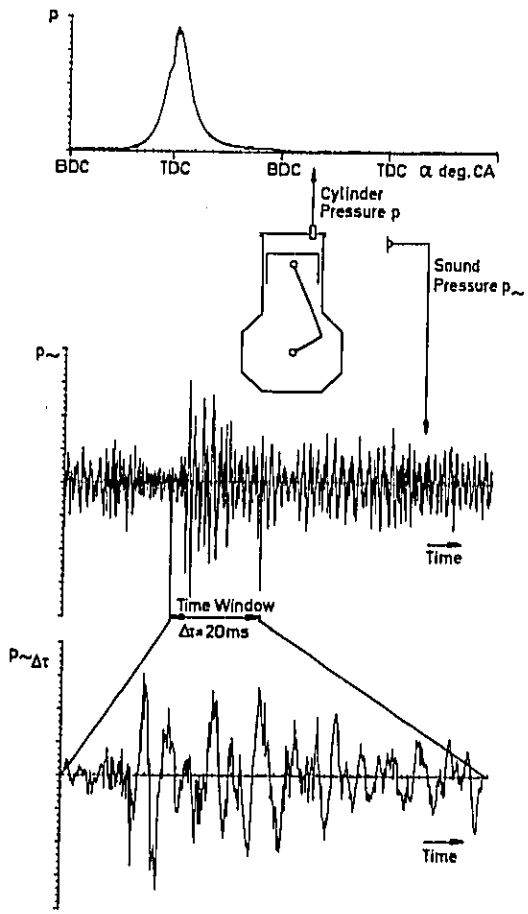

Fig. 3 - Tuning-out of the combustion noise
p cylinder pressure, $p_{\sim}$ sound pressure,
$P_{\sim\Delta T}$ sound pressure within time window

range near combustion TDC and includes the combustion noise. It is only from this cut-out signal period, that a narrow band spectrum is established with the aid of a digital Fourier analyser. Similar to the quantitative time-frequency analysis, the highest level for each frequency band is used to determine the combustion noise.

The computation steps for the analysis of the combustion noise are explained in more detail in Figs. 4 and 5. The sound pressure characteristics for 30 consecutive working cycles are stored in the core memory of the computer. Only two of the confirmed 30 cycles are shown in Fig. 4. Preliminary tests have confirmed that the test results are reproducible if averaged from 30 combustion cycles. The window-signal has a constant time length of $\Delta\tau$ = 20 ms, each signal consisting of 512 digital samples. By

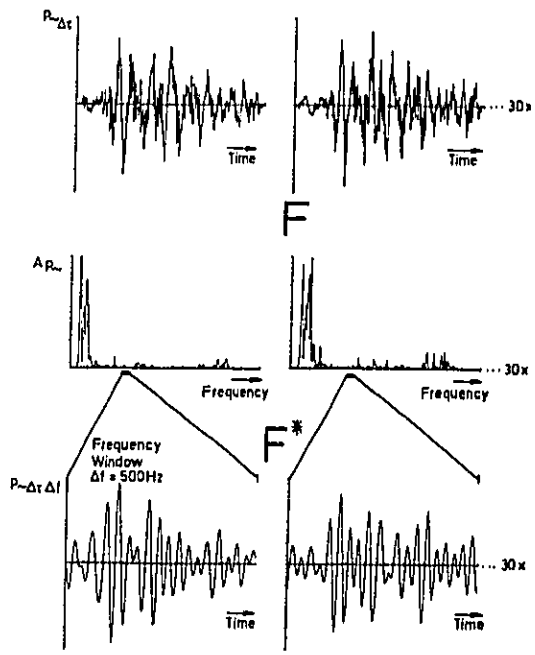

Fig. 4 - Time and frequency window
$A_{p_{\sim}}$ amplitudes of sound pressure,
$P_{\sim\Delta T\Delta f}$ sound pressure within time and frequency window

multiplication with a suitable window function, unsteadiness of the signal at the beginning and at the end are avoided.

The Fourier transformation (F) provides the narrow band spectrum of the window signal (amplitude $A_{p_{\sim}}$ and phase - phase not shown in Fig. 4). After erasing the frequency components outside a suitably chosen frequency window an inverse Fourier transformation (F*) is carried out. The result is a bandpassed time signal. The individual 30 time signals are squared and averaged (Fig. 5). By this method also the frequency error of analogous filters is avoided.

An integration window is slid over the averaged quadratic sound pressure characteristics and the level is determined for each effective value obtained in this way. An integration time of 6 ms has proved to be favourable. Again the maximum value of the noise level $L_{V\Delta f}$ is defined as combustion noise level for the frequency band Δf. This signal processing is carried out for each of the 500 Hz wide frequency ranges between 0.5 and 10 kHz. The result is the averaged narrow band spectrum of the combustion noise (Fig. 5 below).

If the values are not averaged the individual spectra of the combustion noise of consecutive engine cycles are obtained. In this case the cyclic variations occurring from engine cycle to engine cycle can be investigated, or the

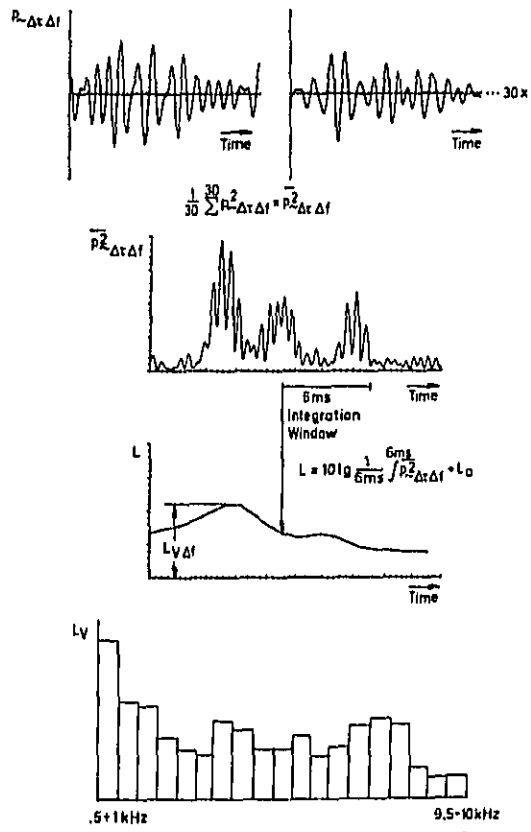

Fig. 5 - Computation steps for the determination of the combustion noise spectrum, L_V combustion noise level

combustion noise with the engine operating under transient conditions - e.g. during transition from part load to full load - can be examined.

This measuring method can be used only as long as the noise impulses caused by the combustion process can be separated in terms of time from other impulses. In the case of 1 to 4-cylinder engines, this can be done over wide engine speed ranges by appropriately choosing the time window. In general this is not the case for 5 and 6-cylinder engines because of interference of other noise sources, for instance valve opening and closing noise. Here suitable measuring conditions must first be provided by means of additional measures carried out on the engine, such as partial encapsulation.

It should be mentioned here, that the sound originating from piston slap near TDC cannot be separated by this method. As the combustion chamber pressure causes the traverse motion of the piston across the clearance space, the resulting airborne sound is associated with the combustion noise.

An example for the effectiveness of the time-frequency-windows method is shown in Fig. 6. Part a) shows the A-weighted sound pressure level of the one-cylinder Diesel engine for two loads versus injection timing, as it is determined by conventional sound level measuring devices. In addition, the curves for the combustion noise (L_V 0.5...10 kHz) are shown as the sum of the band levels of the combustion noise measured by the time-frequency-windows method. About the same gradient results for all curves, but the time-frequency-windows method yields about 6 dB higher levels. An increase of 6 dB shows that the combustion noise predominates over the mechanical noise, which is the case at n = 1200 min^{-1}. Fig. 6b shows the levels for two different timings at n = 1700 min^{-1}. As the combustion noise here is not predominant, the noise level L_A provides no clear-cut result. Conversely, the level L_V 0.5 ...10 kHz indicates a distinct dependency on the

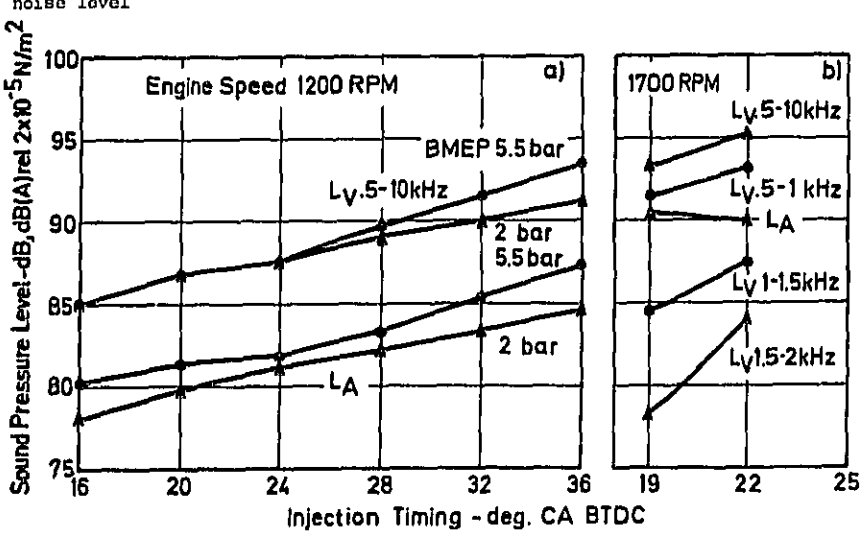

Fig. 6 - Comparison of combustion noise level L_V with the A-weighted sound pressure level L_A

injection timing as it is the case also with L_V 0.5...1 kHz. Higher frequency bands (1...1.5 kHz and 1.5...2kHz) further clarify the influence of injection timing on combustion noise.

TEST EQUIPMENT

The time-frequency-windows method was developed in connection with testbench evaluations of a single-cylinder engine. Testbench arrangement and data as well as some first results are given below.

TEST CELL AND TEST ENGINE - The acoustic measurements were carried out on a test cell, the walls and the ceiling being covered with noise insulating material (limit frequency 100 Hz). A heavy foundation supported by coil springs is let into the nonabsorbing floor. Thereby solid borne sound bridges between test cell floor and foundation are eliminated.

An eddy-current brake and an electric motor for motoring the test engine are installed in a neighbouring acoustically isolated test cell. The aerodynamic noise sources of the test engine are eliminated by suitable damping units so that only noise in the test cell is the airborne sound emitted from the engine surface.

The tests described in this paper were carried out on a water-cooled single-cylinder engine with the following technical specifications:

Cylinder diameter	$D = 125$ mm
Stroke	$s = 130$ mm
Cubic capacity	$V_h = 1.595$ dm^3
Compression ratio	$\varepsilon = 16.5$
Injection timing (static start of fuel delivery)	$\alpha_E = 15^\circ$ crankshaft before TDC

RECORDING AND STORAGE OF MEASURED VALUES - The measuring equipment used for the tests is shown in Fig. 7 as a functional diagram. The fundamental sources of information are the airborne sound pressure characteristics and for comparison the cylinder pressure characteristics.

The airborne sound signal is picked up by a capacitor microphone (13) in 1 m distance of the engine surface and fed to a pre-amplifier and a measuring amplifier (14). The cylinder pressure is measured via a piezo-electric pressure pickup (8), a charge amplifier (9) and a high-pass filter (10). A 1-inch tape recorder (15) equipped with 7 FM channels and 1 direct channel is available for storage of the signals. The photocell (11) produces one needly pulse per revolution at BDC of which only that at compression BDC is transmitted by the triggering unit (12). This serves as a trigger signal during signal processing with a digital Fourier analyser (16).

To enable measurements under transient operating conditions as well as under steady-state conditions, a device is installed for quick adjustment of the injection pump control rod. By means of a pneumatic cylinder (4) it is possible to bring the control rod from a given steady-state part load operating point into the full load position within one working

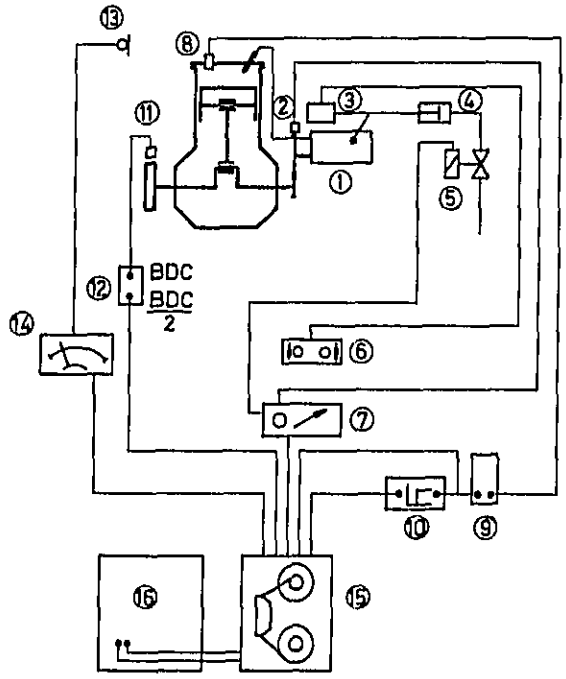

Fig. 7 - Block wiring diagram for the acquisition and storage of measured values
1 Injection Pump, 2 Photocell, 3 Actuator, 4 Hydraulic Cylinder, 5 Magnetic Valve, 6 Controller, 7 Accelerator, 8 Pressure Transducer, 9 Charge Amplifier, 10 High Pass Filter, 11 Photocell, 12 Triggering Unit, 13 Microphone, 14 Measuring Amplifier, 15 Tape Recorder, 16 Fourier-Analyzer

cycle. During the short measuring time of transient operation, the engine speed varies so little that one can assume that only the combustion noise and not the mechanical noise is affected. The use of a photocell (2) and a logical circuit ensure that the sudden movement of the control rod could take place only during the period of charge changing between two working cycles.

MEASURING RESULTS

First results obtained with the described time-frequency-windows method, which are presented below, shall demonstrate the applicability for engine noise evaluation. In this connection speed and load dependence of the combustion noise, correlation between combustion noise and cylinder pressure spectra, cyclic variation of the combustion noise and combustion noise under transient conditions have been investigated.

SPEED AND LOAD DEPENDENCE OF THE COMBUSTION NOISE - Fig. 8 shows in map form lines of constant combustion noise level Lv 0.5...10 kHz. Important conclusions can be drawn from this graph, regarding

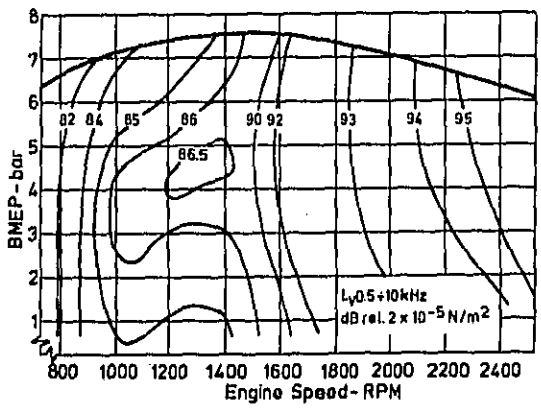

Fig. 8 - Map of combustion noise levels

for example the correlation of the combustion noise with engine operational parameters like peak pressure, rate of pressure rise, etc.

In the lower engine speed range the levels up to a mean effective pressure p_{me} = 5 bar are dependent only on the engine speed. Above this, a load increase produces a decrease in levels. This tendency is reversed in the speed range above n = 1600 min^{-1}. Up to a BMEP of 5 bar the combustion noise levels show a marked dependency on load, whilst for higher mean effective pressures only the engine speed has any effect. The range between n = 1200 min^{-1} and n = 1600 min^{-1} appears to be of particular interest. Pure load and speed dependencies are found close together in narrow areas of the graph, and this is expressed in the form of large gradients dLv/dn, particularly for the speed dependency. This operating range would have to be subjected to more detailed investigation in the future in order to clarify the causes of this characteristic.

It must be emphasised that the combustion noise levels in Fig. 8 correspond to the noise levels according to equation (3) and therefore to only one working cycle not taking into account the series of the cycles. For comparison with the usual measurements one has to add therefore 3 dB per doubling of RPM. The increase of about 10 dB/octave according to Fig. 8 corresponds therefore well with measurements of engines with predominating combustion noise which have shown increases of about 13 dB/octave (2).

FREQUENCY ANALYSIS OF CYLINDER PRESSURE AND COMBUSTION NOISE - Figs. 9 and 10 show for 1200 RPM engine speed in three-dimensional form narrow-band frequency spectra - averaged from 30 working cycles - of the cylinder pressure and the com-

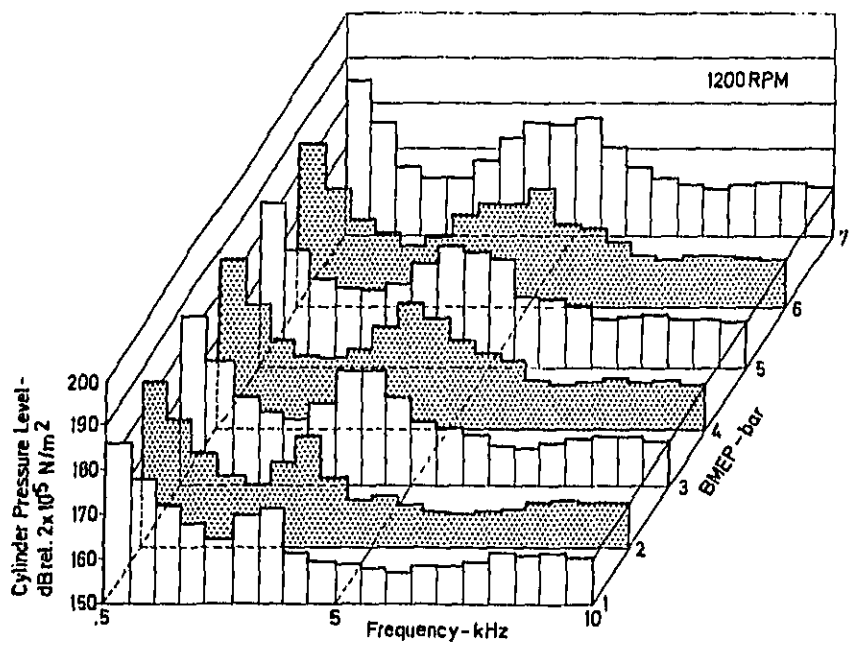

Fig. 9 - Narrow-band cylinder pressure spectra plotted versus load

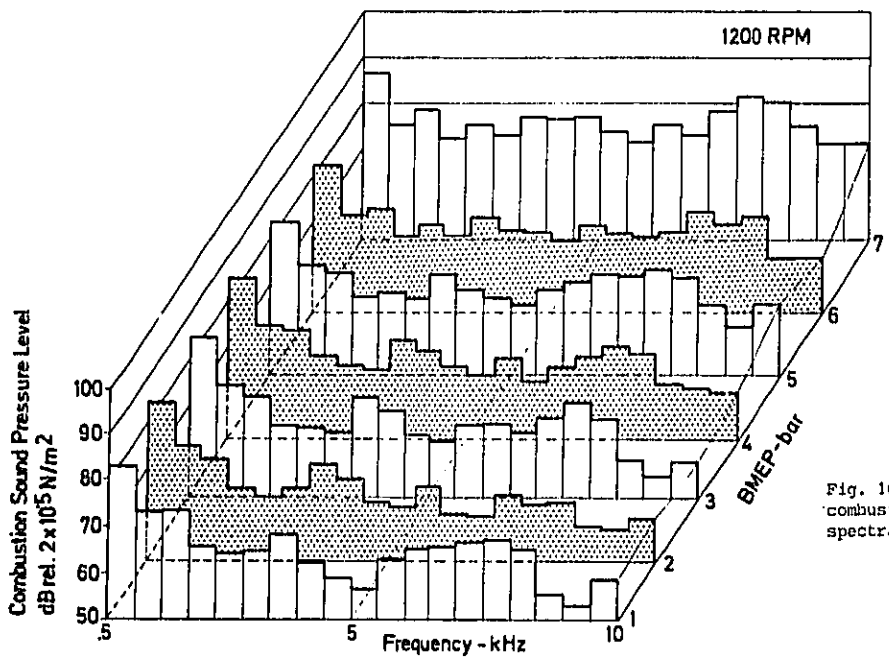

Fig. 10 - Narrow-band combustion sound pressure spectra versus load

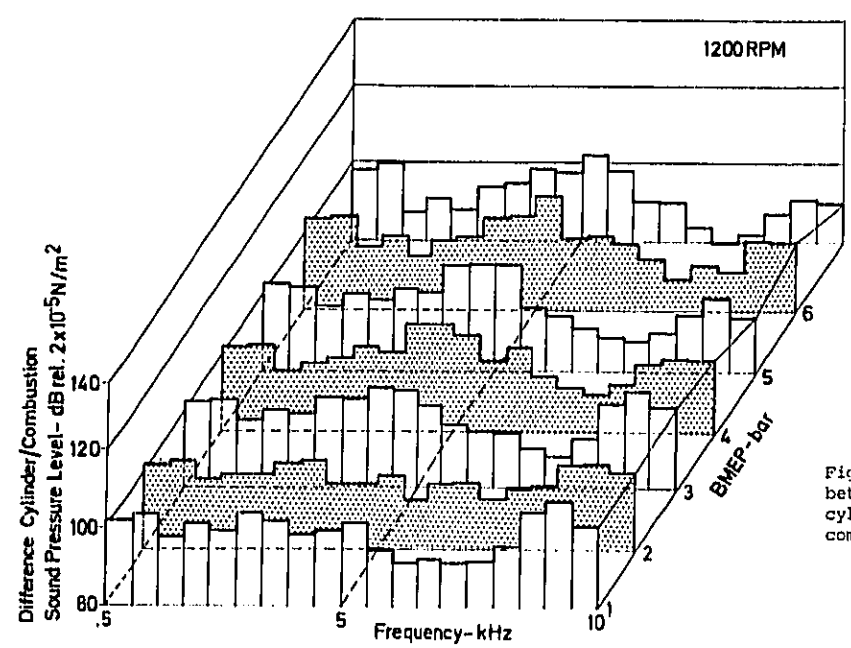

Fig. 11 - Difference between spectras of cylinder pressure and combustion sound pressure

bustion noise versus the mean effective pressure. The band width is 0.5 kHz in all cases. The spectra of the cylinder pressure (Fig. 9) show for the low frequencies the highest levels of approx. 185 dB. As frequency increases, these fall to values of around 160 dB. Worth noting is an increase of about 10 dB in the frequency range 3...4 kHz. As the load increases, this frequency range shifts to higher values. For 7 bar BMEP the increased levels ly between 3.0 and 6.0 kHz. Apart from this phenomenon, no marked load dependency can be detected for the frequency spectra.

Fig. 10 shows the corresponding levels of the combustion noise. In the frequency range up to 5 kHz one finds relationships between cylinder pressure and combustion noise. The frequency component 0.5...1 kHz is a decisive factor for the levels, but the level increase in the range 3.5...5 kHz is not as pronounced as the combustion chamber spectrum might lead one to expect. On the other hand a second increase is indicated in the frequency range 7...8.5 kHz for which the cylinder pressure spectrum offers no explanation. Investigations at other engine speeds showed that the frequencies of these increases are independent of engine speed, and it must therefore be a case of natural frequencies of the engine structure.

Fig. 11 shows the level difference between the cylinder pressure and the combustion noise spectrum. Assuming a linear transmission system between excitation (cylinder pressure) and system response (combustion noise), only one frequency dependency should result. However, in many frequency ranges a load dependency is shown. This would suggest the conclusion that the frequently used model theory of the existence of an invariable transmission function should be given careful thought.

CYCLIC VARIATIONS UNDER STEADY-STATE CONDITIONS - Fig. 12 shows by means of examples the cyclic variations of the total combustion noise level (0.5...10 kHz) and some selected frequency band levels for six consecutive working cycles. It becomes evident that in the level-determining frequency range 0.5...1 kHz as well as in the range 1...1.5 kHz, only very small variations occur. Conversely at higher frequencies there is scatter of values, which differ up to above 10 dB, their temporal sequence being of a statistical nature.

It is presumed that the subjective annoyance factor of Diesel engine noise is to be looked for in these cyclic variations.

CYLINDER PRESSURE AND COMBUSTION NOISE UNDER TRANSIENT CONDITIONS - Figs. 13 and 14 show the overall levels and selected frequency band levels of the cylinder pressure or the combustion noise during the sudden transition from a part load operating point to full load. Between the 3rd and 4th recorded working cycles, the control rod of the injection pump was shifted to full injection quantity at the time of engine breathing.

In the example shown for the cylinder pressure (Fig. 13) no reaction to the load

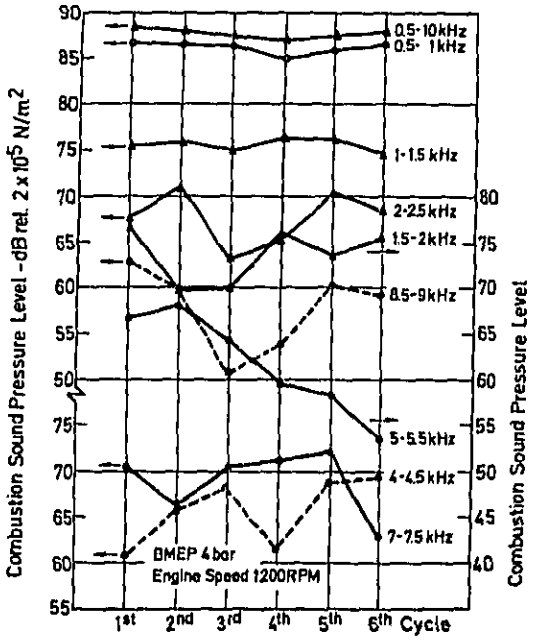

Fig. 12 - Cyclic variations of the combustion sound pressure level

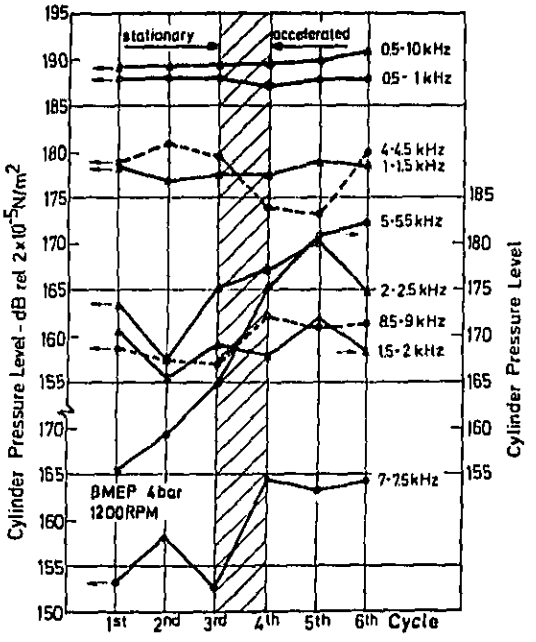

Fig. 13 - Cylinder pressure levels under transient conditions

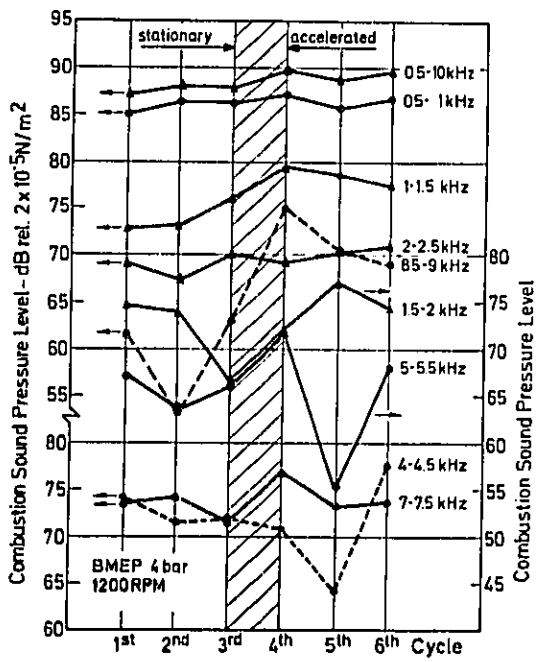

Fig. 14 - Combustion sound pressure levels under transient conditions

change is shown in the overall level and in the level-determining frequency band. Some bands of higher frequency, on the other hand, indicate a clear increase in levels (e.g. 5...5.5 kHz). In other cases, however, the level increase seems to be covered by the cyclic variations (e.g. 1.5...2.0 kHz). Fig. 14 shows the relationship of the combustion noise for the corresponding working cycles. Here the overall level increases by about 2 dB because of the load change. For the bands of higher frequency, the same applies as has already been mentioned in connection with the cylinder pressure.

SUMMARY AND CONCLUSIONS

1. The time-frequency-windows method is suited for direct determination of the combustion noise out of the airborne noise of a Diesel engine. Means for digital frequency analysis provided the method is applicable for testbench investigations for 1 to 4-cylinder engines. For higher cylinder numbers additional measures have to be taken on the engine.

2. The time-frequency-windows method shows up influences on the combustion noise also in cases of predominant mechanical noise.

3. Comparison of combustion noise and cylinder pressure spectra on a direct-injected single-cylinder Diesel engine shows the influence of the engine structure on the airborne combustion noise. An invariable transmission function as it is frequently used must be questioned for the engine investigated.

4. Cyclic variations of the combustion noise spectrum can be detected by the time-frequency-windows method. A marked scatter of values for several high frequency bands is of statistical nature, the level determining low frequency bands showing only very small variations for the investigated engine.

5. The method is also suited to follow transient operating conditions of the engine.

6. The time-frequency-windows method should be used to further investigate engine combustion noise phenomena and their interdependence with engine parameters.

REFERENCES

1. W. Pflaum and W. Hempel, "Geräuschverteilung bei Dieselmotoren ohne Aufladung", MTZ No. 9, 1966

2. F.W. Leipold and H.O. Hardenberg, "Noise Emissions and Performance of the Diesel Engine - A Comparison between DI and IDI Combustion Systems" SAE-Paper 750796 p. 13 - 23

3. T. Priede, "Relation Between Form of Cylinder-Pressure Diagram and Noise in Diesel Engines" Proc.Instn.Mech.Engrs. (A.D.), No. 1, 1960/61, p. 63 - 77

4. E.W. Huber and E. Wodiczka, "Bestimmung des Verbrennungsgeräusches von Dieselmotoren mit verschiedenen Verbrennungsverfahren" MTZ 33(1972), No. 9, p. 351 - 356

5. G. Hauser, "Schmalbandige Frequenzanalyse einmaliger und impulshaltiger Schwingungsvorgänge am Beispiel von Dieselmotorengeräuschen" Doctor Thesis, University Hannover, 1975

790268

Reducing Diesel Knock by Means of Exhaust Gas Recirculation

H. Oetting and S. Papez

Volkswagenwerk AG

ABSTRACT

The different impacts on Diesel knock were investigated. The main parameters were fuel quality, ambient and engine temperature, quantity of fuel injected, compression ratio, and injection timing. One of the most reasonable methods to decrease cold knock is exhaust gas recirculation (EGR). The mechanism of the EGR effect was explained and the limitations of Diesel application of EGR was estimated.

THE TWO PROBLEMS of reducing exhaust emissions and improving fuel economy of motor vehicle engines have in recent times been joined by a third, that of noise. And wherever manufacturers decide to improve the fuel economy of their vehicles by switching to Diesel engines the noise problem gains in significance. For the combustion process peculiar to Diesel engines sometimes involves a steep rise in combustion pressure which results in the well-known 'rattle' of Diesel engines, a special kind of noise emission.

This loud noise is especially pronounced when Diesel engines are running cold at low loads and rpm's. They then produce a noise which is termed 'cold knock', and the lower the loads and engine speeds, the less heat is generated in the engine, so that it takes much longer to warm up and cold knock is prolonged in consequence. Naturally, this effect is enhanced as the ambient temperatures at which the engine is started drop progressively.

Should the owner of a Diesel car decide one bright Sundy morning in winter to take a weekend trip it is likely that the whole neighborhood will be awakened by the sound of the engine starting up.

It is only natural, therefore, that there is an urgent desire to reduce the intensity of cold knock, and the prerequisite for that is to know exactly what causes cold knock.

Normally, the mixture in a Diesel engine is ignited by the high temperature which the air reaches during the compression stroke. After a brief ignition delay, combustion commences when the first fuel particles enter the combustion chamber, and it proceeds as more fuel reaches the combustion area. Of course it is necessary that there is enough oxygen, and that all fuel molecules come into contact with a sufficient number of oxygen molecules. One of the aims of fuel injection design is to time the injection process so that the pressure generated by combustion is optimally converted into mechanical work. All design parameters are geared to that goal.

Ignition delay is longer in a cold engine, which means that before combustion begins much fuel will have reached the combustion chamber and formed an air/fuel mixture. Combustion, therefore, once it starts proceeds relatively quickly, pressure increases steeply, and cold knock is generated. The two pressure diagrams in Fig. 1 (a and b), and especially diagram b, where the two oscillograph pressure curves of diagram a are superimposed, show clearly that the pressure gradient in cold engines is much steeper.

MEASURING EQUIPMENT-In order to study more closely the causes of cold knock and to investigate ways of eliminating it we ran a series of tests on a Rabbit Diesel engine which had indicator bores in all four cylinders. Compared to standard engines its displacement was slightly higher, 1.6 instead of 1.5 liters. By modifying the heads of four pistons we manufactured an alternative set, one set being designed for a compression ratio of $\varepsilon = 19.6$, the other for $\varepsilon = 23.1$. All measurements were taken with the engine idling. Injection was timed at a crankshaft angle of 5° before TDC.

Fig. 2 shows the measuring equipment which we used in testing this engine. Depending on the setting of the heat exchanger, it would either keep the temperature of the recirculated exhaust gas constant at approximately +10 °C or heat it up to +190 °C. Moreover, we had the option of routing part of the intake air throught the heat exchanger instead of the exhaust gas.

In all four cylinders, continuous pressure measurements were taken by quartz pressure gages, amplified, and stored on tape.

SAE/P-79/80/$02.50

Copyright © 1979 Society of Automotive Engineers, Inc.

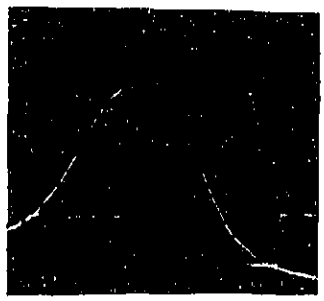

Cold Engine

a

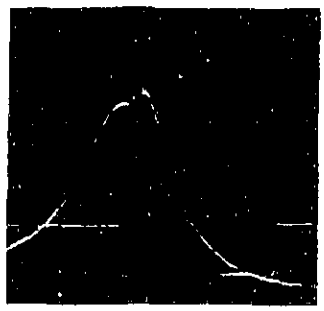

Hot Engine

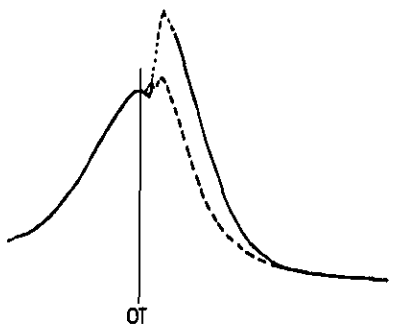

b

Fig. 1 - Cold and hot engine pressure traces

While cylinder pressure was measured, the noise emission of the engine was measured simultaneously via a microphone placed at a distance of 50 cm from the center of the radiator grille. The noise signals were stored on tape as well. The last measurement signal also stored on tape was the one which indicated cylinder 1 reaching TDC.

All pressure and noise measurements were taken in the free field sound room of the VW Acoustic Center. To simulate a road surface reflecting noise from below, both the vehicle and the microphone were placed on a chipboard basis.

We also took emission measurements in order to evaluate CO_2 content in the intake and in the exhaust gas for computing the quantity of exhaust gas recirculated. Furthermore, from the concentration of O_2 in the exhaust

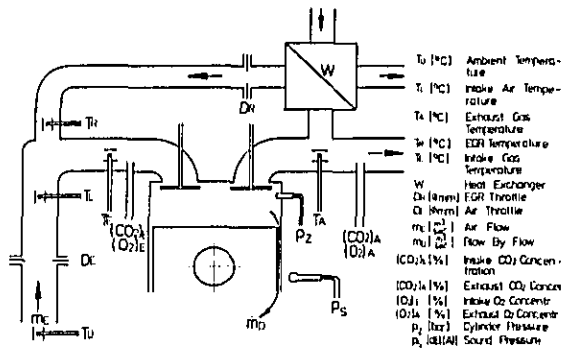

Fig. 2 - Engine and measuring equipment

we drew conclusions to the combustion air/fuel ratio. As these tests could not be run in the free field sound chamber we had to go elsewhere, taking care to ensure that thermodynamic conditions remained the same throughout.

Our test procedure was to record the pressure and noise signals from the engine for one minute after starting, after which we let the engine run at idle for precisely 19 minutes to stabilize its temperature, followed by another minute of noise and pressure measurements.

Our pressure and noise measurements were always accompanied by temperature readings by thermocouples as well as by measurements of the air throughput and blow-by rates by means of rotary gas meters.

Some of the tests were run with the vehicle at the temperature of the free field sound chamber (+20 °C), and for the other part the vehicle was cooled down to -12 °C in the cold chamber. After cooling, the vehicle was towed along a prescribed route from the cold chamber to the free field sound chamber and tested immediately.

Depending on the engine temperature, the engine speed varied between 750 and 1100 rpm. It would have been possible to try and keep the engine speed constant, but this would have meant changing the injection rate in an arbitrary manner, and so the attempt was not undertaken. We did, however, record the way in which pressure curves and noise emissions varied as the engine speed fluctuated between 700 and 1200 rpm, and we used these measurements to eliminate the factor of engine speed from our subsequent recordings.

We limited our frequency analyses to octaves, because we found after some experiments with thirds that the individual frequency bands obtained were too narrow to reflect any influences from the engine.

FREQUENCY ANALYSIS-In a large number of tests in which all sorts of passenger car Diesel engines were examined the frequency spectrum of cold knock was determined. All tests were conducted in the low-resonance chamber, where we first recorded the noise of the cold engine and then the sound of the hot engine, with no cold knock involved. We then com-

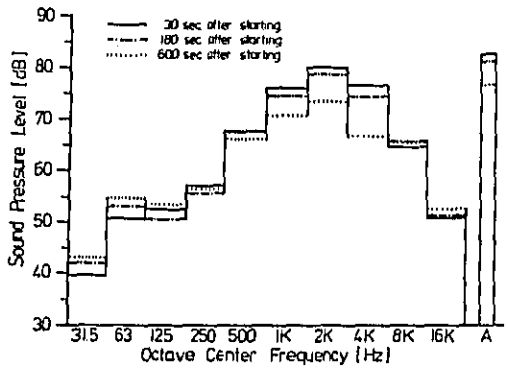

Fig. 3 - Idling sound pressure versus octave for 30 to 600 s after starting (Rabbit Diesel, without EGR)

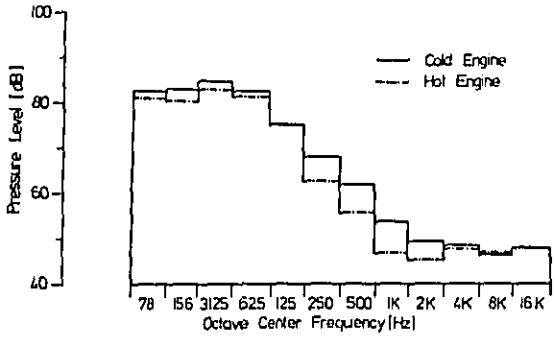

Fig. 4 - Idling indicated pressure versus octave for cold and hot Rabbit Diesel

pared the octave analyses of the two recordings, and we found in all cases that cold knock occurs mainly at 500, 1000, 2000, and 4000 cps. There is no trace of it at 250 and 8000 cps. Whether the main emphasis was on the higher or the lower frequencies depended on the engine type involved.

Without EGR, all sound pressure curves obtained from the Rabbit Diesel engine and weighted in dBA were similar to the one shown in Fig. 3, which shows sound pressure vs. octave center frequencies. The uninterrupted line represents a frequency diagram taken 30 seconds after starting the engine cold at -10 °C, so that cold knock is quite pronounced. The dot-dash line shows the frequencies emitted after 180 seconds, when cold knock is still clearly audible, and the dotted line shows the frequencies after 600 seconds, when cold knock had disappeared completely. The diagrams indicate that in the Rabbit Diesel engine cold knock is limited to 1000, 2000, and 4000 cps.

We also analysed the correlation between the pressure curves recorded together with the noise pressure level measurements and the frequencies emitted. We found that the range of frequencies where the noise emitted varies depending on whether the engine is cold or hot is wider than that found during our noise tests, and that it is shifted slightly towards the lower frequencies. Fig. 4 exemplifies this situation. The fact that lower frequencies are more extensively involved is due to the high injection rate, which makes for a high overall pressure level. This fact must necessarily have its effect on the pressure frequency analysis, especially in the lower frequency range, but it seems as if it is filtered out somehow during the transmission of the noise from the interior of the combustion chamber to the microphone.

HEAT RATE-The pressure curve of the expansion has a peak generated by combustion. The shape of this peak depends on so called 'heat rate'. The actual shape of the heat rate mainly depends on non-design parameters of the engine, such as start of injection, injection quantity, ignition delay, and delivery curve (Fig. 5).

As a rule, the start-of-injection parameter varies with the engine speed, and the injection quantity depends mainly on the torque which is to be generated by the process of combustion, i.e. from the torque demanded by the intentions of the driver, and from the torque required to overcome engine friction. Ignition delay is mainly governed by two parameters, the delay which is due to the kind of fuel used, and the delay which is due to the thermodynamic state of the air and the combustion chamber walls at the beginning of injection.

Lastly, the delivery curve itself depends on the design parameters of pump, piping, and nozzle.

The state in which the walls of the combustion chamber and the air in it are in as injection begins varies with the following factors: The state of the gas before compression, the compression ratio, the time elapsed since the engine was started, and the loads and speeds at which the engine has been running since.

IMPACT ON DIESEL KNOCK-The phenomenon of cold knock is caused mainly by what is represented by the uninterrupted lines in Fig. 5, i.e. delivery curve, ignition delay, injection quantity and start of injection.

Tampering with the injection curve would mean changing the design of both pump and nozzles and, as the pressure involved is fairly high, any design changes in this field are complicated and expensive, so that they are better avoided.

The injection quantity is dependent on the torque requirements, including engine friction. With the engine idling, the injection quantity will fluctuate widely, because a cold engine requires much fuel to run smoothly, whereas a warm engine requires much less. The pressure diagrams in Fig. 1 (a and b) illustrate some of the differences. It is obvious from this figure that cold knock would be much less obtrusive if there were an engine lubricant whose viscosity would be equal to its high-temperature state even when it is cold. To investigate

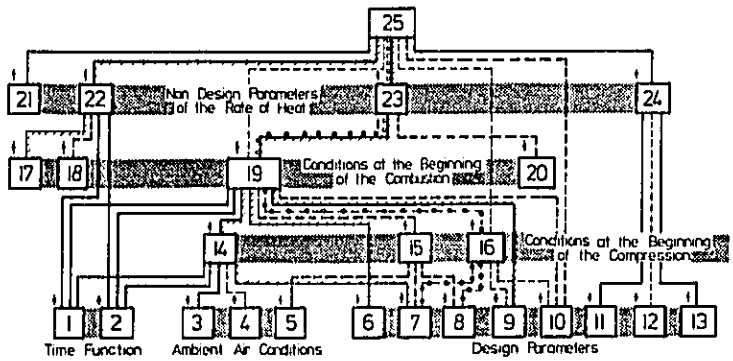

Fig. 5 - Impacts on heat rate at constant speed

this assumption, we ran a test involving two different lubricants with the following viscosity data:

	Standard Summer Oil	Non Standard Oil (Full Synthetic Multigrate)
+20 °C	355 c.St.	125,7 c.St.
-10 °C	5270 c.St.	876 c.St.

With the standard oil, the difference found in the intensity of cold knock with engine and lubricant at +20 °C and after 20 min. of idling was 3 dB, whereas with the non-standard oil with engine and lubricant at -10 °C and after 20 min. of idling it was 0 dB. Most impressing was that with -10 °C and non-standard oil not one octave shows higher sound pressure than with -20 °C and standard oil.

By way of conclusion, one has to state that one of the outstanding factors influencing cold knock is the viscosity of the lubricant, which is why we cross-hatched the lines indicating this in Fig. 5. True, the cold knock of winter oils is already lessened because of its lower viscosity, but it still remains a disturbing factor.

The next parameter to deal with influencing cold knock is the start of injection. To flatten out the pressure gradient it would be possible to delay the start of injection and to compensate for the resultant loss of power by increasing the injection quantity. Although this manoeuver generally produces the desired result it is not recommended because it is accompanied by a noticeable increase in the emission of hydrocarbons, so much so that blue smoke may be noticed leaving the exhaust. To avoid this phenomenon, designers in the past have advanced the start of injection, especially with the engine running cold. They accepted the resultant steep pressure gradient and loud knock as being preferable to the emission of blue smoke. Which means that modifying the start of injection is not a suitable way of combating cold knock.

For the time being, the only remaining suitable factor is ignition delay. Ignition delay may be reduced by selecting appropriate fuels. One of the ways in which this is taken into account is that the gasoline companies change the chemical composition of their Diesel fuels in winter so that it will ignite more easily (cross-hatched lines in Fig. 5). But all this in no way changes the disturbing quality of cold knock.

Other ways of reducing ignition delay are limited to various methods of increasing the temperature of the combustion chamber walls and the air in it before injection begins (also cross-hatched lines). Increasing the temperature is generally accomplished by installing lubricant, coolant or intake air heating or preheating equipment, and by increasing the compression ratio.

The influence of the compression ratio should be presented by a sample test. We used two compression ratios, 19.6 and 23.1. The engine was started at the same temperature in both cases, and with $\varepsilon = 23.1$ we found the cold knock intensity to be lower by 2 dBA.

So it is possible to reduce cold knock slightly by increasing the compression ratio, although this is not a solution to be recommended without reservation: Generally speaking, Diesel engine compression ratios are far and away beyond the ratio of optimum efficiency, which would be around $\varepsilon = 16$. So to improve the efficiency of Diesel engines their compression ratios should be lowered, if anything. But this is impossible because engines must be capable of starting at low temperatures. Therefore, increasing the compression ratio is not a good way of combating cold knock.

Consequently, we are thrown back on the

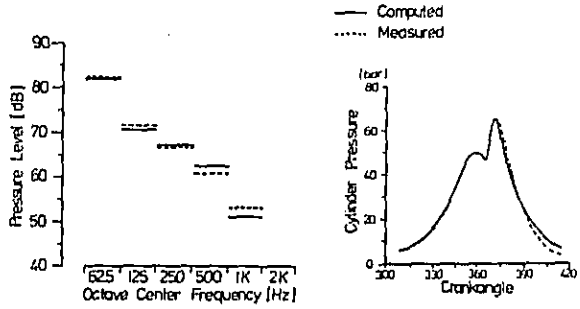

Fig. 6 - Computed simulation of measured pressure trace and its frequency analysis

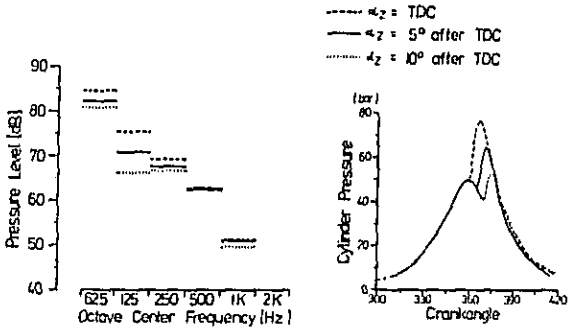

Fig. 8 - Computed variation of start of combustion

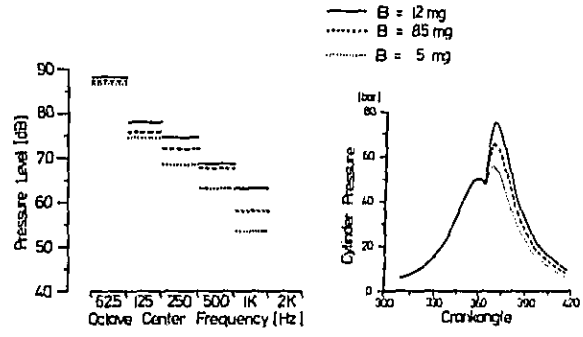

Fig. 7 - Computed variation of injection quantity

remaining ways of increasing temperature. The first one which comes to mind is to increase the quantity of exhaust gas present during the combustion process.

THE INFLUENCE OF THERMODYNAMIC CONDITIONS ON DIESEL KNOCK-Before considering the influence of the exhaust gas it seems proper to study the extent to which thermodynamic conditions for combustion process influence cold knock, with the heat rate assumed constant. This assumption cannot be realised experimentally because the thermodynamic conditions influence the heat rate in the real engine. Therefore we chose computations.

To begin with, we simulated on the computer a pressure cycle derived from a measured indicator diagram (Fig. 6). The test in question had been run on the engine at a compression ratio of 23.1, without EGR, at idle, at an engine speed of 950 rpm, and at a starting temperature of +20 °C. The heat rate established in this simulation was taken over unchanged in all our following studies, i.e. the quantity of heat induced per degree of crank angle either remained unaltered, or else was reduced or increased in proportion to any change in the total quantity of fuel injected. Our study concerned itself with the following parameters: Injection quantity, start of combustion, compression ratio, and intake air temperature.

All pressure curves were subject to a harmonic analysis. From that octave centre frequencies were computed. Fig. 6 shows a comparison between the octave analysis derived from both, the measured and the computed pressure curves. In the lower frequencies, the two analyses agree quite well, which is due to the fact that the computed pressure curve was modified until computed and measured curves were in a good agreement. In the higher frequencies it was only to be expected that some bias would occur. At all frequencies above 1000 cps errors were found, which were unavoidable because the scan frequency was 1 per degree of crank angle. However, Fig. 4 shows that an analysis of the 250, 500, and 1000 cps octaves will suffice to assess Diesel knock in the pressure curve.

In the following versions of our computation we only changed one condition at a time and studied the effect on the frequency analysis of the pressure cycle.

Variations of the Injection Quantity-As was mentioned before, there is more friction in cold engines, which is why more indicated power is required, which in Diesel engines means an increased injection quantity. And increasing the injection quantity has a considerable influence on the noise level. Fig. 7 shows the results computed for fuel quantities of 5, 8.5, and 12 mg per power stroke. The result: The injection quantity has a powerful influence on cold knock. The lower frequencies are affected by the pressure increase caused by more fuel being injected, and the higher frequencies reflect the steeper gradient of the pressure curve.

Variations of the Start of Combustion-The start of combustion varies with the injection point and the ignition delay, the latter being generally sub-divided into two components,

a) a physical component reflecting the properties of fuel treatment and evaporation, and
b) a chemical component reflecting the preliminary reactions in the course of which unstable intermediary products are formed.

At low engine speeds, physical properties predominate, the physical ignition delay generally being inversely proportional to the final

compression pressure and the final compression temperature.

The result of this computation is presented in Fig. 8: If combustion begins at TDC, it will produce high pressures, but hardly steeper pressure gradients, a conclusion which can be drawn from the fact that there are hardly any differences in the noise levels measured at higher frequencies.

If actual hardware is tested, the results may deviate from this computation in two points:

1 - Early ignition is accompanied by high temperatures and high pressures, which may result in the heat rate being changed so that heat transformation is speeded up. This, of course, would mean steeper pressure gradients and, therefore, more cold knock.
2 - Late combustion may be due to much ignition delay. If so, a relatively large quantity of fuel would reach the combustion chamber before the onset of combustion, and if ignited would burn very quickly, having previously undergone several physical and chemical reactions. This again would result in steep pressure gradients and loud knocking.

Variations of the Compression Ratio-The compression ratio exerts considerable influence on the pressure and temperature of the charge at the end of the compression stroke. If the valves are opened before or closed after the two dead centers, part of the charge will be lost. Further losses are incurred because of the gaps in the piston rings. All these losses have their influence on final compression pressure and final compression temperature.

Thus, for instance, it was found that in an idling Diesel engine which was started at a temperature of + 20 °C so much of the charge will be lost that with a volumetric compression ratio of 23,1 the actual compression ratio will be no more than about 18. And at lower temperatures the discrepancy may be expected to be even greater.

Fig. 9 shows the outcome of our computer analysis of actual compression ratios of 18, 20.5, and 23. We can see that less compression leads to lower noise levels in the frequency ranges which are of interest. This, of course, does not agree with the experience and with our measurements, because the fact that ignitablity is affected by low compression ratios was not taken into account, the heat rate and the ignition delay being kept constant during this investigation. Yet our results are plausible, because they demonstrate the effect which lowering the compression could have: Pressure gradients could be much gentler if ignition were not so dependent on a high compression ratio.

Variations of the Intake Air Temperature-The results of this computation are presented in Fig. 10. When looking at this graph we must keep in mind that injection point and heat rate have not been modified, so that the ignition delay could not be influenced by any change in the intake air temperature.

Consequently, varying the intake air temperature between +20 °C and +180 °C does not

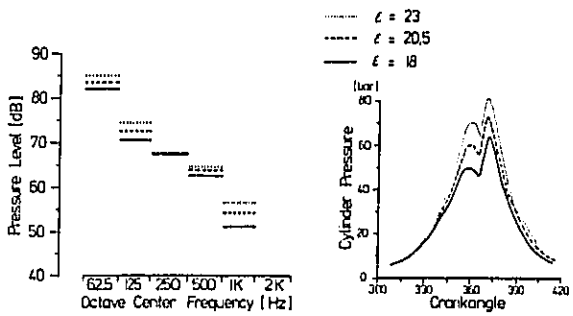

Fig. 9 - Computed variation of compression ratio

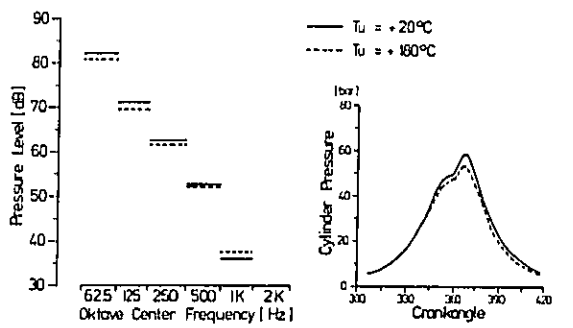

Fig. 10 - Computed variation of intake air temperature

affect the steepness of the pressure gradients at all if the influence which temperature exerts on ignition delay is blotted out. It seems unreasonable to expect any other result, because if the heat rate remains unchanged, a mere increase in temperature will hardly affect the pressure curve.

INCREASE IN THE AMOUNT OF RESIDUAL GAS-Another practicable way of attaining higher temperatures at ignition point is under discussion, that of increasing the amount of exhaust gas remaining in the combustion chamber for the following combustion cycle. This step should not raise any problems, especially at engine speeds close to idle, for because of the high air/fuel ratio the exhaust gas contains a high percentage of oxygen. By being present in the combustion chamber during one or more combustion cycles it has reached a fairly high temperature, and if it were possible to feed it into the combustion process without too much loss of heat through contact with cold walls it should go towards reducing the ignition delay and, consequently, cold knock.

The best way to achieve this end seems to be to change valve timing so that the quantity of remaining gas is increased. This might be accompanied by the installation of some sort of control organ, a throttle plate, for instan-

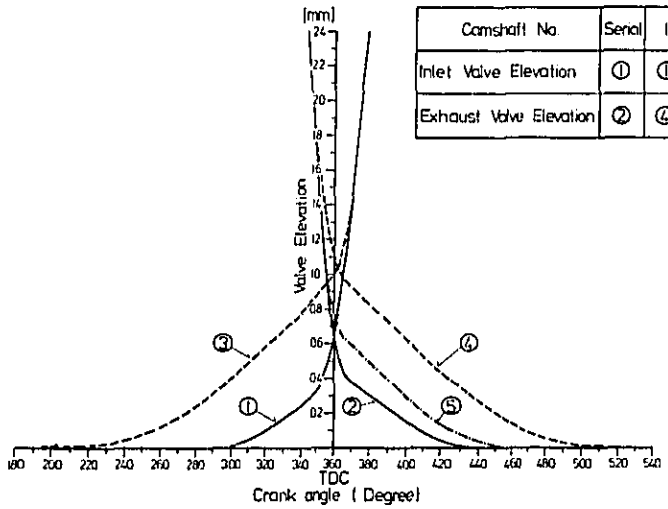

Camshaft No.	Serial	1	2	3	4
Inlet Valve Elevation	①	①	③	③	①
Exhaust Valve Elevation	②	④	②	④	⑤

Fig. 11 - Camshaft variations

Camshaft No.	Serial	1	2	3	4
Residual Gas in Cylinder 1500 rpm	5.1%	10.2%	11.8%	18.2%	64%
Volumetric Efficiency at Full Load 4500 rpm	100%	96.2%	95.8%	91.5%	99.0%

Fig. 12 - Computed results of camshaft variations

ce, in the inlet or outlet system. Installing a throttle plate alone might even be sufficient to increase the quantity of residual gas and to lower the intensity of knock, because if there is a throttle in the intake system some exhaust gas will flood into the intake system during the valve overlap period, and this gas would be the first to enter the combustion chamber during the subsequent induction stroke. Installing a throttle in the outlet system, on the other hand, would first of all have the same effect as an inlet throttle, and it would increase the density of the gas residue remaining at the end of the exhaust stroke. And if the camshaft geometry were to be changed into the bargain, this effect would surely be enhanced even more.

We tested all these assumptions. First of all, we established the extent to which cold knock may be reduced by intake and outlet throttles alone. If the throttles were adjusted so as to bring the engine close to stalling at low temperatures of -10 °C (high emission of black smoke), cold knock the 1000, 2000 and 4000 cps range was reduced by about 1.5 dBA by inlet as well as by outlet throttles. Once the engine temperature at idle had stabilized the throttles became ineffective as regards reduction of noise.

We then computed whether or not manipulating the valve overlap, i.e. changing the downward gradient of the outlet cam and the upward gradient of the inlet cam, would be suitable for increasing the quantity of residual gas without reducing the peak horsepower of the Diesel engine by more than 2 %. We investigated all the variations shown in Fig. 11, and we found that version # 4 was the only one where the air delivery rate deterioration remained below 1 % (Fig. 12), so that the loss of peak horsepower was less than 1.5 % approx. With a camshaft geometry like this, the proportion of residual gas increases by about 25 % in the lower rpm range, and if this effect were enhanced by throttles it should be possible to double it.

Our tests showed, however, that with a camshaft geometry of this kind the loss of peak horsepower was more extensive than our computations had indicated, it being 4 instead of 2 % and increasing as the engine speed fell (Fig.12 +13). Without throttles, cold knock was not influenced at all, and with them it was muted by about 4 dBA if the engine was throttled down close to stalling (considerable increase in the emission of black smoke). This was an important result (lines indicating this on Fig. 5 are identified by circlets), but we thought that the loss of torque was to excessive and abandoned the attempt.

EXHAUST GAS RECIRCULATION-Once we had chosen suitable diameters for the pipes conducting the EGR, it quickly brought excellent results. We were able to reduce cold knock 10 seconds after starting by up to 5 dBA.

These were startling results, especially so because the first EGR system featured relatively long pipes, so that much heat was lost in warming them before the gas fed into the cylinders became noticeably hotter. To investi-

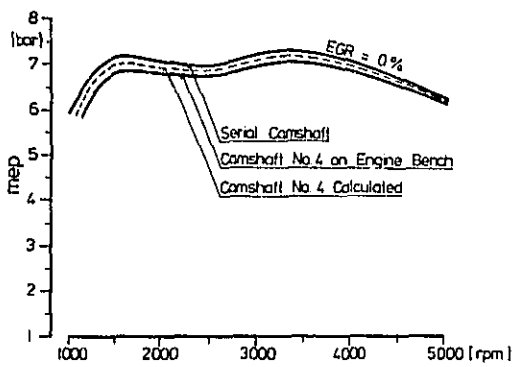

Fig. 13 - Full load versus speed for camshaft No. 4

gate this, we ran temperature tests which indicated that if the engine was started at -10 °C the temperature at the intake port was around 0 °C as late as 60 seconds afterwards, in spite of 40 % of the exhaust gas being recirculated. Still there was a massive effect on cold knock, because the noise emitted by the engine was muted by 4 dBA. It seemed logical to conclude that the effect of EGR extended to fields other than temperature.

In our attempts to explain this phenomenon we fell back on the experiences gathered when trying to combat the nitrogen oxide emissions of spark ignition engines by means of EGR. Then, we had found that a high concentration of inert gas in the combustion chamber would reduce the speed of combustion with flatter pressure gradients, lower peak temperatures, and earlier freezing of the NOx-formation rate. What is decisive of all these factors is the flattening of the pressure gradient. If this effect is the same in Diesel engines it might explain the extent to which EGR influences cold knock.

EGR Quantities in Diesel Applications- The first question raised here concerns with relative quantities. Why is it that 20 % EGR is ineffective, while 40 % may already serve to reduce noise by as much as 4 dBA? Therefore we considered the quantitative aspects starting from the following assumptions:

1 - Air consists of nitrogen and oxygen, the ratio generally being 79/21.
2 - If the air/fuel ratio is higher than 1, combustion in Diesel engines is complete as a rule, so that the exhaust gas will contain nothing but N_2, O_2, CO_2, and H_2O.
3 - N_2, CO_2, and H_2O are inert gases.
4 - The formation of black smoke begins as soon as the percentage of oxygen E in point (2) of Fig. 14 is equal to A, i.e. to the percentage of the air which is consumed by the combustion process.

Sometimes, a deviant assumption is made, namely that black smoke begins at an equivalence air/fuel ratio of 1.15, as in the Diesel Rabbit. The black-smoke limit, in this case, is of course E = 1.15 x A.

If we take the nominations of Fig. 14 to these assumptions into consideration we have

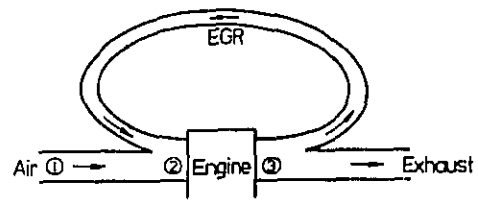

S = Oxygen Percentage at ① (normally 21%)

E = Oxygen Percentage at ②

EGR = EGR Percentage at ② and ③

X = Oxygen Percentage at ③

A = E - X = Air Percentage in Engine Consumed for Combustion

Fig. 14 - Nominations for EGR quantity consideration

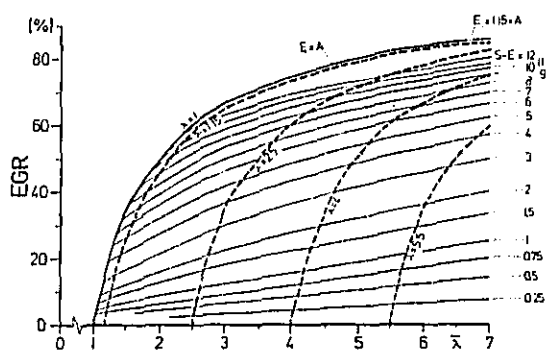

Fig. 15 - Oxygen dilution by Diesel-EGR

$$E = EGR \times \frac{X}{100} + (100 - EGR) \times \frac{S}{100} \qquad (1)$$

and

$$X = E - A. \qquad (2)$$

In a different notation, This reads

$$E = S - \frac{A \times EGR}{100-EGR} \qquad (3)$$

Now if we remember that the seeming equivalence air/fuel ratio, i.e. the one which stems from the assumption that the quantity of fuel injected is burned in pure air, can be expressed as

$$\bar{\lambda} = \frac{S}{A} \qquad (4)$$

or

$$A = \frac{S}{\bar{\lambda}} \qquad (5)$$

we have

$$\bar{\lambda} = \frac{S \times EGR}{(S-E)(100-EGR)} \qquad (6)$$

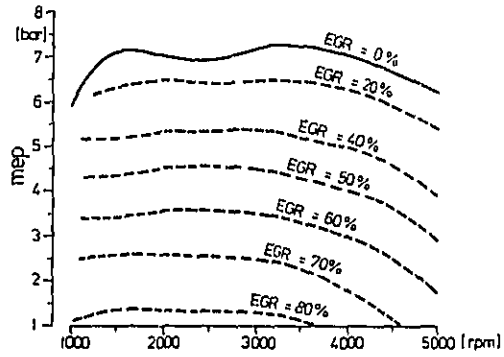

Fig. 16 - Permissible EGR-rates in Diesel application

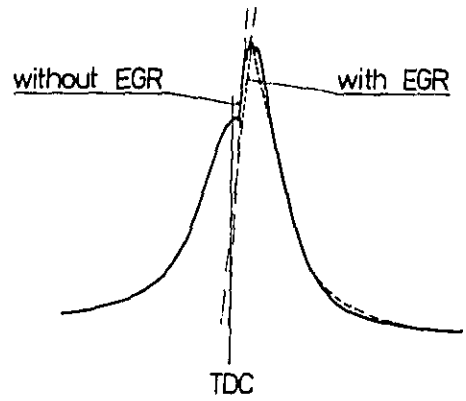

Fig. 17 - Diesel pressure traces with and without EGR at idle

Using an S value of 21 % it is easy to draw up Fig. 15. The parameter expressing the difference between the uninterrupted lines below the smoke limit is S - E, the amount by which the oxygen content of the intake air is diminished through EGR. The uninterrupted smoke limit is derived from the expression E = A. This applies under conditions of stoichiometric combustion, with a real equivalence air/fuel ratio of 1. The outward interrupted line approximately indicates the smoke limit of a Diesel Rabbit at a real equivalence ratio of 1.15.

We ran a test on a Diesel Rabbit not fitted with EGR, the lubricant being SAE 10 W. We started the engine cooled down on -10 °C but with an ambient air temperature of +20 °C and let it come up to constant temperature at idle. Immediately after starting, the engine consumed 5.75 % oxygen, and 2.9 % after temperature had stabilised. The corresponding air/fuel ratios range from 3.7 to 7.2, with EGR = 0. This explains why we did not extend Fig. 15 to include any higher air/fuel ratios.

We see that at λ = 6, which is a not unrealistic figure in the idle range, the oxygen content of the intake gas will be reduced by an amount equal to S - E = 1 % only if the EGR rate is stepped up to 22 %. Spark ignition engines, which are generally operated at an equivalence air/fuel ratio of approximately 1.0 will show the same effect at an EGR rate of about 4.5 % (marked by the intersection point of the S - E = 1 % and the λ = 1 line). A 15 % EGR rate in a spark ignition engine therefore will produce the same oxygen dilution effect as a 48 % rate in a Diesel engine at idle. As the EGR rates commonly used to reduce the NOx emissions of spark ignition engines vary between 5 and 15 % we have an explanation why Diesel knock at idle will only be influenced noticeably by EGR rates in excess of 25 %. In addition to this, we now have corroboration for our assumption that the effect which EGR has on cold knock is due to the immission of inert gases, just like its effect on the formation of NOx.

In Fig. 16, which is an engine map of the Rabbit Diesel, we show the way in which the smoke limit is displaced as the EGR rate increases. If there is no EGR, the full-load curve is also the smoke limit, the air excess in this case being about 15 %. We now assumed that these 15 % are our minimum requirement, and we consulted Fig. 15 to see what seeming air/fuel ratios (λ) would be associated along the smoke limit with what EGR rates. These seeming air/fuel ratios are the same as the real ratios obtained from engines without EGR. Our investigations showed that even with EGR rates of up to 60 % the engine may be run up to the middle load range without producing any exhaust gas opacity more intensive than that under full load.

The same considerations can be applied, of course, to the problem of using EGR to reduce NOx emissions. It may even especially interesting to do so, because it is hardly likely that EGR will ever be used to combat cold knock in the middle load range, and if this is done at all, it will apply only to a very brief time after starting.

Even admitting that high EGR rates are possible in Diesel engines we must not forget that exhaust gas recirculation leads to increased particulate emission. If its application is limited to idle speeds only its influence on particulate emission will surely be restricted, but even so, if Fig. 16 were to reflect the changes in the emission of particulates we may safely assume that the permissible EGR limit would drop considerably.

Analysis of Pressure Diagrams-Our assumption that the immission of inert gases is the most decisive effect which EGR has on Diesel knock is confirmed by a look at the pressure curves. Fig. 17 shows a typical sample selected from a large number of records. The uninterrupted line above represents the pressure curve in a Rabbit Diesel cylinder (compression ratio 23.1) a few seconds after starting the engine at a temperature of +20 °C. The interrupted line is a pressure curve measured in the same cylinder and under the same conditions,

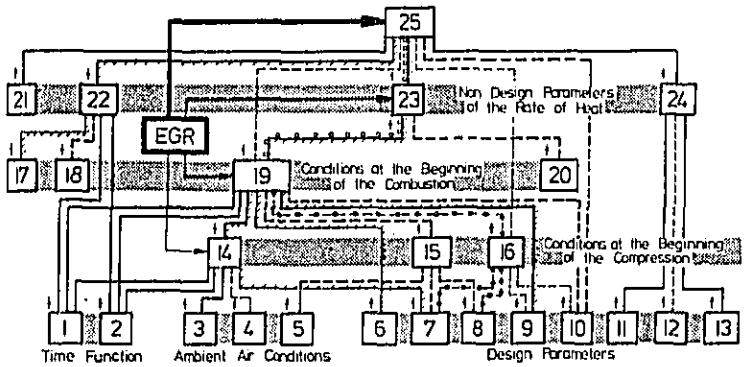

Fig. 18 - Impacts on heat rate at constant speed EGR including

the only difference being a 60 % EGR rate. At this rate, oxygen is diluted by no less than 25 % approx.

The two pressure curves show that there are extensive differences of ignition delay and combustion pressure gradient.

If we define delay as the amount of time which elapses between the start of injection and the onset of the steep pressure gradient, then this time corresponds to a crank angle of approximately 10.5° in the EGR engine, whereas it is down to about 8° in the engine without EGR. Now the first conclusion to be drawn from this is that EGR has failed to meet expectations being that oxygen heated up by previous combustion processes would reduce ignition delay. The true effect went in the opposite direction: Ignition delay tends to be prolonged by the inert gas effect.

Another argument in support of the inert gas assumption is furnished by a comparison of the speeds of pressure increase over that section of the curve where the increase in pressure is due to combustion. Without EGR, pressure increases at a speed of approximately 15 bar per degree of crank angle, whereas with EGR it is down to 5 bar. The conclusion is that pressure with 60 % EGR can increase a third as steeply as without.

It would be natural to assume that such a flattened pressure gradient would be accompanied by very decreased cold knock; but this was not the case here. Noise emission in the specific cold knock frequencies (1000, 2000, and 4000 cps) dropped by a mere 4 dBA. This is due to the fact that cold knock was not very intensive even without EGR, because the starting temperature of the engine was +20 °C, and its compression ratio was 23.1.

By way of summing up, we should turn back to Fig. 5 and widen its scope to include the influence of EGR (Fig. 16). We can state categorically that there is no doubt that EGR does influence the temperature of the intake air before compression, the state of the air and the combustion chamber walls at the start of injection, and the ignition delay. But everything we know now seems to indicate that all these influences are irrelevant as far as Diesel knock is concerned. The only important factor influencing this phenomenon being that the introduction of exhaust gas will delay the process of combustion.

CONCLUSION-By experiment as well as by computer analysis, we evaluated a number of ways of reducing cold knock in Diesel engines. EGR seems to be a comparatively cheap way of attaining this goal, especially considering that its installation may be required anyhow to meet emission standards. The effect which EGR has on Diesel knock is not due to a reduction of the ignition delay, which would be a temperature phenomenon, but to a flatter combustion pressure gradient. The EGR rates required to produce this effect are high; they vary between 25 and 60 % of the intake gas quantity. This is only feasible because Diesel engines run at very high equivalence air/fuel ratios when idling.

ACKNOWLEDGEMENTS-The method of measuring Diesel knock is developed by the VW Measuring Department together with the VW Engine Testing Department. Main part of the measuring work was done in the free field sound chamber of the VW Measuring Department. The measuring group has carried out the sound and the pressure analyses.

The computer work has been done by the engine calculation group on VW's CDC 173 Cyber.

REFERENCES

1. Dr. Gerhard Thien, "Beurteilung der geräuscherregenden Eigenschaften der Verbrennung an Diesel- und Ottomotoren mittels Frequenzanalyse des Brennraumdruckes", MTZ 25 (1964) 7, S. 289
2. Dr. E. Mühlberg, "Abgasrückführung bei Verbrennungskraftmaschinen, insbesondere bei Dieselmotoren", MTZ 32 (1971) 5, S. 166
3. Charron Francis, "Verfahren zur Erhitzung der Ansaugluft eines aufgeladenen Dieselmotores", German Patent 24 38 118, Assigned to: Societe d'Etudes de Machines Thermiques S.E.M.T., Saint Denis (France), 1974
4. FVV-Literaturrecherche Verbrennungskraftmaschinen: "Kaltstart- und Warmluftverhalten von Dieselmotoren", Heft 175, 1975
5. Dr. H. Seifert, EDV-Programmsystem, FISITA-Kongress, Tokio 1976
6. H. Groß, "Einfluß der Verbrennung auf das Geräusch", ATZ 79 (1977) 4, S. 133
7. B. Wiedemann, R. Schmidt et.al., "Data Base for Light-Weight Automotive Diesel Plants", Final Report, Volume I: Executive Summary, DOT-TSC-NHTSA-77-3,1 , 1977
8. Dr. H.P. Lenz u. G. Akiskalos "Der Einfluß der Abgasrückführung auf die Abgasemissionen und das Klopfgeräusch an einem PKW-Golf-Diesel", Report No 30615, Institut für Verbrennungskraftmaschinen und Kraftfahrwesen der Technischen Hochschule Wien, 1977
9. Dr. H.P. Lenz u. G. Akiskalos, "Verfahren zum Vermindern des Verbrennungsgeräusches von Dieselmotoren im Leerlauf", German Patent P 27 50 537.9-13 (Application pending), Assigned to Audi NSU Auto Union AG, 1977
10. Dr. R. Beckmann, Dr. H. Oetting, "Verfahren zur Vermeidung des Nagelns von Dieselbrennkraftmaschinen", German Patent (Application pending), Assigned to VW AG, 1978

790269

DI DIESEL ENGINE BECOMES NOISIER AT ACCELERATION

- THE TRANSIENT NOISE CHARACTERISTIC OF DIESEL ENGINE -

Yoshito Watanabe
Hideaki Fujisaki
Toyohiro Tsuda

Nissan Diesel Motor Co., Ltd.
Ageo, Saitama, Japan

ABSTRACT

An acceleration mode in measuring vehicle pass-by noise was simulated on an engine test bed in an anechoic room. The accelerated running noise of various types of diesel engines was measured and compared with the steady running noise. The measurement results show that naturally aspirated DI engines become noisier at acceleration, while IDI engines change only slightly. In turbocharged DI engines, the response lag of the turbocharger causes an especially big noise level difference immediately after acceleration start. This paper deals also with the mechanisms of higher level of accelerated running noise in DI engines.

MOTOR VEHICLES HAVE A CLOSE RELATION with the daily lives of people nowadays. However, the fact that those convenient vehicles emit noise which is seriously affecting our living environment has been a common problem in the world. Meanwhile, the oil crisis in 1973 made the public turn their attention to diesel engines as a means of economizing on fuel. Since then, dieselization has been a steady trend not only in heavy duty trucks but also in medium and light duty trucks and in some passenger cars (1)*. In general however, diesel engines emit louder noise than gasoline engines due to their characteristic combustion mechanisms. In light of the fact that the engine is a major noise source in vehicles, reduction of the engine noise has been a vital problem for diesel development engineers.

Measurements of engine noise levels are essential for studying noise reduction, and in the past we measured noise levels on engines operated in a steady condition, i.e. keeping load and engine speed constant. On the other hand, vehicular noise regulations in Japan are prescribed in terms of noise levels measured during accelerated running as in ISO R362 and SAE J366b. This paper deals with the effects of these different operating conditions on engine noise measured with several engines in our anechoic chamber.

ACCELERATION TEST METHOD

ACCELERATION MODE - This acceleration mode simulates on the engine test bed the engine load and speed progress during acceleration in a vehicle pass-by noise test. The Japanese test procedure for the road vehicle noise is prescribed in JIS D1024. As far as "the measurement with vehicle in acceleration" is concerned, the method in JIS D1024 is practically identical with that of ISO R362. According to the test procedure, before the start of acceleration, the engine is driven at 75 % of its rated speed and road load condition, then the fuel control rack is pulled rapidly to the full position to accelerate the engine. In the case of a bare engine noise test, acceleration starts from a little lower engine speed taking into account the overshoot of the acceleration device.

EXAMINATION OF ACCELERATION METHOD - The use of inertia disks which correspond to the inertia mass of a vehicle has been widely adopted so far as a measure to exactly reproduce an accelerated running of a vehicle in engine operation on a test bed. However, as there are a variety of engines with different outputs, and various combinations of gear ratio and vehicle weight are assumed for each of the engines, inertia disks of all sizes would have to be prepared. Not to speak of flexibility in their choice, the space for their storage, and handling and safety measures would require careful consideration. In anticipation of these problems, we gave up the adoption of inertia disks and searched for another method. We found with the engineers of a manufacturer of dynamometers that the regulating unit of the existing eddy-current type dynamometer could be modified to allow an acceleration mode running in which acceleration time could be changed freely by a purely electrical and electronic means.

ACCELERATION EQUIPMENT - The mechanisms of the eddy-current dynamometer are such that when direct current is flowed as an exciting current, starting power is generated and produces an eddy current in an eddy ring, and thereby electric power is consumed. This dynamometer can be controlled in two ways, by automatic speed regulation and automatic current regulation. In the former method, the speed of a test engine is controlled to keep it equivalent to the setting dial speed. Namely, if the engine speed is lower than the set speed, brake horsepower of the dynamometer is reduced by decreasing the exciting current flowed

*Numbers in parentheses designate References at end of paper.

SAE/P-79/80/$02.50
Copyright © 1979 Society of Automotive Engineers, Inc.

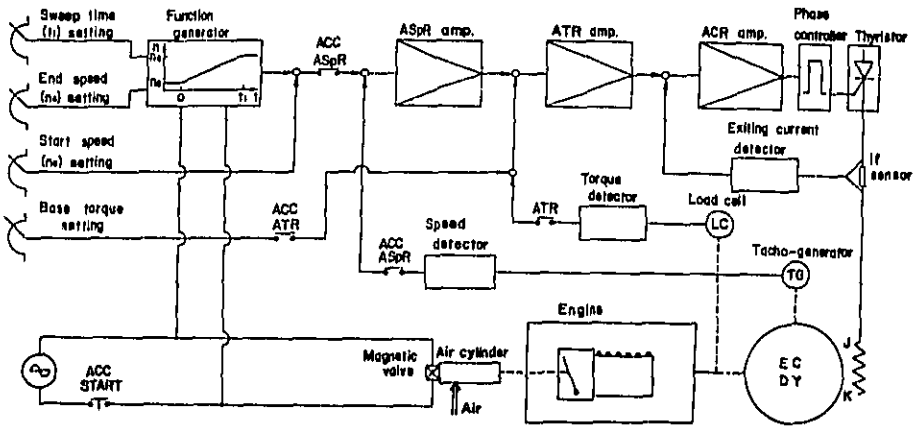

Fig. 1 – Schematic diagram of the acceleration simulating system

in it so that the engine speed will increase. On the other hand, when the engine speed is higher than the set speed, the exciting current is increased, thereby increasing brake horsepower of the dynamometer to decelerate the engine. In the automatic current regulation method, the exciting current is kept constant to match the setting dial scale. Nearly steady torque characteristics can be achieved with this method.

The acceleration regulating unit we employ performs both of these regulating functions at the same time, and its block diagram is shown in Fig. 1. An acceleration starting button actuates the air cylinder, which then momentarily brings the fuel control rack of injection pump up to the full quantity position. Following this the engine generates full torque, all of which, unless absorbed, would be used to accelerate the engine at an angular acceleration speed determined by inertia mass of the engine and dynamometer. The acceleration thus determined, however, would be too fast for ordinary cases. So the automatic speed regulation should be applied here to check the increase of engine speed, but its response is not quick enough to meet this purpose. Then, in order to generate brake torque corresponding to 60 to 80 % of the full torque (we call this base torque), the necessary quantity of exciting current is flowed into the system without feedback. In this condition, the automatic speed regulation can work effectively to keep the engine rotating at the set speed. This is swept by the function generator from the beginning to the end of acceleration.

Fig. 2 shows reproduced engine speed and measured brake torque of the dynamometer in this system. Though a slight overshoot is observed immediately after acceleration begins, the subsequent nearly straight line indicates that a constant acceleration is realized.

This system can provide an acceleration time of 1.5 to 18 sec. per unit engine speed rise of 1000 rpm and a base torque of up to 150 kg-m.

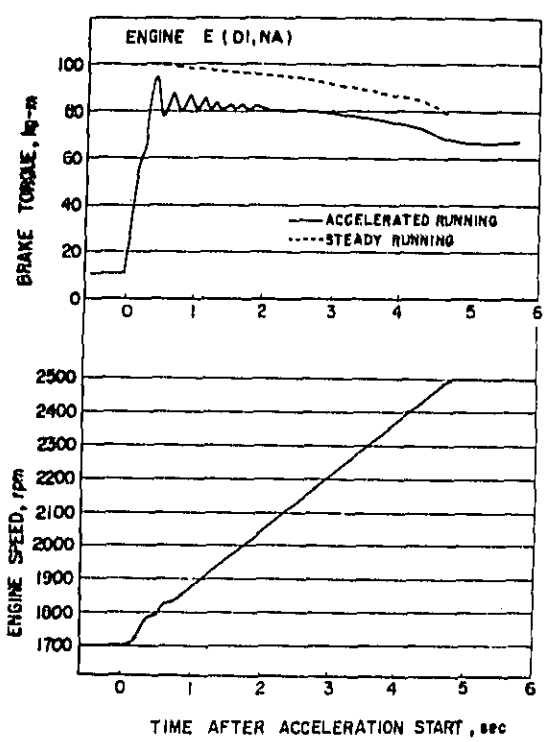

Fig. 2 – Regulation performance of the acceleration simulating system

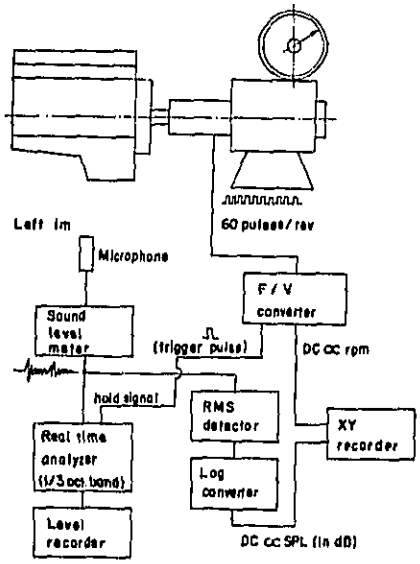

Fig. 3 - Block diagram of noise measurement equipments

Table 1 - Test Engines

Engine	Cyl. Configuration	Combustion Type	Swept Volume (l)	Max. HP at Rated Speed (HP/rpm)
A	Inline - 4	IDI (SC)	2.16	65/4000
B	Inline - 4	IDI (PC)	2.40	65/4200
C	Inline - 4	IDI (SC)	2.96	85/3600
D	Inline - 6	DI - NA	11.67	220/2300
E	Vee - 6	DI - NA	14.31	300/2500
F	Vee - 8	DI - TC	14.31	330/2500

RECORDING IN NOISE MEASUREMENTS - The block diagram of noise measurement equipments is shown in Fig. 3. By a magnetic pick-up and a sixty-tooth gear incorporated into the dynamometer, sixty pulses are obtained per engine revolution. F/V (Frequency/Voltage) converter generates DC signals proportional to the pulse frequency. The DC signals are then input as X-axis signals of an X-Y recorder. On the other hand, noise level is measured by microphone 1 m away from the engine surface, and the outputs of sound level meter (AC signals) are converted to DC signals through an AC-DC converter, and via a log converter are recorded on the Y-axis. Thus sound pressure level of noise affected by change in engine rotating speed is expressed on the X-Y recorder.

If frequency analysis of a given rotating speed is required, the measurement is done as follows : First, the dial of F/V converter is set for a certain engine speed. When the engine speed which is increasing by acceleration reaches the set point, the equipment generates a pulse, which then works as a trigger signal to hold the output of the frequency analyzer.

QUASI-STEADY NOISE TEST - For the purpose of comparing noise levels of an acceleration condition and a steady condition, a noise level was measured on an engine which was running with full load under automatic speed regulation, and gradually accelerated by manual operation of the setting dial. Since this condition can be regarded as almost identical with the steady condition, we call the noise measured in it a quasi-steady noise.

ACCELERATED RUNNING NOISE OF VARIOUS ENGINES

THE INFLUENCE OF COMBUSTION MODE - The acceleration noise, together with the quasi-steady noise for comparison purposes, was measured in an anechoic chamber on various engines with different combustion modes and sizes. The engine specifications and test conditions are shown in tables 1 and 2, respectively. The measurements were made without fan, excluding the effect of intake and exhaust noise, and keeping the oil, water and exhaust temperature just before acceleration nearly constant. Though the measurements were carried out on four (right, left, front and upper) sides of the engine, as the tendency being the same, the left side noise will be discussed as a representative in this paper.

Table 2 - Measuring Conditions

	Accelerated				Quasi-steady		
	Engine Speed (rpm)		Rate of Rising Engine Speed (rpm/sec)	Load before Acceleration Start (% of full load)	Engine Speed (rpm)		Time (min)
	Start	End			Start	End	
Engine A	2800	4000	469	34	1000	4000	20
Engine B	2800	4000	125	34	1000	4000	20
Engine C	2500	3600	150	17	1000	3600	16
Engine D	1500	2300	105	10	1000	2300	8
Engine E	1700	2500	170	11	1000	2500	10
Engine F	1700	2500	170	11	1000	2500	10

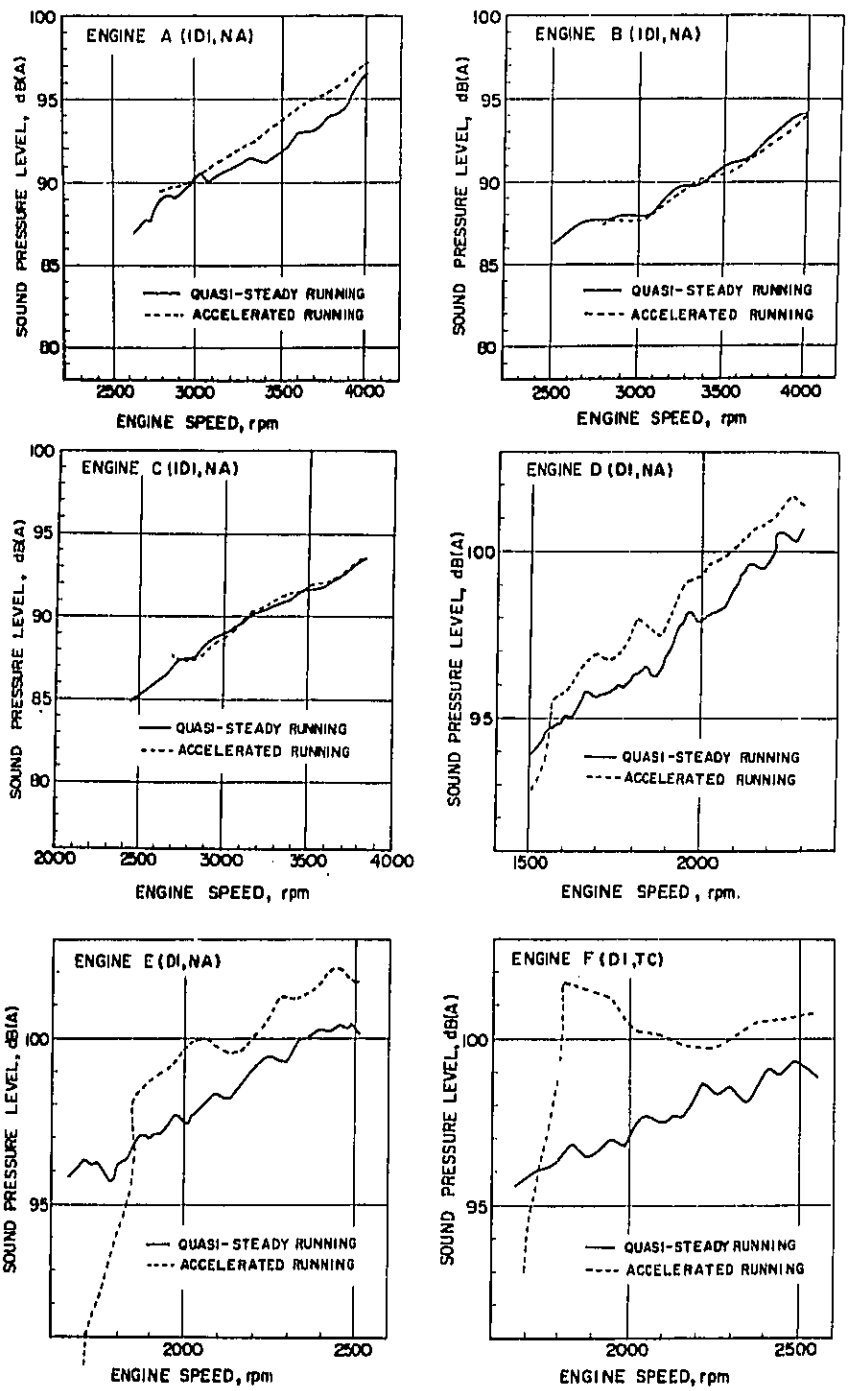

Fig. 4 - Comparison of the noise level between accelerated and quasi-steady running

The test results are shown in Fig. 4. As seen here, in indirect injection engines (Engine A, B and C), no significant increase of noise level was observed immediately after acceleration and the accelerated running noise scarcely differs from the quasi-steady running noise through all the engine speed. On the other hand, in naturally aspirated direct injection engines (Engine D and E), a significant increase of noise level of a few dB(A) was observed immediately after acceleration and the accelerated running noise is about 2 dB(A) higher than the quasi-steady running noise. As for turbocharged direct injection engine (Engine F), such an increase of noise level is very big. The acceleration noise is loudest immediately after acceleration due to response lag (2) of the turbocharger and differs as much as 5 dB(A) from the quasi-steady noise. The difference gets smaller around the rated speed, where the turbocharger begins to work fully.

Fig. 5 shows frequency analyses at 2000 rpm during acceleration on E (DI, NA) and F (DI, TC) engines. In naturally aspirated engine E (DI, NA), the accelerated running produces 2 to 3 dB(A) higher sound pressure level than the quasi-steady running in the almost whole frequency range. In turbocharged engine F (DI, TC), the tendency is almost the same, but an especially big difference of 4 dB(A) is observed in the frequency range of 500 Hz to 2 kHz, where the sound pressure level virtually contributes to noise.

THE INFLUENCE OF ACCELERATION STARTING SPEED - The acceleration starting speed was varied on E (DI, NA) and F (DI, TC) engines to see how it affects the noise level. The results are shown in Fig. 6, where the acceleration time per unit increase of engine speed is constant. It can be seen from this figure that in naturally aspirated engines, noise levels follow the same curves even if acceleration starts from different engine speeds, but in turbocharged engines, noise level curves show a slight change up to a certain point according to the difference of starting speed, which

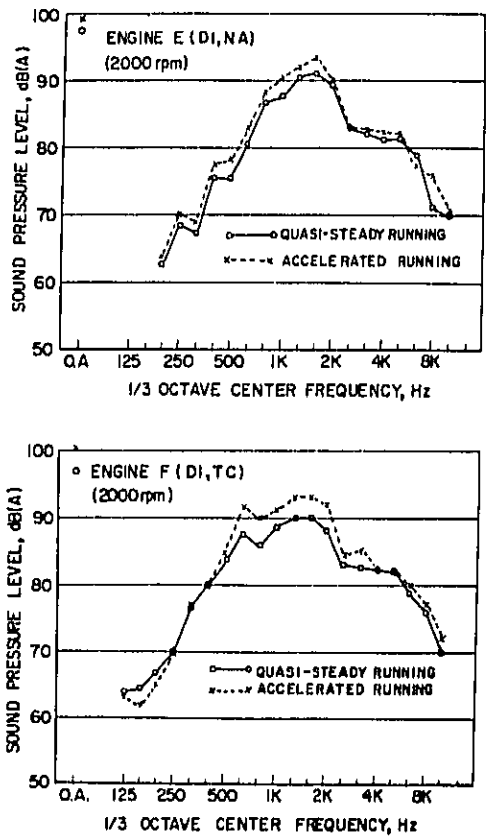

Fig. 5 – Comparison of the noise spectra between accelerated and quasi-steady running

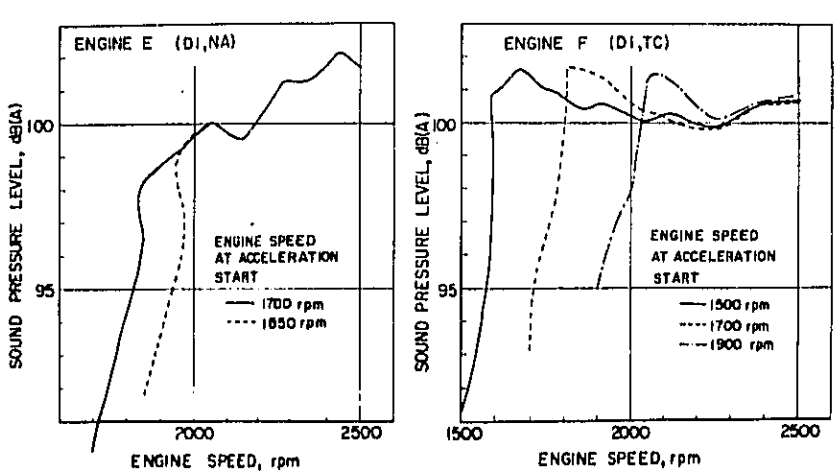

Fig. 6 – Influence of acceleration starting speed on noise

may be caused by the response lag of the turbocharger.

THE INFLUENCE OF ACCELERATION TIME - Fig. 7 shows the influence of acceleration time on noise tested with E engine (DI, NA). There seems to be little influence, but generally the shorter the acceleration time, the higher the sound pressure level.

THE INFLUENCE OF THE LOAD AT WHICH ACCELERATION STARTS - Fig. 8 shows the influence of the load at which acceleration starts on noise level tested with E engine (DI, NA). Generally the higher the load, the lower the sound pressure level.

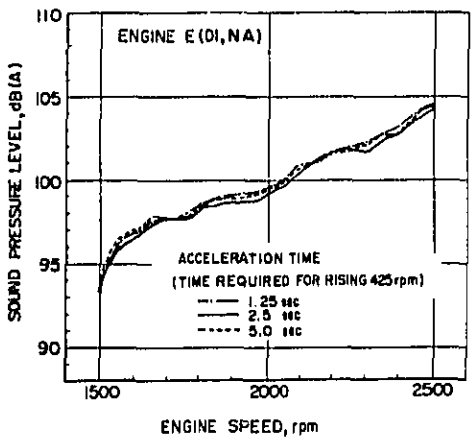

Fig. 7 - Influence of acceleration time on noise

THE COMBUSTION STATE ANALYSIS OF DIRECT INJECTION ENGINES AT ACCELERATED RUNNING

CYLINDER PRESSURE AND NOZZLE NEEDLE LIFT - So as to investigate the mechanisms in which the accelerated running noise is higher than the quasi-steady running noise, we carried out a cylinder pressure analysis on the E engine (a naturally aspirated direct injection V8 engine) as a representative. The cylinder pressure and nozzle needle lift at engine speed of 2000 rpm were measured in acceleration and quasi-steady states, and are compared in Fig. 9. Fig. 10 rearranges the results derived from the indicator diagrams and

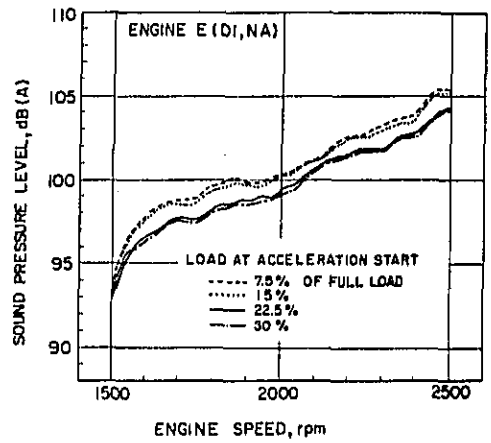

Fig. 8 - Influence of load at acceleration start on noise

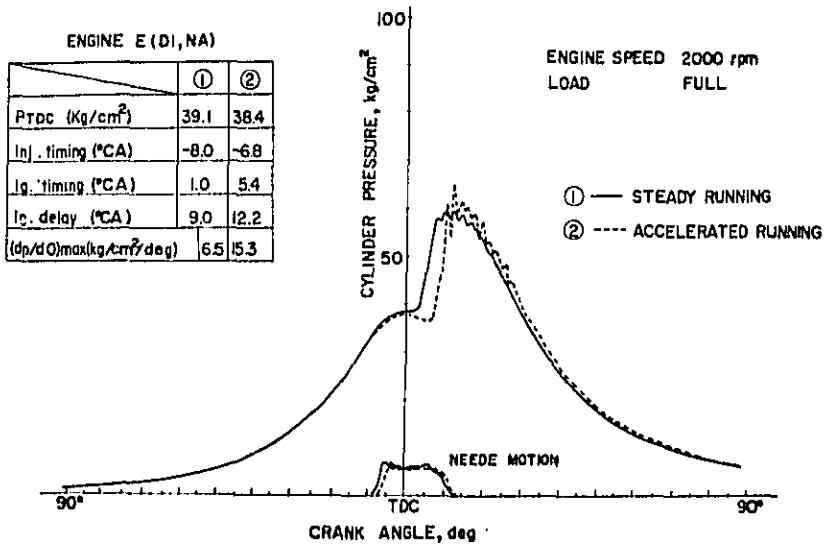

Fig. 9 - Comparison of cylinder pressure diagram between accelerated and steady running

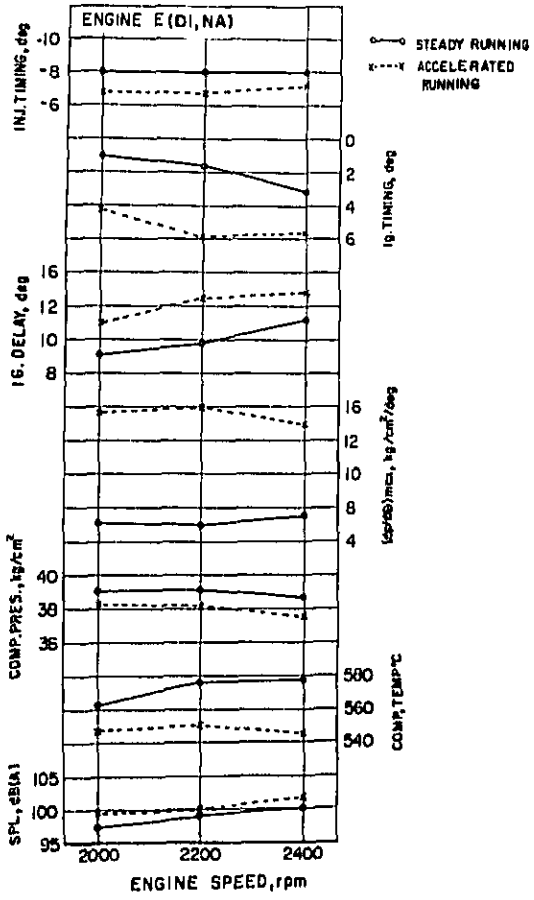

Fig. 10 - Comparison of combustion characteristics between accelerated and steady running

nozzle needle lift diagrams for three engine speeds. As shown in those figures, the compression pressure and temperature at TDC in the acceleration state decrease by about 1 kg/cm^2 and 20° to 30°C, respectively. Injection timing delay of about 1 degree in acceleration is offset by ignition timing delay of about 3 degrees and results in about a 2 degree ignition delay. Consequently the max. rate of cylinder pressure rise ($dp/d\theta$) increases considerably by 2 to 3 times and noise level also increases. It is found from Fig. 11 which shows the frequency analysis of cylinder pressure at 2000 rpm that frequency components increase in the range from 250 Hz to 2 kHz. This region agrees well with the results obtained from frequency analysis of noise, Fig. 5, indicating the frequency region where the noise level becomes higher.

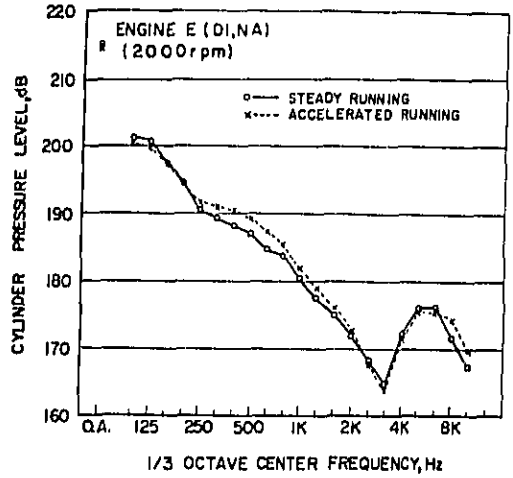

Fig. 11 - Comparison of cylinder pressure spectra between accelerated and steady running

THE RELATION BETWEEN CYLINDER PRESSURE AND ENGINE NOISE - Murayama and Kojima proposed equation (1) as an attempt to separate combustion noise from mechanical noise (3, 4).

$$ESP = MSP + TRC \cdot CP \qquad (1)$$

where, ESP : Sound pressure of engine noise
MSP : Sound pressure of mechanical noise
TRC : Transfer coefficient
CP : Cylinder pressure

Based on the above equation, we calculated MSP and TRC at every 1/3 octave band. Since the equation (1) is considered to be valid only for pure tone, while it is better to suppose adding in energy unit when calculation is done by every 1/3 octave band, we used the following equation in the actual calculation.

$$(ESP)^2 = (MSP)^2 + (TRC)^2 \cdot (CP)^2 \qquad (2)$$

In a steady state with engine speed constant at 2000 rpm, CP and SP were measured for every band by varying load and injection timing. Then we calculated MSP and TRC by minimum involution method, which are shown in Fig. 12. Assuming the MSP and TRC values thus obtained can also apply to an acceleration state, we substituted cylinder pressure values measured in an acceleration state into the equation (2) and predicted engine noise levels in an accelerated running. Fig. 13 shows a comparison between the predicted and measured values of engine noise levels. There are discrepancies at some of the frequencies, but the general tendencies agree fairly well and especially the overall values are quite identical. Therefore, it is considered that the change of combustion state in the cylinder may be a major cause for higher noise level in accelerated running.

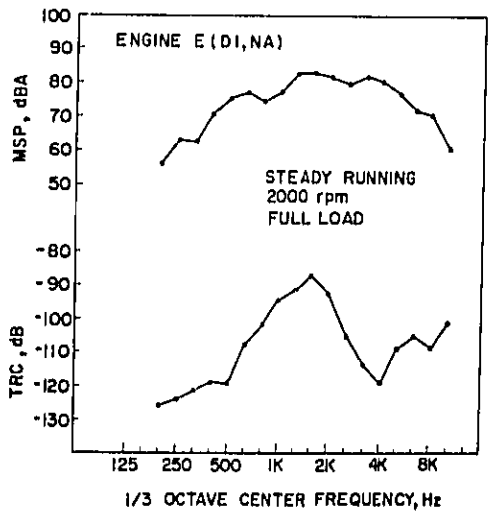

Fig. 12 – MSP and TRC obtained by varying operating conditions in steady running at 2000 rpm

MECHANISMS OF COMBUSTION NOISE RISE IN ACCELERATED RUNNING

In the study conducted so far, it was shown that an increased ignition delay in accelerated running of direct injection engines is a major cause for an increase in max. rate of cylinder pressure rise and a higher noise level as its consequence. We then investigated factors affecting the ignition delay.

VOLUMETRIC EFFICIENCY - According to Wolfer's equation (3) (5), which is well known as an equation of ignition delay, the ignition delay is a function of cylinder pressure and temperature.

$$\tau = 0.44\, p^{-1.19}\, e^{\frac{4650}{T}} \qquad (3)$$

where, τ : Ignition delay
p : Cylinder pressure
T : Cylinder temperature

As has already been seen in Fig. 10, compression pressure and temperature at TDC are low in an accelerated running. One possible reason for this may be that since acceleration is a transient phenomenon, a decrease in suction air quantity occurs due to the influence of inertia mass of air particles. Air flow in air intake duct was measured by a hot wire anemometer to compare the volumetric efficiency in accelerated running with that in quasi-steady running. The results are shown in Fig. 14. It is clear that air flow actually decreases right after acceleration, but it recovers at once, and moreover, air flow even increases on the high speed range. The volumetric efficiency at the beginning of acceleration is high because the combustion chamber wall temperature is low, which is the case with light load.

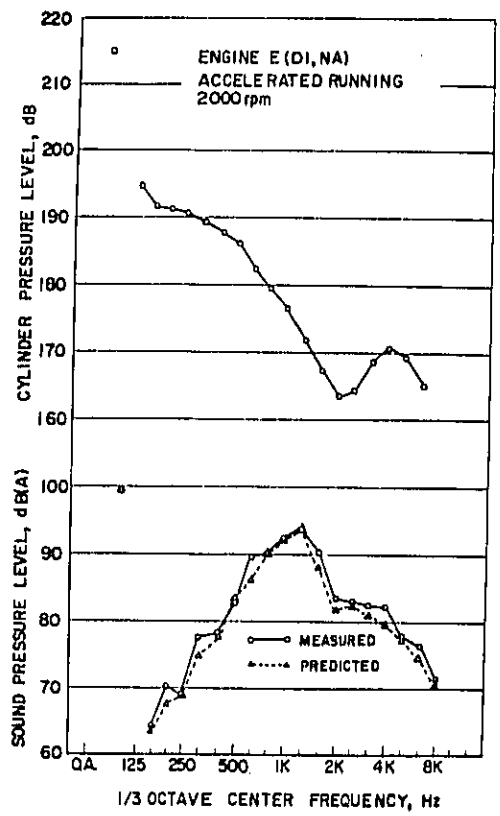

Fig. 13 – Comparison between predicted and measured SP

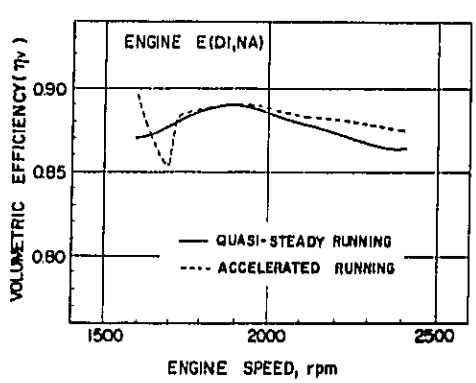

Fig. 14 – Comparison of volumetric efficiency between accelerated and quasi-steady running

WALL TEMPERATURE - As a cause for low cylinder pressure and temperature at TDC, we assumed a bigger heat loss through the combustion chamber wall as a result of the low wall temperature at the beginning of acceleration. Cylinder head wall was chosen for temperature measurement. A CRC thermocouple was buried between valve bridges and wall temperature was measured both in acceleration and quasi-steady states. Fig. 15 shows the results. Through acceleration, the wall temperature goes up almost linearly with the rise of engine speed. But the temperature difference between acceleration and quasi-steady states remains about 100°C in the whole engine speed range ; in other words, the temperature difference of 110°C which exists immediately before acceleration is hardly reduced.

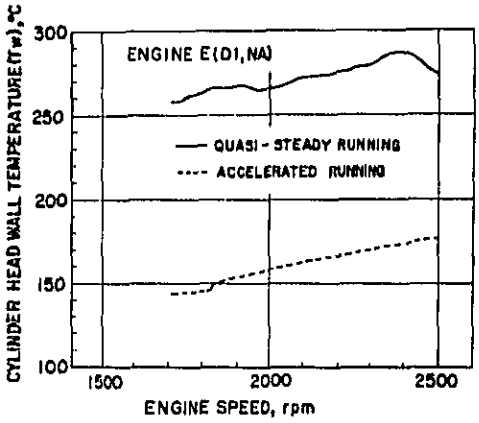

Fig. 15 - Comparison of cylinder head wall temperature between accelerated and quasi-steady running

THE RELATION BETWEEN WALL TEMPERATURE AND NOISE - In order to investigate the relation between combustion chamber wall temperature and noise, the following test was done on the E engine (DI, NA) under an automatic speed regulation running. First, the temperature of engine cooling water as well as the engine load and speed was sufficiently lowered so that the cylinder head wall temperature could be reduced to 100°C, which was still lower than the 160°C at 2000 rpm in accelerated running. Then, the fuel control rack was rapidly brought to the full position to operate the engine at 2000 rpm and with full load. Fig. 16 shows how the engine noise changed with a rise in cylinder head temperature in the test. The noise level at the wall temperature corresponding to that at 2000 rpm in the accelerated running is very much in agreement with the accelerated running noise level at that speed. The cylinder pressure indicator diagram, frequency analysis of the cylinder pressure and sound pressure level are shown in Figs. 17, 18 and 19, respectively. Each of them makes a comparison with the accelerated and quasi-steady running at the same engine speed, 2000 rpm. From those figures, it is clear that both cylinder pressure and noise agree fairly well in accelerated and automatic speed regulation running if compared at the same wall temperature. Fig. 20 shows the relation between the steady noise and wall temperature measured by varying load In this case, however, the noise level at the load corresponding to that at the wall temperature of 160°C in the accelerated running is lower than the accelerated running noise. Therefore, it is assumed that factors other than the wall temperature such as the injection fuel quantity or premixed fuel quantity are working.

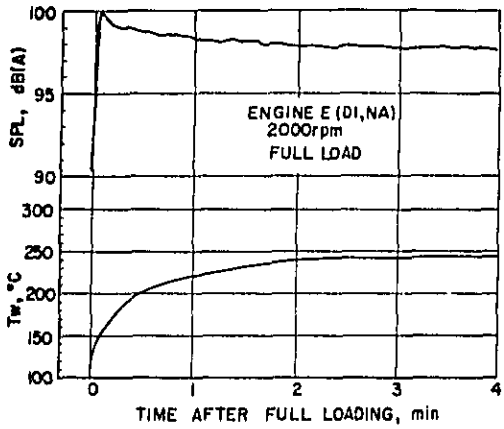

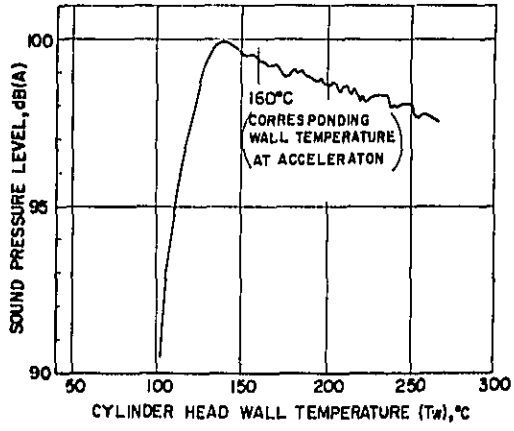

Fig. 16 - Relation between noise level and wall temperature in constant speed running

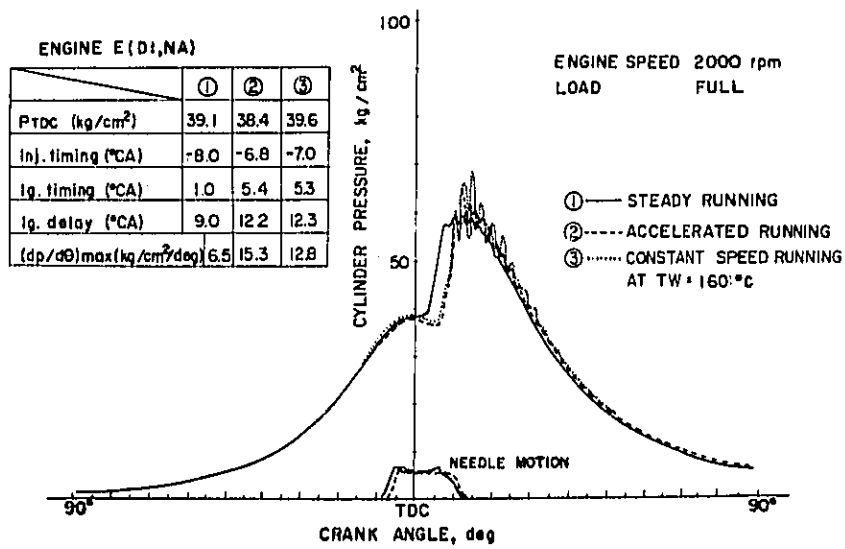

	①	②	③
P_{TDC} (kg/cm²)	39.1	38.4	39.6
inj. timing (°CA)	-8.0	-6.8	-7.0
ig. timing (°CA)	1.0	5.4	5.3
ig. delay (°CA)	9.0	12.2	12.3
(dp/dθ)max(kg/cm²/deg)	6.5	15.3	12.8

Fig. 17 - Cylinder pressure diagram in constant speed running at Tw=160°C, compared with accelerated and steady running

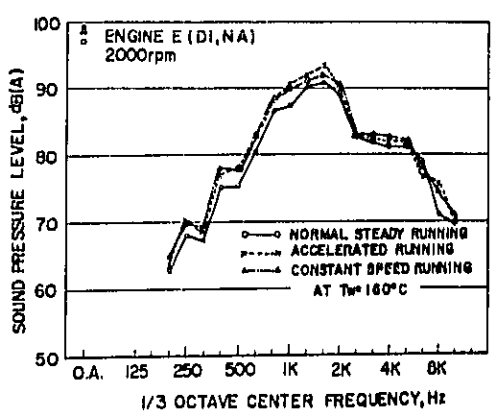

Fig. 18 - 1/3 octave band noise spectra in constant speed running at Tw=160°C, compared with accelerated and steady running

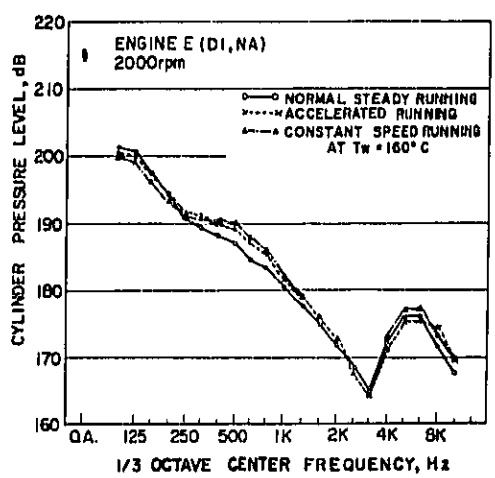

Fig. 19 - 1/3 octave band cylinder pressure spectra in constant speed running at Tw=160°C, compared with accelerated and steady running

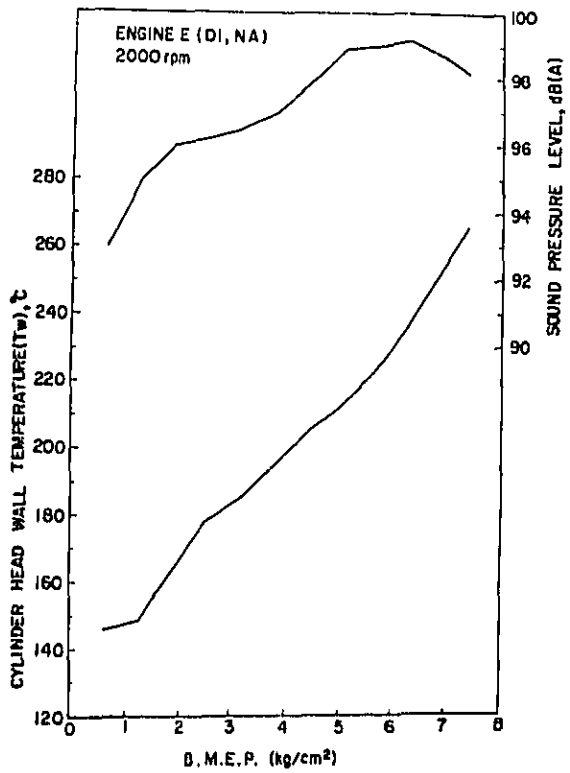

Fig. 20 – Noise level and cylinder head wall temperature versus BMEP in steady running

After measurements of accelerated running noise levels in several engines, we carried out analytical experiments on naturally aspirated direct injection engines to study the mechanisms which produce higher noise level in an accelerated running. This research work is now in progress and there are many points which remain to be solved.

CONCLUSIONS

The acceleration state of engine during a vehicle pass-by noise test was simulated on the engine test bed in an anechoic chamber. The accelerated running noise in the simulation mode and quasi-steady noise (the engine noise emitted during a slow acceleration with full load) were measured on several types of engines. The measurement results clarified the following points:
1) In indirect injection engines, there is very little or no noise level difference in accelerated and steady running. While in naturally aspirated direct injection engines, the accelerated running noise is about 2 dB(A) higher. And in turbocharged direct injection engines, due to the response lag of the turbocharger, noise immediately after the start of acceleration is very high, as much as 5 dB(A) higher than the steady noise, and the difference gradually becomes smaller as the acceleration continues.
2) The influences on noise level of the acceleration time and engine speed at acceleration start were examined on direct injection engines. Though the influence of the acceleration time was small, the noise in general became slightly louder as the acceleration time was shortened. The engine speed at acceleration start had substantially no effect on naturally aspirated engines, but in turbocharged engines, the response delay by turbocharging led to a noise level difference.
3) From the measurement results of cylinder pressure and nozzle needle lift in naturally aspirated direct injection engines, it is seen that the ignition delay increases by about 2 degrees in an accelerated running. The relation between CP and SP in a steady state was calculated from actual CP and SP values measured for different loads. Based on the relation, SPs in accelerated running were predicted from measured CPs at the same engine speed in the course of acceleration. The predicted values agreed well with the measured SPs, thus a change in combustion state was proved to be a cause of louder noise in accelerated running.
4) Using naturally aspirated direct injection engines, the volumetric efficiency and cylinder head wall temperature were measured in accelerated and quasi-steady running. The compared results show that the volumetric efficiency in accelerated running decreases immediately after acceleration but recovers again at once, which means there is no substantial difference between the two running states.
5) The cylinder head wall temperature during acceleration was lower than that in a quasi-steady running by about 100°C, and this low temperature was proved to be a factor in increasing the ignition delay. By running the engine at a constant speed with full load and letting the wall temperature change, sound pressure level and cylinder pressure were measured. Comparison of these results with an accelerated running (at the same engine speed) shows that if the wall temperatures are the same, not only the engine noise levels but cylinder pressure diagrams almost agree.
6) Noise and wall temperature were measured varying load in a constant speed for comparison with those at the same speed during acceleration. At the same wall temperature, the noise level in constant speed running was found to be much lower than the accelerated running noise. This fact indicates that the injected fuel quantity as well as wall temperature has an effect on the combustion noise.

FUTURE WORK

From our present point of view and areas so far clarified, the future problems may be summarized as follows: Though the combustion chamber wall temperature has been proved to be one of the factors affecting the ignition delay, its precise mechanism is yet to be solved. It might be explained simply as the low wall temperature increases the heat loss through walls, which in turn lowers the cylinder pressure and temperature,

and consequently the ignition delay occurs. Or the combustion chamber wall temperature itself may be directly related to vaporization or ignition of injected fuel. As future work we would like to confirm the following point: If compression pressure and temperature in accelerated running could be made identical with those in steady running of the original engine by, for example, an increase of compression ratio or heating of intake air, the ignition delay and resulting noise can be lowered accordingly.

ACKNOWLEDGEMENT

The authors would like to thank the directors of Nissan Diesel Motor Co., Ltd. for permission to publish this paper. They also thank the company's staff in the engine noise research section, especially Messrs. M. Fujimori and K. Shiraishi for their support and cooperation, and Mr. Y. Hayashi for helpful comments on this work and Miss M. Kawaguchi for typing the manuscript.

REFERENCES

1. Y. Hayashi, "A Series of Light Duty Indirect Injection Diesel Engines." SAE Paper 760212 presented at SAE Automotive Engineering Congress & Exposition, Detroit, February 1976.

2. G. J. Hawksley and D. Anderton, "Studies into Combustion and Noise in Turbocharged Engines." I Mech E C72/78 presented at the Conference on Turbocharging and Turbochargers, London, April 1978.

3. T. Murayama and N. Kojima, "Studies on the Combustion Noise in Diesel Engine - 1st Report, Separation of Combustion Noise from Engine Noise." Bulletin of the JSME, Vol. 18, No. 118, 1975.

4. T. Murayama, N. Kojima and Y. Satomi, "A Simulation of Diesel Engine Combustion Noise." SAE Paper 760552 presented at SAE Fuels and Lubricants Meeting, St. Louis, Missouri, June 1976.

5. H. H. Wolfer, "Ignition Lag in the Diesel Engine." VDI-Forschungsheft No. 392, 1938.

790270

RELATION BETWEEN COMBUSTION SYSTEM AND ENGINE NOISE

D. Anderton

I.S.V.R., University of Southampton

ABSTRACT

From measured overall I.C. engine noise levels and corresponding measured combustion (cylinder pressure) levels the paper illustrates the major influence that the combustion system has on the engine radiated noise. The basic 'noisiness' of normally aspirated and turbocharged two- and four-stroke D.I. systems, normally aspirated I.D.I. (swirl chamber) diesel and gasoline systems are compared by a normalised frequency spectrum method. Using a simple linear model for calculating the direct combustion noise level of each combustion system the relative levels of noise are calculated. The results show good agreement with measured noise levels for normally aspirated two-stroke and four-stroke D.I. engines and indicate that combustion noise is low in turbocharged diesels, I.D.I. diesels and particularly gasoline engines.

COMBUSTION IS A CONTROLLED EXPLOSION. In the case of the internal combustion engine the control is in the form of an iron or aluminium structure which does not allow the explosion to communicate itself directly with the surrounding air until the pressure is reduced to a few atmospheres by an expansion and heat loss process. During the controlled explosion, the containing structure is forced to expand and deflect slightly, causing a pressure wave many times less than that of an open explosion and the pressure wave is perceived as noise rather than a destructive pressure blast. The form of this noise depends on the characteristics of the explosion, the containing structure deformation and its ability to radiate noise.

In order to allow the controlled explosion to take place repeatedly it is necessary to use mechanical devices which operate at high speed and produce noises of their own. The balance between these two major noise sources determines whether an engine is 'combustion noise controlled' or 'mechanical noise controlled'. To the user it is not particularly important which noise source is predominant, but to a manufacturer seeking to control the noise of his product it is. The answer will determine the direction in which the manufacturer's considerable efforts and time will be spent.

Unfortunately devising reliable methods by which combustion and mechanical noise can be separated on running engines has proved extremely difficult. Basically three tests are at present used:

(a) Establishing 'critical cylinder pressure' levels by several tests in which the injection or spark timing is altered to modify the form of the combustion, and the changes assessed from the resulting cylinder pressure spectra and noise (1).*

(b) Monitoring the engine without fuel supply to assess the mechanical noise (2).

(c) Modification of engine running parts, e.g., chain drive for gears, close tolerance pistons, stiffer fuel pump drives, etc., to modify engine mechanical noise (3).

In many cases even on completion of all of these lengthy tests there can still be uncertainty about the balance between mechanical and combustion noise.

More recently, many workers are experimenting with the coherency techniques in which random signal analysis methods developed to separate uncorrelated 'noise' from the wanted signal are used to separate combustion from mechanical sources. The main difficulty here is in applying the techniques to fundamentally periodic signals, all of which bear a relationship to one another (4,5,6). At the present time these methods have not shown anything that was not known previously and we must await further advances.

Since the combustion development in an engine can be measured directly (unlike piston slap, gear noise, etc., where it is difficult to measure the direct forces involved in deflecting the structure) then for this noise source alone many quantitative relationships can be derived. Vibration measurements have shown that up to the moderate force inputs obtainable with electrodynamic shakers the engine structure response and noise radiation is linear (7). Therefore, based on a linear model of the engine structure the general characteristics of I.C. engine noise which arises solely as a result of combustion can be predicted. This information, when used in conjunction with the measured engine noise characteristics, can also be used to augment other information to estimate the balance between 'combustion noise' and 'mechanical noise'.

NOISE PRODUCED BY I.C. ENGINES

The overall noise at full load of some 44 different I.C. engines, measured at the ISVR over

*Numbers in parentheses designate References at end of paper.

SAE/P-79/80/$02.50
Copyright © 1979 Society of Automotive Engineers, Inc.

the last 12 years, is shown in Figure 1 as a function of engine speed. The engines tested include two-stroke diesels, normally aspirated and turbocharged four-stroke diesels, indirect injection (swirl chamber) diesels and gasoline engines.

(generally a frequency of maximum noise level in engine noise) are compared it can be seen that there is some 26 dB difference in the level. The engine structure itself, however, is loaded by a force down the connecting rod determined by the

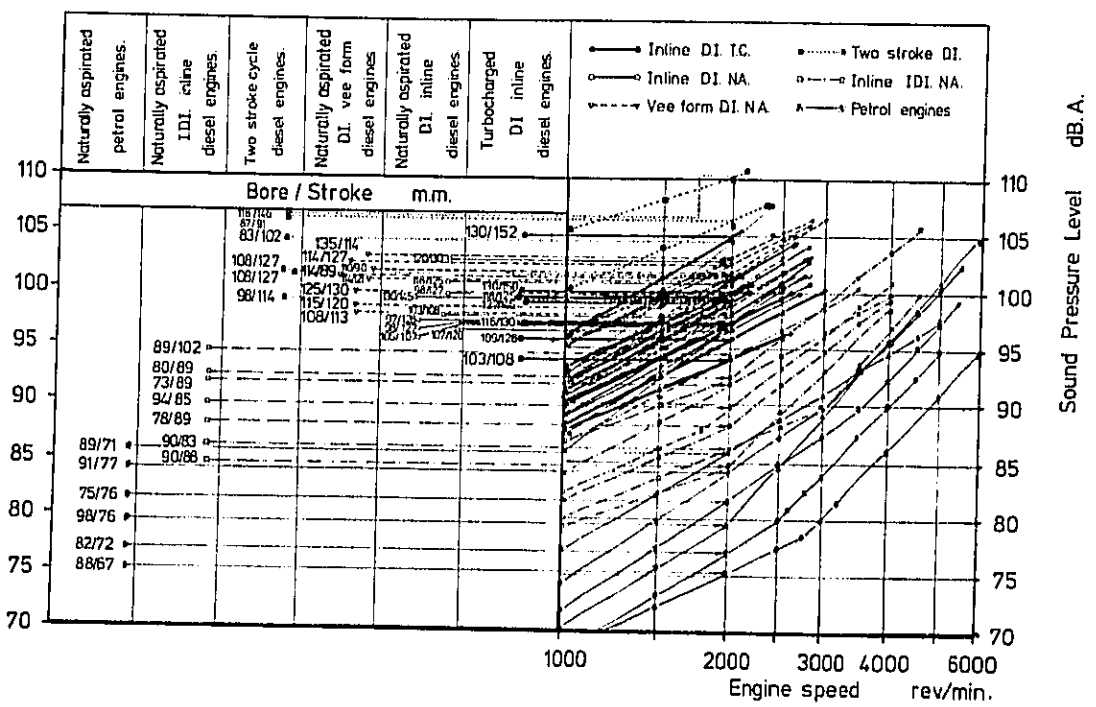

Fig. 1 - Noise versus speed at full load for a range of engine types

For all engines at rated speed the variation in overall noise measured 1m from the engine surface is from 95 to 110 dBA. The importance of engine speed in controlling engine noise is clear from the figure, but even at a constant engine speed of 2000 rev/min, for example, there is a 35 dBA spread in overall noise level according to engine type. It is well known that combustion noise in normally aspirated direct injection diesels is the predominant noise source. From Figure 1 the average noise level for this type of engine at 2000 rev/min is about 100 dBA. For the level of a gasoline engine to be 75 dBA at 2000 rev/min (the lowest noise level measured) it therefore follows that the combustion noise in this gasoline engine must be at least 25 dBA lower than the diesel. It is therefore clear from Figure 1 that very large differences in combustion excitation level should be measured in the various I.C. engine combustion systems. If, for example, the cylinder pressure spectra for a normally aspirated diesel engine of 12.2 litres 130 mm bore is compared to that of a 1.6 litre 91 mm bore gasoline engine then this is indeed shown to be true, especially at frequencies above 500 Hz (Figure 2). If the levels at 1000 Hz

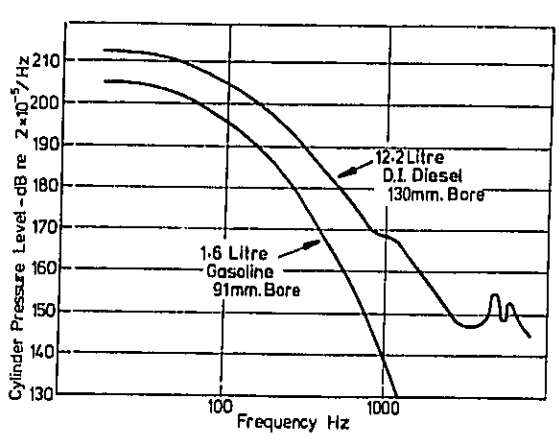

Fig. 2 - Cylinder pressure spectra for D.I. diesel and gasoline engine

product of cylinder pressure level and piston area. This applied force is shown in Figure 3. For the

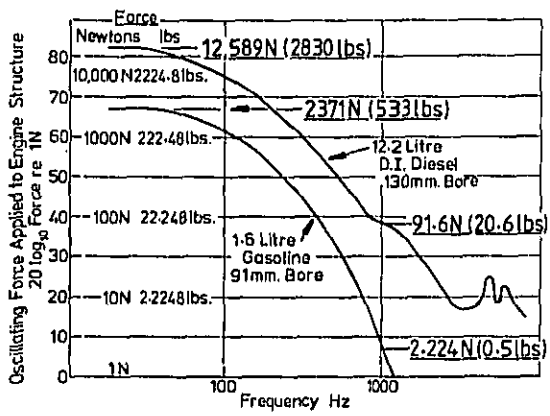

Fig. 3 - Combustion force spectra for D.I. diesel and gasoline engine

diesel engine the root mean square oscillating force applied to the structure at cycle firing frequency (16.6 Hz) is some 2830 lbs (12,589 N), whilst at 1000 Hz the applied loading is some 20.6 lbs (91.6 N). For the gasoline engine at cycle firing frequency the rms oscillating force applied is some 533 lbs (2371 N) whilst at 1000 Hz it is only 0.53 lbs (2.22 N). Thus the square of the force input to the gasoline engine structure at 1000 Hz is some 33 dB lower than that of the diesel. For a linear system the noise due to combustion at 1000 Hz would also be lower by 33 dB, provided that no other noise sources were present.

ASSESSMENT OF COMBUSTION INDUCED NOISE

Priede (8,9) showed, some 20 years ago, that the noise of diesel engines could be related to changes in the level of the high frequency components of the frequency spectrum of the cylinder pressure development. Making sure to use flush mounted pressure transducers such measurements have been found to be remarkably repeatable. Figure 4 shows the relationship between cylinder pressure development, rate of heat release and cylinder pressure spectra. The frequency analysis is carried out using an analogue analyser of 1.5% bandwidth, but bandwidth corrected, i.e., results appear as a spectral density plot. When combustion is abrupt, the rate of pressure rise and initial peak rate of heat release are large and the level of the high frequency (above 500 Hz) cylinder pressure spectrum components are also high (10, 11, 12). There is a direct relationship between initial peak of heat release and rate of pressure rise when combustion is abrupt (Figure 5) and under these conditions combustion noise can be related to either (12,13). However, when the combustion is smooth, as in gasoline, well matched full load turbocharged diesel or high speed two-stroke, the combustion noise can only be related to the form of cylinder pressure development and peak pressure (7). At present the only fully reliable method of combustion noise assessment is by the full frequency analysis of the exact cylinder pressure development. Priede (8,9) also showed that the noise of engines (and machines) increased rapidly with speed because of the rapidly sloping frequency spectra which shifted upwards in frequency as the cycle fundamental frequency increased, giving rise to higher force inputs to the structure in the high frequency range (10,11). This indicated that comparisons of combustion excitation were very dependent on

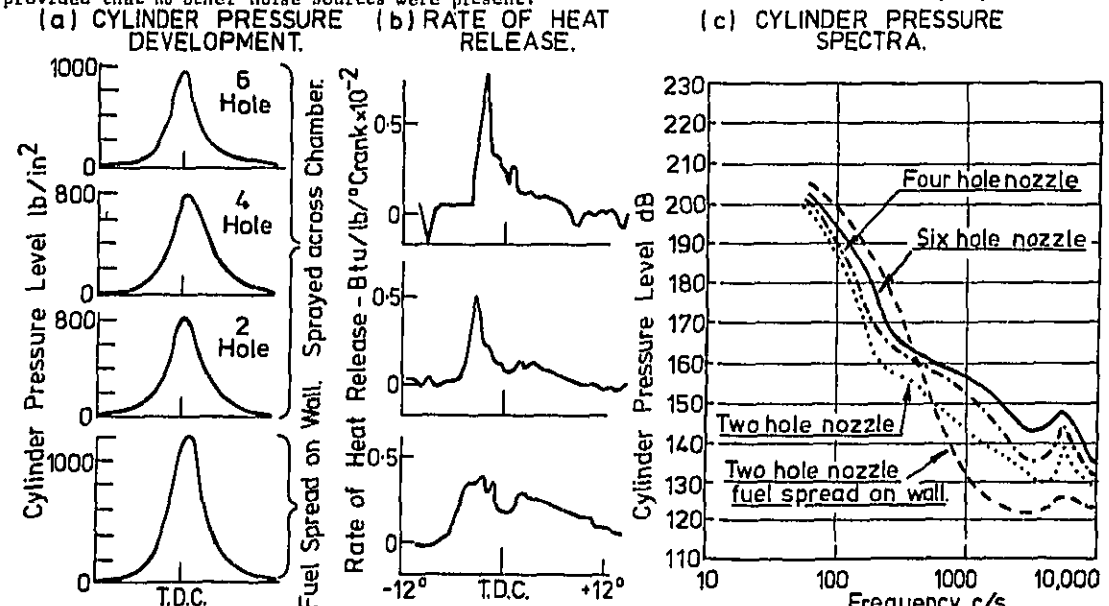

Fig. 4 - Relation between cylinder pressure development, rate of heat release and cylinder pressure spectra

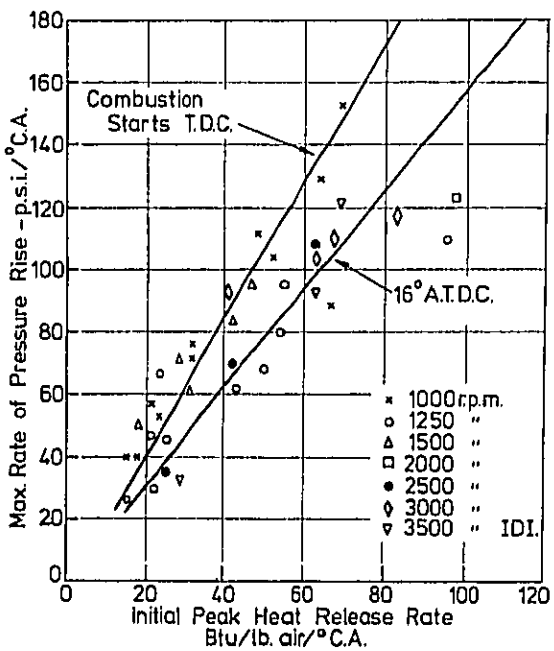

Fig. 5 - Relationship between rate of pressure rise and initial peak heat release rate for normally aspirated diesel engines

engine speed. In order to compare the various combustion systems it is necessary to reduce them to a standard form which is independent of speed. It is the level of the harmonic components between 800 and 3000 Hz (the predominant range of engine structure resonances) that determines the importance of the cylinder pressure spectrum. Figure 6a shows that the cylinder pressure spectra can be approximated to a straight line representing the best fit over the frequency range. Figure 6b shows this simplified spectrum normalised for engine speed which defines the cylinder pressure level as a function of both frequency and speed. Figure 6c shows measured cylinder pressure levels for a D.I. engine taken at various speeds plotted on a base of normalised frequency. As can be seen all spectra are coincident in the important frequency range and can be approximated by a single straight line. A comparison of the simplified and normalised cylinder pressure spectra derived from full load measurements taken over the entire engine speed range for a variety of engines provides a method of rating the combustion systems as noise sources - the higher the level the higher the noise at any given speed. In Figure 5 the simplified and normalised spectra for 13 different normally aspirated diesel engines are shown. The variation in combustion excitation level at 1000 Hz ranges from 27 dB at 1000 rev/min to about 20 dB at 3000 rev/min depending on the combustion system used. Two-stroke diesel engines have the highest excitation levels with Direct Injection four-strokes slightly lower and Indirect Injection four-strokes lower still. In general it can be seen that the multiple hole nozzle low swirl chamber configuration gives rise to higher levels of combustion excitation than does the high swirl single hole nozzle chamber configuration. Figure 7 shows a similar comparison between normally aspirated four-stroke diesels and turbocharged four- and two-stroke diesels. In this case the effect is most marked with the turbocharged levels much lower than those of normally aspirated engines, there being little difference between high swirl and low swirl chamber configurations in this respect. Finally, Figure 9 shows a comparison between the normally aspirated four-stroke diesels and six gasoline engines. The very marked reduction in combustion excitation level with gasoline operation is clearly shown.

CALCULATION OF COMBUSTION INDUCED NOISE IN I.C. ENGINES

Over the last ten years the computation of the harmonic cylinder pressure spectrum from a cylinder pressure time history has become possible and therefore a combustion model which can accurately predict the initiation of combustion as well as later burning allows the computation of combustion induced noise (10,14). Such a model has been developed by Ogegbo and is primarily based on a physical representation of fuel preparation and combustion initiation (15). This I.S.V.R. model is a two zone model based on modified single droplet and simplified jet theories. It assumes that the physical processes such as atomisation, vaporisation and mixing rates control diesel combustion. Figure 10 shows a typical comparison between measured and predicted cylinder pressure development and spectra for a shallow bowl D.I. engine. Figure 11(b) shows the error in cylinder pressure spectrum prediction, in one-third octave bands as a function of frequency and engine speed for two combustion models, firstly model I (a modification of Austen and Lyn's approach relating the injection rate and the rate of burning) and secondly, the I.S.V.R. model in which the physical processes leading to combustion control the heat release rates (16). A $\pm$ 7 dB scatter in the higher one-third octave bands results in both cases but in summing over the frequency range to give overall level predictions accuracies of $\pm$ 2.5 dBA are found. The advantage of the I.S.V.R. model over model I is that predictions for new ranges of engines can be made at the design stage.

RELATION BETWEEN CYLINDER PRESSURE SPECTRUM AND COMBUSTION INDUCED ENGINE NOISE-During the compression and power stroke all clearances are taken up and the engine structure can be considered as linear. It can be shown that the overall noise is proportional to the square of the direct gas force and consequently to the fourth power of engine bore (7). A structure attenuation factor linking the

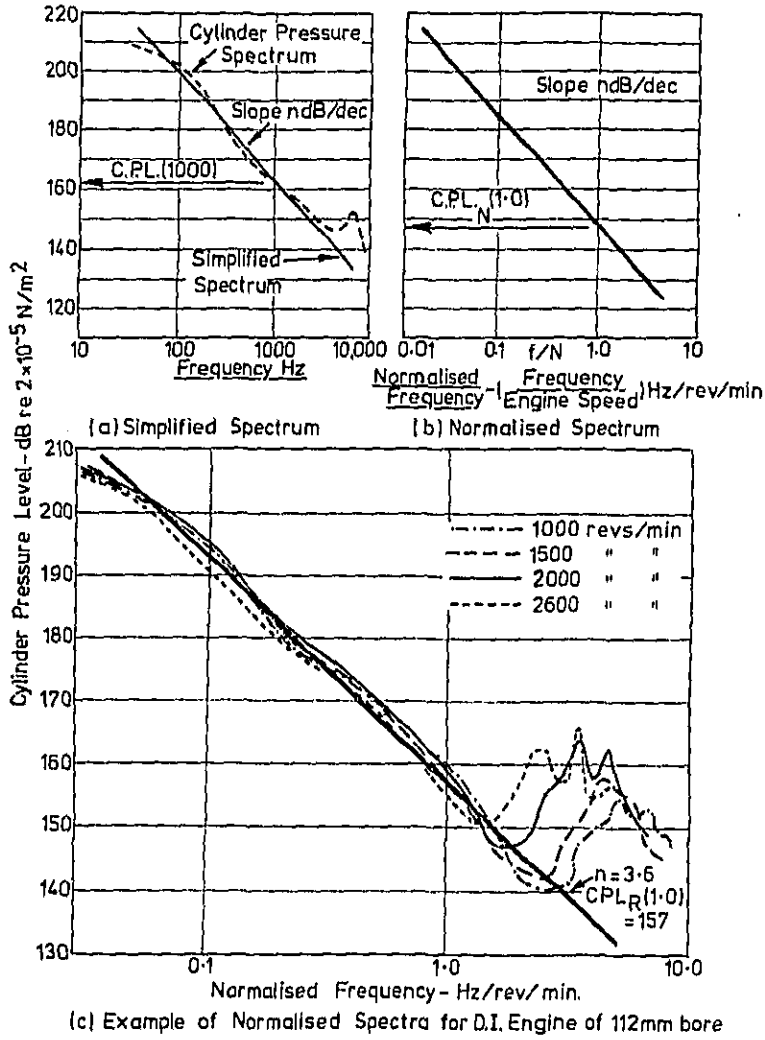

Fig. 6 - Normalised and simplified cylinder pressure spectra

direct combustion force and the engine noise can then be defined and typical measured values are shown in Figure 12(a), (7). An average 'standard' structure attenuation can be specified from such measurements taken on engines with abrupt cylinder pressure diagrams and this is shown in Figure 12(b). The use of a structure attenuation factor with a known cylinder pressure spectrum will then allow the noise level due to combustion to be predicted (14).

The cylinder pressure at frequency f can be calculated from the reduced spectrum by the relation

$$(C.P.)^2 = \frac{(C.P._R(1.0))^2 . A \log_{10}(3n) . (N/f)^n}{f^n} \qquad (1)$$

where (C.P.) = cylinder pressure at frequency f Hz

$C.P._R(1.0)$ = cylinder pressure level of reduced spectrum at f/N = 1.0

n = slope of simplified cylinder pressure spectrum - combustion index

N = engine speed rev/min

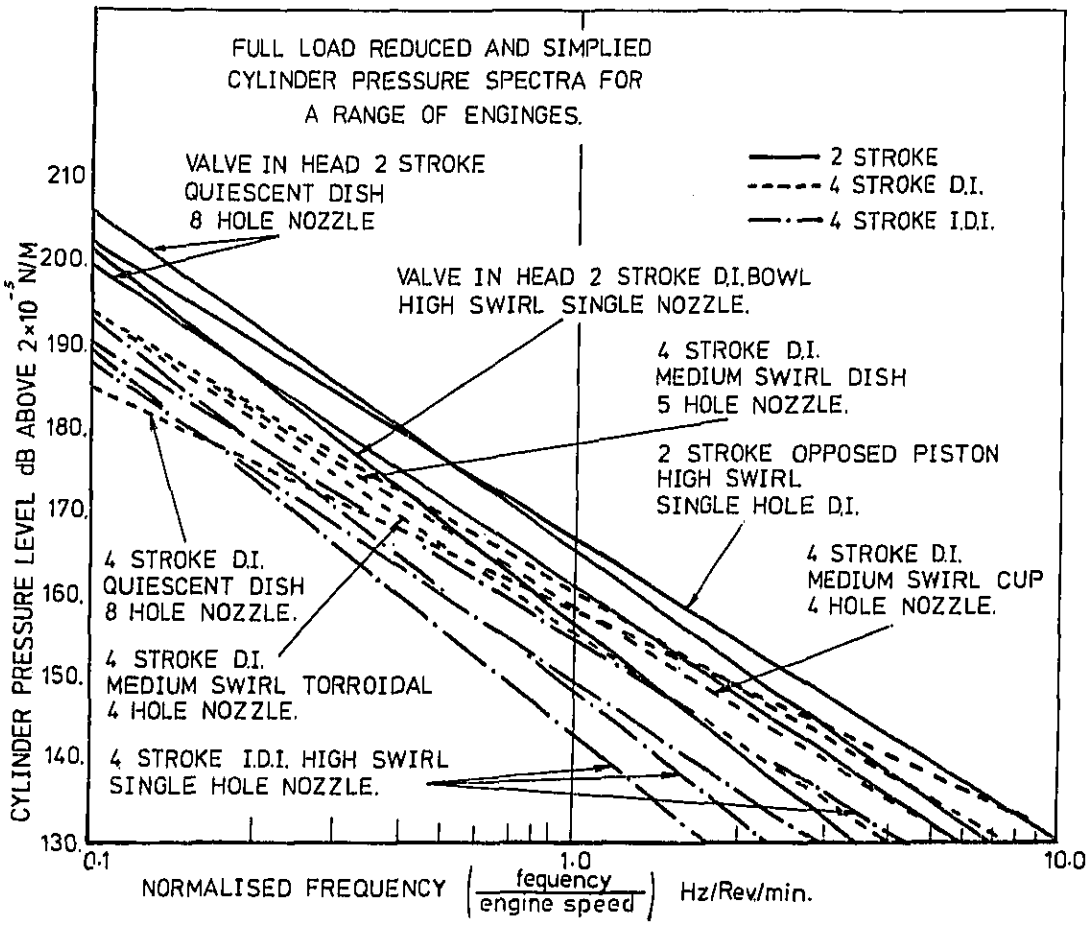

Fig. 7 - Full load normalised and simplified cylinder pressure spectra for a range of normally aspirated engines - D.I., I.D.I. and two stroke.

In a similar manner the structure attenuation at frequency, f, for the standard attenuation curve can be specified in two parts by:

$$S = \frac{A \log_{10}(S_{1000/10}) \; A \log_{10}(3q)}{f^q} \qquad (2)$$

where S_{1000} = value of attenuation at 1000 Hz dB/Hz

q = slope of attenuation curve dB/decade

by definition at frequency f

$$(\text{Sound Pressure, P})^2 (f) = \frac{(\text{cylinder pressure} \times \text{bore}^2)^2}{S} \qquad (3)$$

Therefore $P^2(f) =$

$$\frac{(C.P._R(1.0))^2 \; A \log_{10}(3n).(\frac{N}{f})^n.B^4}{A \log_{10}(S_{1000/10}).A \log_{10}(3q)} \; f^{q-n} \qquad (4)$$

The overall sound pressure level is given by

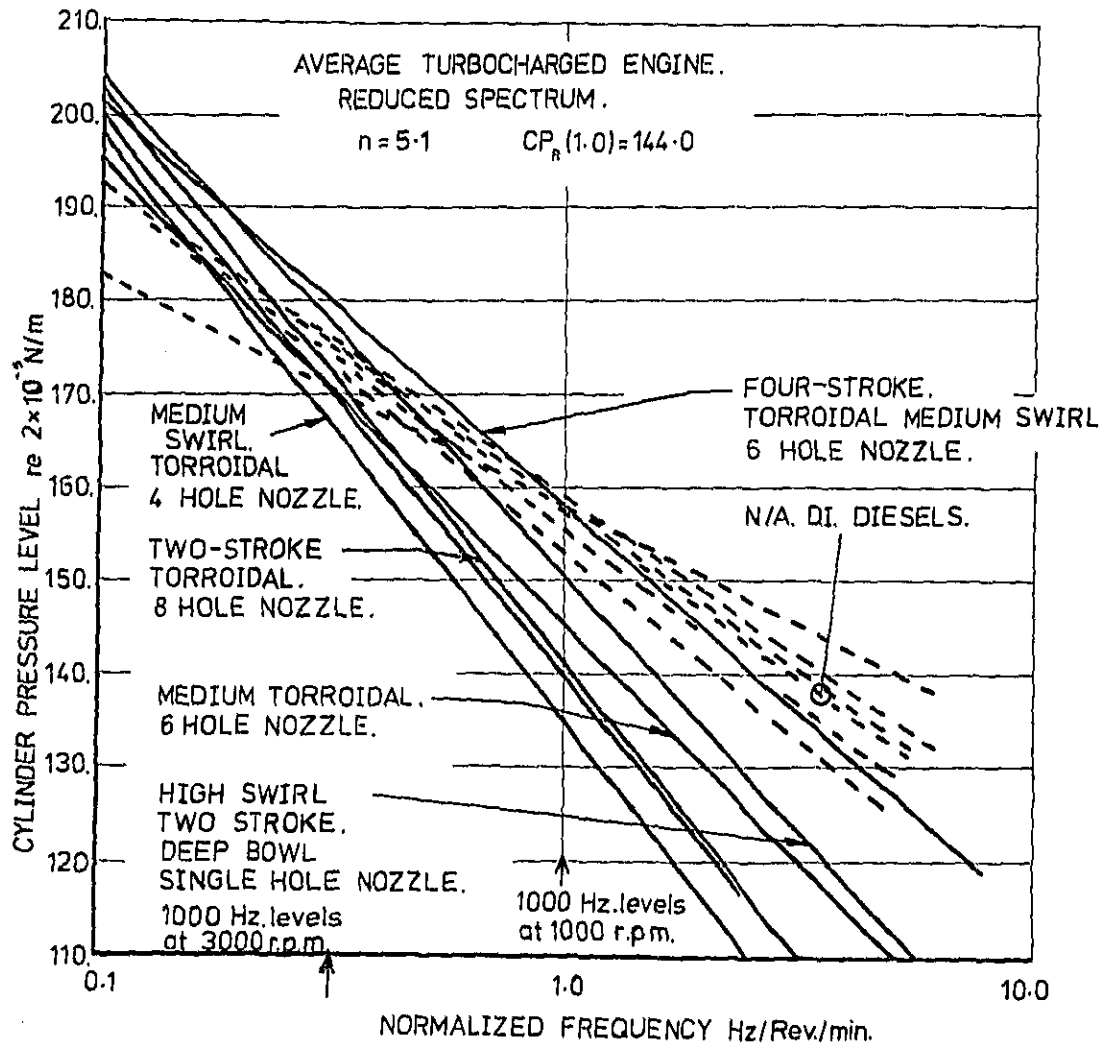

Fig. 8 - Normalised and simplified spectra for turbocharged diesels (two- and four-stroke)

$$p^2(\text{overall}) = \int_{f_1}^{f_2} p^2 \, df \qquad (5)$$

Using the general form of the structure attenuation factor shown in Figure 12(c) the overall combustion noise level calculated from a measured or computed simplified and reduced cylinder pressure spectrum at an engine speed of N rev/min becomes

$$(S.P.L.)_{\text{overall}} = 20 \log_{10} \times \left| \frac{(C.P._R(1.0))^2 . A \log_{10}(3n) . B^4 . N^n}{P_{ref} \; A \log_{10}(S_{1000/10})} \right| \times \left| \frac{|1000^{(q_1-n+1)} - f_1^{(q_2-n+1)}|}{(q_1-n+1) A \log_{10}(3q_1)} + \frac{f_2^{(q_2-n+1)} - 1000^{(q_2-n+1)}}{(q_2-n+1) A \log_{10}(3q_2)} \right| \text{dB} \qquad (6)$$

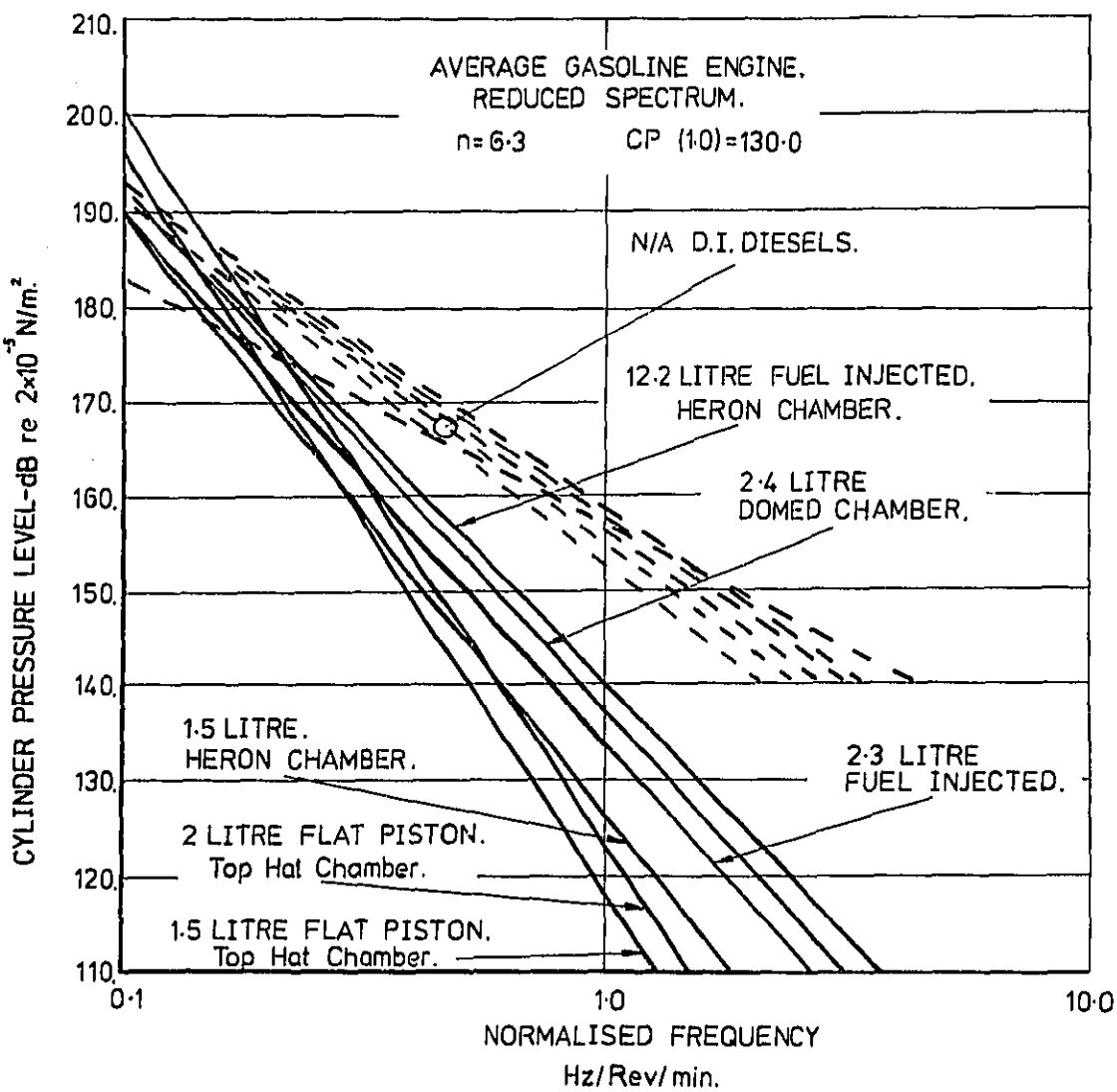

Fig. 9 - Normalised and simplified spectra for gasoline engines

Equation (6) can be divided into three parts. One specifying the cylinder pressure level, an engine bore term and a shape factor which is purely dependent on the chosen attenuation curve levels and slopes, the combustion index and the frequency range and weighting networks chosen. For the standard structure attenuation shown in Figure 12 (b) and both the A and linear weighting networks the value of the shape factor as a function of combustion index is shown in Figure 13.

The predicted noise will vary as the fourth power of bore for direct combustion noise whereas (Figure 15) the measured noise levels of diesel engines vary as the fifth power of bore. This implies that the structure attenuation factor is not constant but varies directly with bore size. A model for the prediction of combustion induced noise based on measured or estimated simplified cylinder pressure spectra, the engine bore and a structural attenuation factor which varies directly with bore and has the value shown in Figure 12(b) for a bore size of 100 mm can be put forward. The overall level of direct combustion induced noise at 1 metre is given by the following relations:

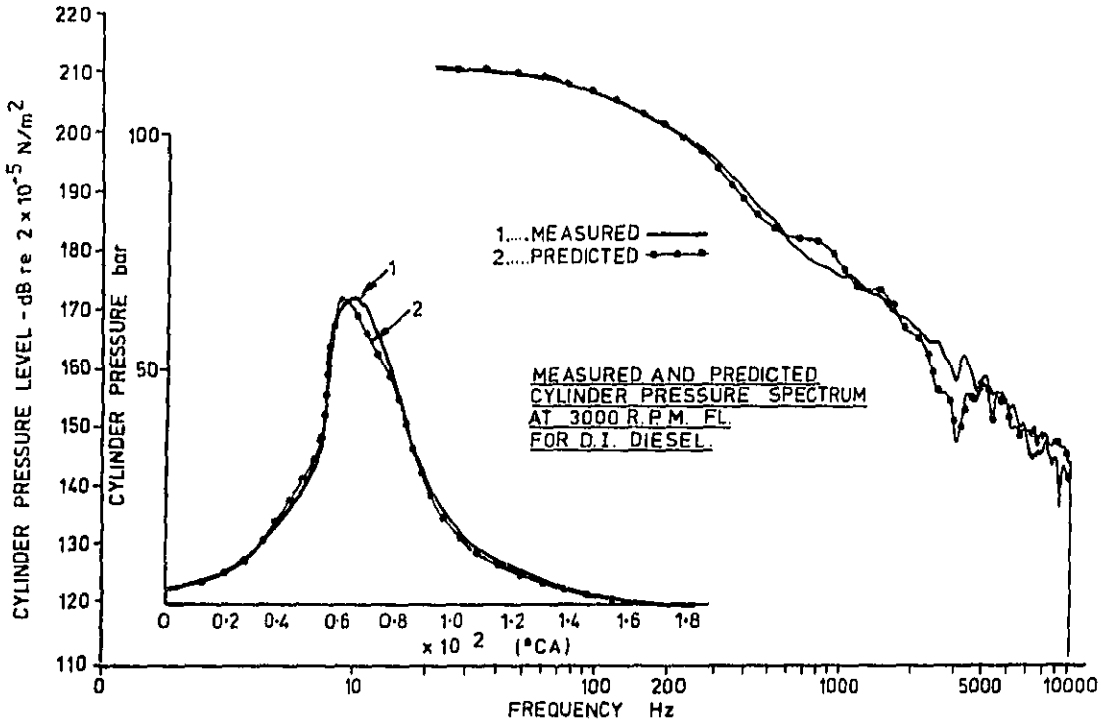

Fig. 10 - Comparison of predicted and measured cylinder pressure development and spectrum

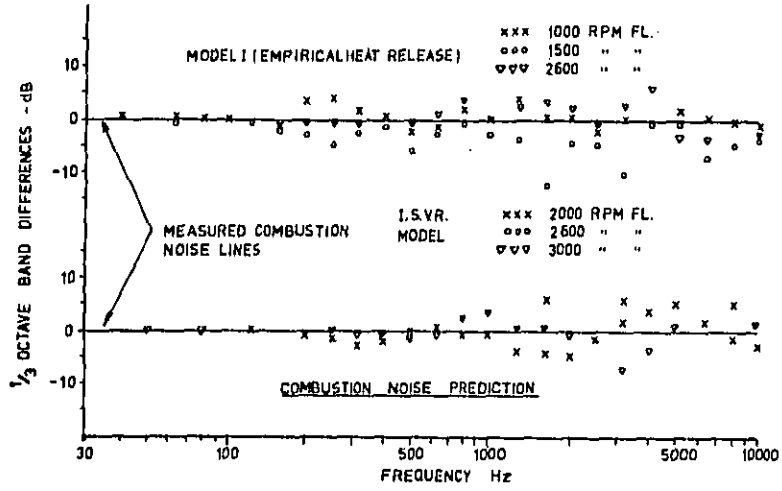

Fig. 11 - Prediction of cylinder pressure spectrum levels from combustion models

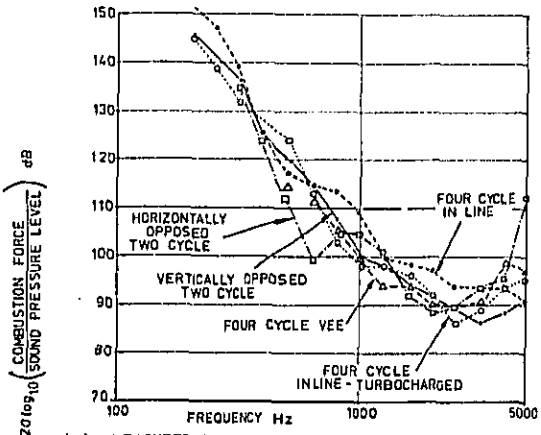

(a) MEASURED STRUCTURE ATTENUATION FACTOR FOR VARIOUS ENGINE CONFIGURATIONS.

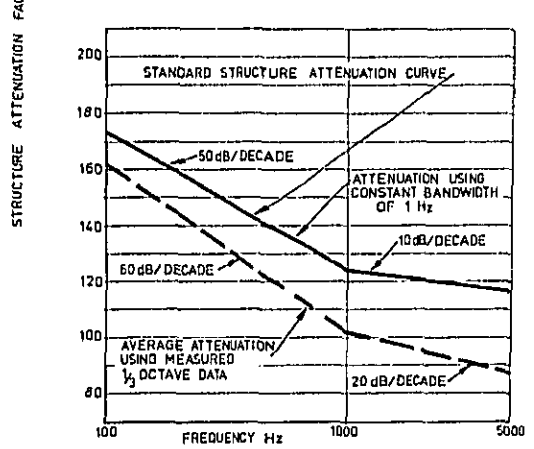

(b) STANDARD STRUCTURE ATTENUATION FACTOR ASSOCIATED WITH A BORE SIZE OF 100 mm

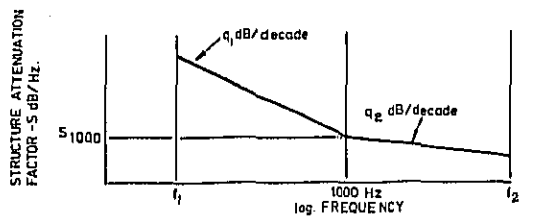

(c) GENERAL FORM OF STRUCTURE ATTENUATION FACTOR.

Fig. 12 - Structure attenuation factor

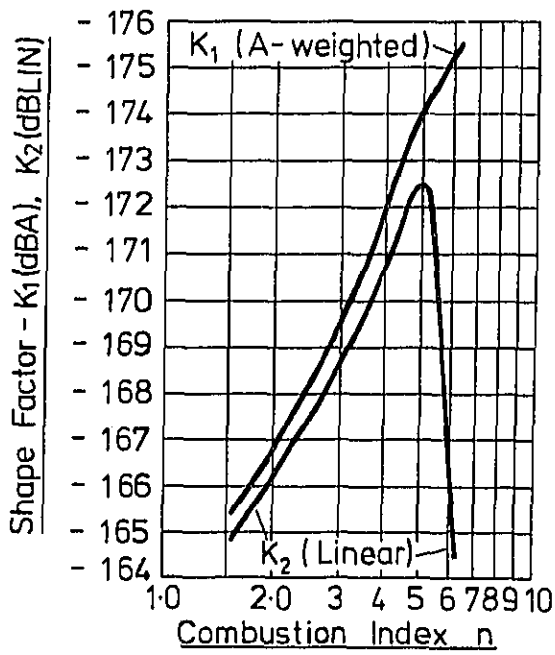

Fig. 13 - Spectrum shape factors K_1 and K_2

Based on simplified cylinder pressure spectrum

$$\text{Overall Noise} = CPL_{(1000)} + 50 \log_{10} B - K_1 \text{ dBA} \quad (7)$$

and

$$\text{Overall Noise} = CPL_{(1000)} + 50 \log_{10} B - K_2 \text{ dB(LIN)} \quad (8)$$

where B = bore in mm
K_1 = A-weighted spectrum shape factor shown in Figure 12.
K_2 = Linear spectrum shape factor shown in Figure 12.
$CPL_{(1000)}$ = level of cylinder pressure spectrum at 1000 Hz

Based on normalised cylinder pressure spectrum

$$\text{Overall Noise} = CP_R(1.0) + 50 \log_{10} B + 10n \log_{10} \frac{N}{1000} - K_1 \text{ dBA} \quad (9)$$

and

$$\text{Overall Noise} = CP_R(1.0) + 50 \log_{10} B + 10n \log_{10} \frac{N}{1000} - K_2 \text{ dB(LIN)} \quad (10)$$

where N = engine speed N
n = combustion index
$CP_R(1.0)$ = level of normalised cylinder pressure spectrum at value 1.0

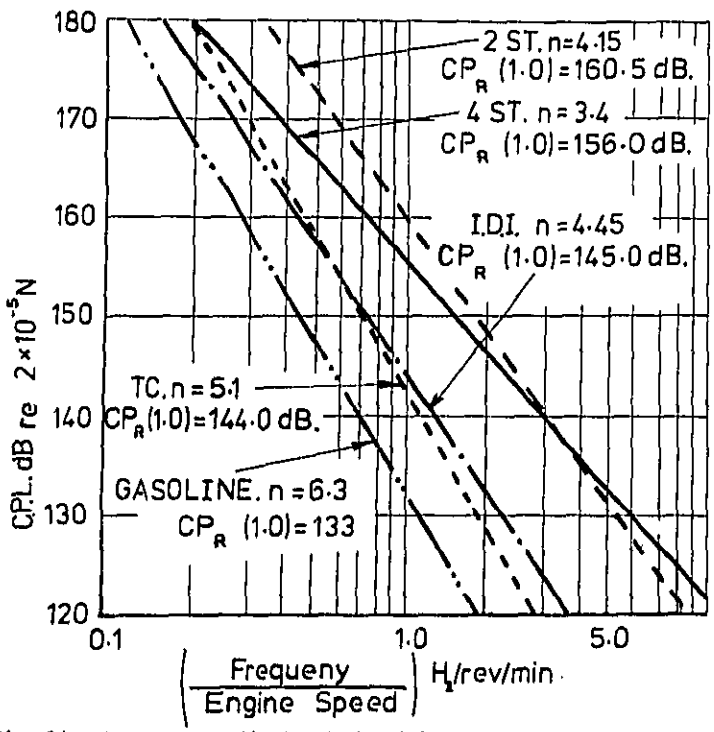

Fig. 14 - Average normalised and simplified spectra as a function of combustion system

$$dBA_1 = CP_R(1.0) + 50 \log_{10} B + 10n \log_{10} \frac{N}{1000} - K_1 \quad (9)$$

where $CP_R(1.0)$ = value of the simplified and reduced cylinder pressure spectrum at 1.0 Hz/rev/min dB re 2×10^{-5} N/m^2

B = engine bore mm

N = engine speed rev/min

n = combustion index = one tenth of the slope of the simplified and reduced cylinder pressure spectrum in dB/decade

K_1 = shape factor (Figure 13)

In the case of opposed piston designs in which two separate crank arrangements are

These relations, because they include the absolute level as well as slope of the cylinder pressure spectrum, can be used to predict the level of combustion induced noise in diesel engines of each combustion class at any speed or load. A more exact computation can be obtained by using the exact cylinder pressure spectrum values, as calculated according to the ISVR combustion model, and an exact structure attenuation factor which, at present, can only be obtained experimentally.

CATEGORISATION OF COMBUSTION SYSTEMS FOR NOISE

The overall noise level of an I.C. engine with a standard structure (as defined in Figure 12) is given by the relation:

Overall noise in dBA at 1m from the engine surface, dBA_1

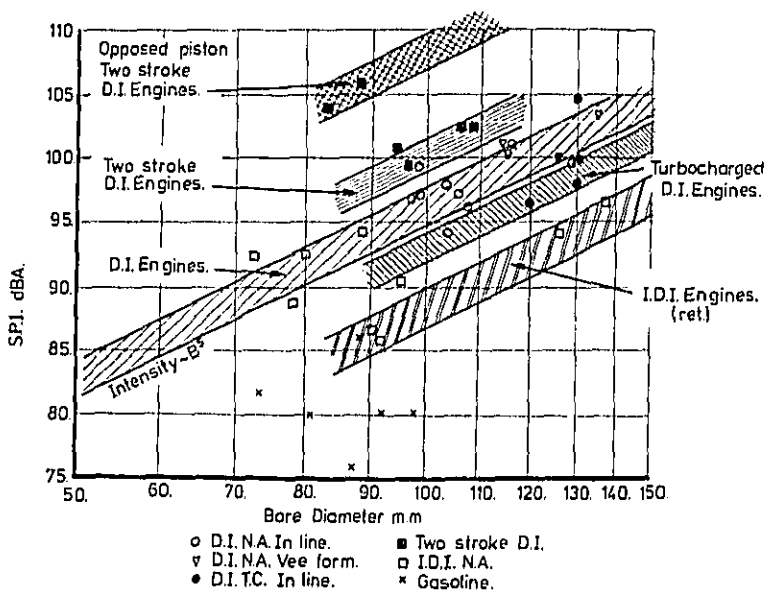

Fig. 15 - Relation between measured overall noise and bore size of engines in the various groups at 2000 revs/min

used an equivalent bore B_e must be used in equation (1) where $B_e = \frac{B^e}{\sqrt{2}}$. The normal bore dimension is used for single crankshaft opposed piston designs.

The normalised spectra shown in Figures 7, 8 and 9 can be grouped according to the form of combustion and then be averaged to give a single line representation of the average combustion excitation level in that group. This comparison of combustion systems is shown in Figure 14. The average combustion excitations are defined by:

Normally aspirated two-stroke diesels

Combustion index n = 4.15, $CP_R(1.0)$ = 160.5dB

Normally aspirated direct injection four-stroke diesels

Combustion index n = 3.4, $CP_R(1.0)$ = 156 dB

Normally aspirated indirect injection (swirl chamber) diesels

Combustion index n = 4.45, $CP_R(1.0)$ = 145 dB

Turbocharged two- and four-stroke diesels

Combustion index n = 5.1, $CP_R(1.0)$ = 144 dB

Gasoline engines

Combustion index n = 6.3, $CP_R(1.0)$ = 130 dB

Using these average values, measured directly from the engine combustion system, in combination with equation (9) the average noise levels likely to be associated with each combustion system can be calculated and the results compared to the actual measured noise of the engines.

To illustrate this the noise data of Figure 1 for an engine speed of 2000 rev/min are plotted as a function of bore size (Figure 15). For the diesel engines the variation of noise with $(\text{bore})^5$ can be clearly seen as also can the grouping of the noise levels according to the form of combustion.

It can be seen that the measured overall noise levels of the engines do fall into specific groups:-

(a) All normally aspirated DI engines fit within a 3 dB band of slope $(\text{bore})^5$. It is clear that there are no differences between the overall noise of vee-form and in-line engines. Some of the IDI engines also fall within this same band but these generally have 'abrupt' or 'advanced' pressure diagrams.

(b) The turbocharged engines occupy a band just below.

(c) The remaining IDI engines fall within a band some 8 dBA below the DI engines. These engines generally have smooth or retarded type pressure diagrams.

(d) Two-stroke cycle engines fall within a band some 4 dBA higher than the DI engines.

(e) Opposed piston two-stroke cycle engines (separate crankshaft arrangements) fall in a band 12 dBA higher than DI engines.

(f) Gasoline engines show considerable scatter but are about 15 dBA below the DI engines.

It is clear that the effect of engine structural configuration (for current production engines) on noise is small. Figure 16 shows a comparison between the measured noise levels and those calculated to be due to combustion induced noise from equation (9). For conventional and opposed piston two-stroke and normally aspirated direct injection four-stroke diesels the calculated combustion noise levels correlate very well with the measured data. However, the levels calculated for the IDI, gasoline and turbocharged engines lie below those measured, particularly in the case of the turbocharged engines (full load).

RELATIVE CONTRIBUTION OF COMBUSTION AND MECHANICAL NOISE IN THE VARIOUS ENGINE TYPES

The comparison of measured overall noise levels with those predicted to be due to direct combustion excitation, shown in Figure 16, can be used to indicate the general level of mechanical noise associated with the engine types. At 2000 rev/min it is clear that mechanical noise is generally just below that due to combustion in the DI four-stroke and two-stroke engines. For the IDI engines (matched for low emissions) the mechanical noise is of the same level as combustion. For the turbocharged engines mechanical noise is almost wholly predominant. For the gasoline engines there is some scatter but it can be concluded that mechanical noise tends to dominate the total noise.

Since the average cylinder pressure spectra have been used to construct Figure 16 it is useful to note the variations in combustion level for each system. This can be done approximately by examining the values of $CP_R(0.5)$ (1000 Hz value at 2000 rev/min). From the spectra shown in Figures 7, 8 and 9 the following variations can be placed on the calculated combustion noise levels shown in Figure 16 at 2000 rev/min.

Normally aspirated two-stroke diesels

Variation $\pm$ 4.0 dBA.

Normally aspirated DI four-stroke diesels

Variation $\pm$ 2.5 dBA.

Normally aspirated IDI four-stroke diesels

Variation $\pm$ 5.0 dBA.

Turbocharged two- and four-stroke diesels

Variation $\pm$ 5.5 dBA.

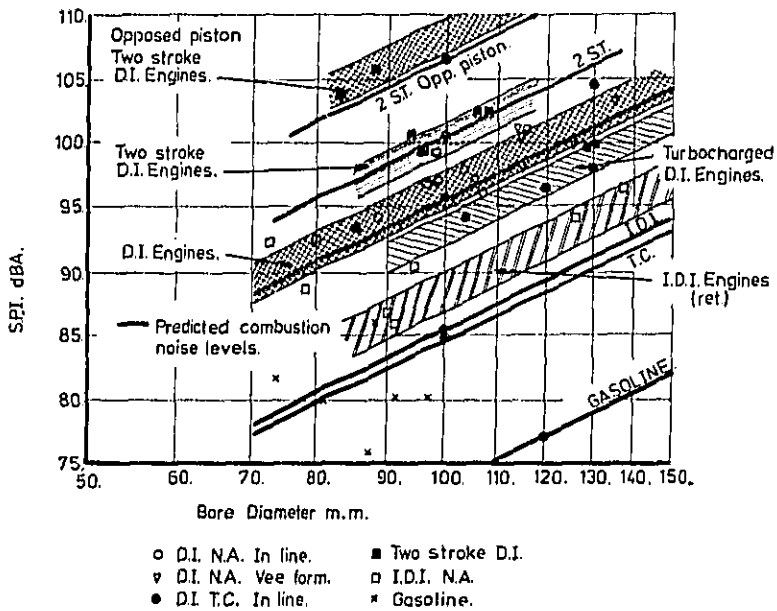

Fig. 16 - Measured and predicted overall noise versus bore size for engines in the various groups at 2000 rev/min

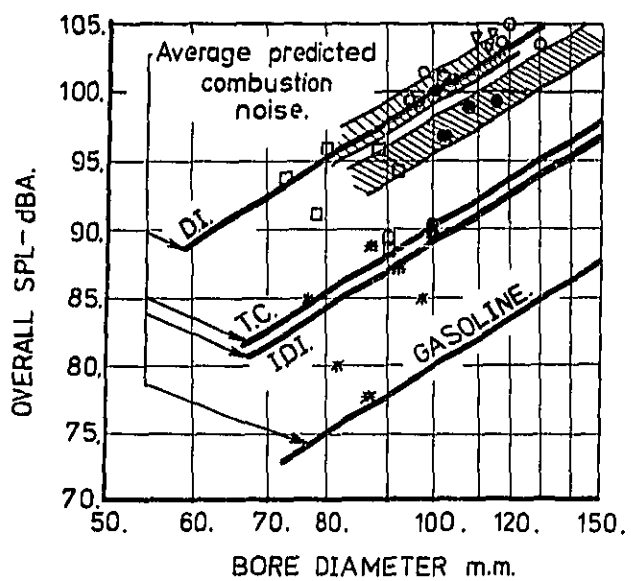

Fig. 17 - Measured and predicted overall noise versus bore size for engines in the various groups at 2500 rev/min

Gasoline engines

Variation ± 6.5 dBA.

Despite the spread of combustion excitation levels it is clear that the general conclusions regarding mechanical noise levels are valid. For instance the measured noise levels of turbocharged engines are considerably greater than the predicted average combustion noise level plus variation.

At 2500 rev/min the general picture is similar (Figure 17). The DI four-stroke engine measured noise is coincidental with the calculated combustion noise and the measured turbocharged engine noise is just below. The calculated turbocharged combustion noise levels are some 6 dBA below those measured at this speed. The IDI engine noise shows more scatter at this speed with only a few results near the calculated combustion noise levels. The same result for gasoline engines can be seen. At 2500 rev/min the measured variation in combustion noise is lower than that found at 2000 rev/min. The variations are:

Normally aspirated DI diesels

Variation = ± 2.0 dBA.

Normally aspirated IDI diesels

Variation = ± 4.0 dBA.

Turbocharged two- and four-stroke diesels

Variation = ± 5.0 dBA.

Gasoline engines

Variation = ± 5.5 dBA.

At 4000 rev/min the measured IDI noise values (Figure 18) lie a little above that calculated for combustion noise again indicating a predominance of mechanical noise. For the gasoline engines (Figure 18), however, the measured noise levels are almost included within the band of calculated combustion noise plus maximum variation, indicating that some degree of combustion noise con-

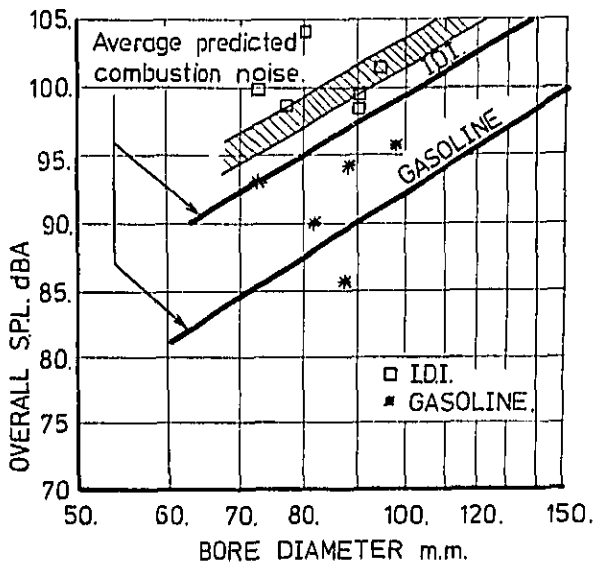

Fig. 18 - Measured and predicted overall noise versus bore size for engines in the various groups at 4000 rev/min

trol is present at high engine speeds. At 4000 rev/min the measured variation in combustion noise is less than that at 2000 or 2500 rev/min. The variations are:

Normally aspirated IDI diesels

Variation = ± 3.5 dBA.

Gasoline engines

Variation = ± 4.5 dBA.

CONCLUSIONS

(a) From the results of the measured overall noise levels of some 44 IC engines it is clear that, for a given engine speed and bore, there is a very large variation in overall noise, of the order of 25-30 dBA, and that this variation is associated with particular combustion systems.

(b) From measured cylinder pressure spectra for 26 IC engines it is clear that there is a corresponding variation in the combustion excitation levels associated with the various combustion systems.

(c) From the measured reduced and simplified cylinder pressure spectra the average combustion excitation spectra for the various combustion systems are:-

Normally aspirated two-stroke diesels

Combustion index n = 4.15, $CP_R(1.0)$ = 160.5 dB

Normally aspirated direct injection four-stroke diesels

Combustion index n = 3.4, $CP_R(1.0)$ = 156.0 dB.

Normally aspirated indirect injection (swirl chamber) diesels

Combustion index n = 4.45, $CP_R(1.0)$ = 145.0 dB.

Turbocharged two- and four-stroke diesels

Combustion index n = 5.1, $CP_R(1.0)$ = 144.0 dB.

Gasoline engines

Combustion index n = 6.3, $CP_R(1.0)$ = 130.0 dB.

(d) Using a linear combustion model, in which a constant structure attenuation is used, the general variation in measured overall noise levels is reflected in the calculated overall noise levels based on combustion excitation alone.

(e) A comparison of measured overall noise and calculated combustion noise levels can be used to indicate the general level of mechanical noise for engines designed for different combustion systems. For normally aspirated Direct Injection two- and four-stroke diesel engines the results suggest that combustion noise is predominant. For the IDI four-stroke diesels, combustion noise and mechanical noise are about equal. For turbocharged engines the mechanical noise is completely predominant at full load, whilst for gasoline engines this is also true at the lower engine speeds but combustion begins to become important at the higher engine speeds.

(f) The measured overall engine noise levels show clearly that it is quite possible to design lower noise engines, even using conventional structures, if maximum engine speed is limited and the intrinsically quieter combustion systems used.

REFERENCES

1. Priede, T., "Relation between form of cylinder pressure diagram and noise in diesel engines". Four papers on diesel engine fuel injection, combustion and noise. Proc. I. Mech. E., London (AD), 1960-61.
2. Khan, I.M. et al, "Prediction of diesel engine noise" Paper C15/77 Conference on Land Transport Engines, I.Mech. E., London, January 1977.
3. Priede, T., Grover, E.C., "Application of acoustic diagnostics to internal combustion engines and associated machinery", I. Mech. E., Symposium - Acoustics as a diagnostic tool, 1970.
4. Chung, J., Crocker, M.J., and Hamilton, J.F. "Measurement of multiple coherence function and the

separation of the coherent engine noise from the total noise of a diesel engine". Proc. Inter-agency sym. on Univ. Research in Trans. Noise, Raleigh, N.C., June 5-7, 1974.
5. Seybert, A.F., Crocker, M.J. "The use of coherence techniques to predict the effect of engine operating parameters on diesel engine noise". ASME paper no. 75-DET-33.
6. Strahle, W.C., Handley, J.C. "Stochastic combustion and diesel engine noise". SAE paper 770408.
7. Anderton, D., Baker, J. "Influence of operating cycle on noise of diesel engines". SAE paper 730241, 1973.
8. Austen, A.E.W., Priede, T., "Origins of diesel engine noise". Proc. Instn. Mech. Engrs. London 1959, 173, 19.
9. Priede, T., "Noise and engineering design". Philosophical Transactions of the Royal Society of London, A., vol. 263, pp. 461-480, 1968.
10. Priede, T., Grover, E.C., Anderton, D. "Combustion induced noise in diesel engines". Diesel engine users association, London, Publ. 317, March 1968.
11. Anderton, D., Grover, E.C., Lalor, N. Priede, T., "Origins of reciprocating engine noise - its prediction and control". ASME paper 70-WA/DGP-3, 1970.
12. Anderton, D., "Rate of heat release and diesel engine noise", US Department of Transport Report No. DOT-TSC-OST-77-56.
13. Hawksley, G.J., Anderton, D. "Studies into combustion and noise in turbocharged engines". Paper C72/78 Conference 'Turbocharging and turbochargers'. I. Mech. E., London, April 1978.
14. Anderton, D., "Combustion as a source of diesel engine noise", Ph.D. Thesis, University of Southampton, 1974.
15. Ogegbo, A.M., "Automotive diesel engine combustion and noise". Ph.D. Thesis, University of Southampton, 1973.
16. Austen, A.E.W., Lyn, W.T. "Relation between fuel injection and heat release in a direct injection engine and the nature of the combustion process". Four papers on diesel engine fuel injection, combustion and noise. Proc. I. Mech. E., London (AD), 1960-61.

790271

ESTABLISHING A TARGET FOR CONTROL OF DIESEL COMBUSTION NOISE

M F Russell, Lucas Industries Noise Centre
E J Cavanagh, Lucas CAV Research Department

Lucas CAV Limited
London, England

ABSTRACT

The minimum practicable levels of diesel combustion noise and mechanical noise, which might be achieved by control at source, are estimated for direct injection engines of 1 litre per cylinder capacity, as used in trucks and tractors of European manufacture. These levels are compared with targets derived from proposals for more stringent noise legislation for such vehicles. The targets might be achieved by a combination of control of combustion and mechanical noise at source and reduction of the engine structure response to these sources.

EFFECT OF FUTURE VEHICLE NOISE LEGISLATION ON TRUCK DIESEL ENGINES

Proposals are being discussed at national and international levels for further legislation to limit noise from road vehicles, and to alter the test procedure by which vehicle types are approved. Proposals to limit noise from big trucks to levels below that currently required in the Common Market countries for cars, will undoubtedly improve the urban acoustic environment, if these levels are achievable in volume production. Legislation has been drafted to reduce the noise limits by 3 dB(A) below present levels, for all classes of vehicles in EEC countries, and for medium and heavy trucks in the U.S.A., in the early 1980's. Even lower levels have been suggested for the middle and late 1980's.

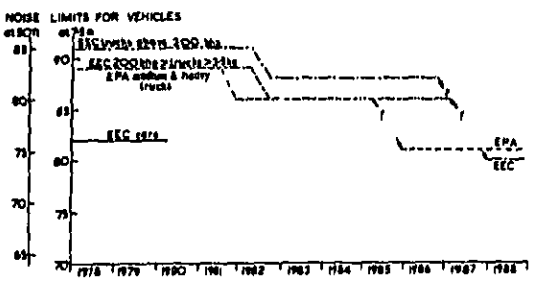

Fig. 1 - Draft legislation and proposals for future limits

For example 80 dB(A), measured at 7.5 metres, has been suggested for all trucks in the U.K. by 1988 (1)* and 75 dB(A), measured at 50 feet, has been suggested for medium and heavy trucks in the U.S.A. by 1985 (2). If the two sets of proposals are compared, they turn out to be very close, as shown in Figure 1. Over the last few years, other countries have issued proposals for reductions in noise limits, and if these are taken together, a noise reduction "staircase" might be constructed as shown in Figure 2. From this it is possible to derive target levels for noise radiated by the engine surface by making certain assumptions. This paper discusses the origins of this noise, and

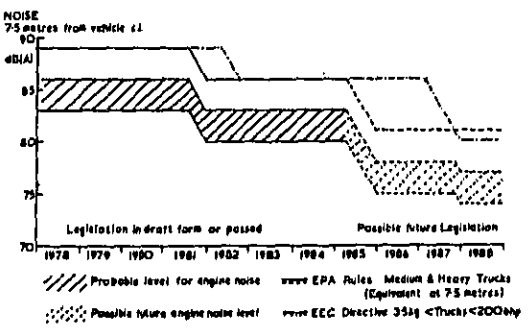

Fig. 2 - Engine noise limits inferred from future noise legislation

separately how it may be controlled at source with the aim of meeting the legislation largely by control at source.

The total vehicle noise is the sum of noise radiated from the exhaust, engine surfaces, cooling fan, engine air intake, gearbox and bell housing surfaces, tyres, etc. During the current test procedures in use in Europe and North America, the vehicle is travelling comparatively slowly in a low gear such that the engine is pulling full load in the top quarter of its speed range. Thus the engine, and the accessories driven from the engine, are emitting noise levels close to their maxima, whereas tyre and rolling noise are well below their maximum levels. With improved cooling system

* Numbers in parentheses designate References at end of paper

SAE/P-79/80/$02.50
Copyright © 1979 Society of Automotive Engineers, Inc.

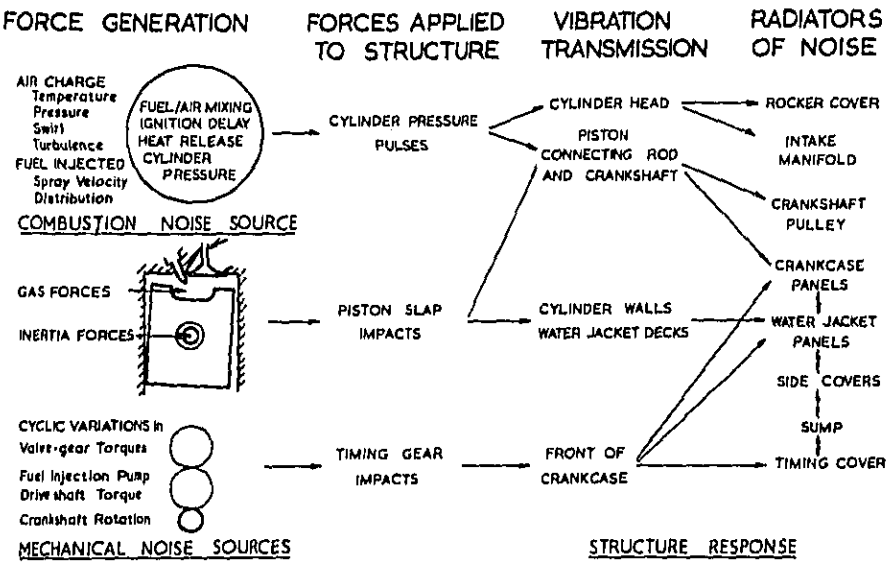

Fig 3 NOISE GENERATION PROCESSES IN DIESEL ENGINES

design, and temperature-controlled fan clutches, the noise from the cooling fan can be reduced considerably. If the maximum fan speed could be halved, the fan noise might be reduced by 16 dB(A) from a typical value of 80 to 90 dB(A) at 7.5m (3). Effective control of exhaust and intake noise, by silencers, may be accomplished if sufficient space is available. Although unsilenced exhausts from 4 stroke engines can emit noise levels as high as 100 dB(A) at 7.5m, silencers have been made with an insertion loss of up to 30 dB (4) and further reductions in the exhaust noise may be obtained from the turbines of turbochargers. If these reductions, based on existing results, are put together with truck coasting noise levels (5, 6) two possible combinations of noise sources, to achieve 80 dB(A) at 7.5 metres, might be:-

	70 dB(A)	70 dB(A)
Fan	70	74
Engine Exhaust	70	74
Engine Intake	65	65
Coasting Noise 30-40 miles/hr	73	75
Engine Noise	77	74
TOTAL	79.7	79.8

Clearly these levels can only be used as guides, and an allowance for variation between samples has to be made for each individual contribution, as the degree of variation is not necessarily the same for all noise sources.

It seems not unreasonable therefore to expect the noise radiated by the engine surfaces to contribute between one quarter and one half of the total vehicle noise power. This would set target levels for engine noise between 6 and 3 dB(A) below the vehicle noise limits.

In the common situations where noise from diesel engines is obtrusive, it is often made worse by the impulsive character of "diesel knock". If the character of the noise could be altered until it was not obtrusive, this would constitute an improvement in the noise. However, while this is easy to state in qualitative terms, it is very difficult to put numbers to such subjective assessments. British Standards suggest that noises which contain a predominant tonal or impulsive component should be considered as the equivalent of a continuous, broad band, noise 5 dB(A) more intense (7). It seems worth taking any opportunities which arise to reduce such impulsive or tonal components in order to improve the character or quality of the noise, and to reduce the nuisance or disturbance which such noises may cause.

ORIGINS OF DIESEL ENGINE NOISE

Noise radiated by the engine surface originates from:-

1. Combustion
   compression, combustion and expansion transient pressures acting on cylinder head and piston top face.
2. Mechanical
   (i) piston slap against cylinder wall.
   (ii) timing gear rattle.
   (iii) fuel injection pump torque reaction applied to engine structure.
   (iv) inertia forces due to acceleration of piston and connecting rod applied to main bearings.

Some of the processes which combine to produce these force pulses are complex. The shape and size

of the cylinder pressure pulse, which determines the noise originating from the combustion process, can be altered dramatically by many factors. In a direct injection diesel engine, fuel which is injected and mixed during the ignition delay period*, profoundly affects the shape of the cylinder pressure pulse; and the fuel which is burned before the cylinder pressure reaches its peak value controls the peak height of the cylinder pressure pulse. To be more specific, the peak rate of heat release determines the rapid rise in cylinder pressure which occurs immediately after ignition. The peak in the heat release is the result of fast combustion of the fuel which has been injected and premixed with the air during the ignition delay period. The rapid pressure rise after ignition contributes most of the energy in the high frequency components of the Fourier Analysis of the periodic diesel cylinder pressure pulse (8). The fuel which is premixed during the ignition delay period, and hence the peak rate of heat release and peak rate of increase of cylinder pressure, depend upon:

1. Duration of ignition delay period, which in turn depends upon:
   (a) Temperature and pressure of intake air.
   (b) Engine compression ratio.
   (c) Heat imparted to air charge during induction and compression, by engine surfaces.
   (d) Cetane number of fuel.
2. Fuel quantity injected and mixed with the air charge which in turn depends upon:-
   (a) Rate of fuel injection, which is likely to vary the ignition delay period.
   (b) Fuel spray velocity, and proportion of fuel deposited on combustion chamber wall, and/or distributed in regions of mixture which are too lean to burn.
   (c) Droplet size and spacial distributions.
   (d) Air motion such as swirl, squish, subsidiary and transient vortices and turbulence.
   (e) Air charge temperature and pressure.

Much research remains to be done in the field of diesel combustion, but some of the more important factors which control the noise originating in the combustion process are summarised in Fig. 3.

The major mechanical noise sources in current conventional diesel engines are usually impacts between working parts and the structure, such as piston slap and timing gear rattle. These impacts occur as clearance, or backlash, is taken up when forces, or torques, change direction. The sum of the gas and inertia forces acting on the piston changes sign or direction, several times during the engine cycle, causing the crown or skirt of the piston to move across the clearance and strike the cylinder wall. Timing gear rattle occurs as backlash in the timing gear train it is taken up during torque reversals between gears which are providing the cyclically varying torques required to drive the valves and fuel injection pump. The forces generated by the combustion and mechanical noise sources are applied to the engine structure, causing vibration of the moving parts and the crankcase/cylinder-block casting. These components have to be stiff enough to prevent excessive deflection under gas and inertia forces; and they transmit vibration from the sources to the external surfaces of the engine (9 and 10). Figure 3 indicates how the vibration energy may travel through conventional engine structures. This vibration excites resonances in the surface structures such as cast panels, cast metal covers and sheet metal covers. The resulting vibration levels of the thin section areas of the engine surface are sufficient to radiate noise of considerable intensity. The dynamic magnification factors of the resonances in conventional engine structures are usually in the range of 5 to 40 (10); so the normal modes of the cast panels and covers control the noise radiated by the engine surfaces. Each normal mode has a radiation efficiency and directional radiation. The effects of radiation efficiency can be seen in Figure 4 where the noise 0.9m from an engine is compared with the "noise radiating potential" of the engine surfaces. The maximum mean square surface velocity (normal to the surface) of each panel was multiplied by the density of air (ρ) and the speed of sound in air (c) to give the notional sound intensity which would be radiated by each panel if the radiation efficiency were unity (noise radiating potential). The surface velocity varied over the audio frequency range, so the procedure was applied to 1/3 octave band filtered velocity levels. The low efficiency of noise radiation below 1600 Hz can be seen from Fig. 4. A typical cylinder pressure spectrum is plotted in Fig. 4 to show the relative importance of attenuation of vibration within the engine structure, by the processes summarised in Fig. 3, and the inefficient radiation of sound at middle and low audio frequencies for a conventional inline, U.K. truck engine. The symbols for maximum surface vibration (noise radiating potential) indicate the areas with maximum vibration levels in each 1/3 octave band. Up to 800 Hz, the sump vibrates most; from 1 to 2 kHz, the side covers predominate; between 2 and 5 kHz, the crankcase panels, front (timing) cover, side cover, water jacket panels, intake manifold and rocker cover all contribute significantly; above 5 kHz the intake manifold surfaces predominate.

It is more convenient to refer the noise radiated by an engine to a constant spectral level of cylinder pressure when working on the engine structure, and this is the Structure Response for the engine, which is inversely proportional to structure attenuation. Some examples of the structure response functions of engines measured at Acton are shown in Fig. 5.

There is a strong commercial pressure to optimise specific power (in terms of both linear dimensions and weight), reliability and efficiency of truck engines. This leads to similar peak cylinder pressures, scantling thicknesses, rated speed and external cast panel dimensions. Furthermore metal flow considerations in conventional casting techniques restrict the minimum panel thickness. It is not surprising therefore

* Ignition delay period is measured in degrees crank angle between the beginning of injection, with a rate greater than 0.5 cu.mm. of fuel per degree crank angle and the beginning of the rapid pressure rise after ignition.

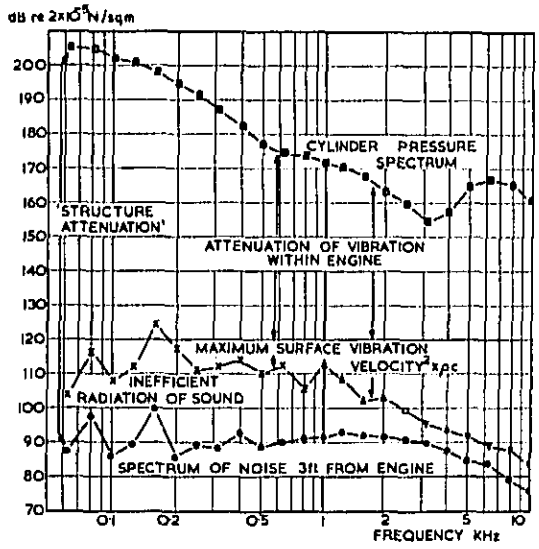

Fig. 4 - Structure attenuation

that truck engines from different manufacturers have crankcase and water jacket panel resonances in similar frequency ranges. Furthermore noise from conventional valve gear covers, sump, crankshaft pulley etc., have so many resonances in the mid and high audio frequency range that together they radiate noise over a broad spectral band. Much of the vibration damping for these resonances comes from the joints with the cylinder block casting which are, in principal, common to many conventional designs. Thus the structure responses of conventionally constructed truck engines will show much similarity of level and frequency dependence as shown in Fig. 5 (unless treated as described in Ref. 9).

The structure attenuates the combustion pressure signals very considerably at low frequencies, but the structure response increases rapidly to a peak near 2.5 kHz for the following reasons:-

1. For automotive engines, the piston, connecting rod, and crankshaft have a fundamental resonance in the region of 2 to 3.5 kHz, depending upon their size (9).

2. The surface structures of the engine, that is crankcase and water jacket panels, valve gear covers, and timing covers, have strong panel resonances above 1 kHz on many engines. (Engine flexural modes and sump panel resonances often occur below 1 kHz.)

3. The acoustic radiation efficiency of the stiff panels, and at higher frequencies the more flexible covers, increases with frequency to reach a peak at 1 kHz or above.

DETERMINING THE RELATIVE IMPORTANCE OF COMBUSTION AND MECHANICAL NOISE

The structure response of an engine exerts a controlling influence over the noise radiated by the engine surfaces. The structure response to combustion pressure pulses is different to that for piston slap and different again for timing gear rattle, it is impossible to ascertain the source of the noise by subjective judgement of the noise, or by spectral analysis of many, if not most, diesel engines. The measurements to compare noise contributions from combustion and mechanical sources should be carried out with the engine running, to ensure that changes in clearance between working parts due to temperature effects are minimised. Fortunately there is a simple means for varying combustion noise at source, which allows simple and rapid correlation of changes in external noise with changes in combustion noise. It is possible to separate combustion and mechanical noise as defined above, by recording cylinder pressure and external noise simultaneously, as the injection timing of the engine is varied over an extended range. As the injection timing of a diesel engine is advanced, the noise from the combustion process becomes larger at a rate much greater than the increase of noise from mechanical sources (9). The noise external to the engine will consist of combustion noise plus contributions from the various mechanical noise sources. As the level of combustion noise is increased, by advancing the injection timing, the level of external noise will remain approximately constant if mechanical noise is predominant and will rise when combustion noise is predominant. If both the cylinder pressure pulse and the external noise signals are subjected to spectral analysis, as illustrated in Fig. 4, the Structure Attenuation (or Structure Response) spectrum may be found from the difference in decibels between the two spectra at each frequency. It is preferable to use a narrow band analysis for both spectra, alternatively a Transfer Function may be found if a suitable analyser is available. When combustion noise is predominant, the structure attenuation will remain constant, as the injection timing is advanced. If mechanical noise makes a significant contribution to external noise, the structure attenuation measured will be less than

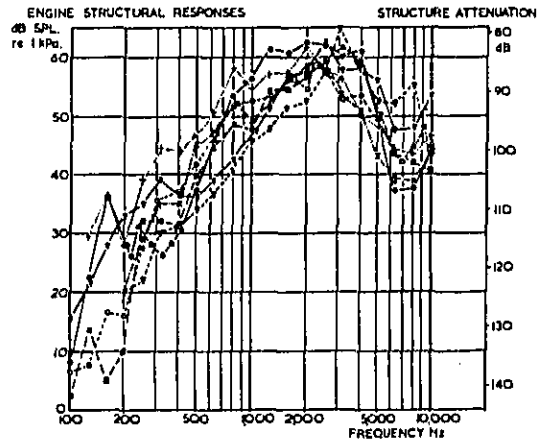

Fig. 5 - Structure responses of in-line truck and tractor engines

the "true" structure attenuation. As the injection timing is advanced the structure attenuation will increase until the combustion noise becomes predominant. Thus the true "maximum" structure attenuation is found by progressively advancing the injection timing. When the injection timing is subsequently returned to that specified for each speed for best fuel consumption, low emissions, etc., the contribution to the external noise from the combustion process may be found by subtracting the "true" structure attenuation spectrum from the cylinder pressure spectrum at the desired timing.

This process is illustrated in Fig. 6 using overall noise levels in dB(A). The actual noise level measured (solid points on graph at 5^{o} timing intervals) was a combination of combustion noise and timing gear rattle. The contribution from the combustion process (aa) was calculated from the cylinder pressure spectra at each timing and the "true" structure attenuation spectrum from a very advanced timing. The resulting noise spectrum was A-weighted and summed to give dB(A) values. It was noticed that combustion noise contributed less than 77.5 dB(A) to the total noise of 93 dB(A) at 5^{o} ATDC timing. The mechanical noise level must therefore be 92.9 dB(A) at this timing. It was assumed that this mechanical noise level remained constant as the injection timing was advanced, and the contributions from combustion sources (aa) and mechanical sources (bb) were added, to give the calculated total noise shown as the solid line in Figure 6. This curve is a tolerable mean level for the experimental points, which suggests that the assumptions were reasonable. The levels of mechanical and combustion noise contributions at normal running timings, between 15 and 20^{o} BTDC, can be read off from "aa" and "bb" in Fig. 6. Mechanical noise was predominant at these timings. This technique was used to find the mechanical noise of several engines under full load steady speed running conditions.

The relative importance of mechanical noise and combustion noise has been determined for a number of engines in the last few years. The mechanical noise levels for these engines are shown in Figure 7 and a typical combustion noise at high speeds. However, the lowest published levels (11) and a set of results from a 1 litre direct injection engine which was both run and

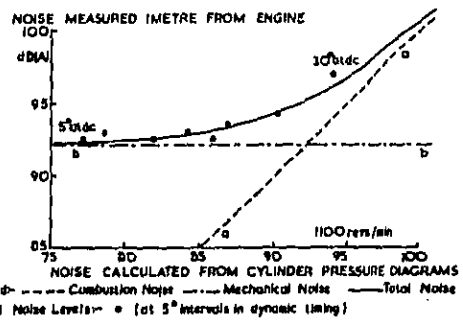

Fig. 6 - Source diagnosis by variation of injection timing

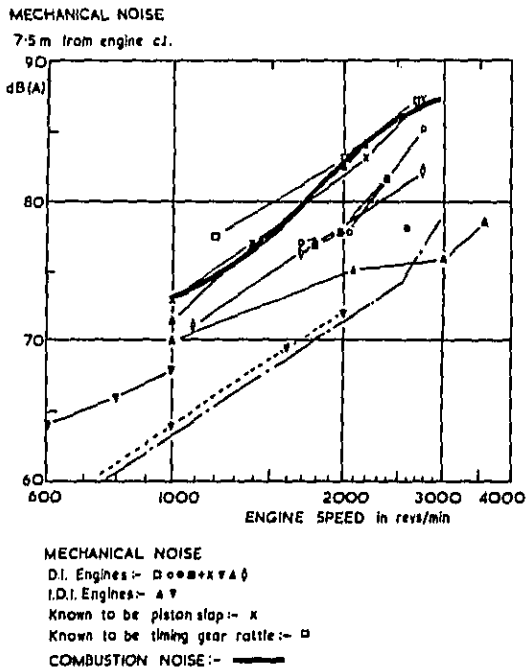

Fig. 7 - Mechanical noise levels of diesel engines measured at Acton

motored, show that lower mechanical noise levels are achievable. These results have been corrected for test cell acoustics, and the noise level at 7.5 metres has been estimated from test bed measurements, assuming simple hemispherical radiation. 15 dB(A) was subtracted to convert corrected test cell levels to estimated levels at 7.5. This includes directivity and ground plane reflection but ignores the partial shielding of the of the engine which leaves the sump the most important radiator of noise in many truck installations. The sum of combustion and mechanical noise levels in Fig. 5 may be compared with the target levels in Fig. 2. Any shielding from the truck or coach body will give additional noise reductions of up to 3 to 6 dB(A) for simple side shields (12, 13).

MECHANICAL NOISE CONTROL AT SOURCE

It appears from Fig. 7 that there is little point in reducing combustion noise at present since mechanical noise is predominant in so many engines. However, engines exist in volume production with conventional components which do not give rise to high mechanical noise levels, and much work is being done to control mechanical noise (14, 15)

Toothed rubber belts are becoming an acceptable alternative to gears for the small diesel engines used in cars and light vans. In two cases with which Lucas CAV have been associated,

reductions of at least 7 dB(A) have been achieved at and near idling conditions by changing from a gear to a toothed rubber belt timing drive. The timing drives for truck engines, and particularly heavy duty types, have to transmit higher torques with a longer life than light vehicle engines, so other means of control may be more attractive, such as:-

1. Reduction in cumulative backlash between gears in timing drive by close control of machining tolerances.
2. Lightweight, low-inertia gears.
3. Gears made from materials with inherent resilience (Tufnol, or moulded plastics), or gears with anti-backlash devices.

It seems likely that further advances in the analysis of structural dynamics of engines could suggest ways in which timing gears might be mounted, which would minimise the injection of vibratory forces into the engine structure.

The other major mechanical noise source is piston slap which has been the subject of considerable investigation. It is well known that piston slap noise may be reduced considerably by reducing the clearance between the piston and the bore over the temperature range through which the piston and bore have to operate. This implies control of the expansion of the piston to match that of the bore. Other workers (16, 17) have indicated that articulated pistons, pistons with offset gudgeon pins or angled rings, can reduce the severity of piston to cylinder impacts. Yet another approach is to cushion the impact between piston and wall with various forms of resilient construction (17). It seems likely that the choice between such alternatives will be made on the basis of a "trade-off" between noise control and friction horsepower. Piston slap is probably the mechanical source which will prove most difficult to treat.

Noise control from the fuel injection equipment has been the subject of intensive research at Lucas CAV (18), and two quiet fuel pumps are in volume production. Both these pumps cater for the top end of the market, but the principles embodied in them can be applied to other pumps in the Lucas CAV range. The fuel injection pump causes a sudden torque reaction which is a direct result of the requirement to inject fuel rapidly into the cylinder, for a short period during the engine cycle. It is important that the pump is mounted in such a way that it does not excite significant vibration in the engine structure. This is the subject of another investigation at present, which will be reported separately.

The ultimate limit on control of mechanical noise at source may be the forces developed at the main bearings in order to accelerate the connecting rod and piston during their reciprocating action. At high engine speeds, the higher harmonics of this force could excite structural resonances. The excitation levels will rise rapidly with speed because the forces themselves increase with the square of rotational speed, and their spectra attenuate rapidly with frequency. This might give rise to a Minimum Mechanical Noise level (MMN) for any particular engine structure, which cannot be bettered. Apart from using lighter components and restricting the engine speed, the only practical way to reduce noise from this source is by control of the structure response, which has been the subject of considerable investigation in the past (9, 10, 19). A lot of work is being done to control mechanical noise at source and if, as seems likely, this work is successful, some comparable reduction in combustion noise will be required.

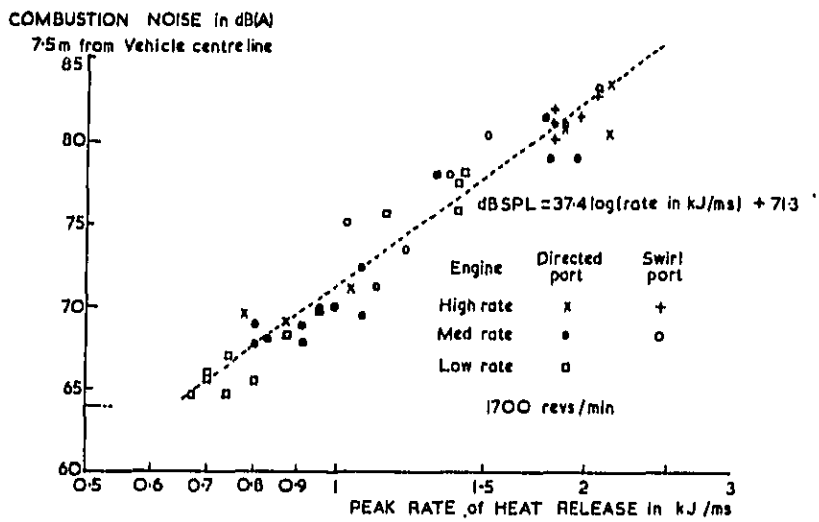

Fig. 8 - Relationship between combustion noise and peak rate of heat release for two naturally aspirated direct injection engines

COMBUSTION NOISE CONTROL AT SOURCE

The noise from the diesel combustion process is usually said to be loud because fuel injected and mixed during the ignition delay period burns immediately after ignition, giving a rapid increase in cylinder pressure which is a salient feature of many diesel cylinder pressure diagrams. At advanced timings this rapid rate of pressure rise may become the dominant characteristic of the cylinder pressure diagram, and it has been used by some workers as a measure of combustion noise. However at retarded timings, and when smooth cylinder pressure pulse diagrams are being investigated, the peak rate, and the average rate, of pressure rise have proved unreliable as a measure of combustion noise.

In a study involving two direct injection engines of similar size but with different combustion systems, the effect of peak rate of heat release per unit time was investigated. One combustion system utilised directed ports to achieve air motion in the combustion chamber and the other used swirl ports, shaped like part of a snail shell, to achieve a different air motion which promoted better mixing. The cumulative heat release was calculated from recordings of cylinder pressure diagrams, and the rate of heat release was calculated from the cumulative heat release. In all cases only one sample diagram was used for each computation, whereas it is desirable to compute an average of twenty heat release diagrams, as is the Lucas CAV practice for combustion noise calculations. The rate of heat release was calculated at intervals of 0.7 crankshaft degrees, giving adequate definition of the rate of heat release diagram. The engines were run with conventional fuel injection equipment (medium rate of injection) and a high rate of injection system which has been devised for low emissions engines. The directed port engine was also run with a low rate of injection and an experimental pilot injection system to extend the range of results towards the quietest combustion diagrams obtainable. The noise levels computed from the cylinder pressure diagrams are plotted against peak rate of heat release in Fig. 8 for both engines, and all injection systems. There is a close relationship between combustion noise and peak rate of heat release in these results over a 20 decibel range.

When the swirl port engine was run at different speeds, the combustion noise (uncorrected for speed) was plotted against the peak rate of heat release in kilo Joules/millisec., in Fig. 9. There appears to be a close relationship between combustion noise and peak rate of heat release over the speed range 1100 to 2800 revs/min for this engine. Furthermore, the best straight line through this set of data gives a very similar line to the best straight line through the data of Fig. 8. This suggests that the peak rate of heat release is closely related to the combustion noise over a very wide range of combustion noise levels, and therefore over a very wide range of cylinder pressure diagram shape.

Four of the heat release diagrams which were used to give the peak rate of heat release are shown in Fig. 10 (the timings quoted are nominal, set at the pump). With conventional injection systems the peak rate of heat release reduces rapidly as the injection timing is retarded. If a number of these curves are plotted together, the peak rates of heat release follow a smooth curve closely. Another feature of these diagrams is the very similar shape of the initial heat release for the directed port engine and the swirl port engine, with conventional (single) fuel injection per stroke. Thus peak rate of heat release

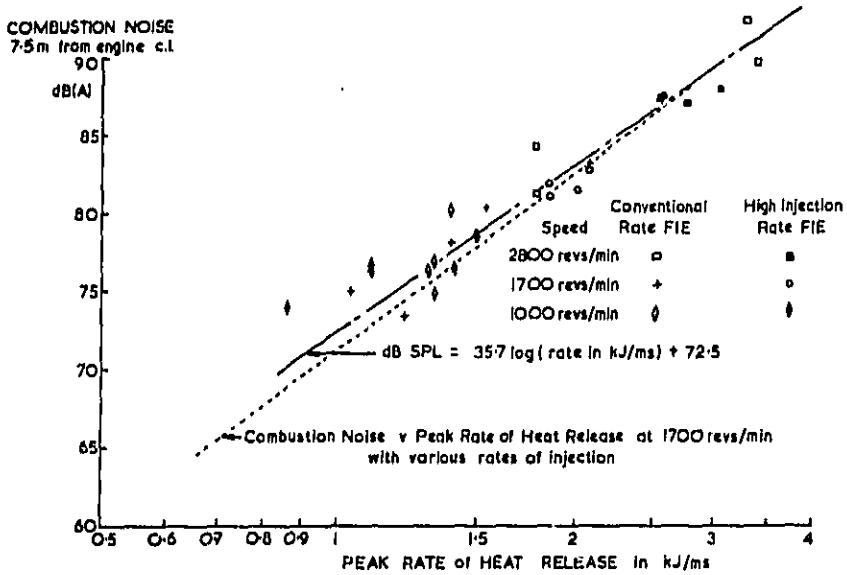

Fig. 9 - Relationship between combustion noise and peak rate of heat release: swirl-port

describes the cumulative heat release in the first five degrees crankangle of the heat release diagram for both engines with conventional injection systems. Furthermore since the peak rate of heat release reduces smoothly with timing, there is a relationship between peak rate of heat release and the fuel injected before top dead centre.

With very smooth cylinder pressure diagrams, the noise level tends to be controlled by the peak cylinder pressure. Since such smooth diagrams have to be produced by heat release diagrams which have no large peak in the early stages of combustion, the heat release tends to vary much less around, and shortly after, top dead centre by comparison with those for conventional DI engines. Hence the heat release before top dead centre, or some similar measure, may be closely related to the peak cylinder pressure. The heat release diagram for the experimental pilot injection system at 15° BTDC timing for main injection, shown in Fig. 10 has an initial rate of increase for the rate of heat release which is similar to that of the diagrams for conventional fuel injection systems. It seems possible that the peak rate of heat release may be closely related to the peak cylinder pressure by reason of this symmetry; so the relationship with combustion noise from typical naturally aspirated cylinder pressure diagrams is more complete than is the case with

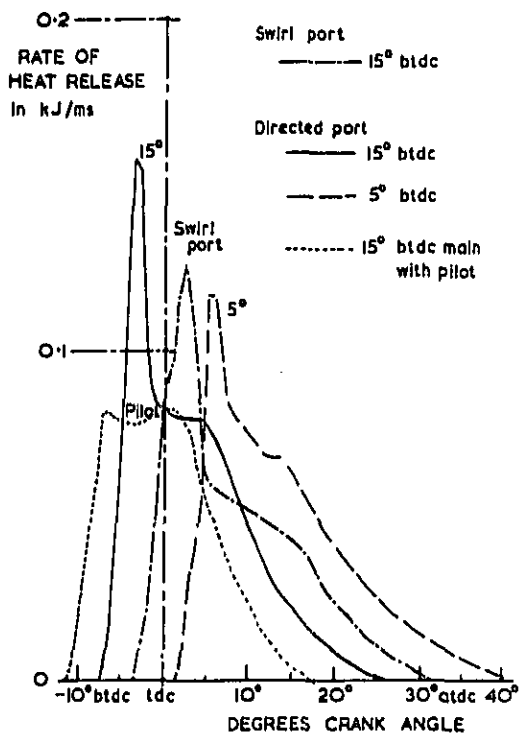

Fig. 10 - Smoothed heat release diagrams

peak rate of rise of cylinder pressure.

A series of "theoretical" heat release diagrams were constructed to explore the relationship between combustion noise and peak rate of heat release, over a wider range of diagrams than is possible with experimental results from currently available engines and fuel injection systems. With the aid of a digital computer, they were combined with a 16:1 compression ratio combustion system to give a series of computed cylinder pressure diagrams. The combustion noise which would be generated by such diagrams was calculated using the same structure response as used for the experimental results. The theoretical cycle efficiency was computed assuming no heat loss or gain to the combustion chamber walls. Figure 11 shows three typical diagrams, which were arranged to have heat release over a long period (in terms of crank angle) to explore the possibilities of very quiet combustion noise levels. Values for efficiency at 10° ATDC are shown on the timing swings, together with the timings required to achieve a cycle efficiency of 0.55. The maximum noise levels produced by the heat release diagrams with a peak rate of 0.17 kJ/°ca (that is 2.86 kJ/ms.) reproduces the results of Fig. 9 tolerably well. (The calculated results were for 2800 revs/min.) As the peak rate of heat release is reduced, the noise level reduces in the same way as those shown in Figs. 8 and 9. However when the middle and bottom diagrams are compared, the noise levels generated are 5 to 12 dB(A) different, even though they have the same peak rate of heat release. If however noise is compared with the cumulative heat release in the first few degrees after ignition, then the noise levels produced at a timing of 5° before top dead centre (start of heat release timing) relates closely to cumulative heat release up to 9° after ignition. Clearly this relationship does not hold as the heat release (or injection timing), is swung over a wide range relative to the compression curve, as shown by the timing swings in Fig. 11. Despite the considerable influence which peak rate of heat release, or cumulative heat release during the early stages of combustion, has on combustion noise, no unique relationship has been found which covers all likely parameters. Peak rate of heat release may be used as a guide to reduce combustion noise but it cannot be used as a predictor by itself. It does not therefore provide a target for combustion noise.

It is interesting to note that the widely differing heat release diagrams of Fig. 11 can give cycle efficiencies of 0.55 if a sufficiently early timing is selected, at the expense of 6 dB(A) increase in combustion noise as the timing is advanced from 4° to 16° BTDC. No account has been taken of the smoke output from the heat release diagrams shown in Fig. 11, which would probably be considerable. In order to achieve rather more practical diagrams which might lead to a target for combustion noise, a series of cylinder pressure pulse shapes were produced with heat release diagrams which were short in duration.

Two sets of diagrams were produced which had combustion pressure rises which varied over a wide range as shown on the cylinder pressure diagram in Fig. 12 by the differences between "aa" and "bb". One set of diagrams had a peak cylinder pressure of

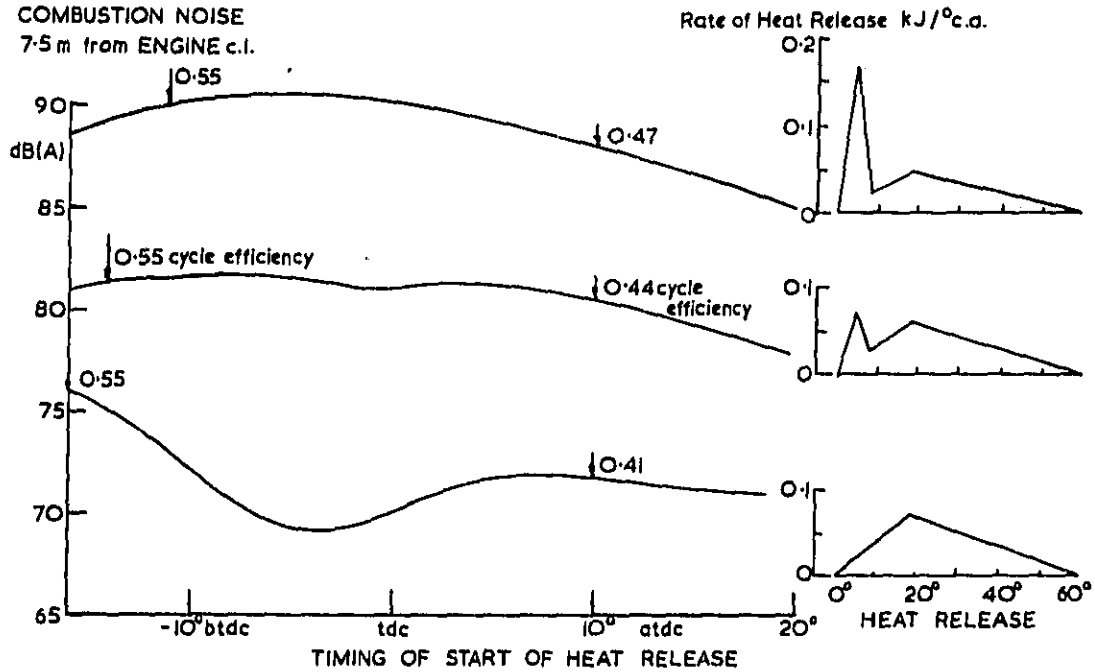

Fig. 11 - Noise from theoretical heat release diagrams over a wide timing range 2800 revs/min SA2

10 MN/sq.m. (1450 Lb/sq.in.) and the other set had a peak cylinder pressure of 9 MN/sq.m. (1305 Lb/sq.in.). The effect of varying the rate of pressure rise after ignition on the combustion noise calculated from the complete cylinder pressure diagram, using the same structure response as used for the experimental results, is shown in Fig. 12 also. In order to remove unwanted effects from very high harmonic components caused by sharp edges in the diagrams, the cylinder pressure pulse diagrams were smoothed by a weighted average before the estimates of combustion noise were made. As the graphs in Fig. 12 show, the rate of pressure rise is the dominant characteristic above 7 MN/sq.m. per ms., and that the effect of peak cylinder pressure becomes dominant at lower rates of pressure rise. Since the aim of engine designers is usually to achieve a high efficiency within the structural constraints of peak cylinder pressure, the range of peak cylinder pressure chosen was limited. When different engines are being compared, however, a much wider range of peak cylinder pressure can be encountered, and the effect of peak cylinder pressure on combustion noise over the whole range of available engines may be considerably more than that shown in Fig. 12.

All the test results in this paper were obtained with U.K. diesel fuel with a Cetane Number of 53. Reduction of Cetane Number to 40 would add 3 dB(A) (20).

MINIMUM COMBUSTION NOISE LEVEL

In order to establish an ultimate target for combustion noise, the noise which would be radiated by an engine in response to the smoothest cylinder pressure diagram which can be obtained in an engine with fixed compression ratio has been calculated. The factored compression curve represents one of the smoothest diagrams which may be achieved, and it simulates the expansion curve which may be expected with a given compression ratio. Even when displaced somewhat from top dead

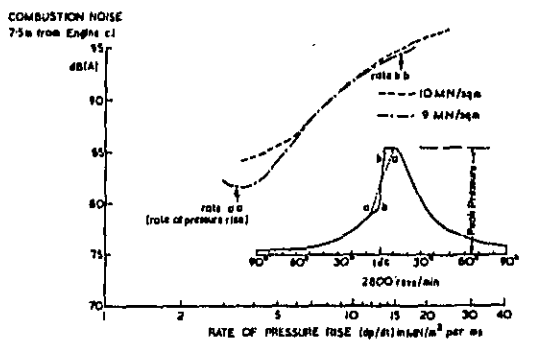

Fig. 12 - Combustion noise from cylinder pressure diagrams with various rates of pressure rise and the same peak pressure

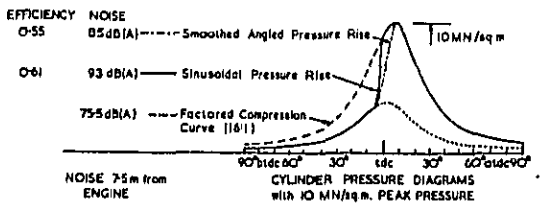

Fig. 13 - Noise levels calculated from some theoretical cylinder pressure diagrams

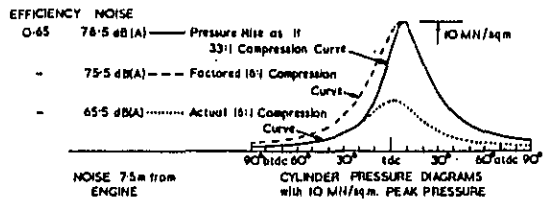

Fig. 14 - Noise levels calculated from some theoretical cylinder pressure diagrams

centre, it is impractical for thermodynamic reasons as the diagram in Fig. 13 shows. In order to retain a smooth expansion curve only small displacements from top dead centre may be tolerated so the net work with such a diagram would be small, taking into account the "negative work" done on the working fluid before top dead centre. Furthermore it would be extremely difficult to produce the controlled heat release from 90° before top dead centre to give an exact factor of the compression curve. However it does

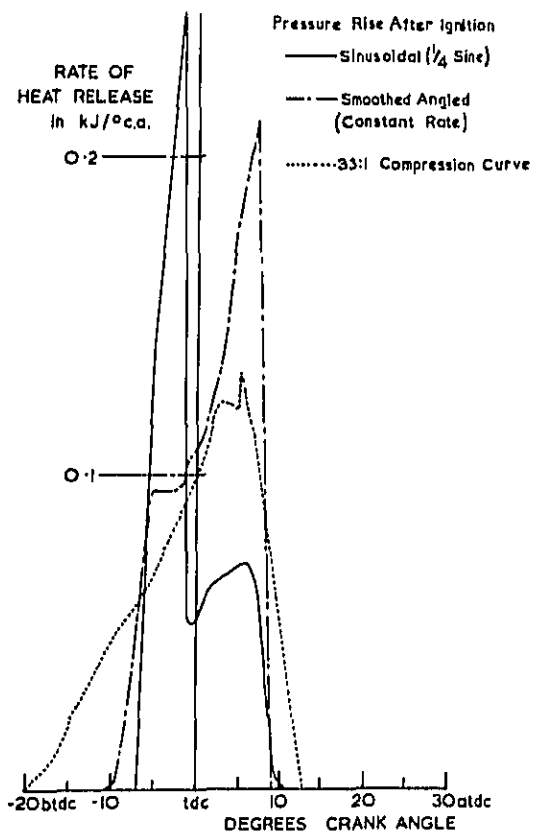

Fig. 15 - Heat release diagrams for 2800 revs/min theoretical cylinder pressure diagrams

represent the minimum achievable noise level with a given compression ratio and peak cylinder pressure, and for the purposes of assessing the combustion noise produced by other cylinder pressure pulse shapes, it is useful to define this as the Minimum Combustion Noise level (MCN). It has been assumed that the designer will aim for an efficient engine within the constraints imposed by structure of the engine, so all comparisons have been made with the same peak cylinder pressure (10 MN/sq.m. or 1450 Lb/sq.in.). Such an assumption effectively fixes the quantity of nitric oxide produced by the engine.

The best of the constant rate of pressure rise (smoothed, angled, pressure rise) diagrams from Fig. 12 was compared with a quarter sine pressure rise and the factored compression curves in terms of combustion noise and cycle efficiency. Neither of the more practical diagrams approaches the low noise level of the factored compression curve (MCN) in fact the constant pressure rise diagram is over 10 dB(A) louder. If the pressure rise is calculated as if it were a compression curve of 33:1 to give the appropriate peak cylinder pressure, followed by a 16:1 expansion curve, the noise level approaches that of the factored compression curve more closely. Such an approach requires a much more carefully tailored heat release diagram and this may present practical problems. The heat release diagrams for these theoretical cylinder pressure curves are shown in Fig. 15. In two cases the heat release has been completed shortly after its peak value, at 7° ATDC, which would make for low smoke levels. The 33:1 compression curve requires a steadily increasing rate of heat release, with a very much slower initial slope, than has been achieved with the practical diagrams in Fig. 10. This suggests that considerable development of the conventional diesel process would be required to achieve such a diagram, involving perhaps assisted ignition and control of the heat release by rate of injection and/or mixing.

There is a 10 dB(A) difference between the actual compression curve and the factored compression curve due to peak cylinder pressure differences, as shown in Fig. 14. If the peak cylinder pressure is allowed to fall, at some conditions of load and speed, then a further reduction in noise may be expected below that from factored compression curve (MCN). However, this would detract from other aspects of the performance, notably efficiency. It is proposed therefore to take the factored compression curve as a target level for combustion noise of typical diesel

engines with a compression ratio of 16:1 when running under full load conditions.

ENGINE NOISE UNDER TRANSIENT CONDITIONS

Much work has been done on engine noise with the engines running at steady speeds and constant loads on test beds. However the vehicle noise legislation requires the vehicles to be accelerated over a test track at full fuelling with an intermediate gear ratio selected. (e.g. the middle ratio.) The engine speed will vary over approximately the top quarter of its speed range during such a test, and if the approach to the test is prolonged, or if the engine has been idling for some time previously, the engine may be appreciably cooler than it would be under steady speed, full load, conditions in a test cell.

In an attempt to test the importance of this effect, an engine was accelerated from idling to rated speed, with full fuelling. The load varied up the speed range as the water brake used provided little load at low speeds and the load built up rapidly with speed. The noise was recorded continuously, during the acceleration, on a magnetic tape recorder, and it was plotted against speed on a graphic level recorder. The spot levels for constant speed, full load, conditions were recorded and plotted with the same equipment. When the engine was allowed to idle for five minutes before each acceleration test the noise external to the engine exceeded the noise produced under steady speed conditions by approximately 4 dB(A) as shown in Figure 16. In a second acceleration test, the engine was run at rated speed, full load, until the oil and coolant temperatures had stabilised, whereupon the engine was held at idle for no more than five seconds before commencing the acceleration test. The noise levels measured outside the engine in the "hot" acceleration test were very close to those measured under steady speed conditions except at 1000 revs/min, where they were lower as shown in Fig. 16. The engine was cooler when running at 1000 revs/min under full load, (with the test cell cooling system) than it was during the hot acceleration run.

One of the reasons put forward for this noise increase has been the increased clearance between components, such as the piston and bore, due to differential expansion (12). However work in progress at Acton suggests that combustion noise increases also under transient conditions. When setting target levels for combustion noise, some allowance will have to be made for the transient effects unless methods of control of combustion noise overcome the increase in noise level due to transient conditions as well as reducing steady state noise levels. Alternatively if better thermal control of the engine can be achieved, the increasing combustion noise due to transient conditions may be minimised.

When an engine is fitted with a turbocharger, the transient performance is often limited by the rate at which the turbocharger may be accelerated to provide additional air flow, and in some cases boost pressure. If a turbocharged engine is run with a lower boost pressure than was intended for the (steady speed) design conditions, the noise level from the combustion process will increase. This increase will be particularly marked if the engine has been designed with a low compression ratio and high boost pressure. The effect is analogous to running a simple engine and turbocharger combination at part load, when the noise level rises above the full load level (20). Such problems may be overcome with waste gates or more sophisticated turbocharger systems, but otherwise an allowance should be made for transient tests over steady state results, amounting to as much as 5 dB(A) for turbocharged engines and perhaps 3 dB(A) for naturally aspirated engines with a 16:1 compression ratio.

COMPARISON OF COMBUSTION NOISE FROM DIRECT INJECTION ENGINES, MINIMUM COMBUSTION NOISE AND TARGET LEVELS DERIVED FROM LEGISLATION

An assessment of the ability of current and future engines to meet proposed legislation may be obtained by generating curves of combustion noise versus engine speed from theoretical and measured

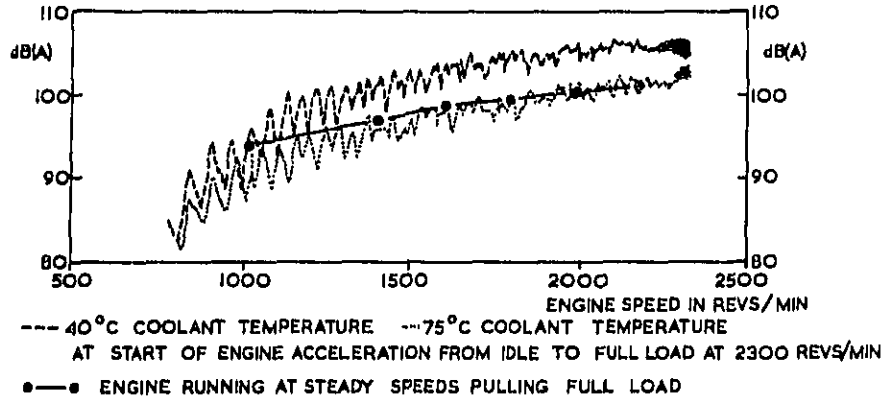

Fig. 16 - Effect of water temperature on engine noise during free acceleration

cylinder pressure diagrams. A "Minimum Combustion Noise Level" has been obtained from the factored compression curve appropriate to peak pressures and compression ratios of typical U.K. truck engines. These noise levels may be compared with estimates of probable limiting levels of noise for engines which are installed in vehicles, which have to conform to future noise legislation requirements. The combustion noise levels from a current, conventional, naturally aspirated direct injection engine with pilot injection, and a turbocharged engine, are compared with the probable engine noise levels required in the foreseeable future in Fig. 17. The direct injection engine with pilot injection is within 7 dB(A) of the Minimum Combustion Noise Level over most of the speed range and the turbocharged engine (which had effectively the same level of turbocharging over the whole speed range) comes within 4 dB(A) of the Minimum Combustion Noise Level at high speeds.

The lowest mechanical noise level which has been found in the literature has been plotted in Fig. 17 also. This level should be added to the combustion noise levels (giving approximately 3 dB(A) increase in the level of turbocharged engine in the speed range 2000 to 2500 revs/min.) to obtain the total noise from the engine. When this total noise is compared with the probable noise from engines which will be required to meet future noise legislation, it can be seen that the turbocharged engine could just meet the 1988 requirements, and both engines could meet the 1983 requirements, under steady speed, full load conditions. The proximity of the Minimum Combustion Noise curve to 69 dB(A) at 2800 revs/min indicates how difficult it will be for combustion systems to be quiet enough to meet the proposed legislation without sacrifice of efficiency (by reducing the peak cylinder pressure) or reducing the compression ratio and increasing the boost pressure (which will require extra equipment for starting). It is also clear that the lowest published mechanical noise levels will prevent the achievement of the probable levels of engine noise required to meet the suggested vehicle legislation levels, with conventional engine structures. Furthermore any increase in combustion noise under transient conditions, as in the drive-by test, would prevent turbocharged or naturally aspirated direct injection engines from meeting these levels, with conventional structures. It seems unlikely, therefore, that control of combustion noise at source alone will allow truck engines to meet the probable requirements derived from the suggested limits for legislation on vehicle noise for 1988, without going to less efficient engines or lower compression ratios. Furthermore, the lowest mechanical noise levels, which have been published so far, exceed these levels.

So far no account has been taken of the known effects of improvements to the structure of conventional truck engines. These reduce the resonances of the surfaces of the engine, and retune certain important noise radiating normal modes to frequencies where they radiate noise less efficiently. Previous work (10) has shown that 5 dB(A) reductions in overall noise, whether mechanical or combustion in origin, may be achieved by developments to conventional engine structures. These developments involve re-engineering the cast panels, cast metal covers and sheet steel covers which comprise much of the surface structure of the engine. The modifications to crankcase and cylinder block castings were designed to fit into the constraints of the existing transfer lines.

Such improvements to conventional structures would enable engines with quiet combustion systems, as indicated by the turbocharged and experimental pilot injection curves in Fig. 17, to meet the suggested future limits. Furthermore no account has been taken of the possible shielding from vehicle structures and truck cabs. Fairly simple modifications to cab structures to shield, rather than enclose, the engine might achieve reductions of the order of 3 to 6 dB(A) without adversely affecting the accessibility of the engine. It seems possible therefore that engines with quiet combustion systems and matching low mechanical noise levels, with some structural improvement or shielding, might meet the probable noise levels for engines derived from the suggested future legislation limits. Since the sources of "diesel knock" would have been treated in such engines, and particularly if the structural resonances of the engine are damped as well, it seems likely that the noise will be less offensive subjectively, which will give an additional significant improvement in the noise environment in urban areas.

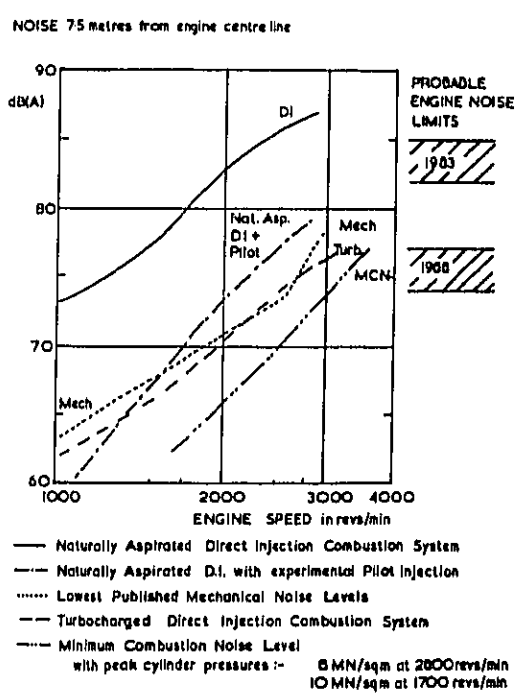

Fig. 17 - Simulated combustion noise levels for 1 litre/cylinder diesel engines

ACKNOWLEDGEMENT

The authors would like to thank the directors of Lucas Industries and Lucas CAV Limited for permission to publish this paper. They are pleased to have the opportunity of thanking Messrs A J Herbert, G P Bulfour and J D Wake of Lucas Industries Noise Centre, Mrs S Kennedy, Miss A Dore, Miss N Hutchinson, and Mr L Piasecki of Lucas CAV Research Department, and Mr W May and Mr D Lemon of SCRD Limited for their invaluable assistance.

REFERENCES

1. Minutes of meeting of Council Ministers of EEC, 8th March 1977 concerning Directive 77/212/EEC amending Directive 70/157/EEC and letter to U.K. Truck Manufacturers from U.K. Department of Transport VSE 780/2, 4 Oct. 1977.
2. EPA Proposed Standards for Medium and Heavy Trucks, Transportation Equipment Noise Emission Controls 40 CFR part 205, Section VII and 205.52 (USA) Federal Register, Oct. 30 1974, Vol. 39, No. 210. FRL 281-6 p 38343 & 38351. Together with 40 CFR 205, published April 13 1977, FRL 511-6 and EPA Proposed Standards for Buses, 40 CFR 205 published Sept. 12 1977, pt IV, FRL 796-3 pp 45777.
3. P.E. Rentz, D.P. Pope, "Description and Control of Motor Vehicle Noise Sources". BBN Report 2739 NCHRP 3-7/3, Vol. 2 of Establishment of Standards for Highway Noise Levels, Feb. 1974.
4. R.E. Hunt, F.C. Kirkland, and S.P. Royle, "Truck Noise via Diesel Exhaust and Air Intake Noise". Report No. DOT-TSC-OST-73-12. Department of Transportation, Transportation Systems Centre, Cambridge, Massachusetts.
5. D.G. Harland, "Rolling Noise and Vehicle Noise". Journal Sound and Vibration (1975) 43(2) 305-316.
6. C.H.G. Mills, "Noise Emitted by Coasting Vehicles". Motor Industry Research Bulletin 1970-3.
7. British Standards Institute, "Method for Rating Industrial Noise Affecting Mixed Residential and Industrial Areas". BS4142 1967, Amended 1975.
8. A.E.W. Austen, and T. Priede, "Origins of Diesel Engine Noise". Symposium on Engine Noise Suppression, Oct. 1958, Proc. Istn. Mech. Engrs., London 1959, 173 19.
9. M.F. Russell, "Automotive Diesel Engine Noise and its Control". Paper No. 730243, SAE Int. Automotive Eng. Congress, Jan 1973, Detroit.
10. M.F. Russell, "Reduction of Noise Emissions from Diesel Engine Surfaces", Paper No. 720135, SAE Automotive Engineering Congress, Jan 1972, Detroit.
11. E.W. Huber and E. Wodiczka, "Bestimung des Verbrennungsgerausches von Dieselmotoren mit Vershiedenen Verbrennungsverfahren". MTZ 33, 9, Sept. 1972.
12. B.J. Challen, "The Effect of Combustion Systems on Engine Noise". Paper No. 750798 in SP397, SAE Diesel Engine Noise Conference, Milwaukee, Oct. 1975.
13. D.T. Aspinall, and J. West, "The Reduction of External Noise of Commercial Vehicles by Engine Enclosure". Motor Industry Research Association Report No. 1966/17.
14. T. Usami, S. Wada, and S. Sonoda, "Piston Slap Noise of Indirect Combustion Diesel Engines". Paper No. 750801 in SP397, SAE Diesel Engine Noise Conference 1975.
15. S.D. Haddad, "Some Methods for Controlling Impact Noise in Engines". Internoise 77, Zurich March 1977.
16. R. Munro and R. Parker, "Transverse Movement Analysis and its Influence on Diesel Piston Design", Paper No. 750800 in SP397, SAE Diesel Engine Noise Conference, Milwaukee, Sept. 1975.
17. M.D. Rohrle, "Affecting Diesel Engine Noise by the Piston". Paper No. 750799 in SP397, SAE Diesel Engine Noise Conference, Milwaukee, Sept. 1975.
18. M.F. Russell, "Noise Control Stategy for Manufacturers and Users". Paper No. C252/77 at I.Mech.E. Conference "Limiting Noise from Fans, Pumps and Compressors". London, Oct. 1977. Published by Inst. Mech. Engrs.
19. T. Priede, A.E.W. Austen and E.C. Grover, "Effect of Engine Structure on Noise of Diesel Engines". Proc. Inst. Mech. Engrs. 1964-5 Vol. 179, No. 4.
20. M.F. Russell, "Recent CAV Research into Noise Emissions and Fuel Economy of Diesel Engines". Paper No. 770257, SAE International Automotive Eng. Congress, March 1977, Detroit.

790272

PISTON MOVEMENT AND ITS INFLUENCE ON NOISE OF AUTOMOTIVE ENGINES

W. Sander, W. Steidle and E. Wacker

Karl Schmidt GmbH
Neckarsulm (Germany, W.)

ABSTRACT

This paper compares the calculated and measured piston transverse movement in a spark ignition engine. The induction of engine vibrations by the piston slap is studied by measuring the lateral forces at the piston skirt during the impact on the cylinder. The application of a piston movement computer program for piston development is demonstrated in the case of engine noise due to piston top land slap. The pressure differences in the main combustion chamber of an IDI-diesel engine are measured, and the effect on the piston attitude is analysed. Examples of low-noise piston design for diesel engines are presented.

LOW PISTON NOISE IS GIVEN a most careful attention in automotive engines of today. Due to the high rated speed of those engines the mechanical noise becomes predominant compared to the combustion noise. The piston noise is part of the overall engine noise which makes the identification by measuring techniques very difficult. Radiated noise spectra do not give concise information about the piston as a source of noise. The human ear is often used to detect piston noise by its typical sound. This method applied either on the test bed or in the vehicle is suitable as a final check but not sufficient as tool to determine the mechanisms of piston-induced noise. An alternative approach therefore is made by analysing the dynamics of the piston moving in the cylinder. This method explains the piston slap as one of the origines of mechanical vibrations in the engine structure.

PISTON TRANSVERSE MOVEMENT DYNAMICS

Both analytical and experimental methods have been applied to study the piston movement for years. Computer programs have been developed which simulate the piston attitude relative to the cylinder wall and allow a quantified approach to the dynamics of piston slap (1, 2, 3, 4, 5, 6, 7, 8, 9)*. In this way a number of design and operation parameters have been analysed in respect to the impact of piston slap on mechanical engine noise. Data of piston transverse movement measured in the engine are less completely available which might be attributed to the difficulty and cost of the measuring methods (4, 10, 11, 12). Most comparisons between calculated and measured movements were made for truck diesel engines.

Prospects of the energy situation are favouring the diesel engine and its application in passenger cars. In many cases such engines have been converted from gasoline engines running at high speeds, and generally without major changes of the powertrain components. The research work of which some results will be reported in the following section was undertaken therefore using a watercooled 4-cylinder in-line spark ignition automotive engine, featuring linerless cylinder block design and expansion controlled pistons.

TRANSVERSE MOVEMENT ANALYSIS - The calculation methods used for this analysis have been reported in detail by (5). Fig. 1 reviews the idealization of the piston and the forces considered. In relation to the cylinder wall the piston will have a transverse and a rotational motion as far as clearances and elastic deformations of the piston permit it. The major force is the gas load acting on the piston crown, having an alternating transverse component which is a function of the connecting rod inclination. Gas load and inertia forces originating from the oscillating connecting rod are both acting on the piston pin. The inertia forces of the piston are considered and are acting on the center of gravity.

* Numbers in parentheses designate References at end of paper

SAE/P-79/80/$02.50
Copyright © 1979 Society of Automotive Engineers, Inc.

In addition to those forces which can be determined with great accuracy the influence of friction is also incorporated in the analysis. Estimated friction coefficients are used which may differ significantly from the actual friction coefficients during some portions of the piston movement.

As a further simplification the continuously distributed contact pressure between the skirt and the cylinder is replaced by two discrete contact forces near the top and bottom end of the skirt respectively. It can be checked whether the top land will touch the cylinder wall but no contact forces are assumed to occur in this case.

Piston Clearances at Operating Temperatures - The actual clearances between piston and cylinder evidently have a decisive influence on transverse movements and inpact magnitude. The nominal skirt clearance is existing only at the lower end of the skirt and in the cold engine condition. The upper end of the skirt, in this condition, has a larger clearance due to the taper (and barrel) skirt profile, as shown in fig. 2 for the test piston. It is useful also to take wear and plastic deformation of the skirt into account.

A thermal expansion test rig is used in order to determine the hot piston profile. In this rig the operational temperature distribution in the piston is simulated by heating the crown and cooling the skirt. As it is to be seen in fig. 2 the clearances are significantly reduced, even at no load operation. The cylinder distortions are not regarded in fig. 2. At full load, the diameter of the lower skirt end comes into interference with the cylinder wall.

Cylinder Distortion - The assembling forces between cylinder block and cylinder head are responsible for the cylinder deformation which was measured as shown in fig. 3. The piston is affected only by the cylinder deformation measured in the thrust direction (fig. 3 a) having a roughly conical expansion of the bore diameter in the upper third of the cylinder with 0.04 mm maximum. The thermal distortion of the cylinder profile is estimated to be conical with an additonal expansion at the top of 0.03 mm. Deformations due to the cylinder pressure during combustion are not considered. The cylinder profile evaluated so far is incorporated in the analysis.

Skirt Flexibility - The skirt of low-weight automotive engine pistons has a flexibility which cannot be neglected. There are two basic modes of elastic skirt deformation as shown in fig. 4. An interference (overlap) between the piston skirt and the cylinder exists due to differences in thermal expansion, mode 1, which then reduces the initial ovality of the skirt, and causes prestressing at the thrust sides of the skirt. The lateral components of the connecting rod forces acting on the piston pin cause the skirt to deflect according to mode 2. This way the skirt clearance increases at the opposite, unloaded side and the piston tilts due to different stiffnesses of upper and lower end of the skirt. The elastic skirt deformations are measured in a rig applying the skirt load on half cylinders in both modes. The measured deformations of the test piston are also shown in fig. 4.

CALCULATED RESULTS - Results of the analysis will be presented and compared with measured results at full load and a speed of 3000 1/min. This load condition was chosen because the piston noise of the test engine was most critical there. The piston pin was offset 1.3 mm to the major thrust side.

Lateral Forces - They are displayed in fig. 5 a) for the upper and lower end of the skirt. The prestressing force acting on the lower end of the skirt due to the overlap, shown in fig. 2, is not incorporated in this plot.

Transverse Movements - The piston transverse movement is plotted in respect to three planes, i. e. bottom skirt, top skirt, and top land. All plots represent the movement of the piston center in the respective plane.

At the lower end of the skirt (fig. 5 b) the piston center performs part of its movement while the skirt is still in contact with the cylinder wall. This part of the movement is marked by the hatched area which represents the width of interference between the lower end of the piston skirt and the cylinder.

If the lateral forces exceed the prestressing force, the unloaded side of the skirt moves away from the cylinder wall. When the lateral forces then decrease and the skirt comes into contact with the cylinder, an impact is occuring.

The movement of the upper end of the skirt (fig. 5 c) consists of an unrestricted transverse movement within its clearance and an additional elastic deformation during cylinder wall contact (see hatched area). The calculated movements of the skirt ends correspond to the respective lateral forces shown above.

The movement of the top land (fig. 5 d) is derived from the calculated skirt movements. It is very similar to the movement of the upper end of the skirt. However, the amplitudes are considerably larger due to tilting of the piston.

Impulses of Skirt End Impacts - The transverse velocity of the skirt end at the time of impact combined with the corresponding part of the piston mass is used to calculate the impulse figures shown in the histogram of fig. 5 e). This gives information on time, i. e. the location, and order of magnitude of the impacts during

one engine cycle.

TRANSVERSE MOVEMENT MEASUREMENT - Various alternative methods were reported in the past (1, 10, 13). It was decided to use inductive transducers in the piston and a linkage transmission system for connecting the wires from the piston to the crankcase. The linkage, shown in fig. 6, consists of two rods of which one is connected to the piston pin, the other to the crankcase. The advantage of this arrangement is that very small additional inertia forces are acting on the piston (13) and it allows to run high speed in excess of 5000 rpm. Highly flexible steel cables are used as transmitting wires.

Fig. 7 shows the transducer configuration in the test piston. In each of the two measuring planes a pair of motion pickups is installed. This provides temperature compensation and linearisation of the output signal. The calibration curve is slightly dependant on the clearance. Additionally two pairs of strain-gauges in T-configuration are applied at the skirt end, located in an area where maximum bending strain occurs due to the lateral forces on the skirt. The strain versus force curves allow to determine the dynamic skirt loading from the measured strain.

MEASURED RESULTS - The engine measurements were taken at full load and at an engine speed of 3000 ^{1}/min. The pin of the test piston was offset 1.3 mm to the major thrust side.

Lateral Forces - The plot of measured lateral forces, fig. 8 a), indicates simultaneous loading of both the major and the minor thrust sides during large periods of the engine cycle. This confirms the assumption of prestressing forces originating from the interference of the skirt. To achieve a suitable comparison, the calculated lateral force of the bottom end of the skirt, fig. 5 a), is shown once more in fig. 8 b), but this time the prestressing force is included. The calculated and the measured forces conform fairly in respect to time and amplitude. There is a rapid increase of the lateral force at TDC (firing) which has a steeper angle in the measured plot and shows as well a small vibration at maximum level, indicating impact influence.

Transverse Movements - The measured and the calculated transverse movements of the top and the bottom end of the skirt are compared in fig. 9 a and b. The bottom skirt movements do not conform completely, particularly in the lower part of the cylinder, i. e. near BDC, because the applied transducer configuration cannot transmit the actual elastic motion of the piston center at zero clearance.

The conformity of the measured and calculated top skirt movements is very satisfactory, both concerning the number of side changes and size of amplitudes. In addition the assumption of movements during cylinder wall contact due to elastic skirt deformation is confirmed. The variable movement of the piston during contact is mainly caused by a skirt flexibility and to some degree by the cylinder wall distortion. The measured velocities of the side changes are generally lower than calculated. This effect might be explained by the barrel shape of the skirt profile and by the presence of lubricating oil between the skirt and the cylinder. That means that the actual impulse size of the skirt impacts is lower than the one obtained by the analysis.

The top land movement, shown in fig. 9 c, is again derived from the measured movements of top and bottom skirt end.

VARIATION OF ENGINE CONDITIONS -

Load - The effect of load variation is demonstrated in fig. 10, showing the no load condition at an engine speed of 3000 ^{1}/min. The plot of the calculated movement of the top skirt end correlates well with the measurements (fig. 10 b). Because of the low cylinder pressure at no load the inertia forces (fig. 10 a) are able to initiate an additional couple of side changes near TDC (firing). The motion amplitude is about 20 % lower than at full load. This is caused by the counteracting effects due to the reduced skirt loading and due to higher clearances.

Speed - Fig. 11 shows the effect of reduced speed of 1500 ^{1}/min at full load for the top skirt end, in comparison to fig. 9. The smaller inertia forces result in smaller side change amplitudes at TDC (intake/exhaust) and BDC. The amplitude at TDC (firing) still is high, however, the velocity of side change is lowered significantly. Major impacts at lower speeds are confined to TDC (firing).

EVALUATION OF PISTON SLAP-INDUCED ENGINE VIBRATION

The analysis of the piston transverse movement outputs a large number of impacts of different magnitude. The comparisons have shown that larger impulses are obtained by the analysis neglecting the presence of lubricating oil than by the measurements.

The ability of a piston impact to generate vibration in the engine structure is depending basically on two parameters:

a) the force-time curve during impact

b) the vibrational response of the structure.

Data concerning the force-time curve were obtained by the strain gauge measurements. Supplementary measurements in the test engine were conducted with an acceleration transducer on the major thrust side of the cylinder wall. Records were taken first with the complete set of four pistons and second, after removing the piston of the measured cylinder, with the three remaining pistons. One result of these measurements representing the engine condition full load and a speed of 3000 1/min is shown in fig. 12.

Part of the engine cycle, including the critical side change of the piston at TDC (firing), plottings of the measured piston transverse movement are compared with the measured force versus time curves and the cylinder vibrations. The vibrations, filtered by a 12 to 20 kHz bandpass, indicate an impact about 40° after TDC caused by the piston in the measured cylinder. Regarding the top land movement there is found a good correlation between its side change to the major thrust side (marked by an arrow and the measured impulse at the cylinder.

The top skirt end comes into contact with the cylinder wall about 20° earlier where no cylinder vibration is found. This can be confirmed by analysing the measured side force curve during the time of impact. The duration of the increase of the lateral force, regarded as impact duration, amounts to 5 ms. An impact of this duration will be able to cause vibrations in a structure the resonance frequency of which does not exceed 200 to 400 Hz. The measured resonance frequency of the test engine cylinder is 16 kHz so that no induction of cylinder vibration is to be expected in this case. In this regard it should be noted that engines with wet liners usually have lower resonance frequencies (15).

PRACTICAL USE OF THE PISTON MOVEMENT ANALYSIS

GENERAL CONSIDERATIONS - Using the piston motion computer program it is possible to analyse a variety of parameters in respect to piston noise. The main piston design parameters are listed in table 1. Engine operation parameters like speed, load or transient conditions may be considered as well as engine design parameters like cylinder distortions, connecting rod length and weight or cylinder pressure variations.

Predicting noise from the program output data one has to observe the natural limitations of the analysis. It has been demonstrated in the above section that a skirt impact will not necessarily create vibrations in the engine structure. On the other hand, vibrations of the cylinder wall do not in every case significantly contribute to the noise radiated from the engine surface.

All those factors which determine the effect of a piston slap on the radiated noise may be summarized in a complex piston noise transfer function of the engine. Having generally no analytical knowledge of this function, practical noise experience of the studied engine is required.

If piston noise is occuring in an engine the piston motion program could be advantageously applied to analyse the noise generating pattern of the piston as well as to study the influence of the actual design variables at critical engine conditions. This is to be shown in the following section reporting a practical case.

ANALYSIS OF A PISTON NOISE AT COLD START CONDITION - During evaluation tests on a 4-cylinder spark ignition engine a typical piston noise was noticed by listening at the test bed. The critical condition of the engine was experienced after cold start at 50 % load and a speed of 3500 1/min. The piston pin was offset 1.5 mm to the major thrust side. A piston movement analysis was performed basing on the respective piston and engine data. The result is shown in fig. 13. The movement of the piston is plotted relative to the cylinder liner using different lines for the planes of top land, top skirt and bottom skirt on both thrust sides. A histogram of the skirt impact impulses is shown by the side of it. The diagram indicates two alternative sources of piston noise:

a) the impulse of the top skirt 15° after TDC on the major thrust side.

b) the top land contact 10° before TDC on the minor thrust side (arrow).

After disassembling the engine the appearance of the piston ring area, fig. 14 a, verifies the statement (a). Such hard marks, as shown, are typical for a noise-inducing top land slap.

STUDY OF NOISE-REDUCING PISTON DESIGN VARIABLES - Before starting the analysis, a second run using a piston with 1.8 mm pin offset to the major thrust side was made. The piston noise, however, was not significantly reduced. Fig. 15 demonstrates that this result can be predicted by the analysis since the top land still gets into contact with the cylinder. The impulse of the top end of the skirt is neither reduced not changed enough timewise shifting the impact in an area of better lubrication. Based on the analysis it was decided to increase the top land clearance by a fraction of the calculated interference between top land and cylinder. A further increase of clearance was considered detrimental to the sealing effect and the life of the piston rings. In order to reduce the tilting amplitude of the piston and this way to prevent the top land from touching the cylinder wall, the

stiffness of the skirt was increased too.

Fig. 16 shows the analysis of the improved piston. The top land is no longer touching the cylinder. After running the piston ring area, fig. 14 b, is clean which is a sign for a tight fit between top land and cylinder wall, but no hard marks are seen any longer. The noise emission of the engine has been satisfactory since then.

EFFECT OF THE IDI-DIESEL COMBUSTION ON THE PISTON ATTITUDE

In the piston movement analysis the gas loading on the piston is assumed to act on the piston center. This is correct for most spark ignition engines. But indirect injecting diesel combustion systems commonly use a pre-chamber. During compression and especially during combustion an intense gas flow takes place to and from the main combustion chamber. The pre-chamber being located in most cases on the minor thrust side a significant pressure drop from the minor to the major thrust side acting on the piston crown is to be expected.

PRESSURE MEASUREMENTS - In a single cylinder swirl-chamber (Ricardo Comet V) diesel engine pressure measurements have been taken in two locations shown in fig. 17, at various speeds and loads (16). A typical result is presented in fig. 18 for a speed of 4000 ^{1}/min and a mean effective pressure of 4.7 bar. The first line presents the cylinder pressure in location (1), near the throat of the swirl-chamber. The second line presents the differential pressure in respect to the location (2), opposite to the swirl-chamber. If pressure vibrations are neglected, the maximum differential pressure measured is 5 bar. The engine speed is influencing the pressure differential significantly while the load effect may be neglected. The duration of the asymmetrical pressure on the piston crown amounts to about 50° crank angle.

EFFECT ON THE PISTON MOVEMENT - Using the asymmetrical gas load as a function of the cank angle as input in the computer program the effect of the IDI-diesel combustion on the piston movement was studied. A simple linear extrapolation of the measured gas pressure was employed to simulate the pressure distribution on the piston crown.

The result of this analysis is shown in fig. 19 for the case of a pre-chamber located at the minor thrust side. For comparison the effect of a 1.3 mm piston pin offset to both thrust sides is simultaneously shown for the case of symmetrical gas load. It is evident that the pre-chamber combustion has s similar effect as this pin offset to the major thrust side, as far as the crank angle range at and after TDC (firing) is regarded.

From low-noise requirements it is therefore recommended not to use a piston pin offset in IDI-diesel engines. This is contrary to symmetrically burning spark ignition engines which usually have an optimum piston pin offset of 0.8 to 1.5 mm to the major thrust side.

It is assumed that direct injecting diesel engines using excentric combustion bowls in the piston crown also have a certain asymmetrical effect on the piston attitude. However, measured data are not available at this time.

LOW-NOISE PISTON DESIGN

During part-load and transient engine conditions the piston noise is strongly influenced by its clearance. The minimum safe cold clearance of an eutectic all-aluminium piston should be 0.07 % of the cylinder diameter, depending on the cylinder distortions. Using expansion controlled pistons the cold clearance may be reduced to 0.04 % of the cylinder diameter.

Fig. 20 shows an expansion controlled automotive diesel engine piston of 76.5 mm diameter. It has comparable low weight as a full-skirt piston. Unrestricted heat flow from the crown is allowed (no slots). The steel insert supports the loaded skirt area which results in high stiffness required for low tilting under lateral loads. For turbocharged diesel engines a more rigid piston skirt design is necessary like it is shown in fig. 21. This piston of 98.5 mm diameter was designed and successfully tested for a specific rating of 0.3 kW/cm^2 piston area and a peak combustion pressure of 140 bar. In spite of the rigid design a thermal expansion coefficient of the skirt of $16 \cdot 10^{-6}$ mm/mm °C is maintained.

Further design features reducing piston slap and tilting amplitudes are a large guiding length and a cam and barrel profile favouring the lubrication of the skirt. By these means, the increase of clearance by wear is avoided and an optimum damping effect of the skirt by the lubricating oil film is obtained. The top land clearance has to be matched carefully in order to prevent the piston crown from a hard cylinder wall contact.

Nodular cast iron as a piston material is offering an attractive potential for the design of low-noise pistons running in standard cast iron cylinders due to similar thermal expansion rates of both materials. Fig. 22 shows a piston of 85.0 mm diameter for a direct injection automotive diesel engine. The piston requires spray nozzle cooling at the interior surface. There is only a modest increase in piston weight,

because the size of the piston pin may be reduced due to the higher fatigue strength of the nodular cast iron piston pin boss. Furthermore the hot crown of the nodular cast iron piston may help to increase the thermal efficiency of the engine.

CONCLUSIONS

Measured and calculated transverse movements of an automotive engine piston show good conformity at all load and speed conditions. The calculation method based on simplifications like two point support of the skirt and no lubrication is considered to be suitable for automotive applications if realistic assumptions for the piston clearances at operational temperatures and the elastic deformations of the piston skirt are made.

The impact velocities, calculated by the program have a tendency to be larger than in reality. Measured side forces on the piston skirt during impact show a relatively slow increase of force over time which does not cause vibrations in the cylinder. However, if the piston crown comes into hard contact with the cylinder, vibrations and noise are most probably induced.

Data are available on the piston attitude, regarding the effect of the asymmetrical combustion in IDI-diesel engines. For the most common case of the pre-chamber being located at the minor thrust side, no piston pin offset is recommended from a low noise point of view.

REFERENCES

1. A. Meier, "Zur Kinematik der Kolbengeräusche". Automobiltechnische Zeitschrift (ATZ) 54, No. 6, pp 123 - 128, June 1952.
2. E.E. Ungar; D. Ross, "Vibrations and Noise due to Piston Slap in Reciprocating Machinery". Journal of Sound and Vibration, No. 2, 1965, pp 132 - 146.
3. W. Hempel. "Ein Beitrag zur Seitenbewegung des Tauchkolbens". Motortechnische Zeitschrift (MTZ) 27/1, pp 5 - 10, Jan. 1966.
4. A.M. Laws; D.A. Parker and B. Turner, "Piston Movement in the Diesel Engine". 10th International Congress on Combustion Engines, CIMAC Washington, D.C. April 5 - 9, 1973.
5. W. Steidle; e. Wacker, "Kolbengeräusche". ATZ 77, No. 10, pp 293 - 298, Oct. 1975.
6. R. Jacobs, "Ölhaushalt des Tauchkolbens". Forschungsbericht der FVV, Heft 196, 1975.
7. R. Munro; A. Parker, "Transverse Movement Analysis and its Influence on Diesel Piston Design". SAE-paper 750800.
8. T. Usami; S. Wada and S. Senoda, "Piston Slap Noise of Indirect Combustion Diesel Engine". SAE-paper 750801.
9. H. Tschocke, "Berechnung der Kolbenbewegung in schnellaufenden Hubkolbenmotoren unter besonderer Berücksichtigung der Kurbeltriebsschränkung und der Kolbenschaftgeometrie". Automobil-Industrie Vol. 1, pp 59 - 69, 1978.
10. H. Steinbrenner, "Messung des Kolbenringflatterns in schnellaufenden Kolbenmaschinen" MTZ 22 (1961) 7, pp 261 - 265.
11. S. Furuhama "Piston Slap Noise, its Causes and Reduction". Nainen Kikan, Vol. 13, No. 153, July 1974, pp 42 - 52.
12. M. D. Röhrle, "Affecting Diesel Engine Noise by the Piston". SAE-paper 750799.
13. U. Essers, "Meßtechnische Untersuchung der Kolbenquerbewegung an Verbrennungsmotoren". Habilitationsschrift TH Aachen, 1969.
14. S. Furuhama and J. Enomoto, "Die Messung der Kolbentemperaturen eines Benzinmotors im fahrenden Kraftfahrzeug". Transactions of J.S.M.E., Vol. 39, No. 317, Jan. 1973, pp 324 - 337.
15. J. Haasler, "Geräuschverhalten von Viertakt-Dieselmotoren". VDI-Forschungsheft 505/1964.
16. "Simultanious Measurement of Cylinder and Swirl-Chamber Pressures and Pressure Differences in a Small COMET Diesel". D. P. 76/258 Ricardo Consulting Engineers.

Table 1 - Piston Design Parameters in the Transverse Movement Analysis

Piston skirt	clearance profile thermal expansion (control) flexibility total length
Piston pin	offset vertical piston pin position
Piston inertia	total weight vertical position of gravity center offset of gravity center
Piston crown	clearance

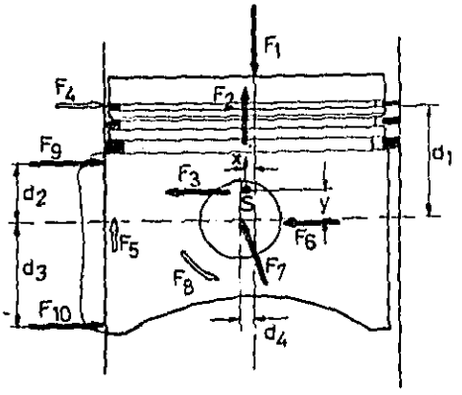

forces due to gas pressure and inertia, supporting forces

friction forces, friction torque

F_1 =	cylinder pressure	F_8 =	friction pin - boss
F_2 =	vertical inertia	F_9 =	top skirt reaction
F_3 =	horizontal inertia	F_{10} =	bottom skirt reaction
F_4 =	friction ring-groove	x, y =	position of center of gravity
F_5 =	friction skirt - cylinder	$d_{1,2,3}$ =	piston dimensions
F_6 =	conrod inertia	d_4 =	piston pin offset
F_7 =	conrod reaction	S =	center of gravity

Fig. 1 - Forces acting on the piston

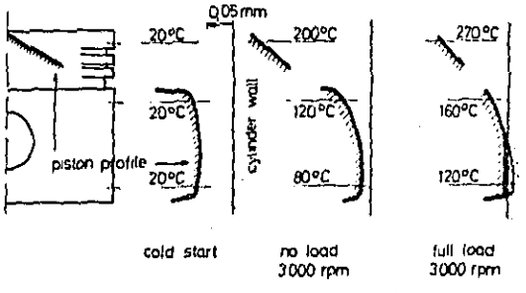

Fig. 2 - Piston temperatures and clearances

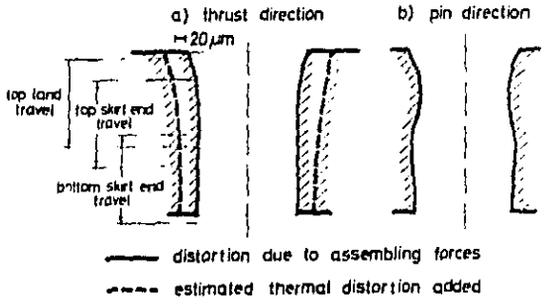

Fig. 3 - Cylinder distortions

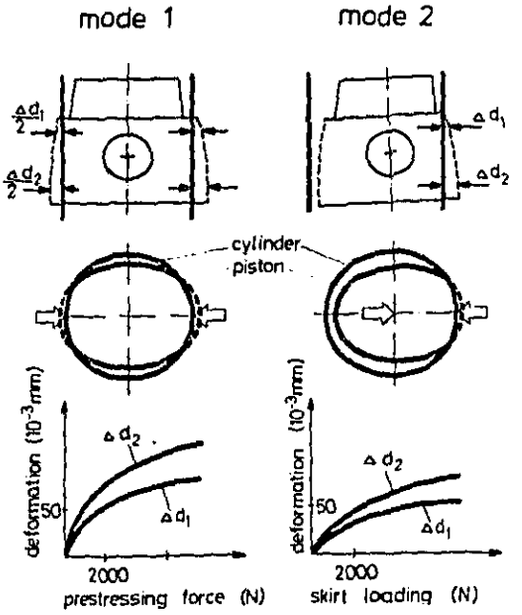

Fig. 4 - Elastic deformations of piston skirt

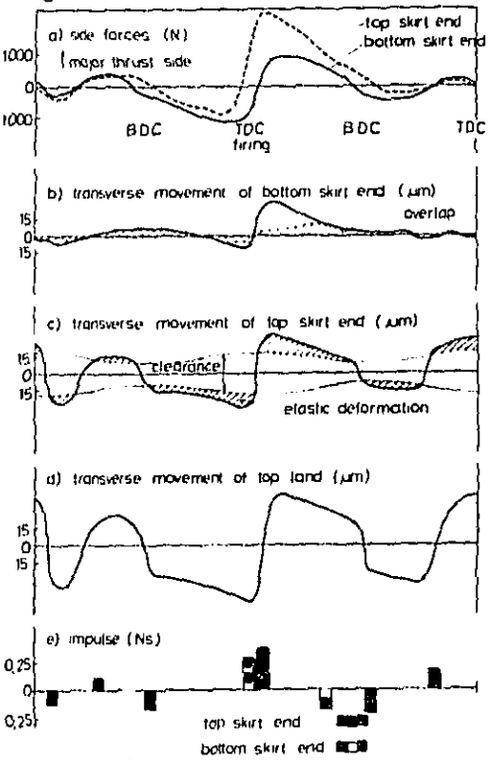

Fig. 5 - Computer program output (full load, 3000 rpm)

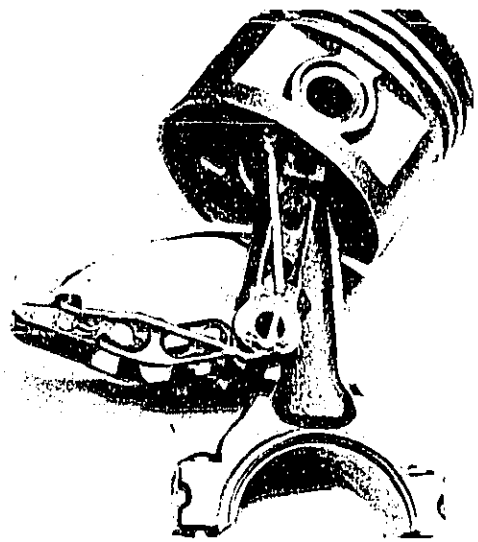

Fig. 6 - Linkage system

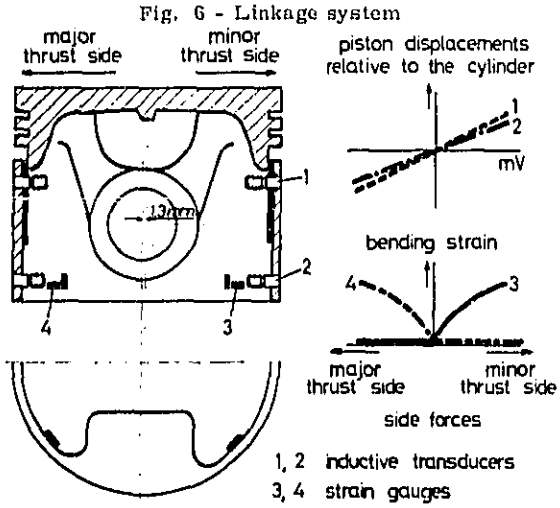

Fig. 7 - Piston with transducers

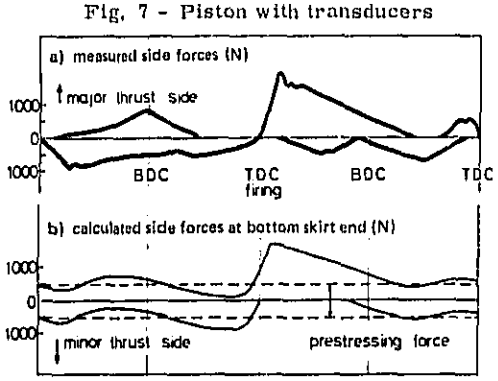

Fig. 8 - Comparison of measured and calculated lateral forces (full load, 3000 rpm)

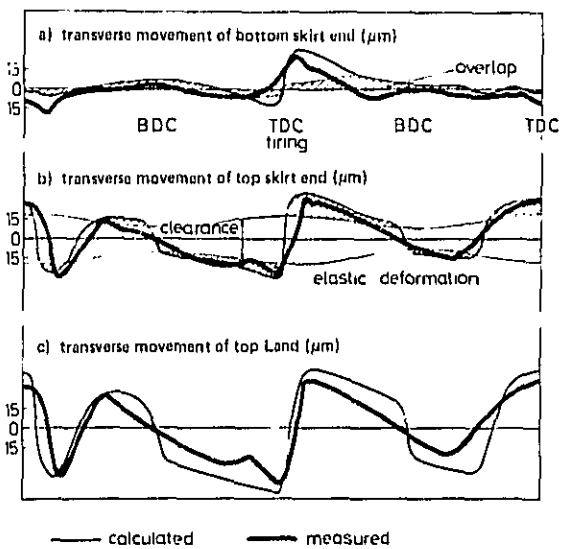

Fig. 9 - Comparison of measured and calculated transverse movements (full load, 3000 rpm)

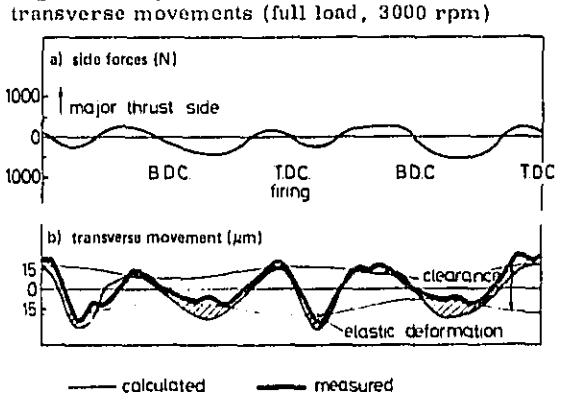

Fig. 10 - Transverse movement of top skirt at varying load (no load, 3000 rpm)

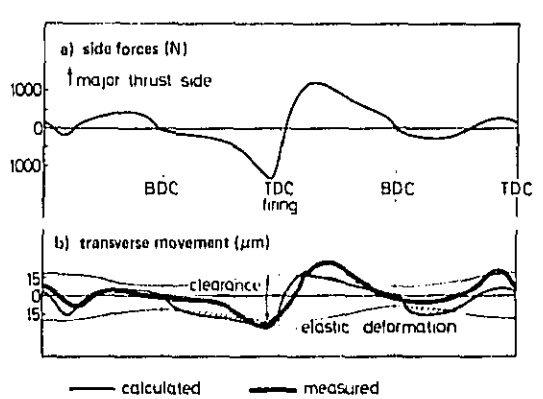

Fig. 11 - Transverse movement of top skirt at varying speed (full load, 1500 rpm)

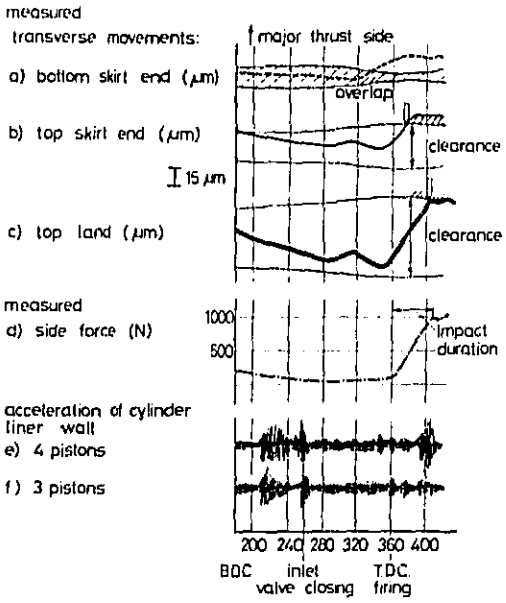

Fig. 12 - Transverse movements, side force and cylinder vibration (measured at full load, 1500 rpm)

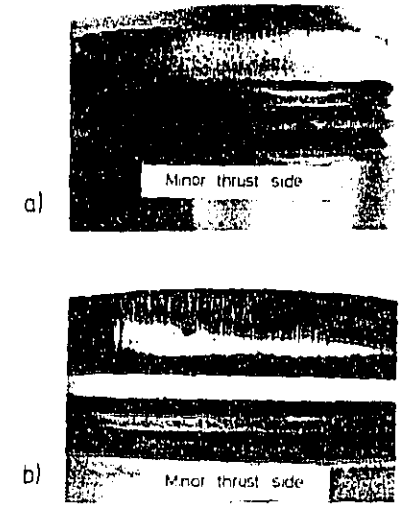

Fig. 14 - Appearance of piston top land (minor thrust side)
a) slap marks, b) improved piston

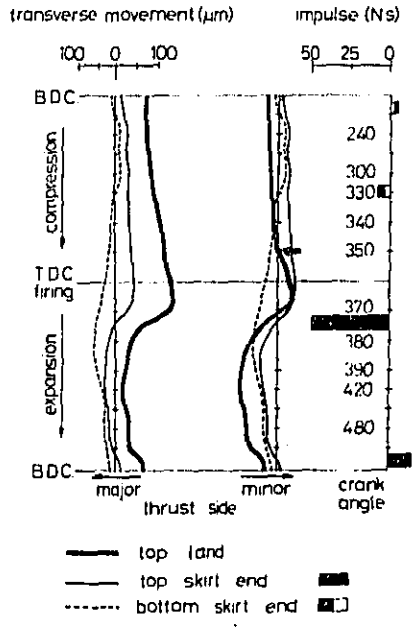

Fig. 13 - Transverse movement plot of noisy piston (half load, 3500 rpm)

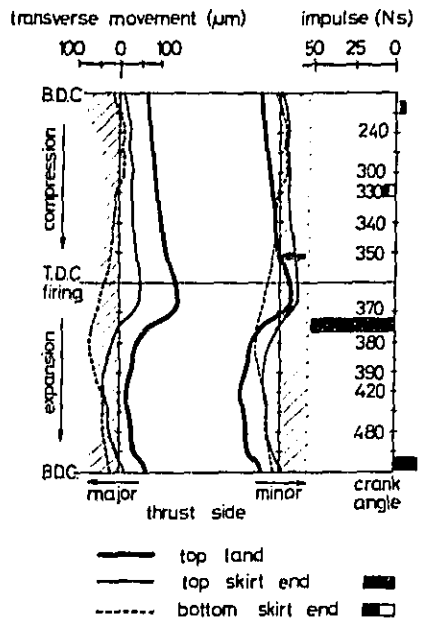

Fig. 15 - Transverse movement plot of piston with increased pin offset 1,8 mm (half load, 3500 rpm)

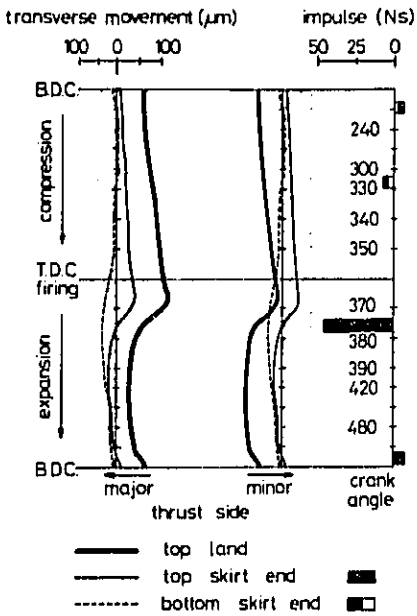

Fig. 16 - Transverse movement plot of improved piston: larger top land clearance and stiffer skirt (half load, 3500 rpm)

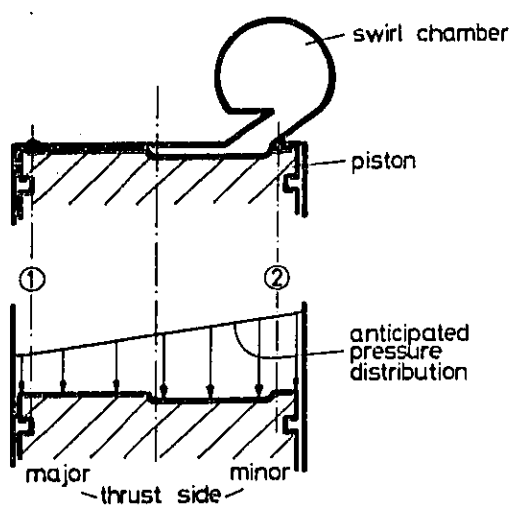

Fig. 17 - Asymmetrical cylinder pressure of IDI-diesel engine

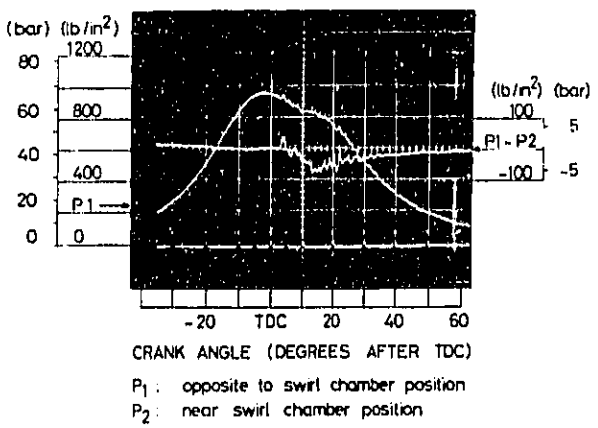

Fig. 18 - Measured cylinder pressures (4,7 bar m.e.p., 4000 rpm, swirl-chamber system Ricardo Comet V b)

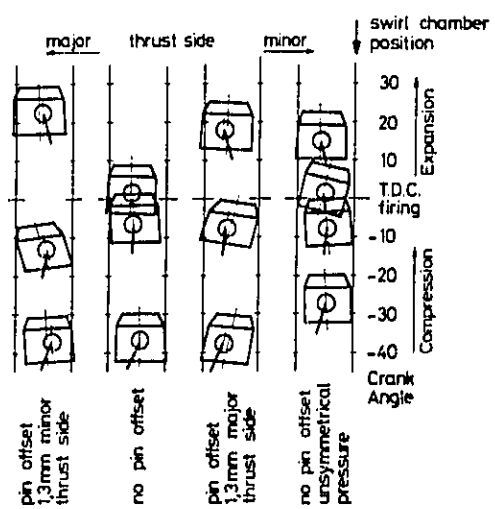

Fig. 19 - Effect of asymmetrical pressure versus piston pin offset on piston attitude (4,7 bar m.e.p., 4000 rpm)

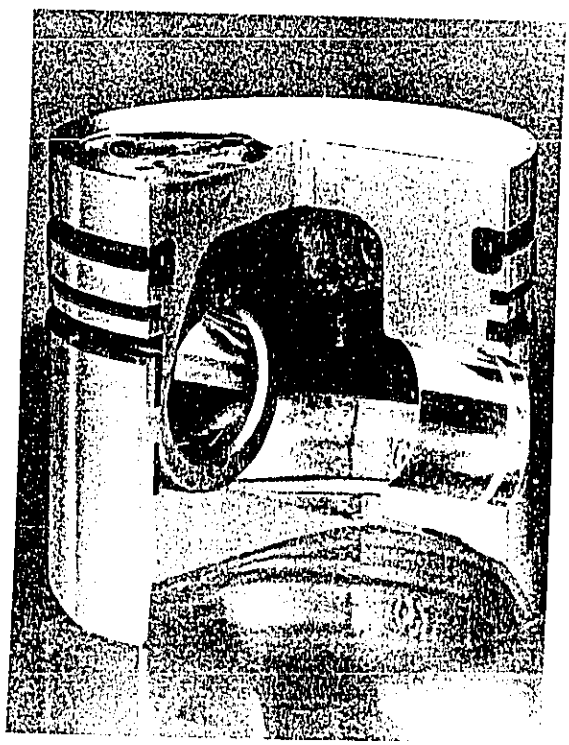

Fig. 20 - Expansion controlled aluminium piston for automotive IDI-diesel engine of 76.5 mm cyl. dia.

Fig. 21 - Expansion controlled aluminium piston for turbocharged diesel engine of 98.5 mm cyl. dia.

Fig. 22 - Nodular cast iron piston for automotive IDI-diesel engine of 85.0 mm cyl. dia.

790273

THE INFLUENCE OF MOUNTINGS ON INJECTION PUMP NOISE

M F Russell, BSc, MSc
Lucas Industries Noise Centre

Lucas CAV Limited, Acton

H L Pullen
Institute of Sound and Vibration Research

Southampton University

ABSTRACT

As new designs of diesel engine, which emit less noise, are evolved to meet increasingly stringent noise legislation, noise from diesel fuel injection equipment could become a significant proportion of the total noise from the engine. Quieter fuel injection pumps are being produced for such engines by Lucas CAV, however their potential will not be realised unless special care is taken in the design of pump drive and mounting brackets. Impacts from the sudden take-up of backlash in the drive to the pump, and vibration of the engine surfaces to which the pump is secured, can increase pump-radiated noise considerably.

RESEARCH INTO NOISE EMITTED BY DIESEL ENGINES has established how the noise originates from combustion, and from mechanical impacts (1,2)*. Further research has shown how noise is transmitted through the engine structure as vibration, (3) and how this vibration excites resonances in the thin-section panels and covers which comprise the external surfaces of conventional engines (4). To meet future legislation, new and improved engine designs can embody one or more of the three basic approaches to structure-borne noise control:-

1. Control at source, of all major sources:-
   (i) Smooth cylinder pressure development (5).
   (ii) Elimination of timing drive impacts (3).
   (iii) Minimal piston slap impacts (6).
2. Quiet structures, either:-
2a Vibration isolation of external surfaces from all sources (7), or:-
2b Combination of treatments for all thin section surface areas of structures:
   (i) Crankcase/cylinder block resonances tuned to frequencies at which excitation is least (4), plus
   (ii) Vibration damping treatments to sump, valve gear covers, etc., when made of flexible sheet material (4), plus
   (iii) Vibration isolation of sump, valve gear covers, pulleys, etc., when made flexurally stiff (4).
3. Enclosures, either
3a Closely-fitting enclosure made from flexible, damped, material which does not radiate sound efficiently, supported from engine via vibration-isolating mounts. Little or no acoustic absorbent in small gap between engine and enclosure (8), or
3b Ventilated sound-proof "tunnel" around engine and gear box, lined with acoustic absorbent (9).

Noise from the fuel injection pump will be attenuated if the engine is enclosed overall. However if either or both of the first two approaches is adopted, the pump will be free to radiate noise; and must itself be treated to match the noise reduction of the engine as a whole. To meet this need, new fuel injection pumps have been developed which emit low noise levels (10). These have been developed with the aid of a specially-built "quiet rig" which is described later in this paper, which allows accurate measurement of pump noise to be made. When a fuel injection pump is mounted on an engine, the noise which it radiates may be increased due to vibration originating from the engine. Similarly vibration originating in the pump may cause the engine surfaces to radiate noise.

Quite apart from vibration transfer between pump and engine, the bracket, drive coupling, and other parts of the mounting, may affect the noise generating and radiating properties of the pump itself. The investigations reported here, were aimed at finding the effect on pump-radiated noise of mounting inline pumps to engines.

The paper outlines the noise-generating mechanisms of inline fuel injection pumps, and indicates how these may be affected by future, more stringent, legal limits on exhaust emissions. The techniques used to measure pump-radiated noise in the laboratory and on running engines are discussed in detail, with results for both large and small in-line fuel injection pumps. The technique for calculating pump-radiated noise from surface vibration, was improved to give reliable measurements when the pump was driven by a running engine. This technique was used to compare the noise radiated by a flange-mounted Minimec pump on a truck engine with that from a base-mounted Minimec on an engine of similar size and rating. The pumps were driven by a hydraulic motor on the stationary

* Numbers in parentheses designate References at end of paper.

SAE/P-79/80/$02.50
Copyright © 1979 Society of Automotive Engineers, Inc.

engines, as well as by the usual drive arrangement from the engines when they were running. This enabled the influences of mounting brackets and drives to be separated. In all the diagrams in this paper, solid points indicate engine running, and open points indicate pump motored on a stationary engine.

The differences between the noise radiated from flange-mounted pumps and base-mounted pumps, were considerable; even when one engine was modified to mount the same pump either by its flange or its base. However, other factors affect the pump-radiated noise, and results are given which show the influence of:-

(a) Vibration of engine surfaces to which the pump mounting bracket is secured.
(b) Backlash in the pump drive.

When these effects have been removed by employing the hydraulic drive to motor the same pump in flange and base-mounted configurations on the same stationary engine, there remained a difference between flange and base mountings. The spectrum of the noise from the base-mounted pump was similar to the spectrum of the noise measured from the same pump in the laboratory on a special quiet rig.

NOISE GENERATING MECHANISM

ORIGINS OF NOISE - The diesel fuel injection pump develops high pressure hydraulic pulses, by a cam and roller-tappet which forces a plunger along a barrel which has a radial port drilled part way along the plunger stroke. Fuel trapped above the plunger, as the top of the plunger passes the port, is forced into the injector pipe at high pressure until a helical groove, connected to the fuel space above the plunger by drillings, uncovers the port to release pressure in the barrel. The pressure required to inject fuel into a direct injection diesel engine is usually greater than 200 Bars; and it is commonly 500 Bars on current conventional European truck diesel engines, over much of the load and speed range. Injection pressures are higher for larger engines and peak line pressures of 700 Bars are common for larger pumps.

It is necessary that the hydraulic pressure pulse be terminated abruptly to shut off the flow of fuel into the combustion chamber as quickly as practicable. If fuel is injected into the combustion chamber at a low rate, at the end of injection, it does not mix with the remaining air charge, and it burns incompletely, giving soot which appears as visible smoke in the exhaust. The period of injection is kept short (typically 1 to 2 ms.). When a jerk pump is employed to produce this hydraulic pulse, a large force is developed between the cam and roller which is at an angle to the axis of the tappet. A lateral reaction is supplied by the tappet block to the tappet, and this force has a similar, but not identical, waveform to the hydraulic pressure pulse.

An example of the hydraulic pressure pulse developed in the barrel of an inline pump is shown on the left of Figure 1. When such a repetitive pulse is subjected to Fourier Analysis, a series of spectral lines results, with the fundamental at firing frequency. The lower harmonics are of similar level to the fundamental. Harmonics above the frequency at which the pulse duration is half the period, form a typical pulse spectrum with modulated harmonics. The overall envelope of the harmonics falls at approximately 40 decibels per decade increase in frequency as shown in Fig. 1. Components above 2.5 kHz are below the self-noise of the instrumentation used to measure the pulse shown in Fig. 1. If the pulse were perfectly triangular, it would have a spectrum envelope which

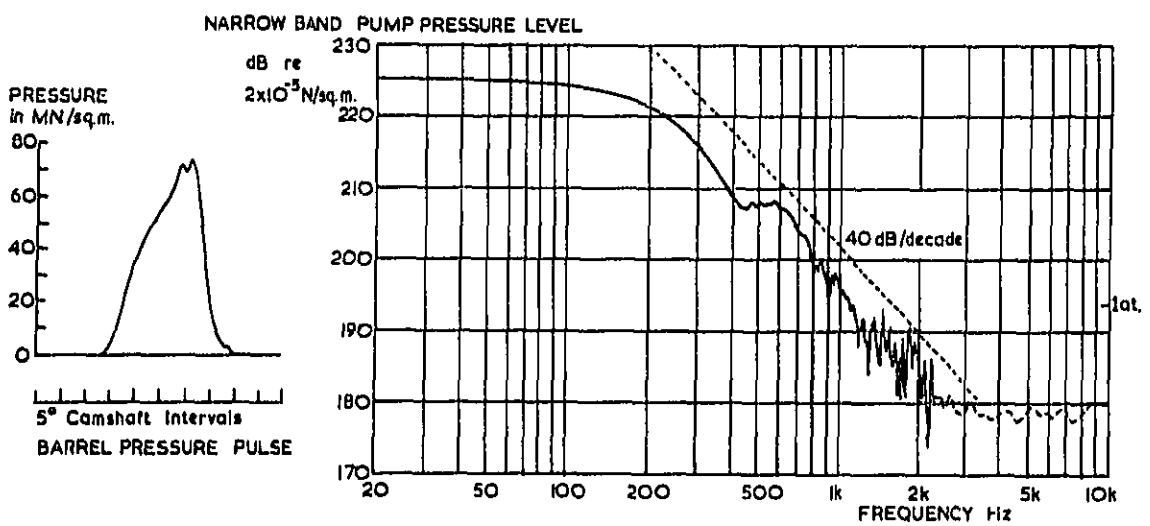

Fig. 1 - Barrel pressure spectrum from an in-line pump at 1100 revs/min

would fall at 40 decibels per decade increase in frequency.

The major noise-radiating resonances of the pump housing, and most other structures attached to the pump, lie in the frequency range between 300 Hz and 5 kHz, so the overall noise radiated by the pump and other structures will rise at 40 decibels per decade increase of speed. (Under full fuelling conditions.)

In addition to the hydraulic pressure pulse excitation, there is a mechanical impact as the delivery valve seats after unloading the high pressure pipe to the injector. To ensure rapid closure of the injector needle, and therefore a "dribble-free" end to the injection, the delivery valve must move rapidly to unload the high pressure pipe, when the pumping pulse terminates. As a result, the impact between delivery valve and seat occurs when the delivery valve is moving at high velocity. The resulting impulsive force is large, and can excite high frequency resonances in the pump and also attached structures. This excitation force is nearly independent of speed and it can become predominant at light load conditions. (When the hydraulic pulse is small by comparison.)

EFFECT OF EMISSIONS LEGISLATION ON PUMP NOISE- In a conventional direct injection engine, much of the mixing between the fuel and the air charge is a result of penetration of the air charge by high velocity jets of fuel in droplet form. The effectiveness of this mixing controls the rate at which the fuel burns; this has a direct bearing on the efficiency of the engine, and the smoke level. The effect of legislation controlling gaseous emissions, such as oxides of nitrogen, is to restrict peak temperatures achieved during the cycle. This is most conveniently achieved in practice by retarding the injection timing. At late injection timings there is a greater tendancy for the fuel injected towards the end of the injection period, to be incompletely burnt. This gives high levels of smoke, unburnt hydrocarbons and particulates in the exhaust. This undesirable consequence of controlling gaseous emissions may be overcome if the mean spray velocity of the injected fuel is increased, to improve the mixing of fuel and air within the plume of droplets formed from each injector hole (11). Research has shown that the rate of fuel injection may be increased, in current conventional diesel engines, to achieve an optimum economy, or low levels of oxides of nitrogen, depending upon the timing of the injection (12). To achieve this increased rate, the hydraulic pressures within fuel injection equipment will increase as conventional combustion systems are developed to meet the more stringent legislation which is proposed to control emissions.

RADIATION OF NOISE FROM PUMP SURFACES - The pump structure as a whole, and in particular the thin-section pump surfaces, respond to vibration which originates from within the pump by deflecting under the applied forces, and resonating in a multitude of normal modes of vibration when the force is suddenly removed at spill. The amplitude of each mode depends upon the level of exciting force at its natural frequency, the point in the normal mode at which the excitation force is applied, and the modal damping factor. These normal modes may be excited also by vibration originating from within the associated engine, via the pump mounting. Similarly vibration originating in the pump may be transmitted via the mounting to the engine, and it may cause the crankcase panels and attached structures to vibrate in their normal modes, to radiate yet more noise. Thus on the running engine, both the pump surfaces and the engine surfaces respond together to vibration developed within the pump and the engine.

MEASUREMENT OF NOISE FROM FUEL INJECTION PUMPS

LABORATORY MEASUREMENTS WITH QUIET RIG - The noise from the fuel injection pump surfaces excited by forces developed within the pump may be measured by running the pump on a "quiet rig". On the quiet rig, every effort is made to ensure that the pump noise may be measured without interference from other vibration sources. Furthermore the rig is constructed to radiate little noise in response to pump vibration. The pump is mounted via solid blocks to a massive cast iron table which is supported on a stiff frame. The pump body is thus rigidly held. The drive torque is supplied from a motor outside the sound-proof test cell in which the rig is situated. A toothed rubber belt connects the primary drive shaft with a secondary (pump) driveshaft which is on approximately the same axis as the pump camshaft. The pump driveshaft, running in stiffly mounted bearings, is equipped with a large flywheel. It is connected to the camshaft of the pump via a special coupling with high torsional stiffness. The coupling consists of two sets of thin spring discs separated by a length of shaft which allows misalignment between pump camshaft and pump driveshaft to be taken up. There is an ISO document for discussion (DIS 4008/1) which lays down stringent limits for the stiffnesses of drives and mountings for fuel injection test equipment. The shafts and structure of the rig are enclosed by sound-proof guards made from a laminate of steel and plastic, which are lined with acoustic absorbent. It is not possible to cover the cast iron table completely without introducing excessively high mounting blocks, but noise from this area has been controlled by careful detail design. The guards are necessary to allow engineers to operate the rig without injury from rotating shafts, belts etc., as well as to reduce the rig noise.

When a new type of pump is fitted to the quiet rig, one of the first measurements is that of "rig noise". For this, the pump is encased in a lead jacket, lined with an acoustically-absorbent plastic foam, to reduce the noise radiated by the pump as much as possible. The remaining noise, measured at the standard measurement positions, is a combination of residual noise transmitted through the lead jacket, and noise from the rig surfaces. Most fuel injection pumps are too small to radiate much noise at low frequencies, and rig noise often predominates up to 200 or 300 Hz. Pump noise usually predominates above 500 Hz when the pump is mounted on the quiet rig. The quiet rig provides a stiffer mounting, and a much larger drive inertia and stiffness, than typical engines. With such a stiff mounting, the hydraulic pulse developed by the pump is likely to be larger and shorter than

when the pump is mounted on a running engine. This will be offset to some extent by the restraint to the pump vibration afforded by the stiffer mounting arrangement.

NOISE FROM A LARGE PUMP MOUNTED ON A PROTOTYPE QUIET ENGINE - The Maximec pump has been developed by Lucas CAV Limited for the quieter engines required to meet future noise legislation. It is capable of injecting 400 cu.mm. per stroke at pressures up to 1000 Bar and is exceptionally quiet for its size. When the noise from a Maximec pump was measured on the quiet rig, it was found to be 11 to 15 dB(A) quieter than the total noise of the large naturally aspirated engine to which it was fitted as shown in Fig. 2a. Noise control treatments had been designed into the structure of the engine by the manufacturers. This foreshadows situations which will be more prevalent when stringent noise limits are enforced.

The surfaces of the engine were covered completely with a sealed lead jacket lined with acoustic absorbent, which reduced the noise by 7 to 10 dB, at and around 1 kHz, and by up to 12 dB at high frequencies. When the pump surfaces were exposed, leaving the lead jacket around the rest of the engine surfaces, the noise measured to the side of the engine might be expected to emanate solely from the pump surfaces. However, the lead jacket (which was much larger than that over the pump on the quiet rig) vibrates as a result of the forces transmitted through the absorbent. Furthermore small "leaks" in the jacket allow more engine noise to reach the microphone than was intended. Both these effects lead to inaccurate results for pump radiated noise. In the current investigations, illustrated in Fig. 2a it has been found that the noise level with only the pump exposed on an otherwise lead jacketed engine, was 1 to 3 dB(A) above the noise when both pump and engine were covered with a lead jacket. The noise radiated from the engine through the lead jacket would have been sufficient to increase the apparent pump-radiated noise from the levels measured on the quiet rig to those measured on the engine, as shown in Fig. 2a. The differences between noise apparently radiated by the pump on a running engine, and the noise when the same pump is mounted on the quiet rig can be seen more clearly from the spectra on the two noise measurements in Fig. 2b. In order to assess the validity of these results, a further measurement of noise radiated from the pump surfaces was made. To obtain this estimate, 1/3 octave band vibration spectra were measured at 29 points on the side of the pump and governor, on the side facing the microphone. These measurements may be made conveniently either with the pump mounted upon the engine or on the quiet rig. The mean square values of vibration acceleration were found in each 1/3 octave band between 100 Hz and 10 kHz. The noise in each 1/3 octave band was estimated from the expression:

$$1/3 \text{ oct. S.P.L.} = 10 \log_{10}\left[\frac{\overline{u^2}\rho c A \eta_{rad}}{2\pi r^2}\right] + D$$

where $\overline{u^2}$ is the mean square vibration velocity, calculated from the measured acceleration values (α) ($u = \alpha/2\pi f$)

ρ is density of air

c is speed of sound in air

A is area of noise-radiating surface

η_{rad} is the radiation efficiency of the normal modes of surface area A.

r is the radius, from pump centre, to the measurement microphone position

d is the directivity factor expressed in decibels.

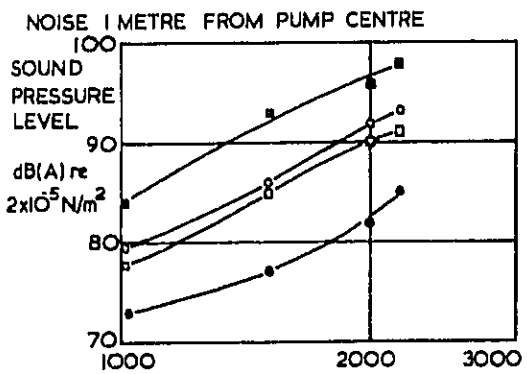

Fig 2a

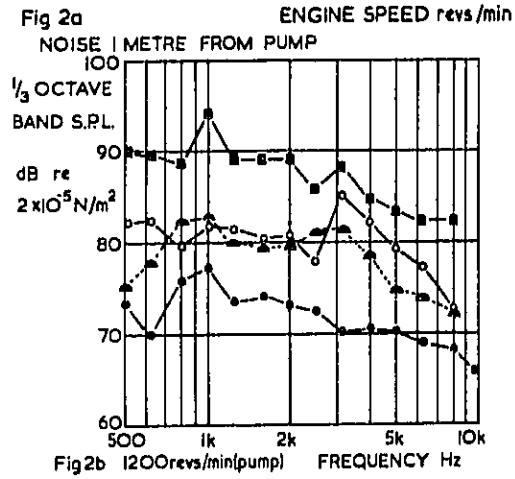

Fig 2b

- ○ Noise Measured with Pump Exposed on a Lead-Covered Engine with the Engine Running
- ● Noise Measured with Pump on Quiet Rig
- ▲ Noise Radiated from Pump on Running Engine Calculated from Surface Vibration
- ■ Noise Measured with No Covers over Engine or Pump with the Engine Running
- □ Noise Measured with both Engine and Pump Covered with a Lead Jacket with the Engine Running

Fig. 2 - Noise radiated from pump and engine surfaces, engine A with large in-line pump

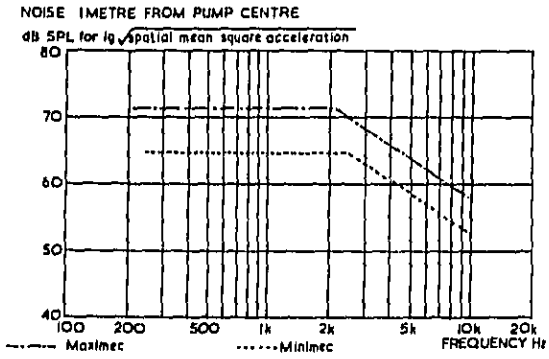

Fig. 3 - Noise radiated by vibration of pump surfaces measured 1 metre from pump centre

Comparisons of noise measurements and noise derived from surface vibration of pumps mounted on the quiet rig have given experimental values for the radiation efficiency and directivity of each pump. The measurements are taken in rooms with known acoustical properties. The radiation efficiency (and directivity) rise from a low value at low frequencies to a peak at a frequency between 1 and 4 kHz (depending upon the size and stiffness of the fuel injection pump). The slope below this frequency is approximately 20 decibels per decade increase in frequency. The slope above the peak is approximately zero. The radiation efficiency is similar to those for fundamental and odd numbered harmonics calculated by Wallace (13). The structure of the pump has a large number of normal modes and it is quite possible that odd-numbered modes (which are shown by Wallace to radiate more efficiently than even-numbered modes, just below the frequency for peak radiation efficiency) are responsible for most of the noise radiated by the pump.

Simplified frequency-dependent relationships are drawn in Fig. 3 to convert the spatial mean square acceleration, measured in decibels re 1g (9.81 metres/sec^2) to the noise measured opposite the middle of the pump, to the side of the pump, and 1 metre from the centre of the pump. The noise radiated by the whole of the pump surface (both sides, top, bottom and ends) is assumed to radiate over a hemisphere for a distance of about 1 metre from the pump due to reflections from the engine surface. At larger distances, reflections from acoustically hard floors or the road surface may interact with the directly radiated noise. The directivity of both Maximec and Minimec is small (less than 3 dB).

The noise spectrum derived from spatial mean square vibration levels is compared with the noise radiated by a pump exposed on an otherwise lead jacketed engine in Fig. 2b. There is reasonable agreement over the spectral range 800 Hz to 2.5 kHz and at 8 kHz. There are significant differences below 630 Hz where the pump is less able to radiate noise, and at 3.15 kHz. However the results confirm the results from the partial lead jacket experiment, indicating that the pump radiates more noise when mounted on a running engine than it does when mounted on the quiet rig. This might be due to extra vibration excitation from sources within the engine, or it might be some effect of the mounting.

NOISE FROM SMALL PUMP MOUNTED ON TWO TRUCK ENGINES - The results from the preliminary work with the large pump warranted a more detailed investigation to discover why the pump was radiating more noise on a running engine. In addition, it seemed desirable to compare base and flange mounted pumps to find if the type of mounting made a significant difference to the noise radiated by the pump. Since the Maximec is not yet in production in a flange-mounted form, this comparison had to be made with the smaller Minimec pumps.

A very similar Minimec pump specification is fitted to two 6 cylinder inline engines, made by different truck manufacturers, which have similar rated power output.

It was felt desirable to compare again the noise spectra estimated from mean square spatial vibration levels with noise measurements when the pumps were exposed on otherwise lead-jacketed engines. The comparison is made for the flange-mounted pump (engine B) in Fig. 4. The spectra at the top of Fig. 4a show the spectrum of noise from the pump exposed on a lead-jacketed engine (solid circles) compared with the noise of the complete engine without any lead jacket (solid squares) and the noise measured when both engine and pump were covered by the lead jacket (crosses). The crosses are too close to the solid circles for accurate measurements to be made over much of the frequency spectrum. This indicates that the noise transmitted through the lead jacket from the engine surfaces is as high or higher in level than that radiated by the pump surfaces. This result shows

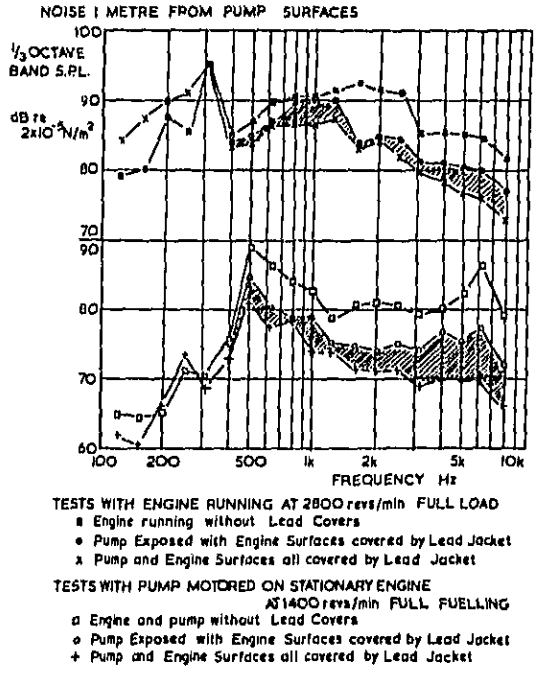

Fig. 4a - Flange-mounted in-line pump on engine 'B'

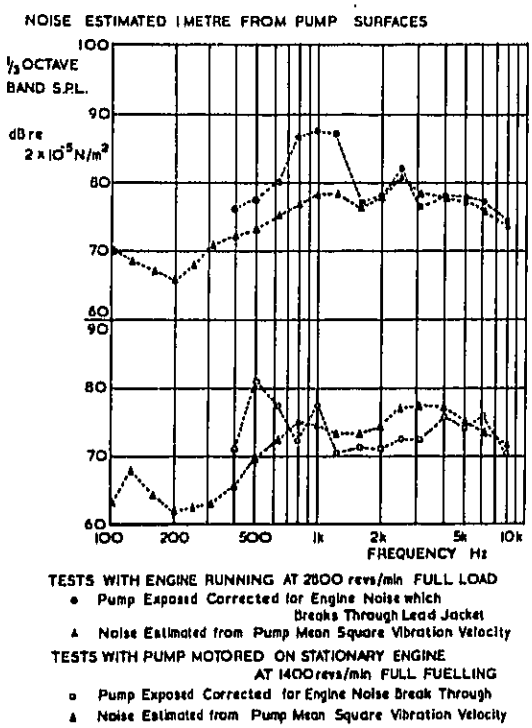

Fig. 4b - Improved estimates of noise radiated by surfaces of flange-mounted inline pump on engine 'B'

how the lead jacket technique is even less accurate for small pumps that it was for the Maximec in Fig. 2.

An alternative drive has been arranged for the fuel pump, so the pump may be run on a stationary engine. To do this, the idler gear was removed from the timing gears and a hydraulic motor was connected to the gear which was mounted on the pump camshaft. This preserved the flywheel effect of the drive gear. In these early tests, an Oldham Coupling* was used to allow for misalignment between the hydraulic drive motor and the camshaft axis. By driving the pump on a stationary engine, the noise radiated by the engine surfaces was reduced, and it was expected that the pump-radiated noise might be measured more accurately. To prove this point, the noise radiated by the pump when it was exposed on an otherwise lead jacketed engine (open circles in Fig. 4a) was compared with the overall noise from pump and engine surfaces without any lead jacket (open squares) and with noise radiated when both pump and engine were covered by lead jackets

* A coupling permitting parallel misalignment of coupled shafts. It consists of a pair of flanges carrying diametrally disposed dogs on their opposed faces. These dogs mate with 4 slots in a floating disc; the slots are arranged at right angles to each other on a common pitch circle, illustrated in Fig. 7.

(addition signs). Despite the elimination of engine excitation, the noise radiated by engine surfaces, through the lead jacket, was high enough to preclude accurate measurement of pump-radiated noise over much of the frequency range. Another result from this test is that noise excited by the pump forces and radiated by the engine surfaces, contributes significantly to the overall engine noise in the 500 Hz, 630 Hz, 5 kHz, 6.3 kHz, and 8 kHz 1/3 octave bands, on engine B with a flange-mounted pump. Although unsatisfactory as measurements of pump-radiated noise in their own right, the spectra in Fig. 4a were used to check noise levels estimated from pump surface vibration. The noise levels measured with the pump exposed on a lead-jacketed engine, were corrected by subtracting the intensity of noise radiated when both pump and engine were covered by lead jackets. These corrected levels for pump-radiated noise are shown in Fig. 4b. The corrected noise measurements agree closely with pump noise estimated from vibration measurements above 1.4 kHz, when the engine was driving the pump. When the same comparison is made for the pump motored on a stationary engine, the results are close where pump-excited, engine-radiated noise was high (below 1 kHz and around 6.3 kHz). Between 1.1 kHz and 3.5 kHz the comparison is less encouraging but still within 5 dB.

An attempt was made to repeat this check procedure for the base-mounted pump and its engine but the levels of noise with the pump exposed on a lead-jacketed engine were so close to the noise with both pump and engine covered with a lead jacket, that no useful results could be obtained by this method.

This work has confirmed the conclusions drawn from the preliminary measurements on the Maximec and large naturally aspirated engine (engine A) and

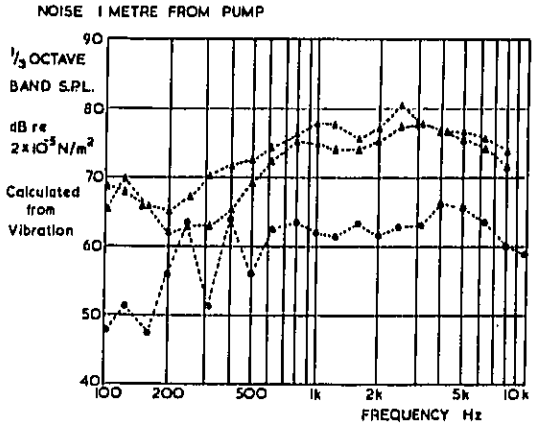

Fig. 5 - Noise radiated from pump surfaces with different mountings and drives

leads to the conclusion that pump-radiated noise may be estimated more accurately from measurements of surface vibration and a simplified radiation efficiency curve, than it may be measured by load jacket techniques. Accordingly all comparisons between engines B and C were made with noise spectra estimated from mean square surface vibration levels.

COMPARISON OF PUMP-RADIATED NOISE WITH DIFFERENT MOUNTING BRACKETS AND DRIVE COUPLINGS

FLANGE-MOUNTING ON ENGINE COMPARED TO BASE-MOUNTING ON QUIET RIG - Measurements of pump-radiated noise have been compared with the same pump in three mounting/drive configurations on engine B in Fig. 5:-

(i) Pump mounted and driven by a running engine.
(ii) Mounted on a stationary engine and driven by a hydraulic motor.
(iii) Mounted and driven by the quiet rig.

The increase in noise (above that measured on the quiet rig) due to mounting the pump on the engine is large above 400 Hz; it is larger than the similar results obtained for engine A (Fig. 2). The noise radiated by the pump when motored upon a stationary engine is similar to the noise radiated by the pump whilst driven by a running engine above 500 Hz (within 3 dB over most of this frequency range). For these tests the coupling between the hydraulic motor and the gear mounted on the pump camshaft was an Oldham coupling with

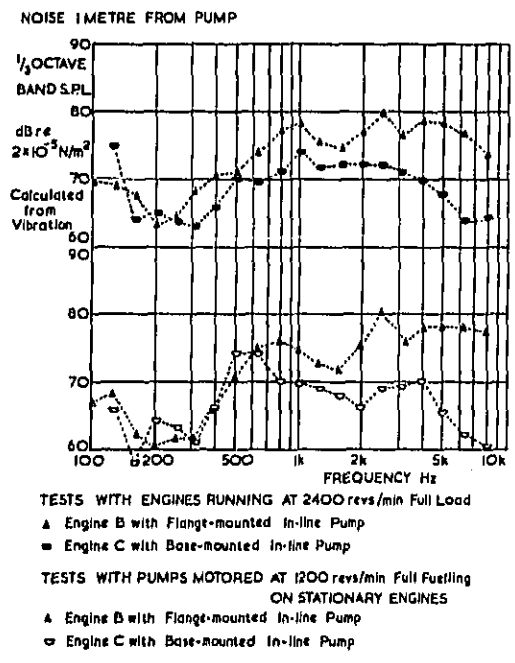

Fig. 6 - Comparison of noise radiated by two 6-element pumps mounted on two engines with similar rated power

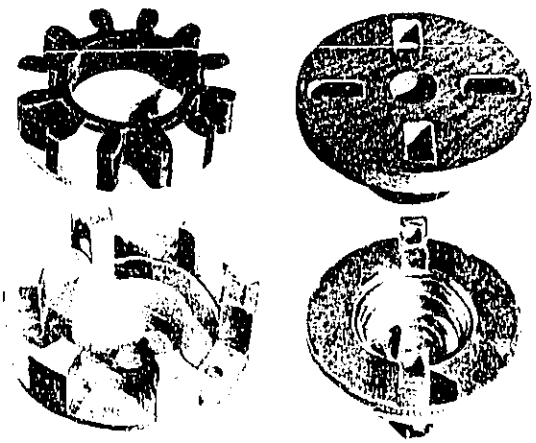

Lucas CAV CR coupling designed to drive pumps

Oldham coupling adapted for driving pumps

Fig. 7 - Couplings used to drive fuel injection pumps

a Tufnol* disc which was a tight press fit on the sliding dogs. This result suggested that some feature of the mounting was responsible for causing the pump to radiate more noise, although it was possible that residual backlash in the Oldham Coupling and timing gear rattle might cause drive line impacts which were not present on the quiet rig.

FLANGE MOUNTING COMPARED WITH BASE MOUNTING ON SIMILAR ENGINES - Noise levels derived from pump surface vibration measurements were compared for two pumps with similar ratings mounted on two engines of similar size and rating but of different manufacture.

A Minimec pump was mounted to one engine by the flange, (part of the governor chamber end plate) which was bolted to a cast aluminium timing cover. The camshaft of this pump carried a gear wheel which acted as a flywheel, and which meshed with the timing gear idler of the engine. When this pump was being motored whilst mounted on the stationary engine, the idler gear was removed and a hydraulic motor drove a shaft attached to the gear via an Oldham coupling. The coupling was arranged to be a tight press fit to minimise backlash.

A similar Minimec pump was mounted to the engine crankcase via an L-shaped aluminium alloy bracket, which was stiffened by two webs. Four bolts secured the bracket to the engine crankcase panels and four more bolts secured the base of the

* Tufnol is a proprietary plastic material which is reinforced by laminated cloth fabric. It has high strength and stiffness.

Minimec to the bracket. This pump was driven via a short shaft from the timing gear case with a coupling similar in principle to that used on the quiet rig, but with the addition of hard rubber-bushes, to accommodate any misalignment between gear and camshaft centre lines.

The comparison between the noise radiated by the pumps (estimated from pump surface vibration) is shown in Fig. 6 with both pumps being run at 1200 revs/min, full fuelling, which corresponds to the maximum rating of engine C. The base-mounted pump radiated less noise than the flange-mounted pump when driven either from the running engine (solid points) or when driven by a hydraulic motor via an Oldham coupling whilst mounted on stationary engines (open points). This result seems to indicate that base-mounting configuration is superior in some way to flange-mounting, both with the manufacturers drive arrangements from running engines, and with similar drives from a hydraulic motor. However the mounting may not be the only influence of work; and an attempt was made to establish a common basis for mounting comparisons between flange and base mountings on the same engine with the same pump and with similar drive arrangements.

COMPARISON OF FLANGE AND BASE MOUNTING CONFIGURATIONS ON ENGINE B

The mounting for the fuel injection pump on engine B was changed from the original flange mounting to a new base-mounting configuration, similar to that of engine C. A special pad was prepared, on the crankcase of engine B, to take the bracket from engine C, which was bolted to the crankcase. The base of the pump (for engine B) was bolted to this bracket such that the camshaft axis was the same as in the flange-mounted configuration, but the pump was 100mm further away from the timing cover of the engine. There was no contact between the pump flange and the timing cover ear to which it had been secured in the flange-mounting configuration.

The drive to the pump camshaft was from the same gear in the timing gear train, via a short shaft and a Lucas CAV CR100 coupling. This coupling was chosen as the closest equivalent of the pump drive shaft used on engine C, which could be installed in the space available. This type of coupling, which is compared with an Oldham coupling in Fig. 7, consists of two flanges each with 4, 6 or 8 dogs which are separated by a rubber annulus carrying 8, 12 or 16 lobes respectively. The lobes fit between the dogs when the flanges are brought together. The drive places the rubber lobes in compression, giving a torsionally stiff drive. The coupling is able to take up small misalignments of the driveshaft and pump camshaft. The noise radiated by the pump was estimated from surface vibration measurements with the engine driving the pump through the CR coupling, and with the hydraulic motor driving the pump through the CR coupling. The pump was driven by the hydraulic motor through the CR coupling in the flange mounted configuration also to provide a base/flange comparison in which the drive, pump and engine were the same. This comparison is also free of torsional vibration from the engine crankshaft and valve gear.

When the base-mounted pump was motored on the stationary engine, the spectrum of pump-radiated noise was 5 to 15 dB lower than noise radiated from flange-mounted pump, over the frequency range 700 Hz to 8 kHz (Fig. 8). This represents a very large improvement in pump radiated noise, and it brings it within 5 dB of the noise radiated by the same pump on the quiet rig above 700 Hz. However, when the pump was driven by the engine, the noise radiated by the base-mounted pump was similar to that radiated by the flange-mounted pump (Fig. 8).

EFFECT OF COUPLING

Results from tests with the Minimec pump flange-mounted to engine B, driven by a hydraulic motor via a CR coupling may be compared with results from similar tests in which the flange-mounted pump was driven via an Oldham coupling in Fig. 9 (top). There is a reduction in pump-radiated noise of 5 dB or more in the 1/3 octave bands centred on 1.25 kHz, 1.6 kHz, 2.5 kHz and 3.15 kHz when the rubber CR coupling is substituted for the Oldham coupling; even though the Oldham coupling was a tight press fit. The effect of coupling backlash was explored more thoroughly in the base-mounted configuration.

An Oldham coupling which had been in use for some time, which had discernable backlash, was compared with a new coupling which was machined to give a force fit between dogs and mating slots in the tufnol disc. With the aid of a stroboscope, it could be seen that the backlash was taken up as pumping torques were applied, with an impact as the

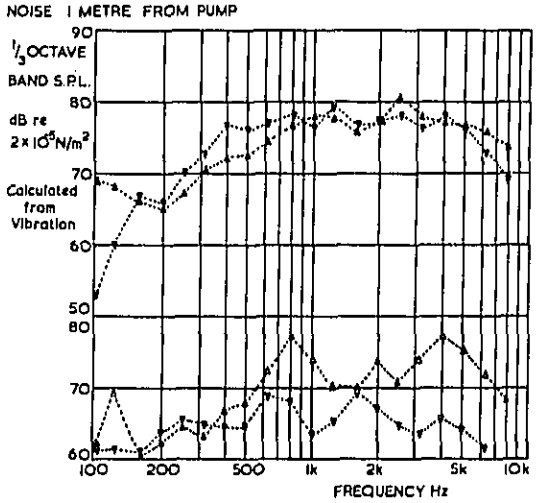

Fig. 8 - Comparison between flange- and base-mounting of same in-line pump on engine B

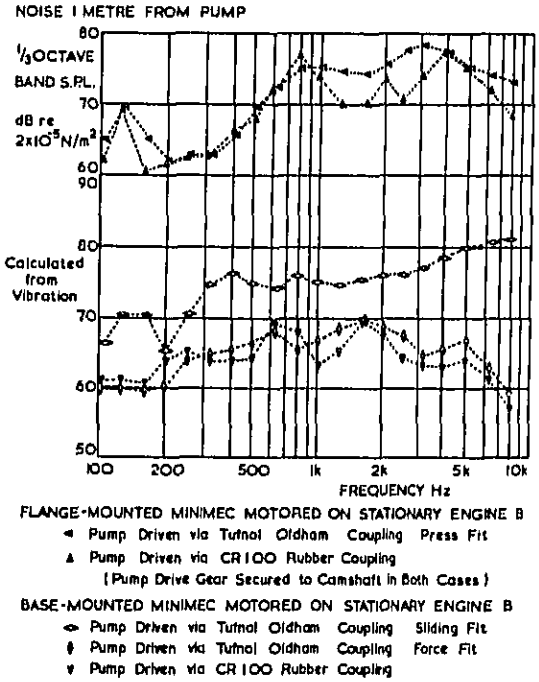

Fig. 9 - Effect of backlash in drive to pump camshaft

drive was taken up. The spectra of pump-radiated noise, derived from surface vibration measurements, measured with these two couplings showed a large difference in pump-radiated noise, Fig. 9. It must be emphasised that this noise is not radiated from the coupling itself, due to impacts as the coupling backlash is taken up, when the pump begins to force fuel into the injector pipe. (This is a separate problem and it has been a well-known source of noise on pump test benches.)

When the Oldham coupling was replaced with a Lucas CAV type CR100 rubber coupling, the noise radiated by the pump was even less than that with the special tight Oldham coupling, over most of the frequency range. This small difference could be the effect of changes in coupling stiffness rather than backlash. It is possible that the flange mounted pump was excited by impacts between drive gears whilst the engine was running. Apart from the effect of drive line backlash on noise, it increases line-to-line, and shot-to-shot, scatter in pump delivery; on these grounds alone it must be avoided.

EFFECT OF ENGINE VIBRATION ON PUMP-RADIATED NOISE

When the pumps were driven by engine B in flange-mounted and base-mounted configurations, the spectra of pump-radiated noise were similar. Examination of the spectra in Fig. 8 shows that the noise from the base-mounted pump has been increased as a result of running the engine. This suggests that vibration originating from the engine has increased the pump surface vibration, over the levels measured when the pump was motored on a stationary engine. A similar but smaller trend is evident in Fig. 6.

A comparison (Fig. 10) of the crankcase vibration spectra, measured on the securing bolts for the base-mounting bracket shows that the crankcase of engine B vibrated much more than that of engine C. (The vibration levels measured have been converted into equivalent pump-radiated noise using the same procedure and radiation efficiency as used for pump surface vibration, as if the pump radiated noise as a rigid body in response to crankcase vibration.) The difference between the vibration spectra of two engine crankcases is similar to the difference between noise spectra of base-mounted pumps driven by the engines B and C whilst they were running (within 3 dB between 400 Hz and 1.8 kHz and above 3.5 kHz). These test results show that base-mounted pumps on both engines B and C radiate less noise than the flange-mounted pump on engine B when the excitation is from internally-generated pump forces alone. Unfortunately the crankcase of engine B vibrates much more than that of engine C, so when the pump was mounted to the crankcase of engine B, engine excitation increased the noise levels to match those of the flange-mounted configuration.

CONCLUSIONS

To measure noise from fuel injection equipment on a running engine by the "lead jacket" technique, a jacket is required which is capable of attenuating engine-radiated noise by 15 to 20 dB over the frequency range 500 Hz to 10 kHz. This might be achieved with a multiple layer jacket supported away from the engine (without absorbent in contact with engine surfaces); but there would be difficulties in sealing the surfaces of the lead jacket around the pump and pump drive shaft, and the overall jacket might have to be so thick that it would change the acoustic radiation from the rear of the pump. Assessment of the noise radiated by the pump

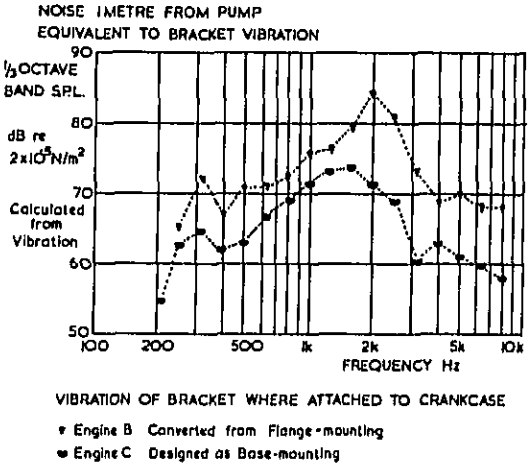

Fig. 10 - Vibration of Brackets with Engines Running

surfaces from the spatial mean square vibration velocity levels seem to be a better alternative for estimating pump-radiated noise. The efficiency of noise radiation has been derived from measurements on a quiet drive rig; and it is in agreement with published formulae for radiation resistance of beams.

One of the major factors which influences the noise radiated by the pump is backlash in the drive system. This backlash is taken up as pumping commences and large impulsive torques are transmitted into the pump structure, via the cam and roller-tappet, which can increase the vibration levels of the pump surfaces by 10 decibels at high frequencies.

Vibration imparted to the pump mounting bracket by the engine can increase the noise radiated by the pump considerably. In the particular case investigated, crankcase vibration was responsible for an increase in pump radiated noise of at least 5 dB(A) by comparison with another engine, which itself suffered from the same effect to a lesser degree. It is essential that the pump bracket is secured to the engine where there are low vibration levels.

Vibration originating within the fuel injection pump can excite engine surfaces into vibration. In the case for which valid data is available, pump-excited, engine-radiated noise, did not contribute significantly to the overall engine noise level in dB(A) terms but it did contribute to the lower levels of the engine noise spectrum. It is highly desirable that the pump torque reaction be taken by the engine in such a way that major structural resonances of the engine are not excited. Alternatively the response of the engine structure may be reduced as described in previous work (3, 4) which will reduce not only the noise originating from the fuel injection pump but also that originating from the combustion process, piston slap and timing gear rattle.

After the influence of drive line backlash and engine vibration had been removed, one test remained which compared the effects of flange and base-mounting; the same pump was driven on the same engine by the same hydraulic motor via the same coupling. This one result indicated that the pump-radiated noise, due to vibration excitation originating within the pump was less in the base-mounting configuration than in the flange mounting configuration. This result has not been reproduced on an engine running under normal operating conditions.

ACKNOWLEDGEMENT

The authors would like to thank the directors of Lucas Industries and Lucas CAV Limited for permission to publish this paper. They gratefully acknowledge the advice and assistance freely given by Professor T Priede, Dr B A Jarrett, Mr W Clifton and Dr A Waring.

REFERENCES

1. A E W Austen and T Priede, "Origins of Diesel Engine Noise". Symposium on Engine Noise Suppression. Proc. Instn. Mech. Engrs., London 1959, 173, 19.

2. R Monroe and A Parker, "Transverse Movement Analysis and its Influence on Piston Design". Paper No. 750800 in SP397. Society of Automotive Engineers, Diesel Engine Noise Conference, Milwaukee, Sept. 1975.

3. M F Russell, "Automotive Diesel Engine Noise and its Control". Paper No. 730247. SAE International Automotive Engineering Congress, Detroit, Jan. 1973.

4. M F Russell, "Control of Noise Emissions from Conventional Diesel Engines". Paper No. 720135 SAE Automotive Engineering Congress, Detroit, Jan. 1972.

5. M F Russell, "Establishing a Target for Control of Diesel Combustion Noise". SAE Automotive Engineering Congress, Detroit, Jan. 1978.

6. M D Rohrle, "Affecting Diesel Engine Noise by the Piston". Paper 750799 in SP397, Society of Automotive Engineers, Diesel Engine Noise Conference, Milwaukee, Sept. 1975.

7. T Priede, A E W Austen and E C Grover, "Effect of Engine Structure on Noise of Diesel Engines". (Figs. 1, 13c, 14, 15, 16, 17, in particular). Proc. Instn. Mech. Engrs., London 1964-5, Vol. 179, part 2A No. 4.

8. G E Thien, "Use of Specially Designed Covers and Shields to Reduce Diesel Engine Noise". Paper 730244, Society of Automotive Engineers International Automotive Eng. Congress, Detroit, Jan. 1973.

9. D T Aspinall and J West, "The Reduction of External Noise of Commercial Vehicles by Engine Enclosure". (UK) Motor Industry Research Association Report No. 1966/17.

10. D Williams, "The Design of Inline Fuel Injection Equipment for Automotive Diesel Engines". Paper No. 780769, Society of Automotive Engineers Conference, Milwaukee, Sept. 1978.

11. H C Grigg, "The Role of Fuel Injection Equipment in Reducing 4-stroke Diesel Emissions". Paper No. 760126, Society of Automotive Engrs. Automotive Engineering Congress, Detroit, Feb. 1976.

12. G Greeves, "Response of Diesel Combustion Systems to Increase in Fuel Injection Rate". Paper to be presented at Society of Automotive Engineers Congress Feb. 1979.

13. C E Wallace, "Radiation Resistance of a Baffled Beam". Journal Acoustic Soc. Am., Vol. 51 No. 3 (part 2) pp 936-952.

790274

A COHERENCE MODEL FOR PISTON-IMPACT GENERATED NOISE

P. A. Hayes, Cummins Engine Co., Columbus, Indiana, U.S.A.

A. F. Seybert, Dept. of Mech. Eng., Univ. of Kentucky, Lexington, Kentucky, U.S.A.

J. F. Hamilton, Dept. of Mech. Eng., Purdue University, W. Lafayette, Indiana, U.S.A.

ABSTRACT

An experimental study was conducted to investigate piston-impact generated noise in diesel engines. A coherence model was used to represent the noise generating mechanisms of the engine. The model was applied to an in-line turbo-charged diesel engine. Frequency response functions were measured between the cylinder liner vibration and the engine noise, and between the combustion pressure and the engine noise. The noise coherent with piston impacts was separated from the noise coherent with combustion. Guidelines are presented showing how the results of the coherence model may be used for engine design and noise prediction.

SINCE THE INTRODUCTION OF THE DIESEL ENGINE as a power plant, engine designers have been very attentive to performance characteristics. This need is satisfied by the high-performance power plants in commercial use today. Until the early 1960's the noise output of these commercial diesel engines was marginally acceptable to the public. However, recent concern for public health has forced legislation on noise reduction. This legislation has necessitated substantial research in the area of diesel engine noise.

Prior to 1940, most diesel engine noise research pertained to reducing "engine knock" by means of improving the burning properties of the cylinder combustion process (1-4)*. Over the last decade, most of the diesel engine noise sources have been isolated. Jenkins (5) has ranked the various noise sources according to their importance. In general, for naturally aspirated engines, the combustion pressure excitation is the greatest contributor to noise, with the piston impact source a close second, and the other mechanical impacts (such as bearing impacts, valve train and oil pan vibrations) third. This fact has resulted in research in the area of combustion noise (5-9). For turbo-charged engines Haddad, Priede, and Pullen (10) have shown that piston impact is the predominant noise source. Anderton and Duggal (11) also found that turbo-charging can reduce combustion noise emissions to the level that reduction in mechanical noise is needed to further reduce engine noise.

Piston impact, i.e., the impacting caused by the lateral motion of pistons across the cylinder clearances, has been shown to be a major noise source in internal-combustion engines (10-12). This fact is especially true in turbo-charged engines where, despite the very smooth cylinder pressure development, the piston side-force increases at a much higher rate and achieves a higher peak value immediately following TDC. The change in piston side-force is due to the high cylinder pressures. The widespread acceptance of turbocharging suggests that research in the direction of reducing the noise produced by piston impacts is needed.

Some analytical studies have been carried out on the motion of the piston across the cylinder clearance (13-16). Fielding (16) provides the most elaborate equations of motion for the piston by accounting for the lateral and angular motion of the piston. References (15) and (16) use the final velocity of the piston to calculate an "impact energy" (kinetic energy on impact). They use this quantity to estimate noise reductions for changes in engine parameters. Haddad and Fortescue (17) used an analog computer simulation to illustrate the liner displacement (using a two-mode expansion) caused by piston impact. Using this simulation, the effect of engine load and cylinder clearance on liner vibration was illustrated.

A considerable amount of experimental research has also been carried out on piston-impact noise (18-22). Most of this research is involved with experimentally varying engine parameters and noting changes in engine noise. Some experimental research has been done on the actual motion of the piston across the cylinder clearance (23-24). However, this experimental research was directed at a particular type of diesel engine and is very empirical. This information, though useful, is not generally applicable to engines of different size or geometric configuration.

Recently, a large portion of the research on diesel engine noise has been in the area of "noise source identification." In this type of qualitative research, a noise source of interest is isolated either by masking contributions of other noise sources or by removing the noise source and noting the difference between the original and modified sound. With this technique, the contribution of the noise source to the total noise

*Numbers in parentheses designate References at the end of paper

SAE/P-79/80/$02.50
Copyright © 1979 Society of Automotive Engineers, Inc.

can be estimated. The limiting factor in this method of source identification is that the phase information accounting for the interaction between sources (providing reinforcement and cancellation of sound pressure) is not taken into account. Because of the loss of the phase information, the total sound predicted by summing the contributions of each source usually results in an erroneous total sound prediction. The coherence function and frequency response techniques are potentially useful in this regard. Recently these techniques have been used to diagnose noise sources on complex vibrating machinery (25-27) and to estimate the structural-acoustical response of diesel engines (28-30). Utilizing these techniques, the total coherent noise can be divided into portions uniquely coherent to each source and a portion arising from the common coherence between sources.

In this paper the problem of piston impact noise is approached using a coherence theory technique. The overall objective of the study was to develop a semi-empirical model useful for predicting piston-impact noise from basic design information such as combustion characteristics and piston/cylinder liner geometry. The coherence theory is used to develop a two-input, single-output model of diesel engine noise. This paper discusses the formulation of that model and the experimentation required to determine certain frequency response functions relating the input and output variables of the model for an in-line, turbocharged, six-cylinder diesel engine. A future paper* discusses a piston impact and cylinder vibration model that is used in conjunction with the coherence model to predict piston-impact noise.

TIME DOMAIN AND AUTO-SPECTRA ANALYSIS

As a preliminary to the coherence model, several experiments were conducted to determine the characteristics of piston-impact induced cylinder liner vibration and noise. As a part of the experimental study, accelerometers were mounted on the thrust side of the cylinder liners at a position 70 mm (2.75 in.) from the top of the cylinder liner. A typical full load (2100 rpm, 865 ft.lb.) liner vibration time-history is shown in Figure 1a, for approximately 720° of crank angle. As can be seen from Figure 1a, the most significant region of vibration (typically 125 G's maximum) begins slightly prior to TDC (top dead center), and has a duration of about 5 msec. Additional vibration can be seen throughout the time-history. This vibration is due to five other piston impacts that may occur during the intake, expansion, and exhaust cycles, as well as vibration caused by other mechanical impacts. Since the liner vibration during combustion is much greater than the other vibrations, the research in this project has focused primarily on the piston impact and vibration near TDC.

Cylinder liner vibration during combustion consists of two parts, a high-frequency vibration lasting about 2 msec, followed by a much lower frequency vibration lasting about 3 msec. These characteristics are illustrated in Figures 1b, c, and d. The auto-spectra for the four

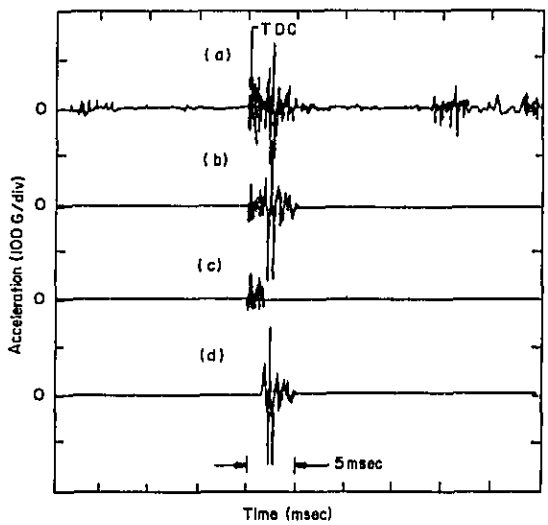

Fig. 1 - Typical cylinder liner acceleration time-histories for full-load engine condition: (a) one complete cycle (720° of crankshaft rotation), (b) major piston impact response near TDC during combustion, (c) high-frequency portion of vibration, (d) low-frequency portion of vibration

vibration signals in Figure 1 appear in Figures 2a, b, c, and d. It is evident that while the total vibration near TDC (Figure 2b) contains both low-frequency content and high-frequency content, the first two milliseconds (Figure 2c) contain only high-frequency vibration centered around 6500 Hz. Also, from time domain sample averaging, this high-frequency vibration was found to be a random vibration, probably due to random fluctuations in the cylinder pressure. The last three milliseconds of the signal contain vibrations in the 1500-3000 Hz frequency range, which is characteristic of piston impact (15).

An important point in the analysis is illustrated by comparing the auto-spectra in Figures 2a and 2b. The only difference in the spectral processing used to compute the spectra in Figures 2a and 2b is that in Figure 2b the noncombustion piston impacts, and background vibration, were cleared from the data. This procedure essentially eliminated the random error that is superimposed on the spectrum in

*"A Model of Piston Impact for Internal Combustion Engine Noise Reduction," A.F. Seybert, J.F. Hamilton, P.A. Hayes, Submitted for ASME Conference on Mechanical Vibration, St. Louis, Mo., Sept. 9-12, 1979

Figure 2a. This procedure yields an improved estimate of the true auto-spectrum (Figure 2b) with smooth characteristics that are desirable for data interpretation purposes.

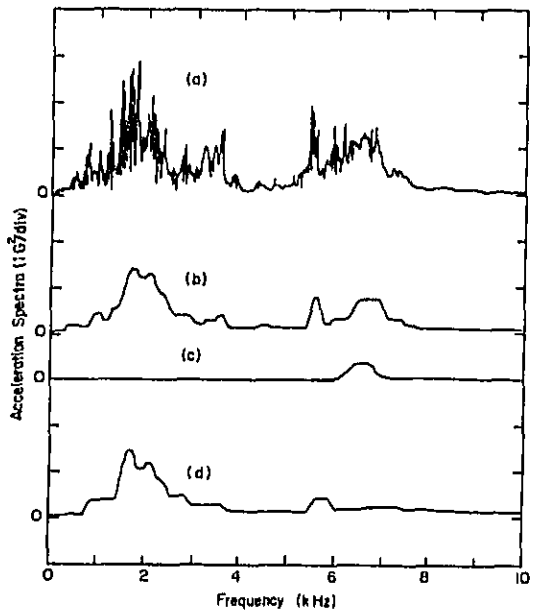

Fig. 2 - Spectra of cylinder liner vibration: (a) one complete cycle, (b) major impact near TDC, (c) high-frequency portion, (d) low-frequency portion

Piezoelectric pressure transducers were mounted in the cylinder head to study the cylinder pressure. Figures 3a and 3b show typical unfiltered and filtered cylinder pressure time-histories. The filtered cylinder pressure time-history was obtained by passing the pressure transducer signal through a high-pass filter with a break frequency at 500 Hz to reduce the dynamic range of the signal. Both the filtered and unfiltered cylinder pressure signals were very repeatable from cycle to cycle.

Also included in Figure 3c is a typical time-history of the full-load engine noise. Due to the complexity of the noise signal, visual correlation between it and the cylinder pressure and liner vibration time-histories is impossible. Clearly, a more sophisticated approach is required to determine the relationship between piston impacts and noise and between cylinder pressure and noise.

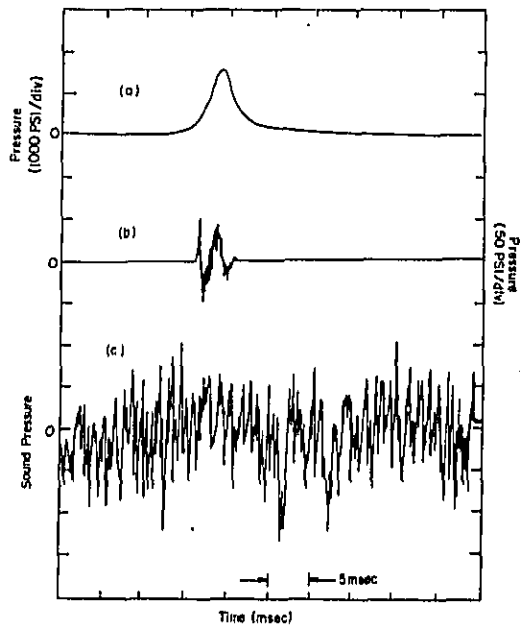

Fig. 3 - Typical cylinder pressure time-histories: (a) unfiltered, (b) high-pass filtered at 500 Hz, and (c) typical engine noise time-history

Figure 4 shows the full-load cylinder pressure and noise auto-spectra. These spectra are ensemble averages of 50 individual time records. Each record was sampled for exactly one full engine cycle (57 msec) to minimize leakage error; the frequency bandwidth was 1/57 = 17.5 Hz. Low-pass filters were used to minimize aliasing errors.

It can be seen from Figure 4a that the cylinder pressure spectrum shows evidence of the presence of large peaks near 2400, 4600, and 5500 Hz. Independent tests of this engine and other engines using one-third octave spectrum analysis confirmed that these peaks are not a result of digital aliasing error. Most diesel engines exhibit these so-called combustion or "bowl" resonances. These resonances are particularly noticeable for turbo-charged engines because the cylinder pressure spectrum is reduced at frequencies above 1000 Hz. Only the first resonance (2400 Hz) is usually observed for naturally-aspirated engines. It is difficult to predict from theory the resonant frequencies of the combustion chamber, because the frequencies are highly dependent upon the temperature of the combustion gases. However, theoretically, the second and third resonant frequencies are related to the first resonant frequency by ratios of

1.7 and 2.1 respectively*. The corresponding frequency ratios from Figure 4a are 1.9 and 2.3.

From Figure 4b it can be seen that the noise spectrum generally decreases with increasing frequency. However, it is evident that an A-weighted sound level will be dominated by noise in the 500-2000 Hz frequency range.

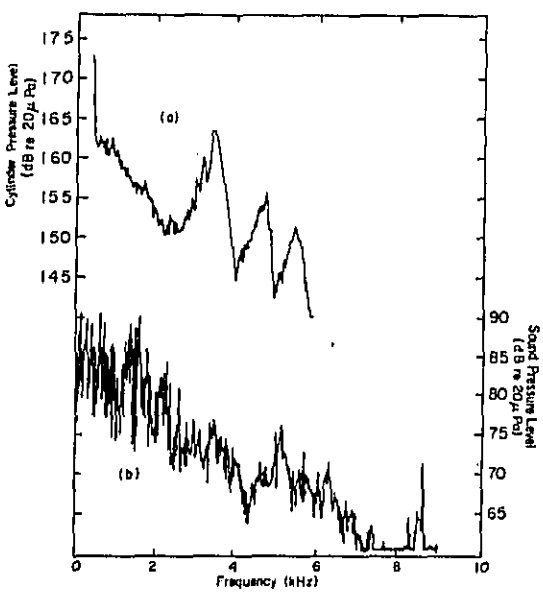

Fig. 4 - (a) Cylinder pressure spectrum, (b) engine noise spectrum

APPLICATION OF COHERENCE THEORY

The ordinary coherence function $\gamma^2_{xy}(f)$ between two quantities x(t) and y(t) is defined as:

$$\gamma^2_{xy}(f) = \frac{|S_{xy}(f)|^2}{S_{xx}(f)\, S_{yy}(f)} \qquad (1)$$

where

$S_{xy}(f)$ = cross-spectrum between x(t) and y(t)
$S_{xx}(f)$ = auto-spectrum of x(t)
$S_{yy}(f)$ = auto-spectrum of y(t)

*See, for example, "Theoretical Acoustics," P.M. Morse, K.U. Ingard, McGraw-Hill, 1968, Section 9.2.

It can be shown that $0 \leq \gamma^2_{xy}(f) \leq 1$. Physically, the ordinary coherence function between two quantities x(t) and y(t) is a measure of the degree of linear dependence between the quantities. For complete linear dependence between x(t) and y(t) the ordinary coherence function is unity. The presense of extraneous signals in either x(t) or y(t) will cause the ordinary coherence function to be less than unity.

It was found that when computing coherence functions involving either cylinder liner vibrations or cylinder pressures, a much smoother coherence function could be achieved by clearing all of the signal except the major portion of interest. As with the auto-spectra, one period (57 msec) of each signal was used in computing coherence functions with lowpass filtering at 4000 Hz. The cylinder pressure from another cylinder was used to trigger all of the signals to insure repeatability, and all spectra were calculated by averaging 40 samples.

A typical ordinary coherence function estimate between two cylinder pressures is shown in Figure 5a. Figure 5a shows high coherence at low frequencies and a loss of coherence above 2000 Hz. The loss of coherence is due to the dominance of random combustion pressure variations at high frequency.

A typical ordinary coherence function estimate between two liner vibration signals is shown in Figure 5b. Figure 5b shows a high coherence ($\gamma^2(f) > 0.7$) from 500-3000 Hz.

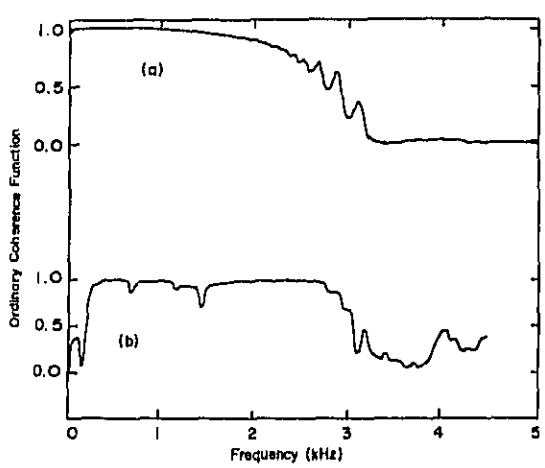

Fig. 5 - (a) Ordinary coherence between cylinder pressures, (b) ordinary coherence between liner vibration

The cylinder pressures and liner vibrations producing noise can be considered as a multiple-input, single-output system. Since cylinder pressures are almost fully coherent below 2500 Hz, and since liner vibrations are almost fully coherent for frequencies below 3000 Hz, all cylinder pressures can be combined into one single input, and all liner vibrations can be combined into another single input. A two-input, single-output model representing combustion noise and piston impact noise is shown in Figure 6. Y(t) is the total noise output, N(t) is the extraneous noise (background and other noise not coherent with either the cylinder pressures or liner vibrations), p and v are the typical cylinder pressure and liner vibration inputs, and H_v and H_p are the frequency response functions between respective inputs and the engine noise. Y'(t) is the noise coherent with liner vibration and cylinder pressure.

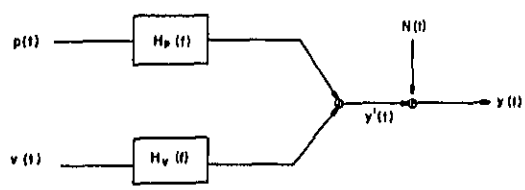

Fig. 6 - Coherence model for a two-input, single-output system

Some caution must be exercised in using the model shown in Figure 6. The output Y'(t) is the noise coherent with, but not necessarily caused by, piston impact or combustion pressure. This distinction is important because it means that one must have prior knowledge regarding the importance of the two inputs p(t) and v(t) in producing the coherent noise Y'(t). In this study other tests showed that the major noise sources were indeed combustion and piston-impact generated. Figure 7, for example, shows the results of replacing the standard pistons with pistons having a minimal running clearance. This was achieved by using teflon inserts on the thrust and anti-thrust sides of each piston. Approximately a 3dB reduction in noise was obtained in the 1000 to 3000 Hz frequency range. One might question the value of the coherence model in Figure 6 if supplementary testing is required to justify the model. The coherence model allows one to determine the frequency responce functions $H_p(f)$ and $H_v(f)$ relating the inputs and the output of the system. This quantitative information is quite useful in design models for assessing the relative importance of structural and combustion parameters affecting noise.

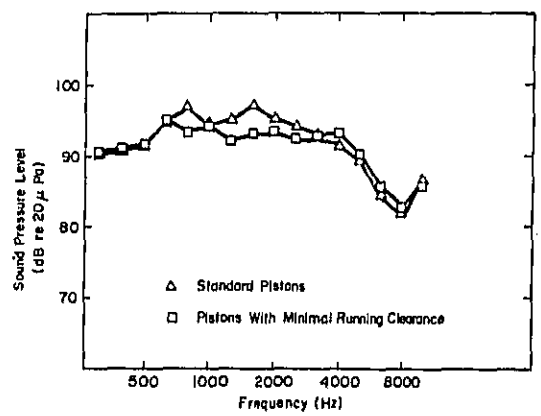

Fig. 7 - The effect of piston/cylinder liner running clearance on engine noise

Since p and v in Figure 6 are themselves partially coherent, the system equations are (31):

$$S_{vy}(f) = H_v(f)\, S_{vv}(f) + H_p(f)\, S_{vp}(f) \qquad (2)$$

$$S_{py}(f) = H_v(f)\, S^*_{vp}(f) + H_p(f)\, S_{pp}(f) \qquad (3)$$

where S_{pp}, S_{vv}, and S_{vp} are the input auto- and cross-spectra, where S_{vy} and S_{py} are the cross-spectra between each input and the output, and where * denotes complex conjugate.

These equations can be solved for the frequency response functions H_v and H_p:

$$H_v = \frac{S_{vy}S_{pp} - S_{vp}S_{py}}{S_{vv}S_{pp} - S_{vp}S^*_{vp}} \qquad (4)$$

$$H_p = \frac{S_{vv}S_{py} - S_{vy}S^*_{vp}}{S_{vv}S_{pp} - S_{vp}S^*_{vp}} \qquad (5)$$

All spectra were calculated using the following smoothing techniques: (1) low-pass filtering at 4000 Hz, (2) using one period to reduce leakage error, (3) clearing uncorrelated or insignificant data, and (4) ensemble averaging of 50 individual spectra to reduce random error. The noise output y(t) was shifted 3.1 msec to account for the time delay between inputs and outputs (32).

The liner vibration and cylinder pressure frequency response functions (magnitude only) appear in Figure 8. Because H_p is the ratio of two pressure spectra, it is dimensionless and is plotted as a decibel quantity. The quantity H_v was made dimensionless by dividing by the reference pressure (20 μPa) and the acceleration of gravity.

Both frequency response functions show that the engine structure responds to excitation over a wide frequency range. Because there is a loss of coherence between the cylinder pressures and between the cylinder liner vibrations below 500 Hz and above 3000 Hz, these frequency response functions are inaccurate in these regions. The assumption that multiple inputs (either cylinder pressures or liner vibrations) can be respresented by a single input is valid only in the 500-3000 Hz range.

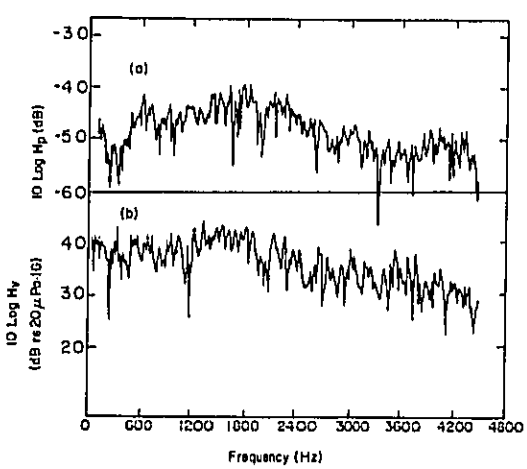

Fig. 8 - (a) Frequency response between cylinder pressure and noise, (b) frequency response between cylinder liner vibration and noise

The noise that is coherent with the cylinder pressure and liner vibration can be calculated using:

$$S'_{yy}(f) = |H_v(f)|^2 S_{vv}(f) + |H_p(f)|^2 S_{pp}(f) + 2 \text{ Real } [H^*_v(f)H_p(f)S_{vp}(f)] \quad (6)$$

where * denotes a complex conjugate quantity, and where $S'_{yy}(f)$ is the pressure-vibration coherent noise. Note that the total noise $S_{yy}(f)$ is given by:

$$S_{yy}(f) = S'_{yy}(f) + S_{nn}(f) \quad (7)$$

where $S_{nn}(f)$ is the spectrum of the extraneous noise. The first term on the right side of Equation 6 is the noise coherent with liner vibration only; the second term is the noise coherent with cylinder pressure only. The third term accounts for any interaction between combustion and piston-impact noise. This term can be positive or negative depending on the phase angle of the complex quantity $H^*_v(f)H_p(f)S_{vp}(f)$.

Figure9 shows the noise coherent with cylinder pressure and the noise coherent with liner vibration. These data were calculated using the first two terms in Equation 6. From Figure 9 it can be concluded that the noise coherent with cylinder pressure is significant over a broad frequency range below 2500 Hz, whereas the noise coherent with liner vibration is significant only in a frequency range from 1200 to 2200 Hz.

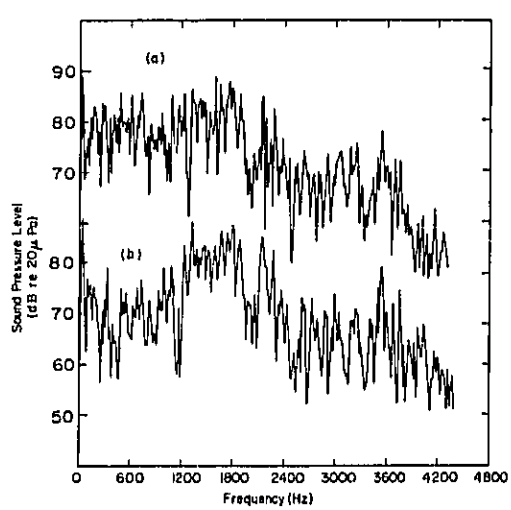

Fig. 9 - (a) Noise coherent with cylinder pressure, (b) noise coherent with cylinder liner vibration

Figure 10 shows the total noise S_{yy}(measured) and the coherent noise S'_{yy}(calculated using Equation 6). Below 2500 Hz most of the noise is coherent with liner vibration and cylinder pressure, but above 2500 Hz there is a significant amount of noise that is not accounted for by the model in Figure 6 (i.e., this noise is lumped into the noise component N(t) and is not identified with either combustion pressures or cylinder liner vibration). It should be noted by comparing Figures 9 and 10 that at certain frequencies the total noise is less than the noise coherent with either cylinder pressure only or liner vibration only. At these frequencies the phase angle of the third term in Equation 6 is between $\pi/2$ and $3\pi/2$; therefore, the third term is negative. Physically this means there is phase cancellation between the noise coherent with combustion and piston impact.

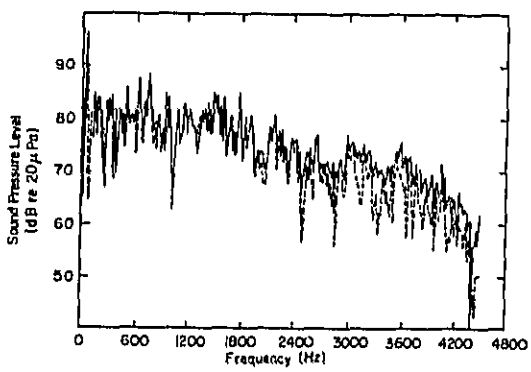

Fig. 10 – Total measured engine noise (solid line) and coherent noise S'_{yy} (dashed line)

APPLICATION TO DESIGN

The frequency response functions in Figure 6 are a description of how well the engine structure responds to an input of a certain type. This response also includes the radiating characteristics of the structure (i.e., the radiation efficiency, the radiation directivity, etc.). If the liner vibration input had been integrated to yield a velocity, the calculated frequency response function $H_v(f)$ would be the acoustical cross-impedance between the cylinder liner and the acoustic field. It should be possible to identify natural frequencies as peaks in the frequency response function, but the data in Figure 8 have too much statistical error to make this possible. Had it been possible to maintain the engine operating parameters constant for a longer period of time (on the order of one minute), smoother estimates of the frequency response functions could be obtained.

The model in Figure 6 can be used for design purposes if the frequency response functions are known. Ideally, the frequency response function would be determined analytically, but, in practice, this is currently not feasible. It appears that the most realistic estimates of the frequency response functions are obtained from running-engine data, but frequency response functions have been estimated from static engine tests (28).

A model of piston impact has been developed by Hayes (33). This model predicts cylinder liner vibration as a function of specified input parameters such as piston/cylinder geometry and combustion characteristics. A model such as this could be used, along with estimates of the frequency response functions $H_v(f)$ and $H_p(f)$, to predict piston-impact and combustion noise, using Equation 6, for a wide range of piston/cylinder liner geometries and combustion parameters. Important piston-impact parameters such as piston mass, piston/cylinder liner running clearance, cylinder liner stiffness, injection timing and peak cylinder pressure could be examined.

SUMMARY

A two-input, single output model has been used to represent the combustion generated and piston-impact generated noise of an in-line, turbo-charged diesel engine. Experiments were conducted to determine frequency response functions between the combustion pressure and between the cylinder liner vibration. The engine noise coherent with each source (combustion and piston impact) has been determined. These data showed that the engine structure responds most strongly over a wide frequency range from 500 to 3000 Hz. Similar conclusions were reached from frequency response measurements on a different engine (7,28). Additional measurements showed that piston-impact vibration occurs mainly in the 1000 to 3000 Hz frequency range. Therefore, it is not surprising that piston impact generated noise is important in the same frequency range (Figures 7 and 9b).

More study should be devoted to measuring and using experimental frequency response functions. At present, the data base is quite limited, and it is not known how the frequency response functions depend on structural factors such as engine configuration, stiffness, and damping.

ACKNOWLEDGEMENT

This paper is the result of research sponsored by Cummins Engine Company at the Ray W. Herrick Laboratories, Purdue University.

REFERENCES

1. G. D. Borelage and J. J. Boreze, "The Ignition Quality of Fuel in Compression Ignition Engine," Engineering, 132-602, 1931.

2. L. J. LeMesurier and R. Stanfield, "Combustion in Heavy Oil Engines," Paper read at North East Coast Institution of Engineers and Shipbuilders, England, Feb. 26, 1932.

3. C. C. Minter, "Flame Movement and Pressure Development in Gasoline Engines," S.A.E. Journal, 30-80, 1935.

4. W. Wilke, "Investigation Concerning the Burning of Diesel Fuels," M.T.Z. 1-43, 1939.

5. S. H. Jenkins, "Analysis and Treatment of Diesel Engine Noise," Symposium on Noise in Transportation, Univ. of Southampton, Paper 9, 1974.

6. B. J. Challen, "The Effect of Combustion System on Engine Noise," S.A.E., SP-397, 750798, 1975.

7. A. F. Seybert, "Estimation of Frequency Response in Acoustical Systems with Particular Application to Diesel Engine Noise," Ph.D. Thesis, Purdue University, 1975.

8. J. Chung, "Measurement and Analysis of Diesel Engine Noise," Ph.D. Thesis, Purdue Univ., 1974.

9. W. C. Strahle and J. C. Handley, "Stochastic Combustion and Diesel Engine Noise," S.A.E., 770408, 1977.

10. S. D. Haddad, T. Priede, and H. L. Pullen, "Relation Between Combustion and Mechanically Induced Noise in Diesel Engines," 15th FISITA Congress, Paris, 1974.

11. D. Anderton and V. K. Duggal, "Effect of Turbocharging on Diesel Engine Noise, Emissions and Performance," S.A.E., SP-397, 750797, 1975.

12. W. W. Soroka and C. F. Chien, "Automotive Piston-Engine Noise and Its Reduction - A Literature Survey," S.A.E. Paper 690452, 1969.

13. P. H. G. Crane, "The Initiation of Diesel Engine Cylinder Liner Vibrations by Piston Transverse Motion," ARL/R2/B10, 1959.

14. E. E. Ungar and D. Ross, "Vibrations and Noise Due to Piston-Slap in Reciprocating Machinery," J. Sound Vib., 2(2) pp. 132-146, 1965.

15. W. J. Griffiths and J. Skorecki, "Some Aspects of Vibration of a Single Cylinder Diesel Engine," J. Sound Vib., I(4), pp. 345-364, 1964.

16. B. J. Fielding, "Identification of Mechanical Sources of Noise in a Diesel Engine," Ph.D. Thesis, Univ. of Manchester, England, May 1968.

17. S. D. Haddad and P. W. Fortescue, "Simulating Piston Slap by an Analogue Computer," J. Sound Vib., 52(1), pp. 79-93, 1977.

18. B. J. Fielding and J. Skorecki, "Identification of Mechanical Sources of Noise in a Diesel Engine: Sound Originating from Piston Slap," Proc. Instn. Mech. Engrs., Vol. 184, pp. 857-873, 1969-70.

19. S. D. Haddad and H. L. Pullen, "Piston Slap as a Source of Noise and Vibration in Diesel Engines," J. Sound Vib., 34(2), pp. 249-260, 1974.

20. E. E. Ungar, F. F. Alvarey, and D. Ross, "Piston-Slap Noise in Reciprocating Machinery," Bolt, Beranek and Newman, Inc., Report No. 1106, 1964.

21. D. Ross and E. E. Ungar, "Recent Experimental Studies of Mechanical Noise in Diesel Engines," Bolt, Beranek and Newman, Inc., Report No. 1139, 1964.

22. T. Usami, S. Wada, and S. Sonoda, "Piston Slap Noise of Indirect Combustion Diesel Engine," S.A.E. SP-397, 750801, 1975.

23. R. Munro and A. Parker, "Transverse Movement Analysis and Its Influence on Diesel Piston Design," S.A.E. SP-397, 750800, 1975.

24. M. Rohrle, "Affecting Diesel Engine Noise by the Piston," S.A.E. SP-397, 750799, 1975.

25. A. C. Eberhardt and W. F. Reiter, "Application of the Coherence Function in Truck Tire Noise Analysis," Proceedings, Second Interagency Symposium on University Research in Transportation Noise, N.C. State Univ., June 5-7, Vol. II, 1974.

26. L. L. Koss and R. J. Alfredson, "Identification of Transient Sound Sources on a Punch Press," J. Sound Vib., 34(1), pp. 11-33, 1974.

27. D. L. Brown and W. G. Halvorsen, "Application of the Coherence Function to Acoustic Noise Measurements," Proceedings, Inter-Noise 72, Washington, D.C., October 4-6, pp. 417-422, 1972.

28. E. T. Buehlmann and M. J. Crocker, "Noise Measurement on a V-6 Diesel Engine," Proceedings, Inter-Noise 74, Washington, D.C., September 20-October 2, pp. 217-220, 1974.

29. J. Chung, J. F. Hamilton, and M. J. Crocker, "Measurement of Frequency Response and the Multiple Coherence Function of the Noise Generation System of a Diesel Engine," JASA, 58(3), p. 635, 1975.

30. A. F. Seybert and M. J. Crocker, "The Use of Coherence Techniques to Predict the Effect of Engine Operating Parameters on Diesel Engine Noise," Trans., ASME 97, B, 4, 1976.

31. J. S. Bendat and A. G. Piersol, Random Data: Analysis and Measurement Procedures, Wiley-Interscience, New York, 1971, Section 5.3.3.

32. A. F. Seybert, J. F. Hamilton, "Time Delay Bias Errors in Estimating Frequency Response and Coherence Functions," J. Sound Vib., 60(1), pp. 1-10, 1978.

33. P. A. Hayes, "Experimental and Analytical Investigation of Diesel Engine Piston Impact and Noise," M.S. Thesis, Purdue Univ., 1977.

790360

MODELING OF VIBRATION TRANSMISSION IN ENGINES TO ACHIEVE NOISE REDUCTION

R.G. DeJong
J.E. Manning

Cambridge Collaborative
Cambridge, Massachusetts

ABSTRACT

The vibration transmission in engine structures has been studied to develop analytical models which predict changes in the noise related vibration of the engine as a function of design changes in the engine components. The models are based on vibration measurements made on non-running engines. This paper outlines the basic procedures for the necessary vibration measurements and for the development of the models. Two examples are given of models developed for different vibration transmission paths in different engines. The vibration transmission from the cylinder pressure to the engine block is modeled for a 4 cylinder DI diesel engine and compared with a simulated vibration transmission measurement with the engine not running. The vibration transmission from the engine block to covers and shields is modeled for a 6 cylinder in-line diesel and compared with the measured vibration transmission with the engine running.

THE NOISE GENERATION MECHANISMS of internal combustion engines continues to be a subject of much interest and study. For purposes of investigating the causes and cures of engine noise, the noise generation mechanisms can be divided into three stages: internal source, transmission path, and external radiation. The internal sources of noise in engines are forces which generate vibration and can be grouped into two categories: gas forces and mechanical forces (1)*. The major gas force, the cylinder pressure due to combustion, has been studied in great detail in the past and its dependence on the operating conditions of the engine has been well documented (2,3). The major mechanical source is generally considered to be piston slap which has been the subject of considerable investigation (4,5) although the mechanism and its dependence on design and operating parameters of the engine is not fully understood. Attempts to modify these internal sources to reduce the engine noise have had some success with an overall noise reduction limited to about 5-6dBA. However, because the internal sources are closely connected with the performance of the engine, reduction in the noise level often adversely affects the performance.

The internal sources do not generate noise directly but instead they generate vibration which is transmitted to the external surfaces where the noise is radiated. The noise radiation from mechanical structures is well understood analytically only for relatively simple geometries such as rectangular flat plates and thin-walled cylinders (6). For complex structures such as engines, the present understanding of the noise radiation process is limited to experimental results comparing the surface vibration levels to the radiated noise (3, 7). The most effective method of reducing the radiated noise has been to add shields over the engine surfaces which can give up to 20dBA noise reduction in certain cases (8). However, the addition of shields is often unsatisfactory because of the increase in weight and the reduction of accessibility of the engine.

The vibration of the engine is transmitted from the internal sources to the external surfaces by means of various transmission paths through the mechanical components of the engine. These transmission paths are not easily identified and their characteristics are not well known. However, the modification of these transmission paths to reduce the vibrational energy flow from the internal sources to the external surfaces appears to be the most promising method of noise reduction in the future. Some attempts have been made to modify the transmission paths by increasing the stiffness of the crank case or isolating engine covers (2,9) with promising results.

This paper outlines a procedure which can be used to measure the various transmission paths in the engine and develop analytical models which can give quantitative estimates of the changes in vibration transmission as a result of mechanical design changes in engine components. If the design changes do not affect the way the engine surfaces radiate noise, then a

*Numbers in parentheses designate References at end of paper.

SAE/P-79/00/$02.50
Copyright © 1979 Society of Automotive Engineers, Inc.

reduction in vibration transmission to the external surfaces will result in a corresponding reduction in the radiated noise.

MEASUREMENT OF VIBRATION TRANSMISSION PATHS

The measurement of the transmission of vibration in any mechanical structure involves the measurement of the response (velocity) at one point for a given excitation (force) at another point. The ratio of velocity to force is called the mobility

$$Y = V/F \qquad (1)$$

The mobility (inverse of impedance) is convenient to use as the transfer fraction of a mechanical system because the resonances of the system appear as peaks in the mobility function. The ratio of velocity to force is a function of frequency and a complete representation involves both magnitude $|Y|$ and phase ϕ.

The development of digital signal analysis equipment has greatly facilitated the measurement of vibration transmission (10). The instrumentation used for the measurements in this study is shown in Fig. 1. A force impulse is used to excite the structure and an accelerometer is used to record the response. The impulse hammer is equipped with a force gauge to measure the input force signal. Fig. 2 shows a typical time history and frequency spectrum of the force impulse. The force spectrum indicates that the impulse has enough energy to excite the structure at all frequencies from 0-5000 Hz.

The transient force and response signals are recorded and transferred to a mini-computer where the frequency spectra of each signal and the mobility ratio are calculated. The results are plotted and stored on disk for future usage. For the measurements reported here the frequency resolution of the spectral data is approximately 25 Hz constant band width.

Figs. 3-6 show examples of the measured mobility functions for several components in a four cylinder diesel engine. Each component was measured while removed from the engine and freely suspended by flexible cords. The piston-connecting rod assembly (Fig. 3) shows a resonance at about 4000 Hz. Below this resonance the vibration transmission characteristics of the piston-connecting rod assembly is controlled by the stiffness of the connecting rod. Fig. 4 shows the drive-point mobility (force and velocity measured at the same point) of the piston top. Comparing this with Fig. 3 indicates the difference in the velocity level at either end of the piston-connecting rod assembly.

The crank shaft (Fig. 5) has several resonances in the frequency range of interest. To aid in understanding the vibration of the crank shaft a shaker was used to excite it at the resonances and the mode shapes of the vibration were measured. Below 3000 Hz these resonances were found to be bending modes with the crank shaft acting basically like a beam. Above 3000 Hz the modes shapes were difficult to measure because of the complicated motion coupling torsional, bending and axial modes. This complexity would undoubtedly increase for crank shafts in engines with more than four cylinders.

The transfer mobility of the oil pan (Fig. 6) shows a large number of resonances which are too close together to count from a measurement of this resolution. The average spacing between the modes can be calculated for a flat plate with the same surface area S and thickness h as the oil pan using the formula (11)

$$\Delta f = \frac{0.57\ hc}{S} \qquad (2)$$

where c is the longitudinal wave speed in the material. Although the exact frequency value of a given mode in the oil pan will be different from that of the corresponding mode in the flat plate, the average spacing between modes remains the same. For the oil pan measured in Fig. 6 the calculated average frequency spacing is 20 Hx.

MODELING THE VIBRATION TRANSMISSION PATHS

Having measured the vibration transmission characteristics of the individual components of the engine, it is possible to combine the measurements numerically to predict the overall vibration transmission of the assembled components. However, this does not give any information on how the physical designs of these components effect the vibration transmission. Therefore it is more useful first to construct analytical models of the individual components and then to use the representation of the model to predict the overall vibration transmission. In this way changes in the design parameters of the engine components can be directly related to changes in the vibration transmission within the engine.

Two types of models can be used to represent the vibration transmission characteristics of the individual components. First, when the component has relatively few resonances below the maximum frequency of interest a lumped parameter or finite element model (depending on the complexity of the component) can be used to match the transfer mobility function over the frequency range desired. As the number of resonances increases it becomes more difficult to match the mobility function with this type of model. However, it may not be necessary to match exactly every resonant frequency if all one is interested in is the average transmission in a frequency band (such as a one-third octave band). In this case, if there are more than about

three resonant frequencies in the frequency band of interest, it is possible to use a statistical model of the component using Statistical Energy Analysis (SEA) (12). With this type of model the mobility function is matched only on the average over each frequency band. The following gives some examples of both types of modeling.

PISTON MODEL - A lumped parameter of the piston-connecting rod can be constructed using a method similar to that for synthesizing electric networks (13). The vibrational motion is assumed to be purely longitudinal and a series of mass-spring elements are combined to match the resonance and anti-resonance frequencies in the drive point mobility of the piston top (Fig. 4). Dashpots are then put in parallel to the springs to match the peak amplitudes of the resonances. The resulting model of the piston and the comparison of the measured and predicted transfer mobility are shown in Fig. 7 (14).

CRANK SHAFT MODEL - A similar model of the crank shaft can be made assuming that the motion is transverse to the axis and that the crank model is then constructed to match the drive point mobility at the center journal. The resulting model of the crank shaft from the four cylinder engine and a comparison of the measured and predicted transfer mobility between two points are shown in Fig. 8. The comparison becomes poor at higher frequencies because of the break down in the assumption of purely transverse motion.

A comparison of the measured and predicted mode shapes of the crank shaft is shown in Fig. 9 for the first four resonant frequencies. Whereas the model is symmetric, the crank shaft does not have exactly symmetric modes shapes. However, the match in the first four mode shapes is fairly good.

OIL PAN MODEL - A statistical model is used for the oil pan because of the large number of resonant frequencies below 5000 Hz (Fig. 6). Since the average resonant frequency spacing of the oil pan was calculated to be about 20 Hz, any frequency band greater than 60 Hz in width will have a sufficient number of modes for the SEA model. In using one-third octave bands this corresponds to a lower frequency limit of 250 Hz.

The average drive-point mobility of a plate-like structure can be given by

$$\langle Y \rangle = \frac{1}{4\ \Delta f\ M} \qquad (3)$$

where Δf is the average frequency spacing of the resonances and M is the total mass. Since the drive point mobility at the edge of a plate-like structure is approximately 4 times the average mobility (11), equation (3) can be modified appropriately to model the average response of a structure by matching the drive point mobility at the edge. This is convenient for a component such as an oil pan which is normally connected to the engine along its edges.

In order to construct an SEA model for the oil pan, the drive point mobility was measured at seven points along the connection flange and the results were averaged. The model can then be used to predict the average transfer mobility from the edge of the oil pan to other points on the surface. Fig. 10 shows a comparison between the model predictions and two measured transfer mobilities on the oil pan. The comparison becomes increasingly better at higher frequencies as the number of resonances in each band increases.

CONSTRUCTING THE COMPLETE TRANSMISSION PATH

The individual component models can be used to analytically connect the elements together to predict the overall vibration transmission of the engine by again using the methods of network synthesis (14). For each component with an input and output point defined as in Fig. 11, the velocity V and force F at the two points can be related by the matrix equation.

$$\begin{bmatrix} V_1 \\ V_2 \end{bmatrix} = \begin{bmatrix} Y_{11} & Y_{12} \\ Y_{21} & Y_{22} \end{bmatrix} \cdot \begin{bmatrix} F_1 \\ F_2 \end{bmatrix} \qquad (4)$$

where Y_{11} and Y_{22} are the drive point mobilities at either end and Y_{12} and Y_{21} are transfer mobilities. For linear, passive, bilateral systems $Y_{12} = Y_{21}$ (12). Components with more than one input or output can be handled by letting the mobility functions themselves be matrices.

When two components, "a" and "b", are connected together at a point with the output of "a" attached to the input of "b", the conditions at the interface are considered to be such that $V_2^a = V_1^b$ and $F_2^a = -F_1^b$ (using superscripts to denote the component). In this case the overall transfer mobility of the assembly is given by (14)

$$Y_{12}^{(a+b)} = \frac{Y_{12}^{b}\ Y_{12}^{a}}{Y_{11}^{b} + Y_{22}^{a}} \qquad (5)$$

The usefulness of this result comes from the fact that the mobility functions used in equation (5) are obtained from analytical models in which the physical parameters have been derived from actual measurements of the components being modeled. This enables the engine designer to use the models to determine how to change the physical design parameters of the various engine components to achieve a reduction in the vibration transmission within the engine and thereby reduce the noise radiated by the engine. The following are some examples of the use of such models to iden-

tify quantitatively the amount of vibration transmission reduction which can be achieved through redesign of various engine components.

COMBUSTION PRESSURE TRANSMISSION

In many direct injection diesel engines the major source of noise is the high frequency component of the cylinder pressure which excites the engine structure to vibrate. Two paths can be identified through which this vibration is transmitted to the external surfaces of the engine block. 1. The cylinder pressure exerts a force directly on the cylinder head which transmits vibration to the engine block through the head gasket and bolts. 2. The cylinder pressure exerts a force on the piston top which transmits vibration through the connecting rod, crank shaft and bearings into the block. In several cases the path through the piston has been found to be the dominant one. This has been reported in other work (15) and is shown in Fig. 12 for our measurements on a non-running 4 cylinder DI diesel.

The measurement of the transfer mobility through the piston-crank-bearing path was made with the piston at top dead center and an artificial static load applied to the piston with flexible couplers through holes in the head where the valves were removed. Heavy grade oil was used in the bearings during the measurements. This simulated as best as possible the conditions under which the high frequency component of the cylinder pressure, which occurs at the onset of combustion, is transmitted through the piston path. The vibration transmission was also measured with the crank shaft at various angles between $\pm$ 30 of TDC and very little change in the result was observed. Therefore, it is assumed that the vibration characteristics of the crank shaft at TDC represents the conditions during the entire combustion process. This may be true only in the case of four cylinder engines and other crank shafts with more complicated geometries need to be studied as well before a more general conclusion can be made. In all measurements the piston was isolated from the cylinder wall with a plastic sleeve to prevent impacts between the piston and the wall from contaminating the results.

A complete model of the vibration transmission path through the piston-crank-bearings was then constructed in order to identify a means of reducing the vibration transmission to the engine block. For simplicity only forces normal to the connection interfaces between the components were considered which is consistent with what would be expected at journal bearings. Also for simplicity only two connections were considered between the crank shaft and the block-those being at the bearing on either side of the piston being modeled. Since a statistical model was used for the block, the output of the complete model is a prediction of the average transfer mobility from the piston top to the engine block surface averaged over one-third-octave bands. Fig. 13 shows a comparison of the model prediction with measurements averaged over the same frequency bands of the vibration transmission to two points on the engine block sides. The accuracy of the model below 500 Hz is poor because the engine block does not have many resonant modes there.

In order to gain insight into what types of design changes would reduce the vibration transmission through the piston-crank-bearing path, it is necessary to look more carefully at the interaction which occurs at the connection points between the various components as indicated by equation (5). This equation states that the overall transfer mobility of two connected components is equal to a ratio with the product of the component transfer mobilities in the numerator and the sum of the drive point mobilities at the connection point in the denominator. In order to reduce the vibration transmission either the transfer mobilities need to be reduced or the drive point mobilities need to be increased, or both.

In the case of the connection between the piston-connecting rod assembly and the crank shaft, the drive point mobility of the connecting rod big end is generally much greater than that of the crank shaft. Therefore the latter can be dropped from the equation as an approximation. Also, over most of the frequency range the transfer and drive point mobilities of the piston-connecting rod are nearly equal in magnitude so that they tend to cancel each other out. The result is that the overall transfer mobility of the piston-connecting rod-crank shaft assembly is approximately equal to that of the crank shaft alone. This is a result of the fact stated earlier that the piston-connecting rod assembly acts like a spring below its first resonance at 4000 Hz and any force which is applied to the piston top is directly transmitted to the crank pin. Therefore, modifications to the piston-connecting rod will have little affect on the overall vibration transmission of that path unless the first resonant frequency is lowered by at least a factor of two or three. This is unlikely because of the constraints on the piston mass and connecting rod stiffness.

As a result the overall transfer mobility from the piston to the block is dominated by the connections at the crank shaft journals and the main bearings. The bearings are considered as inputs to the engine block model. Again referring to equation (5) the interaction of these con-

nections can be studied to determine if design changes can be made to reduce the vibration transmission. Because of the complexity of the crank shaft design it is not clear at this time if design modifications could be made which would significantly change the mobility functions. Therefore only changes in the block design are considered here.

One means of reducing the vibration transmission is to decrease the transfer mobility of the block. This can be done by increasing the stiffness, mass, or damping of the block. Increasing the stiffness of the block at the main bearing supports has been tried by others with some success (8,16) and appears to be worth further investigation. Increasing the mass or damping of the block appreciably is an unlikely solution.

A second means of reducing the vibration transmission into the block is to increase the drive point mobility of the main bearings by increasing their flexibility. Although the bearings are by nature required to have high stiffness for load bearing capabilities, it may be possible to achieve a sufficient amount of resilience at higher frequencies. An attempt at such a design was implemented in the 4 cylinder engine by using a constrained layer of silicone rubber between the bearing rings and the bearing caps as shown in Fig. 14 (17). Although this design could not be directly implemented in a running engine, it was used to demonstrate the prediction capabilities of the model.

Using the resilient bearing design a change in the overall vibration transmission from the piston to the block was predicted and measured on the non-running engine shown in Fig. 15. Above 1000 Hz the vibration reduction is inversely proportional to the stiffness of the bearings. A comparison of the effective stiffnesses of the standard and modified bearings as a function of frequency is shown in Fig. 16.

VIBRATION TRANSMISSION TO COVERS AND SHIELDS

The method of statistical modeling was applied to the noise radiated by engine covers in a study conducted at Calspan Corporation under contract to the Department of Transportation (18). One of the engines studied was a turbocharged 6 cylinder in-line diesel engine and the noise levels radiated from the individual surfaces and external components at 50% rated load were measured by the method of lead wrapping in an anechoic test cell. The results of the source identification are shown in Table I.

The noise radiated by the block sides was treated by the addition of shields of various constructions. A variety of combinations of steel plates with and without damping treatment, with and without foam absorption on the block side, with and without isolation mountings were tried. The measured mobility of a shield constructed with 16 gauge steel with ½" foam backing is shown in Fig. 17 as compared with the drive point mobility of the engine block at a typical connection point.

Rather than use equation (5) to evaluate an overall vibration transmission, in the case of the analysis of covers it is more convenient to modify the equation slightly to evaluate the ratio of the average cover velocity to the engine block velocity. This is done by multiplying equation (5) by Y_{12}^{a} resulting in

$$\frac{V_{rms}^{b}}{V_{rms}^{a}} = \frac{Y_{12}^{b}}{Y_{11}^{b} + Y_{22}^{a}} \qquad (6)$$

where component "a" is the engine block and component "b" is the cover. In the case of light weight covers the magnitude of the drive point mobility of the cover will be much larger than that of the engine block so that

$$\frac{V_{rms}^{b}}{V_{rms}^{a}} \simeq \frac{Y_{12}^{b}}{Y_{11}^{b}} \qquad (7)$$

This result leads to some well known and frequently tried solutions to cover noise reduction which are the addition of damping to the cover to reduce the transfer mobility Y_{12}^{b} and the use of isolated mountings to increase the drive point mobility Y_{11}^{b}. However, equation (7) is useful in that it gives quantitative estimates of the noise reduction achievable.

In the case of the block side shields the foam gives enough damping to bring down the velocity of the shields to about 10dB below that of the block. This will reduce the block side radiated noise proportionately provided the radiation efficiency is not significantly changed. A 10dBA reduction in the block side source level would bring the overall engine noise level down by 2dBA which is essentially the maximum achievable reduction possible by complete elimination of that source until other sources are also reduced. This was demonstrated in the measurements taken with the variety of block side shields mentioned

previously. For all measurements taken with foam between the block and the shields an overall noise reduction of about 2dBA was achieved. Without the foam between the block and shield the noise reduction was significantly reduced, apparently because of the build up of noise behind the shield and leakage around the edges of the shield.

Similar measurements and analysis were done for the valve covers as shown by the average mobility function in Fig. 18 and a comparison between the measured and predicted ratio of the cover and block velocity levels in Fig. 19. The statistical model of the valve cover loses accuracy in the lower frequency range due to the lack of resonant modes. Specifications can be obtained from equation (7) to determine the necessary treatment to reduce the valve cover source level by 10dB. This can be achieved by using isolation mountings with a point stiffness of 5×10^5 N/m (3000 lbs/in) and the addition of damping to obtain a critical damping ratio of 0.05 in the frequency range of interest.

The oil pan was also studied with the mobility functions shown in Fig. 20 and the velocity ratio comparison shown in Fig. 21. This particular oil pan was made of aluminum, and it was found that by going to a steel pan with the same bending stiffness, the drive point mobility could be increased by a factor of 2. Combined with an increase in the oil pan damping factor to 0.03 critical, a noise reduction of 10dBA was predicted for the oil pan source level. Such an oil pan was constructed and installed on the engine with a reduction in total engine noise of 1dBA. Unfortunately the new oil pan source level was not measured individually. However, a total reduction of 1dBA would require at least a 10dBA reduction in the oil pan radiation, although the actual oil pan reduction cannot be determined accurately by this method.

CONCLUSIONS

The following conclusions can be drawn from this study:

1. The vibration transmission paths in engine structures can be modeled with sufficient accuracy to predict changes in vibration transmission with changes in design parameters of the individual engine components. The component models can be constructed from measurements of the mobility on the individual components while freely suspended by flexible mounts. For components with only a few resonant modes below the maximum frequency of interest a model is used which matches the mobility functions over this frequency range. For components with many resonant modes a statistical model is used which matches the average of the mobility function in a given number of frequency bands.

2. Although the models used in this study were limited to point force transmission at the connection points, conceptually the models can handle both moment bearing and line connections. However, at this time there is no readily available method for measuring moment and line mobilities which would be necessary to construct such models.

3. The modeling of the vibration transmission has the potential to be extended to predict the total noise produced by the engine. In order for this to be accomplished two additional things are needed. First, the force strength of the internal sources must be known along with an identification of the appropriate transmission paths to the external surfaces. Second, the nature of the noise radiation from the vibration of the external surfaces must be better understood in terms of its relationship to the physical parameters of the engine structure.

REFERENCES

1. E.C. Grover and N. Lalor, "A Review of Low Noise Diesel Engine Design at I.S.V.R." J.S.V. Vol. 28, No. 3, pp 403-431, 1973.

2. D.D. Tiede and D.F. Kabele, "Diesel Engine Noise Reduction by Combustion and Structural Modification." SAE Paper 730245.

3. D. Anderton and J. Baker, "Influence of Operating Cycle on Noise of Diesel Engines." SAE Paper 730241.

4. S.D. Haddad and H.L. Pullen, "Piston Slap as a Source of Noise and Vibration in Diesel Engines." J.S.V. Vol. 34, No. 2, pp 249-260, 1974.

5. T. Usami, S. Wada, and S. Sonoda, "Piston Slap Noise of Indirect Combustion Diesel Engine." SAE Paper 750801.

6. L.L. Beranek, "Noise and Vibration Control." McGraw-Hill Book Company, New York, N.Y., 1971.

7. M.G. Hawkins and R. Southall, "Analysis and Prediction of Engine Structure Vibration." SAE Paper 750832.

8. G.E. Thien and H.A. Fachback, "Design Concepts of Diesel Engines with Low Noise Emission." SAE Paper 750838.

9. T. Priede, E.C. Grover, and N. Lalor, "Relation Between Noise and Basic Structural Vibration of Diesel Engines." SAE Paper 690450.

10. G.F. Lang, "Understanding Vibration Measurements." Sound and Vibration Vol. 10, No. 3, 1976.

11. L. Cremer, M. Heckl, and E.E. Ungar, "Structure-Borne Sound." Springer-Verlag, Berlin, 1973.

12. R.H. Lyon, "Statistical Energy Analysis of Dynamical Systems: Theory and Applications." The MIT Press, Cambridge, Mass., 1975.

13. V.H. Neubert, "Series Solutions

for Structural Mobility." J.A.S.A. Vol. 38, pp 867-876, 1965.

14. R.G. DeJong, "Vibrational Energy Transfer in a Diesel Engine." Sc.D. Thesis, Massachusetts Institute of Technology, 1976.

15. H. Gross, "Noise Control of Air-Cooled Diesel Engines." Presented at the Tenth Annual Noise Control in Internal Combustion Engines, April 27-28, 1978.

16. D.F. Kabele and G.A. Anderkay, "Techniques of Quieting the Diesel." SAE Paper 750839.

17. R.H. Lyon and R.G. DeJong, "Designing Diesel Engines For Reduced Noise." Proceedings of the EPA-University Noise Seminar 1976, NTIS #PB-265-114.

18. Work sponsored by DOT Contract No. DOT-TSC-1013 carried out at Calspan Corp.

ACKNOWLEDGEMENTS

This work is supported in part by DOT Contract No. DOT-TSC-1013. We are grateful to the staff at Calspan Corporation and Mr. B. Challen of Ricardo & Co. for their assistance in the acquisition of the data used in the analysis of engine covers.

Table I - Source Identification of 6-Cylinder Diesel Engine

RADIATING SURFACE	A-WEIGHTED SOUND POWER LEVEL (dBA RE. 10^{-12} WATTS)
BLOCK SIDES	101
VALVE COVERS	98.5
ENGINE FRONT	98
OIL PAN	97.5
ALL OTHERS	99
TOTAL	106 dBA

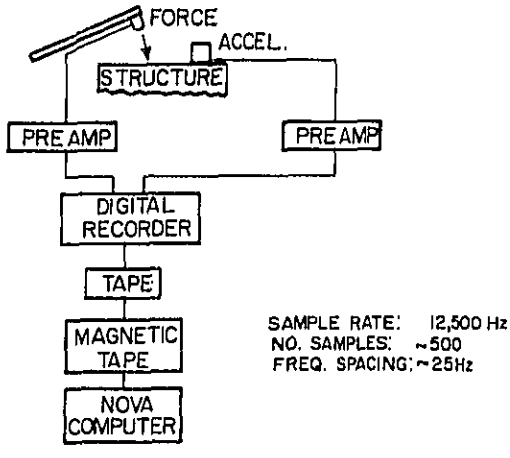

Fig. 1 - Instrumentation for mobility measurements

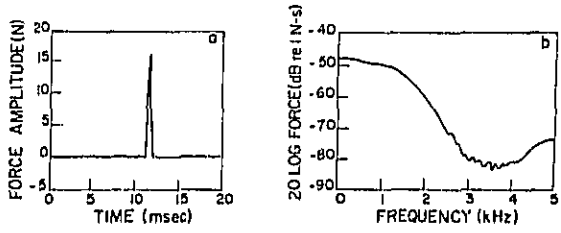

Fig. 2 - Typical force impulse used to excite vibration in engine structures a.-Time History b.- Frequency Spectrum

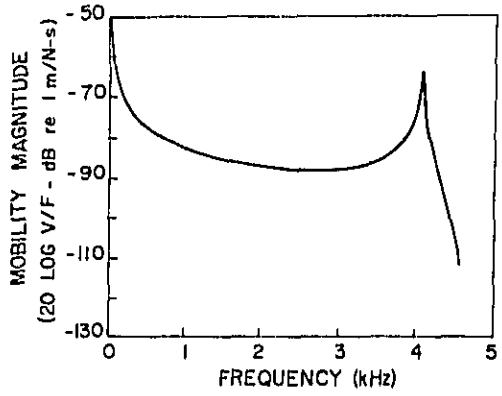

Fig. 3 - Measured transfer mobility of piston from top surface to big end

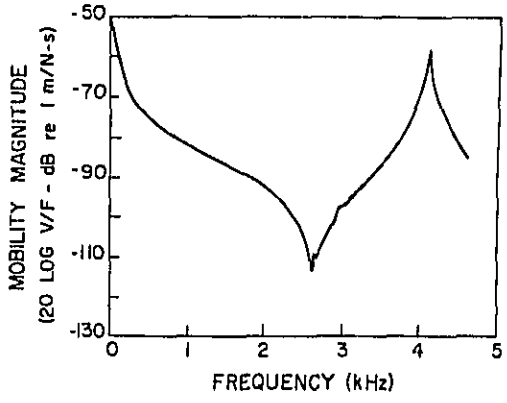

Fig. 4 - Measured drive point mobility of piston top surface

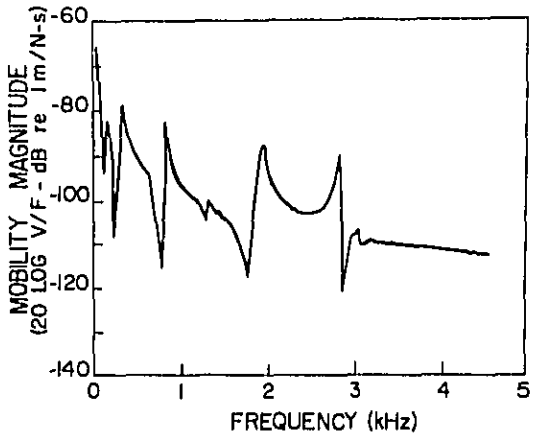

Fig. 5 - Measured transfer mobility of crank shaft from pin #2 to Journal #2

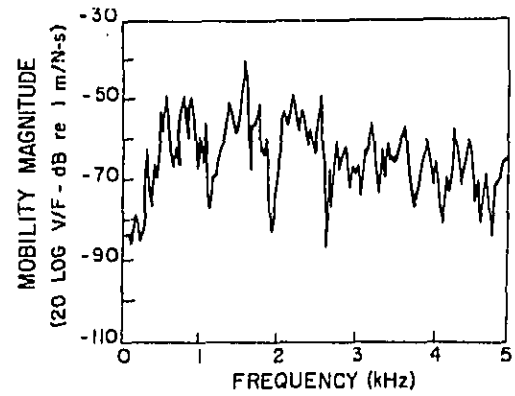

Fig. 6 - Measured transfer mobility of oil pan from flange to surface point

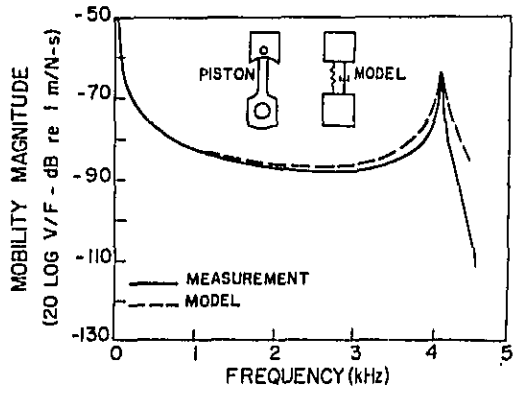

Fig. 7 - Comparison of measured and predicted transfer mobility of piston

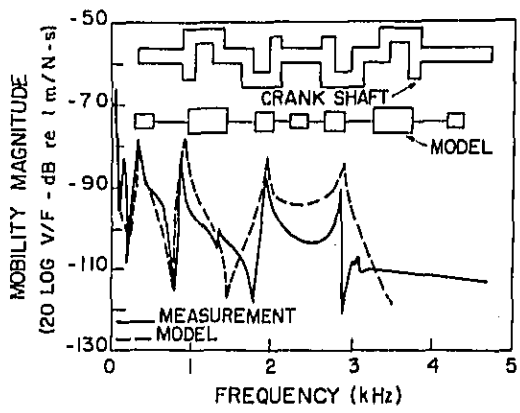

Fig. 8 - Comparison of measured and predicted transfer mobility of crank shaft

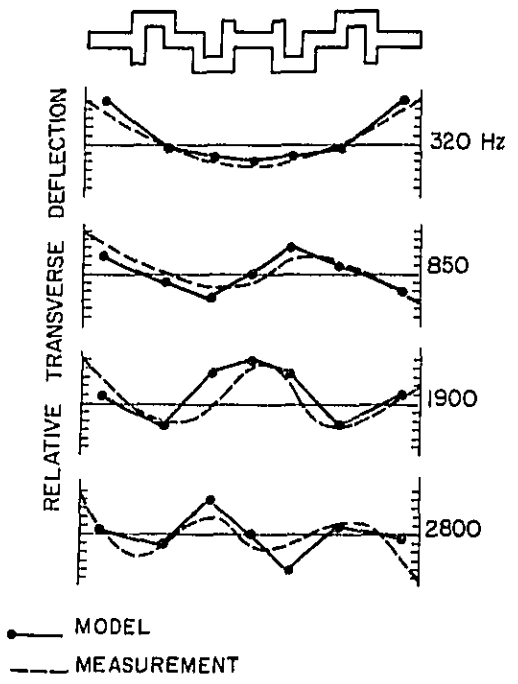

Fig. 9 - Comparison of measured and predicted mode shapes of crank shaft

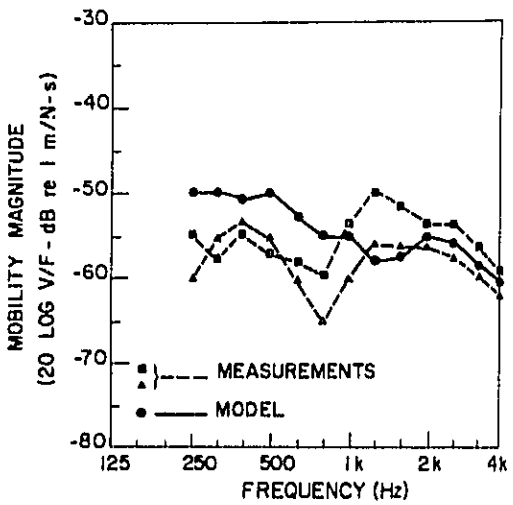

Fig. 10 - Comparison of measured and predicted transfer mobility of oil pan

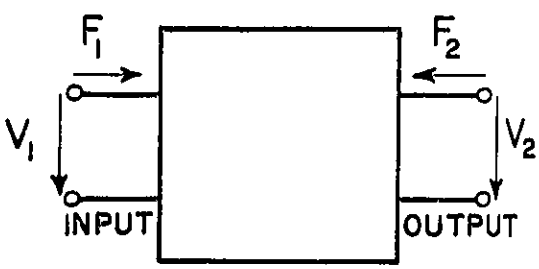

Fig. 11 - Input, output model of individual components

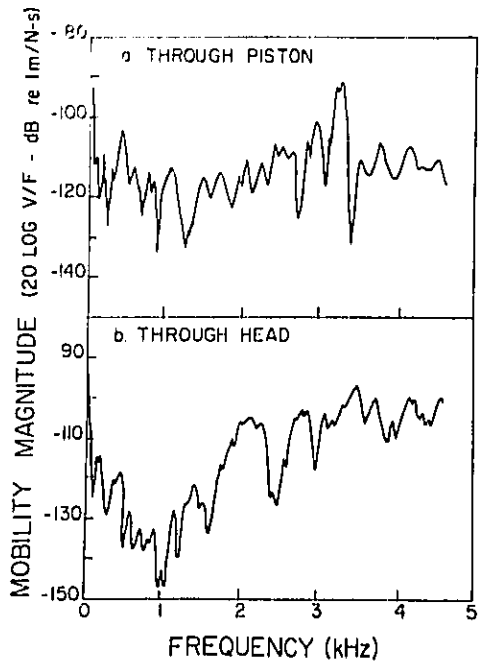

Fig. 12 - Comparison of transfer mobility for two paths from the cylinder pressure to the block side walls

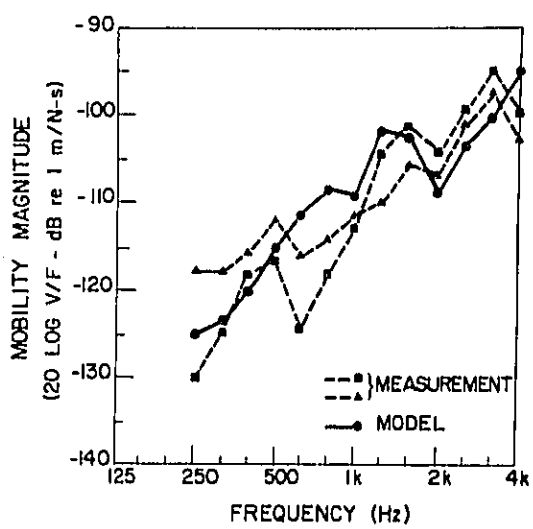

Fig. 13 - Comparison of measured and predicted transfer mobility from piston top to block side walls

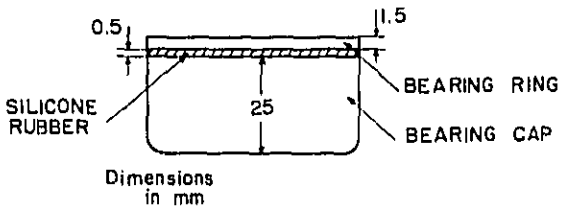

Fig. 14 - Cross section of constrained layer resilient bearing design

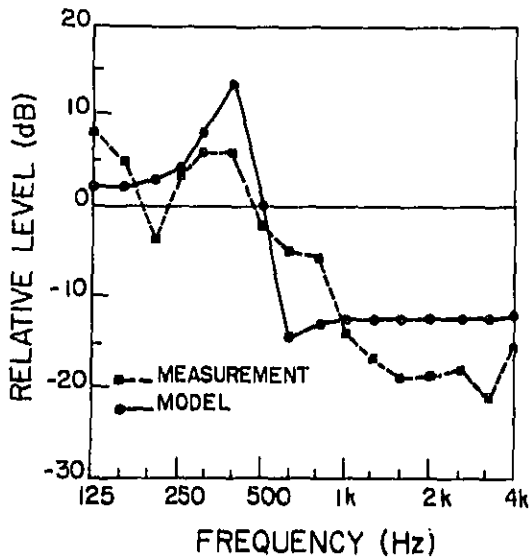

Fig. 15 - Comparison of measured and predicted change in vibration transfer from piston top to block side walls

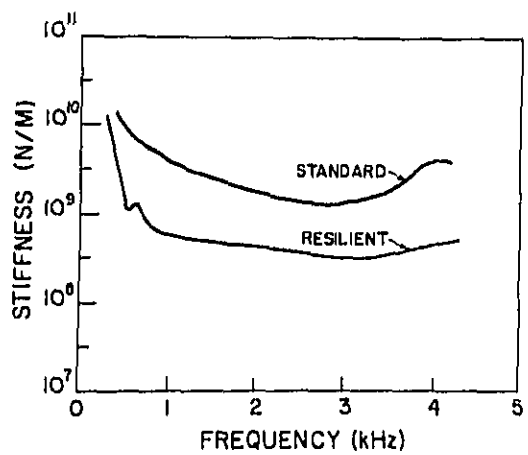

Fig. 16 - Comparison of effective stiffness of standard and resilient bearings

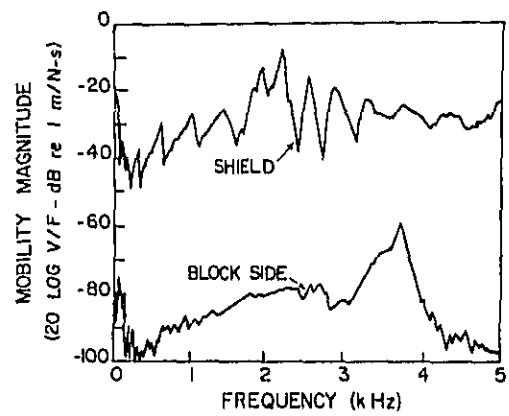

Fig. 17 - Comparison of measured drive point mobilities of engine block side and block side shield with foam backing

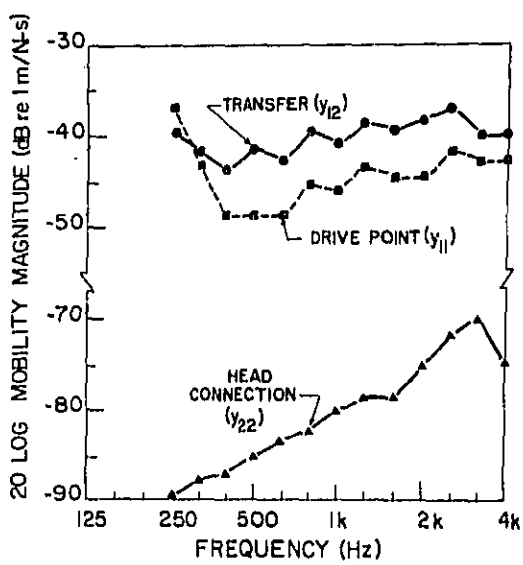

Fig. 18 - Valve cover mobility functions

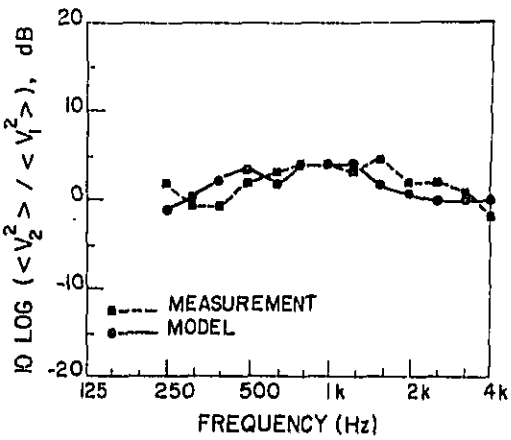

Fig. 19 - Comparison of measured and predicted velocity ratio of valve cover and engine block

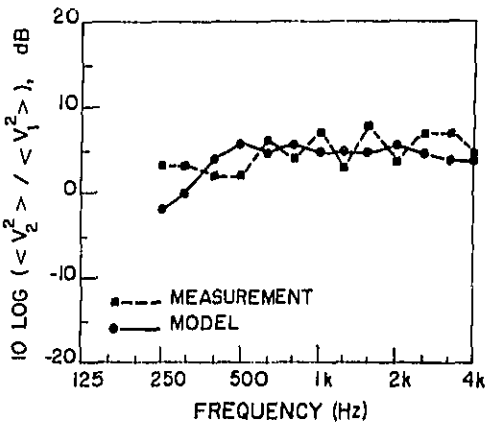

Fig. 21 - Comparison of measured and predicted velocity ratio of oil pan and engine block

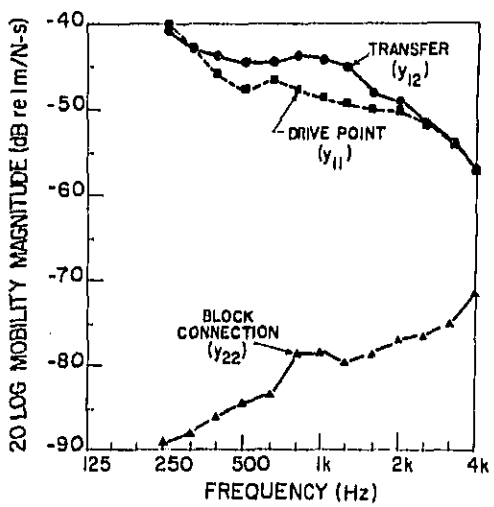

Fig. 20 - Oil pan mobility functions

790361

Vibration Mode Analysis for Controlling Noise Emission from Automotive Diesel Engine

Fujio Aoyama, Shinichi Tanaka
and Yasuo Miura

Hino Motors, Ltd. (Japan)

ABSTRACT

The vibration mode analysis of an automotive diesel engine for the purpose of obtaining a lower level of noise emission will be described in the paper.

Since the noise emission corresponds to the vibration of certain components of the engine, the vibration of engine structure was analyzed in several running conditions.

Vibration distribution shows a natural vibration mode which was proven by coincidence with the result obtained by modal analysis.

When measurement of the vibration mode is very difficult due to the high mechanical impedance and especially the big damping factor of the component, a new method of vibration mode analysis for the engine component excited by cylinder pressure was proven to be useful.

Some attempts for controlling the noise and an analysis of damping effects will also be described in the paper.

THE NOISE EMISSION from heavy vehicles which is attributable mainly to the engine has become of great concern in recent years. As a way of reducing the engine noise, the feasibility of using a partial or full enclosure for the engine has already been studied by many researchers in addition to modification of the engine structure itself. (1)(2)*

Described here is an analytical approach toward obtaining a lower level of noise emission from the diesel engine by controlling the vibration of its structure.

The procedure includes

1) An investigation of the relationship between vibration level and noise radiation efficiency of the engine surface.
2) An investigation of the relationship between the vibration distribution of engine components in several running conditions and their natural vibration modes.
3) An investigation of natural vibration modes of engine components by applying cylinder pressure which are obtained by a new method of vibration mode analysis in firing condition.
4) Some attempts at noise reduction of engine by controlling vibration of engine components.

* Numbers in parentheses designate References at end of paper.

TEST ENGINE, EXPERIMENTAL SETUP AND MODAL ANALYSIS

In the experiment a direct injection type diesel engine was used, whose specifications are shown in Table 1.

Table 1 - Specifications of Test Engine

Engine type	4 Stroke cycle, Water cooled Direct injection
Number of cylinders	6 in line
Bore and stroke	137 mm x 150 mm
Swept volume	13.3 litres
Compression ratio	1 : 17.9

Information from the experiments was mostly processed by a Hewlett Packard Fourier Analyzer Model 5451B of 64Kbytes which enabled modal analysis. Tests were carried out in an anechoic room of 9m x 9m x 6m which provided a free field condition for measuring engine noise.

The noise and vibration measurements were carried out by general procedure with a Brüel & Kjaer type 2209 sound level & vibration meter,

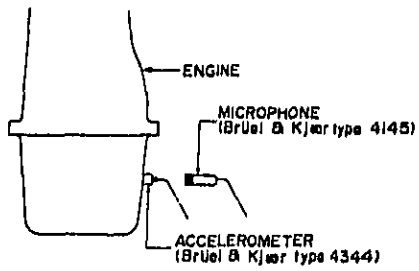

Fig. 1 - Schematic diagram for measurement of sound and vibration

type 2113 frequency analyzer and type 2305 level recorder. A type 4344 accelerometer set on a surface as shown in Fig. 1 was also utilized for measuring vibration.

The modal analysis of some components was carried out by impulse-frequency response technique which measures the response of an impulsive force applied to several points as

SAE/P-79/00/$02.50
Copyright © 1979 Society of Automotive Engineers, Inc.

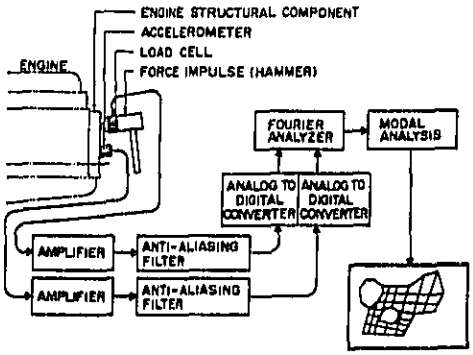

Fig. 2 - Schematic diagram of experimental apparatus for modal analysis (impulse-frequency response technique)

schematically illustrated in Fig. 2.(3)(4) The signals from accelerometer and load cell on the hammer were passed through anti-aliasing filters before analog to digital conversion.

The amplitude and phase angle at each point on the structure at natural frequency can be evaluated by modal analysis from the stored transfer function of the disk memory. This function is in turn obtained from the time domain sampled via analog to digital converter.

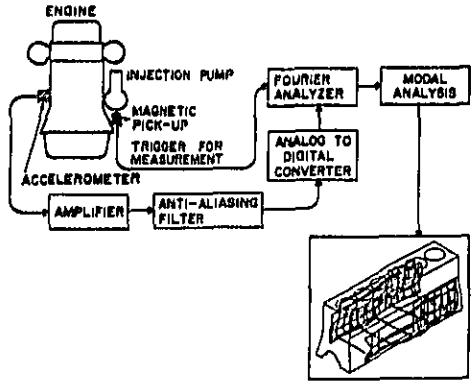

Fig. 3 - Schematic diagram of experimental apparatus for modal analysis (firing condition)

The animated mode shapes can be generated in this way, giving a true picture of how a part is distorted at each key frequency.

For the analysis of firing condition of the engine, the vibration mode of engine structure affected by combustion was also processed by modal analysis as schematically shown in Fig. 3. The signal of the acceleration at each point on the grid covering the structure surface was processed for animated mode shaps through the same procedure as described before.

During these treatments, the magnetic pick-up set on the injection pump functions as a trigger for measuring vibration affected by combustion of a certain cylinder. The detailed procedure will be described later.

RELATION BETWEEN VIBRATION AND NOISE LEVEL RADIATED FROM ENGINE SURFACE (Example on oil sump)

Prior to vibration analysis of the engine structure, it is necessary to ascertain acoustical effects caused by vibration of the engine surface.

According to a preliminary test which clarified that one of the main sources of noise radiated from the engine surface is the oil sump, the vibration and sound level from it were measured at numerous points on its side wall. The accelerometer for the vibration measurement was set up on each point one after another while the sound pressure level was measured at 7 mm

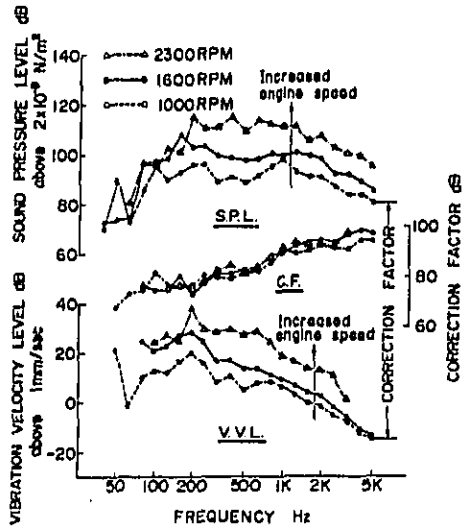

Fig. 4 - Noise characteristics of oil sump (4/4 load)

above each of the points.

This sound measurement procedure is well known as the close field microphone technique which aboids the influence of noise from any other source. In our tests, a 1.6 mm thick stamped steel oil sump was used and the engine was run at full load condition.

An example of the relation between vibration and sound pressure level at various points on the wall surface of the sump is shown in Fig. 4. Though both vibration and sound pressure level become greater with increased engine speed at any frequency band, the difference between them, which the authors call "Correction Factor (C.F.)" as had been expressed by Priede, was not influenced by engine speed as indicated in the figure.(5) Namely, this Correction Factor is almost constant at any frequency band.

The Correction Factors obtained at many points on the side wall of a 1.6 mm thick stamped steel

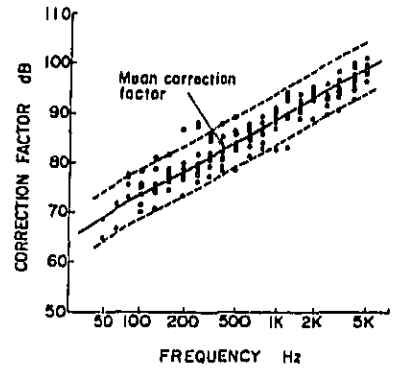

Fig. 5 - Correction Factors of stamped steel oil sump (t = 1.6 mm) (4/4 load)

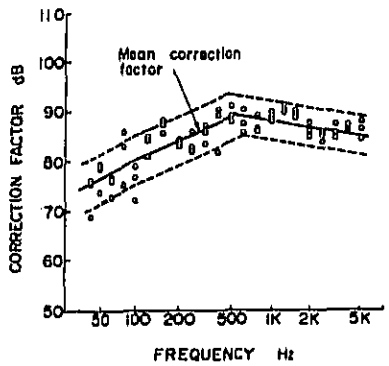

Fig. 6 - Correction Factors of aluminum cast oil sump (t = 5 mm) (4/4 load)

oil sump are shown in Fig. 5. In spite of randomly selected measurement points on the wall, the Correction Factors increased equally at heightened frequency with small dispersion.

These results mean that the level of sound pressure emitted from some area can be estimated from the vibration level measured on it at any frequency band. Namely, the vibration level is closely related to the sound pressure level.

Fig. 6 shows the Correction Factors in the case of an aluminum sump with 5 mm wall thickness obtained by the same measurement technique. In this case, the Correction Factor has a refraction point at a frequency around 500 Hz. This phenomenon can be explained as a coincidence effect which will occur at a definite frequency (coincidence frequency) determined as wall thickness and rigidity.(6) Since the aluminum sump has a comparatively lower coincidence frequency than the stamped steel one, it would give a refraction point within analyzed range of frequency as shown in the figure.

Now, if the Correction Factor is determined, sound pressure radiated from the vibrating area of wall surface can be estimated.

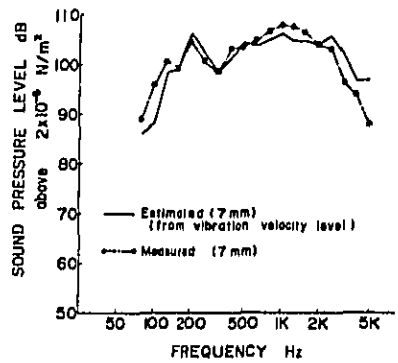

Fig. 7 - Sound pressure level of stamped steel oil sump (4/4 load, 2,300 rpm)

Fig. 7 shows both estimated and measured sound pressure level radiated from the side wall of stamped steel oil sump on a running engine. The two sound pressure levels show very good coincidence at every frequency band. The estimation of sound pressure was carried out as described before using the obtained mean Correction Factor shown in Fig. 5. In this case, the vibration velocity level was measured at 87 points on the wall of the oil sump, and the sound pressure levels were also measured at 7 mm distance from the surface at each point. The mean value of 87 points at every frequency band is shown in the figure. Only the oil sump wall was exposed from the lead plate which covered the whole remaining

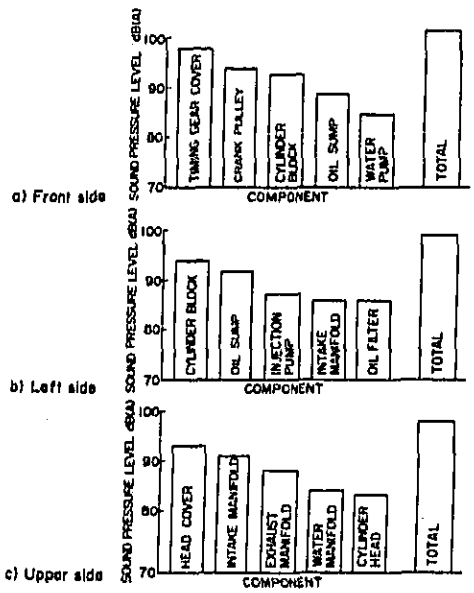

Fig. 8 - Noise radiated from major engine components (1 m distance from engine surface) (4/4 load, 2,300 rpm)

area for protection from interfering noise, which is known as the lead covering technique. (7)(8)

These experimental results indicate that both analysis and control of the vibrating surface are very important for noise reduction, because the sound pressure level of the surface has a very close relation with vibration velocity.

MODE AND DISTRIBUTION OF VIBRATION OF ENGINE STRUCTURE (Example on timing gear cover)

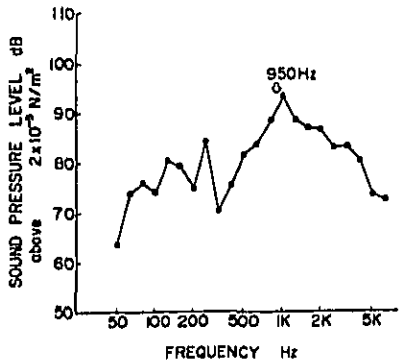

Fig. 9 - Front side noise emitted from timing gear cover (4/4 load, 2,300 rpm)

Fig. 8 shows the contribution of major engine components to the total noise of the experimental engine in some directions. Due to its being one of the main contributors to the noise radiated from the front of the engine, the timing gear cover was chosen for the analysis of vibration mode and distribution.

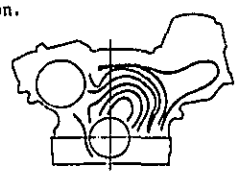

a) 950Hz, 4/4 load, 2300 RPM

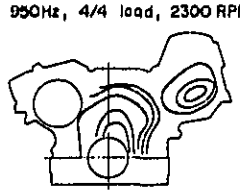

b) 950Hz, motoring, 2300 RPM

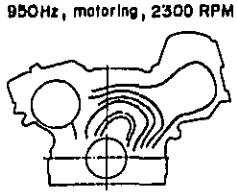

c) 950Hz, 4/4 load, 1600 RPM

Fig. 10 - Vibration distribution of timing gear cover

A peak level of sound pressure was detected at 950 Hz by a narrow band frequency analyzer after a one third octave band frequency analysis as shown in Fig. 9. This survey was carried out by the lead covering technique and the noise was measured at 1m distance from the cover on a running engine.

An accelerometer measured the vibration acceleration at numerous points on the timing gear cover at 950 Hz in several running conditions of the engine.

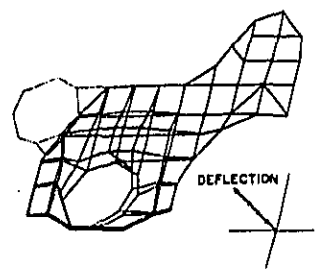

Fig. 11 - Mode shape of timing gear cover obtained by impulse-frequency response technique in assembled condition (950 Hz)

The results can be seen in Fig. 10. A full load and a motoring condition both at rated speed and a full load at medium speed are shown in the figure. The results indicate that the patterns of vibration distribution on the timing gear cover are similar. Namely, it seems to be a natural vibration mode on this engine component.

The natural vibration mode of the timing gear cover when assembled to the engine was obtained by modal analyzer utilizing the impulse-frequency

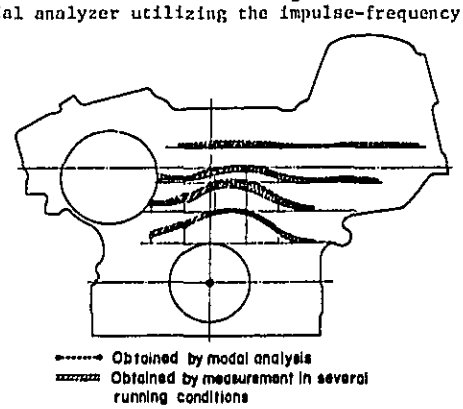

Fig. 12 - Vibration amplitude of timing gear cover (950 Hz)

response technique or the so-called hammering method and is shown in Fig. 11. The chain line in the figure designates the area for water pump where vibration measurement was not performed.

Fig. 12 shows a comparison of vibration distribution of timing gear cover in relative amplitude obtained from actual measurement on the running engine and the natural vibration mode

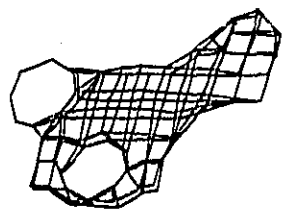

a) 392 Hz

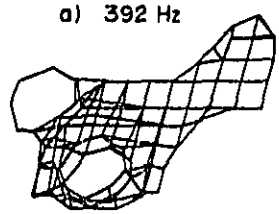

b) 721 Hz

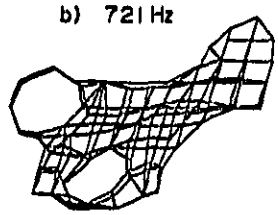

c) 867 Hz

Fig. 13 - Mode shape of timing gear cover by impulse-frequency response technique in free condition

using modal analysis. The two amplitudes show very good coincidence, which means the radiated noise from the timing gear cover was caused mainly by its natural vibration mode.

In the case described above, the modal analysis was carried out for the timing gear cover while assembled to the engine. Therefore, it is necessary to clarify the relation between natural vibration modes of the timing gear cover in assembled state and in free condition.

Fig. 13 shows mode shapes of the timing gear cover in a free condition at a few natural frequencies. In this case, the timing gear cover was suspended by strings and struck by a hammer with a load cell.

This result shows that the natural vibration mode in a free condition has quite a different shape from that in assembled condition at any frequency and therefore it is not possible to estimate from this mode the noise emission from the engine. This indicates that measurement of natural vibration modes of some parts of the engine should be performed with the parts in assembled condition and not free condition.

For effective noise reduction, knowledge of the mode shapes of certain areas on the engine obtained by the procedure described above is very important.

VIBRATION MODE OF ENGINE STRUCTURE INFLUENCED BY CYLINDER PRESSURE DURING COMBUSTION
(Example on cylinder block)

The aforementioned analysis was also tried on the side wall of the cylinder block which is another big contributor to noise emission. The vibration distribution at peak frequency detected by the lead covering technique is shown in Fig. 14.

Though the experimental result showns a comparatively big amplitude at the lower side of the block, it is difficult to comprehend the mode shape of the whole cylinder block owing to difficulty of phase discrimination. Moreover, due to higher mechanical impedance of the cylinder block in general, the vibration mode analysis is very difficult by either impulse-frequency response technique or swept sine excitation technique. (7)

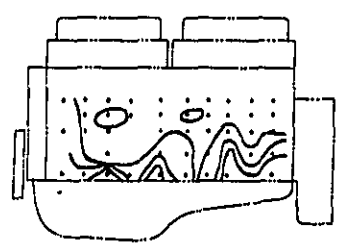

a) Left side

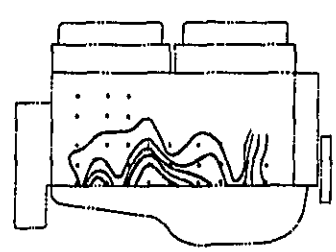

b) Right side

Fig. 14 - Vibration distribution on side wall of cylinder block (1,050 Hz) (4/4 load, 2,300 rpm)

Due to these circumstances, the authors tried to obtain the mode shape of the cylinder block during combustion of each cylinder by utilizing modal analysis with a Fourier analyzer. The measured vibration acceleration at numerous points on the side wall of cylinder block was transmitted to the modal analysis via Fourier analyzer as already shown in Fig. 3. This system was used to display the mode shape as an animation on the screen.

The vibration acceleration on the side wall of the cylinder block is strongly affected by combustion of each cylinder as shown in Fig. 15-a). For analyzing the vibration mode caused by the combustion of a certain cylinder, effects of other

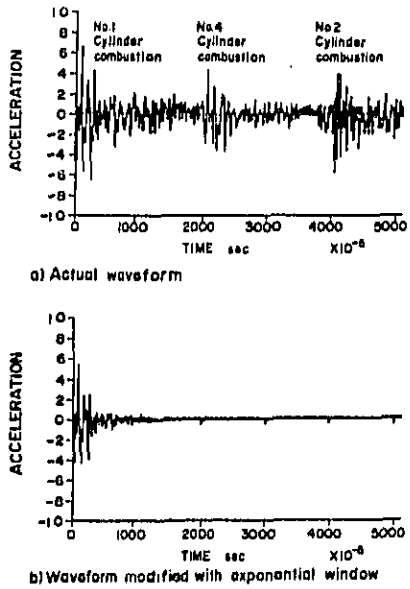

Fig. 15 - Vibration acceleration measured on cylinder block (4/4 load, 1,000 rpm)

firing cylinders must be eliminated.

To fulfill the above described requirement, the time domain of vibration acceleration sampled to Fourier analyzer was multiplied by a decreasing exponential function (called an exponential window) as illustrated schematically in Fig. 15-b). Though the exponential window was applied to eliminate the effect from other firing cylinders, it cannot disturb the relative amplitude and phase

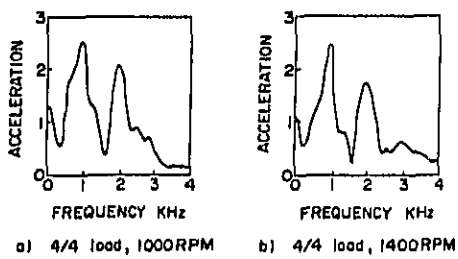

Fig. 16 - Frequency spectrum of acceleration on cylinder block (No. 1 cylinder combustion)

angle among the frequency domains obtained at numerous points. The sampling of the signal of vibration acceleration measured at each point of the cylinder block is triggered just before the combustion of a certain cylinder.

The frequency domain of vibration acceleration for different engine speeds at a point on the wall during combustion of No. 1 cylinder is shown in Fig. 16. Because these experimental results show that the acceleration spectra were very similar for the two speeds shown, the following analysis was performed at an engine speed of 1,000 rpm.

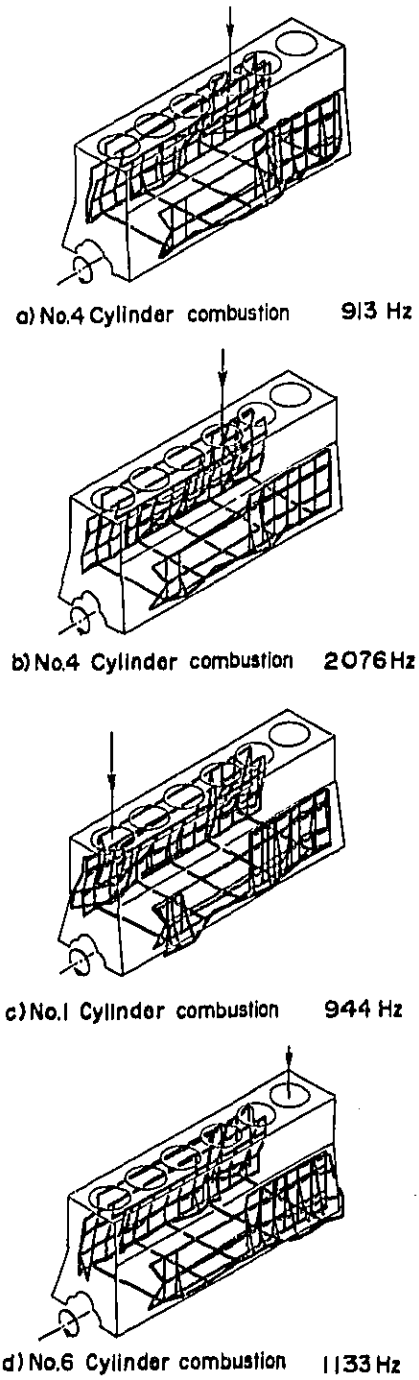

Fig. 17 - Mode shape of cylinder block caused by combustion

This method of analysis was verified by comparison with the mode shape obtained by impulse-frequency response technique as described in appendix A.

The vibration modes of cylinder block were obtained at preferred natural frequencies for an engine speed of 1,000 rpm at full load condition. The vibration modes of cylinder block caused by combustion of No. 1, 4 and 6 cylinders are quoted as an example in Fig. 17.

The following results have been obtained.

1) Vibration modes caused by combustion of each cylinder differ from one another.
2) The vibration modes include several vertical conical shapes and horizontal bending shapes.
3) The conical shape mode which is located around the firing cylinder occurs in every frequency range, while the bending vibration mode disappears at higher frequency (above 1.6 kHz) as shown in Fig. 17-a) and b).
4) The vibration amplitude of both conical and bending modes tends to decrease with increased distance from the firing cylinder as typically shown in Fig. 17-c) and d).
5) The amplitude at lower side of cylinder block is very large at any vibration mode.

SOME ATTEMPTS AT NOISE REDUCTION OF ENGINE

Due to the beforementioned results, it can be considered that reinforcement of the lower side of the cylinder block would be effective for controlling the vibration. An underplate of which the optimum shapes were determined by finite element method was chosen so as to provide five times the usual stiffness of cylinder block. Fig. 18 shows the underplate.

The increase of horizontal stiffness of cylinder block by attachment of the underplate causes a decrease of vibration velocity at the side wall of the engine as shown in Fig. 19. Though the vibration velocity at the lower side of the cylinder block and oil sump is reduced as expected, the effect of noise reduction of engine is not so remarkable and is shown in Fig. 20 together with the effect of the damping treatment in the following description. These results indicate the necessity of a more effective means to control vibration.

Fig. 18 - Underplate for reinforcement of cylinder block

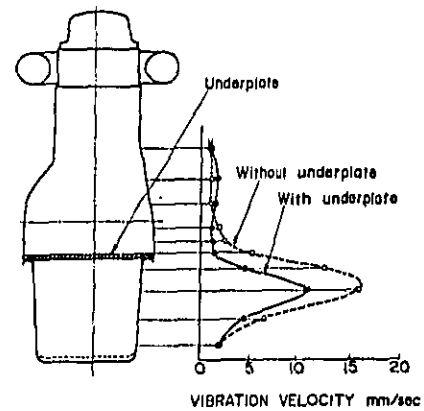

Fig. 19 - Effect of underplate on vibration velocity of cylinder block and oil sump (1,000 Hz, 4/4 load, 2,300 rpm)

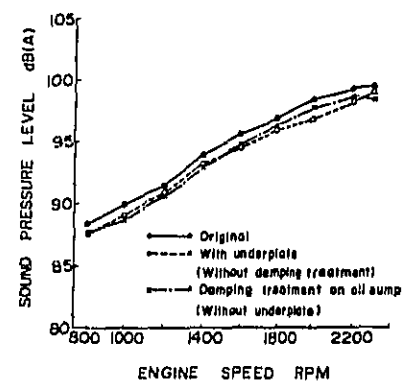

Fig. 20 - Effect of underplate and damping treatment on noise reduction (1 m distance from left side, 4/4 load)

Vibration control by attaching damping materials on the surface of oil sump was tried. Such damping treatment as a way to control the natural vibration modes has been mentioned by many researchers. (8)(9)

The effect of noise reduction by such damping treatment with 8 mm thick vinyl chloride plate attached on the oil sump is shown in Fig. 20 together with the effect of the underplate.

The authors quote the following formula for noise attenuation by damping treatment which is described in appendix B.

$$A = 8 \log_{10} \frac{\zeta_2}{\zeta_1}$$

Where

A ; noise attenuation in dB
ζ_1 ; damping factor of the component before damping treatment
ζ_2 ; damping factor of the component after damping treatment

The damping factors ζ_1 and ζ_2 were obtained by impulse-frequency response technique in heated (or warmed) condition the same as when the engine is running.

This formula shows that the noise attenuation effect largely depends on the damping factors of the component before and after damping treatment.

So far as noise reduction of the cylinder block is concerned, the damping treatment will not give so good a result due to the high mechanical impedance and especially the big damping factor of the component. (10)

CONCLUSIONS

The following conclusions can be drawn from this study;

1. Because the noise level of an engine has a close relation with its vibration level, the noise control can be made by analyzing and controlling the vibration.
2. Observation of the vibration mode of a component should be made with the component assembled to the engine.
3. The new method of analyzing the vibration mode influenced by combustion with modal analysis via Fourier analyzer is convenient for a direct comprehension of vibration mode of a running engine especially in case of components with higher mechanical impedance.
4. The effect of the vibration control is influenced largely by the damping factor of the component itself before attachment of damping material, not only by the damping factor of the damping material.

ACKNOWLEDGEMENTS

The authors wish to thank Professor emeritus F. Nagao of Kyoto University and Dr. Y. Tokita of Kobayashi Institute of Physical Research for their valuable comments on the study. The authors are also thankful to their colleagues who assisted in the studies and to the directors of Hino Motors, Ltd. for their permission to publish this paper.

REFERENCES

1. G. E. Thien and H. A. Fachbach. 'Design Concepts of Diesel Engine with Low Noise Emission', SAE Paper 750838 presented at SAE Diesel Engine Noise Conference, Detroit, August 1975.

2. S. H. Jenkins, N. Lalor and E. C. Grover. 'Design Aspects of Low-Noise Diesel Engines', SAE Paper 730246 presented at SAE International Automotive Engineering Congress, Detroit, January 1973.

3. M. Richardson and J. Kniskern, 'Identifying Modes of Large Structures from Multiple Input and Response Measurements', SAE Paper 760875 presented at SAE Aerospace Engineering Meeting Town and Country, San Diego, November - December 1976.

4. Hewlett Packard Company, 'Modal Analysis Operating and Service Manual Option 402 for 5451B Fourier Analyzer', January 1976.

5. T. Priede, Ph. D., A. E. W. Austen, B. Sc, Ph. D., and E. C. Grover. 'Effect of Engine Structure on Noise of Diesel Engines', Proc. Instn Mech Engrs. Volt Pt 2A No4 1964 - 1965.

6. 'Noise Control Hand Book (Japanese)' third edition 1968 pp. 279 - 280.

7. T. Priede, E. C. Grover, and N. Lalor, 'Relation Between Noise and Basic Structual Vibration of Diesel Engines', SAE Paper 690450 presented at SAE Mid-Year Meeting, Chicago, May 1969.

8. R. S. Lane, S. E. Timour and G. W. Hawkins, 'Technique of Structual Vibration Analysis Applied to Diesel Engine Noise Reduction', SAE Paper 750835 presented at SAE Diesel Engine Noise Conference, Detroit, August 1975.

9. John Pofit, 'Composites for Noise Control-Sound-Deadened Steel', Sheet Metal Industries, January 1974 pp. 44 - 50 presented at the Annual Conference of ISME, October, 1973.

10. M. G. Hawkins and R. Southall, 'Analysis and Prediction of Engine Structure Vibration', SAE Paper 750832 presented at SAE Diesel Engine Noise Conference, Detroit, August 1975.

APPENDIX A.

Comparison of Vibration Mode obtained by Modal Analysis via Fourier Analyzer and by Impulse-Frequency Response Technique

Fig. A-1 shows the vibration mode shape of the timing gear cover which was caused by cylinder pressure of No. 1 cylinder. The result was obtained by modal analysis via Fourier analyzer. Due to good coincidence of this figure with Fig. 11 in the paper, the procedure could be verified.

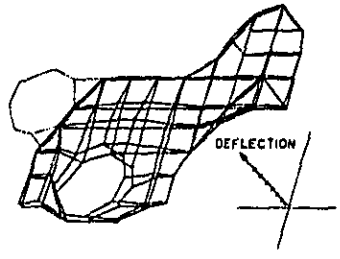

Fig. A-1 Vibration mode of timing gear cover caused by combustion pressure in No. 1 cylinder (950 Hz, 4/4 load)

APPENDIX B

Effect of Dampling Factor on Noise Attenuation

A similar damping treatment applied to several kinds of engines gives different noise attenuation

Table B-1 - Noise Attenuation obtained by Damping Treatment (distance of 1m, 4/4 load, rated speed)

	Engine		Noise Attenuation dB(A)		
	Number of cylinders	Swept volume (litres)	Front side	Left side	Upper side
A	6 in line	13.3	0.9	0.9	0.1
B	6 in line	6.4	0.1	0.6	1.9
C	8 vee form	15.9	0.3	0.1	0.2

Table B-2 - Damping Factor obtained by several Experiments (at preferred natural frequency)

Engine	Component	Damping treatment	Damping factor (%) ζ_1	Damping factor (%) ζ_2
A	head cover	8mm thick coat	2.1	4.5
A	timing gear	8mm thick coat	2.9	5.3
B	head cover	8mm thick coat	0.6	4.3
B	head cover	8mm thick half coat	0.6	3.3
B	head cover	4mm thick coat	0.6	2.2
B	timing gear cover	8mm thick coat	1.5	3.5
C	head cover	8mm thick coat	3.8	5.0
C	timing gear cover	8mm thick coat	3.8	4.6

ζ_1 ; damping factor before damping treatment
ζ_2 ; damping factor after damping treatment

as shown in Table B-1. In this case, the damping treatment with 8mm thick vinyl chloride plate was made on oil sump, timing gear cover and head cover in each engine respectively. This phenomenon will be influenced by different damping factor of each component at its preferred natural frequencies.

Table B-2 shows the damping factors of the components before and after damping treatment which were obtained in heated condition the same as a running engine.

Fig. B-1 shows noise attenuation versus the ratio of damping factors obtained from these engines. In this case, the noise measurement was performed at 1 m from the surface of the compoent in the frequency range of one third octave band including its natural frequency in several running conditions, when the component was exposed from lead covered engine. By such procedure, the relation between the damping factor before treatment of the component at preferred natural frequency and the attenuation of noise radiated from the component was also obtained as shown in Fig. B-2.

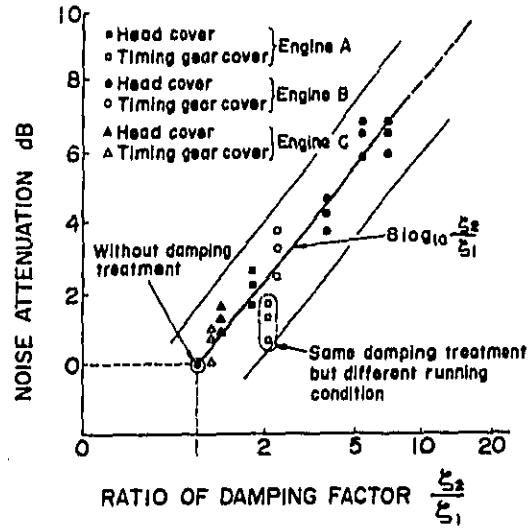

Fig. B-1 Effect of ratio of damping factors on noise attenuation

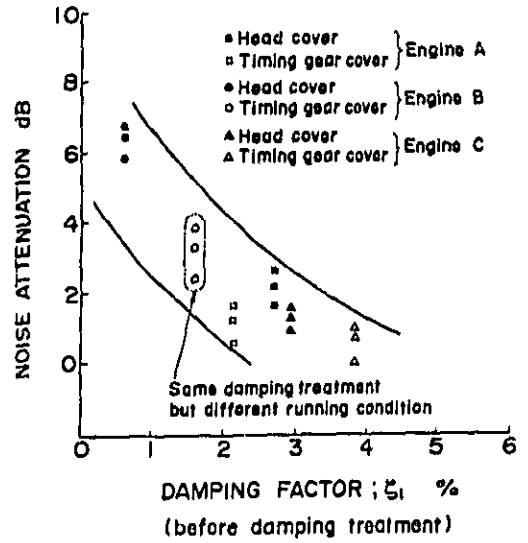

Fig. B-2 Effect of damping factor before treatment on noise attenuation

790362

MODELING OF DIESEL ENGINE NOISE USING COHERENCE

Malcolm J. Crocker
James F. Hamilton

Ray W. Herrick Laboratories
School of Mechanical Engineering
Purdue University
West Lafayette, IN 47907, USA

ABSTRACT

A diesel engine can be modeled as a multiple-input, single output system, sometimes known as a coherence model.

Theoretical models for multi-input, single output systems are quite well developed, but only recently have attempts been made to apply these models to practical noise cases such as diesel engines. The results of these models can be used to predict changes in engine noise as cylinder pressure - time history is varied or to attempt to identify sources of noise in the engine. Practical difficulties and simplifying assumptions which must be made are discussed.

WHILE DIESEL ENGINE NOISE has received considerable attention in the last twenty years, most of the effort has been in noise source identification. Much of this work has been empirical and has mainly involved experimental studies of which some have been quite sophisticated. Similarly, noise sources of interest have been either covered, removed, or disconnected, and by comparing the noise spectrum of the engine before and after the changes, conclusions were reached about the relative source contributions to the complete engine noise.

Such early studies by Priede and his colleagues [1,2,3,4]* and by other workers [5-11] have lead to a qualitative understanding of the noise production process in a diesel engine and also to the design of some reduced noise engines. However, a complete understanding of the noise generation process is still far away.

The need for additional understanding of the noise generation process lead to the present coherence studies, many of which have been conducted at the Herrick Laboratories, in which the engine was modeled as a multiple-input, single output system [12-24]. The object was to utilize the coherence model to provide information about noise sources of a running engine without the undesirable requirement sequentially to cover, remove or disconnect the noise sources which is both time consuming and can possibly alter the noise generation process. The model developed could then be used in a parameter study to determine which factors were important in noise generation; for example, to evaluate the relationship between engine noise and the cylinder pressure time-history.

The multiple-input, single-output prediction model developed involves a mathematical model in which the transfer functions between the multiple-inputs (sources) and the single-output (far-field microphone) must be determined experimentally. It is normal to formulate the model in the frequency domain, in which case the approach is usually called the coherence technique. In this case the transfer functions between the sources and the far-field microphone are called the frequency response functions $H_n(f)$ for the n sources. These functions are dependent on the frequency f, Hz.

It is also possible to formulate a similar multiple-input, single-output model in the time domain where it is known as the correlation technique. Goff was the first to use this technique for noise source identification in 1955, [25]. Although correlation has been used widely and successfully in other applications such as turbulence study, it has not been used widely in noise control studies. However, Kumar and Srivastava did use the correlation technique recently to study noise source identification on diesel engines, and reported some success with this approach [26].

Since the ear tends to behave as a frequency analyzer, it is generally preferable to formulate the noise problem in the frequency domain and to use the coherence technique. The remainder of the paper discusses the coherence approach to modeling diesel engine noise and to noise source identification and discusses some of the difficulties encountered and simplifying assumptions which must be made.

*Numbers in brackets designate References at end of paper.

SAE/P-79/80/$02.50
Copyright © 1979 Society of Automotive Engineers, Inc.

THEORY

The multiple input, single-output model is shown in Figure 1. Here the inputs are x_1, $x_2 \ldots x_i$ and $y' = y_1 + y_2 + \ldots y_i$ is the output which is correlated with the inputs. We define z as the noise measured at the output which is uncorrelated with any of the inputs and assume that no input has been missed in the modeling process.

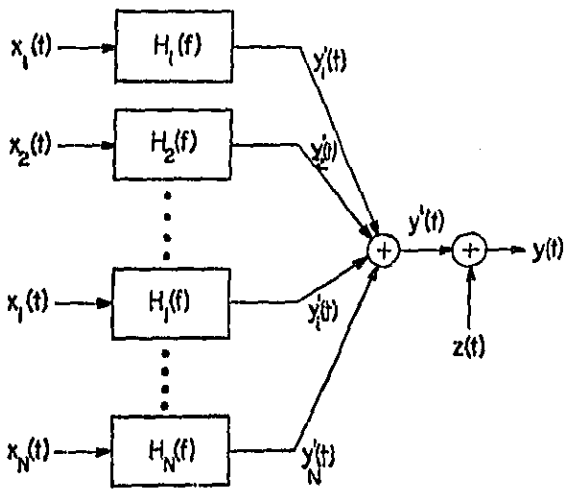

Fig. 1 - Multiple-input, single-output system with uncorrelated noise z(t) in output.

Single Input Case

If we reduce the number of inputs in Figure 1 to 1, (or consider just one path), the theory is more easily understood. The single-input, single-output system is shown in Figure 2.

In the frequency domain, the Fourier transforms $F(f)$ of the time-domain output and input signals $y'(t)$ and $x(t)$ are related by:

$$F_{y'}(f) = H(f)\, F_x(f). \qquad (1)$$

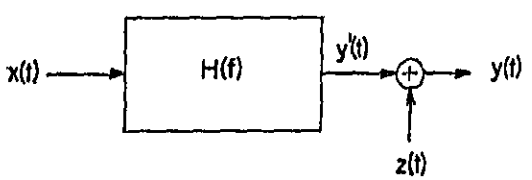

Fig. 2 - Single-input, single-output linear system with uncorrelated noise z(t) in output.

By multiplying by the conjugate of the input signal Fourier transform $F_x^*(f)$, and suitably averaging over the ensemble of records we obtain the frequency response:

$$H(f) = \frac{S_{xy'}(f)}{S_{xx}(f)}, \qquad (2)$$

where $S_{xy'}(f)$ is the cross-spectral density between the input and output, given by:

$$S_{xy'}(f) = \frac{1}{T}\{F_x^*(f) F_{y'}(f)\}, \qquad (3)$$

and $S_{xx}(f)$ is the auto-spectral density of the input given by:

$$S_{xx}(f) = \frac{1}{T}\{F_x^*(f) F_x(f)\}, \qquad (4)$$

where suitable ensemble averaging is again implied. Here T is the record length utilized in the Fourier transformation.

Since uncorrelated noise z may be present at the output then $y = y' + z$. The uncorrelated noise may be caused by ambient background noise, instrumentation noise, nonlinear system response or so-called mechanical noise which is uncorrelated with the input. The signal y' cannot be measured, only y can be measured or the cross-spectral density $S_{xy}(f)$ can be obtained:

$$S_{xy}(f) = \frac{1}{T}\{F_x^*(f) F_y(f)\} \qquad (5)$$

and since $F_y(f) = F_{y'}(f) + F_z(f)$, then Equation (5) gives:

$$S_{xy}(f) = \frac{1}{T}\{F_x^*(f)\left[F_{y'}(f) + F_z(f)\right]\}$$

$$= S_{xy'}(f) + S_{xz}(f). \qquad (6)$$

We note that, in general, cross-spectral densities and frequency response functions are complex quantities, with the exception of the special case of the auto-spectral densities which are real quantities. Since x ans z are uncorrelated, ensemble averaging of $S_{xz}(f)$ will give $S_{xz}(f) = 0$, so that equation (6) becomes

$$S_{xy}(f) = S_{xy'}(f), \qquad (7)$$

and so [using Equations (2 and 7)] the frequency response H(f) can be evaluated from:

$$H(f) = \frac{S_{xy}(f)}{S_{xx}(f)} . \qquad (8)$$

The ordinary coherence function between the input x and the output y is defined as

$$\gamma^2(f) = \frac{S_{xy}(f)}{S_{xx}(f)S_{yy}(f)} . \qquad (9)$$

The ordinary coherence function $\gamma^2(f)$ indicates how well the mean square value of the output is related to the input. If the uncorrelated noise z=0, then $\gamma^2(f)=1$, and if $y'<<z$, so that $y\approx z$, then $\gamma^2(f)\approx 0$.

Multiple Input Case

Figure 1 shows the more general case with N inputs. The total output y(t) is the sum of the individual outputs y'(t) and uncorrelated noise z(t),

$$y = y' + z$$

thus

$$y = \sum_{i=1}^{N} y_i + z \qquad (10)$$

and by Fourier Transformation:

$$F_y = \sum_{i=1}^{N} F_{x_i} H_i + F_z . \qquad (11)$$

Multiplying Equation (11) by its complex conjugate F_y^*, dividing by T and ensemble averaging suitably gives:

$$S_{yy} = \sum_{i=1}^{N}\sum_{j=1}^{N} S_{ij} H_i H_j^* + S_{zz} , \qquad (12)$$

since terms such as $S_{x_i z}=0$ with the ensemble averaging.

Note that the terms F,H, and S are all frequency dependent in Equation (11) and all following equations, however for simplicity this dependency is omitted.

In Equation (12) S_{ij} is the cross-spectral density between the i and j inputs and S_{zz} is the auto-spectral density of the uncorrelated noise z. Multiplying Equation (11) in turn by each value of F_i^*, i=1,2,3...N, and dividing by T gives Equation (13) where suitable averaging is implied.

If there are N inputs, then there will be N equations:

$$S_{iy} = \sum_{j=1}^{N} H_j S_{ij} , \quad i=1,2,3...N. \qquad (13)$$

The frequency responses H_1, H_2, H_3,...H_N can be found by solving Equations (13). For solution by digital computer it is convenient to rewrite Equations (13) in matrix form [14,18].

The multiple coherence function $\overline{\gamma^2_{xy}}$ is defined to be:

$$\overline{\gamma^2_{xy}} = \frac{S_{y'y'}}{S_{yy}} , \qquad (14)$$

where

$$S_{y'y'} = \sum_{i=1}^{N}\sum_{j=1}^{N} S_{ij} H_i H_j^* . \qquad (15)$$

The multiple coherence function γ^2_{xy} represents the fraction of the output which is coherent with all the inputs. From Equations (12,14 and 15) we obtain

$$\overline{\gamma^2_{xy}} = 1 - \frac{S_{zz}}{S_{yy}} . \qquad (16)$$

If $S_{zz}<< S_{yy}$, then $\overline{\gamma^2_{xy}}\approx 1$, but if $S_{y'y'}<< S_{zz}$, $S_{yy}\approx S_{zz}$ and $\overline{\gamma^2_{xy}}\approx 0$.

Partial Coherence

If we wish to determine the amount of noise measured at the output y which is uniquely attributable to each source, then the concepts of the partial coherence function and the residual spectral densities are useful. The partial coherence approach is particularly attractive if the original sources are not very coherent in themselves but if the source signal measurements are contaminated among themselves. (By contamination we mean that in trying to measure one source, we also measure contributions from other sources). Such a situation occurs in practice when microphones are placed close to predominant noise sources on an engine. In the partial coherence approach, the linear effects of the other inputs are removed from each input and output. This approach then is attractive in source identification because contamination can be removed from source signals. However, there is the danger in this process that if the input signals are quite coherent with each other (e.g., engine and exhaust) that some of the true input signals are removed by this process. The theory for the partial coherence approach has been discussed in detail by Bendat [27-29] and Dodds and Robson [30] so it will only be briefly reviewed here.

The residual spectral density represents the spectral contribution of source x_i to the output y when the linear effects of all other sources are removed from both x_i and y, [27-30]. For example consider the case of a noise generating system with three well defined inputs [31,32]. The

unique contributions from source inputs x_1 x_2, x_3 to the output y are respectively:

$$\gamma^2_{1y\cdot23}(f) \cdot S_{yy\cdot23}(f) ,$$
$$\gamma^2_{2y\cdot31}(f) \cdot S_{yy\cdot31}(f) , \text{ and}$$
$$\gamma^2_{3y\cdot12}(f) \cdot S_{yy\cdot12}(f) .$$

The three terms represent the spectral density at y coherent only to x_1, x_2, and x_3 respectively. These three terms may be called the coherent residual spectral density functions of the inputs x_i. Here each term is made of the product of two terms. For example: $S_{yy\cdot23}(f)$ is the residual spectral density of output y when the linear effects due to sources x_2 and x_3 are removed; $\gamma^2_{1y\cdot23}(f)$ is the partial coherence function of source x_1 when the linear effects due to sources x_2 and x_3 are removed from both x_1 and y.

EXPERIMENTAL RESULTS

1. Idealized Experiment

In order to check the above theory an idealized experiment was conducted in an anechoic room with three loudspeakers S_1, S_2 and S_3 driven by three independent random noise generators, see Figure 3. Complete details of the experimental procedure are given by Wang elsewhere [31,32].

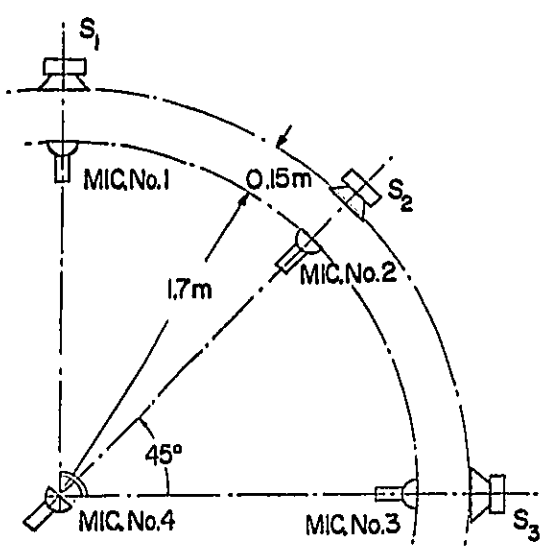

Fig. 3 - The Arrangement of the Sound Sources (Loudspeakers,S) and Microphones (Mic.) in the Idealized Experiment.

In source identification there are two important possibilities; i) Incoherent noise sources with measurement contamination, and ii) Coherent noise sources with measurement contamination. Both these cases could be investigated with the present idealized experiment. The loudspeaker signals could be made completely incoherent or partly coherent by adding part of the output of random noise generator no. 1 to the signals to the other speakers S_2 and S_3 using potentiometers and summers. Three cases with α = 0, 0.5 and 1.0 were studied (α is the fraction of the output voltage of noise generator no. 1 added to the signals fed to speakers S_2 and S_3.) Note that in all cases measurement contamination was present since each microphone received noise not only from the closest loudspeaker, but also small amounts of noise from the other two speakers.

The experimental procedure was as follows: First with all speakers simultaneously in action, $S_{ij}(f)$, $S_{iy}(f)$ and $S_{yy}(f)$ were evaluated. From these measurements the transfer functions H_i, (i=1,2,3) were calculated. Then the contribution of each noise source to the far field noise y was calculated. The calculated contribution $|H_i|^2 S_{ii}$ of each speaker to the far field noise output (y) could be compared with the noise actually measured from that speaker when the other two speakers were switched off. (See Figures 4 and 5). Also shown in Figures 4 and 5 is the output of each speaker predicted by the partial coherence approach. As might be expected, when the sources are incoherent (Figure 4) the two prediction methods give almost the same result which agrees quite well with the measured result. However, when the sources are fairly coherent (Figure 5) where α = 0.5 and $\gamma^2 \approx 0.25$) then the predictions are not so accurate. In all cases, as expected, the partial coherence approach tends to underestimate the noise, while the multiple-input approach tends to overestimate the noise. The two methods used in conjunction can thus be used to give an upper and lower "bound" for the noise of each source.

2. Experiments on Modeling of Diesel Engine Noise

Chung, Seybert, Crocker and Hamilton have used the multiple-input, single-output coherence system to model diesel engine noise, [13-21 and 24].

Six pressure transducers were mounted in the cylinder head of a V-6 naturally aspirated diesel engine which was thought to be combustion-noise dominated. These six transducers were considered to be the inputs to the model. A microphone mounted about 1m. from the side of the engine block in an anechoic room was considered

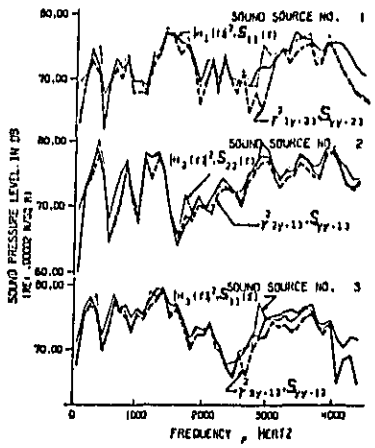

Fig. 4 Predicted spectra compared with the true spectrum, $\alpha = 0.0$. [ref. 32]

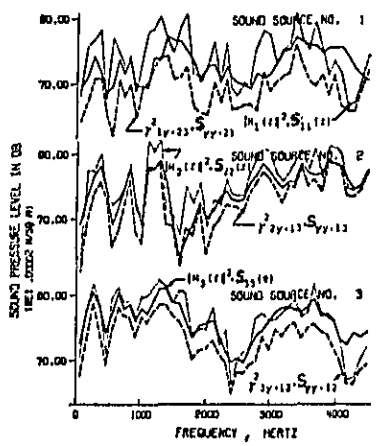

Fig. 5 Predicted spectra compared with the true spectrum, $\alpha = 0.5$. [ref. 32]

to be the output, y. Figure 6 shows cylinder pressure-time histories measured under different loads. The ripples in the time histories were considered to be caused by a chamber resonance also reported by earlier workers. Figure 7 shows the auto-spectrum of the cylinder pressure time history for the lowest load of 7ft-lb obtained using an FFT analyzer. The signal was filtered off below 800 Hz to remove the dynamic range problem and above 5000 Hz to prevent aliasing. The broad peak in the spectrum at about 4000 Hz was found to correspond to the frequency of

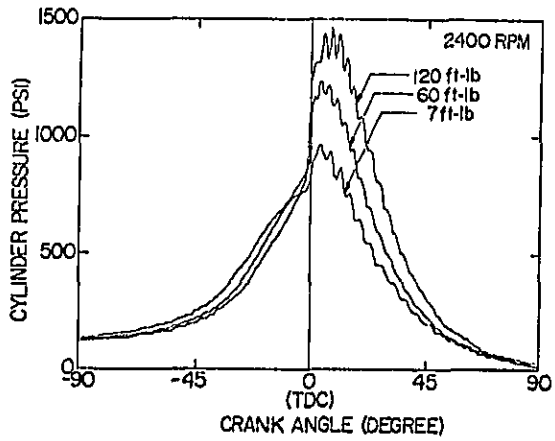

Fig. 6 - The cylinder combustion pressures versus crank angle for several engine load conditions, [19].

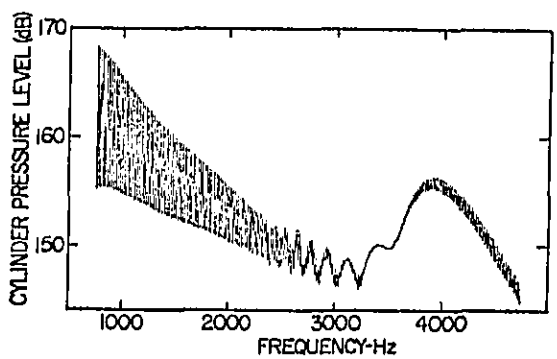

Fig. 7 - Cylinder pressure spectrum for 2400 RPM and 7 ft-lb load with a bandwidth of 10 Hz, [19].

the ripples observed in the 7 ft-lb trace of Figure 6. The peak was thus considered to be caused by the cavity resonance. To investigate this theory, envelopes of the cylinder pressure spectra were obtained using a wider bandwidth for the different loads shown in Figure 6...see Figure 8. Figure 9 shows similar spectra at the same load but different speeds.

The broad peak in the spectrum is seen to be load-dependent but not speed-dependent. The temperature in the adaptor tube before the transducer during combustion may be assumed to be at least 500°C and the resulting transducer adaptor tube resonance frequency must be at least about

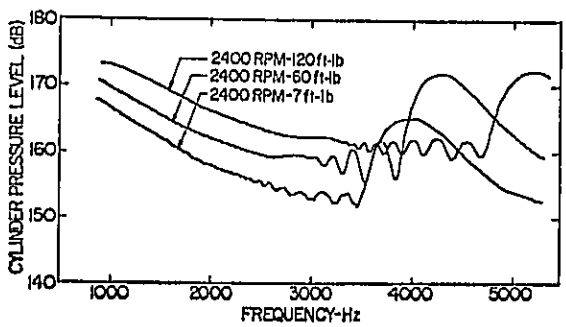

Fig. 8 - High frequency portion of the cylinder pressure spectrum for various loads, [19].

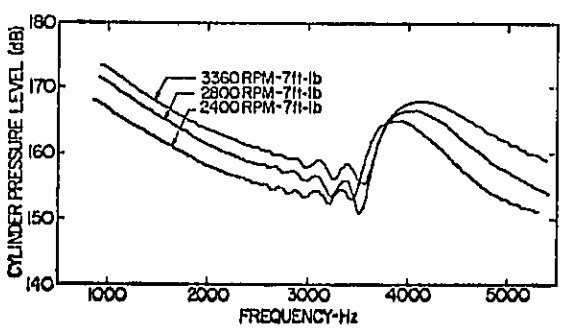

Fig. 9 - High frequency portion of the cylinder pressure spectrum for various speeds, [19].

10,000 Hz which is well above the observed peak in the frequency spectrum. However, the first radial frequency in the cylinder cavity (which is the same as the cut-off frequency of a circular duct) does correspond. At 0°C, this frequency is about 1760 Hz for a 3.5 in diam. duct. Assuming the temperatures in the cylinder are about 1000°C, 1500°C and 2000°C for the low, medium and high loads gives frequencies of $1760 \times \sqrt{1273/273} = 3800$ Hz, $1760 \times \sqrt{1773/273} = 4485$ Hz and $1760 \times \sqrt{2273/273} = 5080$ Hz, respectively. These frequencies seem to correspond quite well with the observed broad peaks in the spectra in Fig. 8. The fact that the peaks are broad may be explained by the fact that the temperature is changing during the combustion phase and so the speed of sound and the first radial resonance frequency will also change. (See Figure 6).

The ordinary coherence function between two different cylinder pressures was measured and is shown in Figure 10. It is seen that up to about 1000 Hz it is about 1.0, but then it decreases steadily until above 3000 Hz it is essentially zero. This would intuituively seem to make sense. At low frequency the pressure signals in the cylinders are composed of multiples of the firing frequency (see Fig. 7) and the process is fairly deterministic. At high frequency the combustion processes become more random. There may be several reasons for randomness in addition to randomness in the combustion. These could include randomness due to slight variations in speed and load from cycle to cycle. Strahle and Handley have recently studied randomness in combustion extensively with a single-cylinder diesel engine [33, 34]. Strahle and Handley concluded that after correcting for speed variations, the remaining randomness in the combustion process was very important in the engine radiated noise in the higher frequency region above about 1200 or 1500 Hz. More-

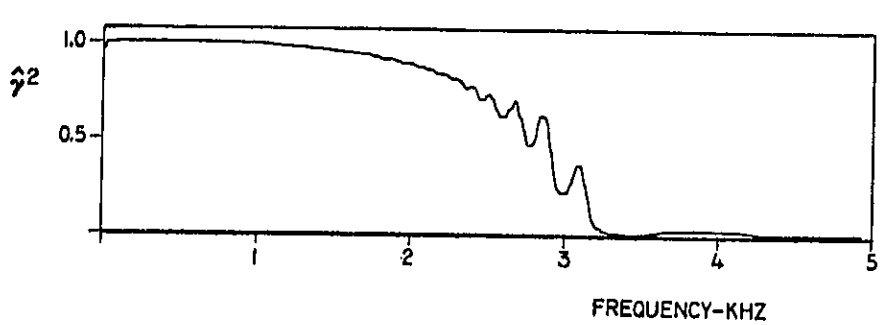

Fig. 10 - Typical ordinary coherence function estimate between cylinder pressures for 2400 RPM and 7 ft-lb load with B_e=20 Hz, [19].

over they concluded that this randomness was possibly caused by turbulence of combustion or randomness in the injection process. They claimed that above about 1200 Hz (with their engine) that the engine noise was dominated by the randomness in the combustion process and that the engine noise and block acceleration were very coherent with the cylinder pressure. They also concluded that the radial resonance in the cylinder was always driven by random combustion processes.

Strahle and Handley's work was conducted with a single-cylinder engine. However, the work of Chung, Seybert, Crocker and Hamilton was with a six cylinder engine. These authors have measured the frequency response of each cylinder, (see Figure 11); the multiple coherence function between all the inputs and the output noise y (see Figure 12) and compared the coherent noise predicted by the model with the measured noise (Figure 13).

Figure 11 shows that the frequency response does not vary much with load (as is assumed in the linear model). Figure 12 shows that the multiple coherence is higher for high loads and is essentially about 1. It is lower for low loads (as also found by Strahle and Handley [34] for the case of ordinary coherence for their single cylinder engine. Figure 13 shows that the model predicts the measured engine noise fairly well.

The theory discussed earlier in this paper assumes random noise in the inputs. However, it is known that at low frequency

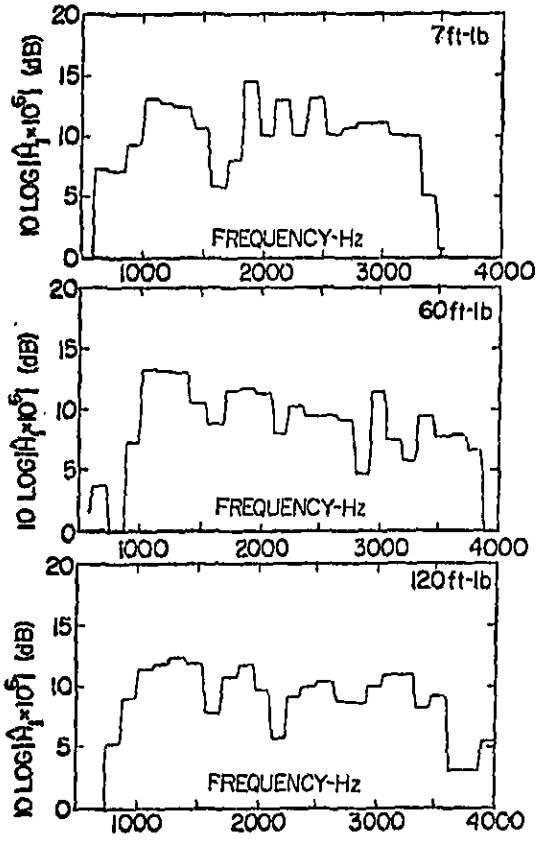

Fig. 11 - Frequency response estimates for cylinder 1 at 2400 RPM, as a function of load, with B_e=140 Hz, [19].

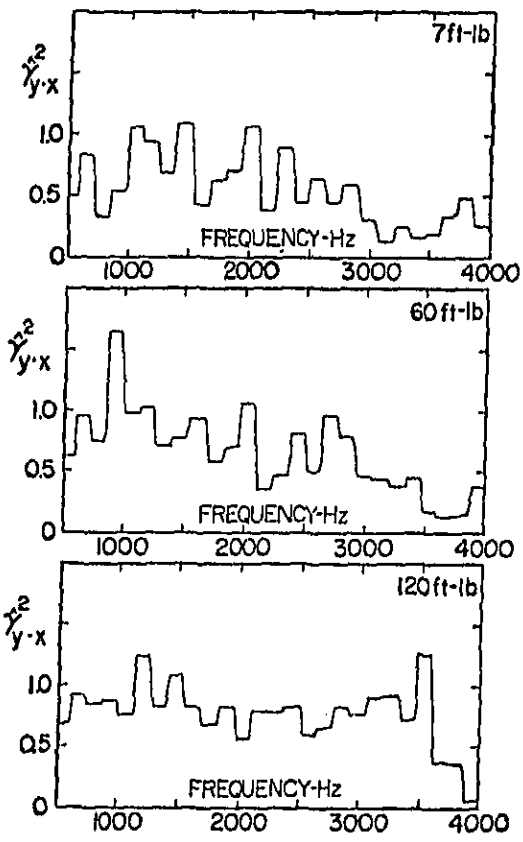

Fig. 12 - Multiple coherence function extimates at 2400 RPM, as a function of load, with B_e=140 Hz, [19].

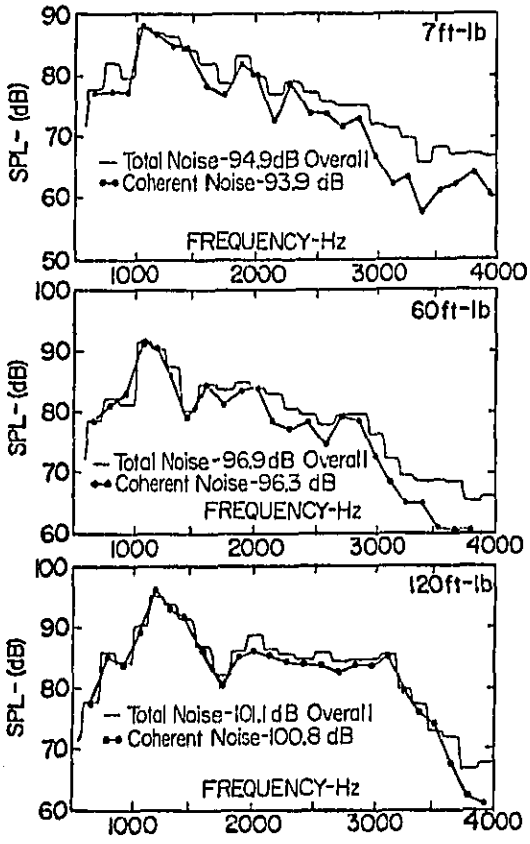

Fig. 13 - Total and coherent engine noise spectra at 2400 RPM, as a function of load, with B_e=140 Hz, [19].

the cylinder signals are composed of line spectra and are generally deterministic. If the input signals were completely deterministic they would become completely coherent with each other and the coherence technique would be unable to separate the contributions of the different inputs. However, recently Seybert, Crocker and Hamilton [35,36] have shown that if there is a known time delay between the signals the spectral density functions can be frequency averaged to reduce the coherency. Even if the signals are deterministic (line spectra) they can be used to obtain frequency responses with loss of resolution in the frequency domain but retaining resolution among the paths.

In Seybert's work [19, 21] allowance was also made for the (propagation) time delays, which occur between the inputs and the output. Seybert and Hamilton have recently shown the magnitude of the bias errors in estimating frequency response and coherence functions involved by time delays [37].

Chung [14, 38] and Seybert and Crocker [19, 21], using the multiple-input single-output model varied the theoretical cylinder pressure-time history and showed that the engine noise was predominantly caused by the pressure jump created at ignition. Chung used an idealized instantaneous pressure rise. Seybert and Crocker used more realistic pressure rises measured on a single cylinder research engine. This result was known qualitatively before, however quantitive predictions of noise were shown by this later work. This shows that if the cylinder pressure rise can be smoothed, considerable noise reduction should occur.

Recently Hayes, Seybert and Hamilton have used the multiple-input, single-output model to try to separate piston slap and combustion noise of a running diesel engine [39]. Such a procedure had been suggested by Chung, et al., earlier [14, 18]. In this procedure the piston slap inputs were measured with accelerometers mounted in the wall of the cylinder liner while the combustion noise was measured with cylinder pressure transducers as before. Because of a limited number of transducers some assumptions had to be made regarding coherence between inputs; however, the approach was useful in separating piston slap noise.

3. Experiments on Source Identification Using the Multiple-Input, Single-Output Model

Koss and Alfredson used such a model in 1974 to try to identify transient noises on a punch press [40]. Later Alfredson [41] working at Herrick Laboratories continued this work on the same V-6 diesel engine used by Chung, Seybert, Crocker and Hamilton. Alfredson used 5 microphones mounted close to the engine and one far field microphone. He mainly concluded that the partial coherence approach was very difficult to use and the results were inconclusive. Although he does not say so directly, it appears that contamination between inputs was a big problem. Also of course the partial coherence approach will give unrealistic results since the "true" signals will be partly coherent and this approach will remove parts of the "true" signals. The contamination problem might be reduced in Alfredson's case by using accelerometers not microphones.

Later Wang and Crocker [31, 32] used the multiple-input coherence approach to try to separate noise sources on a truck (fan, engine, exhausts, intake). They

used six close microphones and one far field microphone. The appraoch seemed to give great difficulty presumably caused by contamination, time delays (between input and output) and insufficient number of inputs. More simple-minded approaches such as the near field approach seemed to work better and give results in close agreement with the source wrapping procedure.

CONCLUSIONS

In this paper uses of the so-called coherence model of diesel engine noise have been discussed. It has been shown that this model has been successfully applied to several different aspects of the noise of diesel engines, which are combustion noise dominated and has yielded the following information:

i) The model can be used to separate the noise from each cylinder (which is given by $|H_i|^2 S_{ii}$). Even if the cylinder pressures are coherent it is still possible to separate the different cylinder contributions to the overall noise because of the known time delays between the cylinder pressure signals. Some frequency resolution is lost in this separation process in the frequency region in which the cylinder pressure signals are coherent (low frequency).

ii) The model can be used to provide theoretically a parametric study of the dependence of engine noise on cylinder pressure-time history. The pressure-time history can be varied theoretically in the computer model thus obviating or reducing the need for much expensive, time consuming, and tedious experimental work.

iii) The coherence model has shown for the first time the quantitative relationship which exists between the engine noise and the abrupt pressure noise occurring at detonation. This relationship was mainly known in only a qualitative way before.

iv) The coherence model has allowed a rigorous determination of the attenuation (frequency response function H_i) between individual cylinder pressures and engine noise. Previous attempts at this must be regarded as approximate at best since only an "average" attenuation could be deduced. Previous attempts must assume that each cylinder pressure is incoherent and equal in magnitude and are thus suspect in the low frequency range where the signals are coherent.

v) The model has allowed a separation of the noise from combustion and piston slap with a running engine. Previous attempts at piston slap noise determination have been empirical and have relied on measuring complete engine noise with several different designs of piston.

vi) Although the model has so far been used on engines which are "combustion-noise" dominated, in principle it can also be used on engines which also have a considerable amount of "mechanical noise" provided the sources of mechanical noise can be identified and measured. In this case the number of inputs to the model must be increased to allow for inclusion of the mechanical sources. It would probably be necessary to measure these source inputs using accelerometer or velocity gauges.

Using idealized experiments with loudspeakers it has been shown that the coherence model can in principle be applied to the identification of the noise sources on the vibrating surfaces of machines, such as a diesel engine. However, in practice so far such experiments with real engines and large multiple sources such as trucks seem to have been mainly unsuccessful. Possibly problems such as contamination between sources, time delays between signals and insufficient numbers of source microphones may be largely responsible.

ACKNOWLEDGMENTS

The support of the National Science Foundation, Cummins Engine Company, Columbus, Indiana and the Office of Noise Abatement and Control of the U.S. Environmental Protection Agency, Washington, DC are gratefully acknowledged for different parts of the work conducted at Herrick Laboratories. Some part of the research was supported internally by Herrick Laboratories funds. The measurements made at Herrick Laboratories described in this paper were mainly conducted by J. Y. Chung, A. F. Seybert, P. A. Hayes, and M. E. Wang while studying as graduate students. The assistance of A. Smith, A. Norfleet and others who constructed the experimental apparatus is gratefully acknowledged.

REFERENCES

1. A.E.W. Austin and T. Priede, "Origins of Diesel Engine Noise," Proc. Symp. on Engine Noise and Noise Suppression, I. Mech. E., London, Oct. 24, 1958, pp. 19-36, and 59-61.

2. T. Priede, "Relation between Form of Cylinder Pressure Diagram and Noise in Diesel Engines," Proc. I. Mech. E., London, No. 1, 1960-61.

3. T. Priede, A.E.W. Austin and E.C. Grover, "Effect of Engine Structure on Noise of Diesel Engines," Proc. I. Mech. E., London, Part 2A, No. 4, 1964-65.

4. T. Priede, E.C. Grover and N. Lalor, "Relation between Noise and Basic Structural Vibration of Diesel Engines," S.A.E. Paper No. 690450, 1969.

5. J. Skorecki, "Vibration Noise of Diesel Engines," ASME Paper No. 63-OGP-2, 1963.

6. W.J. Griffiths and J. Skorecki, "Some Aspects of Vibration of a Single Cylinder Diesel Engine," J. Sound and Vibration, Vol. 1, No. 4, Oct., 1964.

7. B.J. Fielding and J. Skorecki, "Identification of Mechanical Sources of Noise in a Diesel Engine - Sound Emitted from the Valve Mechanism," Proc. I. Mech. E., Vol. 181, Part I, 1966-67.

8. G.E. Thien, "Methods and Problems in Noise Reduction of High Speed Diesel Engines," S.A.E. Paper No. 680407, 1968.

9. D.D. Tiede, and D.F. Kabele, "Diesel Engine Noise Reduction by Combustion and Structural Modification," S.A.E. Paper No. 730245, 1973.

10. G.E. Thien, "The Use of Specially Designed Covers and Shields to Reduce Diesel Engine Noise," S.A.E. Paper No. 730244, 1973.

11. S.H. Jenkins, N. Lalor and E.C. Grover, "Design Aspects of Low-Noise Diesel Engines," S.A.E. Paper No. 730246, 1973.

12. M.J. Crocker, G. Anderkay and J.Y. Chung, "Controlling the Noise Radiated from Diesel Engines," Proc. of First Interagency Symposium on Transportation Noise Research, Stanford University, 1973, pp. 631-647.

13. J.Y. Chung, M.J. Crocker and J.F. Hamilton, "Noise Measurements on a V-6 Diesel Engine," NOISE-CON 73 Proc., Washington, D.C., 1973, pp. 86-91.

14. J.Y. Chung, "Measurement and Analysis of Diesel Engine Noise," Ph.D. Thesis, Purdue University, May 1974.

15. J.Y. Chung, M.J. Crocker and J.F. Hamilton, Measurement of the Multiple Coherence Function and Separation of the Coherent Engine Noise from the Total Noise of a Diesel Engine," Proc. of Second Interagency Symposium on Transportation Noise Research, N. Carolina State Univ., 1974, pp. 562-572.

16. J.Y. Chung and M.J. Crocker, "Study of Diesel Engine Noise Using the Coherence Function Method," Proc. 8th Int. Cong. Acoust., London, Vol. 1, 1974, p. 34.

17. J.Y. Chung and M.J. Crocker, "Noise Source Identification on a V-6 Diesel Engine by Means of the Coherence Function Method," J. Acoust. Soc. Am. 55, 1974, p. 387A.

18. J.Y. Chung, M.J. Crocker, and J.F. Hamilton, "Measurement of Frequency Responses and the Multiple Coherence Function of the Noise-Generation System of a Diesel Engine," J. Acoust. Soc. Am., 58, 3, 1975, pp. 635-642.

19. A.F. Seybert, "Estimation of Frequency Response in Acoustical Systems with Particular Application to Diesel Engine Noise," Ph.D. Thesis, Purdue Univ., December 1975.

20. M.J. Crocker, "Sources of Noise in Diesel Engines and the Prediction of Noise from Experimental Measurements and Theoretical Models," INTER-NOISE 75 Proc., 1975, pp. 259-266.

21. A.F. Seybert and M.J. Crocker, "The Use of Coherence Techniques to Predict the Effect of Engine Operating Parameters on Noise," ASME Paper 75-DET-33, see also Trans. ASME, J. of Eng. Ind., 97, 13, 1976.

22. E.T. Buehlman and M.J. Crocker, "Noise Measurement on a V-6 Diesel Engine," INTER-NOISE 74 Proc., 1974, pp. 217-220.

23. E.T. Buehlman, "Combustion Noise Study on a Diesel Engine," MSME Thesis, Purdue University, May 1975.

24. A.F. Seybert and M.J. Crocker, "Recent Applications of Coherence Function Techniques in Diagnosis and Prediction of Noise," INTER-NOISE 76 Proc., 1976, pp. 7-12.

25. K.W. Goff, "The Application of Correlation Techniques to Source Acoustical Measurements," J. Acoust. Soc. Am. 27, 2, 1955, pp. 336-346.

26. S. Kumar and N.S. Srivastava, "Investigation of Noise Due to Structural Vibrations Using a Cross-Correlation Technique," J. Acoust. Soc. Am. 57, 4, 1975, pp. 769-772.

27. J.S. Bendat, and A.G. Piersol, "Random Data: Analysis and Measurement Procedures," Wiley Interscience, New York, 1971.

28. J.S. Bendat, "Solutions for the Multiple Input/Output Problem," J. Sound Vib. 44, 3, 1976, pp. 311-325.

29. J.S. Bendat, "System Identification from Multiple Input-Output Data," J. Sound Vib., 49, 3, pp. 293-308.

30. C.T. Dodds and J.D. Robson, "Partial Coherence in Multivariate Random Processes," J. Sound Vib., 42, 2 1975, pp. 243-249.

31. M.E. Wang, "The Application of Coherence Function Techniques for Noise Source Identification," Ph.D. Thesis, Purdue Univ., May 1978.

32. M.E. Wang and M.J. Crocker, "Recent Application of Coherence Techniques for Noise Source Identification," INTER-NOISE 78 Proc., 1978, pp. 375-382.
33. W.C. Strahle, "Combustion Randomness and Diesel Engine Noise: Theory and Initial Experiments," presented at Eastern States Meeting of the Combustion Institute, Philadelphia, Nov. 18, 1976, published in Combustion and Flame, 28, 1977, pp. 279-290.
34. W.C. Strahle and J.C. Handley, "Stochastic Combustion and Diesel Engine Noise," S.A.E. Paper No. 770408, 1977.
35. A.F. Seybert and M.J. Crocker, "The Effect of Input Cross-Spectra on the Estimation of Frequency Response in Certain Multiple-Input Systems," presented in part at the 89th meeting Ac. Soc. Amer., April 1975, also published in Archives of Acoustics, 3, 3, 1978, pp. 3-23.
36. A.F. Seybert, M.J. Crocker and J.F. Hamilton, "Effects of Frequency Averaging in Multiple Input-Single Output Problems," paper submitted to J. Acoust. Soc. Amer., 1979.
37. A.F. Seybert and J.F. Hamilton, "Time Delay Bias Errors in Estimating Frequency Response and Coherence Functions," J. Sound Vib., 60, 1, 1978, pp. 1-9.
38. J.Y. Chung, "The Use of Digital Fourier Transform Methods in Engine Noise Research," S.A.E. Paper No. 770010, 1977.
39. P.A. Hayes, A.F. Seybert and J.F. Hamilton, "A Coherence Model for Piston-Impact Generated Noise," paper to be presented at S.A.E. Diesel Engine Noise Conference, Detroit, February 26-March 2, 1979.
40. L.L. Koss and R.J. Alfredson, "Identification of Transient Sound Sources on a Punch Press," J. Sound Vib., 34, 1, 1974, pp. 11-33.
41. R.J. Alfredson, "The Partial Coherence Technique for Source Identification on a Diesel Engine," J. Sound Vib., 55, 4, 1977, pp. 487-494.

790363

TRANSMISSION NOISE REDUCTION USING HOLOGRAPHIC SOURCE IDENTIFICATION AND CONSTRAINED LAYER DAMPING

Ronald W. Hera

Detroit Diesel Allison, Division of General Motors

ABSTRACT

As the noise of various vehicle components is reduced, transmission noise will become more apparent. Most transmission noise is generated by vibration of the transmission housing caused in turn by meshing of gear teeth. To effectively reduce airborne noise eminating from the housing, the critical areas of the housing that act as speakers must be identified.

A photographic technique using laser light, called Double-Pulsed Holography, has been adapted for this purpose. A five-step test program has been successfully completed and has resulted in a quieter prototype through use of constrained layer damping materials at critical points on the transmission housing. Thus, it is expected that holography will be a very useful tool in locating housing areas which are the source of airborne noise.

ALLISON HEAVY-DUTY AUTOMATIC and power-shift transmissions are manufactured for a variety of customers for applications including hauling, cycling, and military uses. A few of the applications are shown in Figure 1. Nearly all of the vehicle manufacturers who specify such transmissions make vehicles that are subject to noise regulations.

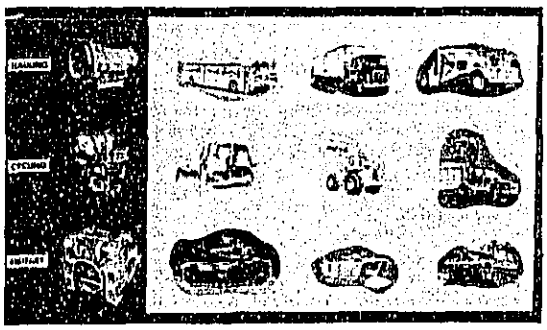

Fig. 1 - Typical applications of three types of Allison Transmissions

The noise standards for many automatic transmission users—line-haul truck manufacturers—are expected to become more severe during the next decade, as shown in Figure 2. Many local standards are already more severe than national standards (1)*. As a result, vehicle manufacturers will continue to select quieter components until national, state and local standards are met.

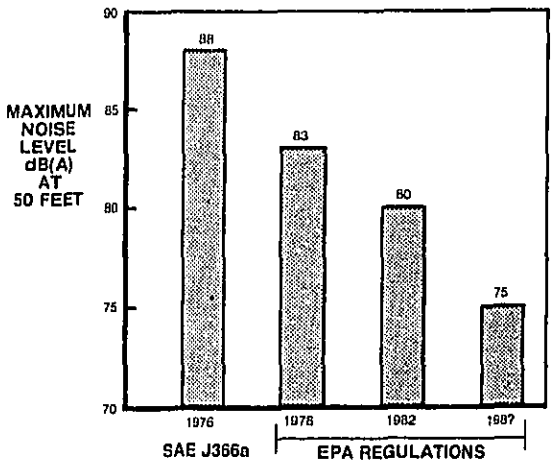

Fig. 2 - EPA noise standards for new trucks

As the noise of other components in vehicles is reduced, transmission noise will become more apparent (2) (3). Figure 3 is a comparison of a production line-haul truck and a quieter prototype. Notice that the transmission noise level was ranked fifth in the 88 dB(A) baseline vehicle, but was ranked third in the 80 dB(A) prototype. Thus, the need to develop quieter transmissions is becoming increasingly important.

Most transmisson noise is generated by vibrations caused by the meshing of gear teeth. These vibrations create vehicle noise in three ways (reference Figure 4).

- Gear mesh torsional vibrations are carried structurally to vehicle panels by drivelines and then converted to airborne sound.
- Gear mesh lateral vibrations are carried structurally by mounts to vehicle panels and then converted to airborne sound.
- Gear mesh vibrations (lateral and torsional) excite the transmission housing and are directly converted to airborne sound.

*Numbers in parentheses designate References at end of paper

SAE/P-79/80/$02.50
Copyright © 1979 Society of Automotive Engineers, Inc.

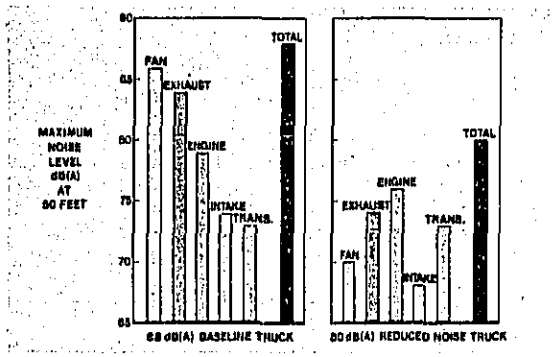

Fig. 3 - Component contribution to overall vehicle noise for two line-haul trucks

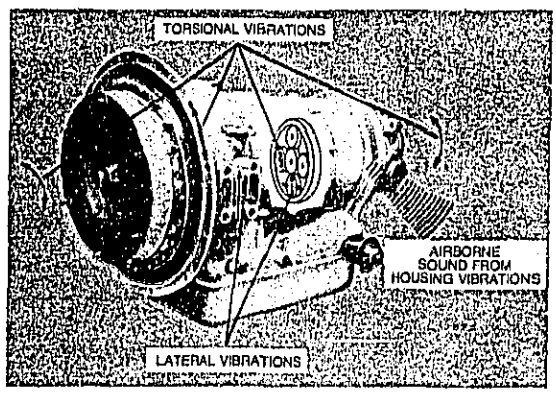

Fig. 4 - Sources of noise from a typical transmission

Much work has been done to reduce the excitation forces caused by the gear teeth, such as modification of tooth profiles, use of overlapping helical gears, and use of counterphased planetary gear sets (4). Driveline and mount improvements have also been helpful in reducing noise.

This paper, however, presents a test program designed to reduce the airborne noise that radiates directly from the transmission housing. To effectively reduce airborne noise from the housing, the critical areas of the housing that act as speakers must be identified and modified to reduce their ability to radiate sound. A photographic technique using laser light, called Double-Pulsed Holography, offers a unique means of visualizing housing surface vibrations and is the test method selected to locate the housing areas acting as speakers (5) (6).

DOUBLE-PULSED HOLOGRAPHY

Holography is a process very similar to photography except that laser light, which is monochromatic (of one color or wavelength), is used. Holography records both amplitude and phase of light, while photography records only amplitude. The most obvious difference is that holography produces a three-dimensional image called a hologram when reconstructed with a laser beam.

The physical arrangement for recording a hologram is shown schematically in Figure 5. The laser emits a beam of light to a beam splitter and becomes two beams, a reference beam and an object beam. The reference beam is guided onto photographic film directly, while the object beam is diffused onto the object and reflected back to the same photographic film. The monochromatic nature of the laser light creates constructive and destructive interference depending on the phase between the two beams, and thus records a three-dimensional hologram. This entire system of laser, mirrors and film holder is called a holocamera.

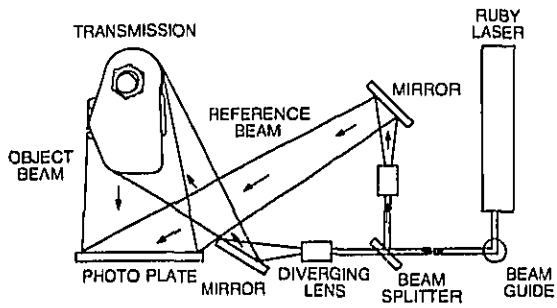

Fig. 5 - Schematic showing the operation of a holocamera

By pulsing the laser in the holocamera, a double-exposure hologram is recorded. If nothing shifted the light paths between pulses, the hologram would be unaltered. However, since the surfaces of the object are vibrating, the object beam's path is longer or shorter by a fraction of a wavelength causing the interference patterns to change. Some light waves are cancelled forming dark areas on the hologram, while others are reinforced causing bright areas. Thus, an image is recorded which is directly related to the motion of the object, i.e., the transmission housing.

To view a hologram, a laser beam is required to reconstruct the reference beam on the film. When the reference beam is reconstructed, a three-dimensional object with dark-fringe patterns can be observed by looking through the photographic film.

THE TEST PROGRAM

For any noise reduction program to be successful, the program must evaluate every possible source of noise. For transmission manufacturers, an organized test program to analyze the vibrational characteristics of the transmission housing is one important part of the over-all noise reduction program.

The analysis of transmission housing vibrations can be done in several ways. Modal analysis using Fast Fourier Transform (FFT) equipment is perhaps the most popular and has proven quite successful. However, the results yield a multitude of closely-spaced resonant mode shapes with little

or no information about forced vibrations. The mode shapes define the general housing motion, but possibly miss some vibrating areas of the housing simply because the areas are not a part of the grid network that defines the housing.

To overcome these problems, the test program at Detroit Diesel Allison used the double-pulsed holography technique. The results of this technique, unlike others, include as much area of the housing as can be photographed and include resonant motion superimposed on forced motion. To observe realistic forced motion, actual running conditions were simulated in the test cell.

The housing noise test program consisted of five steps to produce a quieter transmission by altering the housing only.

(1) An initial noise test to establish a noise baseline and its frequency spectrum.
(2) A holography test to identify areas of the housing with high vibrations.
(3) An accelerometer test to verify that the housing vibration-frequency spectrum is related to the sound-frequency spectrum.
(4) Redesign or treatment of the housing in those areas which were identified using holography.
(5) A final noise test to evaluate the effectiveness of changing or treating the housing.

The housing selected for the test was a transfer gearbox from an Allison CLBT-750 transmission used in off-highway scrapers and trucks. One reason that this transmission was chosen is that the gear mesh consisted of a fourty-second order of the output shaft only. This characteristic simplified the analysis.

INITIAL NOISE TEST

The purpose of the initial noise test, as already noted, was to establish a noise baseline and its frequency spectrum.

The transfer gearbox was installed in a test cell using isolation mounts and special rubber torque couplings to prevent structural vibrations from exciting the bedplate and other objects in the test cell. Thus, the only sound recorded was airborne sound radiating from the housing.

After installation, the gearbox was first operated over its entire speed range at high loads. The resulting noisy operating speeds were noted and the unit was rerun at steady operating conditions at those speed points. The eight noisiest operating points were selected for the holography test.

A three-dimensional plot of sound levels versus frequency for various lines of output speed is shown in Figure 6. Since the only gear mesh order present is the forty-second order, harmonics are easily identified. The vertical dashed lines indicate possible resonances of the housing at those frequencies.

HOLOGRAPHY TEST

The purpose of the holography test was to identify areas of the housing with high vibration levels.

The holography test was conducted in the same

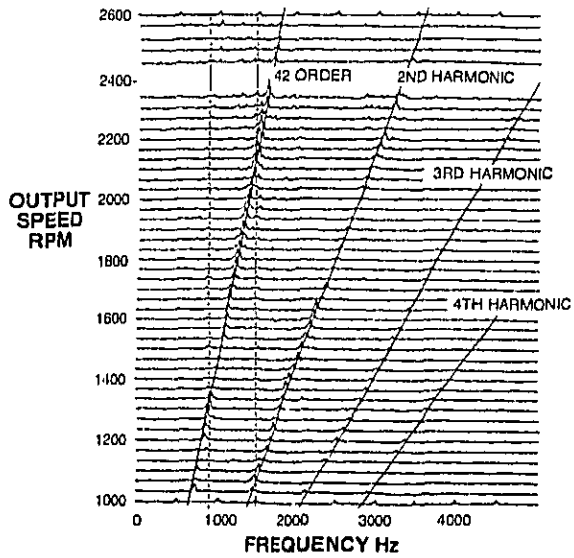

Fig. 6 - Initial noise test results

test cell and under the same running conditions as the initial noise test.

The setup of the holocamera and one microphone is shown in Figure 7. Note that the gearbox housing was painted flat white for better contrast in the holograms. The holocamera consisted of laser, mirrors, and film holder enclosed in the large box on the portable lift. The holocamera used a one-joule, Apollo Model 22 ruby laser with a 76-mm oscillator and a 152-mm amplifier. This holocamera was designed for general applications and is relatively large. A more complete description of the holocamera and related equipment is given in the Appendix.

The video camera in Figure 7 was used during setup to record the laser flash on video tape. The video tape could then be played back slowly to determine if the housing was adequately illuminated

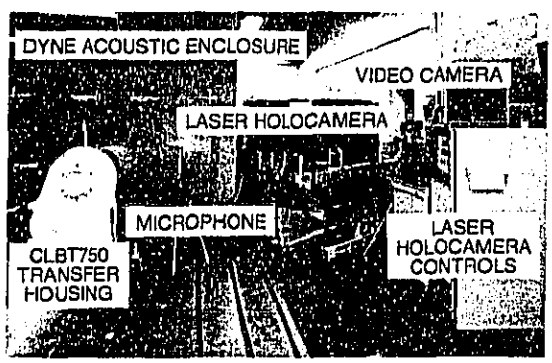

Fig. 7 - Test cell installation for initial sound, holography, and accelerometer tests

by the laser flash. The video monitor and tape were located in a control room adjacent to the test cell, see Figure 8. The red safety light in the control room was illuminated as a safety precaution whenever the laser was in a condition ready to fire.

Reconstruction of the holograms was accomplished using a 15-mW, helium-neon laser as shown in Figure 9. The resulting holograms were photographed using conventional techniques and printed as ordinary photographic prints.

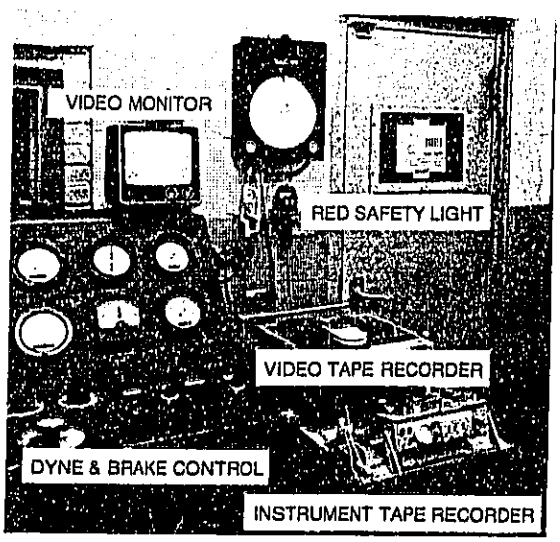

Fig. 8 - Control room layout

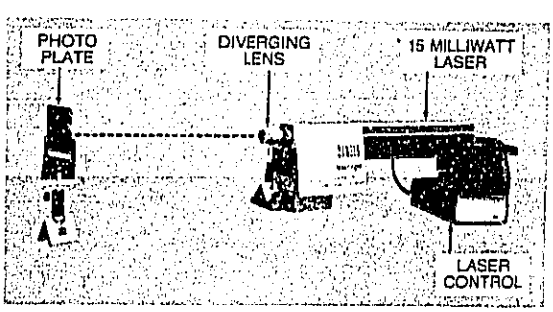

Fig. 9 - Hologram reconstruction setup

Figure 10 is a photograph of a hologram taken from the back of the housing. Note that there is a "bull's-eye" of fringes on the housing at two different locations.

A bull's-eye in a hologram indicates a peak or valley in the displacement pattern on the surface that occurs between pulses. It is much like a peak or valley on a topographical map. Counting dark fringes in a bull's-eye yields the distance a surface moves in the time between pulses.

The velocity (toward the laser) of the vibrating surface of the object at the center of a bull's-eye can be approximated by:

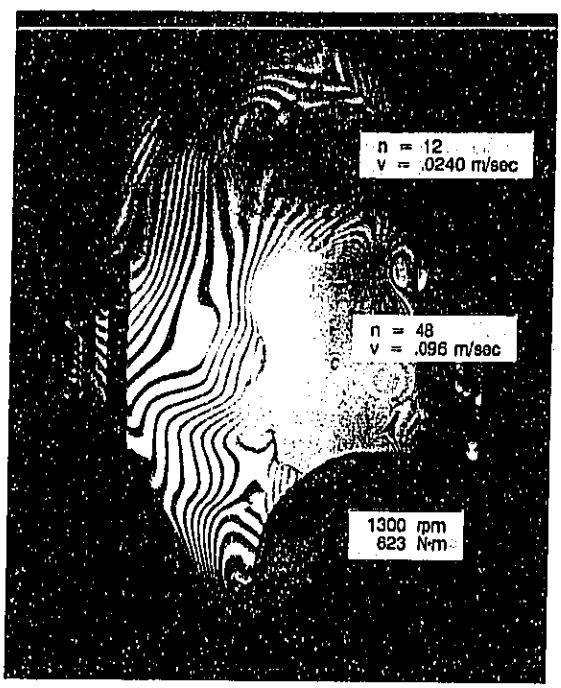

Fig. 10 - Hologram of rear of transfer housing

$$V \text{ (metre/sec)} = \frac{n \ (\lambda/2)}{t \ \cos \phi} \qquad (1)$$

where: n = number of fringes in the bull's-eye forming a complete circle
$\lambda/2$ = half-wavelength of the laser light (.347 μm for this test)
t = time between pulses (200 μsec for this test)
ϕ = bisector angle, defined in Figure 11

For this test, ϕ = 30 degrees when viewing the housing from the rear, as in Figure 10, and 45 degrees when viewing the housing from the front, as in Figure 12.

The top bull's-eye in Figure 10 is located on a steel cover. There are twelve black fringes

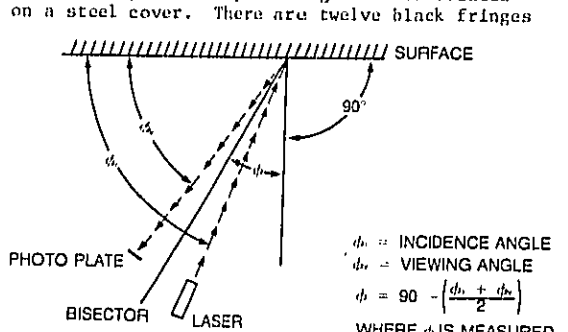

Fig. 11 - Definition of angle

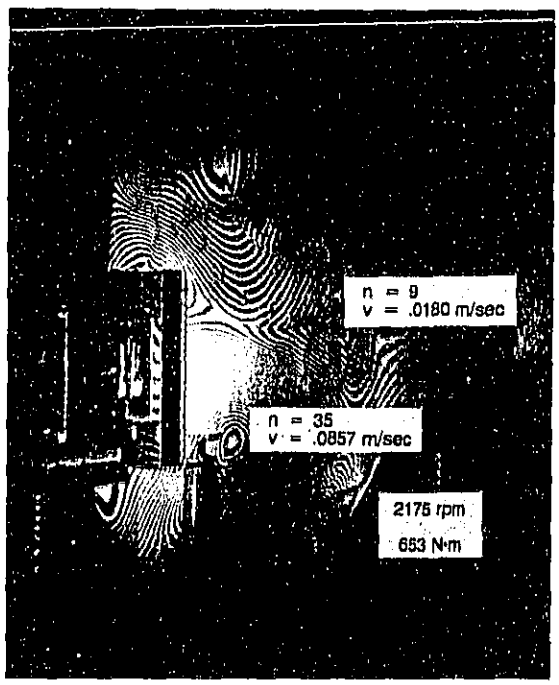

Fig. 12 - Hologram of front of transfer housing

and $\phi = 30$ degrees. Therefore, the velocity at the center of the bull's-eye is .0240 m/s.

The larger bull's-eye indicates greater velocity. The fringes are so closely packed that they are hard to distinguish. There are 48 black fringes for a velocity of .0960 m/s. Certainly the larger bull's-eye is likely to show the major source of sound since it indicates greater velocity.

Thirty-five holograms were analyzed. The patterns were generally different for each operating condition. The differences were caused by various resonant mode shapes superimposed on areas of forced vibration.

Often, there were more bull's-eyes on the front of the housing, as shown in Figure 12, than on the rear, as shown in Figure 10, but they were less severe. More importantly, most of the bull's-eyes occurred on relatively flat surfaces—a trend that existed on all 35 holograms.

ACCELEROMETER TEST

The purpose of the accelerometer test was to verify that the housing vibration-frequency spectrum was related to the sound-frequency spectrum.

The accelerometer location selected for the test was the center of the large bull's-eye in Figure 10. The test was conducted using a slow increase in shaft speed from 1000 to 2600 rpm with the same load as used in the initial noise test.

Figure 13 shows the accelerometer recording of the slow increase in shaft speed from 1000 to 2600 rpm. Note that the forty-second order and

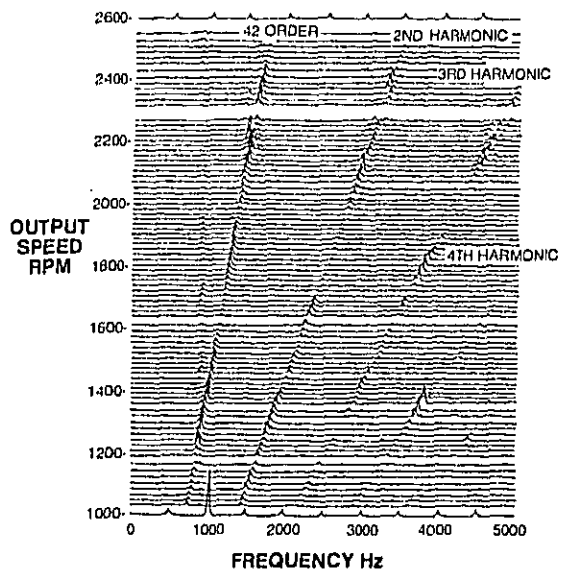

Fig. 13 - Accelerometer test results

its harmonics are present in the housing vibration spectrum just as they were in the noise spectrum shown in Figure 6. Also note that one of the resonant lines in the noise spectrum also appears in the vibration spectrum.

A constant speed point corresponding to the 1300 rpm condition in Figure 10 was also tested to compare the vibration-frequency spectrum with the noise-frequency spectrum at that condition.

Figure 14 shows a comparison of the vibration and noise-frequency spectrums at the constant shaft speed (1300 rpm) running condition. Only three of the noise peaks are present in the vibration spec-

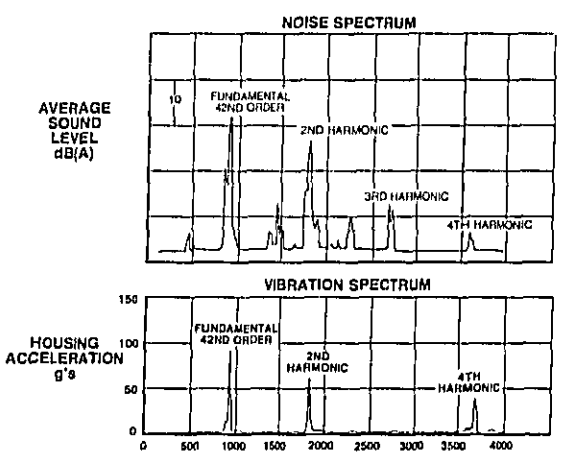

Fig. 14 - Noise and vibration spectrums at 1300 rpm

trum in Figure 14. However, elimination of those three frequency spikes from the noise spectrum would account for a significant reduction in sound.

HOUSING TREATMENT

After reviewing the holograms, a limited area of the housing was selected for treatment. The selection consisted of the relatively flat areas which were the areas of the greatest vibrational activity.

A constrained layer of damping material, shown schematically in Figure 15, was the treatment selected for use in this experiment. The thin damping material flexes between the housing and an outer steel cover. The flexing of the thin damping layer converts the sound-producing energy to sheer stress energy and is dissipated in the form of heat.

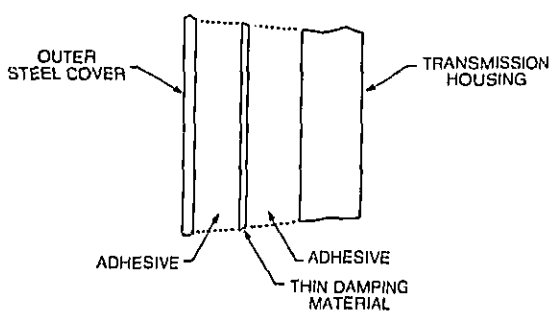

Fig. 15 - Constrained-layer noise reduction treatment

The optimum thickness of the damping layer and outer steel cover is a function of housing wall thickness, temperature and prominent frequency being treated. Since the fundamental frequency and temperature changed with operating conditions and since the housing-wall thickness was not uniform, the treatment was a compromise of those parameters.

Figures 16 and 17 show the housing after applying the constrained layer materials. Notice that all the outer steel covers were simple flat pieces since the holograms showed that the vibrational activity was greatest on flat areas of the housing.

FINAL NOISE TEST

The purpose of the final noise test was to evaluate the effectiveness of treating a limited area of the housing. The final noise test was recorded in the same manner as the initial noise test to assure a fair comparison of the treated housing with the baseline.

The comparison of the noise baseline and the noise after treatment showed a significant noise reduction, see Figure 18. The maximum sound reduction of 8 dB(A) occurred at approximately 1300 rpm. The noise reduction was not constant over the entire speed range since the effectiveness of the constrained layer damping material varied as a function of frequency. High and low temperature extremes would also reduce the ability of the constrained layer to flex and to convert the sound-producing energy to heat.

The constrained layer damping material could possibly be tuned to yield the greatest noise reduction at some specific operating speed.

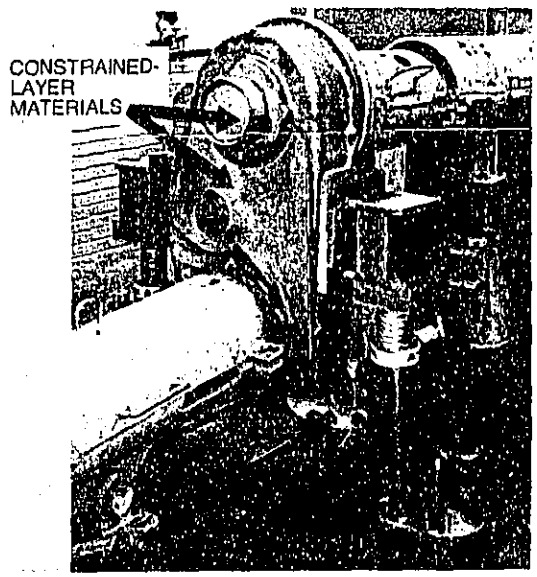

Fig. 16 - Constrained-layer treatment on rear of transfer housing

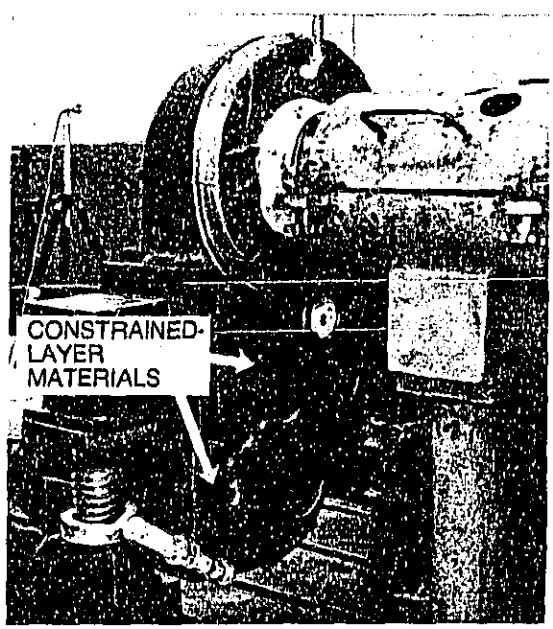

Fig. 17 - Constrained-layer treatment on front of transfer housing

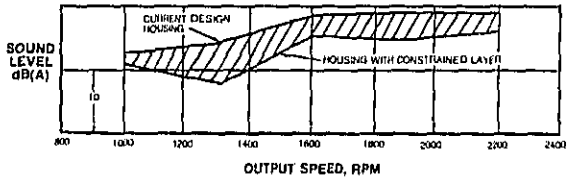

Fig. 18 - Overall transmission sound reduction

SUMMARY

The test objective, to reduce the direct conversion of gear mesh vibrations into airborne noise, was accomplished. The five-step test program was successfully completed and resulted in a quieter prototype using constrained layer damping materials on the gearbox housing.

Two significant points can be made from this test.

- Noise can be significantly reduced by treating a limited area of a housing.
- Holography is a very useful method of selecting areas of transmission housings for noise reduction treatment.

Further development for noise reduction of the CLBT-750 transfer gearbox housing will continue. The next step will be to develop a housing that is stiffer in the areas of high vibration. Any subsequent noise recording will be compared to the previously established baseline noise.

REFERENCES

1. Robert Hickling, "Regulation and Control of Ground Vehicle Noise", G.M. Research Laboratory Report, Fluid Dynamics Research Department, Warren, Michigan, November, 1977.

2. Richard L. Staadt, "Truck Noise Control". Paper SP-386 (740001), The Twentieth L. Ray Buckendale Lecture, presented at the SAE Automotive Engineering Congress and Exposition, Detroit, Michigan, February, 1974.

3. D. F. Rudny, "Meeting European Noise Regulations for Rubber-Tired Front End Loaders". Paper 760599 presented at SAE West Coast Meeting, San Francisco, California, August, 1976.

4. W. E. Palmer and R. R. Fuehrer, "Noise Control in Planetary Transmissions". Paper 770561 presented at SAE Earthmoving Industry Conference, Central Illinois Section, Peoria, Illinois, April, 1977.

5. D. A. Evensen, R. Aprahamean, and K. R. Overoye, "Pulsed Differential Holographic Measurements of Vibration Modes of High-Temperature Panels". NASA Contractor Report NASA CR-2028, National Aeronautics and Space Administration, Washington, D. C., June, 1972.

6. A. Felske and A. Happe, "Vibration Analysis by Double-Pulsed Laser Holography". Paper 770030 presented at the SAE International Automotive Engineering Congress and Exposition, Detroit, Michigan, February, 1977.

APPENDIX

Specifications

Detroit Diesel Allison One-Joule, Double-Pulsed, Ruby Holocamera

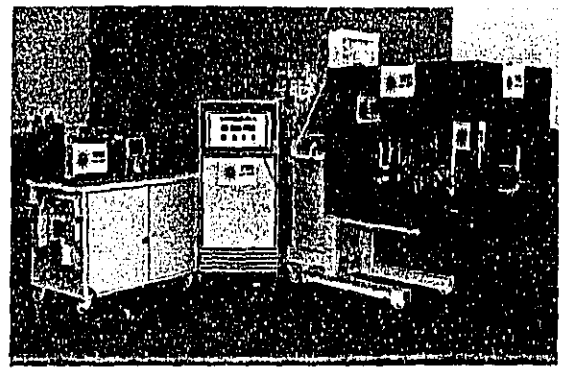

A. Holocamera
   1. Support - 1 megagram-rated shoplifter with manual height adjustment
   2. Table - 0.9x1.2x0.15 metre honeycomb table with magnetic stainless steel top and bottom. Both sides are drilled and tapped 1/4-20 on 25.4-metre centers.
   3. Enclosure - 0.9x1.2x0.9 metre angle-iron frame with removable wood sides for maximizing safety and security.
   4. Optical Components:
      a. Helium-neon alignment laser
      b. Ten mirrors and holders
      c. Ten assorted lenses
      d. Two filter holders with nine assorted filters
      e. Five adjustable platform component mounts
      f. Two film or plate holders
      g. One ten-percent reflection beam splitter that can be mounted in the laser head

B. Ruby Laser - Apollo Model 22 with 76-mm oscillator, 152-mm amplifier and double-pulse Q-switch.
   1. Energy - TEM_{oo} with output etalon
      a. One joule, single pulse
      b. 0.5 joule/pulse, 1 to 800 microsecond separation
      c. 0.07 joule/pulse, 800 to 99,500 microsecond separation (oscillator only using 152-mm head)
   2. Coherence - 50 percent fringe contrast at 1 metre, optional dye cell may be purchased to extend coherence to 7 metres.
   3. Repetition Rate - 1 ppm for pulse repeatability
   4. Pulse Separation Control - 1 megahertz digital clock
   5. Dimensions
      a. Optical Rail - 2 metre with dust cover
      b. Power Supply - 0.7x0.6x1.5 metres

C. Accessories
   1. Autocollimator
   2. Photodiode with integrator circuit to measure pulse energy
   3. Dual-trace storage oscilloscope
   4. Safety goggles
   5. Safety inter-locks and relays for safety lights, etc. to conform to safety standards

D. Holocamera Power Supply and Storage Cabinet
   1. Transformer - 5KVA, 440V to 110V single phase
   2. Two 20A breakers into 16 110V receptacles
   3. 440V cord to transformer 10 metres length
   4. Enclosure - 0.66x1.2x1.4 metres with two storage drawers and one shelf
   5. All accessories and holocamera optics can be locked in cabinet.

790364

COMPUTER OPTIMISED DESIGN OF ENGINE STRUCTURES FOR LOW NOISE

N. Lalor

Institute of Sound and Vibration Research
University of Southampton , England

ABSTRACT

The paper describes a computer optimisation procedure, using static deflection techniques, by which the overall noise level of an engine can be reduced by up to 5dBA by minor modification. The computer program operates within given weight, space and strength constraints and produces a modified design which can be machined by existing plant.

The use of the static deflection technique is justified by the results of running engine damping measurements and by the analysis of the influence of damping on typical third octave vibration levels. This analysis demonstrates that the damping of the block structure has very little influence on running engine vibration levels, which are, in fact, controlled by the stiffness.

A CURRENT ENGINE BLOCK STRUCTURE is designed mainly from strength considerations. It has to be made stiff enough to withstand the direct gas and inertia loads and the torque reaction forces without significant distortions at the various bearing surfaces. As a result of considerable experience and development, a modern engine will continue to operate satisfactorily under these loads for long periods of time before the necessity for overhaul.

Such a technological advance has been due mainly to an economic impetus. On the other hand, until recent legislation, there has been little or no similar pressure to reduce the noise. As a result of this, most of the currently produced engines have no built-in low noise features but rely mainly on palliative measures to make them acceptable. However, such measures tend to be rather expensive extras and are therefore unpopular since they inevitably increase the price of the unit in a very competitive market.

Although the load carrying capacity of the block for a given weight has improved enormously in the past few years because of the advances made in stress analysis, there has been no parallel advance in noise reduction, due mainly to the lack of a suitable systematic technique that could be used at the drawing board stage. Fortunately, since the strength requirement is essentially a low frequency, and noise a high frequency, problem it is possible to alter the performance of the structure to satisfy one without affecting the other. This paper describes a technique for optimising an engine block for low noise without degrading its structural integrity and with little or no weight increase. For an existing design this will mean a reduction of up to a maximum of 5dBA (i.e. bringing the engine down to the bottom of the scatter band for its class). However, the technique can also be used to assess radical changes in design, from a noise point of view.

NOISE REDUCTION OBJECTIVE

Figure 1 shows the third octave noise spectrum of a typical medium sized six cylinder in-line diesel engine running under full load conditions at its rated speed of 2800 rev/min. It can be seen from the figure that the overall "A" weighted noise level

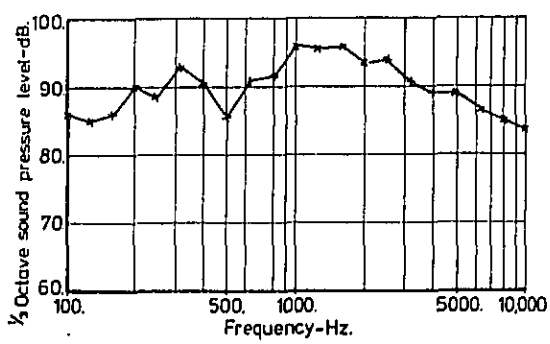

Fig. 1 - Noise of in-line 6 cylinder diesel engine. 2800 rev/min. Full load

will be mainly dominated by the broad high frequency peak between 800 Hz and 2500 Hz, and to a lesser extent by the peak in the 315 Hz and 400 Hz frequency bands. It is clear that if these two peaks alone could be lowered a few dB by structural modification without adversely affecting the rest of the spectrum, then a significant reduction in overall noise level

SAE/P-79/80/$02.50
Copyright © 1979 Society of Automotive Engineers, Inc.

would be achieved. Such a reduction would not, of course, be as great at the 10dBA or so achieved by radical redesign but would nevertheless be well worthwhile if it could be obtained by modifications small enough to allow the block to be machined by existing plant. Before attempting such an exercise, it is necessary to understand in some detail the vibration characteristics of the engine at these frequencies where the noise peaks occur.

VIBRATION CHARACTERISTICS OF ENGINE BLOCK STRUCTURES

If an electro-magnetic shaker is attached to an engine block structure its acceleration response measured at a point will look similar to the spectrum shown in Figure 6. It can be seen that there are a large number of resonant peaks over the frequency range measured, and at the frequency associated with each peak the structure will vibrate in a characteristic mode shape. Although the structural response is clearly very complex it falls into two very distinct groups.

PLATE TYPE MODES - In the first group, which lies typically from zero to around 1000 Hz to 1500 Hz, the engine behaves as if it were a solid, although elastic plate. Thus, each point on one side of the block will be in phase with its corresponding point on the other side. Figure 2 shows, as an example of this type, the fundamental lateral bending mode of a six cylinder in-line engine. It has been found empirically (1)* that the frequency of this mode is given by

$$f = \frac{225}{\ell^{1.5}} \text{ Hz} \qquad (1)$$

where ℓ = Block length in metres.

This mode is also found with vee-form engines although, due to the greatly increased lateral bending stiffness, the expression (2) for the frequency of the mode changes to:

$$f = \frac{600}{\ell^{1.5}} \text{ Hz} \qquad (2)$$

In addition, vee-engines also display a bank-to-bank mode, where the cylinder banks vibrate like the prongs of a tuning fork, which also belongs to this first group. Its natural frequency is given by the expression (3):

$$f = \left(\frac{2.79}{d}\right)^3 \text{ Hz} \qquad (3)$$

where, d = perpendicular distance from crankshaft axis to top face of cylinder block, in metres.

Although the expressions given above are for fundamental modes, the structure will also exhibit overtones of these modes, which extend the influence of this group well up the frequency range. However, when the distance between nodal lines reduces to the span of a typical cast panel (e.g. between the stiff main bearing sections of the crankcase wall) then the block starts to exhibit the second type of mode.

PANEL MODES - In this second, high frequency modal group, each cast panel of the block structure vibrates independently. Figure 3 shows an example of

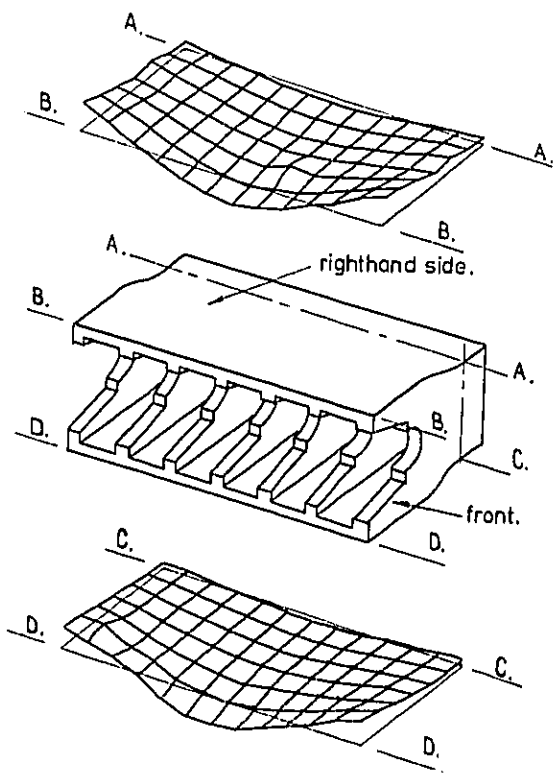

Fig. 2 - Fundamental lateral bending mode of in-line 6-cylinder engine

this type, also for an in-line six-cylinder engine. The natural frequencies of these panels will depend on their size and shape and therefore each engine will have a range of frequencies where its different panels vibrate in their fundamental mode. Empirically it has been found (2) that for both in-line and vee-form engines these lie predominantly in the range

$$f_1 = \frac{45}{(\ell p)^2} \text{ Hz} \quad \text{to} \quad f_2 = \frac{70}{(\ell p)^2} \text{ Hz} \qquad (4)$$

where, ℓp = distance between main bearings in metres

In practice there is usually an overlap frequency range between the two groups where both modal types can be identified. This is particularly true with deep skirted crankcase designs, where the natural frequencies of the crankcase walls below the crankshaft axis can be quite low. In these cases the lower frequency limit of the panel modes (f_1 in equation (4)) is also usually reduced.

*Numbers in parentheses designate References at end of paper.

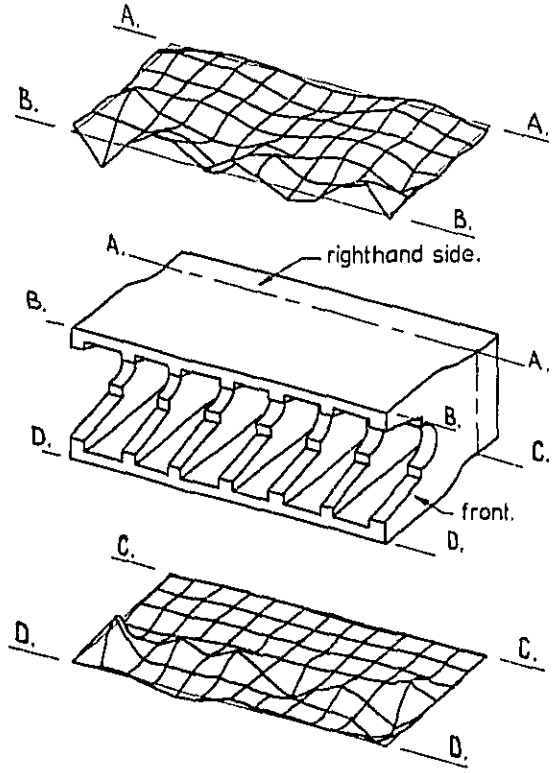

Fig. 3 - Typical panel mode of in-line 6-cylinder engine

IDENTIFYING THE PREDOMINANT NOISE RADIATING MODES ON THE RUNNING ENGINE

The engine described in section 2 has a block length of approximately 0.75 metres and therefore, in general terms, the modal types responsible for the noise peaks (shown in Fig.1) are found (using equations (1) and (4) as a guide) to be :

(a) Plate type block bending modes (315 Hz, 400 Hz and 800 Hz - 1600 Hz)
(b) Crankcase skirt modes (800 Hz - 1600 Hz))Deep)skirted
(c) Panel modes (2000 Hz and 2500 Hz))crankcase)design

The fundamental horizontal bending mode is probably the only one contributing to the noise peak at 315 Hz and 400 Hz, since at these frequencies the third octave bands are quite narrow in addition to the fact that the modal density (number of modes per unit bandwidth) is quite low. However, at 800 Hz and above the modal density is much higher and therefore there will be several modes in each third octave band. This raises the problem of identifying which modes in each band are actually causing the noise. Since it has been established (4) that the noise level is proportional to the mean square velocity of the engine surface, it is clear that the mode with the highest amplitude in each band will be the predominant noise source. Unfortunately this information cannot be obtained directly from either the modal analysis test (using an electromagnetic shaker) or from running engine vibration measurements alone. The reason for this is that although the shaker test is very good for identifying mode shapes and natural frequencies the absolute (and relative) amplitudes are quite unrepresentative of the running engine due to incorrect damping and to the way in which the force is applied to the structure. Conversely with the running engine vibration measurements, although the damping and forcing are, of course, correct the combination of high damping and the harmonic nature of the exciting force spectrum make separation of the modes impossible (due to phase problems). The only practical way out of this difficulty is to use the combined results of both tests and, as an example, Figure 4 shows such a comparison in the case of the fundamental bending mode. Figure 4a shows the mode shape measured on one side of a six cylinder in-line engine during the shaker test. Figure 4b shows the appropriate third octave band acceleration levels measured along the line A-A (Figure 4a) when the engine is running. Although there are differences due to the effect of the flywheel, crankshaft and contamination from other modes, which are not present for the shaker test, it is clear that both modes are basically the same. Thus it is possible to use the shaker test results to identify which mode is producing the third octave vibration pattern on the running engine, since the predominant mode will be mainly responsible for this pattern.

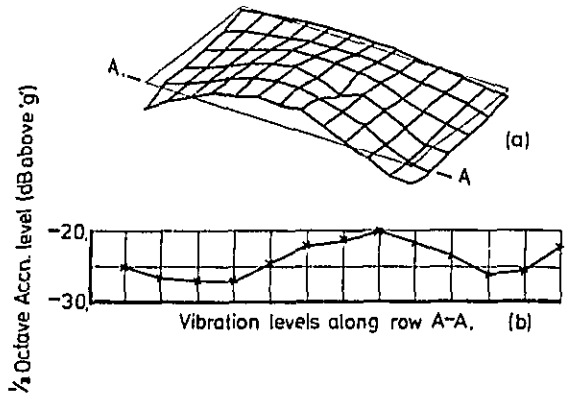

Fig. 4 - Comparison between shaker test and running engine vibration results

MECHANISM OF MODAL EXCITATION

In the previous section a method was described whereby the predominant modes of vibration in the

acoustically important frequency ranges could be identified. Since it is rarely possible to significantly alter a mode (except panel modes) without radical structural changes, the only alternative is to try to influence the way the mode is excited in the first place. For the vibration tests it is most convenient to use an electromagnetic shaker as the source of excitation and this is quite admissible as only a modal analysis was required. In the case of the running engine, however, the excitation is not from some external source but is due to internal loads. Dynamically, these internal loads produce local deformations of the structure at their points of application which then spread out over the engine principally as bending waves. The mechanism of the excitation of the modes of vibration is thus very complex and from the analysis point of view, the situation is further complicated by the fact that on the running engine there are many sources of excitation (e.g. combustion, piston slap, bearing impacts, etc) occurring simultaneously or in rapid succession. It is therefore very difficult to relate cause and effect, particularly because several of the exciting forces are dependent on one another. Thus, results of correlation analysis can be misleading. However, it is most important to know by how much each mode is excited in practice by each cylinder firing. In order to obtain this information, a static deflection test has been devised.

STATIC DEFLECTION TEST - Although this test has been described in detail elsewhere (5) it consists basically of a rig where high pressure oil is pumped into the combustion chamber of an engine, with the piston at the T.D.C. position, and the resultant distorted shape of the structure is measured.

In order to understand the relevance of this test to the dynamic situation it is best to consider static deflection as a vibration phenomenon but at the special case of zero frequency. When exciting the block at a particular frequency the resultant vibrating shape is composed of various amounts of each mode excited and as the frequency of excitation is varied it is only the relative amplitudes and phases of the modal components which change. Of course, at the natural frequency of a particular mode, that mode shape is dominant but, even then, components of all the other modes are also present. This situation also exists at zero frequency although none of the modes is then at resonance.

If the amplitude of the exciting force is constant with frequency then the relationship between the resonant and static deflection amplitudes of a particular mode is given by:

$$[x_o]_{f_n} = Q.x_{ST}$$

where, $[x_o]_{f_n}$ = resonant amplitude of the mode

Q^n = dynamic magnification factor at resonance = $\frac{1}{2\zeta}$

ζ = damping ratio

Figure 5 shows the results of a test (6) carried out at I.S.V.R. to determine the damping ratio of various modes on a running engine. It will be observed that, although the damping is almost

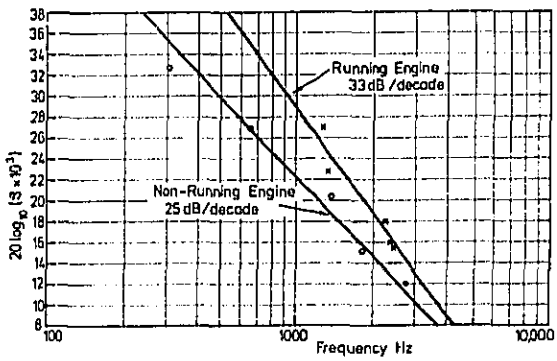

Fig. 5 - Variation of damping ratio with frequency

twice as high as with the non-running engine (due to the influence of the loaded oil films when the engine is operating), it decays at 33 dB per tenfold increase in frequency. Thus, for a constant amplitude exciting force, the Q factor of one mode, say at 2500 Hz, would be 33dB greater than for another having a natural frequency of 250 Hz. However, since the combustion exciting force spectrum (cylinder pressure spectrum) decays at approximately the same rate, the two effects cancel out and the net result is that the Q factor remains sensibly constant with frequency. Thus, any mode which has a high amplitude at its natural frequency will also make an important contribution to the static deflection shape of the engine. Conversely, the dominant modes (when excited by cylinder pressure) of the structure can be identified from the static deflection test.

There is, however, an even more important factor which relates the results of the static deflection test to the dynamic situation. Fig.6 shows a typical acceleration response spectrum measured at a point on an engine structure during a modal analysis test where the shaker force amplitude is kept constant with frequency. The figure also shows a typical cylinder pressure spectrum for an engine running at 2400 rev/min full load.

The resultant response of the engine structure when running will be proportional to the product of the two spectra, so that the engine can only vibrate at the frequencies corresponding to the cylinder pressure spectrum lines. Examination of Figure 6 shows that very few of these lines coincide with the natural frequencies of the modes, particularly in view of the fact that many of the peaks in this modulus spectrum are the resultant of several modes. This is because the natural frequencies are irregularly spaced whereas the cylinder pressure spectrum lines are all at integral multiples of the cyclic repetition rate. Thus the third octave band levels tend to be dominated by the off-resonant contributions (particularly at high frequency, where the number of forcing lines in a band is high) which, although smaller in amplitude, are much greater in number. Since damping only significantly affects the response

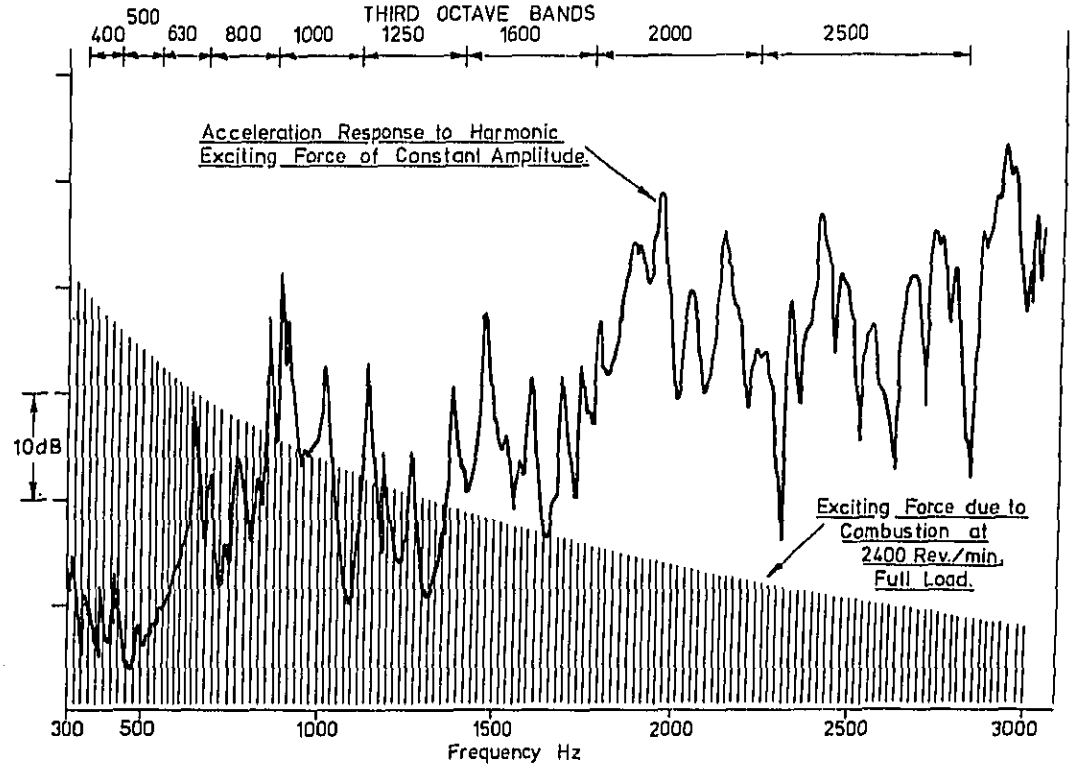

Fig. 6 - Structural response and combustion exciting force spectra 2400 rev/min full load.

of a mode at or near its natural frequency, it would be expected that the third octave response levels would be relatively insensitive to damping. Fig.7 shows the results of a computation carried out for a six-cylinder in-line 4-stroke diesel engine, to verify this. The computer program summed the contributions from 52 modes for each engine firing harmonic that lay in a particular third octave band and the calculation was repeated for several bands at different speeds and damping ratios.

A speed of 800 rev/min (giving an engine firing frequency spacing of 40 Hz) was chosen for this figure since it gave results most sensitive to the damping ratio. It can be seen that even then the damping ratio has very little effect on the third octave band levels over the range of Q factors encountered with the running engine block structure (up to approximately 100 - see Fig.5) and for a typical range of frequencies. This confirms that the band levels are controlled in practice by the off-resonance components. In order to determine the relative importance of the stiffness or mass controlled parts of the response, the calculations were repeated with the mass controlled part removed. Figure 7 shows that this had a negligible effect, so that the modal stiffness is the important factor. Thus the static deflection characteristics are even more relevant to the dynamic case and, in fact, suggest that it may be possible to predict the response of a block structure (and hence its noise) without the very expensive (and as yet not very accurate) modal computations which are at present considered necessary. The figure also explains why previous attempts to apply damping treatments to the block casting have tended to give disappointing results whereas similar treatments to

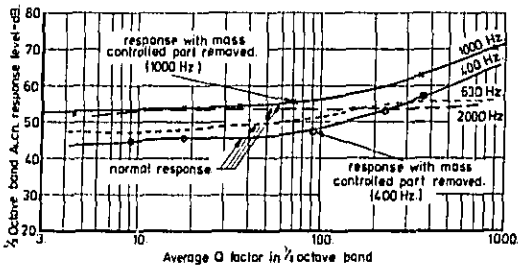

Fig. 7 - Variation of 1/3 octave band acceleration level with modal damping

the light covers (oil pan, valve cover, etc., which have much lower inherent damping) have proved much more effective.

COMPUTER OPTIMISATION

It might appear that the most logical way of meeting the objective set in section 2 (i.e. the reduction of the predominant noise peaks by a few dB without adversely affecting the rest of the spectrum) would be to construct a dynamic forced finite element model of the structure from which the noise spectrum changes due to various structural modifications could be assessed. However, although several researchers (e.g. 5, 7, 8, 9) are actively working along these lines the method, at present, suffers from very high computational cost and insufficient accuracy. The cost is particularly high because of the combined effect of the large number of runs necessary (in the order of two hundred) to achieve an optimum result and the considerable complexity of the model. The lack of accuracy is mainly related to the problem of correctly modelling the structure, particularly at high frequency.

However, having established the relevance of the static deflection analysis to the dynamic situation, it makes possible a much cheaper and, in fact, more accurate method of optimising the structure for low noise. Static deflection analysis also has the advantage that certain parts of the structure, such as the main bearing webs, can be analysed separately because of the relative simplicity of specifying the stiffness boundary conditions. This means that it is possible to perform a very extensive two-dimensional computer optimisation (often involving as many as 200 runs) of, for example, the engine section through a main bearing web, quite cheaply.

THE COMPUTER MODEL - The finite element model used for the optimisation is composed of triangular plate elements for web sections and rod elements for ribs. For a two dimensional analysis of main bearing web sections, rod elements are also used round the outside of the model to take into account the shear load imposed by the outer side walls of the engine. For a three dimensional model this is, of course, not necessary since the side walls are built up from triangular plate elements. Great care must be taken in the design of the model, since the computer can only choose the best combination of the alternatives given to it. Thus, for example, the boundaries between the plate elements must be so positioned as to allow the ideal web thickness contours to be built up by the computer.

THE OPTIMISATION CRITERIA - Once a representative model has been obtained it is then necessary to specify the required deflection pattern of the outer walls of the engine structure. This is done by identifying the modal characteristics which produce the peaks in the noise spectrum as described, for example, previously in connection with Figure 1. The static deflection shape for the modified structure should, ideally, have as little as possible of the mode shapes corresponding to the predominant noise radiating modes. This may mean, quite simply, that the outer wall deflection of the block should be reduced, but not necessarily. For example, if the crankcase panel modes were the predominant source of noise, then any crankcase static deflection pattern along a horizontal row having a rate of curvature corresponding to a half sine wave between main bearings should be avoided. This could be achieved by actually allowing the maximum deflection to increase but be diffused over a wider area so as to avoid the high rate of curvature. This would, in practice, mean a reduction in high frequency noise at the expense of low frequency noise. Of course, if the bending modes of the whole block were also a significant source of noise, then such a solution would not be permissible. Another very important consideration here is the way the deflection pattern of one main bearing section differs from another, due to design differences. This is because if the deflection pattern varies significantly from one main bearing section to another (even though the actual deflections in each case are small) the outer wall of the cylinder block structure will distort, with very adverse consequences if panel modes are an important source of noise.

OPTIMISATION PROCEDURE - Figure 8a shows a section through a main bearing web of a typical in-line six cylinder diesel engine of wet liner construction, similar to that described in section 2. The equivalent two dimensional computer model is shown in Fig.8b and the deflection of the nodes of the model under a cylinder pressure of 70 atmospheres (piston at T.D.C.), in Fig.8c. The deflection pattern is typical for this type of design. Due to the weakening effect of the camshaft bearing hole, the crankcase deflects downwards much more on that side causing a large bodily movement to the right. Above bottom deck level, the block is actually stronger on the camshaft side, due mainly to the partial double-wall construction, and therefore it deflects bodily to the left. Since this engine is similar to the one described in section 2, it is clear that these bodily movements of cylinder block and crankcase will give rise to the plate type bending modes which are a predominant noise source up to 1600 Hz. In addition, since the crankcase skirts move with the rest of the crankcase, they will also be excited by this bodily swing.

Fig.8c also shows that there is a large inwards relative lateral deflection between the left and the right hand outer walls of both the cylinder block and the crankcase. This is mainly because, when a panel is stretched in one direction by a direct loading, it will deflect inwards at right angles to that loading, due to the Poisson's ratio effect. Of course, in the crankcase area, the deflection pattern is modified by the main bearing hole and the lack of any tie between the crankcase skirts so that the oil pan fixing flanges actually deflect outwards away from each other. This overall relative deflection of the side walls is important because it makes a significant contribution to the excitation of the panel modes.

It can also be seen from Fig.8c that the push tube cover deflects inwards by an appreciable amount. This is due basically to the fact that, although not designed as a structural member, it restrains the normal vertical motion of the top fixing flange relative to the bottom. Since the cover is not in the same vertical plane as the outer walls of the block, moments are formed at its top and bottom edges which cause the inwards deflection of the centre.

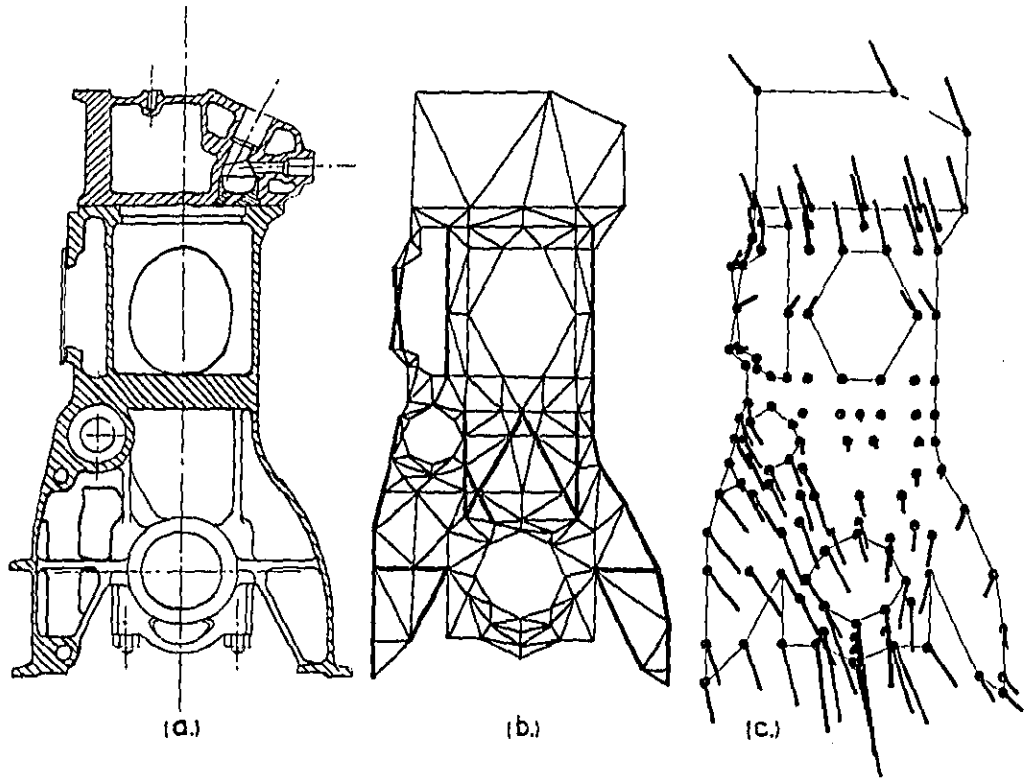

Fig. 8 - 2D computer model of main bearing web section of in-line engine.

It is first necessary to establish that these deflection results obtained on the model are identical to those measured experimentally at the same plane on the actual engine during the static deflection test. If they are it is then possible to optimise the bearing section design on the computer. Since both plate type bending and panel modes contribute to the overall noise of this engine, the best criteria to apply to the section is simply one of minimum deflection.

Fig.9a shows typical design modifications obtained as a result of this optimisation procedure and the resultant deflection pattern can be seen in Fig.9b. It will be observed that the lateral bodily movements of both the crankcase and cylinder block have been significantly reduced by balancing the structure. The modifications have also reduced the relative deflections of the side walls and the inwards deflection of the push tube cover - now this is isolated structurally from the fixing flanges on the block it no longer restrains them.

These modifications will give up to about 2dBA reduction in the noise of the engine for a weight penalty of around 5 per cent of the total weight of the section. It is now necessary to carry out this procedure on all the main bearing sections that differ in design detail from the one described, mainly to ensure that the deflection patterns are as identical as is practicable, for the reasons given above. In addition, the new design of web must be checked for its sensitivity to horizontal loads since these are also important on the running engine.

The final step in the optimisation procedure is to attend to the outer walls of the block structure. The crankcase outer wall panels either side of the loaded cylinder bay tend to deflect inwards more at their centre than at the main bearing positions due to their curved shape in the vertical plane. This is because any vertical load carried by these walls will be seen by the main bearing webs as an upwards shear force in the plane of the wall. Since the wall is not vertical, this shear force will have a horizontal inwards component which, at its centre, is only supported by the bending strength of the wall (i.e. it does not have the support of the main bearing webs). This phenomenon is clearly the major exciting mechanism of the crankcase panel modes and it is best dealt with by horizontal ribbing. Vertical ribs must not be used here because they increase the proportion of load carried by the walls and thus tend to actually increase their

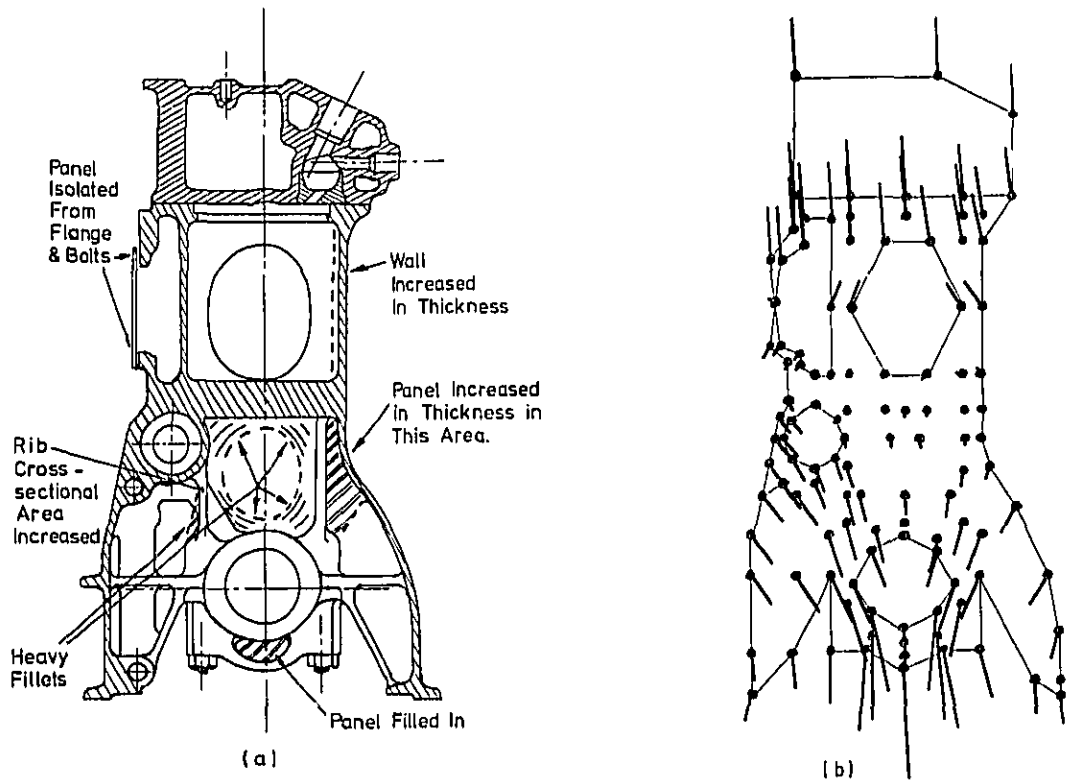

Fig. 9 - Optimised design of main bearing web section

deflection. In general the side walls of the cylinder block do not suffer from this type of deflection due to the fact that they are vertical. Any panel mode problem, which usually occurs with dry liner designs due to the lack of side wall support between the cylinders, can be dealt with by ribbing. Vertical ribs may be used here provided that the correct strength compensation is employed on the camshaft side so that the cylinder block remains structurally balanced.

These measures to control the panel modes of the block will, on the engine described above, also give up to about 2dBA reduction so that the total reduction of block noise will be 3 to 4dBA. Since the oil pan, valve cover, front timing cover, flywheel cover etc., generally get their vibrational energy from the block, the measures described above will also reduce the noise from these components. By how much will depend on the degree to which the deflection at the fixing flanges of the block has been reduced. For example, in the case given above, the horizontal inputs to the valve cover and oil pan have clearly been much reduced, but not so the vertical. To what extent the vertical inputs are important will depend on the cover design but, in any case, the choice of any isolation or damping measure employed will be greatly eased by having the uni-directional input. In general some control of the various covers will be necessary, in addition to the block modifications described above, but the total treatment will, in most cases, give up to about 5dBA reduction in engine noise.

CONCLUSIONS

The following conclusions can be drawn:

(1) The damping ratio of the running engine decays at approximately the same rate with frequency as the combustion gas force spectrum. Thus the dynamic magnification factor at resonance (Q factor) is approximately constant for each mode.

(2) Because the Q factor of the modes is sensibly constant, any mode which is of high amplitude at its natural frequency will also make an important contribution to the static deflected shape.

(3) The third octave vibration levels, particularly in the acoustically important frequency range, are controlled by the off-resonance contributions of the modes. Thus the levels in the bands are relatively insensitive to damping.

(4) The stiffness controlled part of the modal response controls the off-resonance contribution to the third octave vibration levels so that the static deflection analysis is very relevant to the dynamic situation.

(5) Up to a maximum of about 5dBA reduction in block noise level can be achieved by static deflection optimisation of a current engine design. The necessary modifications would be small enough to allow the block to be machined by existing plant.

(6) Up to about 5dBA reduction in engine radiated noise would then be possible by some noise treatment of the various covers.

ACKNOWLEDGMENTS

The author would first of all like to thank his colleague, N. Somkhanay, for untiring help with the computation. Thanks are also due to colleagues, both at I.S.V.R. and Perkins, who have helped by giving their constructive criticisms of the work. Finally, many thanks are due to Mrs. J. Halliday for typing the manuscript at the eleventh hour.

REFERENCES

1. P.E. Waters, N. Lalor, T. Priede, "The Diesel Engine as a source of commercial vehicle noise" Proc.Inst.Mech.Engrs.Symposium - Critical factors in the application of diesel engines, 1970.

2. D. Anderton, E.C. Grover, N. Lalor, T. Priede, "The automotive diesel engine - its combustion, noise and design", Inst.Mech.Engrs. Conference on land transport engines - economics versus environment. Paper C14/77, 1977.

3. N. Lalor, "Origins of reciprocating engine noise - its characteristics, prediction and control" Soc. of Environmental Engrs. Symposium on noise control, 1971.

4. C.M.P. Chan, D. Anderton, "The correlation of machine structure surface vibration and radiated noise". Inter-Noise 72 proceedings, Washington 1972.

5. N. Lalor, M. Petyt, "Modes of engine structure vibration as a source of noise". S.A.E. Paper 750833, Milwaukee 1975.

6. K. Abideen, "Structural damping of a running engine", M.Sc. Thesis, University of Southampton, 1976.

7. M.G. Hawkins, J.M. O'Keeffe, "A method of determining the effect of design change on diesel engine noise" C.I.M.A.C 1975.

8. R. Southall, "A review of engine noise control", p.321-325. Noise control vibration and insulation, November/December 1976.

9. N. Lalor, D.M. Croker, "The use of finite element techniques for the prediction of engine noise", Inst.Mech.Engrs. Conference on Noise and Vibration of Engines and Transmissions. To be published July 1979.

790365

RELATION BETWEEN CRANKSHAFT TORSIONAL VIBRATION AND ENGINE NOISE

Kazuomi Ochiai, Asst. Manager, Research & Engineering Division
Mitsuo Nakano, Staff Engineer, Research & Engineering Division

Isuzu Motors Limited
Kawasaki-shi, Kanagawa-ken, Japan

ABSTRACT

This paper presents the results of the latest investigations carried out at Isuzu Motors Ltd. into the mechanism of radiated noise from an acoustically modified diesel engine. Although the overall noise level of this engine is quite low compared with those of conventional design because noise in the acoustically important range from 800 to 1250 Hz has already been sufficiently reduced by structure modification, predominant peaks appear at 315 Hz and at 1600 Hz third octave bands which now govern the overall noise. To achieve further reduction of engine noise, these two peaks have to be adequately reduced. Therefore the noise generating mechanisms at 315 Hz were studied in detail on the running engine as well as experimentally using modal analysis program and by theoretical analysis. This study revealed the relationship between the vibration behaviour of the crankcase and a torsional vibration of the crankshaft. Also presented are the results of a study into the means of reducing noise peak.

In Japan, diesel engines are predominantly used for commercial vehicles because of their economy and reliability. However, they have been subject to social complaints from the environmental point of view because of their noise and smoke. Reflecting the growing social pressure, legislation on vehicle noise is likely to become more stringent in the future. In order to meet a demand for quieter diesel engines, manufacturers have been devoted to developing more efficient and cost effective methods of reducing noise. Also at Isuzu Motors Limited a considerable amount of work has been undertaken to establish theories for predicting diesel engine radiated noise at an early design stage from the structure vibration characteristics calculated using finite element methods (1)*. To assess the effects of the structure modifications of experimental engines on noise several engines were made and evaluated. Figure 1 shows some results obtained recently at the Isuzu laboratories by applying the novel technique on an in-line, 6 cylinder, 4 cycle, direct injection diesel engine.

The noise reduction at mid-frequencies where predominant peaks exist was so remarkable that components at 315 Hz and 1600 Hz have become dominant and these now govern the overall engine noise. For further reduction of overall engine noise the mechanism producing the 315 Hz peak has to be analysed theoretically in conjunction with experimental results. An outline of such an analysis process is presented in this paper.

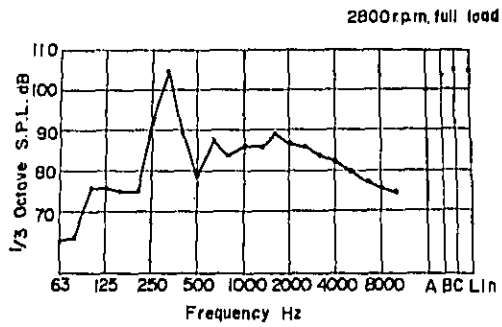

Fig. 1 – Noise spectrum of experimental diesel engine. Noise in the range from 800 to 1250 Hz have been reduced after structure modification and predominant peaks appear at 315 Hz and 1600 Hz

FACTORS AFFECTING NOISE LEVEL AT 315 Hz

The noise of a diesel engine quietened by structure modification is measured in terms of overall noise dB(A) against speed for various cases with different crankshaft torsional dampers as shown in Figure 2.

The harmonic ratio analysis has also been carried out and the noise component of the 7th order of speed are shown in the same figure. It is interesting to note that the overall engine noise in the speed range from 2600 rev/min upwards is strongly affected by the natural frequency of the damper adopted and the trend of the overall noise peak exactly correlates with that of the noise components of the 7th order of speed. It is felt that such phenomena have not occurred so far in conventional diesel engine and it was therefore decided that all efforts should be focused on the analysis of the generating mechanism of the 7th order noise.

* Numbers in parentheses designate References at end of paper.

SAE/P-79/80/$02.50
Copyright © 1979 Society of Automotive Engineers, Inc.

An engine with a torsional damper of natural frequency of 164 Hz was firstly selected for analysis in order to emphasize the problem. Noise spectra measured at 2500 rev/min, 2700 rev/min, 2800 rev/min and 3000 rev/min are shown in Figure 3. It is clearly seen that the predominant peak at each engine speed lies at the frequency of its 7th order, that is, 315 Hz in the case of 2700 rev/min, 329 Hz in 2800 rev/min and 350 Hz in 3000 rev/min respectively. For a better understanding of the characteristics illustrated in the Figure 3, a Cambel diagram can be drawn as shown in Figure 4. From this figure the predominance of the 7th order component (especially in the speed range from 2600 rev/min upwards) can be recognized more clearly.

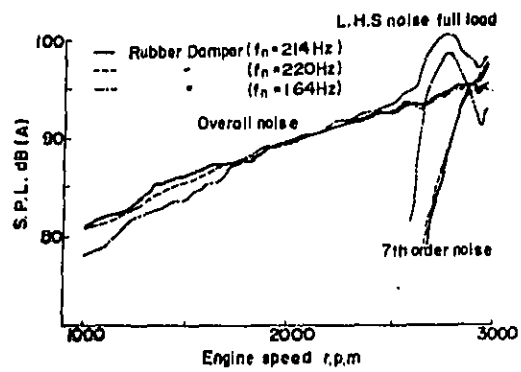

Fig. 2 - Noise speed relationship
Overall noise is considerably affected with the 7th order noise component from 2600 rpm upwards

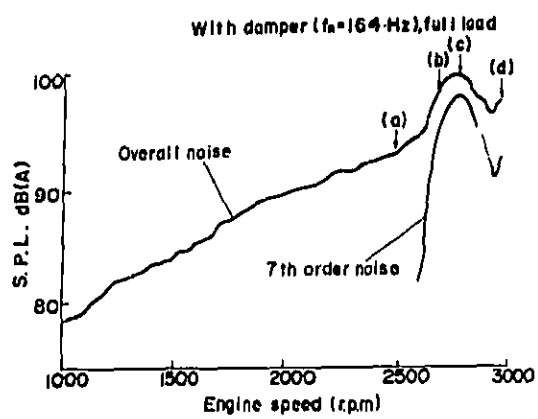

Fig. 3A - Typical noise-speed relationship
Overall noise peak is affected with the 7th order component. Points (a), (b), (c) and (d) are the speeds where narrow band analysis has been carried out.

Fig. 3B - Comparison with noise spectra

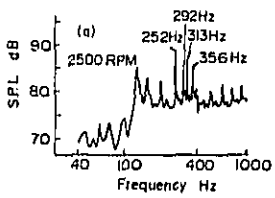

(a) Spectrum has several peaks more than 80 dB level

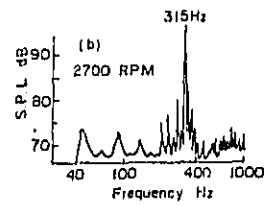

(b) Spectrum has a predominant peak at 315 Hz

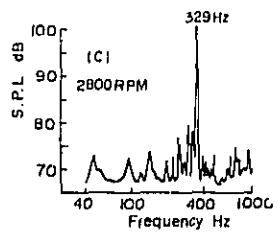

(c) Spectrum has a predominant peak at 325 Hz

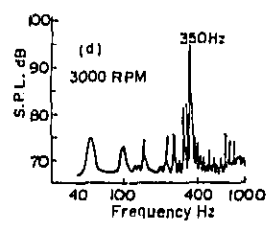

(d) Spectrum has a predominant peak at 350 Hz

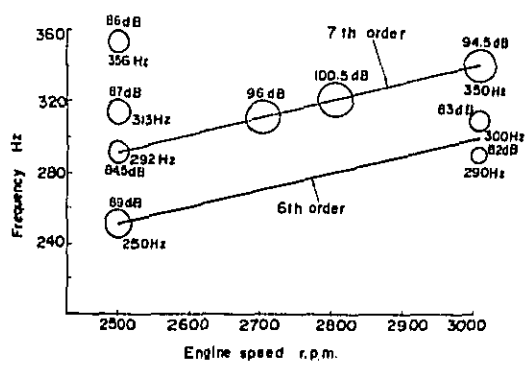

Fig. 4 - Cambell diagram
Noise levels more than 80 dB are shown in the figure

CORRELATION BETWEEN NOISE AND TORSIONAL VIBRATION

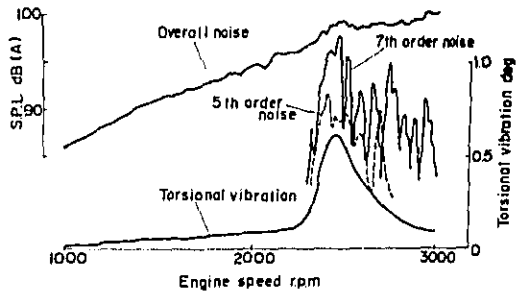

Fig. 5 – Relationship between noise and torsional vibration. Resonance of torsional vibration appears at engine speed where 5th and 7th order noise components are maximum

Figure 5 shows the noise-speed relationship and the torsional vibration-speed relationship. The noise peak is transferred to 2450 rev/min due to the mass of a torsional vibration transducer with FM oscillator attached to the front end of the crankshaft and to the fact that the peak of 6th order crankshaft torsional vibration also appears at this speed. This fact suggests that the 315 Hz noise component is strongly affected by the 6th order crankshaft torsional vibration. As for crankshaft torsional vibration itself a large number of reports have been published. However, none of them seems to have referred to the relationship between engine noise and torsional vibration. Authors have tried to analyse the experimental results theoretically by referring to Kosuge's paper (2). Assuming that an equivalent mass of the crankpin concentrates at its center and that the crankshaft is rotating at a constant angular velocity of two fluctuating forces are excited when torsional vibration is added. One of the two is the fluctuating component of centrifugal force due to the fluctuation of angular velocity caused by torsional vibration, and the other is the inertia force in the tangential direction caused by torsional vibration. Figure 6 shows a section of a crankshaft. From the calculation, which is fully described in the appendix, exciting force due to the n-th order torsional vibration can be represented by equations:

$$Fx + Cx = mrw^2\left\{\frac{\phi}{2}(n+1)^2\cos(n+1)wt - \frac{\phi}{2}(n-1)^2\cos(n-1)wt + \cos wt\right\} \quad (1)$$

$$Fy + Cy = mrw^2\left\{\frac{\phi}{2}(n+1)^2\sin(n+1)wt + \frac{\phi}{2}(n-1)^2\sin(n-1)wt + \sin wt\right\} \quad (2)$$

where suffices x and y denote the component in the X- and Y- direction, respectively. The other nomenclature is as follows;

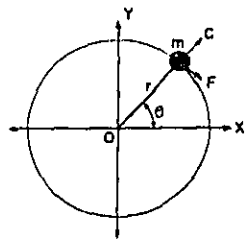

Fig. 6 – Schematic diagram of crank mechanism

F, tangential force
C, centrifugal force
m, equivalent mass of crankpin
r, crank radius
w, angular velocity
n, order of torsional vibration
ϕ, amplitude of torsional vibration

By applying equations (1) and (2), it is seen that the exciting force caused by torsional vibration of nth order has both the (n+1)th and (n-1)th components. Therefore, in the speed range where 6th order torsional vibration is predominant the exciting force of 7th order and 5th order is induced. The measured result on torsional vibration, cylinder block skirt vibration, and noise at 315 Hz third octave band are shown in Figure 7. It is obvious that 7th order block vibration and noise are generated when 6th order torsional vibration occurs.

It can be considered that this may be the reason why the 7th order and 5th order components of overall engine noise peak at 2450 rpm, where the peak of the 6th order torsional vibration appears, as shown in Figure 5.

Figure 8 shows the noise speed relationship of this particular engine under motoring conditions without the torsional damper. From the figure the same tendency can be observed.

As the maximum amplitude of the 6th order torsional vibration can be considered to be approximately ϕ=0.01045 rad (0.6 degree) the 7th and 5th- order components of the excitation force due to 6th order torsional vibration will be represented by equations (3) and (4) using equations (1) and (2):

$$\text{5th order: } \frac{Xn-1}{mrw^2} = \frac{0.01045}{2} \times 5^2 = 0.131 \quad (3)$$

$$\text{7th order: } \frac{Xn+1}{mrw^2} = \frac{0.01045}{2} \times 7^2 = 0.256 \quad (4)$$

Notwithstanding that the magnitudes of the exciting forces induced by the 6th order torsional vibration are only 25.6% and 13.1% of the centrifugal force for the 7th and 5th order components, respectively, the overall engine noise is, in fact, considerably affected by these components, especially by the 7th order.

This fact suggests that the natural frequency of the engine structure coincides with the frequency of the 7th order of speed.

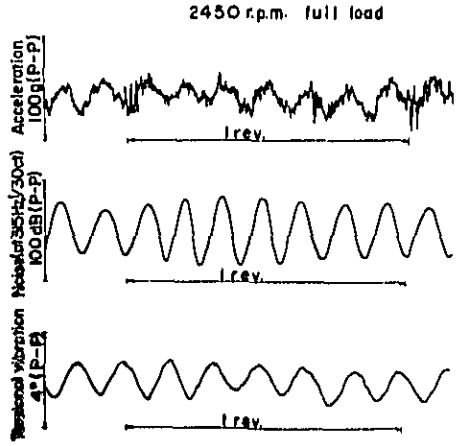

Fig. 7 – Relationship between torsional vibration, Crankcase vibration and noise
Wave forms were measured simultaneously on running engine at 2450 rpm and full load

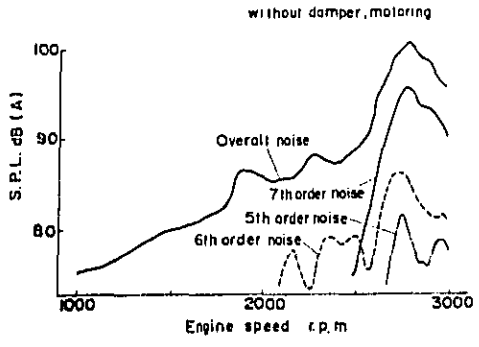

Fig. 8 – Noise-speed relationship with engine motored, and a damper removed

VIBRATION MODES OF ENGINE STRUCTURE

In order to identify vibration modes around 315 Hz, an assembled engine was excited by hammer with an impedance head and the mechanical impedance was measured simultaneously. A schematic of the method used is shown in Figure 9. The response of a point on the structure to a force applied to selected points (as shown in the figure) was recorded. As the force applied is impulsive, all frequencies in the structure can be excited simultaneously. The result obtained at the crankcase of a non-running engine is shown in Figure 10. It can be clearly seen that there is a marked resonance at 340 Hz. Using computer technique and stored mechanical impedances the mode shape at 340 Hz can be "animated" as shown in Figure 11.

It is obvious that the mode at 340 Hz shows a typical bending mode which is well known as a major contributor to the engine radiated noise. The vibration mode on the running engine at 2800 rpm was measured, also as shown in Figure 12. As the mode shape and resonant frequency obtained by using the impulsive excitation method are in extremely good agreement with those obtained on the running engine, it may be concluded that the noise peak at 315 Hz was mainly generated by the crankcase resonance induced by the 7th order excitation force caused by the 6th order torsional vibration of the crankshaft. Accordingly, to reduce the noise at 315 Hz the first measure to be taken is to select an appropriate damper so as to reduce torsional vibration of 6th order as much as possible. Finally a viscous damper was selected which resulted in noise reduction by about 13 dB at 315 Hz third octave band.

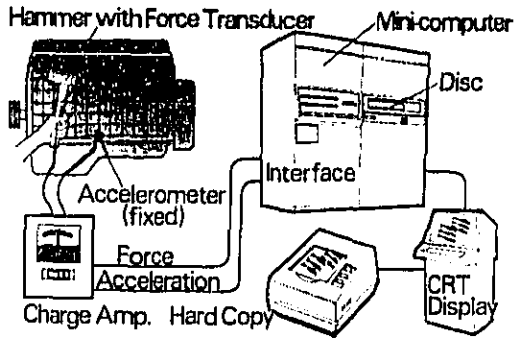

Fig. 9 – Layout of mode animation system
Impulse-frequency response at each grid point is processed using a digital computer, animated modes are displayed on CRT and results are obtained through hard copy

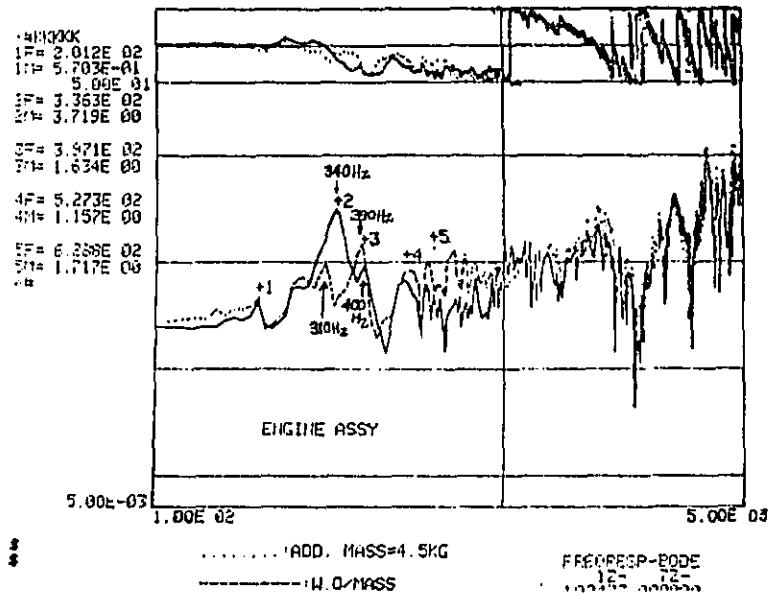

Fig. 10 - Inertance, phase and frequency relationship measured at crankcase. Effects of an additional mass are indicated

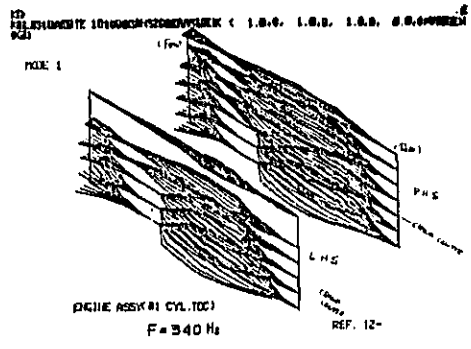

Fig. 11 - Mode shape at 340 Hz animated and displayed on CRT - fundamental bending mode

The second possibility to be tried is to change the above mentioned bending mode by structure modification in order to reduce the noise. Further investigations were carried out on critical factors which control the mode at 340 Hz. If the crankcase is stiffened the resonant frequency will move upwards. However, the weight will be increased excessively. If the crankcase is weakened the resonant frequency will move downwards, but the strength of the crankcase will be sacrificed. Moreover, in both cases described the direct effect on the noise level will be relatively small and not expected to exceed values of more 3 dB. Therefore, investigations were carried out mostly on changing boundary conditions of the vibration system which is composed of a crankshaft, 7 main bearings, and a crankcase. A simple mathematical model was considered to simulate vibration behaviour of the crankcase. The effect of mass on the vibration mode was analysed and this showed that the attachment of an additional inertia mass of 4.5 kg. to the front end of the crankshaft, was promising.

EFFECT OF ADDITIONAL MASS ON NOISE AND VIBRATION

In order to confirm the effect of the additional

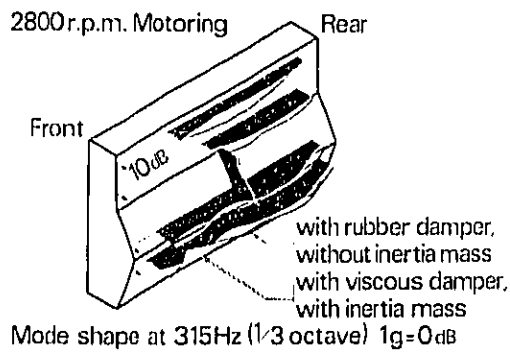

Fig. 12 - Mode shape at 315 Hz on running engine at 2800 rpm and motored

mass on the crankcase vibration characteristics, mechanical impedance measurements were carried out using the mode animation technique.

The results obtained is shown as a dotted line in Figure 10. From this figure it is clearly observed that the peak at 340 Hz is considerably reduced and a new smaller peak appears at 310 Hz when the additional inertia mass is attached to the crankshaft. The peak at 400 Hz is apparently moved to 390 Hz and the mode shape is unchanged.

Mode shapes at 400 Hz, 390 Hz, 340 Hz and 310 Hz were animated as shown in Figures 13, 14, 11 and 15 respectively. From Figure 13 and 14 it is clear that the bending mode at 340 Hz can be successfully changed to a torsional mode at 310 Hz as anticipated.

Comparing Figure 13 with Figure 14 it can be seen that the mode shape is unchanged. In addition the mode shape on the running engine was measured and compared as shown in Figure 12.

The reduction of the crankcase vibration level by some 13 dB at 315 Hz third octave band was obtained. Also the noise measurements were carried out and the results obtained are shown in Figure 16. Using the technique outlined above, noise reductions of up to 13 dB at 315 Hz third octave band can be achieved and the noise generation mechanism also identified. The additional weight represents only 2.5% of the total vibration system of interest and in this sense this technique is quite cost effective.

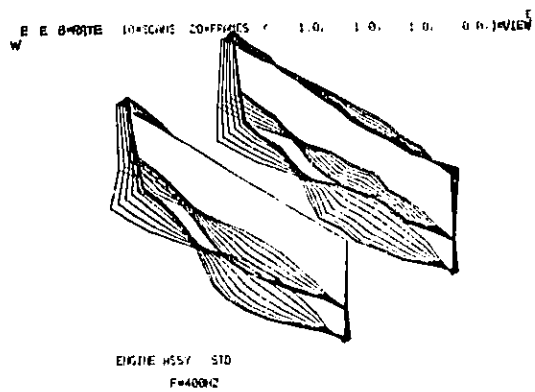

Fig. 13 - Mode shape at 400 Hz, inertia mass removed - bending mode

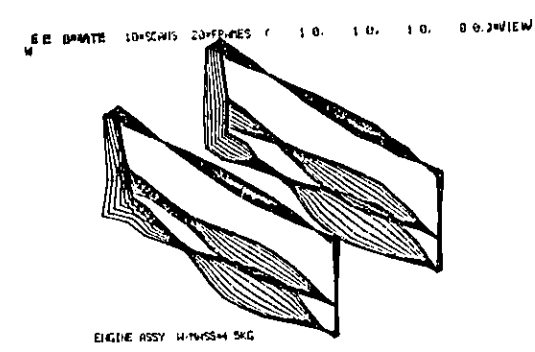

Fig. 14 - Mode shape at 390 Hz, inertia mass applied - bending mode

CONCLUSIONS

As a result of the investigations described in this paper the following conclusions can be drawn:

1. If the crankshaft is rotating at a constant angular velocity and subjected to the nth order torsional vibration, the exciting force is induced which is proportional to an equivalent mass of a crankpin multiplied by amplitude of torsional vibration and $(n\pm1)^2$

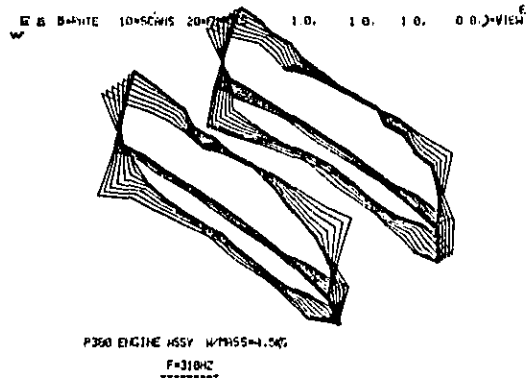

Fig. 15 – Mode shape at 310 Hz, inertia mass applied – torsional mode

2. The mode 'animation' technique has been successfully applied to identify vibration modes of interest and the mode shapes obtained are in good agreement with those obtained on the running engine.

3. The noise generating mechanism at 315 Hz third octave band has been identified by theoretical and experimental studies. With an additional mass representing only 2.5% of the total vibration system of interest the bending mode of the crankcase can be changed into a torsional mode as predicated theoretically and an engine noise reduction of up to 13 dB at 315 Hz third octave band can be obtained. However, further investigations should be carried out to predict the precise weight required to change the bending mode into another one which is of no great importance from the noise point of view.

ACKNOWLEDGEMENTS

The authors wish to acknowledge Mr S Sakata for taking measurements of vibration modes using the mode animation technique. Thanks are also due to Mr. J. Mizusawa, the director, and Mr. T. Iwata, the manager of Isuzu Motors Limited for their encouragement and their permission to publish the results.

REFERENCES

1. K OCHIAI, M AISAKA and S SAKATA, "Simple Model Technique for Better Understanding of Diesel Engine Vibration and Noise" Paper 750834 presented at S.A.E. Meeting, Milwaukee, August 1975.

2. Y KOSUGE, "Secondary Vibration induced by Torsional Vibration of Diesel Engine", Nainenkikan, Vol. 7, No.72, 1968.

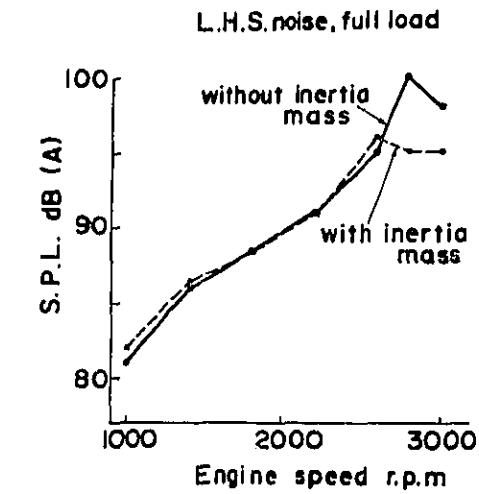

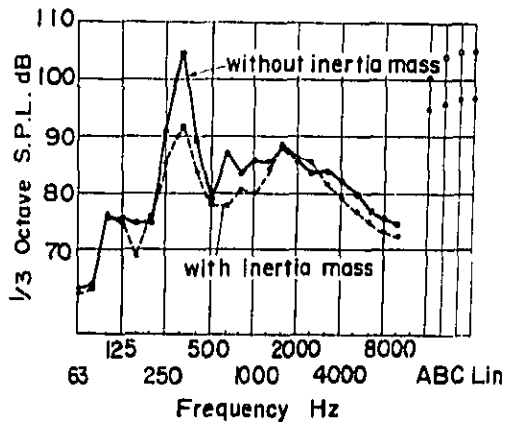

Fig. 16 – Effect of overall engine noise reduction

APPENDIX A CALCULATION

Calculation of inertia forces excited by n-th order torsional vibration. If the crankshaft is rotating at a constant angular velocity(w) and subjected to the n-th order torsional vibration as shown in Figure 6, the inertia forces excited by the torsional vibration can be represented by the following equations;

Inertia force in the tangential direction (F):

$$F = m \cdot r \cdot \frac{d^2}{dt^2}(wt + \varphi \sin nwt) \quad (1)$$

Component in the X - direction:

$$Fx = -m \cdot r \cdot n^2 \cdot w^2 \cdot \varphi \cdot \sin nwt(\sin wt + \varphi \sin nwt \cos nwt)$$

$$\fallingdotseq -m \cdot r \cdot n^2 \cdot w^2 \cdot \varphi \cdot \sin nwt \sin wt$$

$$= -\frac{1}{2} m \cdot r \cdot n^2 \cdot w^2 \cdot \varphi \{\cos(n-1)wt - \cos(n+1)wt\} \quad (2)$$

Component in the Y- direction:

$$Fy = m \cdot r \cdot n^2 \cdot w^2 \cdot \varphi \cdot \sin nwt (\cos wt - \varphi \sin nwt \sin wt)$$

$$\fallingdotseq m \cdot r \cdot n^2 \cdot w^2 \cdot \varphi \cdot \sin nwt \cos wt$$

$$= \frac{1}{2} m \cdot r \cdot n^2 \cdot w^2 \cdot \varphi \{\sin(n-1)wt + \sin(n+1)wt\} \quad (3)$$

Centrifugal force (C):

$$C = m \cdot r \cdot \left\{ \frac{d}{dt}(wt + \varphi \sin nwt) \right\}^2 \quad (4)$$

Component in the X- direction:

$$Cx = m \cdot r \cdot w^2(1+2n\varphi \cos nwt)(\cos wt - \varphi \sin nwt \sin wt)$$

$$\fallingdotseq m \cdot r \cdot w^2(\cos nwt + 2n\varphi \cos nwt \cos wt - \varphi \sin nwt \sin wt)$$

$$= m \cdot r \cdot w^2 \left\{ \cos wt + \varphi (n-\tfrac{1}{2}) \cos(n-1)wt + \varphi (n+\tfrac{1}{2}) \cos(n+1)wt \right\} \quad (5)$$

Component in the Y- direction:

$$Cy = m \cdot r \cdot w^2(1+2n\varphi \cos nwt)(\sin nwt + \varphi \sin nwt \cos wt)$$

$$\fallingdotseq m \cdot r \cdot w^2(\sin wt + 2n\varphi \cos nwt \sin wt + \varphi \sin nwt \cos wt)$$

$$= m \cdot r \cdot w^2 \left\{ \sin wt - \varphi (n-\tfrac{1}{2}) \sin(n-1)wt + \varphi (n+\tfrac{1}{2}) \sin(n+1)wt \right\} \quad (6)$$

Therefore,

$$Fx+Cx = m \cdot r \cdot w^2 \left\{ \cos wt - \frac{\varphi}{2}(n-1)^2 \cos(n-1)wt + \frac{\varphi}{2}(n+1)^2 \cos(n+1)wt \right\} \quad (7)$$

$$Fy+Cy = m \cdot r \cdot w^2 \left\{ \sin wt + \frac{\varphi}{2}(n-1)^2 \sin(n-1)wt + \frac{\varphi}{2}(n+1)^2 \sin(n+1)wt \right\} \quad (8)$$

Nomenclature:

m	equivalent mass of crankpin
r	crank radius
w	angular velocity
φ	amplitude of torsional vibration
n	order of torsional vibration

APPENDIX B INSTRUMENTATION

1 Torsional vibration transducer with F.Moscillator

Make: International Mechanical Vibration Ltd., Japan

Model: VMG100T

2 Harmonic order analyser

Make: Spectral Dynamics Corporation, USA

Model: SD1005A-SR1-2

3 Mode animation system

Time data PDP11 system with MODAMS* by SDRC

*MODAMS; Modal Analysis and Modeling System

790366

ENGINE NOISE REDUCTION BY STRUCTURAL DESIGN USING ADVANCED EXPERIMENTAL AND FINITE ELEMENT METHODS

Dean M. Ford, Senior Engineer - Numerical Analysis
Paul A. Hayes, Engineer - Noise Control Technology
Stephen K. Smith, Technical Specialist - Noise Control Technology

Cummins Engine Company, Inc.
Columbus, Indiana, U.S.A.

ABSTRACT

This paper presents structural analyses performed on an in-line, six cylinder diesel engine for noise reduction purposes. Both finite element modeling and experimental structural analysis using digital techniques were performed on the existing design. By applying both of these methods to the same structure, the accuracy of the structural model can be established. After several iterations the results of each method were made to agree quite closely. The finite element model could then be used for predicting the effect of design changes on the structural response of the block.

THE FEDERAL TRUCK NOISE REGULATIONS have caused the industry to expend much effort to lower the noise levels of current production medium and heavy duty trucks. The diesel engine manufacturers have had noise reduction efforts underway for several years (1)*. Examples of current engine noise reduction hardware in use includes mechanically isolated covers and close fitting panels made of metal stampings and acoustically absorbant liners. In addition to these surface treatments, basic redesigns of the engine structure have resulted in noise reductions (2-4). Lane, Timcoe, and Hawkins (5) report 1/3 octave band velocity reductions of up to 15 dB after structural redesign. Since selected structural modifications can be implemented at moderate costs, significant cost savings and product improvement exist if a surface palliative treatment is no longer necessary. These modifications can be determined by an entirely experimental cut and try approach. This approach does not give confidence that an optimal design has been achieved for cost, weight, ease of manufacturing, or even the structural response itself. A much better approach is to understand the dynamics of the structure by creating an accurate, analytical model. With this model a prediction of the dynamic effect of each modification can be made.

For a Cummins NTC-350 engine (six cylinder, in-line) installed in a vehicle, the highest noise level emanates from the oil pan and cylinder block wall as shown in Table 1. Since the oil pan's vibration and resulting noise are controlled by the interface with the block wall, the area most needing improvement is the lower block wall or crankcase skirt. The dynamic response of the lower block wall surface is influenced by the upper structure of the block. Thus a model of the entire block structure is needed. The dynamic analysis of this complex structure must include many resonant frequencies and mode shapes. A finite element model could be very inaccurate especially in the upper frequency range. A narrow band frequency analyzer, minicomputer, disc storage, graphics terminal, and software package gives us the ability to perform an experimental vibration analysis (determine the natural frequencies and mode shapes) of an existing structure. The results of the finite element analysis were compared to the experimental results to determine the accuracy and completeness of each method. A cylinder block was sectioned into seven segments with each being a piece of the overall block model. Experimental data taken from a segment of the block was also compared to a finite element model. The remainder of this paper discusses the modeling and experimentation done on the NH cylinder block.

Table 1 - Bare NTC-350 Surface Source Ranking
Vehicle J-366B Driveby Test - Left Side

Exposed Surface	Relative Level (dBA)
Oil Pan	0
Block Left Side	-3
Air Comp./Fuel Pump/ Crossover/Rocker Boxes	-9
Valve Covers	-9.5
Flywheel Housing	-9.5
Engine Front	-10.5
Turbo/Exhaust Manifold	-15
Intake Manifold	-20

*Numbers in parentheses designate References at end of paper.

SAE/P-79/80/$02.50
Copyright © 1979 Society of Automotive Engineers, Inc.

In order to develop testing techniques and noise reduction criteria for the block structure, it became obvious that a special block with markedly different vibration characteristics was needed to compare with the standard block. The special block was fabricated and contained several changes, particularly in the crankcase area.

STATIC ENGINE VIBRATION TESTS

In evaluating vibration characteristics of complex structures, a controlled laboratory test rig is generally invaluable. Bench vibration testing allows for quick, economical evaluation of different ideas and designs thus reducing the more expensive and time consuming running engine tests. Typical laboratory vibration tests consist of generating transfer functions between strategic points of interest. An accurate estimation of the transfer function requires simultaneous measurement of a force input and motion output of the structure as a function of frequency. Three basic procedures are used to this end. The classic method of transfer function generation involves swept-sine (shaker) excitation. Good high-frequency resolution and a wide dynamic range can be obtained. This method requires a relatively long time to acquire data over a wide frequency range.

The second method of generating transfer function information is the impulse technique. In this method all frequencies in the structure are excited simultaneously. The transient force and acceleration signals are digitally stored and the transfer function calculated. This method provides a rapid, relatively accurate estimate of the transfer function.

The third method is the random excitation (shaker) technique. In this method a random signal input to the shaker is used to provide a "white" noise input force. The input force and output acceleration are channeled into a narrow band frequency analyzer which processes the signals and performs the required calculations needed to obtain the transfer function. In order to insure an accurate repeatable transfer function, many spectral overlays must be used in calculating the transfer function (6-8). With the use of contemporary digital analyzers these calculations can be made in a matter of seconds and stored digitally for later manipulation. This random excitation technique was used in computing all transfer functions for the static testing of the engine blocks.

It has been shown that the piston/connecting rod/crankshaft transfer path is a major contributor to crankcase vibration and hence, noise (9, 10). With this in mind, a test rig to evaluate this transfer path was designed. The test rig consisted of an engine short block with liners, pistons, connecting rods, crankshaft, oil pan, oil pan gasket and appropriate gaskets and seals (Fig. 1). The block was suspended by an elastic cord in order to insure isolation from the support structure.

The force associated with the high frequency noise generating portion of the diesel engine combustion spectrum is only on the order of 10-30

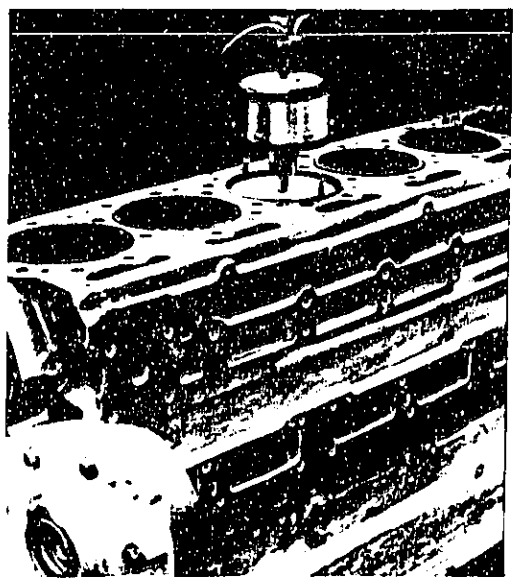

Fig. 1 - Swept-sine shaker excitation of engine structure

pounds (44.5 - 133.5 N) (5) indicating that a low force level excitation can be used on static rigs in order to simulate running engine combustion inputs. With this in mind the shaker input was mounted on one of the piston tops in order to simulate the combustion forces acting on the piston.

Various points along the pan rail were chosen as the output accelerometer locations in order to simulate a composite response of the lower engine and oil pan to combustion pressures.

Transfer functions were then taken from the piston to each of the points along the pan rails for both the standard engine block and the special block. Typical narrow band compliance plots (for both cylinder blocks) are displayed in Fig. 2.

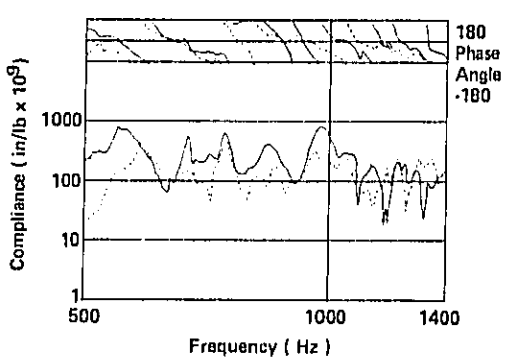

Fig. 2 - Typical compliance plot from piston to crankcase panrail; — standard block; --- special block

This figure clearly indicates there is considerable difference between vibration characteristics of the blocks. By summing the transfer functions between the piston and lower block an average transfer function can be obtained. The 1/3 octave mobility plots for each block are shown in Fig. 3. Again, the differences between the transfer functions indicate a significant difference in vibration characteristics.

RUNNING ENGINE TESTS

Since the two blocks tested displayed such different vibration characteristics of the piston/connecting rod/crankshaft transfer path, the differences should be measureable in running engine noise tests. This assumes that this path is a major contributor to lower engine vibration. The engine blocks tested in the lab were built into two identical model engines. In order to obtain a good measurement of lower engine and oil pan noise the engines were wrapped, using the lead-wrapping techniques, such that the lower three inches of the block and oil pan were exposed. The two engines were run and measured in the same hard test cell and the 1/3 octave noise plots for both engines are also shown in Fig. 3. Note that the reduction in noise occurs over the same frequency range (500-1200 Hz) as the reduction in mobility show in Fig. 3. Also note that the general shape of the mobility plots match the general shape of the respective noise spectra. These similarities tend to verify that the piston/connecting rod/crankshaft transfer path is the dominant crankcase vibration path in this particular diesel engine. The similarities also show that a static laboratory test as performed is an accurate method in evaluating the piston/connecting rod/crankshaft transfer path into the crankcase.

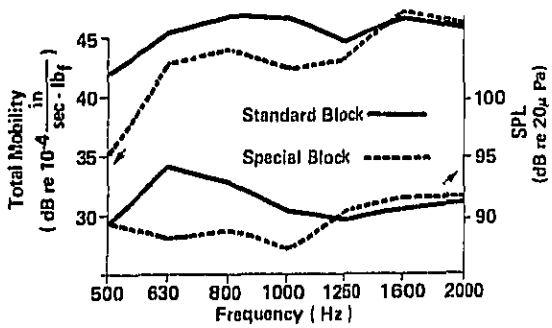

Fig. 3 - Top; total mobility between piston and crankcase panrail; bottom; hard cell engine noise

The laboratory and noise tests indicate that structural modification on the engine block could result in significant noise reduction. These results warranted further investigation into the feasibility of optimizing the block vibration characteristics. The special block, while significantly quieter, was too heavy and could not be machined on present block production lines, suggesting a need to develop a block design which will yield the best vibration characteristics for the least weight. To accomplish this goal, both a finite element analysis and an experimental vibration analysis of the block were performed. The joint analyses allow comparisons and iterations between the results of the two techniques.

EXPERIMENTAL VIBRATION ANALYSIS OF ENGINE BLOCK (1 DIMENSIONAL)

An experimental vibration analysis was performed on the standard engine block. The schematic for the block is shown in Fig. 4. The shaker was mounted on the lower right side of the block, and accelerometers were mounted along each of the five horizontal lines outlining the left and right sides of the block. Transfer functions were obtained for 65 different accelerometer positions (13 along each horizontal line) defining the amplitude and phase of each point's acceleration relative to the random force input. This data was obtained only in the direction normal to the sides of the block assuming that motion in the other two directions would not contribute to noise.

A typical block transfer function is shown in Fig. 5. It is seen that the bare block is lightly damped and contains many well defined resonances below 1200 Hz. Modal coefficients for each point were then generated for each resonance with which mode shapes could be generated. Three typical mode shapes are shown in Fig. 6. The entire block participates in the lower frequency modes as shown by the first bending mode of the block (Fig. 6A). The block modes become more complex with increasing frequency as can be seen by Fig. 6B. Above 800 Hz the block demonstrates a family of crankcase modes, one of which is the crankcase "bulge mode" as shown in Fig. 6C.

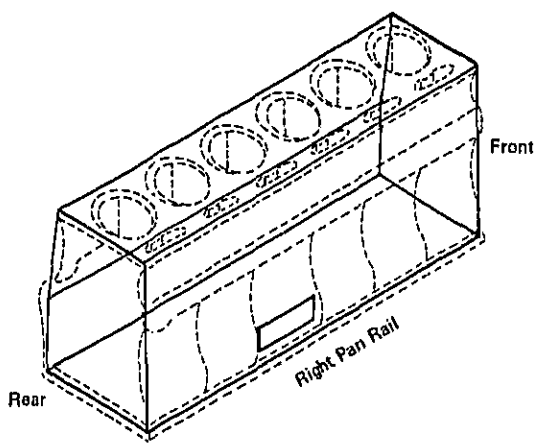

Fig. 4 - Experimental vibration analysis schematic of block (shown in solid lines)

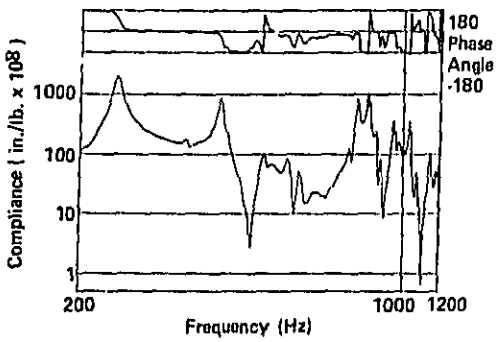

Fig. 5 - Typical compliance plot for standard engine block

BLOCK SEGMENT EXPERIMENTAL VIBRATION ANALYSIS (3 DIMENSIONAL)

As an intermediate check case for the finite element model, an experimental vibration analysis was performed on a section of a standard block. The block was sliced down the center of two adjacent cylinders and contained one of the bulkheads. The shaker was mounted on the left side of the block section and transfer functions were taken in three directions for various points defining the block segment outline for the mode display. These mode shapes were used to compare with the mode shapes predicted by the finite element model of the block segment (to be discussed later).

FINITE ELEMENT ANALYSIS

The function of the dynamic finite element model of the block is to determine how structural changes to the block affect modes shapes and frequencies. This information can then be extrapolated to determine transfer functions which give some indication of the noise characteristics of the block.

DEVELOPMENT OF THE MODEL - In order to establish acceptable confidence in the model, it was necessary to calibrate the model against the existing block. For this exercise to be possible, it is almost imperative that the model and tested hardware be as nearly identical as possible, and that the same boundary conditions are assigned to each. To keep the model as simple as possible, the bare block was modeled with no attached hardware except the main bearing caps. Since the block is rather massive, laboratory fixtures could accurately simulate only a free block. The only complexity which this added to the finite element model was the extraction of the six rigid body modes.

To ease the work of modeling, one can take advantage of the repetitive nature of the block. The total block can be logically divided into seven smaller structures by passing a plane through the center of each cylinder as illustrated in Fig. 7. Except for local bosses, holes, or irregulari-

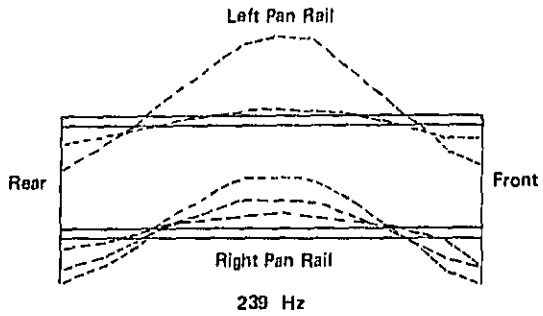

Fig. 6A - Experimentally determined 1st bending mode shape

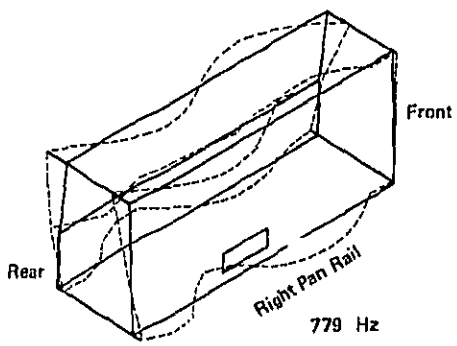

Fig. 6B - Experimentally determined 3rd torsional mode shape

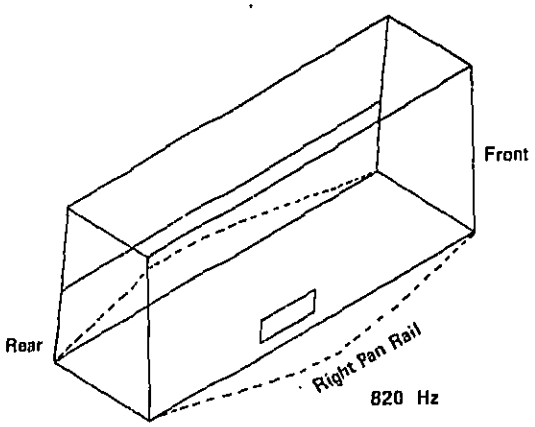

Fig. 6C - Experimentally determined crankcase "bulge" mode

ties, segments 2, 4, and 6 are identical as are segments 3 and 5. The result of ignoring the local irregularities should be insignificant, as localized modes are not of interest. This subdividing suggests the possibility of using the substructuring features of one of the popular finite element programs. We have not done so yet, but substructuring has numerous advantages, especially in the input preparation and computing time.

A physical block was sliced into seven segments. To provide a preliminary indication of the accuracy of the total block model, a single segment (number 2 of Fig. 7) was analyzed by both finite element and experimental techniques. The slice corresponding to segment number 2 was used as a visual aid and provided direct input for wall thicknesses and measurements which were better obtained physically than from the drawing. This finite element model is shown in Fig. 8. The

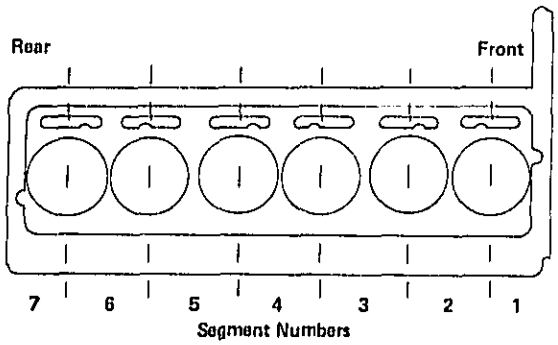

Fig. 7 - Division of block into segments

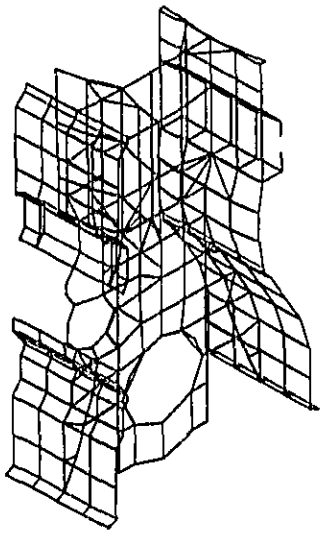

Fig. 8 - Finite element model of segment 2

model was relatively small (283 nodes) and the computer run could be made for a fraction of the cost of the larger model. That segment's mode shapes and natural frequencies were determined experimentally. The correlation between experimental and analytical frequencies is shown in Fig. 9. The sliced block was further used to aid the modeling of the entire block.

An orthographic projection of the complete model is presented in Fig. 10. As many as eighty

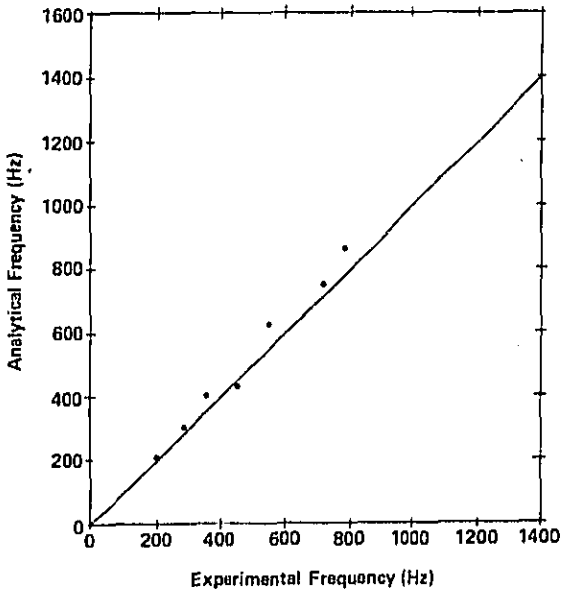

Fig. 9 - Correlation of experimental and analytical frequencies for segment 2

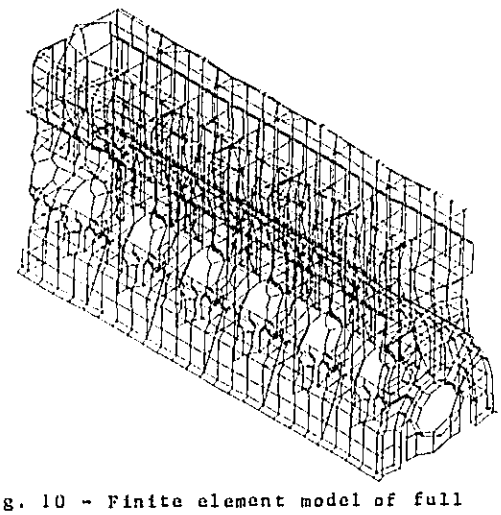

Fig. 10 - Finite element model of full block

frequencies and mode shapes are in the range of interest for acoustic purposes, so that the amount of detail required will be greater than in many dynamics problems where only the lowest few frequencies might be important. The model was generated using quadrilateral and triangular plates, 3 dimensional beams, concentrated masses, and rigid elements. Altogether there are 1604 nodes and 2300 elements.

With 1604 nodes in a 3 dimensional model, there are approximately 9500 degrees of freedom. Obviously, a dynamic reduction, or more specifically a Guyan reduction (11), is required. The dynamic reduction reduces the static degrees of freedom into a smaller set, herein called the dynamic degrees of freedom, so that the eigenvalue extraction is less costly. The underlying assumption is that the retained degrees of freedom are able to describe the mode shapes of the structure. The eliminated degrees of freedom assume the same values as they would under static deformation for the calculated deflection values of the dynamic degrees of freedom. Because of the large number of eigenvalues required and since a dynamic reduction is being used, computing time is reduced if the eigenvalues are determined all at once by a transformation method rather than using one of the tracking methods which determine one eigenvalue at a time (12).

FINITE ELEMENT RESULTS - The first run of the full block dynamic model yielded 144 eigenvalues (equal to the number of dynamic degrees of freedom) and 80 mode shapes (including 6 rigid body modes). In general, the agreement with the known experimental mode shapes was good. The mode shapes were plotted as just outlines of the structure because a complete plot including all of the elements would have included so many lines that it would have been incomprehensible. The 3 mode shapes corresponding to the modes previously shown in the experimental vibration analysis (Fig. 6) appear in Fig. 11. These mode shapes show good agreement as did most modes below 1600 Hz.

An important discovery in the analytical result was a group of eight mode shapes in a narrow frequency band between the first and second bending modes of the block. Plots revealed that each of these modes involved longitudinal (along the crankshaft axis) deflection of the main bearing caps and bending of the bulkheads. One of these modes is shown in Fig. 12. Up to that time, the bulkheads and bearing caps had not been instrumented in the experimental work. The results contained higher frequency modes which exhibited significant bulkhead motion indicating the need for instrumentation on the bulkheads.

Some of the most important modes from a noise standpoint are a group referred to as "panel modes" where the sides of the block are moving in and out between bulkheads. One of these modes has the characteristic that the panels alternate out and in the whole length of the block (Fig. 13). The panels behave very much as if they were pinned at each bulkhead and that the bulkheads themselves have little motion.

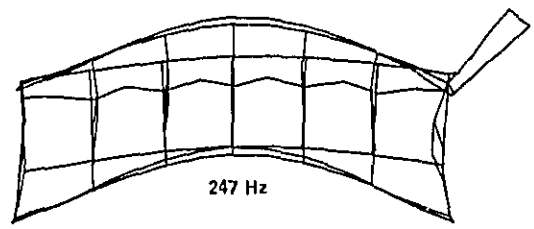

Fig. 11A - Analytically determined 1st bending mode shape

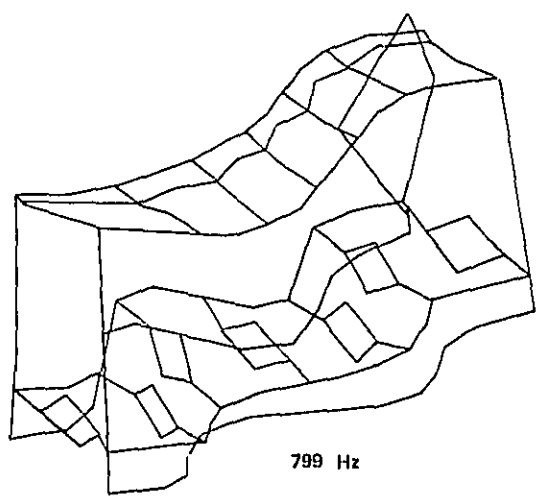

Fig. 11B - Analytically determined 3rd torsional mode shape

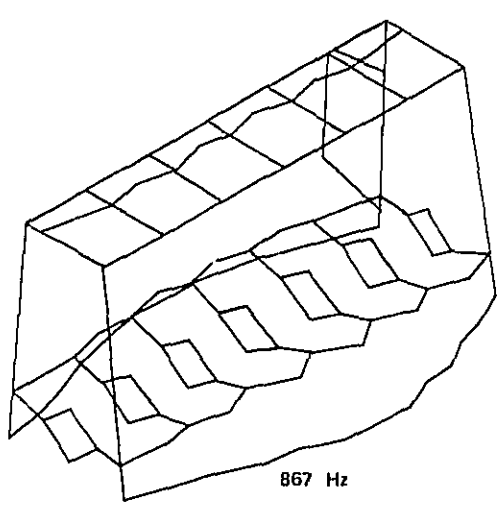

Fig. 11C - Analytically determined crankcase "bulge" mode

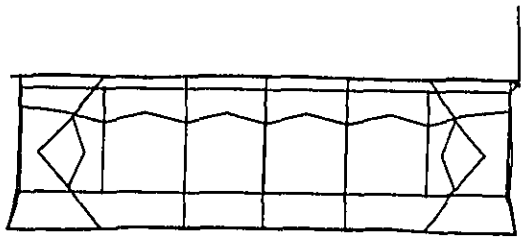

Fig. 12 - Analytically determined "bulkhead" mode

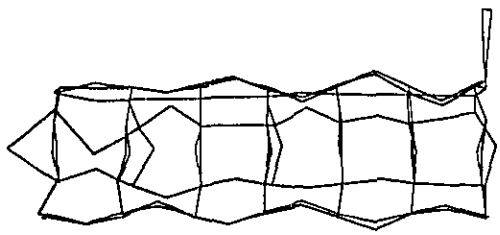

Fig. 13 - Analytically determined "panel" mode

Two of the more important mode shapes acoustically are the crankcase "bulge mode" (Fig. 11c) which has a frequency of about 800 Hz and the panel modes just described. Interestingly, both of these mode shapes are represented in a simpler model if one of the interior segments is fitted with symmetric boundary conditions. This makes a useful tool for calculating how block changes will affect these modes without running the larger and more expensive model.

EXPERIMENTAL VIBRATION ANALYSIS OF ENGINE BLOCK (3 DIMENSIONAL)

Because the finite element model of the block demonstrated that the bulkheads participate in some of the more important modes of vibration, we decided to perform another experimental vibration analysis of the block including bulkhead response data. The finite element model also displayed considerable motion in all three directions, so data was taken in three directions. The schematic of the block is shown in Fig. 14 and data was input on each of the six horizontal lines defining the left and right sides and also on the lower bulkheads (or main bearing caps). A typical transfer function from the shaker input to a bulkhead is shown in Fig. 15. As can be seen the bulkheads do exhibit large responses at resonances just like the block walls. Mode shapes for each resonance were generated and seven modes were seen in which only the bulkheads were in resonance. Fig. 16 shows one of the bulkhead modes which compares very favorably with that computed by the finite element model, Fig. 12.

Further comparison of the finite element versus experimental results are shown in Fig. 17.

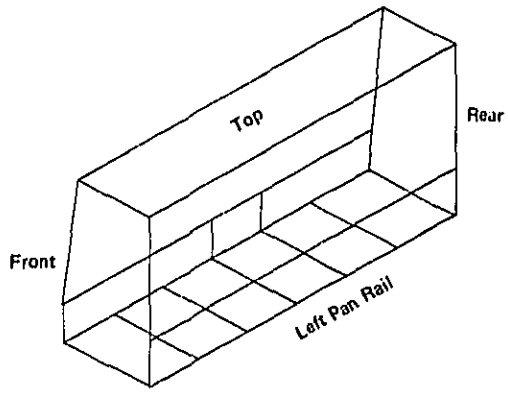

Fig. 14 - Experimental vibration analysis schematic of block with instrumented bulkheads

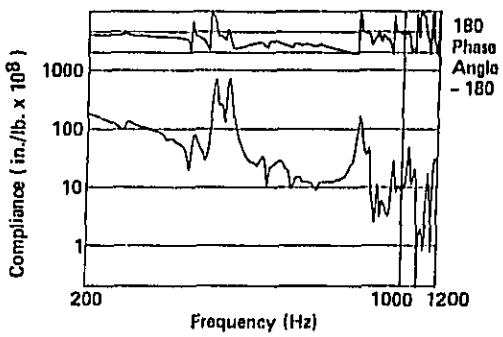

Fig. 15 - Typical compliance plot for bulkhead on standard engine block

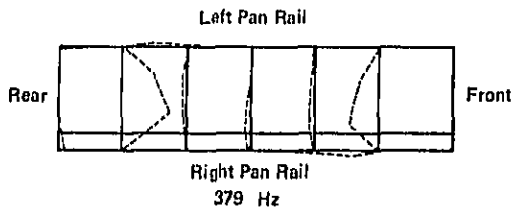

Fig. 16 - Top view of experimentally determined "bulkhead" mode

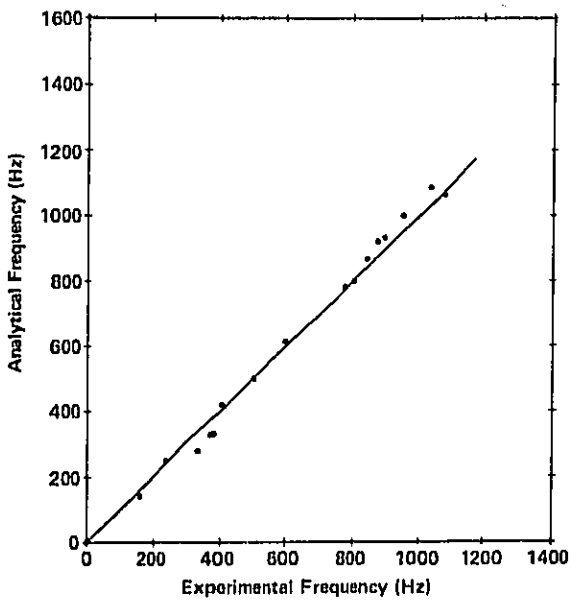

Fig. 17 - Correlation of experimental and analytical frequencies for full block

SUMMARY AND CONCLUSIONS

1. The engine surface noise source identification performed for the NH family of engines during the J-366b vehicle driveby test shows the oil pan and lower block skirt to be the areas producing the most noise.

2. The engine noise testing of the special block cast with crankcase modifications show that noise reductions can be gained by appropriate structural changes.

3. Experimental shaker excited laboratory tests correlated well with the running engine noise measurements.

4. Experimental vibration analysis provides accurate information concerning the dynamic behavior of the cylinder block.

5. A finite element model has been formulated that adequately represents the dynamic characteristics of the NH cylinder block.

6. The interior structure and design of the block were found to be significant as the bulkheads participated in several acoustically important modes.

7. By applying both techniques of finite element modeling and experimental vibration analysis to the same structure, the accuracy and completeness of each method's results can be judged.

8. We have a finite element model of the NH cylinder block which we have used in the design of a new block.

REFERENCES

1. S.H. Jenkins and H.K. Kuehner, "Diesel Engine Noise Reduction Hardware for Vehicle Noise Control." SAE Paper 730681 Presented at Combined Commercial Vehicle Engineering and Operations and Powerplant Meetings, Chicago, Illinois, June 1973.

2. S.H. Jenkins, N. Lalor and E.C. Grover, "Design Aspects of Low Noise Diesel Engines." SAE Paper 730246, SAE Automotive Engineering Congress, Detroit, January 1973.

3. T. Priede, A.E.W. Austen and E.C. Grover "Effect of Engine Structure on Noise of Diesel Engines." Proc. Inst. Mech. Eng. Vol. 179, No. 4 (1964-1965), Part 2A.

4. M.F. Russell, "Automotive Diesel Engine Noise and Its Control." SAE Paper 730243 Presented at the SAE Automotive Engineering Congress, Detroit, January 1972.

5. R.S. Lane, S.E. Timour, and G.W. Hawkins, "Techniques of Structural Vibration Analysis Applied to Diesel Engine Noise Reduction." SAE Paper 730835 Presented at the SAE Conference in Milwaukee, Wisconsin, September 1975.

6. J.S. Bendat and A.G. Piersal, "Random Data: Analysis and Measurement Procedures." Wiley Interscience, New York, 1971.

7. S.H. Crandall and W.D. Mack, "Random Vibration in Mechanical Systems." Academic Press, New York and London, 1963.

8. J.T. Broch, "On the Measurement of Frequency Response Functions." B&K Technical Review, No. 4, 1975.

9. R.G. DeJong, "Vibration Energy Transfer in a Diesel Engine." Ph.D. Thesis, M.I.T., August 1976.

10. E.T. Buehlmann, "Combustion Noise Study on a Diesel Engine." M.S. Thesis, Purdue University, May 1975.

11. R.J. Guyan, "Reduction of Stiffness and Mass Matrices." AIAA Journal, Vol. 3, No. 2, p. 380, February 1965.

12. Richard H. MacNeal, "The Nastran Theoretical Manual"; Editor, December 1972.

790441

AN APPROACH TO A QUIET CAR DIESEL ENGINE

Heinz A. Fachbach and Gerhard E. Thien

AVL Prof. List Ges.m.b.H.
Graz, Austria

ABSTRACT

The paper presents a new development of a low-noise passenger car and small truck diesel engine. As described in the first section of this contribution the new design concept is mainly characterized by the vibration isolation between the vibration excited internal engine structure and the external engine casing, obtained by elastic elements specially developed for this purpose. The external engine casing and the flywheel housing are designed as one part where the gear box can be bolted on in the usual way. An essential part of the paper is dedicated to the description of preliminary theoretical and experimental investigations into the design of the vibration isolating elements between the so-called crankframe and the external housing and to the description of the design of the external housing. In the following the test results gained on a prototype engine featuring the mentioned design principle are discussed. This prototype engine is a water-cooled 2.2 liter diesel engine. The last section finally proves that particularly good results with regard to economic viability can be achieved by using engines of the above design in different vehicles, such as cars, small trucks and farm tractors.

IN IMPROVING OUR ENVIRONMENTAL CONDITIONS and in particular the quality of life of the urban population, concentrated efforts are directed to the reduction of the traffic noise constituting the major noise source in densely populated areas. Satisfying results can certainly be achieved in collaboration of town planning authorities, government, vehicle owners and drivers as well as vehicle manufacturers.

In the past years extensive research and development work was performed to find out possible solutions for the problem of interest, to be realized by vehicle manufacturers (1,2,3,4,5,6,7,8,9,10, 11,12,13)*. Reductions of the total noise emitted by vehicles have to be in the range of 10 dB(A) and more to bring about a perceptible relief to the human ear. Noise reductions of such a magnitude require measures on every single noise source essentially contributing to the total noise. In general, the main noise sources are the exhaust system, the cooling system and the power unit as well as to a certain extent the intake system, vehicle structure, rear axle gear and tires.

The essential findings of previous studies led to the conclusion that a 10 dB(A) reduction of the noise emitted by the surface of the power unit, in particular with regard to diesel engines, cannot be achieved by measures applied to the noise sources of the engine itself nor by measures applied to individual parts of the noise radiating engine surface. To achieve such a high noise reduction it is in any case necessary to eliminate to a large extent the vibration transmission from the load carrying engine parts to the external walls. With conventionally designed engines this principle can only be realized in surrounding the engine itself with an additional enclosure which is attached to the engine in a vibration isolated manner. This enclosure must have a sufficient transmission loss of the air borne sound emitted from the outer engine surface. In the course of the research and development work performed during the past years a new design concept for such an enclosure has been developed (3,5,10,14). It is characterized by the use of 1 mm sheet metal as material for the enclosure walls, by a very small distance to the engine surface, by the lack of sound absorbing lining on the inner side as well as by good accessability to the engine and sufficient operating reliability. With such an enclosure the noise of a vehicle power unit can be reduced by 15 dB(A) to 18 dB(A), the weight increase is about 9 % of the weight of the power unit. The sound reducing enclosure can, either forming a unit of its own, be supported on the engine or it can be integrated into the existing vehicle components in the area of the power unit. In the latter case the flexible engine mounts provide the necessary vibration isolation between engine and enclosure.

Sound reducing enclosures of this kind cause, even if optimized, a certain increase in bulk volume, cost and especially weight depending on the design concept chosen.

With new designs for future engines it is possible to almost completely eliminate the disadvantage of increased weight. The vibration isolated engine casing in this case not only has a sound reducing function, but also provides the lubrication oil sealing to the outside. Therefore, those parts of the conventionally designed crankcase so far providing the sealing can be omitted.

In principle the weight can further be reduced, compared to the additionally enclosed power unit, by sufficiently eliminating the transmission of structural vibrations from the engine to the gear box and therefore by renouncing a transmission gear enclosure under the condition of a low gear noise.

THE NEW DESIGN PRINCIPLE FOR A LOW-NOISE ENGINE

The principle concept for an engine featuring

*Numbers in parentheses designate References at end of paper.

SAE/P-79/80/$02.50
Copyright © 1979 Society of Automotive Engineers, Inc.

the two afore-mentioned advantages is shown in Figs. 1 and 2 on the example of a water-cooled 4-cylinder engine. The vibration excited inner engine structure comprises a skeleton-like so-called central support - which below the bottom of the water space consists only of the main bearing caps - the cylinder head and the crank drive. The engine housing supports the central engine structure and is combined with the flywheel housing. The central support is attached to the enclosure in a vibration isolated manner by means of elastic elements.

With the version shown in Fig. 1, the vibration isolation is effected by one frame-like flexible element horizontally surrounding the engine. It

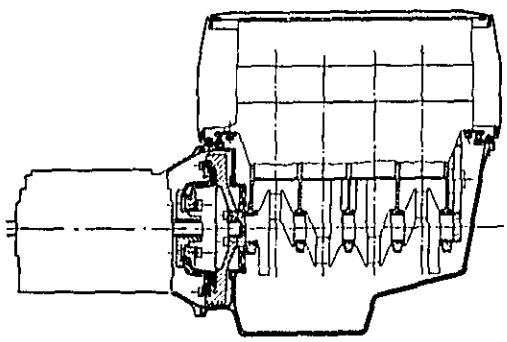

Fig. 1 - Design concept of the low-noise engine, vibration isolation by one frame-like flexible element

is attached to the central support and to the engine housing and provides the sealing of the upper side of the oil chamber. In Fig. 2 individual elastic elements are attached on the front and rear side of the engine, whereas the sealing of the oil chamber is separately provided by a highly elastic diaphragm surrounding the engine in the shape of a frame.

The upper part of the engine where all the accessories are arranged is covered with a thin-

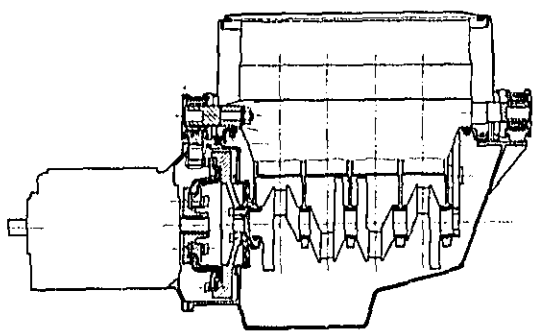

Fig. 2 - Design concept of the low-noise engine, vibration isolation by individual elastic elements

walled enclosure made of sheet steel, similarly to the mentioned enclosures of conventionally designed engines, and is ventilated by a fan, not demonstrated in the figure. Due to the low structural vibrations of the flywheel housing a transmission gear can be bolted on, and as there is no unacceptable vibration transmission an additional enclosure is not necessary.

Because of the elastic connection between the central support and the engine housing displacements may occur between crankshaft with flywheel and engine housing resp. intake shaft of the transmission. Therefore, elastic elements have to be used for the sealing of the penetration of the crankshaft through the rear wall of the engine housing as well as for the connection between flywheel and gear shaft.

THEORETICAL REFLECTIONS

When designing the engine housing and the elastic connection between the housing and the central support certain basic requirements have to be considered:

Sufficient attenuation of the certainly very high air borne sound in the area of the crank drive of the engine by the engine housing.

Highest possible suppression of the structural vibrations by the elastic connection between the central support and the engine housing.

Small relative motion between inner and outer engine structure, in particular between flywheel and flywheel housing, with regard to the connection to the gear shaft.

Lowest possible excitability of the engine housing due to structural vibrations.

SOUND REDUCTION OF THE ENGINE HOUSING - As with small automotive engines low weight is of considerable importance, the so-called engine housing for the new engine type can only be made of aluminium. With regard to stiffness and feasability the thickness of the housing walls was chosen with 5 mm. The sound reduction of the housing of a certain size essentially consisting of plane panels was assumed as follows (15,16,17).

The highest possible transmission loss R is achieved with large undamped panels or with small panels and sufficient damping. (These are panels where the free bending waves reflected from the edges are of no importance). It can be described by the equation:

$$R_{max} = 20.\log f + 20.\log \varrho_w + 20.\log h - 45.3 \quad dB$$

f(Hz), ϱ_w density of wall material in g/cm^3, h wall thickness in mm.

For small panels with low damping the following equation applies:

$$R_{min} = 15.\log f + 10.\log \varrho_w + 5.\log h + 10.\log 2a - 5.\log c_L - 5.6 \quad dB$$

2a smallest panel size in m, c_L velocity of propagation of longitudinal waves in m/sec.

Both equations apply to the important range below the critical frequency amounting to about 2.5kHz for the respective panel size and wall thickness.

Fig. 3 shows the values for R_{max} and R_{min} for

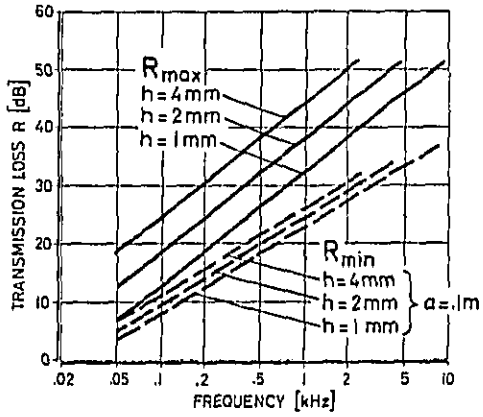

h...THICKNESS OF PANEL
2a..SMALLEST SIZE OF PANEL BETWEEN EDGES OR STIFFENING RIBS

Fig. 3 - Random incidence transmission loss below critical frequency of finite panels of sheet steel

panels of sheet steel with different wall thicknesses. As c_L for steel and aluminium is approximately equal and the weight per unit area of aluminium is about one third the one of steel with the same wall thickness, the transmission loss of the relevant aluminium panels approximately equals the transmission loss of 2 mm sheet steel. On condition that the air borne sound level inside the engine housing does not differ significantly from the sound level in the space between engine surface and the wall of a standard enclosure made of 1 mm sheet steel, as for instance with the upper area of the engine, it could be assumed that the noise contribution resulting from the excitation of the engine housing by air borne sound is of an unsignificant amount (17).

REDUCTION OF VIBRATION TRANSMISSION THROUGH THE ELASTIC CONNECTION BETWEEN CENTRAL SUPPORT AND ENGINE HOUSING - With an engine of a definite size, cylinder number, cylinder arrangement and speed the unbalanced inertia forces of the crank drive as well as the masses of the central support and the engine housing are confined within narrow limits, based on design considerations. For obtaining a satisfactory reduction of the vibration transmission in the frequency range relevant to the noise emission as well as sufficiently small relative displacements between the inner and outer engine structure, particularly between flywheel and flywheel housing the design of the elastic connecting elements between the two engine parts is of considerable importance. For the assessment of the vibration amplitudes at low frequencies the entire engine can be considered as a linear damped two mass spring system. Such a system is demonstrated in the upper part of Fig. 4. The mass M1 corresponds to the inner engine structure, the mass M2 to the engine housing. The elastic connection between the two masses is replaced by the spring $c_{1\,2}$ and the damping d. The engine, in this case the engine housing, is softly supported by means of the spring c_{01} and the damping d. The unbalanced inertia forces of the crank drive are acting on the inner engine structure, with the described 4-cylinder inline engine it is the second order inertia force.

The upper diagram shows the results of the calculation of such a system. $c_{1\,2}$ was considerably higher than $c_{0\,1}$ and deliberately assumed in a way that the resonance frequency of the relative motion of the two masses towards eachother is distinctly above the highest forcing frequency caused by the unbalanced second order inertia forces. It can be seen that at first no relative motion between the two engine parts in the low speed range appears, especially in the speed range corresponding to the natural frequency caused by the engine suspension.

Relative motions only occur above approximately 1000 RPM and increase highly progressively with the speed. At 4000 RPM and under the assumed boundary conditions they amount to 0.8 mm.

The lower diagram exhibits the relative displacements for various realistic spring constants $c_{1\,2}$ as well as realistic damping values of rubber

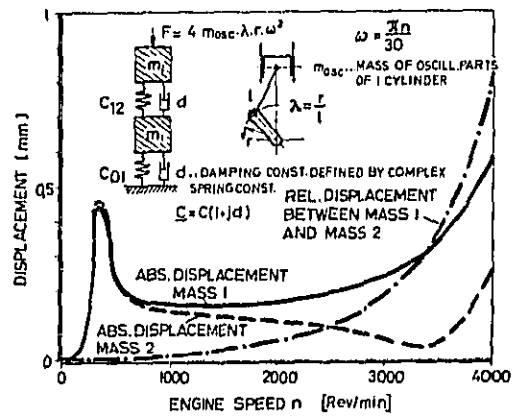

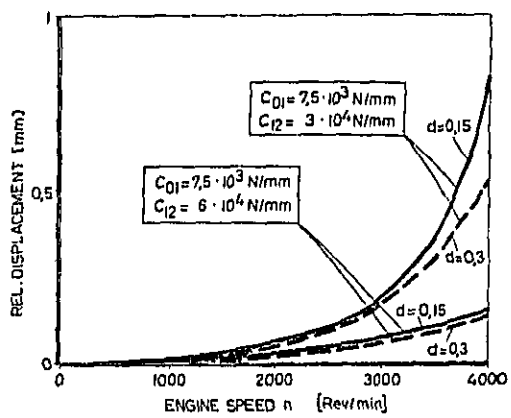

Fig. 4 - Linear damped two mass spring system, displacements with various spring constants and dampings

springs. It can be noted that the relative displacement with $c_{1,2}$ equal 6.10^4N/mm, is considerably smaller than the one with 3.10^4N/mm. With the low spring constant the higher damping at 4000 RPM near the resonance is distinctly more effective than with a higher spring constant.

This calculation model is only related to the vertical motions due to the unbalanced inertia forces and means an extreme simplification compared to the actual conditions. In this case it only serves to illustrate the problems. For the layout of real prototype engines the determination and optimization of the spring constants is carried out by means of a special calculation system which observes all existing degrees of freedom and has been recently introduced at AVL.

The considerations described in the previous section merely concern the lower frequency range where the inner engine structure and especially the engine housing can be considered as rigid masses from the point of view of mechanical input mobility. This cannot be done for the frequency range relative to the engine noise, i.e. above approximately 0.5kHz, as there are the natural frequencies of the different vibration modes of the engine housing and often also the natural frequencies of the elastic elements themselves. A highly simplifying description of this frequency range with a calculation system as in the case of the low frequency solid body vibrations is therefore practically impossible. For this reason it can be established that the vibration isolating connection has to be designed as "soft" as possible with regard to low noise of the engine housing. As this is opposed to the demand for small relative motions at low frequencies an optimum compromise in the selection of spring constants has to be found.

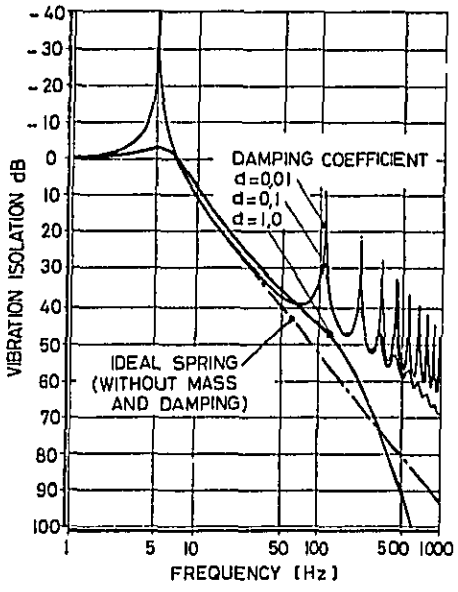

Fig. 5 - Calculated vibration isolation against a rigid mass of real rubber elements with various dampings

Furthermore, it has to be carefully considered that no distinct dip occurs in the vibration isolation of the elastic elements above 0.5 kHz. As it is known, the occurrence of these dips depends on the resonance phenomena in the rubber body itself and is rather controlled by the shape of the rubber body than by the rubber material.

Fig. 5 shows as an example the calculated vibration isolation of a real rubber element with cylindrical rubber body against a rigid mass. It can be seen that above the mass-spring-resonance at 5kHz a close sequence of rubber resonances appears showing more or less deep dips, depending on the magnitude of damping. It has to be pointed out in this connection that such dips, contrary to the mass-spring-resonancies, are independent from the size of the loading mass respectively generally independent from the input impedance of the adjoining component as they represent a pure resonance phenomenon in the rubber body.

EXCITABILITY OF THE ENGINE HOUSING DUE TO BENDING WAVES - Assuming a certain vibration level at the connections of the elastic elements with the central support as well as certain damping properties of the elastic elements the air borne sound emitted by the engine housing mainly depends on the excitability of the housing resulting in bending vibrations. From relevant publications only equations are known (15) which permit the assessment of the average vibration level of thin flexible panels.

The mean square of the vibration velocity (averaged over the panel area) v^2 of a panel, excited at one point by a periodical force, amounts to

$$\bar{v}^2 \approx \frac{\tilde{F}_0^2}{8\omega d S} \cdot \frac{1}{m\sqrt{m \cdot B}} \approx \frac{\tilde{v}_{0.8}^2}{\omega d S}\sqrt{\frac{B}{m}}$$

$\tilde{F}$ ... RMS of exciting force
$\tilde{v}_0^o$ ... RMS of vibration velocity at the point of excitation
ω ... circular frequency
d ... damping constant
S ... panel area
m ... panel surface density
B ... panel stiffness per unit width

The natural bending frequencies of a rectangular panel simply supported on the edges amount to

$$f_{n_x,n_y} = \frac{1}{2\pi}\sqrt{\frac{B}{m}}\left[\left(\frac{n_x \pi}{2a_x}\right)^2 + \left(\frac{n_y \pi}{2a_y}\right)^2\right]$$

n_x, n_y ... number of mode
$2a_x$, $2a_y$ ... panel size

Experience proved however that the average vibration level cannot be described satisfactorily with structures similar to the engine housing in question because of its complicated shape. The only realizable possibility to calculate the excitability of such housings consists, as will be shown later, in the application of a three-dimensional finite element calculation. This calculation cannot be taken as a pre-assessment, but can be carried out only on the basis of a certain design. With the possible assessment method, as mentioned earlier, it can at least be assumed that the fundamental modes of bending vibrations are in the important middle frequency range due to the principal shape of the engine housing (the oil pan is open on top without any transverse bulkheads) and its size.

BASIC INVESTIGATIONS

Before starting with the design of the prototype engines described in the next section a number of questions had to be solved. For this purpose fundamental investigations based on theoretical considerations were carried out.

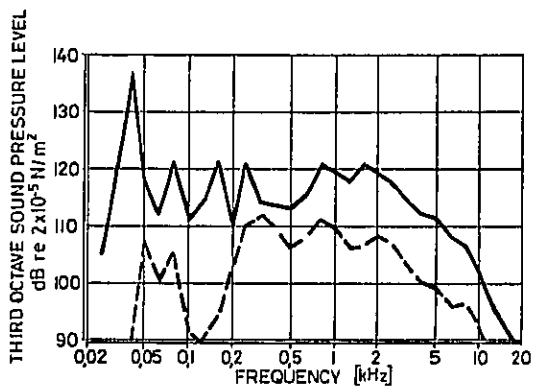

Fig. 6 - Sound pressure level inside and outside the crankcase of a diesel engine

Fig. 6 shows the result of measurements of the average sound pressure level within the crankcase of a diesel engine in comparison with the level outside of the engine taken at a small distance from the engine surface. It can be seen that the level within the crankcase is about 10 dB to 15 dB higher in the middle frequency range than the level outside of the engine. This fact has already been observed on other engines and proves that the assumption described in the previous section is correct, namely that the sound level inside of the engine approximately equals the level between the engine surface and an enclosure wall (16,17). Therefore, it is also more or less certain that the excitation of the engine housing by the air borne sound inside of the housing is of relatively insignificant influence, in accordance with the remarks made in the preceding section.

Further preliminary investigations concerned the design of the elastic supporting elements between central support and engine housing. It was decided to desist from measuring the vibration isolation of frame-like rubber elements, see version 1 in Fig. 1, by means of an electro-dynamic shaker against a rigid mass as in reality the frame-like element is attached to the flange of the engine housing which is open on top and the input impedance of which is supposed to vary widely from place to place. It was therefore resolved to perform the investigations on a test arrangement largely simulating the real conditions. Two test dummies of the engine housing featuring the approximate dimensions of a 4-cylinder inline engine made of aluminium

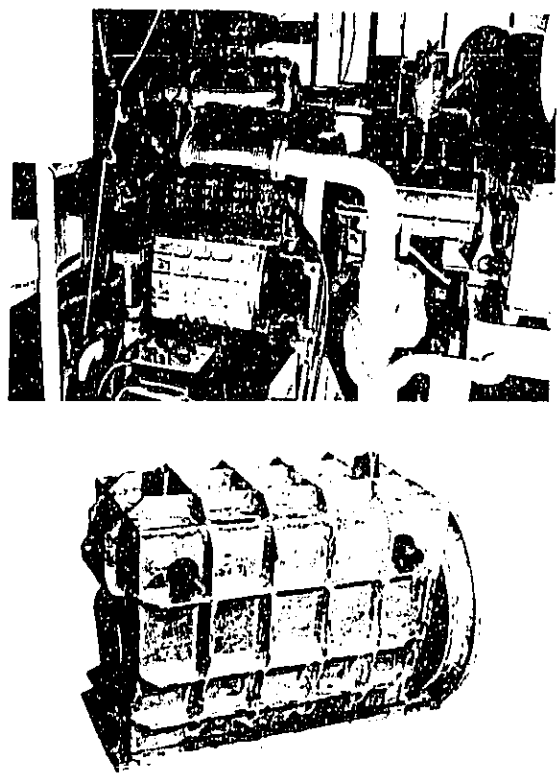

Fig. 7 - Investigation of the vibration excitation of the engine housing, test arrangement and view of a dummy housing

welded structures were manufactured. The two dummies were practically identical, one of them was designed with ribbed external walls. This dummy is shown in the lower part of Fig. 7. The upper part of Fig. 7 shows the detailed test set-up. The housing dummy was attached to the flange of the oil pan of a water cooled 4-cylinder diesel engine by means of the elastic frame-like element to be investigated. The sealing of the lower part of the oil chamber was provided with an oil pan located inside of the dummy. The vibration transmission through different frame-like elements as well as the vibration properties of the engine housing were thoroughly investigated on this test set-up.

Fig. 8 shows as a further example the result from the investigation of the vibration isolation of one design of an elastic frame-like element on the mentioned test set-up. Vibration isolation denotes the difference in vibration velocity level measured in horizontal direction between the two connecting flanges of the vibration isolating frame elements. Due to the nearly symmetrical design of central support and engine housing in relation to the engine center in longitudinal direction only the results of the measuring points demonstrated in Fig. 9 are given. In the lower frequency range at about 0.2 kHz a dip in the vibration isolation of approximately

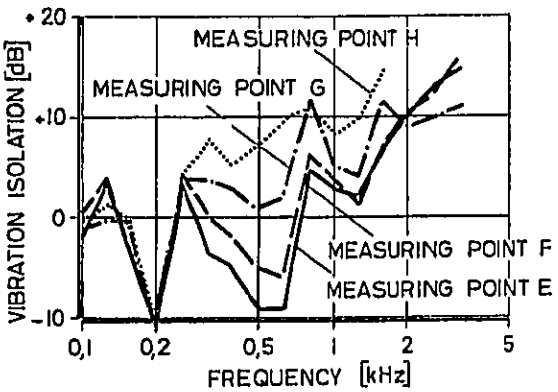

Fig. 8 - Vibration isolation of a frame-like elastic element, connecting inner engine structure and engine housing

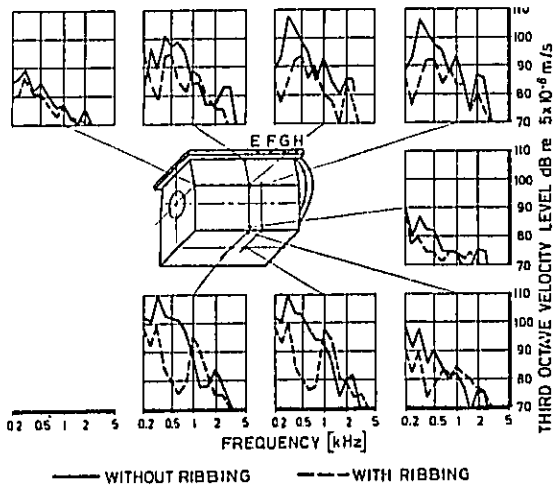

Fig. 9 - Structure vibration on the dummies of engine housing

10 dB can be observed at all measuring points. This dip results from the resonance in horizontal direction of the oscillating system consisting of engine parts and frame element. It is still sufficiently below the middle frequency range decisive for the total engine noise in dB(A). Above 0.31 kHz the vibration isolation varies widely. Due to the higher flexibility of the engine housing in the center compared to the edges the vibration isolation decreases at 0.6 kHz from the outside to the inside by up to 20 dB. This tendency can also be noticed to a lesser extent in the upper frequency range. Above 0.8 kHz the vibration isolation is satisfactory for all measuring points. The frame element which was used for these investigations features a rubber thickness of 12 mm. With a 4 mm thick rubber element satisfying vibration isolation could only be obtained above approximately 4 kHz. In the interest of sufficiently low sound levels in the housing this stiffer frame element was then not used any more. An increase of the elasticity of the frame element would certainly have improved the vibration isolation. But at the same time also a shifting of the fundamental resonance frequency from about 0.2 kHz towards lower frequencies would have occurred, which in connection with the excitations due to the unbalanced second inertia forces at the determined engine speed would have caused inadmissibly high relative displacements between the central support and the engine housing. This could not be accepted with regard to the elastic elements applied to the power transmission from the flywheel to the gear shaft as well as at the penetration of the crankshaft at the rear wall of the engine housing.

For the present analogous tests have not been carried out for version 2 in Fig. 2. It was first attempted to design the elastic connections in such a way that practically no resonances occur in the rubber body at the desired spring constant and loading capacity. By means of a shaker a test series during which a large number of different element designs were examined demonstrated that the best solution consisted in elements presenting circular symmetry. The rubber body of these elements has the shape of a hollow cylinder located between two steel tubes. The results obtained during these tests are not presented in this paper.

Fig. 9 shows the spectra of structural vibration measured on eight characteristic points on the engine housing of the mentioned dummies with and without ribbing. When selecting the demonstrated measuring points care was taken that the vibration velocity was measured at the relatively stiff areas such as circumference of the side wall and the floor as well as in central points of these two walls. Because of the nearly symmetrical design of the engine housing only one side wall was investigated. With the version without ribs the levels of the measuring points at the edges of the side walls (diagrams top left, middle and bottom right) are very low, the spectra clearly show a decrease of the vibration level towards higher frequencies. The level measured at the point in the middle of the upper flange of the side wall is considerably higher because of the low bending stiffness of the open housing at this point (upper row, second diagram from the left). The four central measuring points of the two walls show even higher levels, the highest levels at these measuring points were observed in the range below 0.5 kHz according to the fundamental modes of the bending vibrations of the outer walls.

The levels measured on the ribbed dummy are shown in the diagrams with a dashed line. The increased stiffness causes a reduction of the vibration level especially in the central points of the walls in the just mentioned frequency range of the natural bending frequencies of the walls below 0.5kHz. In the middle frequency range the ribbing has again a positive effect. However, due to the fundamental natural bending frequencies of the ribbed bottom of the engine housing a peak occurs at about 1 kHz exceeding the level of the ribbed wall. A similar effect can be observed in the middle of the upper flange. With the ribbing a certain improvement could also be achieved in the lower frequency range at the edges of the two walls. Here again an insignificant deterioration was registered in the upper frequency range.

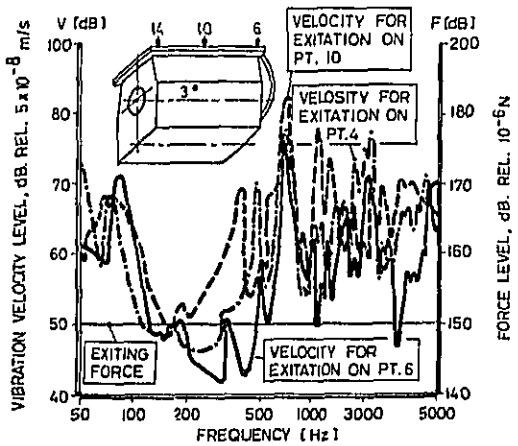

VIBRATION ON PT. 3 FOR DIFFERENT EXITATION LOCATIONS (PT.6,10,14)

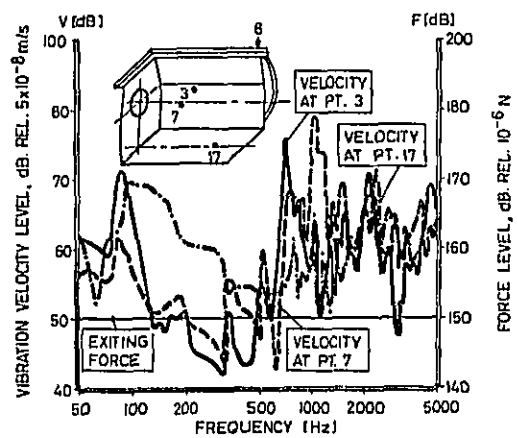

VIBRATION ON DIFFERENT LOCATIONS (PT.3,7,17) FOR EXITATION ON POINT 6

Fig. 10 - Vibration excitability of the engine housing

The test arrangement shown in Fig. 7 made it basically only possible to investigate the vibration behavior of the entire system frame element - engine housing. The excitability of the engine housing was therefore separately examined with an electro-dynamic shaker. The housing was in this case vibration excited at constant force amplitude over the frequency, and the resulting vibration velocity was thus measured at different points of the ribbed engine housing. The upper diagram in Fig. 10 shows as an example the measured vibration velocity levels at one point on the side wall (measuring point 3) with an identical excitation at three different points of the upper flange (excitation points 6, 10 and 14). There are large differences between the curves over the whole frequency range. It is clear that the excitability is highest in point 10, that is in the middle of the flange. Around the front side the levels are already distinctly lower with the same exciting force, the excitability of the engine housing is lowest in the relatively stiff area of the flywheel housing (excitation point 6). The lower diagram shows as an example the vibration velocity levels of three different measuring points of the housing at vibration excitation at one point (point 6). The levels of the demonstrated measuring points located in the flexible area of the wall are very different. The development of the curves is relatively non-uniform, but it can be stated that at each point, although at different frequencies, distinct resonance peaks occur.

To achieve an optimized engine housing by modifying the design a great number of experimental design approaches as well as a time and cost consuming test series would have been necessary. As the main dimensions of the engine housing for the prototype engine described in the next section were already determined at this point of time the finite element calculation could be used for this optimization.

An example is demonstrated in Fig. 11. The finite element calculation method was first used for the determination of possible vibration modes. The upper part of this figure illustrates the unmodified structure as well as the division into finite elements. In the table the vibration modes determined by means of the finite element calculation are shown together with the respective frequencies, once with and once without ribbing. This calculation has mainly proved that the vibration modes are very close together for both designs of engine housings and that the frequencies of the vibration modes with ribbing compared to those without ribbing only differ by the factor 1.1 to 1.3 regarding modes with the same mode number. It can be seen that the frequency range of the modes of natural bending vibrations of such a housing, with given dimensions and wall thicknesses can hardly be shifted out of the most important frequency range of 0.5 kHz to 2.5 kHz due to stiffening measures, such as for instance ribs. This, however, does not exclude that the amplitudes of the vibrations can be reduced by means of this ribbing, as this seems to be the case, considering the results in Fig. 9. In order to be able to investigate this fact by means of a finite element calculation the whole system central support - elastic elements - engine housing must be taken into consideration and real damping must be introduced. Calculations of this kind are presently in the process of preparation at AVL. The lower part of this figure shows as an example, for clarity's sake with a reduced number of points, the mode shape of the ribbed engine housing for the mode number 12 with a resonance frequency of 1480 Hz.

APPLICATION OF THE DESIGN PRINCIPLE TO A HIGH-SPEED LIGHT-WEIGHT DIESEL ENGINE

Fig. 12 shows a prototype engine featuring this new design principle. It is a 4-cylinder inline engine 85 ⌀ x 94 which is designed for low-noise and where a number of other important aspects are taken into consideration. The engine is designed as a D.I. engine equipped with unit injectors instead of the standard injection pump, and central support and cylinder head are designed as one part. However, these design details which are not directly in connection with the noise reduction are not subject of this publication.

m ....MODE NUMBER

f_R, f ...NATURAL FREQUENCY OF VIBRATION MODES WITH AND WITHOUT RIBBING OF THE ENGINE HOUSING

$r = f_R / f$

m	f_R	f	r
1	503	425	1.184
2	550	522	1.054
3	809	563	1.437
4	1031	760	1.356
5	1036	823	1.259
6	1105	931	1.187
7	1125	1030	1.092
8	1141	1044	1.093
9	1190	1057	1.126
10	1210	1068	1.133
11	1378	1190	1.158
12	1480	1222	1.211
13	1515	1237	1.225
14	1597	1292	1.236
15	1618	1387	1.166
16	1736	1446	1.200
17	1854	1499	1.237
18	1889	1519	1.244
19	1906	1543	1.235
20	2038	1576	1.293

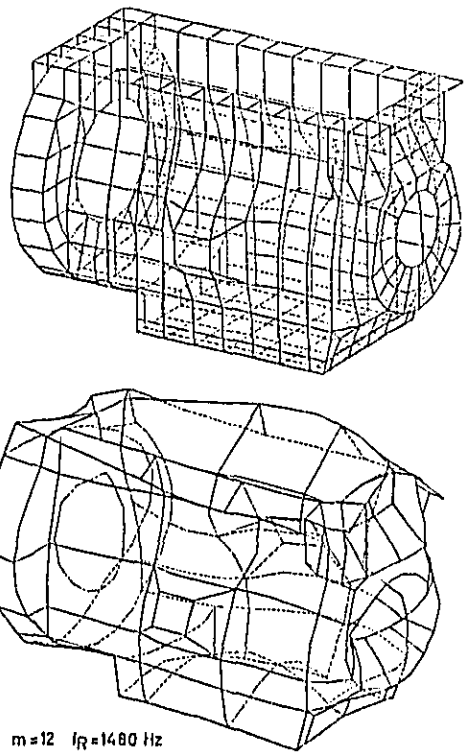

Fig. 11 - Vibration modes of an engine housing, calculated by the finite element method

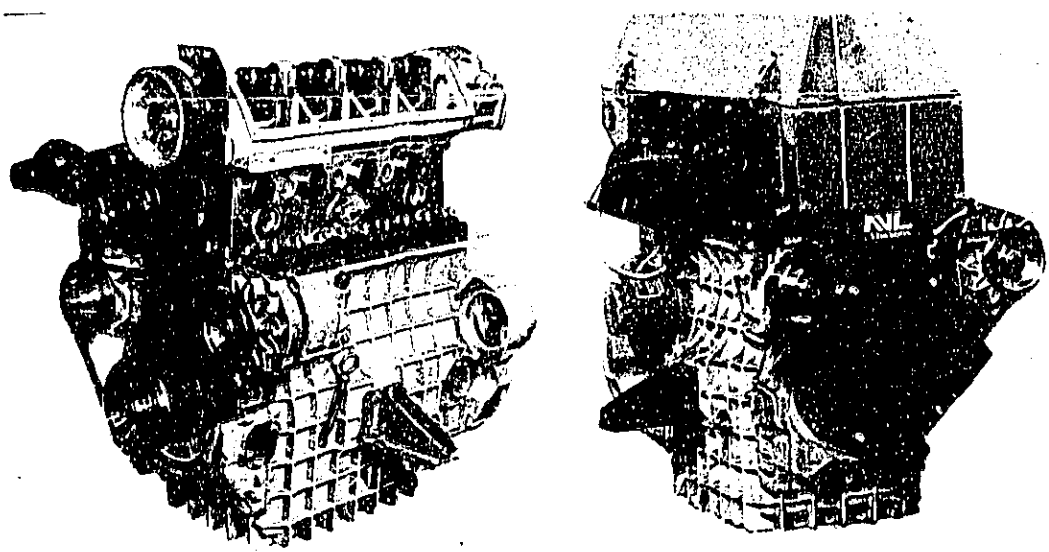

Fig. 12 - Prototype of the low-noise diesel engine

The illustration on the left shows the engine with removed upper enclosure during assembly. The engine housing made of cast aluminium with the engine brackets, the frame-like elastic element between the central support and the engine housing as well as the toothed belt driven overhead camshaft which also drives the unit injectors of the injection system can be seen. The illustration on the right shows the engine fully assembled. For maintenance large covers with quick fasteners are provided. The exhaust as well as intake manifold are located outside of the enclosure. To provide a low manifold noise they are connected in a vibration isolating manner to the inner engine structure. The intake duct for the cooling air is designed like an absorption muffler and is combined with the sound reducing shell of the crankshaft pulley. The cooling fan for ventilating the enclosure is powered by the toothed belt. The cooling air outlet duct also designed as an absorption muffler is located in the area of the exhaust manifold.

TEST RESULTS

The experimental investigations carried out so far were performed on several research engines, also including the prototype engine shown in Fig. 12. The engine test program comprises among other items the complete measurements of the air borne sound, structural vibrations and relative displacements between the central support and the engine enclosure. In these investigations a number of different vibration isolating frame elements as well as different engine casing and enclosure designs are comprehended. The following is a selection of the numerous results gained in the course of these examinations.

Fig. 13 demonstrates the average vibration velocity, obtained from a large number of measuring points, on the central support as well as on two versions of the external casing, once designed with ribbing and once without ribbing. It can be seen that

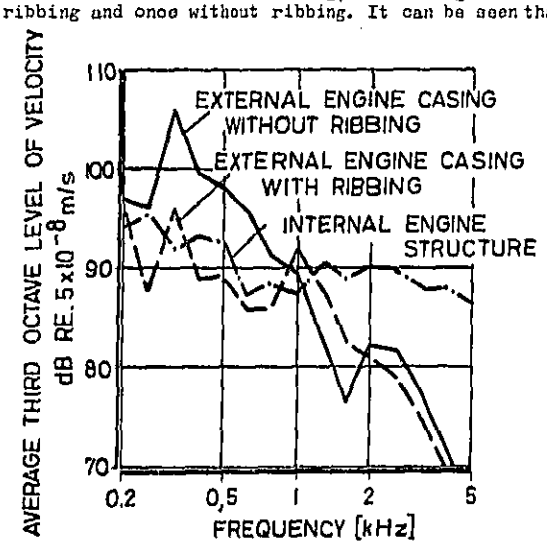

Fig. 13 - Structure vibration of the low-noise prototype engine

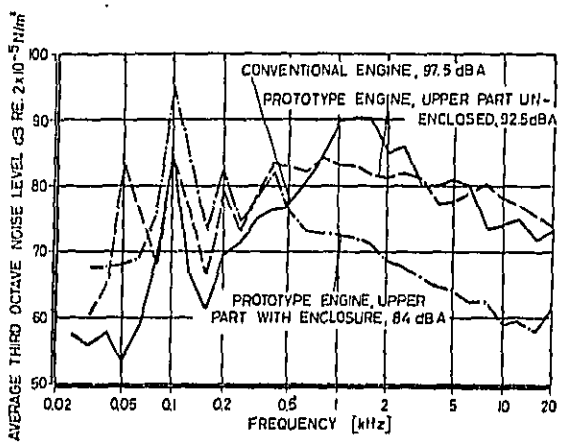

Fig. 14 - Noise of the prototype engine

the sound level of the two different designs of the engine housing is considerably lower in the acoustically important frequency range compared to the level of the inner engine structure. In the low frequency range higher levels, compared to the inner engine structure, occur with the engine housing without ribbing due to the natural bending vibrations. The application of the ribbing resulted in a distinct reduction of the vibration level. The resonance frequencies of the panel modes were shifted upwards, thus causing a certain increase of the vibration level in the middle frequency range.

Fig. 14 gives the average air borne sound spectra, measured at four different points at 1 m distance from the engine surface in the anechoic chamber, in comparison with a conventionally designed engine. The total noise of the prototype engine amounted to 84 dB(A), with the upper part of the enclosure removed 92.5 dB(A). The noise of the conventionally designed engine amounted to 97.5 dB(A) and is therefore 13.5 dB(A) (respectively 5 dB(A) without upper enclosure) higher than the noise emitted from the new engine. An estimation of the noise to be expected with a conventionally designed engine of the same output and speed with the formula of CIMAC resulted in about 100 dB(A) under free field conditions at 1 m distance.

Under consideration of an increase of the sound level by 2 dB(A), if the measurements are carried out in the free field instead of in the anechoic chamber, the noise of the new prototype engine is about 14 dB(A) below the average of conventionally designed engines. The air borne sound spectra show that the sound level of the prototype engine in operating condition is above 0.5 kHz, approximately 15 dB lower than with the conventionally designed engine. In the frequency range below 0.5 kHz the sound level of the new engine is higher. High peaks can be observed at the frequency of the unbalanced second order inertia forces of a 4-cylinder inline engine designed without a balancing system. The comparison with the spectra of the engine the upper part of which is unenclosed shows that these high levels which hardly influence the overall noise are mainly radiated from the upper enclosure made of thin sheet steel. These high amplitudes which pos-

sibly endanger the durability of the enclosure can be eliminated by stiffening or measures on the suspension on the engine casing.

It may be pointed out in this connection that another positive effect of the new engine design consists in the high reduction of the air borne sound level in the upper frequency range where the diesel engine knocking is particularly irritant.

In the spectrum of the engine without upper enclosure the peak at the frequency of the second inertia force (approximately 0.1 kHz) is much lower. In the frequency range between 0.8 and 6.3 kHz the sound level of the prototype engine without upper enclosure is far below the level of the comparable engine, whereas in the highest frequency range it is higher than with the comparable engine. Experience shows that with conventionally designed engines of the size in question the air borne sound levels in the frequency range of 1.0 to 2.5 kHz are mainly controlled by the noise emitted from the crankcase side walls and the rigidly attached oil pan. The low sound levels of the prototype engine without upper enclosure can therefore be particularly related to the vibration isolation of the engine housing. The engine without upper enclosure is, as already mentioned, about 5 dB(A) quieter than the conventionally designed engine. Due to the high sound levels in the upper frequency range the subjective impression of this difference is rather limited, the engine still sounds like a diesel engine.

CONSEQUENCES FOR THE APPLICATION IN VEHICLES - As mentioned at the beginning of this paper, it was attempted during the development of the new engine design to achieve a noise reduction of 10 dB(A) to 15 dB(A)as can be realized by an additional enclosure for the power unit as well as to reduce the weight and ensure good maintenance conditions and operating reliability. Based on the experience with the development of the new engine the set target can be regarded as realizable. The magnitude of noise reduction which can be achieved at present already meets the requirements. The weight of the complete prototype engine in operating condition amounts to 155 kp. The weight per horsepower of the prototype engine amounts to 2.6 kp/HP so that the request for low weight is likely to be met as well. In conclusion the consequences, resulting from the application of such engines, for future vehicle designs and the advantages of the new engine design are discussed.

In principle an engine designed according to the above concept can rigidly be connected with an unenclosed transmission and can be installed in existing vehicles. In this case however, as has been mentioned already, an elastic coupling has to be located between the flywheel and the gear shaft. Relevant design concepts are available, they necessitate however a certain amount of space for installation and additional costs.

One solution that eliminates this disadvantage consists in the relocation of the transmission gear away from the engine to the rear axle gear, a design that has already been realized for other reasons with some modern passenger cars.

Another solution for the application of the new engine featuring a number of advantages is presented in Fig. 15 on the example of a passenger car. The engine is installed in the usual manner. The upper engine enclosure is omitted, and the existing parts of the chassis, engine hood, dashboard and gear box

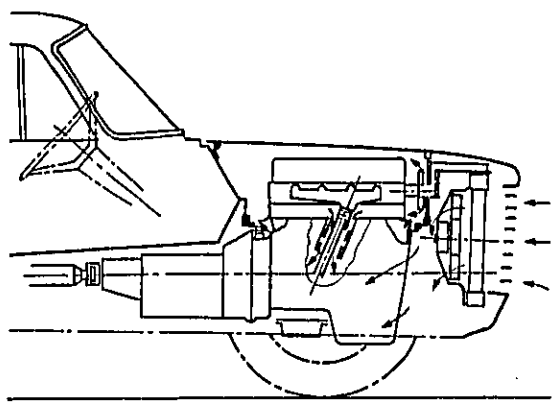

Fig. 15 - Design concept of a quiet passenger car based on the new engine type

are connected with a horizontal partition floor, approximately at the height of the elastic frame element of the engine, and an intermediate wall on the front, thus forming a sound reducing enclosure, in this case only covering the upper part of the engine. This solution offers several advantages: weight saving, enclosed engine and transmission fully exposed to the rain and optimum accessibility of the engine by simply opening the engine hood. The engine cooling system as well as the entire enclosure ventilating system can be arranged as with the additional complete enclosures for power units of conventional design as already mentioned in the beginning of the paper. This concept is demonstrated on the example of a passenger car, but can naturally be applied to other types of vehicles, particularly light-duty trucks.

Finally, another applicability of the new concept, which has already been studied, may be mentioned, i.e. for farm tractors. A conventionally designed farm tractor is characterized by the so-called block-design featuring an engine rigidly connected with the entire transmission - rear axle gear housing. These parts are therefore vibration excited from the engine and cause a high noise level. Merely encapsulating the engine is therefore of limited success in this case. When applying the new engine design to the farm tractor (Fig. 16) the block-de-

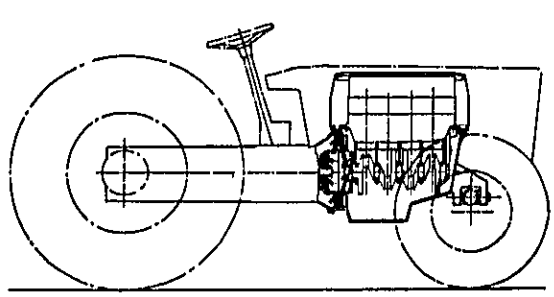

Fig. 16 - Design concept of a quiet farm tractor based on the new engine type

sign can in principle be adhered to. The engine housing must be designed as a pan to be able to carry load as well as the chassis forces. For the power transmission from the flywheel respectively clutch to the transmission gear shaft a short universal shaft can be installed within the housing, as in general there is space enough in axial direction, in contrast to road vehicles. The upper engine enclosure can, modified accordingly, take the function of the engine encasing of the conventional farm tractor which is necessary in any case for weather protection and styling requirements.

REFERENCES

1.W.H.Close, "DOT Quiet Truck Program." INTER-NOISE 74, pp. 473-478.

2.R.L.Staadt, "Truck Noise Control." SAE-SP-386, 1974.

3.G.E.Thien and H.A.Fachbach, "Noise of Diesel and Otto Engines - Generation, Reduction and Consequences to Vehicles and Off Road Machinery." Seminarium "Yttre Buller Fran Vägfordon"("Vehicle Noise"), The Royal Inst. of Technology, Stockholm, Feb. 1975.

4.G.E.Thien and B.Nowotny, "Untersuchungen über den Einfluß von Körperschallvorgängen auf das Geräusch von Dieselmotoren." ("Investigations on the Influence of Structure Borne Sound on Noise of Diesel Engines"), MTZ, 32. Jg., No. 6 (1971), pp. 186-193.

5.G.E.Thien and H.A.Fachbach, "Design Concepts of Diesel Engines with Low Noise Emission." SAE-Paper 750838, Milwaukee, Sept. 1975.

6.F.W.Leipold and H.O.Hardenberg, "Noise, Emissions and Performance of the Diesel Engine - A Comparison between DI and IDI Combustion Systems." SAE-Paper 750796, Milwaukee, Sept. 1975.

7.B.J.Challen, "The Effect of Combustion System on Engine Noise." SAE-Paper 750798, Milwaukee, Sept. 1975.

8.D.Anderton and V.K.Duggal, "Effect of Turbocharging on Diesel Engine Noise, Emissions and Performance." SAE-Paper 750797, Milwaukee, Sept. 1975.

9.R.Munro and A.Parker, "Transverse Movement Analysis and its Influence on Diesel Piston Design." SAE-Paper 750800, Milwaukee, Sept. 1975.

10.G.E.Thien and H.A.Fachbach, "Geräuschverminderung an Dieselmotoren durch Änderung äußerer Bauteile und schalldämmendes Verkleiden." ("Noise Reduction of Diesel Engines by Modification of External Engine Parts and Sound Reducing Enclosures"), MTZ, 32. Jg., No. 5 (1971), pp. 145-152.

11.G.E.Thien and H.A.Fachbach, "Geräuscharme Dieselmotoren in neuartiger Bauweise." ("A New Design Concept of Low Noise Diesel Engines"), MTZ, 35. Jg., No. 8 (1974).

12.G.E.Thien and H.A.Fachbach, "New Design Concepts of High Speed Diesel Engines with Low Noise Emission." INTER-NOISE 75, Sendai, August 1975.

13.H.A.Fachbach and G.E.Thien, "Musterausführungen geräuscharmer Dieselmotoren." ("Prototype Models of Quiet Diesel Engines"), MTZ, 36. Jg., No. 10 (1975), pp. 261-266.

14.G.E.Thien and H.A.Fachbach, "Quiet Automobiles - A Realistic Objective." FISITA 1976, Tokyo.

15.W.Schirmer, "Lärmbekämpfung." ("Noise Control"), Tribüne, Berlin 1971.

16.G.E.Thien, "Elemente zur Abminderung der Schallemission von Verbrennungsmotoren der heute üblichen Bauart." ("Elements Reducing the Sound Emission of I.C. Engines of Conventional Design"), Dissertation Techn. Univ. Graz, Sept. 1977.

17.H.A.Fachbach, "Entwicklung von neuartigen, geräuscharmen Dieselmotoren." ("Development of Newly Designed Diesel Engines with Low Noise"), Dissertation Techn. Univ. Graz, Sept. 1977.

790442

A SURVEY OF PASSENGER CAR NOISE LEVELS

D. MORRISON/B.J. CHALLEN

RICARDO CONSULTING ENGINEERS

ABSTRACT

Results from noise tests on 18 passenger cars are reported. The sample contains both diesel and gasoline engined vehicles and two (a SAAB 99 and Peugeot 504 GLD) are examined in detail over their normal operating range. The effects of vehicle operations are examined and differences between vehicles compared.

For equivalent engines there is shown to be little difference between vehicle noise for diesel and gasoline engines for current legislative test procedures, although idle and low speed noise levels are increased significantly in the case of the diesel engine.

At vehicle speeds above 80km/h in top gear, rolling noise dominates the total vehicle radiated noise.

WITH THE INCREASING TREND towards smaller power units running at higher speeds, together with the advent of diesel engines in passenger cars, concern in the U.S.A. has increased recently over the effects of this trend on vehicle noise levels. The results presented here are from a survey which was mainly concerned with European type passenger cars in which the high speed engine, both diesel and gasoline, is well established. The effects of operational characteristics, particularly as these are reflected in legislative test procedures, are considered.

SELECTION OF VEHICLES

The majority of the tests reported here were funded by a DoT (TSC) contract where two cars were selected for detailed testing. (1)*. These were a SAAB 99GL Injection powered by a 2 litre gasoline engine and a Peugeot 504 GLD powered by a 2.3 litre Comet V diesel engine. Both cars were in 1976 California build, the SAAB engine being fitted with manifold air oxidation and exhaust gas recirculation. An outline specification of both cars is given in Table 1. These cars were chosen as being a common European size and typical of their class. The main objective of this selection was a detailed comparison between diesel and gasoline powered passenger cars. (2)

In addition to these two prime cars, ten additional European passenger cars were selected for abridged testing. These cars were selected on the basis of their popularity in Europe, together with their power and weight, such that a representative cross section of the type of cars used in Europe was obtained.

Brief results from Ricardo research tests on other cars, in addition to those above, have also been included. A list and brief specification of all the cars is given in Table 2.

TEST PROCEDURES

The vehicle noise measurements were made over a hard road surface with the vehicles in their normal road condition. The use of such a hard, acoustically reflecting test area is common to all vehicle noise test standards throughout the world. The test series for the detailed survey of two cars was designed to extract noise levels over the whole operating range of engine load and speed up to the maximum road speed that the approach to the central test zone would allow.

The drive-by tests were made using a comprehensively instrumented test area enabling engine speed, vehicle position and noise levels (at four microphone positions) to be simultaneously recorded on a 7 channel FM tape recorder. The microphone height was 1.2m for the drive-by tests and also for the stationary tests later referred to. A schematic layout of the test site and instrumentation is shown in Fig. 1. The site was calibrated using a sound source, traversed along the zone centre line. Sound pressure level fall-off rates were close to the expected -6dBA per doubling of distance, with an overall mean value of -5.9dBA per doubling. The engine speed signal (obtained from a transducer adjacent to the flywheel ring gear) was relayed to the recording station by means of an FM radio transmitter and receiver. The engine speed was simultaneously displayed on an analogue tachometer, as part of the driver's aid instrumentation mounted on the dashboard. The vehicle speed signal was obtained from a magnetic transducer/slotted brake disc arrangement and fed to an "acceleration meter" system devised by Ricardo, and forming an additional part of the driver's aid instrumentation. Pre-set acceleration or deceleration rates could be selected by a switch box in the vehicle and maintained accurately by driving to keep the needle

*Numbers in parentheses designate References at end of paper.

SAE/P-79/80/$02.50
Copyright © 1979 Society of Automotive Engineers, Inc.

of the centre zero meter at zero deflexion. Vehicle position on the 20m track was achieved by seven phototransistor sensors alongside the track and triggered by one of a pair of sideways-facing spotlights attached to the front of the car.

The data from the tape recorder was processed through appropriate instrumentation and onto a high speed X-Y recorder. Using a synchronising pulse (generated by a spotlight/sensor system ahead of the test zone) multi-pass analysis was used to replay the six data channels individually onto the recorder. The A-weighted noise level signal was passed through a logarithmic amplifier to the recorder. This amplifier had a selectable time constant so that if replay at 1/2 or 1/4 of recorded speed was used, a time constant equivalent to the standard IEC "fast" response (125ms) could be selected. A typical X-Y recorder output for one pass-by is shown in Fig. 2. From this the noise level at any position can be determined. (All sound pressure levels stated in this paper are to a reference pressure of 20μPa).

Not all the vehicles referred to in this paper were tested with the full instrumentation referred to above. In some cases only sound level meter readings were taken and in other cases a compromise between the full instrumentation and basic instrumentation employed (e.g. full noise recording but without the vehicle instrumentation). The two vehicles which were tested in fully instrumented form were the SAAB 99 and the Peugeot 504 GLD.

The drive-by tests carried out were planned to cover a wide range of operating conditions and in addition, certain standard regulatory test procedures were followed (e.g. ISO R362, SAE J986a). In the case of the SAAB and Peugeot mentioned above, detailed mapping drive-by tests were carried out in all gears, at various zone entry speeds. Noise source tests were also made to identify the relative contributions to the overall noise level of the major elements.

An adaption of ISO R362, used by Ricardo for research purposes, is designated a "max. ISO" test and is essentially ISO R362 except that the vehicle entry speed is adjusted so that rated engine speed (i.e. the speed at which maximum power is developed, or the governed speed) is achieved at the end of the 20m zone following a "wide-open-throttle" acceleration. Normally second gear is used for vehicles with four ratio manual transmissions and the lowest ratio for automatic transmissions (the latter chosen for reasons of vehicle speed limitations). Entry and exit speeds are therefore typically some 20-40% higher than for ISO R362. This test method assesses maximum engine noise (i.e. maximum power and rated speed) and is independent of vehicle gearing. As such, it is similar to SAE J366b, but has a defined point where rated engine speed is reached.

INFLUENCE OF VEHICLE OPERATING CONDITIONS

Specification of vehicle noise radiation is complicated by the different end uses to which the information will be put. The choice essentially lies between the use of vehicle speed or engine speed as the main parameter. For any given vehicle, the actual ratios are fixed, but on various models of similar specification different gear ratios may well be used. Fig. 3 shows the difference in appearance of noise radiation from one vehicle plotted in the two forms. The upper part of the figure shows overall noise levels plotted against road speed, which shows the expected trend of noise level increasing as lower gear ratios are used for a given road speed. For comparison, the coast-by noise levels for the vehicle with the engine switched off are included in this figure. The top gear noise levels are asymptotic to this line at 80km/h. In contrast, the lower part of the figure, where the noise levels are plotted against engine speed, shows an almost complete collapse of the data onto a single line. This is clearly the case for 1st and 2nd gear, 3rd gear lies above the line by some 1dBA and top gear by as much as 3dBA. This latter deviation is to be expected due to the asymptotic approach of the overall vehicle noise level to the coast-by level seen above.

This type of behaviour is common to most vehicles. When separating individual noise sources it can be most useful. However, for the manufacturer ensuring that his vehicle complies with noise legislation, this comparison illustrates the influence that gear ratios will have in legislative procedures for "standard" vehicle noise levels. This sensitivity will be dealt with in more detail later.

The data in Figure 3 refers to full power operation, (i.e. maximum vehicle acceleration). Another important parameter is sometimes held to be the vehicle acceleration rate (i.e. engine load) (3). For the two vehicles examined in detail in the present survey this was not found to be the case, apart from the cruise condition. Some of the results produced by the survey are plotted in Fig. 4. The upper section gives results for the SAAB 99 and the lower part the results for the Peugeot 504 GLD. The scatter plot is composed of the results of all the acceleration rates that were tested. In both cases the results refer to noise levels to the left hand side at 7.5m with the vehicle in second gear. The SAAB results show the variation in noise levels for acceleration rates from 0.05g to the maximum acceleration rate possible in that gear. In general, the results fall within a band which is some ± 2dBA wide. An exception to this is the steady state (cruise) condition which is substantially lower. This variation of ± 2dBA should be considered in the context of vehicle-to-vehicle variation which in many cases approaches this magnitude. The noise level produced by the vehicle at a given speed is thus practically constant, irrespective of acceleration rate (i.e. engine load). The non-linear rate of increase of the curve is due, on this side of the vehicle, to the presence of exhaust resonances. For the diesel engined vehicle in the lower part of the figure, the results (both steady state and acceleration) fall within a band which is again some ± 2dBA wide. This might be expected due to the known characteristic of the diesel engine which produces virtually constant noise levels for a given speed irrespective of

load (4,5). Due to the unthrottled operation of the diesel engine, the noise from the intake and exhaust will also not vary as greatly with load as it does for the throttled gasoline engine.

Summarising the noise level measurements for these two vehicles in 2nd gear, Fig. 5 shows the results for both left and right-hand sides, showing the extremes of steady state and maximum acceleration, plotted against vehicle speed. Both vehicles have maximum potential noise levels approaching 85dBA but this is attained at different speeds, reflecting the different engine speed ranges and gearing. The virtually constant noise level produced by the diesel engined car over the acceleration rates is clearly contrasted against the variation in noise produced by the gasoline engined car. For the maximum acceleration case, however, the difference in noise levels for any given speed reaches a maximum value of 5dBA and is generally some 2dBA. There is a difference in the cruise-by noise levels of some 7dBA at low speeds, however, due to the decrease in noise from the gasoline engine when running at low loads.

The variation of engine noise levels with speed and load is shown in Fig. 6, where the noise levels from the SAAB engine are compared with those of a typical high speed IDI diesel engine. These results were obtained in a standard Ricardo anechoic engine test cell, with the exhaust and intake silenced and no fan fitted to the engine. Measurements are made 1m from the engine surface in high accuracy free-field conditions down to 200Hz. It is clear that the variation in noise level of a typical IDI diesel engine with load (generally of the order 2dBA) is much less in the lower speed range than that of a gasoline engine (generally up to 10dBA), and that both types of engine have similar maximum noise levels.

MEASURED LEVELS

REGULATORY TESTS-The results of ISO and "max. ISO" tests on 18 cars are shown in Fig. 7. The results are shown grouped into those of six diesel cars and twelve gasoline cars. The results for a given car are the average of left and right hand sides over at least two repeatable tests. (A test is defined as repeatable if the results for a given side agree to within 1dBA). Table 3 shows the average drive-by, interior noise and exterior idle noise results for various car groups. For the ISO test for all cars the overall average was 78.4dBA with a standard deviation of $\pm$ 2.5dBA and with extreme limits of + 3.2dBA, -4.4dBA. For the diesel car group alone the corresponding figures were 79.9dBA, $\pm$ 1.4dBA, +1.9dBA, -1.4dBA. For the gasoline car group alone, the figures were 77.5dBA, $\pm$ 2.7dBA, +4.1dBA, - 3.5dBA. For this type of maximum load (maximum acceleration) test the diesel engine powered passenger car noise levels are on average some 2½dBA higher than gasoline cars. Comparing the manual transmission diesel and gasoline car groups, however, this difference reduces to only ½dBA. At the high engine speeds produced during the "max. ISO" test the difference between the two group averages is negligible. This narrowing of the difference is largely due to the higher engine rated speeds of gasoline engines than diesel engines, counteracting the inherently noisier diesel operation.

A comparison of the three test procedures, ISO R362, "max. ISO" and SAE J986a is given in Fig. 8. Generally, the "max. ISO" test produces the highest levels, but this is affected in certain cases by gear ratio. For example, the SAE test for the SAAB requires 1st gear to be used (and an entry speed of 50km/h, independent of gearing), resulting in rated engine speed being reached before the end of the zone, whereas, in the "max. ISO" test, the rated speed is reached at the zone exit. ISO R362, because of the gearing factor, generally produces lower levels for those cars with high second gear ratios (in particular for automatic transmission ratios). In isolated cases, however, where the high gearing is accompanied by a very high power/weight ratio, the gearing effect can be outweighed by the acceleration performance and then high ISO R362 levels are produced.

The "max. ISO" test tends to produce results with less scatter but on the other hand does involve an extreme driving pattern, especially for vehicles with three ratio automatic transmissions. The use of such tests is mainly for research purposes in comparing engine noise at an operating condition which produces the highest noise level (i.e. full load, rated speed, transient) and avoids gear ratio effects.

No reliable correlation between test procedures exists because of the heavy dependence on gearing of both ISO R362 and SAE J986a, and also because of the fixed entry speed, independent of gearing or vehicle characteristics for the latter.

STEADY STATE TESTS-The effect of both engine type and rolling noise is clearly apparent from the steady state drive-by results shown in Fig. 9. Two tests are shown: 50km/h in 2nd gear and 50km/h in 4th gear. The three diesel passenger cars are generally 2dBA noisier than the average gasoline car (in one case, 7dBA). This light load operating condition is unfavourable for the diesel engine from a noise comparison point of view due to the decrease of load of gasoline engine noise (light duty diesel engine noise being essentially independent of load). In the case of heavier cars (~1800kg), the steady state noise is often dominated by rolling noise. This is shown clearly in Fig. 9 for the top gear steady state condition for the Jaguar XJ6.

Steady state noise distribution around the moving vehicle may also be shown in the form of a polar plot. An analysis of the drive-by trace, knowing the position of the car on the track relative to each of the four microphones, enables a "dynamic" polar plot of noise distribution to be obtained from the X-Y recorder trace. Examples of such plots, comparing three gasoline cars with three diesel cars, are shown in Fig. 10 for 50km/h, 2nd gear, steady state conditions, where the effect of the diesel engine noise at light load is evident. Polar plots can also be useful in identifying source directionality, for example exhaust noise or fan noise, and have been used for

such purposes when comparing the SAAB and Peugeot sources. The technique is relatively straightforward, complicated only by correction factors for distance and the time delay between position pulse generation and the arrival of radiated sound at the microphone under consideration. Considerable lobing has been found with dominant exhaust systems (2) making this technique a useful adjunct to other analysis techniques.

INTERIOR NOISE-Measured interior noise levels for conditions of 50km/h cruise, 80km/h cruise and idle (car stationary) are summarised in Table 3 for each car group and shown for each individual car in Fig. 11. Considering all 18 cars, the average interior noise level (measured at the driver's ear) was 63.9dBA at 50km/h, 69.4dBA at 80km/h and 48.7dBA at idle. Comparing the diesel and gasoline car groups at the two cruise speeds the average diesel car interior noise is only some 1dBA greater than that for the gasoline car average. At idle, however, this difference increases to more than 3dBA.

EXTERIOR NOISE-Exterior idle noise measurements were made at 3m from the front of the car and at 1.2m microphone height. The results shown in Table 3 and Fig. 12 clearly indicate the high noise levels associated with diesel engine idling. The diesel car average exceeds the gasoline car average by some 8dBA. The problem of diesel idle noise is one which is currently continuing to be examined closely, both from the aspects of measured levels and also subjective tests. It is well recognised that impulsive noise characteristics, as evident in diesel idling, may not necessarily be adequately assessed by an A-weighted sound pressure level.

INFLUENCE OF VEHICLE PARAMETERS

GEARING-To a first order approximation, drive-by noise level at typical regulatory speeds (around 50km/h) is a direct function of engine speed. Assuming a typical rate of increase of noise level with engine speed of 45dBA/decade (for a light duty engine) then a 10% reduction in engine speed as a result of resorting to a corresponding higher gear ratio would suggest a reduction in drive-by noise level by approximately 1½-2dBA. In reality, greater or lesser reductions than this may occur depending on the torque characteristic of the engine. For example, with a substantially higher ratio, the acceleration rate in the zone will be reduced, resulting in a lower ratio of zone exit speed to zone entry speed, and thereby reduced drive-by noise. If a means of testing is introduced which eliminates the gearing effect (e.g. EPA Light Vehicle Testing Program or a "max. ISO" type test) then this approach is no longer effective.

TYRE NOISE-On the strength of the results from the coast-by tests carried out, it has been shown that the rolling noise generally follows the empirical relationship:

$$\text{Coast-by Noise Sound Pressure Level} = 32 \log V + 11.2 \log W - 20 \quad \text{dBA}$$

(V in km/h, W in kg)

This relationship is based on the data from 12 cars with kerb weights ranging from 700kg to 1800kg at coast-by speeds of up to 65km/h. The validity of this prediction is shown in Fig. 13 and indicates an accuracy of ± 1dBA for the vehicles tested. Similar predictions have been made arising from other research work in this field (6).

ENGINE TYPES-As has previously been shown, on the basis of acceleration tests at high engine speeds, the diesel engine on average increases the drive-by level from that of gasoline cars by some 2½dBA. Comparing 8 manual transmission gasoline cars with 5 manual diesel cars, the difference is even less at ½dBA, with very similar standard deviations (see Table 3). The diesel engine is significantly noisier at light load conditions (especially idle) as has been discussed. Drive-by noise levels associated with the larger, lower rated speed gasoline engines typical of current full size U.S. cars are on average approximately 2½dBA less than European passenger cars with "high speed" engines (on the basis of ISO R362 tests). This is largely due to the high intermediate gearing commonly used in automatic transmissions. When compared on a rated engine speed basis, however, these large engines show up as being some 2dBA noisier on drive-by (as in the "max. ISO" tests). This generalisation simplifies the real facts, since many other variables should be considered. For example, to achieve rated engine speed with a relatively high geared automatic transmission, even in the lowest ratio, requires a vehicle speed which by virtue of the high rolling noise on this type of car can significantly influence the overall drive-by noise level. General trends are shown, however, which indicate firstly that diesel car noise levels are not greatly above equivalent gasoline car noise levels and secondly that the larger, low rated speed engine noise potential is not being realised by current test procedures.

POWER/WEIGHT RATIO-From car to car there is no correlation between drive-by noise and power to weight ratio. The car tested with the highest power/weight ratio (the Triumph Dolomite Sprint) did produce the highest ISO R362 drive-by level, but the car with the second highest power/weight ratio (the Jaguar XJ6) produced the second lowest ISO level. Tests were carried out on the SAAB by loading the car progressively up to a gross weight of 2600kg. The drive-by tests subsequently carried out in these varying power/weight ratio builds show a very small effect, when assessed on an engine speed basis. The results from a given test procedure will be dependent on the acceleration performance of the vehicle and the detailed operational requirements of the test procedure, since it is the engine speed opposite the measuring microphone which determines the noise level.

EXHAUST-Exhaust noise can contribute very significantly to the overall drive-by level, particularly where resonances occur in the exhaust system at certain engine speeds and where these speeds are achieved during a test. This was the case for the SAAB 99 where resonances causing locally high noise levels occured at 24, 35 and 46 rev/s engine speed.

Typical exhaust noise contributions for the SAAB and Peugeot under full load and light load conditions are shown in Fig. 14 together with the other major contributions.

INTAKE-Intake noise is generally reasonably subdued in most passenger cars where properly designed intake silencer/filter arrangements are employed. In diesel engines, operating unthrottled, this is even more important, and cases have been known of very high drive-by levels being attributable solely to inadequate intake silencing.

FAN-With the increasing use of thermostatically controlled electrically driven cooling fans, this noise source is becoming less significant, typical fan-only noise levels at 7.5m being around 50dBA. Fans constantly driven by the engine, however, can be a serious noise source and often equal that of the engine, in terms of measured sound pressure level. The remedy is usually relatively straightfoward, the simplest for this class of vehicle being to resort to an electrically driven fan. A coolant temperature sensitive solenoid operated clutch fan is another alternative.

LEGISLATIVE TEST PROCEDURES

There are two extreme approaches in setting a legislative procedure: the maximum noise level possible from the vehicle can be measured, or the noise at a condition which is judged to be representative of typical vehicle operation. The choice between these two approaches is arbitrary, but significant. Although producing higher levels, generally greater repeatability is obtained if the former is adopted.

One method of deciding which is the representative condition for the second approach is to assess the noise levels produced over a typical urban driving cycle. Such a cycle exists for exhaust emission measurement purposes (LA 4) for this class of vehicle and could form the basis. It is not suggested that the noise computation be made over the whole cycle for each vehicle, for this would make the assessment prohibitively expensive. This method could be applied to some sample vehicles to establish the cycle Leq, which could then be related to the most acoustically significant portions of vehicle operation. This could then form the basis for a simple enforcement/testing procedure for that vehicle class.

In weighing the approaches, the authors would suggest that a maximum potential noise method be preferred, since some drivers will operate their vehicles in this manner at some time. Added benefits are that the testing procedure is simplified, it can be less ambiguous than current standards, and repeatability is improved.

CONCLUSIONS

At the road speeds of interest in urban areas with conjested traffic, passenger car noise is controlled by sources proportional to engine speed. Above the steady state cruise condition, radiated noise levels are insensitive to acceleration rate (i.e. engine load) for a given engine speed. Substituting a diesel engine for a gasoline engine has little effect on maximum noise level but does increase low speed noise levels, especially at low loads. This is most noticeable at idling conditions.

Differences due to various test procedures are significant and depend on relatively small vehicle modifications. The test procedure producing the most consistent results is the one where the aim is to assess maximum potential noise levels.

Above 80km/h in top gear, rolling noise tends to dominate radiated noise levels, with engine detail being less important.

ACKNOWLEGEMENTS

The authors would like to thank both DoT (TSC) and the Directors of Ricardo Consulting Engineers for permission to publish this paper. The views expressed are personnal and do not necessarily reflect views of DoT or Ricardo.

REFERENCES

1. "Summary Report Covering Test Work on the SAAB 99 and Peugeot 504 GLD Vehicles", Ricardo Report DP 77/1158, September 1977.
2. B.J. Challen and D. Morrison, "Passenger Car Noise - Diesel and Gasoline", Inter Noise 1978, San Francisco May 1978.
3. "Light Vehicle Noise Emission Program - Measurement Methodology Workshop", U.S. E.P.A. Standards and Regulations Division - Office of Noise Abatement and Control (AW-471), June 1977.
4. B.J. Challen, "The Effect of Combustion System on Engine Noise", Society of Automotive Engineers (SAE)750798.
5. W.M Scott, "Noise of Small Indirect Injection Diesel Engines", Society of Automotive Engineers (SAE) 730242.
6. "Proceedings from the SAE Highway Tyre Noise Symposium", San Francisco, November 1976.

TABLE 1-SPECIFICATION OF SAAB AND PEUGEOT

	SAAB 99CL (Injection)	Peugeot 504 GLD
ENGINE		
TYPE	SPARK IGNITED GASOLINE	COMET V DIESEL
BORE (mm)	90	84
STROKE (mm)	78	89
NO. OF CYLINDERS	4	4
CAPACITY (litre)	1.985	2.304
NOMINAL MAX. POWER (kw)	75	52
RATED ENGINE SPEED (rev/s)	92	75
EMISSION BUILD	CALIFORNIA '76	CALIFORNIA '76
FUEL INJECTION SYSTEM	BOSCH K JETRONIK (C.I.)	CAV (ROTO DIESEL)
TRANSMISSION		
TYPE	MANUAL	MANUAL
NO. OF FORWARD RATIOS	4	4
OVERALL GEARING (km/h per 100rev/s, engine speed)		
1st gear	5.5	4.8
2nd gear	8.9	8.1
3rd gear	11.4	12.1
4th gear	18.1	17.5
KERB WEIGHT (kg)	1200	1 900
WEIGHT AS TESTED (kg)	1415	1560
ODOMETER READING AT START OF TESTS (km) APPROX.	5000	5000

TABLE 2-BRIEF DESCRIPTION OF CARS TESTED

CAR	ENGINE TYPE	ENGINE NOMINAL MAX. POWER *	ENGINE RATED SPEED	TRANSMISSION	KERB WEIGHT kg
SAAB 99GL (EU1)	G	75	5200	M	1050
PEUGEOT 504 GTD	D	52	4500	M	1400
RENAULT 4	G	25	5250	M	645
FORD FIESTA	G	40	6000	M	700
CORTINA 1600	G	54	5200	M	1025
VAUXHALL CHEVETTE GL	G	55	5400	M	845
CHRYSLER ALPINE S	G	65	5600	M	1070
VOLVO 244GL	G	82	5250	M	1125
JAGUAR XJ6	G	154	5500	A	1760
TRIUMPH DOLOMITE SPRINT	G	95	5500	M	1040
BUICK ASPEN	G	75	4000	A	1660
SAAB 99GL	G	120	5500	A	1355
PLYMOUTH VOLARE	G	82	4000	A	1720
V.W. GOLF	G	47	5800	M	840
OLDSMOBILE DELTA 88	G	90	4000	A	1670
MERCEDES 240D	D	58	4500	M	1395
OPEL ASCONA	D	45	4800	M	1112
SAAB 99GL (T/C)	D	65	4800	M	1340

POWER STATED IN kW
SPEED STATED IN rev/m
G = GASOLINE
D = DIESEL
A = AUTOMATIC
M = MANUAL
* = TURBOCHARGED PROTOTYPE

TABLE 3-PASSENGER CAR NOISE SURVEY

VEHICLE GROUP	x	ISO				"max. ISO"				INTERIOR NOISE												EXTERIOR IDLE			
										50km/h				80km/h				IDLE							
		AVE	+	-	s	AVE	+	-	s	AVE	+	-	s	AVE	+	-	s	AVE	+	-	s	AVE	+	-	s
ALL	18	78,4	3,2	4,4	2,5	83,1	2,9	3,3	2,0	63,9	5,1	6,1	3,4	69,4	6,4	5,4	3,5	48,7	6,1	7,7	3,6	58,7	6,8	10,7	4,8
EUROPEAN	15	78,7	2,9	3,7	2,0	82,8	3,0	3,0	2,0	64,8	4,2	7,0	2,8	70,4	5,4	6,4	3,0	49,2	5,6	8,2	3,7	58,4	6,1	10,4	5,0
U.S.	3	76,3	4,6	2,3	4,0	84,5	1,5	1,7	1,6	59,2	1,3	0,7	1,2	64,7	1,3	0,7	1,2	46,3	1,7	0,8	1,4	60,1	5,2	2,8	4,5
ALL GASOLINE	12	77,5	4,1	3,5	2,7	83,0	2,8	3,2	1,9	63,5	5,5	5,7	3,4	69,2	6,6	5,2	3,6	47,6	6,9	6,6	3,6	56,1	3,4	8,1	3,6
ALL DIESEL	6	79,9	1,4	1,9	1,4	83,3	2,7	2,6	2,4	64,6	2,6	6,1	3,5	70,1	2,1	6,1	3,4	50,9	3,9	2,9	2,4	64,0	1,5	1,0	1,0
ALL AUTO	5	75,9	5,0	1,9	2,9	84,3	1,7	1,5	1,4	59,5	2,9	1,7	1,9	64,8	1,0	1,8	1,0	45,3	2,7	4,3	2,6	59,3	6,2	2,3	3,5
ALL MANUAL	13	79,4	2,2	2,7	1,6	82,7	3,1	2,9	2,1	65,5	3,5	3,0	2,1	71,4	4,4	2,4	1,8	50,1	4,7	6,1	3,2	58,5	6,0	10,5	5,4
ALL MANUAL GASOLINE	8	79,1	2,5	2,4	1,7	82,8	3,0	3,0	2,2	65,3	3,7	2,8	2,2	71,1	4,5	2,3	2,2	49,1	5,4	5,1	3,3	55,3	4,2	7,1	4,3
ALL MANUAL DIESEL	5	79,6	1,7	1,6	1,5	82,7	2,4	2,0	2,1	65,9	2,1	3,1	2,0	71,7	0,5	0,5	0,4	51,4	3,4	2,4	2,2	63,7	0,8	0,7	0,8

ALL LEVELS IN dBA

± = extremes of sample

s = standard deviation

ave= arithmetic average of results
x = sample number

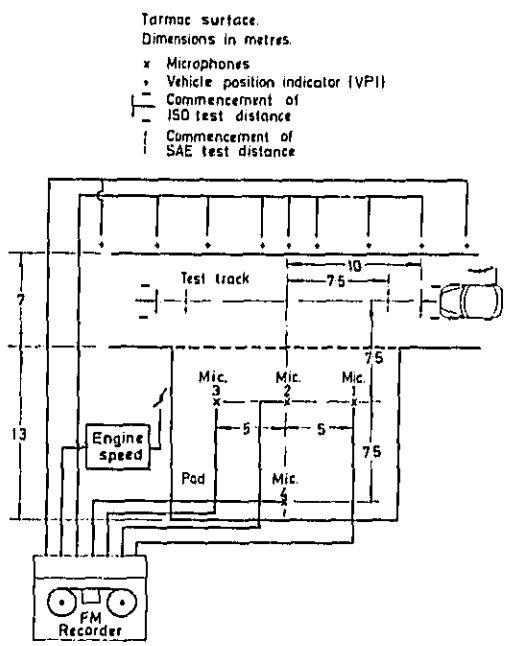

Fig. 1 - Ricardo drive-by noise test site and schematic layout of instrumentation

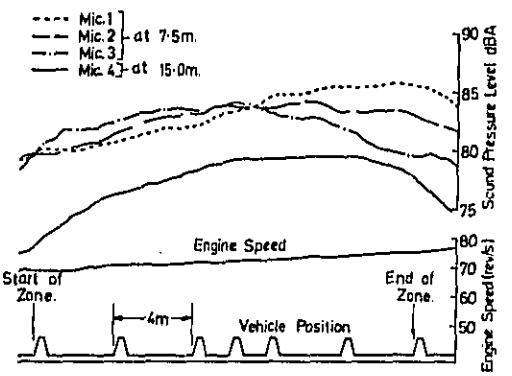

Fig. 2 - Typical drive-by trace (Peugeot 504 GLD) 50km/h entry speed, 2nd gear, (max. acceleration)

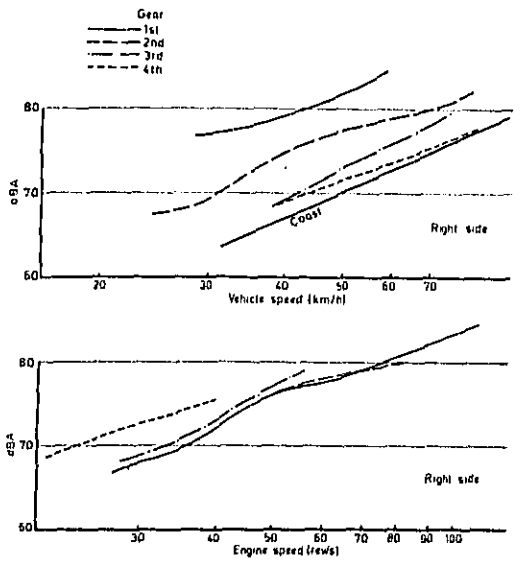

Fig. 3 - SAAB 99 drive-by noise levels at various engine and vehicle speeds

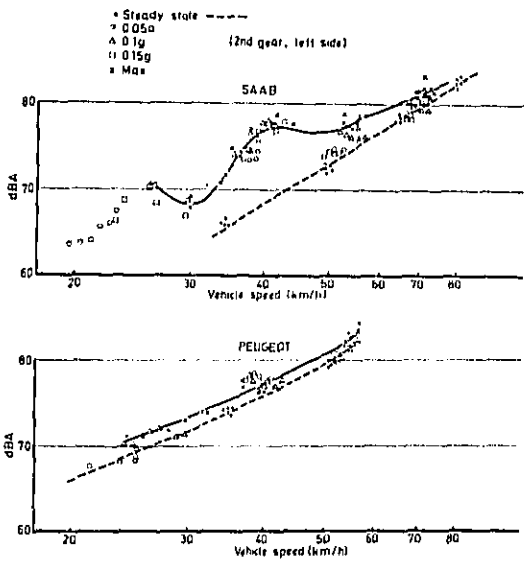

Fig. 4 - Effect of acceleration rate on vehicle noise

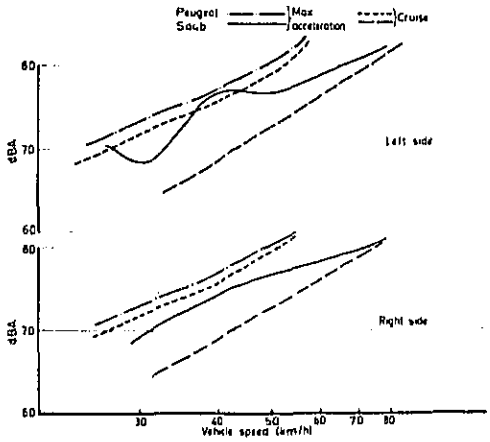

Fig. 5 - Vehicle drive-by noise levels (2nd gear)

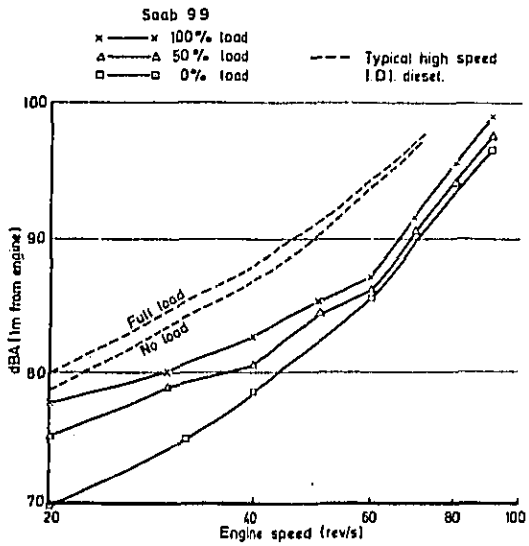

Fig. 6 - Engine noise

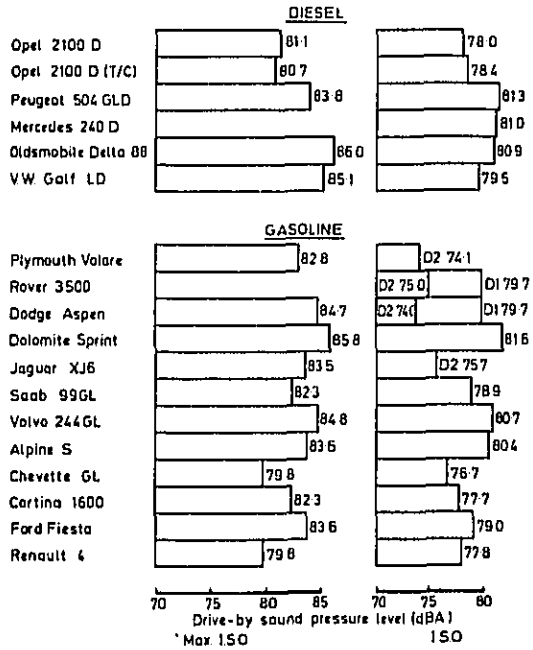

Fig. 7 - ISO and "max. ISO" drive-by levels (averages of left side and right side)

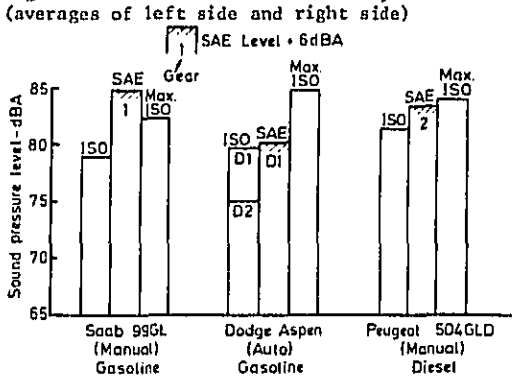

Fig. 8 - Effect of drive-by test procedure on noise level

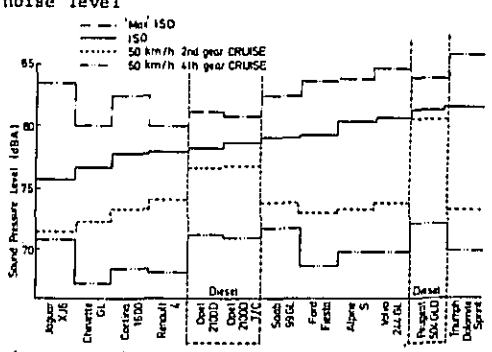

Fig. 9 - Noise levels at 7.5m for various drive-by conditions (averages of left and right hand sides)

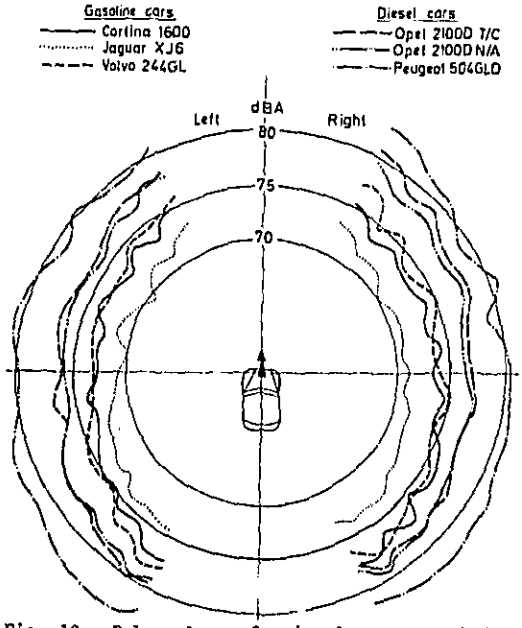

Fig. 10 - Polar plots of noise level distribution (50km/h 2nd gear, steady state, corrected to 7.5m radius)

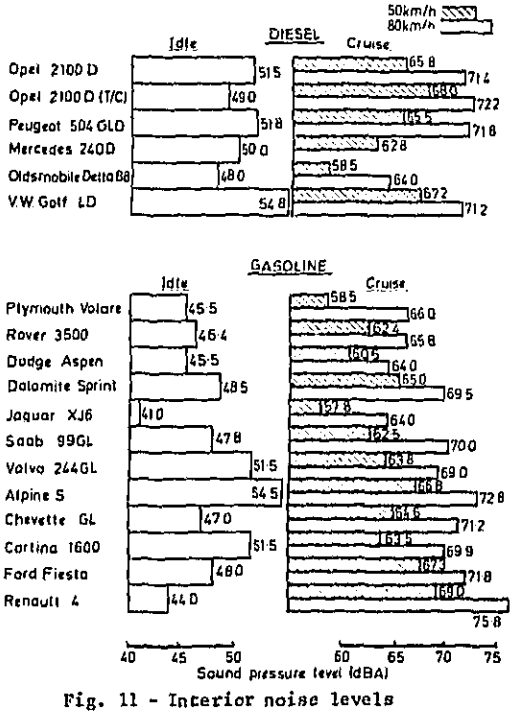

Fig. 11 - Interior noise levels

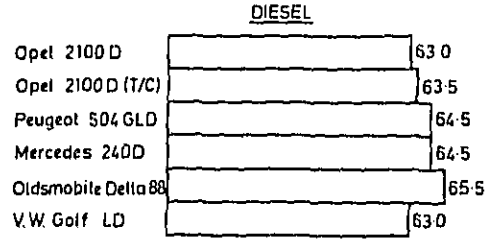

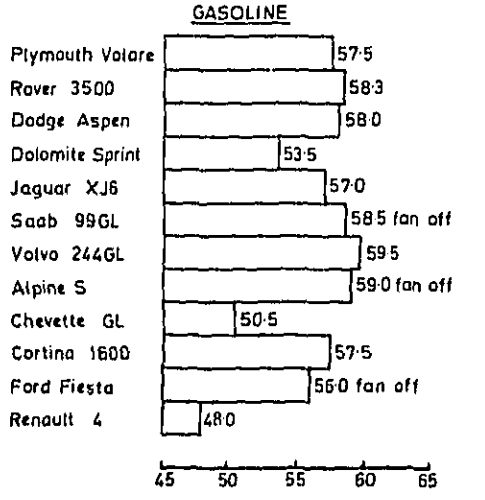

Fig. 12 - Exterior idle noise

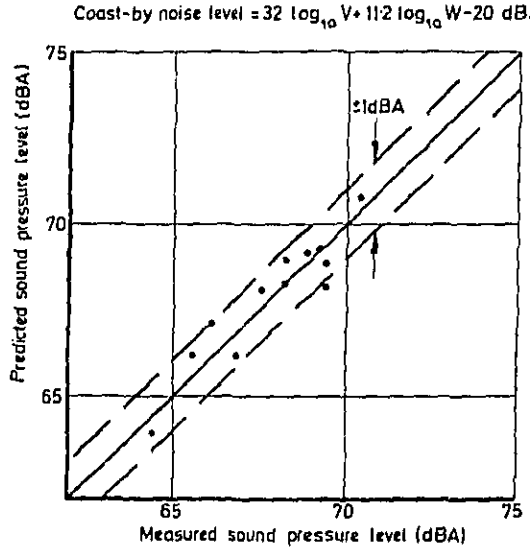

Fig. 13 - Coast-by noise prediction

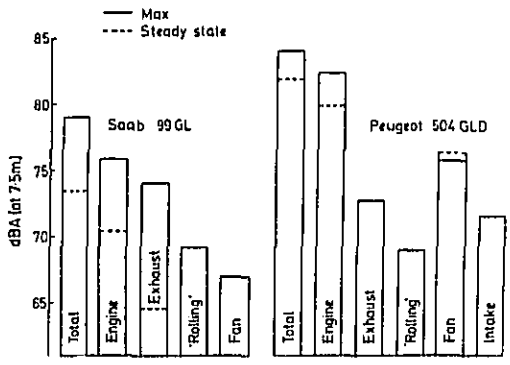

Fig. 14 - Noise source contributions (50km/h 2nd gear, right hand side)

790443

AN EXPERIMENTAL PASSENGER CAR DIESEL ENGINE

E. C. Grover and R. D. H. Perry

Institute of Sound and Vibration Research
University of Southampton.

ABSTRACT

This paper describes the design and initial evaluation of a novel concept of crankcase design applied to a 2 litre high speed diesel engine. This design offers lightweight economic production and low noise without compromising performance.

SINCE THE OIL CRISIS OF 1973 much has been published to exemplify the use of the high speed diesel engine as a means of energy conservation in passenger cars. However, to compete with the modern gasoline engine in real terms the high speed diesel must incur the minimum possible penalties in terms of weight, noise and production cost in addition to the expected benefit of fuel economy.

Over the past twelve years ISVR have designed and built some ten experimental engines to investigate different techniques for noise reduction. These were based on existing diesel engine running components and ranged in size from 1.6 litres to 13 litres. Although the noise reductions of these engines were substantial (ranging from 7 to 11 dB A), weight and manufacturing costs were not essential parts of the designs and the engines were often unattractive for production.

In this paper an experimental engine design is described where lightweight and low production costs are essential features, but a considerable potential for a low noise level is also offered. This work is supported by the National Research and Development Corporation.**

DESIGN CONSIDERATIONS

THE BASIC STRUCTURE. The noise spectrum of the high speed diesel engine is characterised by components in the frequency range from 800 Hz to 3000 Hz resulting from operating forces, whether of combustion or mechanical origin, exciting natural frequencies of the structure. If these operating forces are optimised the radiated noise from the engine can be reduced only by making changes to the vibration response of the structure. This can be done by the use of damping materials and isolation techniques to reduce vibration amplitudes, or by changes in stiffness characteristics so that the basic structure vibration pattern is changed.

The avenues which have been explored in the past at Lucas CAV Ltd and ISVR are summarised in Figure 1. Figure 1a shows the skeleton frame principle where separate highly damped panels are attached by some means to a welded or cast framework (1) * and Figure 1b illustrates the principle of attaining extreme stiffness by the use of low density material (1). Both these techniques incorporate the use of unorthodox production methods and materials. The crankframe engine design is shown in Figure 1c. Here the crankcase is removed and replaced by a damped lightweight cover attached to the lower deck of the cylinder block where vibration levels are characteristically low (2,3,4). The main disadvantages here are the problems associated with the transmission mounting and oil sealing. The use of a main bearing bedplate, to stiffen the crankcase walls (Figure 1d) is successful and practical. This technique has been applied mainly to engines of larger size (5).

The most commonly accepted approach in the design of quieter power units is to increase the engine stiffness by use of ribbing patterns and generally heavier scantlings, so that the response lies generally in a higher frequency range where the levels of the exciting forces are expected to be lower. This inevitably leads to a heavier engine with often only a small noise reduction advantage.

Alternatively, response frequencies could be lowered towards a less important frequency range by reducing stiffness. Within constraints imposed by the need to carry the working loads and the minimum practical casting thicknesses, reducing the thickness of webs and panels of a conventional structure will have little effect on natural frequencies. Moreover the amplitudes of vibration of the less massive structure are likely to be increased resulting in a noisier engine. For a lightweight engine with low natural frequencies an entirely different approach to engine design has to be considered. The core of such a design must, in the first instance, be the determination of an adequately stiff load carrying structure. Then the

* Numbers in parenthesis designate references given at end of paper.

**N.R.D.C. is a U.K. statutory body which finances innovative designs and subsequently licences inventions and knowhow.

SAE/P-79/80/$02.50
Copyright © 1979 Society of Automotive Engineers, Inc.

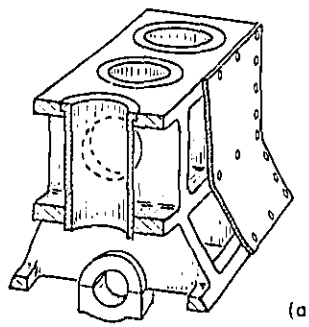

(a) Cast or welded skeleton frame with damped panels.

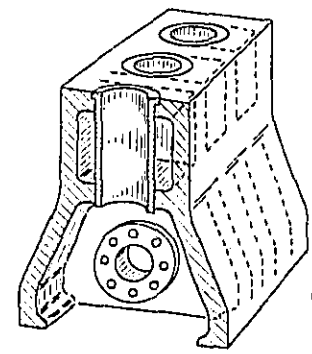

(b) Stiff engine of low density material.

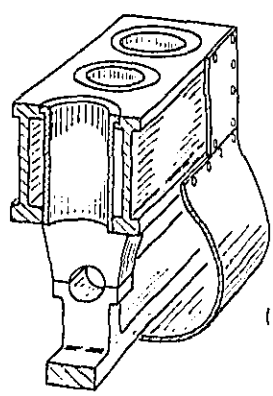

(c) Crankframe engine with high level oil pan and damped block panels.

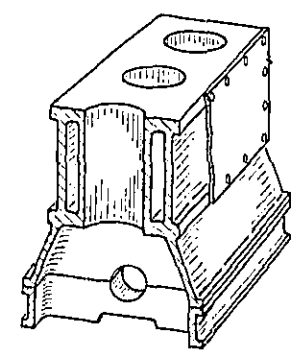

(d) Bedplate engine with stiff crankcase and damped panels on block.

Fig. 1 - Proven schemes for low noise engine design

outer surfaces, which are responsible for the noise emission, can be considered as separate and specific entities.

A test procedure on non-running engines has been developed at ISVR to determine the relative stiffnesses of elements of the block structure (6). Basically, the deflections of the casting are measured when a piston is loaded hydraulically to the equivalent of the combustion force. Figure 2 shows typical distortion patterns for a small symmetrical skirted block. The force, applied to the crankshaft main bearings via the connecting rod causes the bearing saddle A to move vertically dowards elongating the web elements B. The resulting Poisson's ratio effect causes the rib elements C, and consequently the upper part of the crankcase wall, to move inwards and downwards while the lower part of the crankcase wall, acted on through rib element D in turn moves outwards and downwards. The crankcase oil-pan flanges are bowed locally outwards either side of the loaded cylinder.

It can be readily appreciated that on a running engine the rapidly applied force and the varying point of application as each cylinder fires results in a complex vibration of the outer surfaces of the structure and the radiation of high frequency noise.

The above analysis has been somewhat simplified, but nevertheless, it points towards one of the possible mechanisms of crankcase excitation and suggests an obvious way to control it.

If the bearing saddles were to be simply suspended from the lower deck of the cylinder block with no integral connection through webs or ribs to the sidewalls of the crankcase, then vibration excitation of the crankcase walls can result only from travelling waves from the crankshaft bearing supports and block or bending moments at the lower deck where the crankcase walls are attached. That is, the direct force paths from the crankshaft would be eliminated.

ISVR decided to investigate the merits of this basic design concept experimentally. Initially an idealistic design as depicted in Figure 3 was considered. As can be seen, the crankshaft bearing supports were cantilevered from the rigid and well defined lower cylinder block deck. The main bearing bolt axes and head retaining bolt axes were of the same pitch and in the same plane allowing through bolting to be used. Thus a compact basic load carrying structure was formed which would normally be under compressive stress when the bolts were tightened, permitting greater bending forces to be tolerated. This was considered particularly

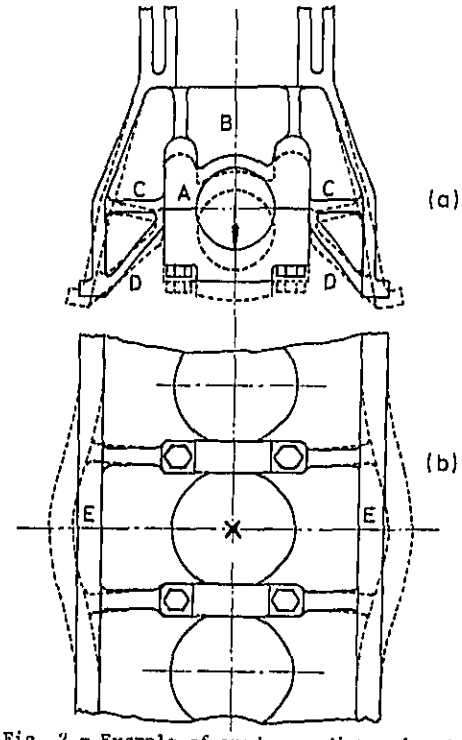

Fig. 2 - Example of crankcase distortion due to static loading

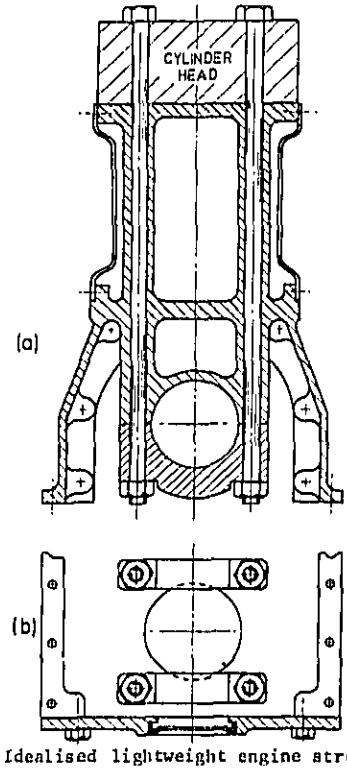

Fig 3 - Idealised lightweight engine structure

important for the cantilevered bearing members. Also the provision of direct and symmetrical load paths from top to bottom would minimise distortion. To maintain a symmetrical structure an overhead camshaft was incorporated. In the cylinder block the direct firing loads were reacted through the cylinder barrels and bolt columns. There were no integrally cast side walls to the cylinder block; the side walls consisted of separate lightweight damped panels.

The crankcase walls were an integral part of the block casting, being suspended from the lower deck and designed to be as lightweight as casting practice permits. The deep skirted arrangement of the crankcase walls would ensure a low natural frequency of vibration so as not to couple readily with the higher frequency vibration expected on the main structure. A curved or cranked form would provide some degree of longitudinal bending stiffness.

Flanges were incorporated in the ends of the crankcase walls to which front and rear oil seal housings were attached. There was no mechanical contact, apart from through the oil seals, between these plates and the crankshaft bearing members (Figure 3b). Gasket layers between the end plates and the crankcase wall flanges gave a means of introducing, and varying, the vibration damping to the structure.

The final design of the block follows these initial thoughts very closely. The main departure being from the through bolting arrangement. For various reasons, not the least being the requirement for a simple and inexpensive casting and cheap construction, the head and main bearing bolt axes could not be maintained in a single plane, therefore separate bolts are used. The cylinder head bolt columns are cast integrally with the cylinder walls as shown in Figure 4a and the main bearing bolts terminate at the lower deck level (Figure 4b), though still satisfying the prestressing requirement of the bearing saddles.

The cylinder block/crankcase is cast in iron and is unlinered. The weights of the principal components are given in Table I and the engine specification is summarised in Table II

Table 1: Weight of Principal Components

Block/crankcase (with bearing caps)	42.0 kg.
Cylinder head	8.62kg.
Crankshaft	19.7 kg.
Flywheel	12.9 kg.
Connecting rods (complete)	3.36kg.
Pistons (complete with gudgeon pin)	2.48kg.
Total engine weight, including starter and alternator andall ancilliaries	166 kg.

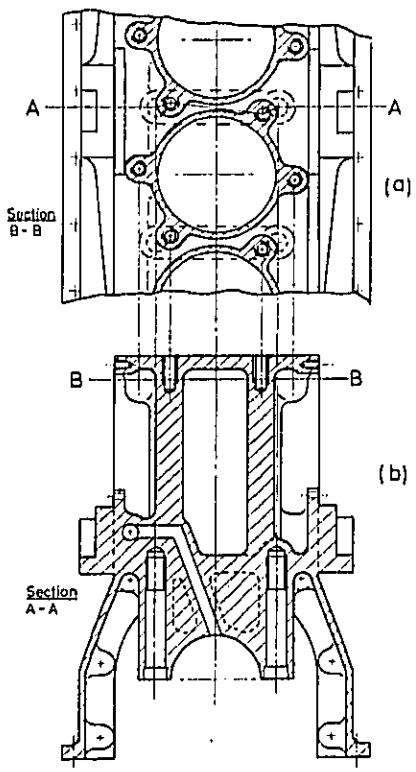

Fig. 4 - Details of experimental design

Table 2: Brief Engine Specification

Bore: 87 mm Swept volume 2.036 litres.
Stroke: 85.7 mm

Combustion system: Ricardo Comet V
Compression ratio: 22/1
Prechamber volume: 47% of compression volume.

Connecting rod length/crank throw: 3.4
Main bearing diameter: 63.5 mm
Big-end bearing diameter: 50.8 mm
Gudgeon pin diameter: 25.4 mm

Valve timing:
Inlet opens: 11° b.t.d.c. Exhaust open 41° b.b.d.c.
Inlet closes: 39° a.b.d.c. Exhaust closes 9° a.t.d.c.
Valve lift (inlet & exhaust) 9.25 mm
Inlet valve diameter: 40.5 mm
Exhaust valve diameter: 37.2 mm

Auxilliary drives:

Camshaft & fuel pump: compound boothed belt.
Water pump & alternator: single v. belt.

PISTON-CRANK MECHANISM. It was decided that the best size of engine on which to evaluate the new structure was a 2 litre high speed unit suitable for any average family car.

To achieve a good power to weight ratio, low mass components were required. This also implied low inertia forces which would minimise mechanical impact noise and tend towards higher mechanical efficiency which would also aid the achievement of a good specific output.

Within the confines of this project, it was necessary to utilize a crankshaft and connecting rods from a production engine. A five bearing, forged steel crankshaft from a quality 2 litre gasoline engine was selected. This, although generously proportioned for a gasoline engine, had smaller bearings than conventional diesel engine practice would suggest. For the required displacement, the resultant bore/stroke ratio is unity. This was considered an acceptable compromise between the requirements for mechanical and indicated efficiency and noise.

The pistons were specially produced in cooperation with a piston manufacturer. They were designed to be as light as the manufacturer considered expedient and finally proved to be only 6% heavier than the equivalent gasoline engine pistons. Two compression and one oil control ring were provided, but neither an iron top ring insert nor any expansion control insert were incorporated. It was hoped that satisfactory gas and oil control could be achieved with three rings, in the interests of minimum friction losses.

CYLINDER HEAD, COMBUSTION SYSTEM & VALVE GEAR. The basic object of the engine design was the evaluation of the crankcase-cylinder block structure. It was therefore considered preferable to incorporate a proven indirect injection system in the design. A conventional Ricardo Comet V system is used.

Light weight was an important design criterion of the cylinder head; therefore the unit was cast in aluminium. To marry with the cylinder bolt column arrangement, a "six bolt" fixing arrangement was adopted. It was hoped that this would give more reliable sealing, but was also considered potentially lighter as a less rigid head could be tolerated.

In the interests of noise and efficiency it was decided to limit the maximum power speed to 4200 rev/min. If an acceptable power to weight ratio was to be achieved, a high mean effective pressure was required. To give good driveability, this high mean effective pressure would have to be maintained, or exceeded, down to as low an engine speed as possible. Therefore the largest possible valves and inclined ports were incorporated. The same camshaft casting as the gasoline engine was used, but with reduced cam period. By these means it was hoped to achieve a good volumetric efficiency over a wide speed range.

The choice of a "six bolt" head retaining system dictated the port and combustion chamber positions, but allowed the use of an efficient cross flow layout. This layout also enabled insulating liners to be incorporated in the exhaust ports. These features should have benefitted volumetric efficiency and heat rejection to coolant.

TEST RESULTS

ENGINE INSTALLATION. The engine was installed with a car gearbox and car type engine mounts in a test cell at ISVR with partial acoustic treatment.

CHOICE OF INJECTION TIMING. The engine was built using a fuel injection system specification that had been developed for an engine of similar size. So far this specification has not been

altered and the only performance development has therefore been the selection of the optimum injection timing.

Although the engine was designed to have a compression ratio of 22/1, it was initially run at a ratio of 19.4/1. For that build the injection pump had to be set such that under full load conditions the dynamic start of injection was about 20° b.t.d.c. in order to achieve stable combustion at high speeds. In this condition full load combustion was rather abrupt and it was not possible to exceed 7.9 bar b.m.e.p., or 44 kW at 4200 rev/min.

When the compression ratio was corrected to 22/1, the same 20° b.t.d.c. dynamic timing at full load was used. An increase in mean effective pressures of about 10% was immediately achieved without adjusting the fuelling, resulting in an output of 50 kW at 4200 rev/min. However, smoke levels were not acceptable and the peak cylinder pressure rose to above 92 bar.

Subsequently the injection timing has been reset to 15° b.t.d.c. In this condition the mean effective pressures are little changed but smoke levels on full fuelling have been reduced by 1.5 Bosch units and the maxim peak cylinder pressure reduced to 73 bar, which approached the design target level. This timing is now the standard setting at which most of the results in this paper were obtained.

The engine was run briefly with dynamic timing of 10° b.t.d.c. at full load. This resulted in a significant loss of performance and generally unstable running at less than full load. Moreover the benefit to noise was insignificant.

Cylinder pressure diagrams and 1/3 octave band spectra at full load for two timings are shown in Figure 5. At all speeds, peak pressures with 15° timing are significantly lower than with 20° timing (Figure 5a). The change in cylinder pressure spectrum levels is small at 3000 rev/min but reductions of 10 dB occur around 2 kHz at 4200 rev/min and at 250 Hz at 1800 rev/min. When the spectra are normalized they are of similar form at the 15° timing (Figure 5c). However, with 20° timing the spectrum slope decreases significantly with rising engine speed. This is not evident from the pressure diagrams which appear similar at different speeds for a given timing.

BRAKE PERFORMANCE. Figure 6 shows the average full load performance levels of the engine with the standard 15° b.t.d.c. injection timing, corrected according to BS AU 141a requirements. The maximum power achieved at rated speed was just under 50 kW, giving a specific output for the engine of 3.34 kg/kW

The shape of the b.m.e.p. (or torque) curve is satisfactory with a peak level of 7.8 bar around 1900 rev/min. The minimum specific fuel consumption is 0.252 kg/kwh at 1900 rev/min with a lowest measured value of 0.235 kg/kW.h at ¾ load 1800 rev/min.

Willans lines at 1800 and 4200 rev/minute gave friction m.e.p. values of 1.65 bar and 2.90 bar respectively. These values suggest that low friction losses have been achieved, which helps explain the good fuel consumption and performance.

The smoke characteristic is satisfactory, although some improvement at high speeds is desirable.

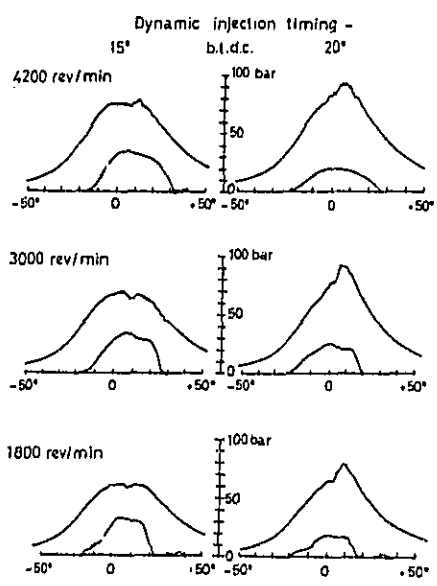

(a) Cylinder pressure diagrams

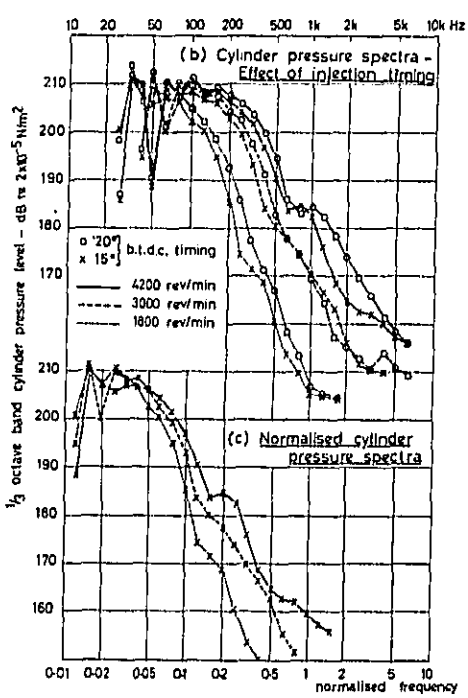

Fig. 5 - Cylinder pressure characteristics at full load

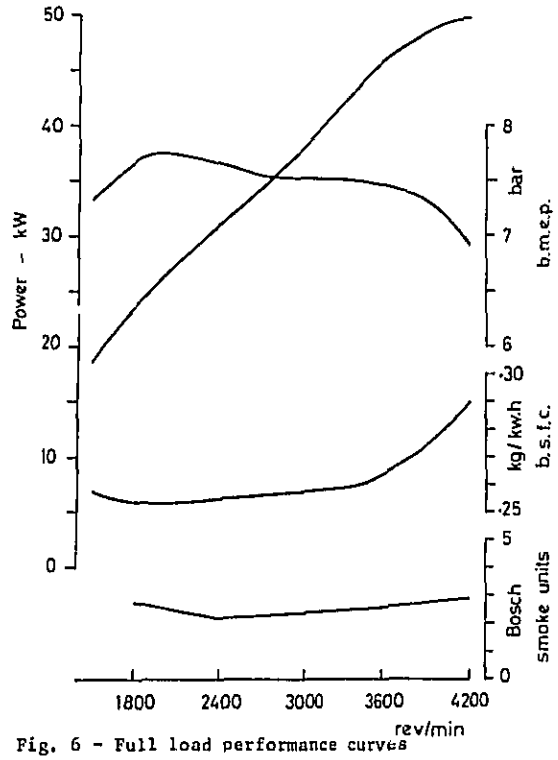

Fig. 6 - Full load performance curves

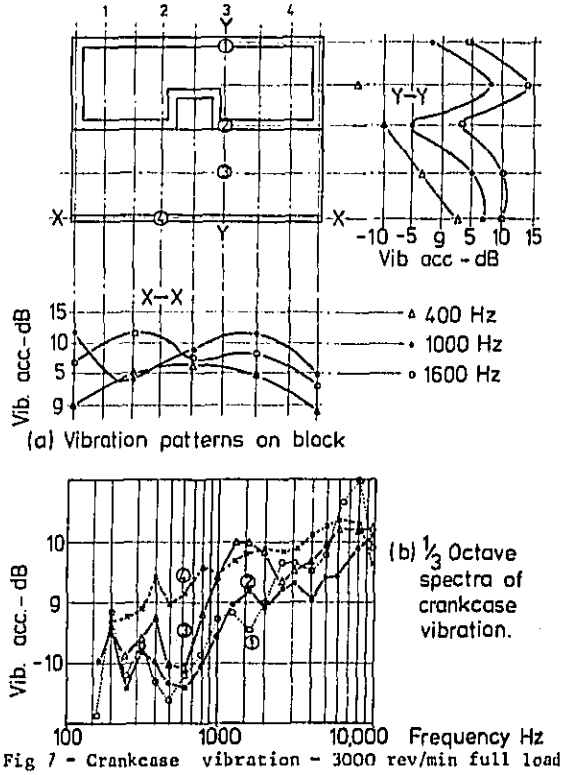

Fig 7 - Crankcase vibration - 3000 rev/min full load

The fall in mean effective pressure below 1800 rev/min reflects the fuel pump delivery characteristic. However, the sharp rise in specific consumption with the corresponding fall in output indicates, along with the smoke levels, that a possibility exists to improve the combustion behaviour at high speeds.

NOISE AND VIBRATION. Vibration. The length and thickness of the crankcase skirts were determined to give a cantilever mode fundamental bending frequency of about 400 Hz. This frequency was chosen so as not to coincide with either the low firing harmonics or the longitudinal bending frequency (which could be estimated for an engine of this length to lie in the 600 to 800 Hz frequency range). The response of the crankcase walls of the fully assembled engine showed a cantilever mode frequency of 418 Hz.

Figure 7a gives the vibration acceleration levels in third octave band frequencies of 400 Hz, 1000 Hz and 1600 Hz on the outer surfaces of the running engine along a vertical line at the plane of No. 2 cylinder and a horizontal line along the pan rail. The level of the 400 Hz component increases down the crankcase to a maximum at the centre of the pan rail, being restrained at the ends of the crankcase by the stiffening/damping effects of flanges and end plates. The 1000 and 1600 Hz components show minimum values at the lower cylinder deck level, which generally increase towards the pan rail (the high levels at the centre of the cylinder block are due to the thin pressed steel side cover). Along the pan rail the vibration patterns suggest higher order bending modes at 1000 Hz and 1600 Hz respectively.

Figure 7b compares third octave band vibration spectra at the indicated points on the structure. Vibration levels on the lower part of the crankcase are higher than on the top and bottom decks by about 10 dB over the frequency range from 500 to 2000 Hz which is an acceptable amplification.

Noise. In the original design concept it was anticipated that specific noise control measures would be necessary for the side covers of the cylinder block water jacket and possibly on the camcover/head surface.

Additional flat damped panels were placed over the water jacket covers, which are dished to reduce block water volume, and attached to the rigid members of the block by the same fixing screws. Thus sealing was not effected and an air gap was provided between the two surfaces.

The cylinder head, cam and valve system is of conventional design and no noise control features are built in. However the system was not developed and subjectively was a major noise source and therefore a simple damped cover was fashioned to enclose these surfaces.

Noise was measured at 1 m from the centres of the sides of an imaginary box enclosing the engine. Figure 8 compares the variation of overall noise with speed at the front and sides for both full load and no load. At all conditions the overall noise increases with speed up to 2400 rev/min, at a rate of about 20 dB per tenfold increase of speed (decade). Above 2400 rev/min the noise increases

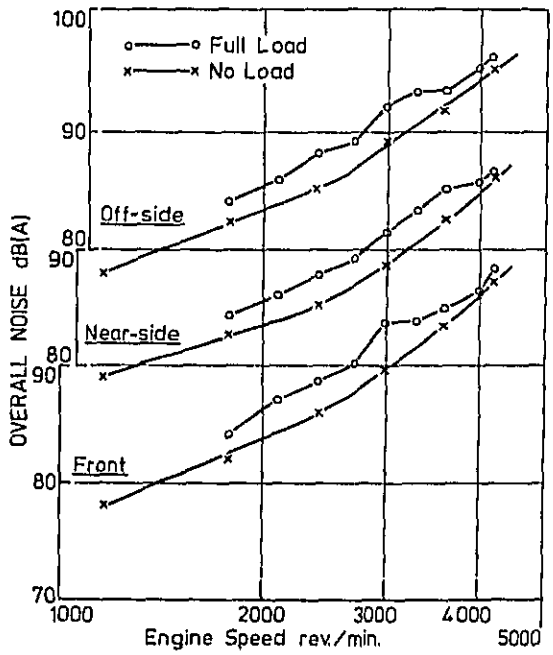

Fig. 8 - Effect of speed and load on overall noise

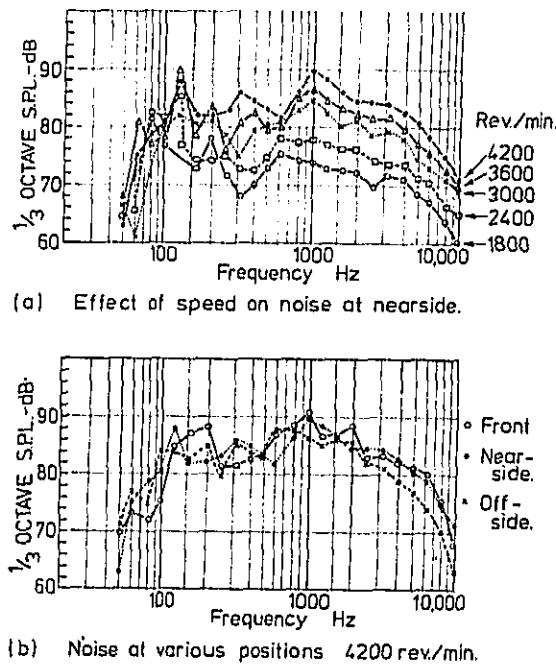

Fig. 9 - Engine noise spectra at full load

at a higher rate of about 40 dB/decade. This is characteristic of small I.D.I. engines and has yet to be fully explained. Apart from a maximum speed where noise levels are nearly the same, the noise increases with load by about 3 dB(A). At the sides the full load noise is at rated conditions, 96 dB(A). At the front it is 98 dB(A). However, no acoustic treatment is applied to any front surface, though in a final version this would be applied in the form of timing belt guards.

In Figure 9a are shown third octave band noise spectra at the near side of the engine at full load over the speed range, 1800 to 4200 rev/min. As speed increases the components in the mid-frequency range, 800 to 2000 Hz, become more predominant due to excitation of the 1000 and 1600 Hz crankcase vibration modes. Significantly, there are no high level components in the low frequency range from 200 to 800 Hz where longitudinal bending modes and the crankcase wall cantilever mode (400 Hz) might be expected to appear. The absence of the bending mode, which might have been a problem with a light flexible structure, is attributed to the fundamental design concept where no direct path exists to transmit the crankshaft side forces to the crankcase walls. The damping given by the engine end plates is a possible explanation for the absence of a marked 400 Hz component in the noise spectra.

Figure 9b compares noise spectra at full load rated speed conditions at the front and sides of the engine. At 1000 Hz and above 2000 Hz, levels are higher by 3 dB at the front and nearside (fuel injection pump side) of the engine which suggests that more detailed attention should be paid to the fuel pump mounting.

CONCLUSIONS

The flexibility inherent in the design of the experimental engine did not give rise to low frequency noise problems, and after more than 80 test bed hours, many at rated conditions, the crankshaft journal bearings showed no indication of abnormal wear.

The test results promise that the simple design philosophy proposed can be viably applied to production automotive engines of high specific performance and low noise characteristics.

ACKNOWLEDGEMENTS

The authors thank the licence holders, N.R.D.C., for the sponsorship which made the project possible and for their permission to publish the results.

Recognition is also given to the following establishments which contributed in various ways:

British Leyland Cars
Wellworthy
Lucas C.A.V.
Uniroyal.

REFERENCES

1. T. Priede, A.E.W. Austen, E.C. Grover, "Effect of engine structures on noise of diesel engines." P4/65 Inst. Mech. Eng. London 1965.

2. T. Priede, E.C. Grover, N. Lalor, "Relation between noise and basic structure vibration of diesel engines." SAE 690450.

3. S.H. Jenkins, N. Lalor and E.C. Grover, "Design aspects of low noise diesel engines." SAE 730246.

4. D.W. Tryhorn, H.L. Pullen, E.C. Grover, "Low noise opposed piston two-stroke engine and blower." SAE 750840.

5. R. Cawthorne, J. Tyler, "T.R.R.L. quiet heavy vehicle project." SAE Feb. 1979.

6. E.C. Grover, D. Anderton, "Implementation of research techniques for low noise diesel engine design." Czechoslovak Scientific and Industrial Society. 1977.

790444

THE EFFECT OF STRUCTURE DESIGN ON HIGH SPEED AUTOMOTIVE DIESEL ENGINE NOISE

D. Anderton, J. Dixon,
ISVR, University of Southampton, England.

C.M.P. Chan,
Search Engineering Ltd., England.

S. Andrews,
British Leyland Cars, England.

ABSTRACT

The paper describes the assessment and testing of two high speed diesel engine structure modifications designed to reduce noise. The modifications tested are a five main bearing version of a standard three main bearing engine and the addition of a sump plate. The results indicate that it is difficult to assess the running engine vibration and noise characteristics using modal analysis techniques but that this is possible when using the banger test techniques. It is shown that noise reductions up to some 4.0 - 5.0 dBA can be achieved both on the test bed and in the vehicle application.

Small high speed (4000-5000 rev/min) diesel engines are finding increasing applications in road transport, primarily because of their good fuel consumption and reliability. Unfortunately this feature is offset by generally higher noise levels than equivalent gasoline engines, as indicated in Fig. 1. Although the maximum noise produced by both types of engine is about the same it can be seen that there is a considerable advantage for the gasoline engine in this respect at part speed conditions. The quieter indirect injection diesel engines (I.D.I.) have similar noise characteristics to the more noisy gasoline engines, but further noise reductions are required if the use of the small high speed diesel is to become even more widespread. This paper describes some investigations into the effect of modified engine structures on high speed diesel engine noise.

What can be done to reduce the engine noise once the air inlet, exhaust, fan noise, alternator noise, etc, have been treated? Further reductions in noise can only be achieved by (a) changes to combustion excitation - choice of combustion system, and (b) engine structure modifications for reduced response. In the case described the combustion system is a modified form of Ricardo Comet chamber i.e. the Rover chamber, which has been developed for low noise and emissions. Further reductions of noise will only be obtained by engine structural changes. On the small high production inline 4, modifications must meet the requirements of low cost and weight without major modification to the existing production line. It is known that by using engine designs with severe weight penalties (underslung beam, bedplate, etc) the engine noise can be substantially reduced. The problem therefore is one of compromise between weight, cost, ease of production and degree of noise control. In the case of this four cylinder 90.5 mm bore 2½ litre engine three modifications have been assessed against the standard engine. The assessment has been carried out on the test bed, using rig tests and in-vehicle tests and it is the purpose of this paper to describe the work carried out.

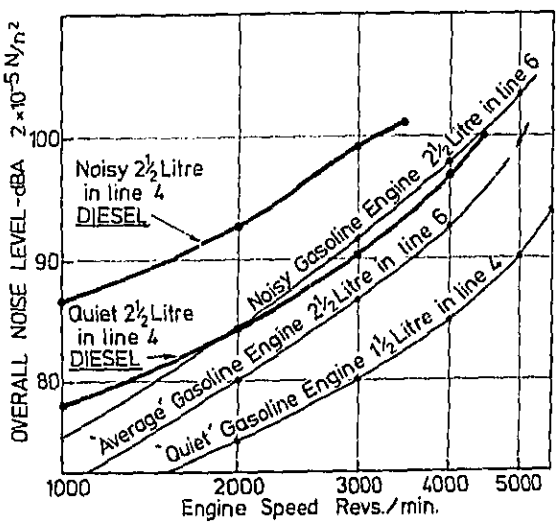

Fig. 1 - Noise of high speed diesel and gasoline engines

DESIGN PHILOSOPHY BEHIND THE ENGINE MODIFICATIONS TESTED

The engine used as a basis for the investigations is the Rover 2½ litre 90.5 mm bore x 87.6 mm stroke indirect injection diesel shown in Fig. 2. This is a 61.5 hp (46 kw) unit rated at

SAE/P-79/80/$02.50
Copyright © 1979 Society of Automotive Engineers, Inc.

4000 rev/min and used in light commercial and cross country vehicles. The block/crankcase is of deep skirted design and the crankshaft is supported in three main bearings. The measured noise balance and cumulative noise reduction for the engine is shown in Fig. 3. As with many small inline engines a great portion of the engine noise is radiated from the engine lower crankcase and sump - some 87% of the total acoustic power on the engine fuel pump side and 49% on the exhaust side. It is therefore clear that structural modifications which should affect noise radiation from the lower crankcase and sump are the primary design aim. Within the constraints imposed by the present production machinery this allows two design approaches.

1. Modifications to the existing crankcase design in the form of internal and external ribbing etc.

2. The design of additional structural components which can be fitted to the existing structure.

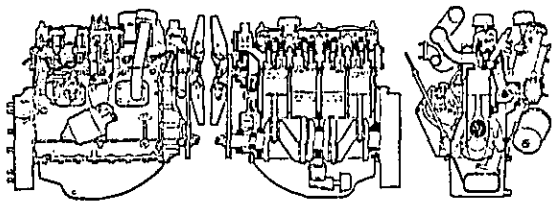

Fig. 2 - Land Rover 2.25 litre 4 cylinder diesel engine

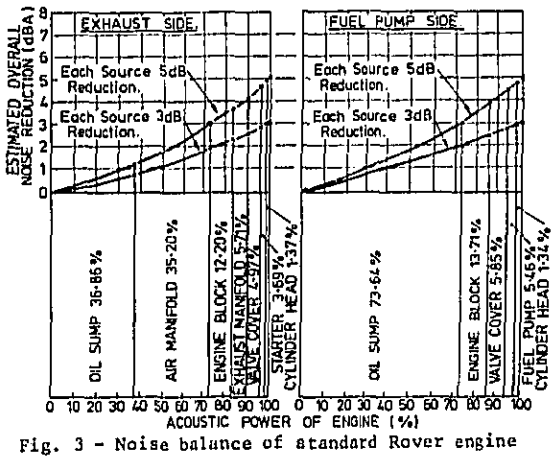

Fig. 3 - Noise balance of standard Rover engine

For the purposes of the investigation it was decided that a five main bearing version of the engine would represent the most that could be achieved by modifications to internal and external ribbing. The incorporation of a cast sump stiffener fitted to and joining the sump flanges would indicate what could be achieved by additional structural components of a 'bolt on' form (Fig. 4). Two sump stiffeners (sometimes referred to as ladder frames (1)*) were constructed, one from cast iron (weight 50 lbs) and one from magnesium (weight 13 lbs), and they were designed to fit either three main bearing or five main bearing engines.

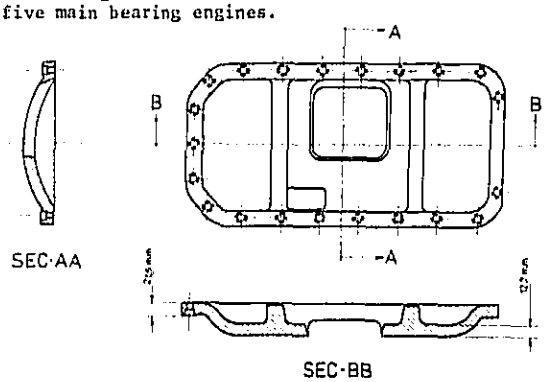

Fig. 4 - Sump stiffener

ASSESSMENT OF THE EFFECTS OF THE ENGINE MODIFICATIONS

Ultimately the overall effects due to the modifications can only be assessed on the running engines. However, there is much that is difficult to assess on the running engine - for example changes to natural frequencies and mode shapes - and therefore rig tests were also carried out with the aim of identifying and measuring the detail changes in noise and vibration. This information could then help in the analysis of future design modifications. Initially it was decided to investigate the response characteristics of modified structures. Previous experience (2), (3), (4), (5) has shown that good mode shapes could be obtained if the block structure alone were tested. Therefore a full mode shape and response analysis was undertaken. This was followed by static stiffness tests, banger tests, running engine (test bed) comparisons and finally vehicle tests.

STATIC STIFFNESS-The engine block with or without cylinder head was supported horizontally by three supports as shown in Fig. 5. A force is applied at the mid-point of the measuring row on the engine block so that the two supports at the two ends of the measuring row and the applied force are in the same vertical plane.

Figs. 6(a), (b), (c) and (d) show the bending stiffness measurements of the three-main and five-main bearing blocks respectively with and without cylinder head. The addition of the cylinder head stiffens the top part of the engine blocks, about an increase of one half of the stiffness at the top edge. The effect of the cylinder head lower down the crankcase can also be seen. Figs. 6(e), (f) and (g) show the bending stiffness measurements of the three-main bearing engine block with the magnesium and cast iron sump stiffener fitted. Since the dimensions of the sump stiffeners are the same the cast iron plate will be four times as heavy as the magnesium one. Since the values of Young's Modulus are approximately in a ratio of 2 to 1, the bending stiffness of the two sump

*Numbers in parentheses designate References at end of paper

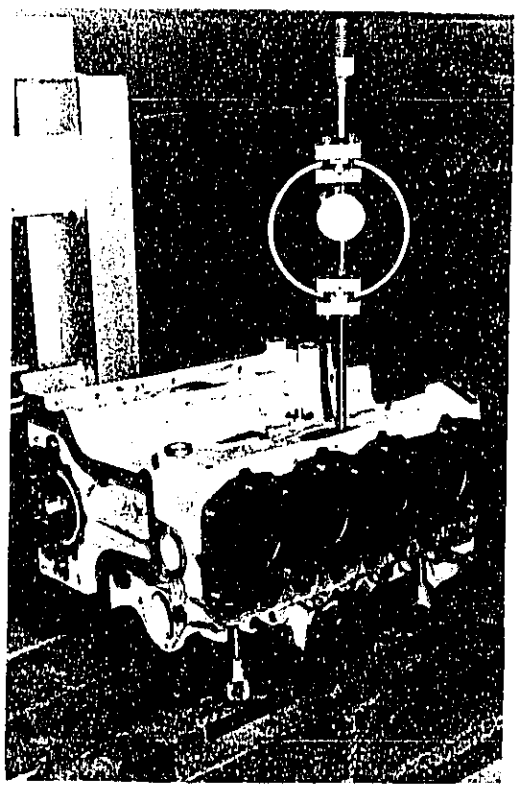

Fig. 5 - The engine bending test system

stiffeners should be of the same ratio as well. Both stiffeners increase the crankcase bending stiffness considerably particularly at the skirt, but influence of the plate on the top part of the engine block was also noticed. The cast iron sump stiffener brings a 4½-fold increase to crankcase stiffness and the magnesium a 3-fold increase as shown in Figs. 6(e) and (f). The measured bending stiffness (simply supported) K can be related to the equivalent area moment of inertia I_e of the engine structure

$$K = \frac{48 I_e}{L^3} \qquad L = \text{engine block length.}$$

The active weight, Wa, of the engine structure for the fundamental bending mode is only a part of the engine dead weight W and can be estimated from the bending frequency, f_B, as

$$f_B = \frac{22.4}{2\pi}\sqrt{\frac{EI_e g}{WaL^3}} \qquad E = \text{Young's modulus}$$

Table 1 shows the measured fundamental bending frequencies, the mean bending stiffness (simply supported) and the calculated active weight for the bending vibration of the two engine blocks.

The maximum measured increase in bending frequency was 39%, provided by a maximum 75% increase in mean bending stiffness. The mass contribution of the additional components bolted onto the block structures (head, sump plate), as shown by the active weight, is a relatively small portion of the total, but the stiffness increases are substantial. Since there is excitation from combustion over the whole audio frequency range, the changes in natural frequency are not sufficient to suppress noise radiation and thus the radiated noise produced will largely be a function of the damping present in the fully built up engine, the ability of a particular mode shape to radiate, and its excitation.

MODE SHAPE ANALYSIS-The resonant frequencies of the freely suspended block and block and head were measured using sinusoidal excitation from a small shaker, measuring the component in quadrature with the applied force. A typical response curve for one point on the engine surface is shown in Fig. 7 showing the frequencies at which mode shapes were measured. The lowest frequency at 570 Hz is the fundamental torsion frequency, the next resonance a 'crankcase mode', (832 Hz) and the next the crankcase fundamental bending (925 Hz). The measured mode shapes for the three bearing and five bearing engine block + head are summarised in Fig. 8 and the first four measured mode shapes shown in Fig. 9. The main differences between three and five main bearing blocks is a general lowering of the natural frequencies in the case of the five-bearing engine plus elimination of the 'crankcase mode' at 832 Hz. An increase in amplitude can also be seen. A comparison of the responses at three different points on the engine blocks is shown in Fig. 10. The 832 Hz resonance is not present in the five-bearing block, but otherwise the general response frequencies and levels are similar.

The effect on the response curves of fitting the sump plates is shown in Fig. 11. Below 900 Hz the effect for both magnesium and cast iron sump plates is extremely marked, but over 1000 Hz there is only an indication of reduced response in the case of the magnesium plate. Above 1000 Hz the cast iron plate shows a considerably reduced response. As a result of the mode shape testing it can be concluded that the response characteristics of the three and five main bearing engines should be very similar, but with the sump plates fitted a reduction in response should occur.

ENGINE TEST BED COMPARISONS

The two engines were mounted on rigid test stands with standard anti-vibration mounts but without gearbox. The exposed rotating flywheel was enclosed in a fibreglass and lead enclosure to reduce its radiated noise. The same valve cover and oil sump were used for both the three main and five main bearing engines. The cylinder pressure of the five main bearing engine was tailored so that the engine block structural vibration and noise emission were compared on the basis of the same combustion excitation levels. This was particularly important in the Rover engine which has proved extremely sensitive to injection timing. The comparisons were made for dynamic timing and not static as backlash produced considerable variation between static and dynamic timings in various engines. The first cylinder of each

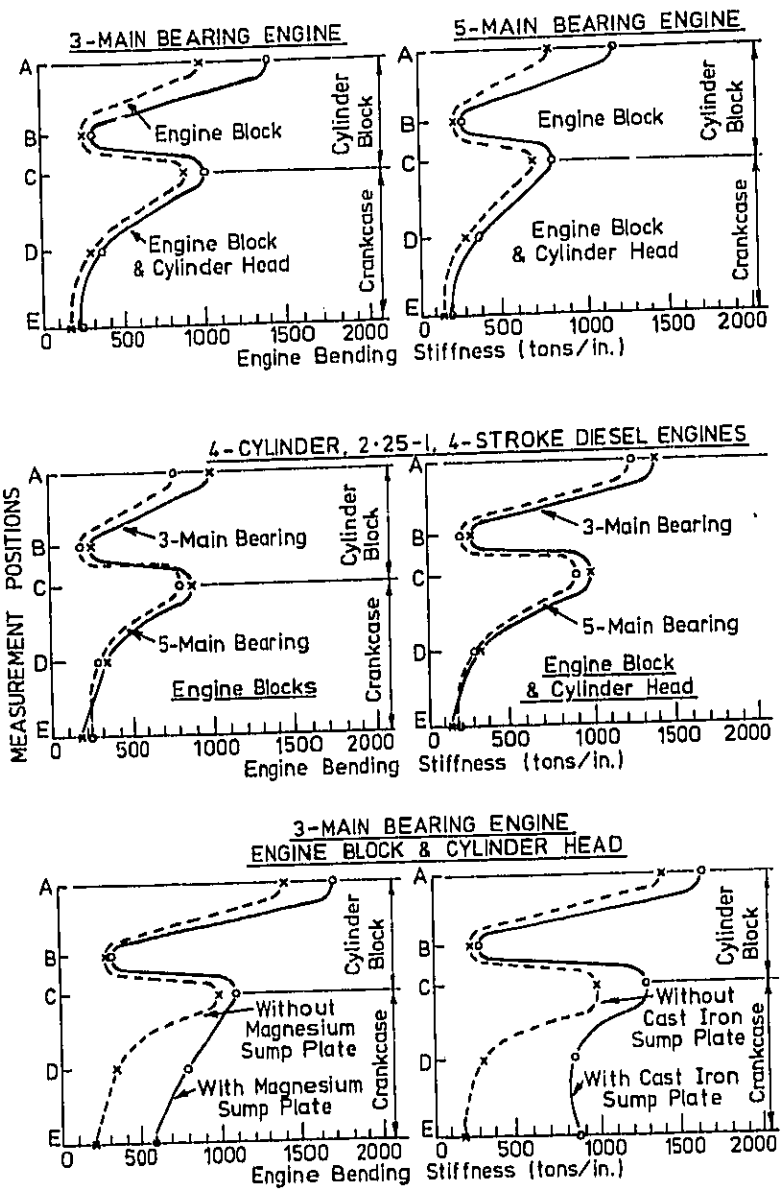

Fig. 6 - Engine bending stiffness

Table 1 - Measured Fundamental Bending Frequency and Mean Bending Stiffness

	THREE-MAIN-BEARING ENGINE				FIVE-MAIN-BEARING ENGINE	
	Engine Block	Engine Block + Cyl. Head	Engine Block + Cyl. Head + Mg. Sump Plate	Engine Block + Cyl. Head + Iron Sump Plate	Engine Block	Engine Block + Cyl. Head
Measured fundamental bending frequency f_B Hz	898 Hz	925 Hz	1251 Hz	1121 Hz	857 Hz	883 Hz
% change in f_B	0.0%	+3.0%	+39.0%	+24.8%	-4.5%	-1.7%
Mean bending stiffness K(Tons/in)	497.8	603.3	869.8	952.7	419.8	570.2
% change in stiffness	0.0%	+21.2%	+74.7%	+91.4%	-15.7%	+14.6%
TOTAL WEIGHT W(lb)	170.0	253.0	266.0	303.0	162.5	245.5
Calculated active weight Wa(lb)	141.5	161.6	127.4	173.8	131.0	167.6
$\frac{Wa}{W}$ (%)	83%	64%	48%	57%	81%	68%

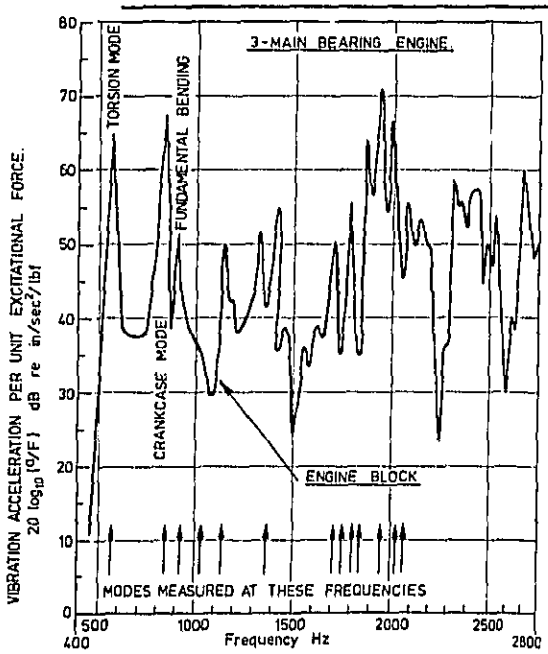

Fig. 7 - Typical engine block vibration response

engine was instrumented with a flush mounted pressure transducer and a needle lift gauge. Fig. 12 shows a comparison of a measured cylinder pressure spectra at 4000 revs/min full load.

EFFECT OF THREE AND FIVE MAIN BEARING DESIGN ON CRANKCASE AND SUMP VIBRATION

The measurement of structural vibration is rather more difficult than noise in that there can be very large differences in vibration acceleration spectra over a very small part of the engine. Because of this the methods previously developed by Chan and Anderton (6) and (7) were used to assess the running engine (8). The average vibration spectra for six rows along the crankcase are shown in Fig. 13 at 4000 rev/min full load. Below 1250 Hz the three main bearing engine is generally of higher vibration level both at the cylinder block and the crankcase. The most interesting frequency region is between 630 Hz and 1250 Hz where the vibration amplitude of the three main bearing engine is well above that of the five main bearing, a difference of 2-4 dB on the cylinder block and up to 13 dB on the crankcase. Above 1250 Hz, the vibration levels of the five main bearing engine are in general slightly higher than those of the three main bearing. Fig. 14 illustrates this effect more clearly. It can be seen that at crankshaft level the increased vibration response of the three main bearing engine between 630-1250 Hz, is due to strong excitation of the crankcase panel mode (measured at 832 Hz for block and head) which

3-MAIN BEARING BLOCK

Frequency (Hz)	Nodal Line Patterns Exhaust Side.	Fuel Pump Side.	Remarks.
582	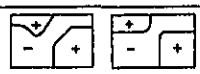		(1,1) Mode, Free-Free Torsional
832			Crankcase Mode
925			(2,0) Mode, Fundamental Bending
1081	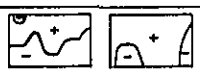		
1253	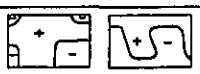		Probably Crankcase Mode
1380			
1727	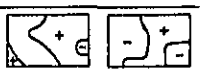		
1757	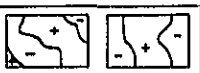		(2,1) Mode Plus Crankcase Skirt Flapping
1806			
1840			Crankcase Mode
1953	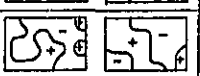		Possibly Crankcase Mode
2006			
2063	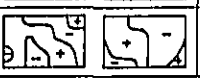		

5-MAIN BEARING BLOCK

Frequency (Hz)	Nodal Line Patterns Exhaust Side	Fuel Pump Side	Remarks.
563	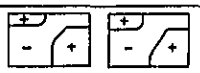		(1,1) Mode, Free-Free Torsional
883			(2,0) Mode, Fundamental Bending
1322	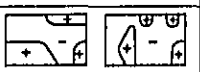		Possibly (3,0) Mode
1516	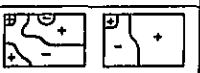		Crankcase Mode
1629			
1791	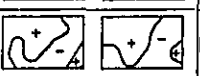		Possibly 
1922			
2480	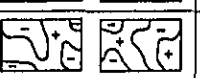		

Fig. 8 - Table of the first few resonance frequencies and mode shapes for three-main and five-main bearing engine blocks

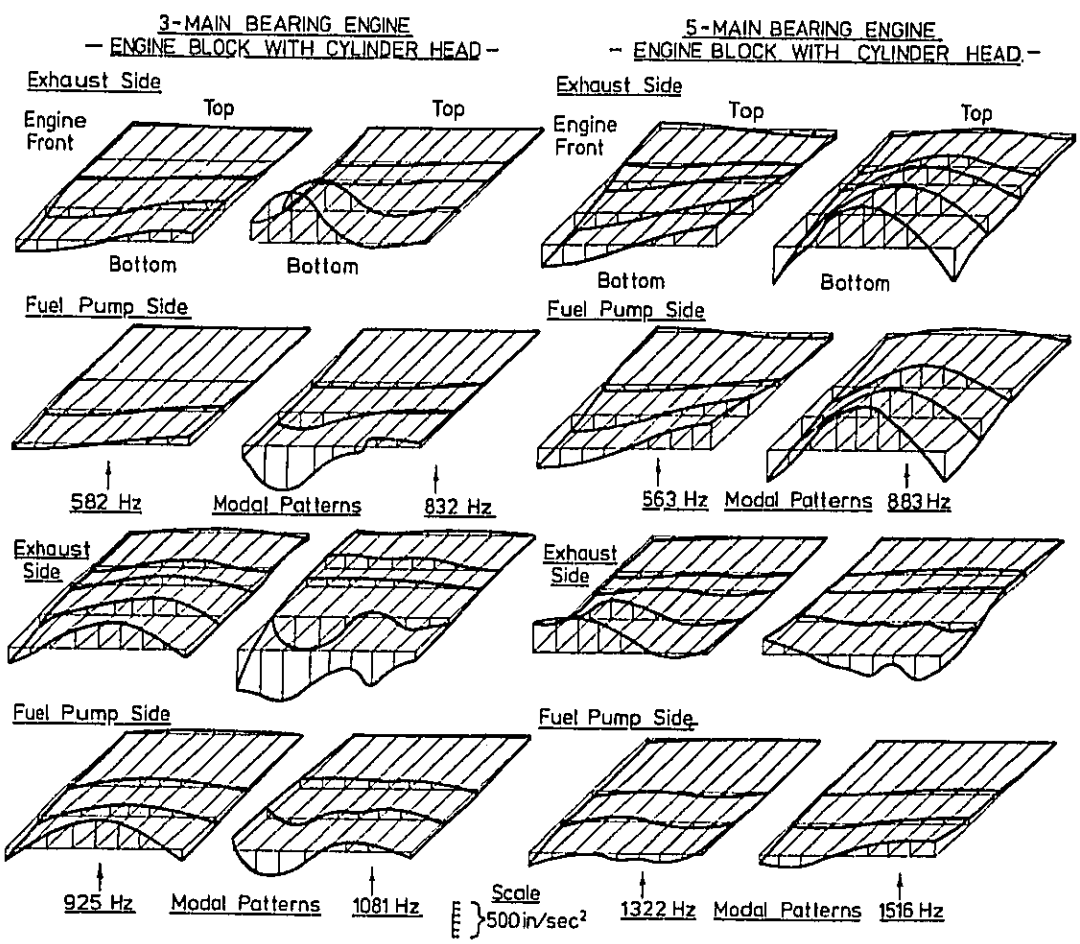

Fig. 9 - First four mode shapes for three-main and five-main bearing engine blocks

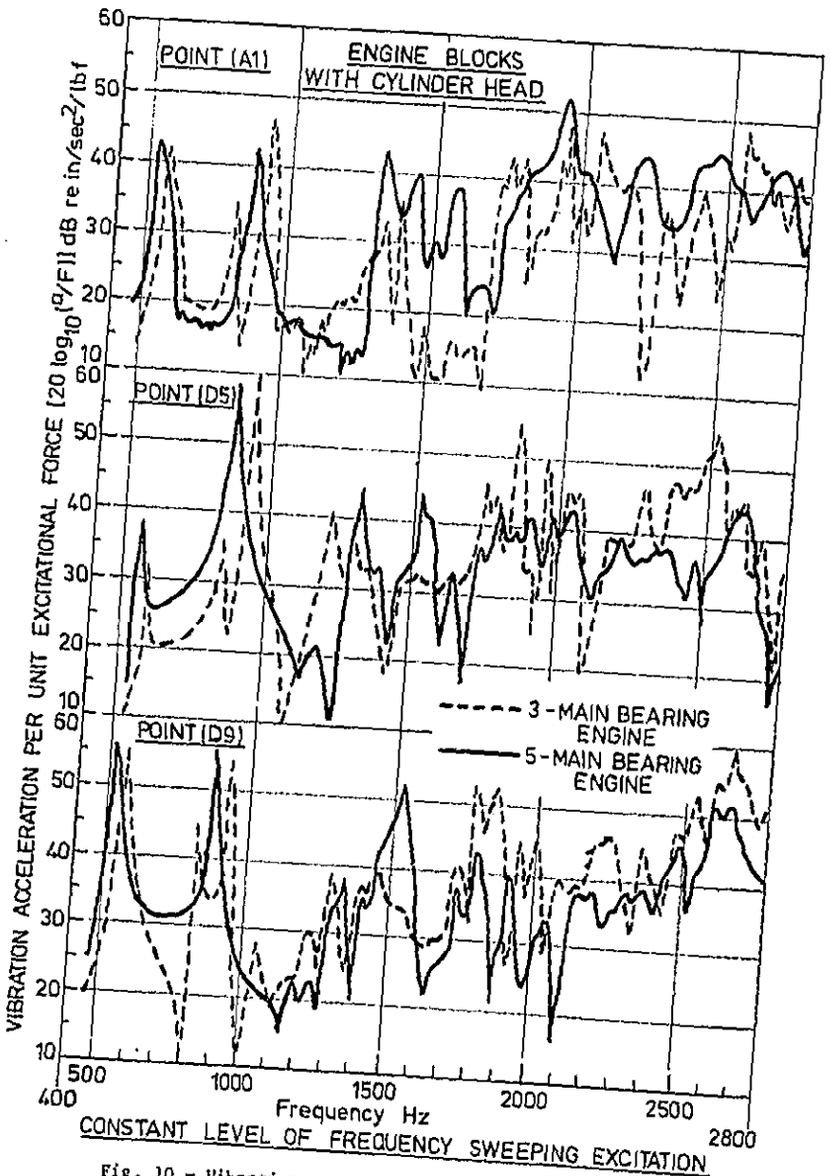

Fig. 10 - Vibration response for the three-main and five-main bearing engine blocks with cylinder head fitted

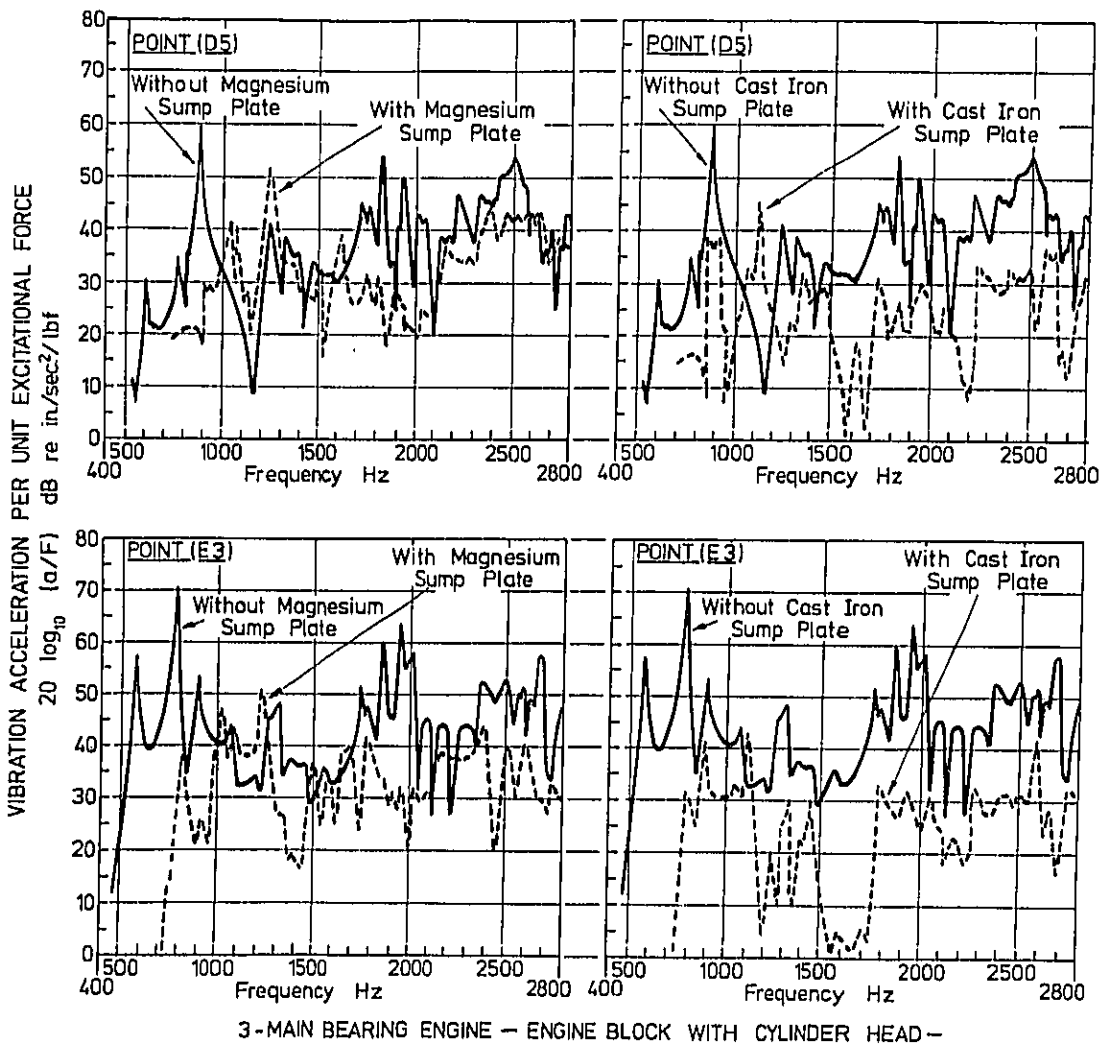

Fig. 11 - Effect of sump plates on engine block vibration response

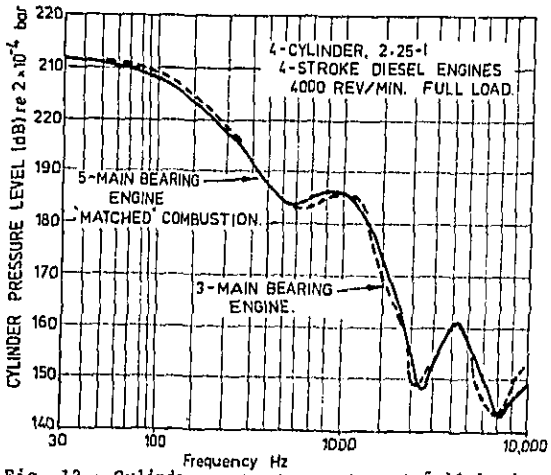

Fig. 12 - Cylinder pressure spectra at full load rated speed for engines tested

is completely suppressed by the introduction of the additional bulkheads in the five main bearing engine. No strong excitation of the fundamental bending mode was found in the running engines. The strong vibration of the crankcase is transmitted to the oil sump (pressed steel) which is a weak structure compared to the block. Fig. 15 shows the comparison of vibration spectra of the oil sump for the two engines. In general, the vibration spectra of the three main bearing engine are well above those of the five main bearing engine particularly at 500-1250 Hz where movement in sympathy with the crankcase mode of the three main bearing engine occurs. The predominant peaks of the oil sump are in the frequency range 1000-3150 Hz.

COMPARISON OF ENGINE NOISE - THREE AND FIVE MAIN BEARING ENGINES

Comparison of the noise spectra for the two engines at 4000 rev/min full load are shown in Fig. 16 after the combustion tailoring process. The overall noise level of the three main bearing engine is 2 dBA higher than the five main bearing engine on the exhaust side and 1.5 dBA higher on the fuel pump side. The difference in noise spectra occur primarily in the frequency range 630-1250 Hz, as was observed for the crankcase vibration. The noise differences were observed throughout the speed range.

EFFECT ON ENGINE NOISE OF ADDING THE MAGNESIUM SUMP PLATE

The effect of the sump plate on engine noise at 4000 rev/min full load was measured for the quieter five main bearing engine and the measured noise spectra are shown in Fig. 17. The plate reduces engine noise by 1.5 dBA on either side of the engine. The reduction occurs over quite a wide frequency range from 800 to 5000 Hz. Again the reduction in noise was found to occur at all engine speeds. The effect of the engine structural modifications on running engine noise at 4000 rev/min full load can be summarised as in Table 2.

Table 2 - Noise Reductions Obtained on the Test Bed at 4000 rev/min Full Load

Engine configuration	Overall noise level at 1m dBA	Overall reduction in noise dBA
Three main bearing engine	101.0-101.5dBA	0
Five main bearing engine (matched combustion)	99.5 dBA	1.5-2.0 dBA
Five main bearing (matched combustion and magnesium sump plate)	98.0 dBA	3.0-3.5 dBA
Five main bearing engine (manufacturer's injection timing & magnesium sump plate)	96.0-97.5dBA	4.0-5.0 dBA

ISO PASSBY TESTS IN A VEHICLE

After the test bed assessments the engines were fitted in a cross country vehicle and the vehicle external passby noise, to ISO R362 and BS 3425:1966 was measured. The results are shown in Table 3.

Table 3 - Engine Noise Reduction achieved on the ISO Passby Test

Engine Condition	Overall noise reduction dBA (average of 6 passby-measurements)
Three main bearing engine	0.0 dBA
Five main bearing engine	2.8 dBA
Three main bearing engine + Mg. Sump Plate	0.8 dBA
Five main bearing engine + Mg. Sump Plate	4.0 dBA

The noise spectra for the maximum noise point during the passby test comparing the three main and five main bearing engines on one side of the vehicle is shown in Fig. 18. Again the major difference in noise occurs between 630 Hz and 1250 Hz as was measured on the test bed. The similarity between engine noise and total vehicle noise measurements shows that in the vehicle, engine noise is predominant.

FURTHER RIG TESTING OF THE THREE AND FIVE MAIN BEARING STRUCTURES

The engine test bed and vehicle measurements have shown a consistent difference between these two engines in the 800-1250 Hz frequency range with both the vibration and noise of the five bearing engine being lower. This is attributed to the removal of the 832 Hz 'crankcase mode' with the five main bearing design. The earlier rig tests (both static and dynamic) - although allowing identification of the mode concerned gave no indication of the actual response which might be expected in the running engine. For instance it might be expected that the fundamental bending mode (at around 900 Hz) would be a major factor controlling noise, if only the modal response of the block and head were used as a guide (Figs. 7, 8,9). Two further rig tests were then completed to find a method of showing, in a rig test, the results obtained on the running engine and vehicle.

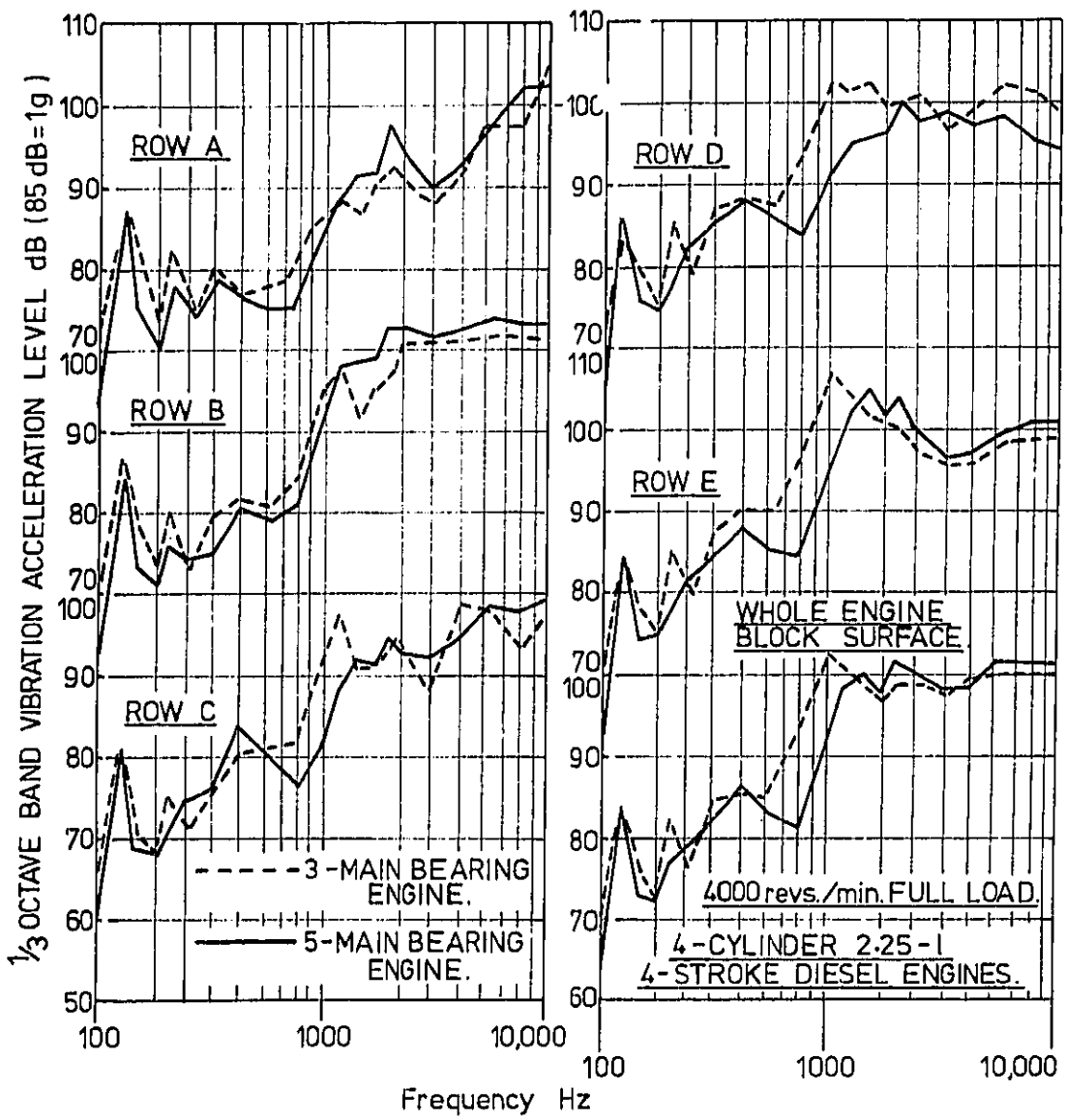

Fig. 13 - Comparison of vibration on running engines

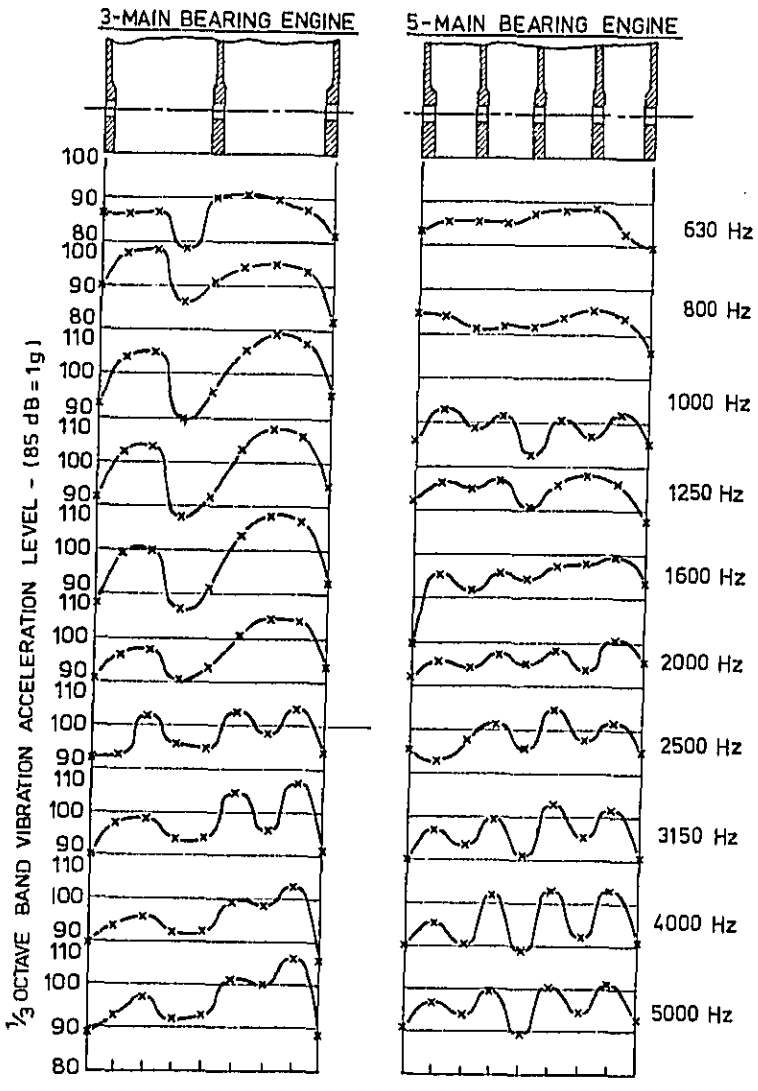

Fig. 14 - Comparison of the time averaged vibration patterns on crankshaft centreline for three and five main bearing engines

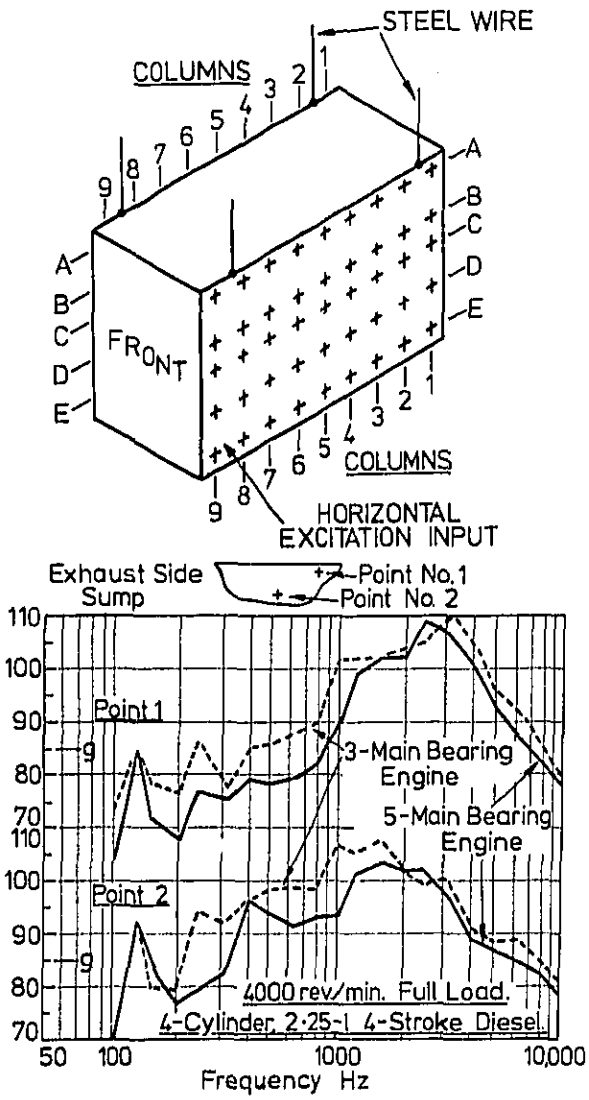

Fig. 15 - Vibration measurement positions and sump vibration for three and five main bearing engines

These tests were firstly to measure the dynamic response of the fully built up engines on the test bed using an electromagnetic shaker and secondly the dynamic response using the 'banger' test (8,9) in which a propane and air mixture is exploded in the combustion chamber of a non-running engine and the resulting structure response assessed.

DYNAMIC RESPONSE OF FULLY BUILT UP ENGINES USING ELECTROMAGNETIC SHAKER

Fig. 19 shows a comparison between the vibration responses for unit force input of the excited three main bearing engine block and cylinder head only and fully built-up engine. The engine block and head were freely suspended but the built-up engine was fixed to the engine test bed with rubber mountings. In both cases the engine was excited at the same point as for the mode shape analysis. When the engine is in the fully built-up condition on the test bed, ready for running, the vibration response under excitation drops tremendously, up to 40dB in the low frequency region, and the damping can be seen to have increased greatly. It is difficult to interpret the structural response at various measurement points to plot the mode shapes, and the fundamental bending mode cannot even be identified. Fig. 20 shows a comparison of the running engine vibration for the three and five main bearing engines with the fully built-up engine response. There can be detected a small increase in response for the three main bearing engine in the fully built-up condition, particularly towards the bottom of the crankcase, but the magnitude is small compared to the running engine measurements. Thus even response measurements on the fully built-up engine structure do not give a true indication of running engine results. This is probably because the input force path and its magnitude is not very representative of the actual engine conditions.

DYNAMIC RESPONSE OF THE FULLY BUILT UP ENGINE USING THE 'BANGER RIG'

The engine structures were in turn excited by means of a gas explosion in the combustion chamber. The response of the cylinder block and piston/crank mechanism was monitored for each engine and then compared. Predetermined quantities of air, oxygen and propane gas were mixed together and fed to the clearance volume of one of the engine cylinders by means of the banger unit. The mixture was then ignited causing a rapid pressure rise in the cylinder. By varying the mixture ratio and pressure both the peak and rate of rise of pressure could be controlled. Thus the effects of the rapid pressure rise part of the diesel cycle was studied on the stationary engine.

A comparison between the running engine vibration and that of the fully built-up when banged is shown in Fig. 21. Although drawn to the same scale, the curves do not have the same datum and so only the shapes of the curves should be compared. Frequencies below 630 Hz were not considered as the vibration levels were beginning to reach those of the background noise (amplifier noise). From 630 Hz to 1000 Hz the response of the three main bearing engine is considerably higher than the five main bearing and the vibration shape shows that it is the crankcase mode which is excited by combustion rather than the fundamental bending mode. From 1250 Hz upwards the reverse is true with the five main bearing engine response being higher than the three main bearing. Comparison with the running engine vibration and noise spectra shown in Figs. 13,14,15 and 16 show that the major trends for the two running engines can be assessed by using the banger rig. The average vibration spectra measured along the crankshaft centre line for the two banged engines are shown in Fig. 22 (c.f. Fig. 13 for running engines). Using this information and correcting for the differences between banger cylinder pressure spectra and that for the running engine the noise levels for the running engines can be predicted.

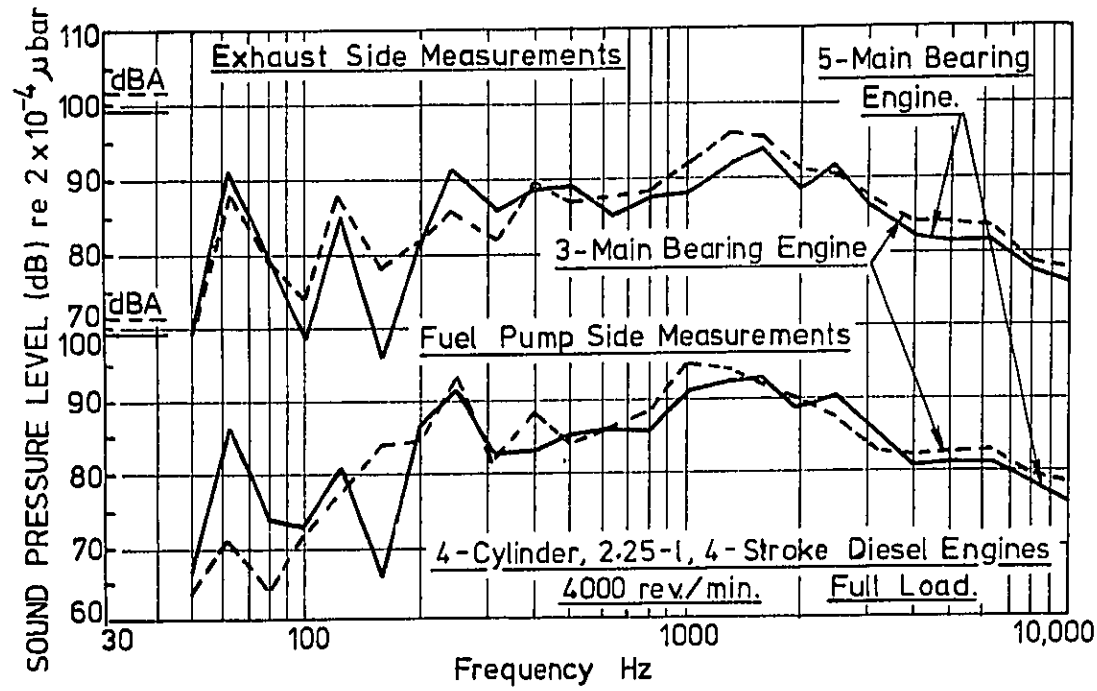

Fig. 16 - Noise measured on the test bed at 1m for three and five main bearing engines

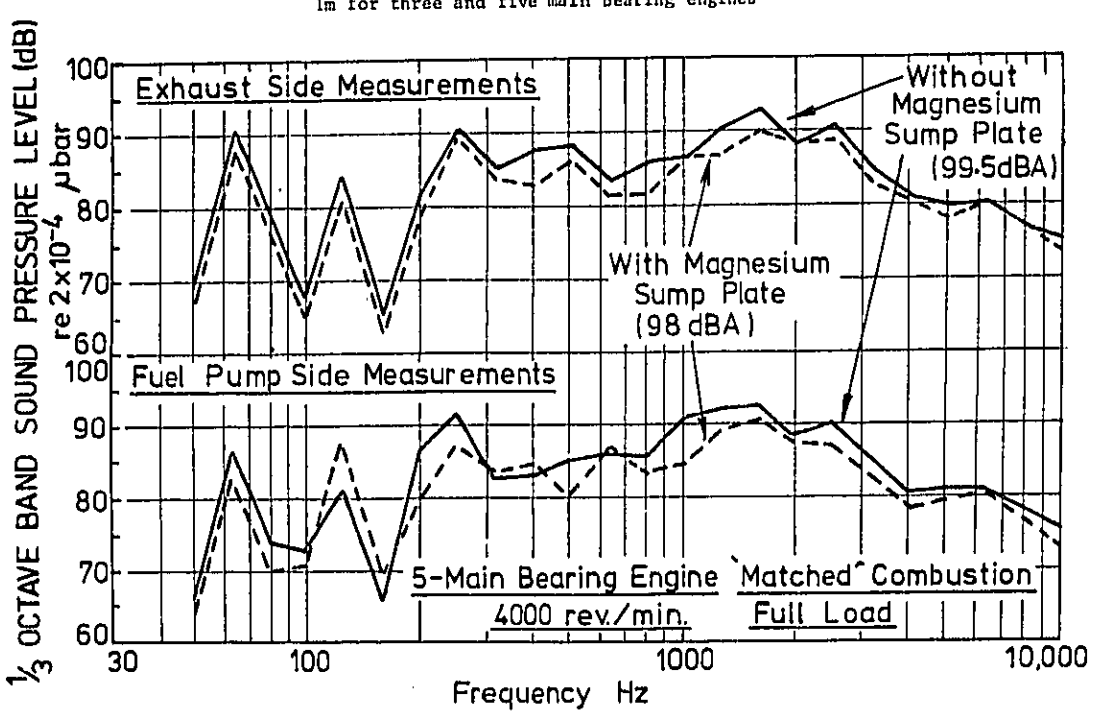

Fig. 17 - Effect of the sump plate on five main bearing engine noise

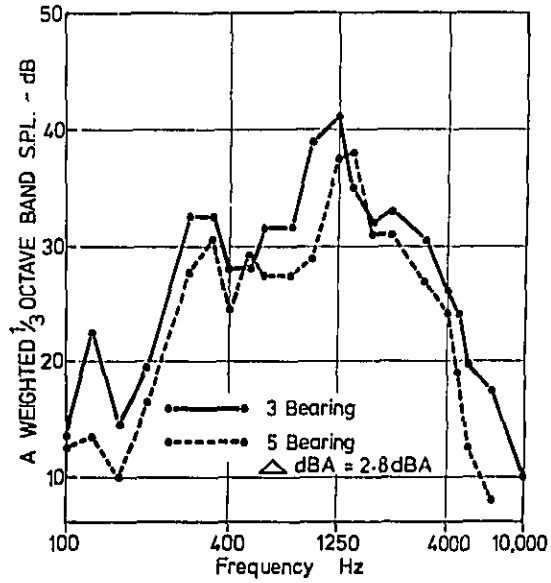

Fig. 18 - Instantaneous ISO passby noise spectra for three and five main bearing engines fitted in the same vehicle

Fig. 23 shows the results. Although only one row of vibration has been used, it can be seen that the banger test has reproduced fairly accurately the 1/3 octave band noise level spectrum for each of the engines, which the shaker tests failed to do.

CONCLUSIONS

1. Structural modifications to a 2½ litre high speed engine have resulted in a 4-5 dBA overall noise reduction at 4000 rev/min full load and over the speed range.

2. This reduction makes the small IDI diesel similar in overall noise level to a current noisy gasoline engine of similar size (Fig. 1).

3. The structural modifications made to the engine crankcase and crankshaft were more effective than the additional bolt on sump plate.

4. The sump plate gave a noise reduction irrespective of the engine block to which it was attached.

5. The major factor giving rise to a noise reduction was the elimination of a crankcase mode which gave rise to high noise radiation over the limited frequency range 630 Hz to 1250 Hz.

6. When vehicle noise is predominated by engine noise the same characteristics are measured during an ISO passby test as are measured on the test bed.

7. Measurements of static stiffness are a useful measure of the fundamental dynamic characteristics of the engine structure, but neither these nor straightforward dynamic response and mode shape testing of partially built engines can be used to predict running engine characteristics.

8. Dynamic response testing of engine structures using the banger technique can be used to assess the likely noise radiating characteristics of running engines. It shows the importance of the rapid pressure rise part of the diesel cycle to the engine noise radiation.

ACKNOWLEDGEMENTS

The authors would like to thank the Science Research Council for its long term support of the work and the Rover Plant of Leyland Cars for the construction and provision of test engines. Thanks are also due to Mrs. G. Pullen for preparation of the manuscript and Mr. P. Prust for preparation of the illustrations.

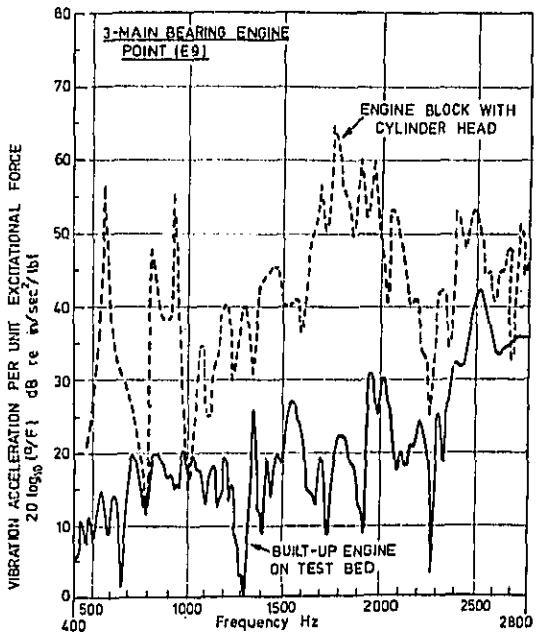

Fig. 19 - Comparison of response between engine block with cylinder head and fully built up engine

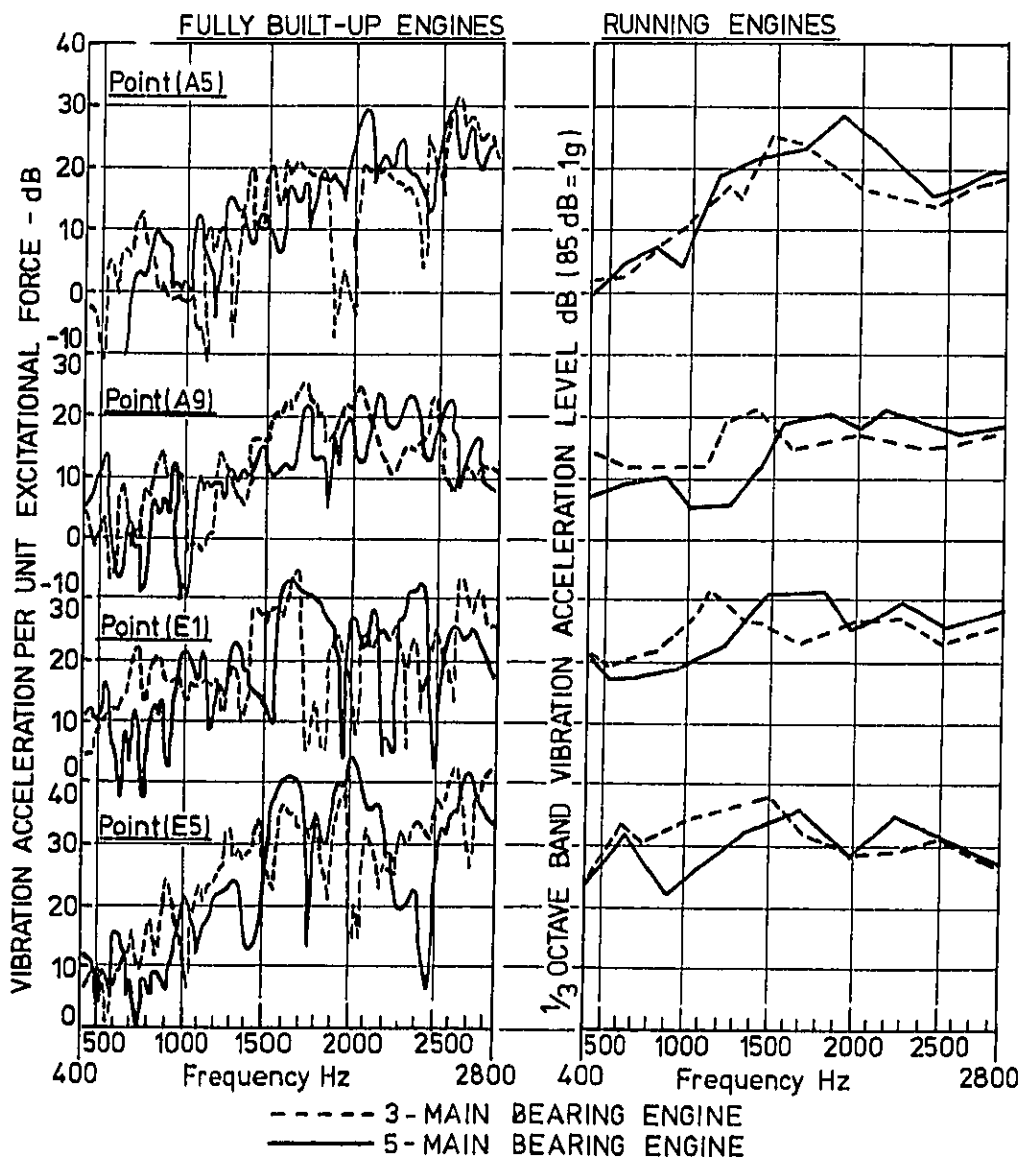

Fig. 20 - Comparison of vibration response and running engine spectra between the 3-main and 5-main bearing engines

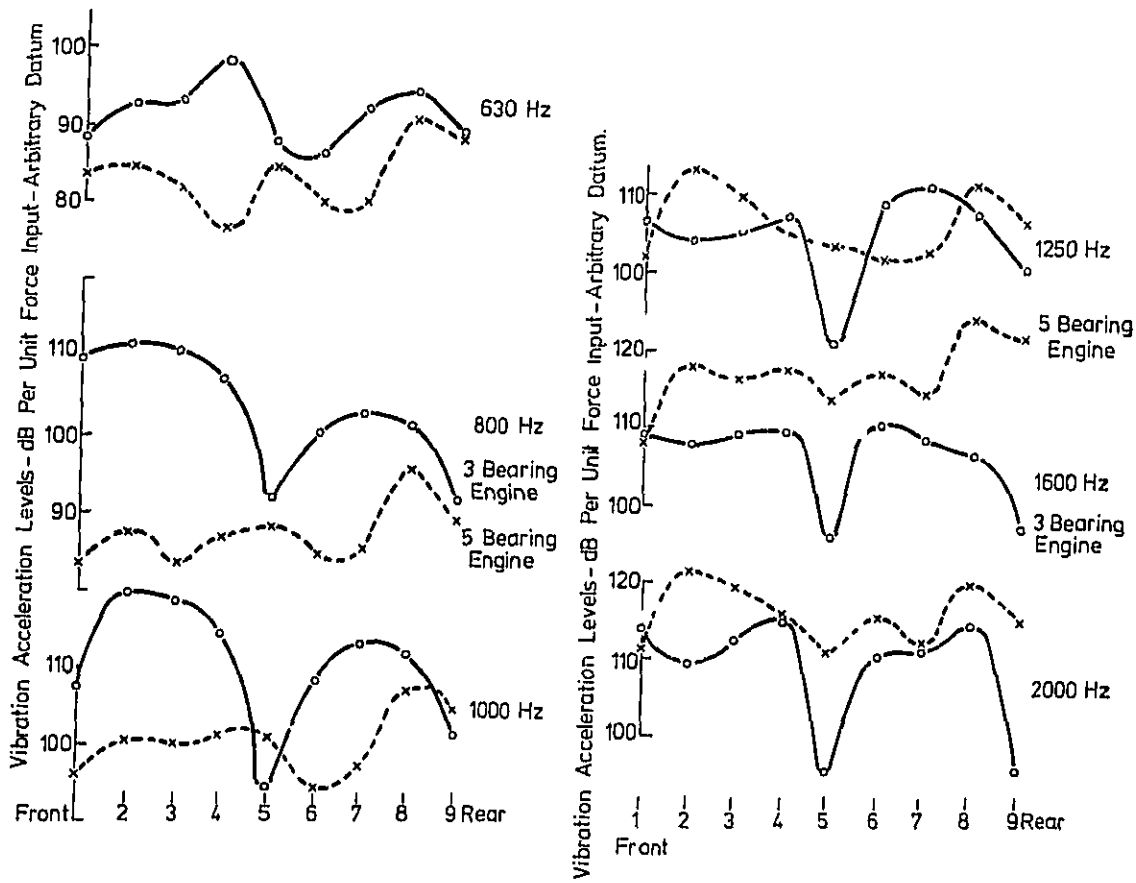

Fig. 21 - Vibration levels along crankshaft centre line for three and five main bearing engines using banger system

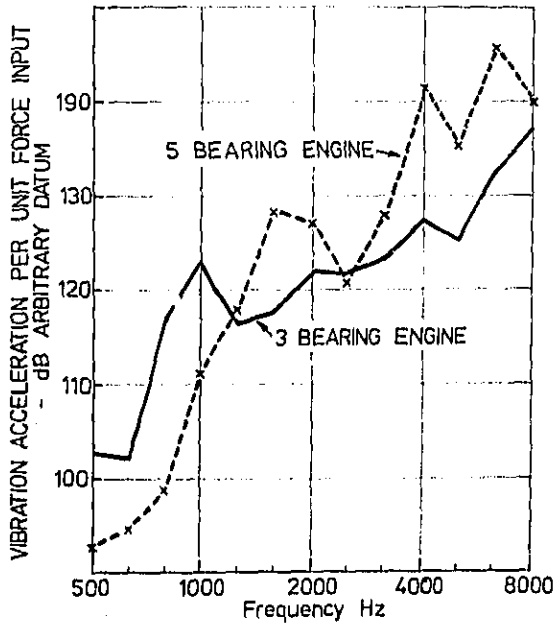

Fig. 22 - Average vibration levels measured on 3 and 5 main bearing engines using the banger system

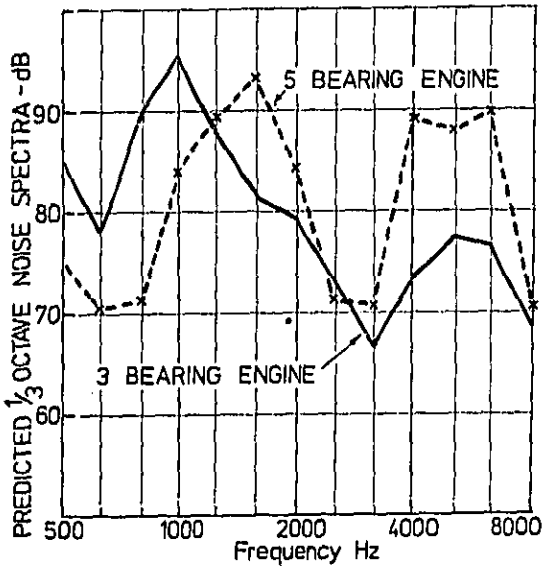

Fig. 23 - Predicted noise spectra of 3 and 5 main bearing engines using the banger system

REFERENCES

1. D. Anderton, T. Priede. "The influence of automotive diesel engine design on combustion, noise and performance". U.S. Department of Transportation conference "Transportation diesel engine fuel economy optimisation". September 1977.

2. M.G. Hawkins and R. Southall. "Analysis and prediction of engine structure vibration". SAE Paper No. 750832.

3. N. Lalor, M. Petyt. "Modes of engine structure vibration as a source of noise". SAE Paper No. 750833.

4. K. Ochiai, M. Aisaka, S. Sakata. "Single model technique for better understanding of diesel engine vibration and noise". SAE Paper No. 750834.

5. R.S. Lawe, S.E. Timour, G.W. Hawkins. "Techniques of structural vibration analysis applied to diesel engine noise reduction".

6. C.M.P. Chan, D. Anderton. "The correlation of machine structure surface vibration and radiated noise". Internoise conference, 1972.

7. C.M.P. Chan, D. Anderton. "Correlation between engine block surface vibration and radiated noise of inline diesel engines". Noise Control Engineering, p.16-24, Winter 1974.

8. C.M.P. Chan, D. Anderton, T. Priede. "Low noise design data for automotive industry". ISVR Memorandum No. 562, September 1976.

790445

Some Aspects Concerning Noise Reduction on Diesel Passenger Cars

Hans-Peter Charzinski and Hermann Hiereth

Daimler-Benz AG

ABSTRACT

The main noise sources of a diesel passenger car are determined and possible noise level reductions are assessed. Primary damping measures such as influencing it by means of modifying the combustion itself as well as secondary measures such as encapsulation are described. A vehicle-supported encapsulation of the engine utilizing parts of the body is discussed in more detail. A research vehicle was built. A description of design function, and practical realization of such a vehicle-supported encapsulation including the necessary development of a new cooling system is given. Finally, the maximum possible reduction of the external noise levels using this design as well as the problems connected with encapsulation - such as the resulting increase in internal vehicle noise and vehicle weight, reduced ground clearance and maintenance accessibility - are reported and critically evaluated.

INTRODUCTION

In view of dwindling crude oil reserves the risen demand for engines with high thermal efficiency is obviously justified.

At present, the Diesel engine complies with this requirement in the best possible way. Outside the U.S., it has since 50 years been the standard engine in the commercial vehicle sector, and it is now increasingly used also as a power plant for passenger cars.

However, one disadvantage of the Diesel engine is its higher noise level compared to that of the gasoline engine. Yet an increasing concern for the environment and ever growing numbers of vehicles on the road together with the effects on account of the downsizing efforts of U.S. cars call for future vehicles with reduced noise levels. Besides, the new future test procedure for external vehicle noise in the U.S. calls for uniform acceleration from a standing start thus biasing Diesel cars, which traditionally have less power installed.

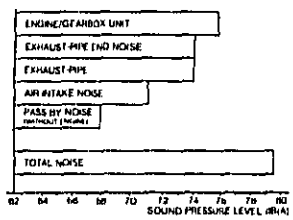

Fig. 1 - Main noise sources of a Diesel passenger car

Therefore it is necessary to investigate all the theoretical possibilities of reducing the noise level of passenger cars with Diesel engines with regard to their practicability.

The following is a report on work carried out toward that goal.

MAIN NOISE SOURCES OF DIESEL PASSENGER CARS

The noise test results in Fig. 1 show the main sources contributing to the total noise of the Diesel passenger car. The individual noise components were determined using the ISO R 362 standard test procedure (maximum acceleration in 2nd gear from 50 km/h, gear selector in position "L"), and evaluating the maximum values of the noise level occuring during the complete test distance. In order to determine these individual components, the other noise sources were in each case elimated by expensive and extensive encapsulation of engine, transmission, and exhaust pipe, and by the use of total silencers for intake and tailpipe noise.

The major part of the total noise of 79.5 dB(A), namely 76 dB(A), is produced by the engine/transmission unit, followed by the exhaust noise and tailpipe ondnoise of 74 dB(A) each and the intake noise of 71 dB(A).

SAE/P-79/80/$02.50
Copyright © 1979 Society of Automotive Engineers, Inc.

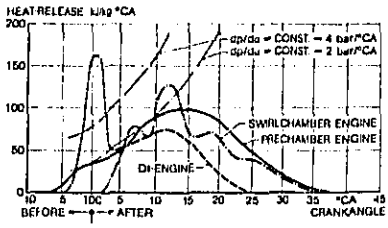

Fig. 2 - Heat release and pressure rise comparing prechamber, swirl chamber and direct injection systems

The pass-by noise (with the engine turned off) of 68 dB(A) measured at an average speed of 50 km/h is negligible considering the fact that the total noise level is relatively high and that its value lies more than 10 dB below the total noise value.

This statement, of course, no longer applies if noise-reducing measures are taken. The extent to which the influence of the pass-by noise increases in this case will be discussed later.

This breakdown into individual noise sources reveals the sequence in which any measures for an effective reduction of the total noise level must be taken since the latter is always determined by the loudest noise component.

ENGINE - As the engine with its intermittent combustion represents the primary noise source, it was first attempted to find out to what extent measures carried out directly on the engine itself contribute to the reduction of the total noise produced by the vehicle.

The type of combustion system is of decisive importance for the combustion noise of a passenger car Diesel engine, since the heat release pattern determines the combustion pressure rise rate over the crank angle ($dp/d\alpha$) and thus the acoustic energy emitted by the engine in terms of both internally transmitted and air-borne sound.

Fig. 2 shows the heat release diagrams of the three respresentative CI-combustion systems, namely the prechamber, the swirl-chamber and the direct injection system.

Also plotted are lines of equal pressure rise rate in accordance with the heat release formula

$$\frac{dq}{d\alpha} = \frac{1}{\varkappa - 1}\left[v \cdot \frac{dp}{d\alpha} + \varkappa p \frac{dv}{d\alpha} \right]$$

As regards pressure rise, which according to some authors, Ref. 1* and 2, can for all practical purposes, be used as an indicator of the combustion noise, the indirect combustion systems using a divided combustion chamber are much favorable than the direct injection system with the prechamber system featuring the lowest pressure rise rate.

Therefore, despite the clear advantages of the direct injection system with regard to fuel consumption, Daimler-Benz has always preferred the prechamber system for the passenger car Diesel engine for reasons of comfort and noise, while all other manufacturers of Diesel cars use the swirlchamber system.

The mechanical noise produced by a Diesel engine can be reduced somewhat by modifications to the valve timing gear and to the injection pump [3] as well as by minimizing the piston clearance by using a termocontrolled piston [4].

A coating of the cylinder head cover and of the oil pan and, if necessary, their elastic separation from the engine load to a further reduction of the noise emission from the surfaces of these parts [5].

While all these direct measures result in a noise level reduction of 5 to 6 dB on the test bed, their effect is hardly measurable in the vehicle during the ISO test, i.e. during the accelerated drive-by test. This may well be a "deficiency" of the test procedure.

Therefore, in order to achieve a marked noise level reduction, it is necessary to encapsulate the engine.

POWER TRAIN - The entire power train - engine, clutch, transmission, drive shaft, differential and rear axle - internally transmits sound via the suspension points into the body where some of it is emitted to the vehicle interior and some to the outside in the form of air-borne sound. In order to keep this solid-borne sound emission as low as possible, it is necessary to optimize each component individually and in particular the interaction of the individual components.

*References appear at end of paper.

Engine, clutch and transmission as a unit must be as rigid as possible in order to keep the vibration amplitudes small and the natural frequencies high.

Engine and transmission mountings must be located at points where bending stresses are lowest, i.e. at nodal points of vibration. The same requirement applies to the supports of the driveshaft. With regard to the transfer of sound from the engine into the driveshaft, the automatic transmission has clear advantages over the manual gearbox because of the damping effect of the hydraulic torque-converter.

TAIL PIPE NOISE - The tail pipe noise measured at an angle of 45° and 22 cm away from the tail pipe end must be reduced by large-volume exhaust mufflers and by tuning the length of the end pipe after the main muffler.

EXHAUST PIPE - The transmission of solid-borne sound from the engine into the exhaust pipe can be reduced by isolating the exhaust system by means of a compensator between the exhaust manifold and the exhaust pipe. Encapsulation or double-wall exhaust pipes and mufflers add to the reduction of noise generated by the pulsation of the exhaust gas [6].

INTAKE NOISE - Large volume air cleaners and damper filters as well as flexible and soft air ducts with generously dimensioned cross sections contribute to reduce the flow noise on the intake side of the Diesel engine.

FAN NOISE - The problem of fan noise can be overcome today by temperature - and speed - controlled viscous-type fan couplings.

PASS-BY NOISE - On Diesel cars of the present generation, the pass-by noise lies so much below the total noise level during accelerated drive-by that it does not affect the measurement of noise on todays production cars.

WIND NOISE - At driving speeds below 50 mph, wind noise can nowadays be neglected once the body has been optimized appropriately in the wind tunnel.

ENGINE ENCAPSULATION

As mentioned above, direct measures on the engine itself, such as the improvement of the combustion process, the mechanical parts and the gas cycle

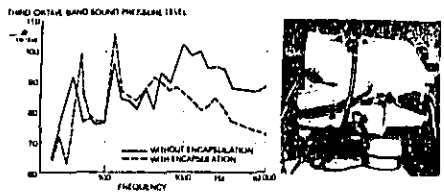

Fig. 3 - Encapsulation of a 2.4 L-Diesel engine noise at rated power (n = 4200/min)
Measuring distance: 1 m in front of the engine

are not sufficient to reduce the dominant noise from the engine itself such that it shows pronouncedly in the vehicle noise test.

A noticeable reduction in the emission of air-borne sound from the engine can only be achieved by additional sound damping measures on the engine.

Possible alternatives for damping air-borne sound from engines are

- partial encapsulation
- complete encapsulation of the engine with the capsule attached to the engine
- complete encapsulation of the engine with the capsule supported by the vehicle.

PARTIAL ENCAPSULATION - A partial encapsulation or covering of individual noise-emitting surfaces is particularly interesting from the point of view of cost, although, of course, its effect is much lower than that of encapsulation of the complete engine [7].

Covering individual portions and components of the engine, such as the belt drive, timing gear cover and injection pump with close-fitting covers results in noise level reductions of 5 to 7 dB when the measurement is taken on the engine test bed at a distance of 1 m from the engine, whereas during accelerated drive-by with the units installed in the vehicle a noise level reduction of only 1 to 2 dB is found.

ENGINE-ATTACHED ENCAPSULATION OF COMPLETE ENGINE - Fig. 3 depicts a fully encapsulated 2.4-Liter Diesel engine and the noise levels measured on the test bed 1 m away from the engine.

The principle of an engine-attached encapsulation is based upon the

excellent damping and insulation properties of a thin-walled casing for the entire engine with only little clearance between the capsule and the engine surface. The capsule components are secured by an intermediate frame which is sound-isolated from the engine by means of rubber elements. A defined flow of cooling air is passed through the inside of the capsule.

In the lower frequency range the acoustic effect is achieved by more isolation of sound in the medium and upper frequency ranges by means of interference damping.

Basic work in this field was carried out by List, [5, 8] at his institute in Graz under contract of the "Forschungsvereinigung für Verbrennungskraftmaschinen (FVV)".

As can also be seen from our test results, noise levels in the frequency range from 500 Hz to 10 kHz can be reduced rather remarkably with the dry capsule shown here, but definite level increases will occur at lower frequencies. These are caused by resonances resulting from the mechanical-elastic properties of the sound isolating support elements.

The following additional problem areas with respect to engine-attached encapsulation have yet to be solved:

- accessibility to the engine for maintenance purposes
- durability of capsule and rubber supports with regard to vibrations, temperature and oil-resistancy
- incorporation of the transmission
- accessory drives
- control and supply line openings
- sealing quality and insulation against solid-borne sound
- cooling of engine, injection pump and acessories
- tuning of capsule resonances to vehicle resonances
- introduction of solid-borne sound from the engine into the body via the supporting elements
- weight
- cost
- space

Besides dry capsule version, where a full casing is provided for an existing engine, capsules for newly developed engines can be split up into a wet and a dry section. The oil pan of a so-called skeleton engine is soundisolated by means of an elastic intermediate frame. The upper part of the engine is encapsulated in sheet metal shells attached to the same auxiliary frame forming the dry section. Thus some of the problems occuring with the engine-attached capsule can be eliminated by separating the capsule supporting from the sealing function.

When the capsule is applied to passenger cars there will undoubtedly remain the drawback of noise peaks in the lower frequency range which may cause unpleasant humming noises in the vehicle interior and which are difficult to eliminate.

VEHICLE-SUPPORTED COMPLETE ENCAPSULATION OF ENGINE - For reasons of function and weight it appears to be favorable, in particular for passenger cars, to use a capsule version which on the one hand utilizes body components as capsule elements and on the other hand avoids the problems arising from the engine supporting and soundisolating elements, namely the resulting noise peaks at low frequencies, by attachment of the complete capsule to the body.

In addition to this and in contrast to the engine-attached encapsulation this version simplifies maintenance because of easier access to the individual engine components and accessories, while durability of the capsule components is improved due to more favorable design and reduced vibration. Another advantage is the clearly lower cost when body components are used as capsule elements.

In general, the vehicle-supported capsule must be designed with the following criteria in mind:

- incorporation into the capsule design of all vehicle components which are suitable for this purpose, such as hood, firewall, and wheelhouse covers
- additional shells to cover the lower end of the engine compartment plus transmission, attached to the vehicle
- suitable sound-absorbing channels for the cooling air.

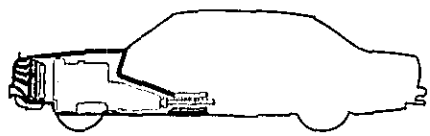

Fig. 4 - Engine compartment encapsulation
Basic sketch of vehicle-supported capsule

Fig. 5 - Engine compartment encapsulation
Air inlet gate

Fig. 6 - Engine compartment encapsulation
Cooling air absorption path rear end

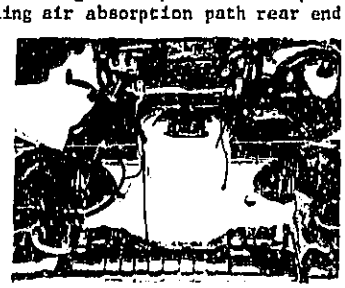

Fig. 7 - Engine compartment encapsulation
Engine compartment without engine

The main effect of a vehicle-supported encapsulation is the reduction of external noise achieved through insulation, damping, and reflection both when the vehicle is stationary (i.e. idling at normal or higher engine speeds), and under accelerated drive-by conditions.

Of course, in any kind of capsule design the noise level inside the capsule increases due to lack of sound dissipation. In the case of the vehicle-supported capsule this leads automatically to an increase of the noise level inside the passenger compartment. For this reason additional measures are required to retain the internal noise at the acceptable level of todays standard production vehicles.

RESEARCH VEHICLE WITH VEHICLE-SUPPORTED CAPSULE - In accordance with Fig. 4 and the above design criteria a 2.4-Liter Diesel passenger car was equipped with a vehicle-supported encapsulation for research purposes.

Some major points of this research project will be commented in more detail below.

COOLING AIR SYSTEM - In order to prevent air-borne sound from escaping to the outside via the inlet and outlet openings required for the cooling of engine coolant, engine oil and automatic-transmission fluid and those for engine compartment ventilation, the corresponding sound absorption paths were optimized in preliminary tests. Flow measurements were carried out to determine pressure drop, the most favorable shape and material combinations were selected by measuring the absorption coefficient in a sound box, and the required flow areas were determined.

Fig. 5 depicts the air intake gates on the research vehicle, Fig. 6 shows the underfloor layout with the air outlet ducts, and Fig. 7 the inside of the capsule, i.e. the engine compartment, without the engine installed.

COOLING SYSTEM - In the initial stage a conventional cooling system comprising a downdraft core type radiator together with an axial fan was used. In addition to this, an external crossdraft radiator was mounted outside the capsule and below the frontal cross member, which - without an additional fan - accounted for approx. 30 % of the cooling capacity.

Cooling capacity measurements carried out with this system, however, revealed excessive coolant temperatures occuring under specific driving conditions, i.e. particularly at maximum speed and at idle.

Thus a new cooling system had to be developed in order to satisfy the increased cooling requirements and the additional pressure requirements imposed upon the cooling fan due to the complete encapsulation of the engine

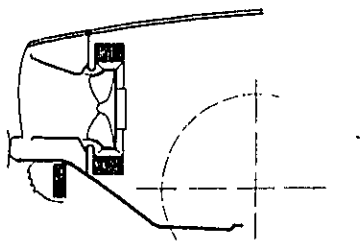

Fig. 8 - Cooling system
Annular radiator/radial flow fan

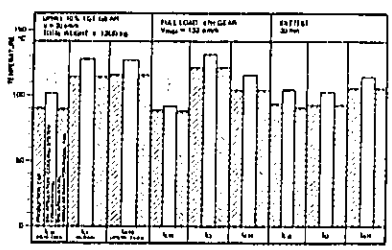

Fig. 9 - Measurement of cooling capacity, results

compartment up to the rear end of the transmission, and because of the smaller air flow sections and the sound absorption paths.

This new cooling system, as shown in Fig. 8, was designed in cooperation with the Behr Corp., and features a combination of an annular radiator with a radial fan, since the radial fan not only produces higher pressures but also exhibits a noise level ranging approx. 6 dB below that of an axial blower with identical performance, measured at 1 m distance.

The flow noise and the power absorbed by the fan can be reduced further by controlling its speed as a function of temperature and engine speed.

With this modified cooling system tests for cooling efficiency were conducted in the wind tunnel. The results for an uphill driving condition, maximum speed and idle are recorded in Fig. 9.

When the conventional cooling system supplemented by an external radiator was used, the coolant temperatures in the vehicle with encapsulation rose to unacceptable levels after the engine was shut off, particularly following maximum speed and idle tests.

With the annular radiator and radial fan combination, however, the

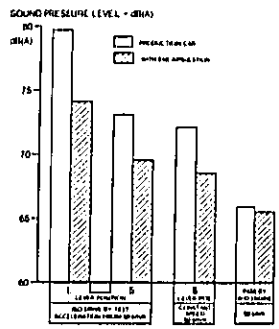

Fig. 10 - Exterior noise

measured temperatures remained within the permissible limits for current non-encapsulated vehicles.

EXHAUST SYSTEM - In order to keep the introduction of solid-borne sound from the engine into the exhaust system to a minimum, a compensator connector was installed between the exhaust manifold and the exhaust pipe.

The emission of sound from the exhaust system induced by exhaust gas pulsation was reduced by encasing the pipes and by using double-walled mufflers.

To reduce tail pipe end noise, additional muffler volume was provided, and the tail pipe length optimized.

RESULTS - The following noise levels were recorded with the research vehicle described above.

EXTERNAL NOISE - Fig. 10 shows the results of external noise measurements under conditions of accelerated drive-by as defined by ISO R 362. These values refer to an encapsulated vehicle with conventional cooling system and an additional external radiator.

In both test series, the vehicle was equipped with automatic transmission.

With the gear selector in "L" which corresponds to 2nd gear a noise level reduction from 79.5 dB(A) to 74 dB(A) was achieved. In "S" (3rd gear) the drive-by noise level was reduced by 3.5 dB from 73 dB(A) to 69.5 dB(A). The same difference resulted when driving at a constant 50 km/h in "S". The drive-by levels of 73 dB(A) of the standard vehicle and 68.5 dB(A) of the encapsulated vehicle in these cases are only 1 dB

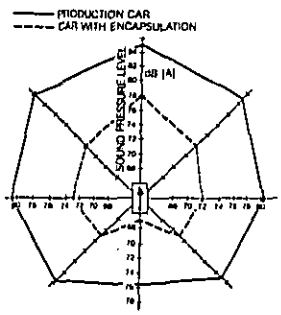

Fig. 11 - Engine compartment encapsulation
Distribution of external noise
7 m distance, n = 4200/min

lower, because the engine speed increase during accelerated drive-by is relatively small for the low powered Diesel vehicles.

The interesting point here is, that on the encapsulated vehicle at a speed of 50 km/h the pass-by noise with the engine switched off of approx. 66 dB(A) now has the same level as the noise generated by the engine, measured under conditions of accelerated and steady-speed drive-by. Engine noise is, therefore, no longer a determining factor for the total noise level, since the addition of two noise sources of the same noise level results in a total-level increase of 3 dB.

Thus the best possible noise level reduction is achieved, inasmuch as the sum of all vehicle noise sources equals the pass-by noise with the engine turned off.

NOISE DISTRIBUTION - Fig. 11 shows the results of the noise distribution around the car recorded at rated engine speed (n = 4200/min) at a distance of 7 m from the stationary research vehicle.

The noise level reductions at the sides, front and rear amount to an average of 6 dB and represent the maximum possible noise reduction.

INTERNAL NOISE - In Fig. 12 the noise in the vehicle interior was recorded as air-borne sound at the location of the front passenger head. In third gear, the noise level of the encapsulated vehicle above an engine speed of 3850/min is higher than that of the standard vehicle. As mentioned above, the fact that the noise level inside the capsule is increased due to lack of noise dissipation must lead to an increase in noise in the passenger compartment.

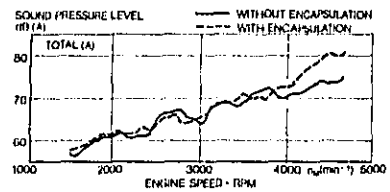

Fig. 12 - Internal noise sound level recorded at front passenger head location third gear, road load

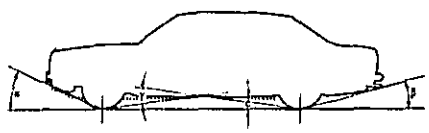

	GROUND CLEARANCE c	ANGLE OF APPROACH α	ANGLE OF DEPARTURE β	RAMP ANGLE γ
PRODUCTION CAR	184 mm	24°	18°	14°
ENCAPSULATED VERSION	134 mm	18°	18°	14°

Fig. 13 - Ground clearance
Angle of approach and departure ramp angle

In the meantime, the internal noise level has been reduced to the usual level of todays standard production vehicles by means of additional modifiactions of the vehicle itself.

PROBLEM AREAS - The following problems concerning the concept of vehicle-supported encapsulation have yet to be solved satisfactorily:

- Reduction of noise level in the passenger compartment to below the values achieved by present production vehicles
- avoiding the temperature rise within the capsule after the engine has been shut off
- design of the steering passage in the firewall
- the capsule shells and larger exhaust mufflers reduce the ground clearance as compared with present production models, as shown in Fig. 13
- additional weight and cost
- reduced fuel economy due to the increase in vehicle weight and in energy required for added cooling performance.

CONCLUSIONS

In order of their significance, the main noise sources of Diesel passenger cars were found to be

- engine and drive line
- tailpipe
- exhaust system
- intake and
- rolling noise.

Furthermore it was shown that the choice of a suitable combustion system can reduce noise, but that in the case of Mercedes-Benz Diesel engines this possibility has already been fully exploited by deciding in favor of the prechamber system which already provides the lowest combustion noise levels.

As regards the encapsulation which is necessary to achieve maximum combustion noise level reductions, the design, effect and major problems involved in engine-attached encapsulation and vehicle-supported encapsulation systems were described.

A research vehicle with a vehicle-supported capsule was built to demonstrate that maximum noise level reductions of approx. 6 dB (selector position "S") and approx. 4 dB (selector position "L") can be achieved during the accelerated ISO drive-by test starting from a speed of 50 km/h. The analysis of the external noise distribution revealed an average reduction by 6 dB. With the aid of special measures it was possible to maintain the interior noise level in the vehicle interior at that of present production vehicles. The problems encountered during maximum noise level reduction with reference to heat balance, ground clearance, ease of accessibility for maintenance and additional weight were principally shown. The results discussed also represent the limits of maximum noise reduction, since in this research vehicle with vehicle-supported capsule in the form shown the sum of all noise sources on the vehicle equals the pass-by noise with the engine turned off, both when driving at a steady speed of 50 km/h and under conditions of accelerated pass-by from 50 km/h with gear selector in "S".

OUTLOOK

The positive results of this research project aimed at reducing the noise generated by a modern Diesel passenger car and at assessing the possibilities of later realization through a first evaluation of the consequences and unsolved problems must not be misinterpreted. The project clearly shows that important principal technical problems remain to be solved, before one could even consider endurance tests.

At this early phase of the program we have purposely not quantified the negative implications of fuel economy, weight and cost.

Another item to consider is the validity of the vehicle noise test procedure used to evaluate the noise level reductions. The ISO R 362 test is meanwhile being criticized by everybody who seriously desires to reduce city noise levels of passenger cars. It was used for purposes of comparison because a large data base exists.

Alternative test conditions have not been finalized as yet, and their validity will have to be evaluated equally critically.

Other regulatory requirements for Diesel cars both existing and in the planning stage - in the areas of NO_x and particulate emissions, together with others must be viewed together with future noise requirements. Even if all technical problems are solvable in time, they will have a direct consequence on the marketability of Diesel cars as obvious economic considerations reveal.

Even today, the higher initial cost of Diesel power exists, so that a careful assessment of economic realities must be conducted, if Diesel cars are to continue to contribute their potentially sizeable share in reducing the amount of fuel used in road transportation.

REFERENCES

[1] Huber/Wodiczka: Verbrennungsgeräusch bei Dieselmotoren
FVV-Forschungsbericht Heft 123, 1972

[2] Hieroth: Vergleich von Dieselverbrennungs- und Aufladeverfahren hinsichtlich ihrer Eigenschaften und Anwendungsmöglichkeiten
Vortrag Wuppertal 1976

[3] Zimmermann: New Robert Bosch Developments for Diesel Fuel Injection
SAE-Paper 760127

[4] Röhrle: Effecting Diesel Engine Noise by the Piston
SAE-Paper 750799

[5] Thien: Elemente zur Abminderung der Schallemission von Verbrennungsmotoren heute üblicher Bauart
Dissertation TU Graz, 1977

[6] Gillet: Hinweise für Schalldämpfer-Einbau, Bemessung und Auslegung
Techn. Information Gillet

[7] Challen: The Effect of Combustion System on Engine Noise
SAE-Paper 750798

[8] Fachbach: Entwicklung von neuartigen geräuscharmen Dieselmotoren
Dissertation TU Graz, 1977

[9] Essers/Liedl: Muß eine leise Reifen-Fahrbahn-Kombination einen Verlust an Sicherheit bedeuten ?
Vortrag Berlin 1976

NOMENCLATURE

p	bar	combustion chamber pressure
φ	$^{\circ}CA$	crank angle
$dp/d\alpha$	bar/$^{\circ}CA$	pressure rise
$d^2p/d\alpha^2$	bar^2/$^{\circ}CA^2$	speed of pressure change
q	kJ/kg	specific heat quantity
v	m^3/kg	specific volume
$dv/d\alpha$		volume alteration
$\varkappa$		polytropic exponent
t_{cw}		temperature, cooling water
t_o		temperature, engine oil
t_{ATF}		temperature, automatic transmission fluid

790446

EXPERIMENTAL STUDY OF A HIGH SPEED DIESEL ENGINE BY THE ACOUSTICAL POWER METHOD

J.M. KINDT (AUTOMOBILES PEUGEOT)
J. MARTY (PSA PEUGEOT-CITROEN)

ABSTRACT

- Reminder of the acoustical power method
- Description of the facilities
- Application to Peugeot engine XD2(2,304 CM3)
  - Relative importance of noise sources
  - Research for improvement
  - The problem of trade-offs between noise, pollution, and fuel economy
- Practical conclusions
  - Results obtained on the engine and on the vehicle
  - Reflexions on various means to reduce the noise level of a passenger car vehicle with a Diesel engine.

I - INTRODUCTION

During the last five years, high speed Diesel engine production has dramatically increased, for application to vans and passenger cars (fig. 1), (fig 2) (1)*. During the same period, an important Research and Development Programme was initiated regarding engine noise at all r.p.m. and loads, in order to improve comfort of passengers and to reduce external noise emissions.

In this paper, we shall particularly insist on the methods for engine noise investigation on the test bench. To complement this, we shall give a brief account of the very important programme of research carried out on a complete vehicle.

II - ACOUSTICAL POWER METHOD

1) Basis of the Method

Idealy, in free field, the acoustical energy passing through a given surface S is proportional to the square of the sound pressure (2) (formula 1) (fig 3)

Let us consider, in those conditions, a sphere of radius R, surrounding the source of noise. The noise pressure can be measured at n points spread over the surface of the Sphere. The total acoustical energy passing through the Sphere is the sum of the partial energies (formula 2) (fig 3).

Assuming that the n points are uniformly distributed over the surface of the Sphere, we can associate with each point an equal area to calculate the acoustical energy. Finaly we obtain the total sound energy, in decibels by the formula 3 (fig 3).

The same acoustical Power Method can be applied to noise measurements of an engine, tested in an anechoic chamber ; in this case, measurements are carried out in n points, predetermined, each being located on a Sphere surrounding the engine (fig 4).

The overall acoustical power is recorded, and spectral analysis is made, (usualy third octave).

2) Interest of the method

Formerly, for engine noise analysis on the test bench, individual measurements were made with a few microphone locations, usualy one in front, one on each side, and one above the engine (3)

The acoustical power method uses a multiplicity of measurement locations distributed around the engine. This yields more complete and more detailed description of the phenomena. The method constitutes a particularly suitable tool of research to identify parts which are the main sources of noise.

The engine being entirely wrapped up, investigated parts are uncovered in succession, one at a time and the corresponding total acoustical power emitted by each is evaluated. It is of course understood that in the study, the individual microphone location is taken into account when the recorded particular acoustical pressure is considered. A local treatment of a part of the engine will be deemed efficient if it has an appreciable bearing on the noise level, as measured at the nearest microphone locations and if it also results in a measurable overall reduction of acoustical power ; all the other noise sources being isolated by means of the wrapping.

* Numbers in parentheses designate References at the end of paper.

SAE/P-79/80/$02.50
Copyright © 1979 Society of Automotive Engineers, Inc.

This kind of study clearly represents a considerable amount of individual measuring data and would be impossible to carry out had we not at our disposal an automatic system of data recording and treatment.

3) Description of the installation

Measurements are performed on an engine test bench installed inside an anechoic chamber. The main features are as follows : the outside shell is of .22 m thick concrete, 5.60 m in length, 5.56 m in width, 5.50 m in height (fig 5).

The concrete shell is set on a slab independant of the building structure so as to eliminate outside vibrations (fig 5)

All the inside surfaces are lined with noise absorbing materials, that are :

- a rock wool fiber lining 12 cm thick
- a system of dihedrons (40 X 40 X 40 cm) constituted by plates of rock wool 4 cm thick glued together to form a stepped aggregate and supported on a metal frame.

The microphone is secured to a mounting formed to a sector of a circumference of 1.20 m radius, rotating around a vertical shaft (fig 6)

The monitoring and data treatment system (fig 6) consists of :

- a real time analyzer with parallel filters
- a band perforator
- a computer
- a printer

III - RESULTS OF THE MEASUREMENTS PERFORMED ON THE XD2 ENGINE

XD2 Engine

XD2 is a 4 cylinders in line Diesel engine, indirect injection, Ricardo system - 2,304 cm3 displacement (fig 7)

This engine is mounted on 504 passenger cars and vans (J 7).

Measurements performed on the XD2 engine (fig 8)

a) The acoustical power measurements first enable to evaluate the engine behaviour in various conditions of speed and torque.

The measured overall noise level follows a near linear law of increase, function of r.p.m. The load factor is noticeable only at low r.p.m. it is very small above 3 000 r.p.m.(fig 9)

1/3 octave spectral analysis at various r.p.m. shows relatively high levels in the medium frequencies, between 1000 and 3000 Hz (fig 10). According to us, the acoustical comfort will be improved if the noise levels are lowered within this frequency range. On the other hand the contribution of medium frequencies is particularly important to the external noise measurements performed according to the present day regulatory procedures (ISO R 362, SAE J 986 a). The ideal spectrum should be flat in the range of 600 to 6 000 Hz.

b) Measurements upon wrapped up engine (fig 11)

These measurements aim to evaluate the contribution of various engine parts to the radiated acoustical power.

The conventional method; as previously stated, consists in completely wrapping up the engine with an acoustical shield and to systematically uncover each part under investigation. Every measurement is carried out by 1/3 octave spectral analysis. The obtained result is given here as a specific example : it shows the important contribution of the oil sump to the acoustical power radiation in the medium frequencies range which is of particular interest according to our view-point. It also contributes in the higher frequencies. (fig 12, 13 14).

All these results enable to establish the relative importance of each part in the overall acoustical power emission at various r.p.m. The fig 14 is given as an example.

For a number of reasons, there is a relatively high percentage of error in the data. In spite of this inaccuracy, a relatively good rating may be obtained, following the order of importance of various parts to consider for noise reduction ; that is : oil sump, cylinder head, rocker cover, timing cover, front pulley and damper and cylinder block.

IV - RESEARCH FOR IMPROVEMENT OF THE ENGINE PHONIC INSULATION

a) First tests

A first series of measures has been taken by insulating to the possible best the oil sump, rocker cover, timing cover and the front pulley with the damper - all the other engine parts excluded.

Important reduction of acoustical power has been actually recorded.

b) Development for industrial production

The following modifications were tried out.

- Oil sump (fig 16)

The production part has been left as it was (press drawn sheet metal) with its mounting means. A plastic shell is bonded to the outside of the sump with a mat of fibrous material 5 mm thick between the two.

- Timing cover (fig 17)

The same solution has been applied : double casing, plastic outside, original cover inside (cast aluminum) - fibrous material in between.

- Front pulley with damper (fig 18)

A shield of compressed fibrous material is fixed in front of the pulley to act as noise vibrations absorber.

- Rocker cover (fig 19)

The cylinder head treatment is limited to that of the rocker cover. The same method as hereabove is applied : plastic shell and fibrous material bonded externally to the sheet metal part as coming from production lines.

The obtained improvement with these four modifications is to be compared to the one obtained previously (according to fig 15).

A rather good efficiency has been evidenced. The acoustical power attenuation was particularly important in the critical medium frequencies, range around 2 000 Hz (fig 20).

We add for precision, that these improvements take place in all engine conditions of use : from idle to high r.p.m. at full load.

V - FUEL INJECTION IMPACT ON NOISE

The effect of fuel injection adjusting parameters upon the engine noise has been investigated specifically in view of urban driving conditions: idle and low r.p.m. low load.

The timing at injection start has an important effect on the pressure evolution inside the combustion chamber (fig 21). Too much advance in injection timing results in a high peak on the pressure diagram with unfavourable consequences on the noise emission (fig 22) (4).

On the other hand injection timing is an important factor in specific consumption and in the exhaust gas composition.

In particular the percentages of HC and NOx vary in important proportions. Each of them varies in opposite directions for a 2 degrees variation of the timing (fig 23).

Cooperation between automobile makers and those of the injection equipment results in marked progress to reduce the amount of pollutants in exhaust gases in view of compliance with ever more stringent regulations. These achievements did not have any adverse effect on engine noise emission. This has not been an easy task. We are willing to improve these results in the future by lowering the typical Diesel noise at idle and low r.p.m. It is not proven that the goal is compatible with the present day projects of more severe antipollution regulation.

Note :

Combustion noise has a very specific nature, which makes quantitative measurements particularly uneasy to appreciate correctly. In this case it is often necessary to revert to subjective appreciation.

VI - PRACTICAL CONCLUSIONS

1) Engine noise reduction

Research on XD2 Diesel engine, applying the acoustical power method, results in possibility to improve the engine noise, by means of relatively minor modifications, without putting in question the engine internal structure. We emphasize the attenuation of noise levels in the medium frequencies which to our mind appears to be particularly important. It is to be stressed that the achieved improvement is observed in all conditions of engine use.

The method is applicable also in the endeavour to improve the characteristic Diesel noise at idle and at low r.p.m. by acting on the fuel injection parameters. However, as we feel it, care should be taken in this particular case when appreciating the results of measurements of the acoustical power. Besides, research to improve this particular combustion noise is difficult due to the complexity of phenomena occuring in emission of pollutants and that of noise.

2) Results on vehicle

Test bench measurements were supplemented by experiments on a complete vehicle. Research centers have at disposal specific facilities for this. Fig 24 shows an anechoic chamber recently put to service for inside and outside noise analysis on passenger cars and on vans. (fig 24)

The reduction of noise level for a complete vehicle is generally less perceived than the one measured on the engine, due to the contribution of various noise sources such as intake, exhaust, transmission, rolling.

In the particular case of the light duty truck J7 (fig 25) equipped with the XD2 Diesel engine, the engine constitutes the main noise source (50 % of acoustic power is emitted by the engine) (fig 26)

Our finding is that the modifications of the XD2 engine have brought a real improvement of external noise of the J7 Vehicle.

The maximum noise level recorded according to ISO procedure was 83 dB A with the original engine (fig 27). After modification of the oil sump, rocker cover, timing cover and front pulley with damper, the recorded noise level was 80 dB A. The 1/3 octave spectral analysis showed the important improvement in the medium frequencies (fig 28).

In the case of 504 passenger car with the same XD2 Diesel engine, we can not expect the same improvement as the vehicle at the start is less noisy (80 dB A viz 83 according to ISO R 362) - and besides the engine contribution is only of 35 % viz 50 % for the external noise.

VII - CONSIDERATIONS ON VARIOUS MEANS TO IMPROVE DIESEL ENGINE NOISE ON A PASSENGER CAR

We have seen here above the means to reduce by a certain amount the engine noise level by external modifications. On a light duty truck, external noise level is lowered by about three decibels A. The effect is less important on a passenger car.

For better improvement, it has been considered to modify the engine internal structure (5), (6). This kind of modification raises big manufacturing problems. Besides we still need more detailed knowledge of the basic vibration phenomena in the heart of the engine, and more specifically in the zone of crankshaft bearings. This knowledge is necessary to establish a research programme for an improved engine structure.

Moreover, turbocharging is more and more widely used with the heavy truck Diesel engines. Turbocharging can also be applied to high speed passenger car Diesel engines. This is a costly but apparently efficient means to combine high power with a not too high noise level.

Other research for improvement may apply to combustion and fuel injection. In this latter field it may be hoped that with the help of electronic devices an improvement will be achieved in the difficult trade off between noise, fuel-economy and antipollution.

Inside the vehicle, an acceptable level of comfort is achieved through a careful treatment of all the passenger compartment parts prone to vibration or to vibration transmission. Good acoustical insulation between the engine and passenger compartment is of prime importance.

External noise reduction must be achieved through the treatment of other sources besides the engine : exhaust for example. External transmission of engine noise is attenuated by the use of noise absorbant materials placed under the hood. In one of our previous papers we have shown that car underside shielding achieves an appreciable attenuation of the external noise.(3) These shields preferably made from synthetic material, basically compressed fibers, must possess sufficient resistance to outside deterioration agents. They should combine insulating and absorbing acoustical properties. Unfortunately, the use of this type of material is not very wide-spread as yet. In fact these shielding reduces the ground clearance and adversely affects engine cooling. In spite of all these drawbacks the under-car shielding stays as of to-day the most effective means to achieve meaningful improvement of external noise level.

AKNOWLEDGMENTS

The authors are indebted to
- Professort T. Priede, ISVR The University of Southampton and
- Doctor G. Thien, Institute Prof. List-AVL

for their assistance and valuable advice in the preparation of this paper and their contribution towards its composition.

REFERENCES

1) Statistic data from "Chambre Syndicale des Constructeurs Automobiles" (France)

2) K. Zaveri Automatic Method of Sound Power Measurement
Bruel and Kjaer Technical Review n° 3 - 1971

3) M. Le Creurer - J. Marty
Practical Means for Reducing the NOise of High Speed Engines
SAE OFF HIGHWAY VEHICLE MEETING - September 1975 - SAE 750 837

4) J.M. Kindt - J. Marty
Etude de la Réduction du bruit d'une voiture particulière à moteur Diesel
Ingénieurs de l'Automobile - n° 5-6 juin-juillet 78

5) D. Anderton, C. Grover, N. Lalor, T. Priede
The automotive Diesel Engine - Its Combustion Noise and Design.

1st Lecture at Institution for Mechanical Engineers

Land Transportation Conference - London - January 1977

6) H.A. Fachbach - G.E. Thien
Ein neuer weg zum Geräuscharmen Fahrzeuzmotor

17. FISITA Congress - Budapest 1978

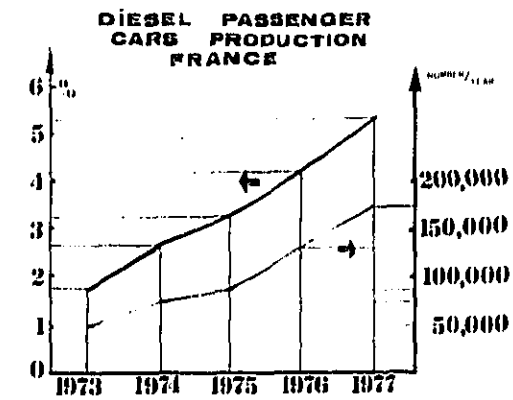

Fig. 1 - Diesel Passenger Cars Production France (last five years)

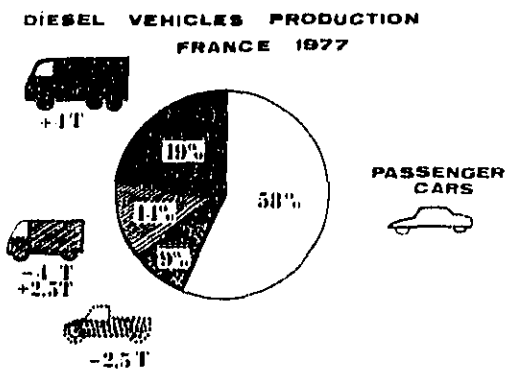

Fig. 2 - Diesel Vehicles Production (Passengers cars and trucks) France 1977

SOUND POWER CALCULATION

S = SURFACE m^2

E_0 = REF 10^{-12} WATTS

p_0 = REF 2×10^{-5} N/m²

1 $$\frac{E}{E_0} = K S \frac{p^2}{p_0^2}$$

n measuring points over a sphere

2 $$\frac{E}{E_0} = \frac{E_1}{E_0} + \frac{E_2}{E_0} + \cdots + \frac{E_n}{E_0}$$

$$S_1 = S_2 = S_3 = \cdots = S_n = \frac{4\pi R^2}{n}$$

$$\frac{E_1}{E_0} = K S_1 \frac{p_1^2}{p_0^2}, \quad \frac{E_2}{E_0} = K S_2 \frac{p_2^2}{p_0^2}, \quad \cdots \quad \frac{E_n}{E_0} = K S_n \frac{p_n^2}{p_0^2}$$

$$\frac{E}{E_0} = K \times 4\pi R^2 \times \frac{1}{n}\left(\frac{p_1^2}{p_0^2} + \frac{p_2^2}{p_0^2} + \cdots \frac{p_n^2}{p_0^2}\right)$$

3 $$10 \operatorname{Log} \frac{E}{E_0} = 10 \operatorname{Log} K \times 4\pi R^2 + 10 \operatorname{Log} \frac{1}{n}\left(\frac{p_1^2}{p_0^2} + \cdots + \frac{p_n^2}{p_0^2}\right)$$

Fig. 3 - Sound Power calculation - formula

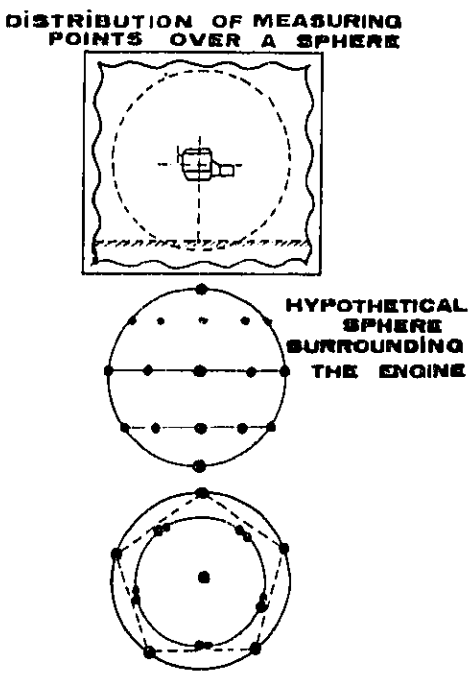

Fig. 4 - Engine Sound Power Measurements - Microphone locations

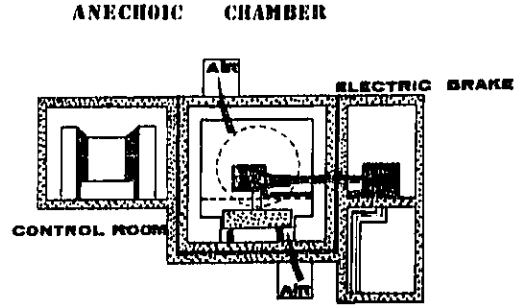

Fig. 5 - Schematic view of the installation

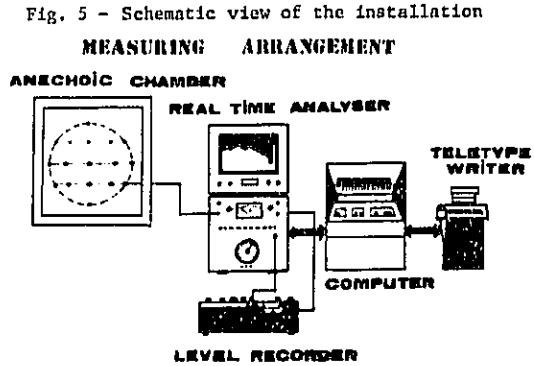

Fig. 6 - Monitoring and data treatment arrangement for sound power method

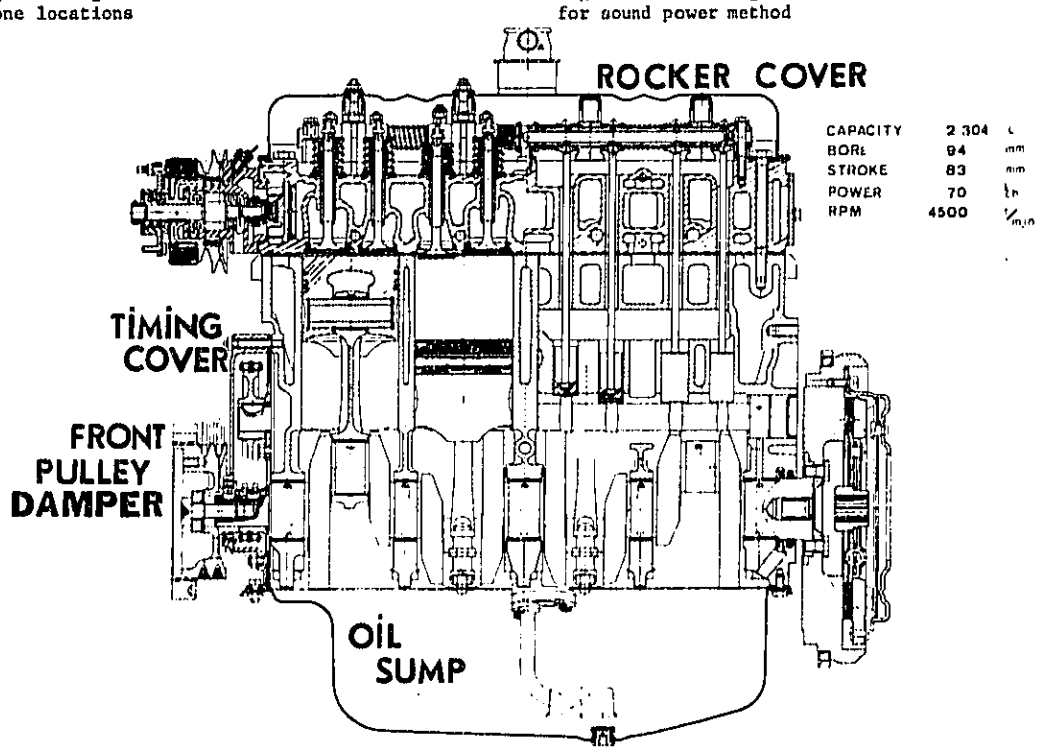

Fig. 7 - XD2 Diesel Engine (axial section)

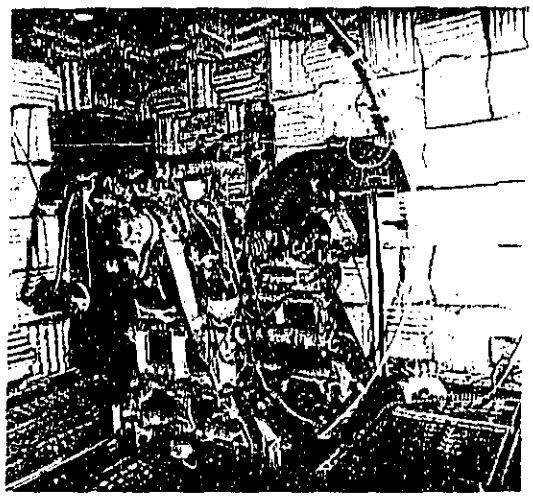

Fig. 8 - XD2 Engine fixed on test bench inside anechoic chamber

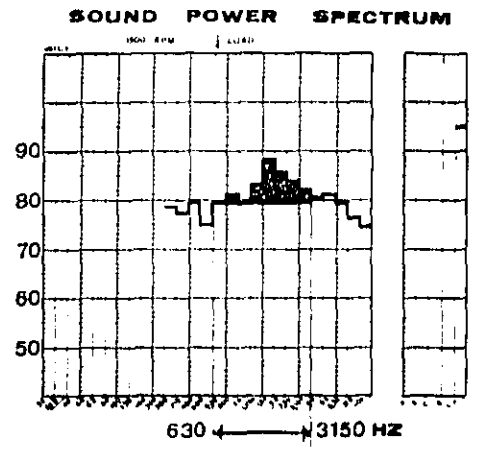

FREQUENCY RANGE TO CONSIDER IN ORDER TO OBTAIN LOW NOISE ENGINE.

Fig. 10 - Third octave spectral Analysis of the overall Sound Power

INFLUENCE OF R.P.M. AND LOAD ON ENGINE NOISE.

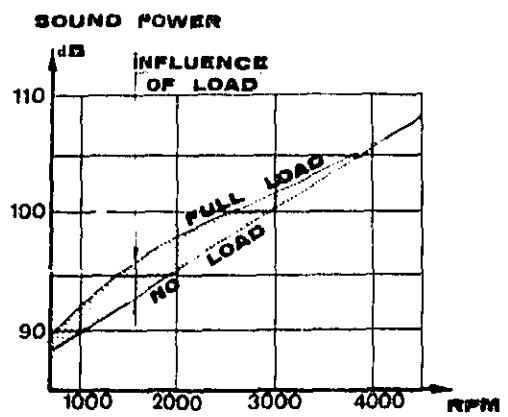

Fig. 9 - Overall noise level as a function of load and RPM

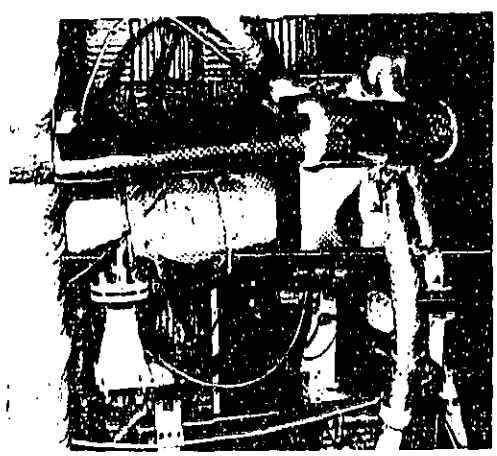

Fig. 11 - View of Engine completely wrapped up

OIL SUMP SOUND POWER TO 1600 HZ

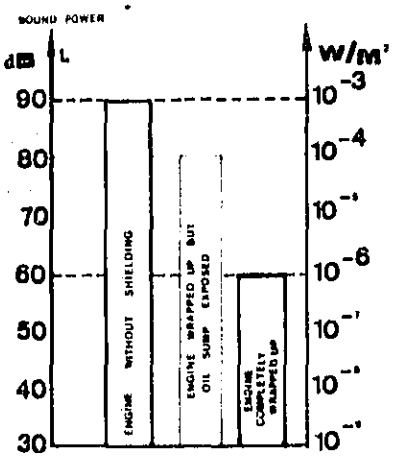

$$\frac{10^{-4} - 10^{-6}}{10^{-3} - 10^{-6}} \simeq \frac{10^{-4}}{10^{-3}} = 10\,\%$$

Fig. 12 - Calculation of oil sump contribution to overall sound power (principle)

OIL SUMP SOUND POWER

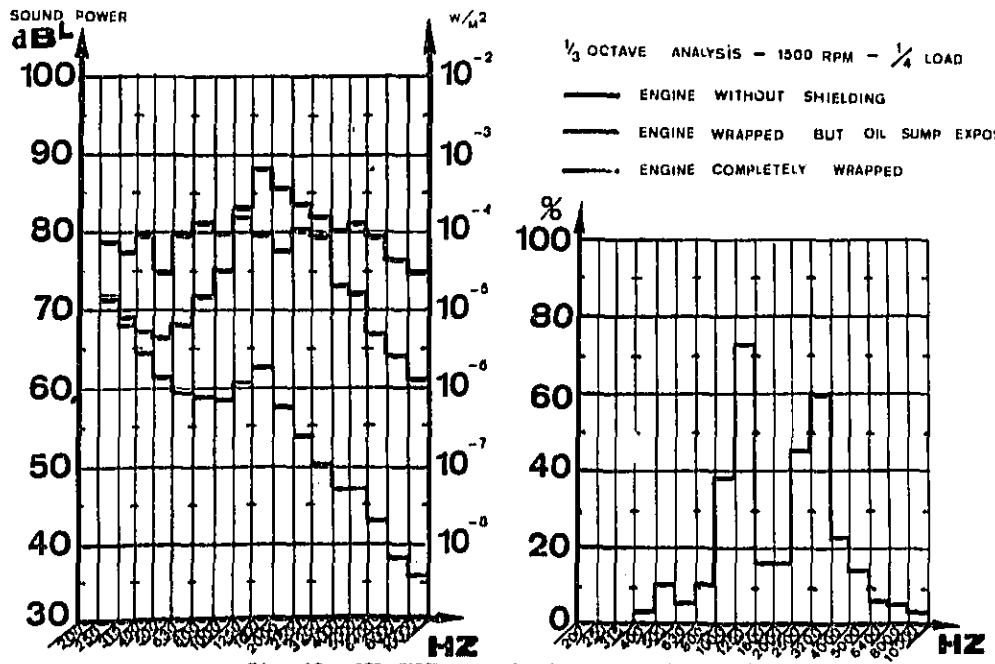

Fig. 13 - OIL SUMP contribution to sound power by 1/3 octave spectral analysis

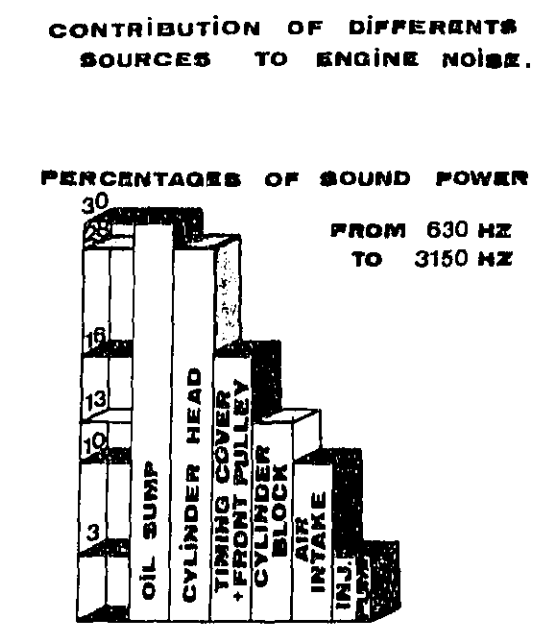

Fig. 14 - The main noise sources of engine emission

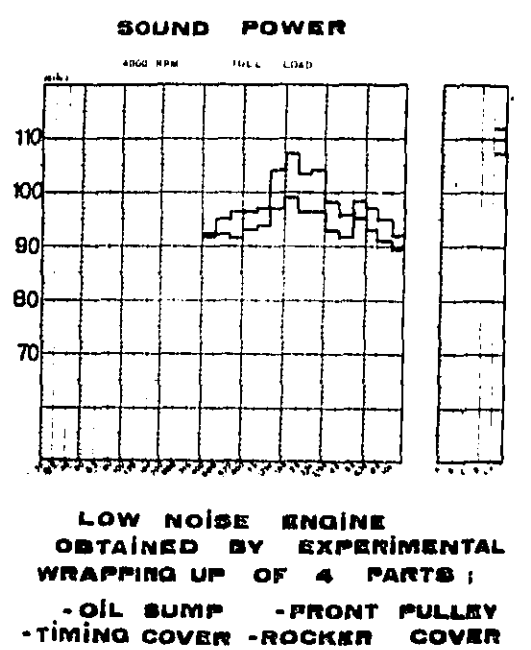

Fig. 15 - Comparison of 1/3 octave spectra with and without experimental wrapping up of main noise sources of the engine

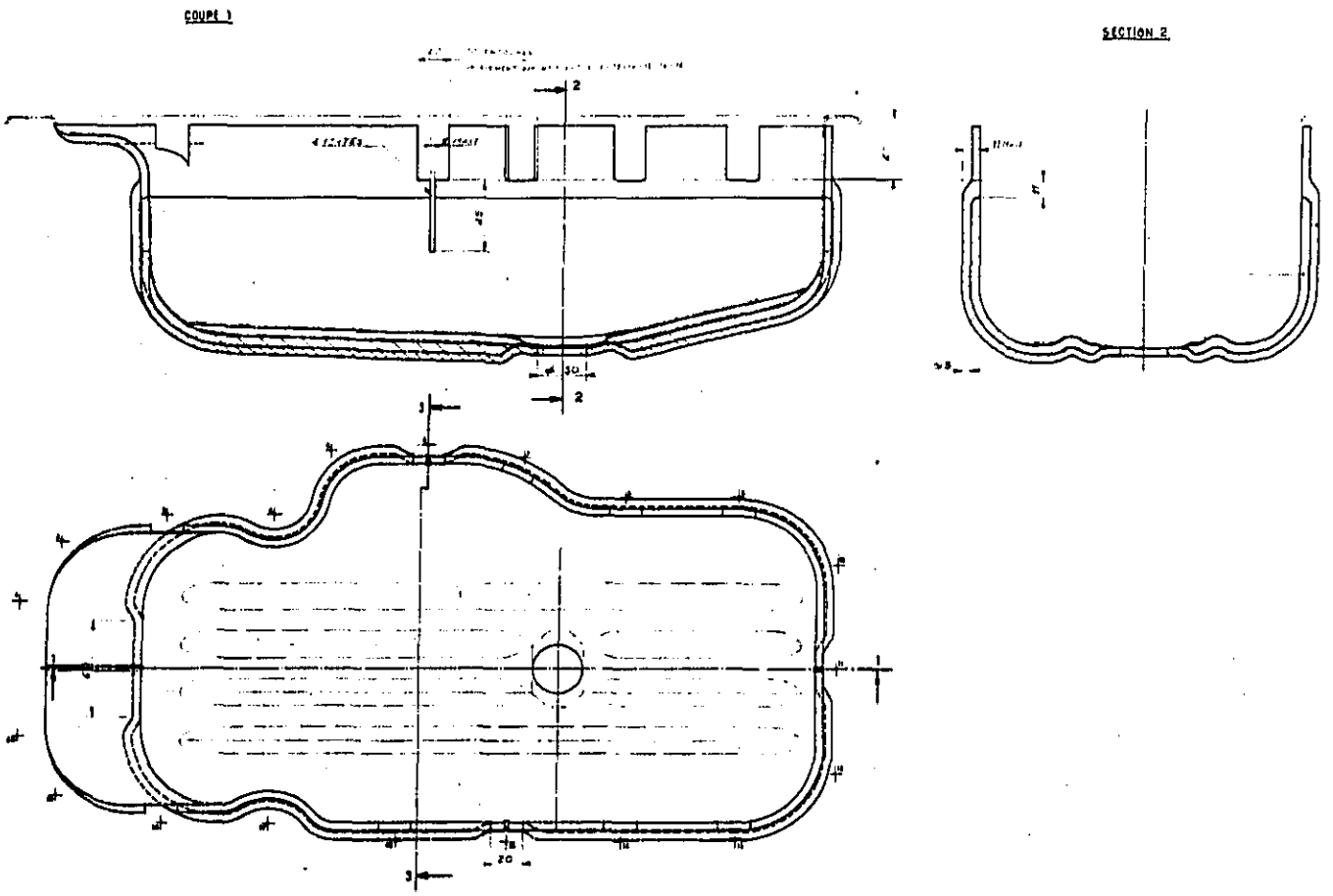

Fig. 16 - OIL SUMP MODIFICATION

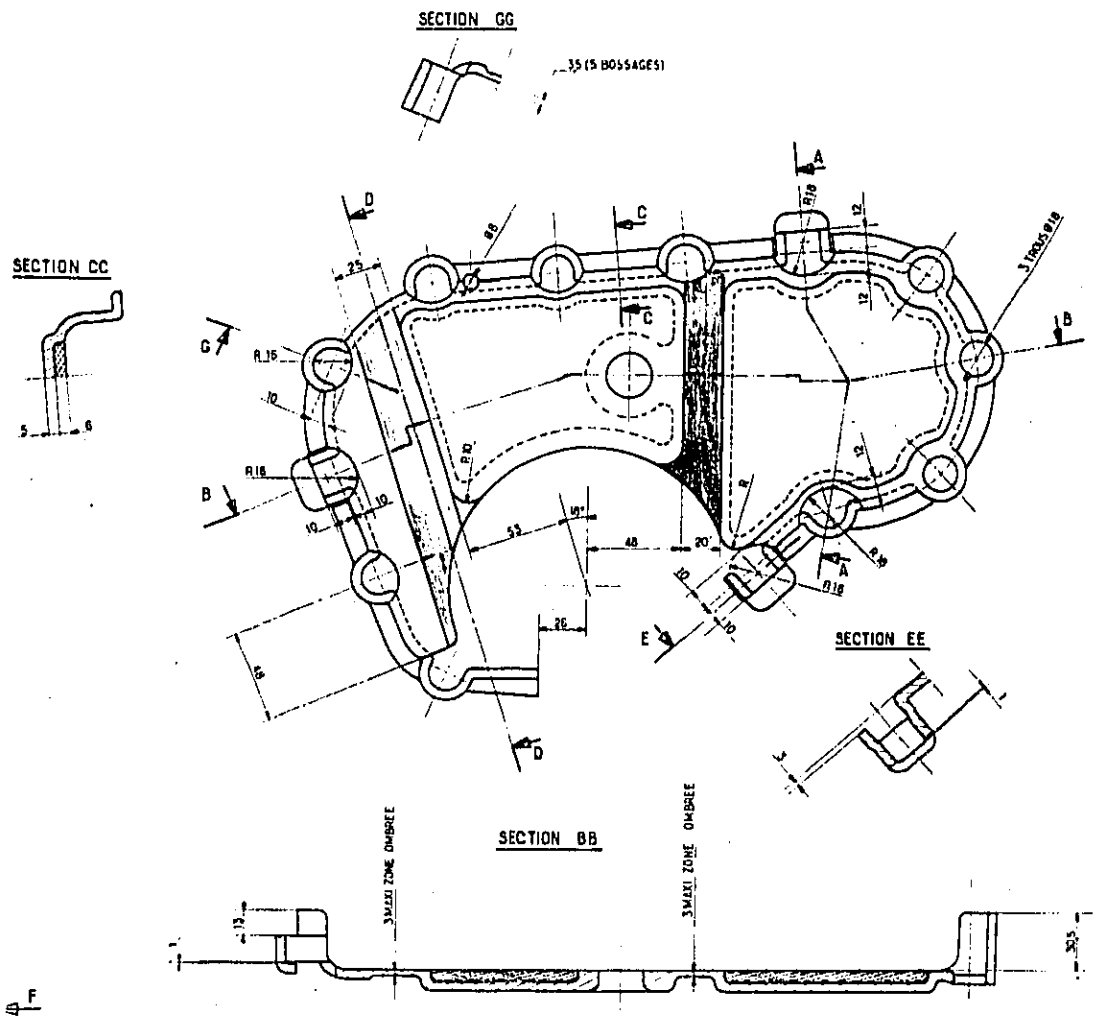

Fig. 17 - TIMING COVER MODIFICATION

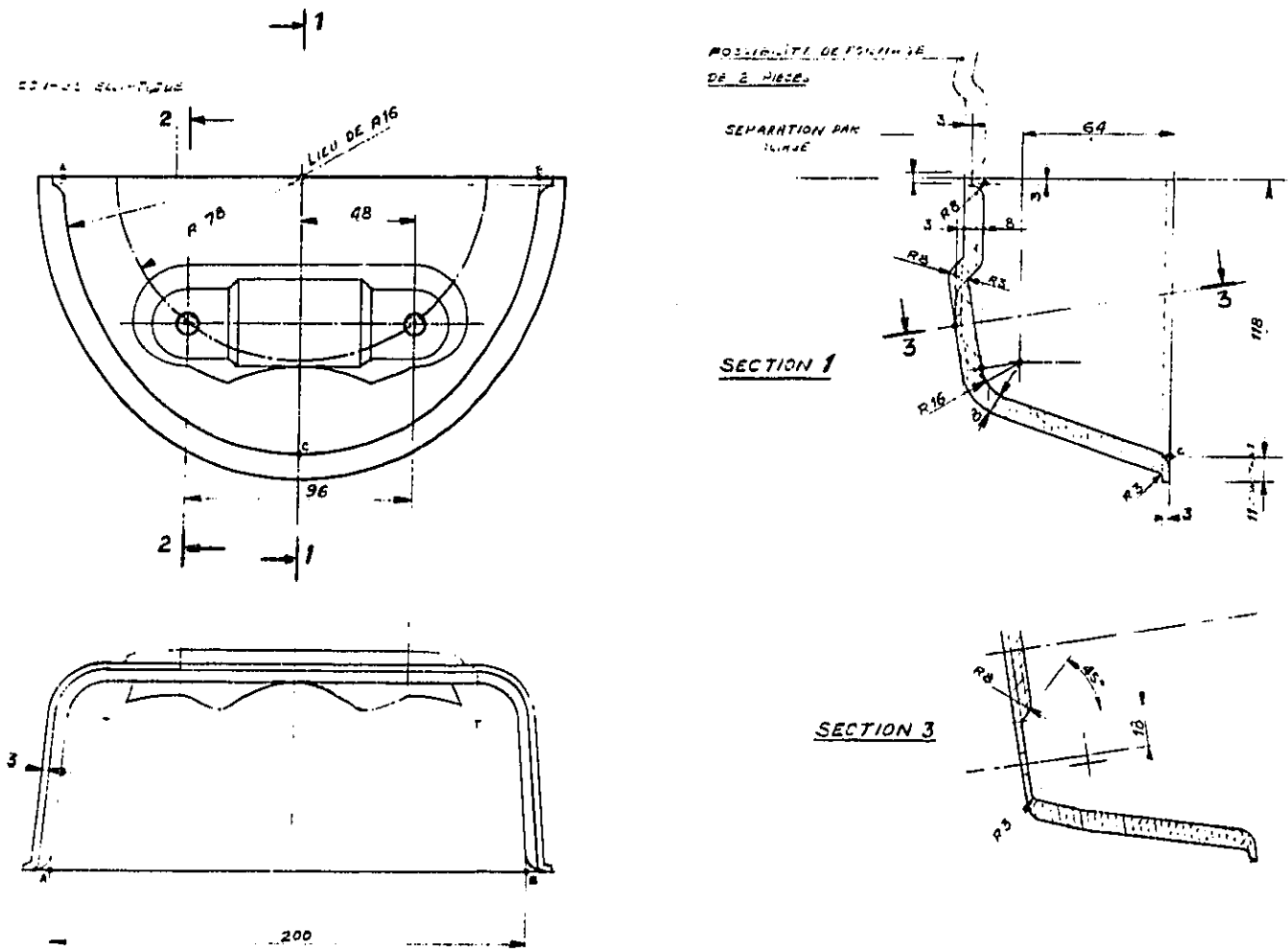

Fig. 18 - External engine modification: Front pulley enclosure

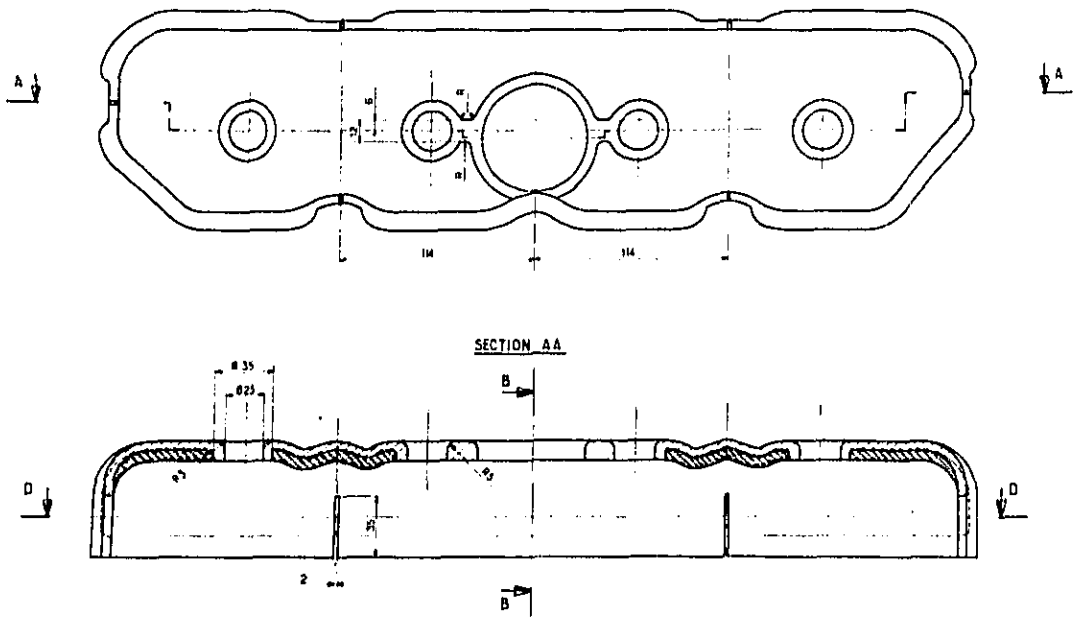

Fig. 19 - Rocker Cover modification

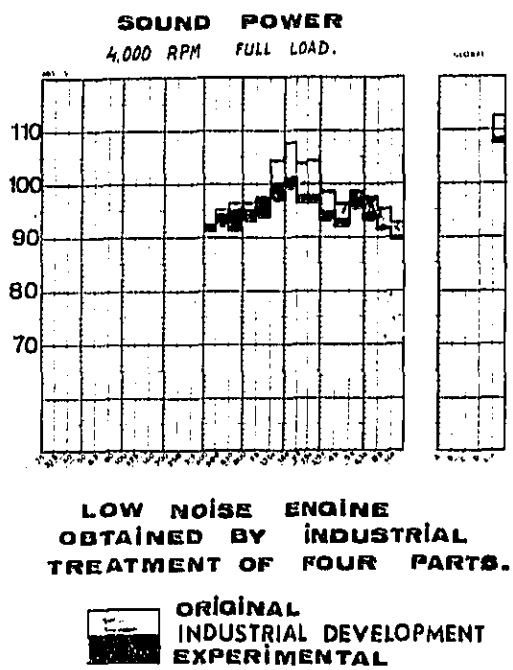

Fig. 20 - Comparison of 1/3 octave Spectra of the engine:
a) with experimental insulation
b) with partial modifications according to Figs. 16, 17, 18, and 19

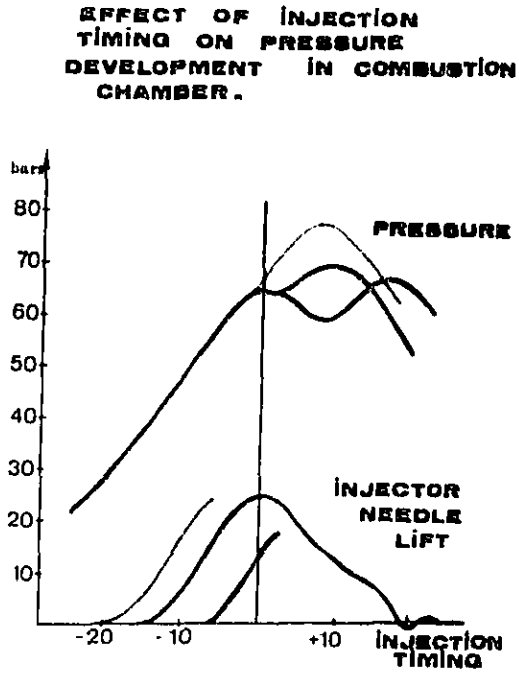

Fig. 21 - Effect of injection timing variation on pressure development in combustion chamber

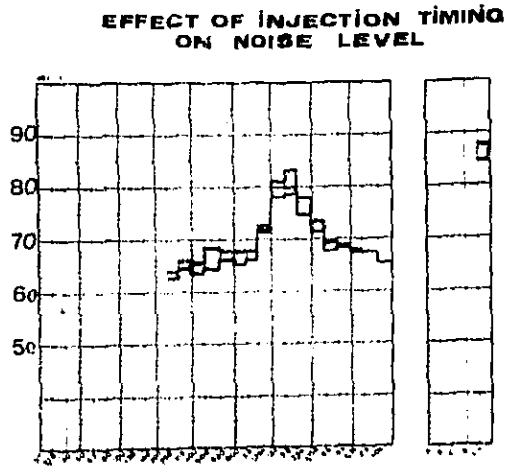

Fig. 22 - Effect of injection timing variation on Noise Level

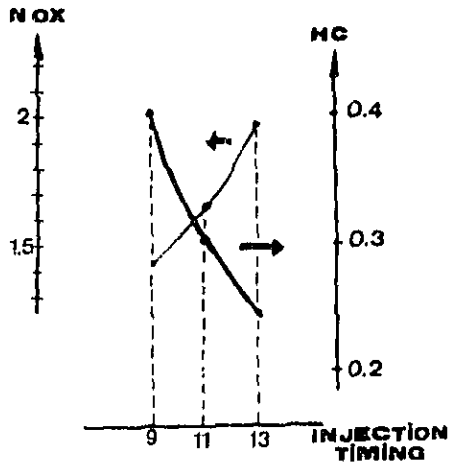

Fig. 23 - Effect of injection timing variation on NOx and HC

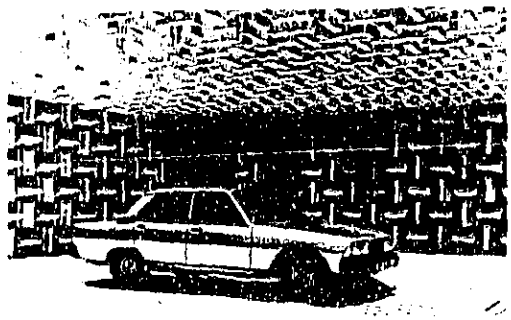

Fig. 24 - Anechoïc Chamber for noise analysis on passenger cars and vans

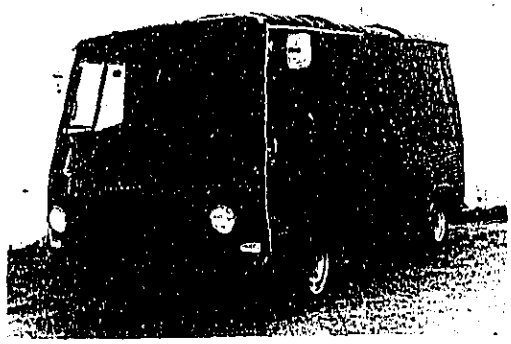

Fig. 25 - View of the light duty Truck "J7"

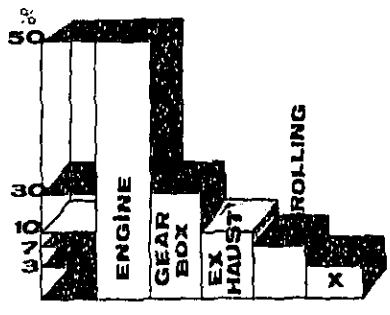

Fig. 26 - The main sources of noise of the "J7" vehicle

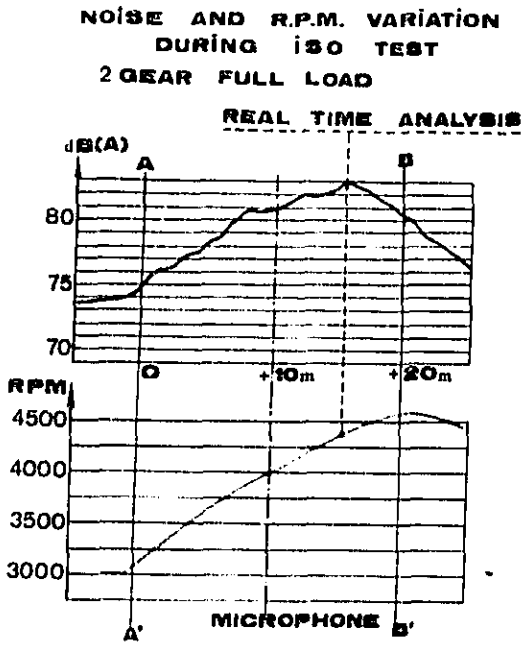

Fig. 27 - External noise of the "J7" vehicle recorded by the ISO procedure

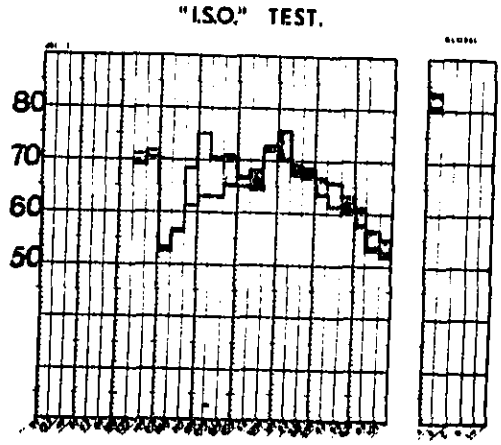

Fig. 28 - 1/3 octave spectral analysis at the maximum noise level recorded by the ISO procedure. "J7" vehicle before and after engine modifications

790447

PRACTICAL INVESTIGATION OF NOISE REDUCTION OF A DIESEL PASSENGER CAR

A. PETITDIDIER

AUTOMOBILES CITROEN

ABSTRACT

The present stage of technique still does not allow the manufacturing of Diesel engines as silent as gasoline engines. However, a rational use of classical insulating processes will enable Diesel engine passenger cars to have, from now on, an acoustic quality close to that of gasoline engine vehicles. The purpose of this paper is to describe a practical example of the insulation of a passenger car with a Diesel engine.

THE RAPIDLY INCREASING number of passenger cars with Diesel engines has incited car manufacturers to give them particular attention as regards the noise problem, and we hope and expect that the work now in progress will allow good results in the near future.

CITROEN is studying the relationship between passenger compartment acoustic and elastic vibrations by finite element method and modal analysis.

This research, which entails considerable means as far as computing and experimenting, will lead us to a better knowledge of noise production processes, but is not yet apt to bring concrete solutions to our problems.

The following paper is therefore not based on such theoretical studies, but is simply aimed at describing the practical means recently used on the CX 2500 Diesel to try and obtain with this vehicle an acoustic quality as close as possible to that of the CX 2400 equipped with a petrol engine of similar cylinder capacity.

To this end, we have developped the following items :

- Improvement of engine suspension.
- Intake and exhaust noise reduction.
- Increase of the acoustic insulation or bulkhead.
- Absorption under engine hood.
- Partial "encapsuling" of engine compartment.

IMPROVEMENT OF ENGINE SUSPENSION

On all the models of CX line the power unit is transversely fitted, as you can see in photo (1). This arrangement leads to considerable stress at the fixing points of the power unit (about 1000 daN when the car starts off quickly).

When the first CX model, which was the CX 2000 equipped with a gasoline engine of 1985 cm3 with 4 cylinders in line, was designed, one of our main concerns was thus to position the fixing points of the engine in very strong areas on the chassis. This led us to choose the 4 point suspension shown in photo (2)

To the extent that it is correctly adjusted, this suspension gives good results. The position of the power unit is determined as soon as 3 points are fixed. The 4th point must therefore be adjustable in order to avoid stress on the engine mounts as the rigidity of these mounts increases greatly with such stress and the insulation of the engine vibrations becomes insufficient.

In the case of the CX 2500 Diesel equipped with a Diesel engine of 2500 cm3 with 4 cylinders in line, it proved necessary to improve the vibratory insulation of the engine. In order to render the quality of the vibratory insulation independant of the assembling process, the 4 point suspension was replaced by a 3 point suspension.

In the photo (3) you can see the 3 points of this new suspension. The difference resides mainly in the removal of the small rod (d) and the change in design and position of the lower gear-box mount (b). This can be seen in greater detail in photo (4).

This new arrangement allows us to achieve a good adjustment more easily during production and, thanks to a better adaptation of the flexibility of the mounts, also permits us to reduce by half the stress transmitted to the body by the vibrations of the engine.

Considered subjectivly, the result has proved to be very satisfactory, and we have not found it necessary to make a more thorough study of this engine suspension, especially as the coupling which arises between the different modes of vibrations (roll, yaw, pitch) makes it very difficult to interpret the results of the experiments.

REDUCTION OF INTAKE AND EXHAUST NOISE

The intake noise is particularly high with a Diesel engine since it always runs with the intake air system wide open. Moreover, in the case of the CX 2500 Diesel there was a connexion between an

SAE/P-79/80/$02.50
Copyright © 1979 Society of Automotive Engineers, Inc.

acoustic resonance of the intake air system and the first mode of stationary waves of the passenger compartment, whose frequency is close to 80 Hz.

This problem was solved by placing a resonator into the air filter, in parallel on the intake pipe.

Fig. 1 - shows the arrangment of the resonator whose neck consist of the annular space (a), which opens into chamber C by the orifice (b).

Fig. 2 - shows the acoustic resonance which existed in the intake air system without the resonator, and the advantage provided by the resonator.

On Fig. 3 - can be seen the interior noise, measured at the level of a rear passenger's ears, with and without the resonator.

The resonance was very high in the rear seat since, in that case, the passenger's ears were close to the maximum acoustic pressure of the 1st cavity mode.

Fig. 4 - shows the distribution of isophonic lines in a longitudinal plane through passenger's ears.

This acoustic mode was also excited by the noise of the exhaust outlet.

A resonator was therefore inserted into the rear muffler in order to appreciably reduce the acoustic excitation in the critical zone of frequencies.

On Fig. 5 - can be seen the neck (a) of the resonator which opens into chamber C by the orifice (b)

After these alterations the low frequency noise level of the vehicle was found to be acceptable.

Then, it was necessary to consider the specific noise of the Diesel engine, rich in middle and high frequencies.

In order to let as little as possible of that noise reach the passenger compartment, 3 means were used :

- Increase of bulkhead acoustic insulation.
- Absorption under engine hood.
- Partial "encapsuling" of engine compartment.

INCREASE OF BULKHEAD ACOUSTIC INSULATION

Generally, the passenger compartment side of the bulkhead of passenger cars is fitted with a spring-mass type padding complex whose acoustic attenuation characteristics are shown on Fig. 6 diagram.

This diagram shows the difference between the acoustic attenuation given by a plane sample of this padding complex, fitted to a steel sheet 1 mm thick, and the attenuation which would be given by the bare steel sheet alone.

In fact, it is well known by specialists that the actual efficiency of such a padding is highly reduced by the many cuttings made to accomodate the various controls (steering, brake, etc ...).

Thus, in order to increase the acoustic insulation of the bulkhead, a padding was added to the engine side of the bulkhead. This padding is composed of the same type of spring-mass padding complex which is used on the passenger compartment side of the bulkhead. It is shown in Phot 5 just after it has been fitted to the bulkhead. Phot 6 shows the padding alone. The cutting in the center (a) corresponds to the position of the heating unit while cutting (b) corresponds to the position of the power steering. In Fig. 7 on can see the level of noise for the front passenger :

- Without padding on the engine side of the bulkhead.
- With a padding of the spring-mass type.

The use of this padding complex decreases the noise level by approximatly 6 dB (A)

In the zone of low frequencies the attenuation is greater than what had been hoped for. This is probably due to the effect ot the damping on the steel sheet.

The attenuation of the two other zones, the middle and high frequencies, contribute to the reduction of the typical noise made by the Diesel engine.

We found, later on, that it was difficult to position this padding due to its lack of rigidity, caused by the many cuttings which had been made in it.

A new padding made of semi-absorbing material is therefore being developped. It offers the advantage of being stiffer and lighter (1.9 daN instead of 5.2 daN), its handling is easier and its positioning can be carried out with greater accuracy (Photo 7).

This is composed of a layer of scraps of cotton impregnated with thermosetting resins and compressed into a sheet which is covered on both sides by a microporous layer of synthetic unwoven fibers.

The total thickness of this sheet is a about 8 mm and its weight is 2200 g/m2.

On Fig. 8 - can be seen absorption characteristics of this material.

Although the acoustic attenuation given by the padding made of semi-absorbing material is weaker in theory than that given by a padding made of a spring-mass type complex, the results obtained by the former type of padding are very satisfying and we are presently trying to perfect this new technique in collaboration with KELLER FRANCE Co.

ABSORPTIONUNDER ENGINE HOOD

The specific of the Diesel engine is due, in large part, to the richness of the noise spectrum in the high and middle frequencies.

By way of comparison , we have measured the noise under the engine hood for a Diesel engine and for a gasoline engine whose characteristics are given in Table 1.

In both cases the noise was measured without absorbing padding under the hood.

You can see in Fig. 9 that the noise level of the high frequencies is much higher for the Diesel engine than for the gasoline engine. This hasled us to use acoustic absorption as a means of dealing with this problem.

The engine hood was chosen to apply an absorbing padding since it is the largest available area (approx. 1.35 m2)

Photo 8 - shows this padding whose absorption characteristics are shown on Fig. 10

Fig. 11 - shaws the influence of the absorbing padding upon the under hood noise, and Fig. 12 shows theinfluence upon the interior noise in the front seats.

At this stage of the research study the aim in view was considered to have been reached as regards the interior noise.

For the reader's interest we have represented on Fig. 13 and 14 the compared noise of the Diesel and gasoline vehicle whose characteristics are given in Table 1.

However, there remained two shortcomings to cope with :

1 - Windows open, the characteristic noise of Diesel engine was still noticeable,
2 - The noise heard from the exterior of the vehicle was too loud when the engine was idling.

It was therefore decided to enclose the engine compartment to a maximum, in order to reduce the acoustic radiation towards the exterior.

This is the so-called "encapsuling".

PARTIAL "ENCAPSULING" OF ENGINE COMPARTMENT

To accomplish the partial enclosure of the engine compartment, we have used a semi-absorbing material of the same type as that which we are planning to place on the engine side of the bulkhead.

Its components have been given above. Compared to shields of steel sheet, the advantages are :

- a smaller weight
- acoustic absorption
- absence of vibrations.

The encapsuling consists of 3 shields :

- one shield under the engine
- one shield in both front wheel arches.

On the Photo 9 one can see the crank-case (a) and gear-box (b) in their previous condition.

Photo 10 - shows the under-engine shield.

On this photo can be seen the large space which was necessary to leave open in front of the shield, to release the cooling air from the water radiator.

Photo 11 - shows the shield of the right front wheel arch. One can see the cuttings which had to be made, particularly at the level of the Damper housing, in order to avoid the destruction of the material by the friction of a wheel equipped with a snow chain.

Photo 12 - shows the shield of left front wheel arch.

Photos 13 - 14 and 15 - show the shields alone on Fig. 15 can be seen the analysis by 1/3 octave bands of the exterior noise, measured stationary, engine running at idle.

This operating condition was chosen since it corresponds to a specific case of Diesel engine noise.

It can be stated that the improvement attained by the shields is considerable from 500 Hz upwards. By way of comparison we have plotted on the same graph the spectrum obtained with a gasoline engine.

Unfortunately, the problem has not been completely solved for, even if we can consider that the obtained noise of 72 dB A is relatively low, it is still definitely higher than that observed in the same conditions with a gasoline engine. We hope that our research, now in progress, will allow us appreciably diminish the difference between the noise of the two types of engines.

EXTERIOR NOISE

According to the procedure defined by the ISO Recommendation R 362, the obtained noise is :

- Without shields : 81 dB (A)
- With shields : 78 dB (A)

These results show that the partial encapsuling of engine compartment allowx to obtain a considerable decrease of the exterior noise.

Without encapsuling, such a decrease could only be achieved by a radical alteration of the structure of the engine.

CONCLUSIONS

The concrete example we just presented shows that, from now on, it will be possible to obtain for passenger cars with Diesel engines a level of acoustic quality fairly close to that of vehicles with petrol engines, regarding the interior as well as the exterior noise.

However, we must admit that, in spite of the improvements achieved, the "Diesel" noise still remains characteristic at low RPM and especially at adling.

We therefore pursue our research work with the confident hope that we vill obtain in the near future more and more silent Diesel passenger cars.

TABLE 1

VEHICLE	CX 2400	CX 2500 D
Engine	Gasoline	Diesel
Number of cylinders	4	4
Bore (mm)	93.5	93
Stroke (mm)	85.5	92
Capacity (l)	2.347	2.5
Compression ratio	8.75/1	22.25/1
DIN Horse power	115hp at 5500 rpm	75hp at 4250 rpm
DIN Torque	18.3 m kg at 2750 rpm	15.3m.kg at 2000 rpm
	Carburettor	Indirect Injection Ricardo system

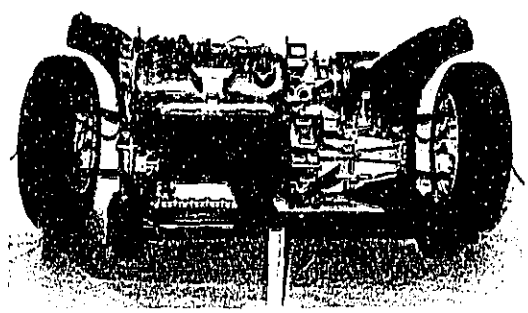

Photo 1 - Transverse arrangement of the power unit

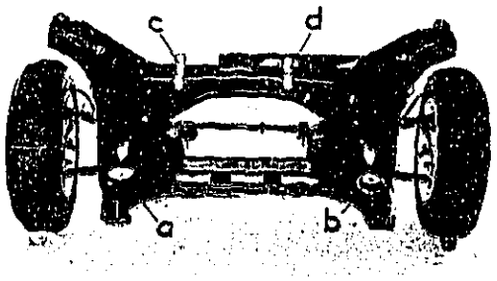

Photo 2 - Layout of four point suspension mountings

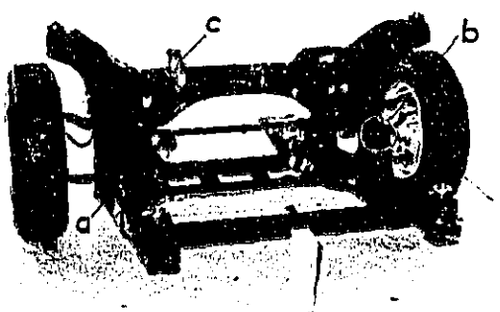

Photo 3 - Layout of three point suspension mountings

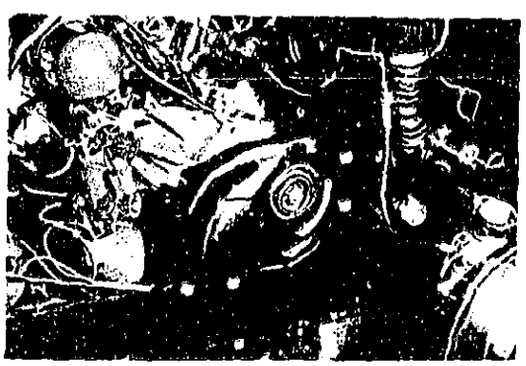

Photo 4 - Gear-box mounting for the three point suspension

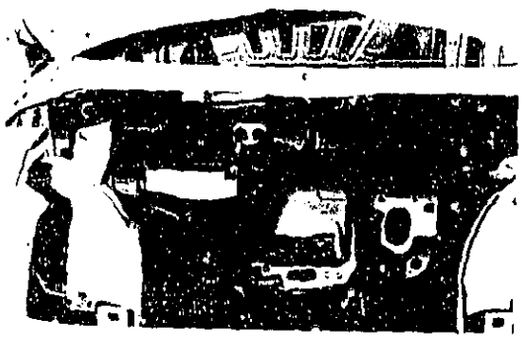

Photo 5 - Bulkhead padding, engine side, with spring-mass type padding complex, on vehicle

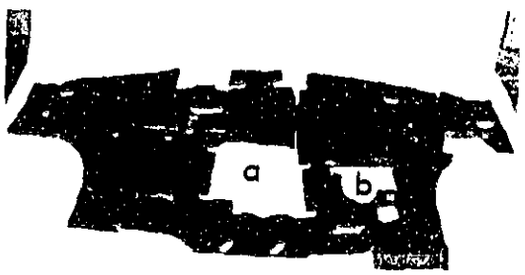

Photo 6 - Bulkhead padding, engine side, with spring-mass type padding complex alone

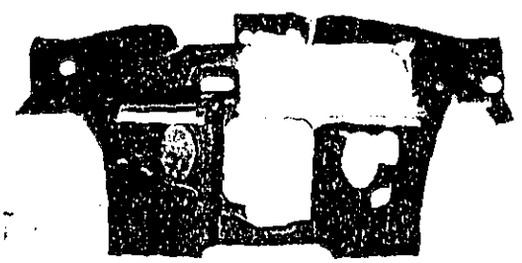

Photo 7 - Bulkhead padding, engine side, made of semi-absorbing material

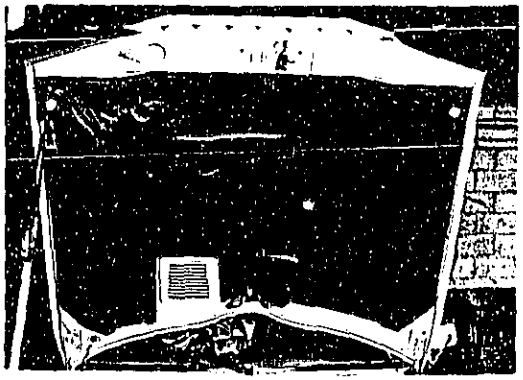

Photo 8 - Under-hood absorbing padding

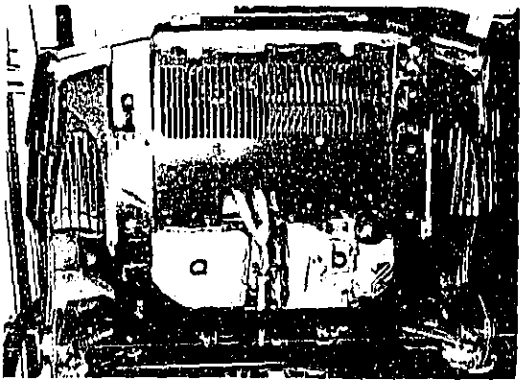

Photo 9 - Under engine view without shield

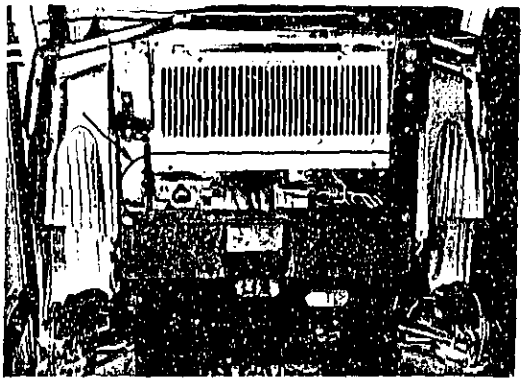

Photo 10 - Under engine shield on vehicle

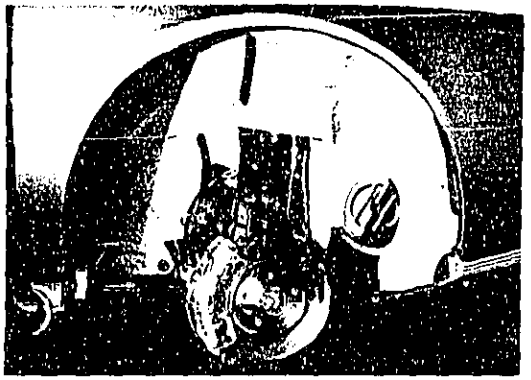

Photo 11 - Shield of right front wheel arch on vehicle

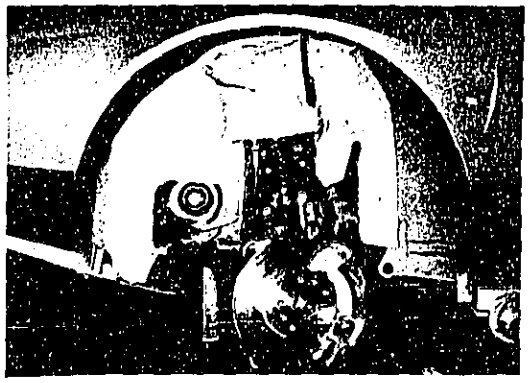

Photo 12 - Shield of left front wheel arch on vehicle

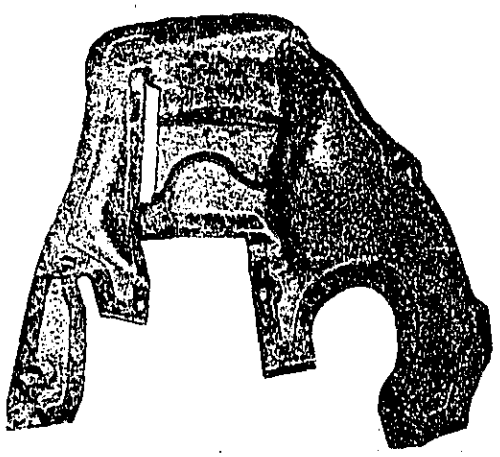

Photo 13 - Shield of right front wheel arch alone

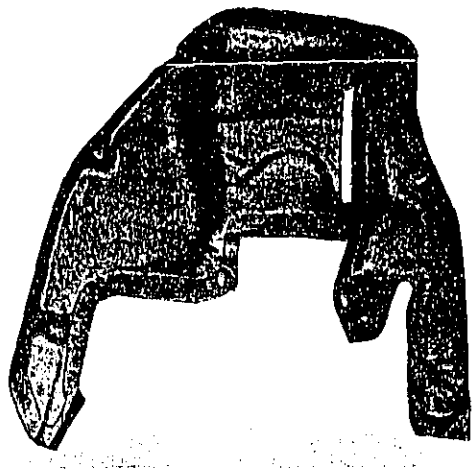

Photo 14 - Shield of left front wheel arch alone

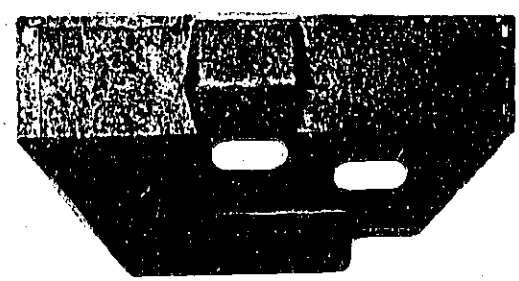

Photo 15 - Under engine shield alone

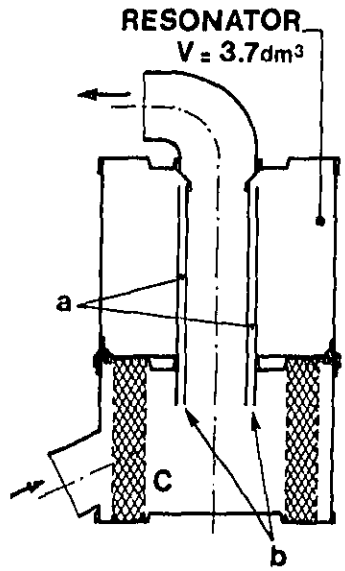

AIR FILTER

Fig. 1 - Air filter with resonator

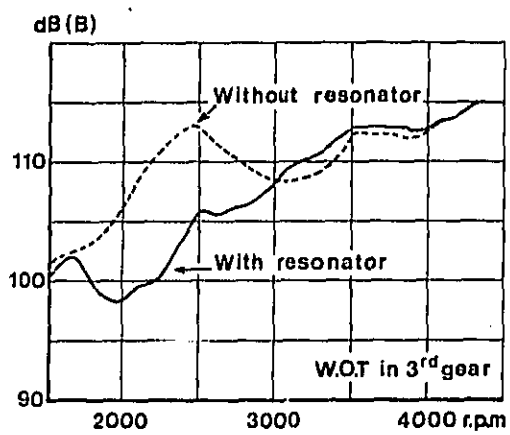

Fig. 2 - Influence of the resonator upon the intake noise at air filter inlet

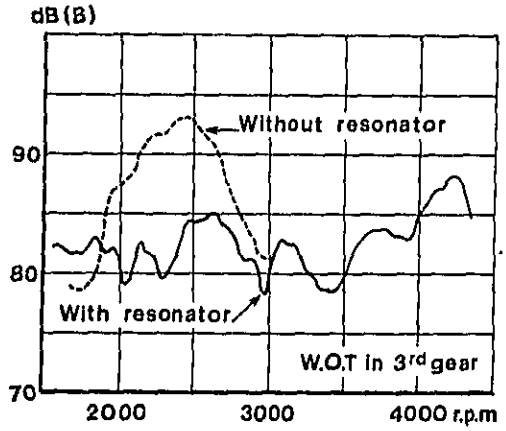

Fig. 3 - Influence of the resonator upon the intake noise at rear passenger's ear

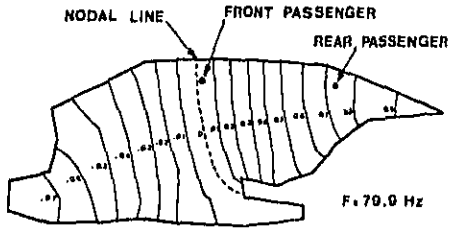

Fig. 4 - Isophonic lines for the 1 st cavity acoustic mode

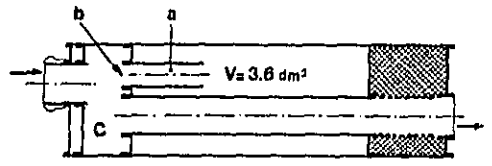

Fig. 5 - Exhaust rear muffler with resonator

1/3 OCTAVE ANALYSIS

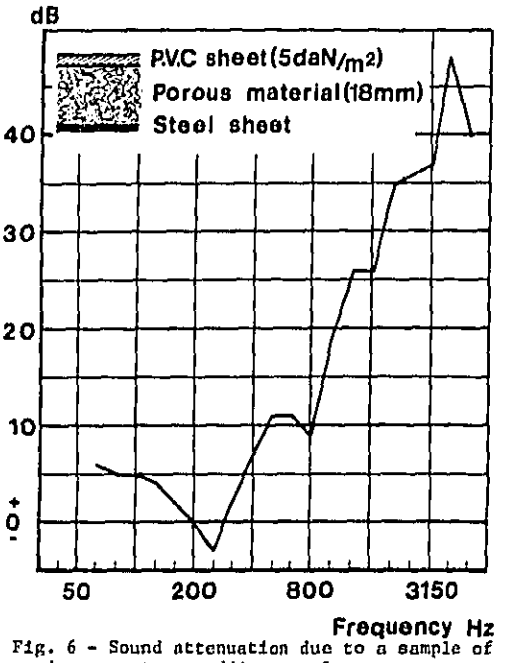

Fig. 6 - Sound attenuation due to a sample of spring-mass type padding complex

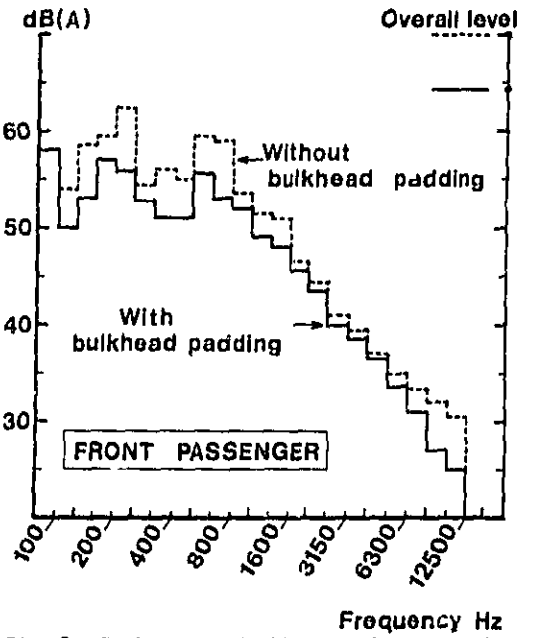

Fig. 7 - Influence of bulkhead padding upon the interior noise at 3000 rpm

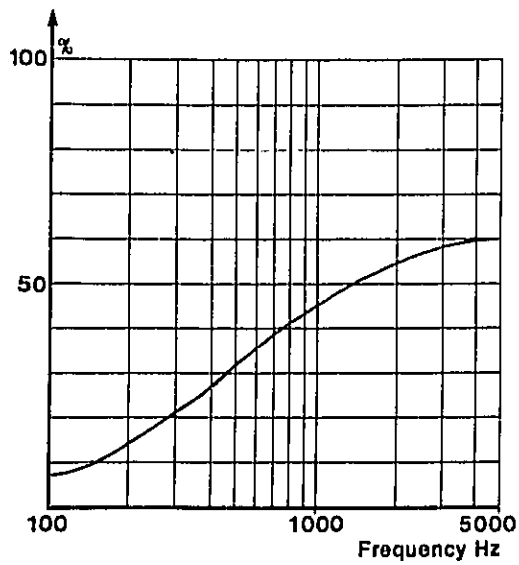

Fig. 8 - Absorption characteristics of the semi-absorbing material

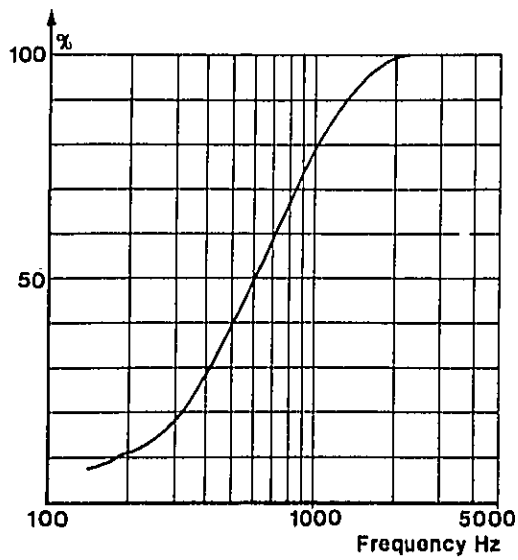

Fig. 10 - Absorption characteristics of the under hood absorbing padding

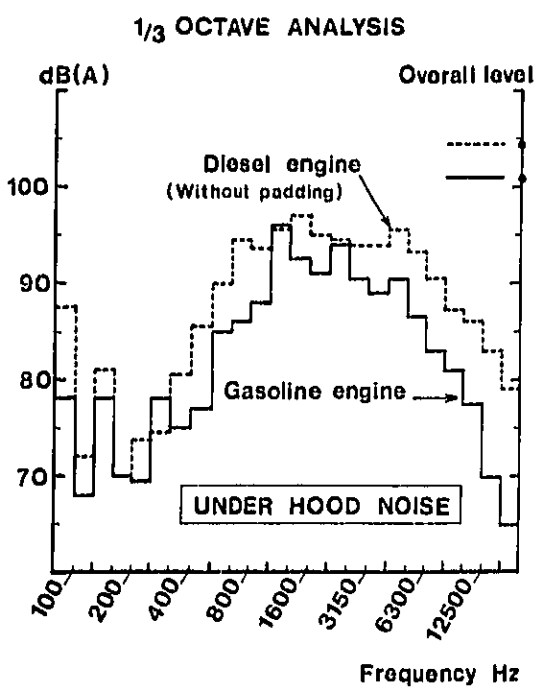

Fig. 9 - Comparison of the spectral analysis of the under hood noise for Diesel and gasoline engines at 3000 rpm

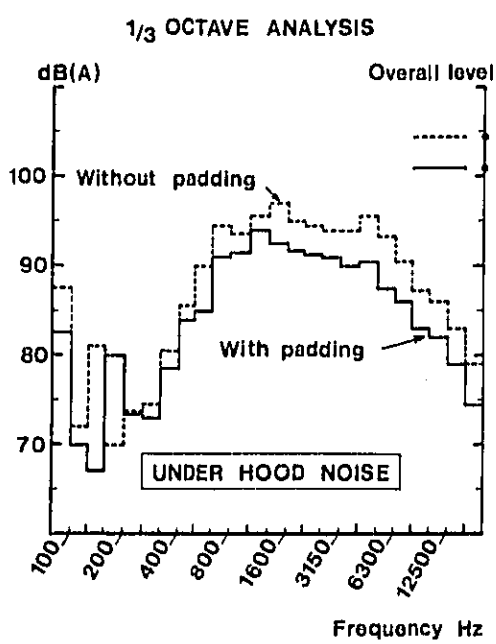

Fig. 11 - Influence of the under hood absorbing padding upon the under hood noise

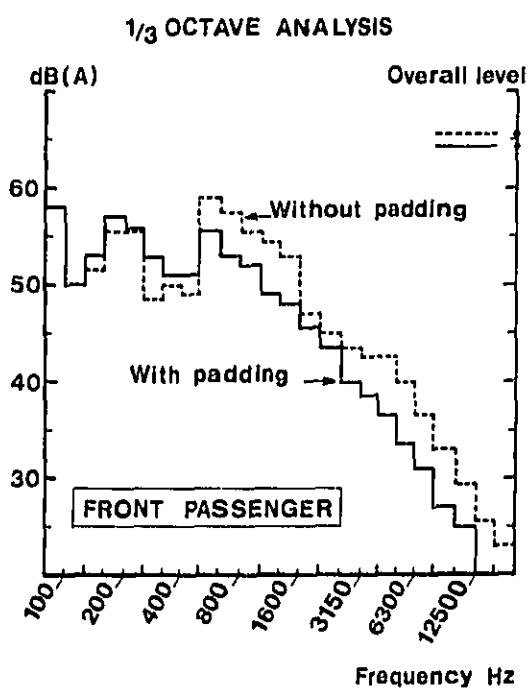

Fig. 12 - Influence of the under hood absorbing padding upon the interior noise

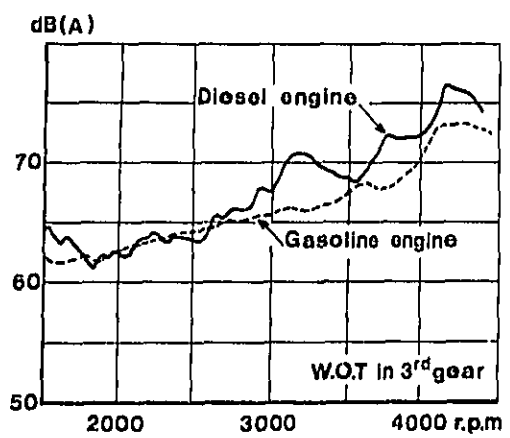

Fig. 13 - Comparison of interior noise at front passenger's ear for Diesel and gasoline engines

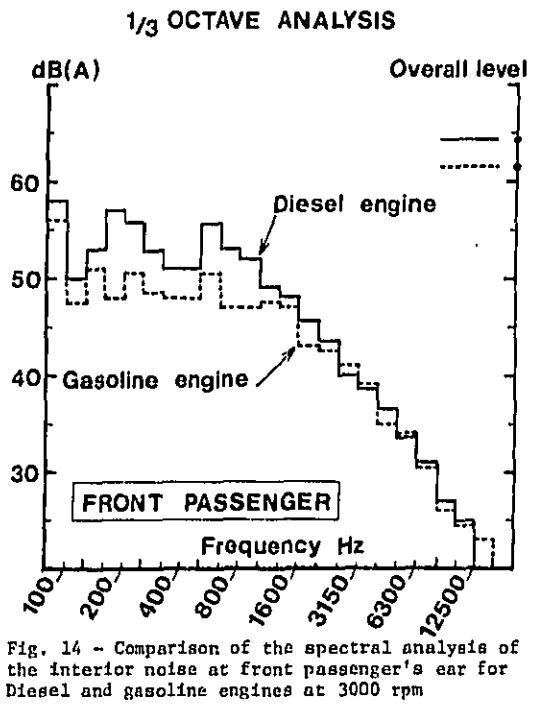

Fig. 14 - Comparison of the spectral analysis of the interior noise at front passenger's ear for Diesel and gasoline engines at 3000 rpm

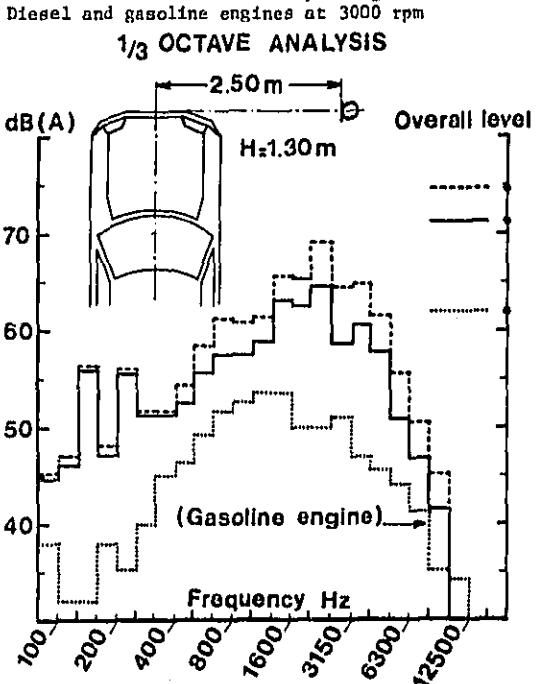

Fig. 15 - 1/3 octave analysis of exterior noise at 800 rpm
Stationary vehicle:
Diesel engine with shields
Diesel engine without shields
Gasoline engine (without shields)

790449

Concept for a Chassis Mounted Capsule of Engine and Gearbox for Heavy Trucks

Gerhard K. Krisper and
Helmut H. Kratochwill

Steyr-Daimler-Puch AG, Austria

ABSTRACT

The proposed reduction of noise by international legislation will probably result in a limit of 80 dB(A), measured according to ISO R 362. In order to obtain a uniform noise level for all categories of vehicles, the 80 dB(A)-limit is also forecast for heavy trucks in about 5 to 10 years. With a high powered conventional Diesel-engine, this limit can only be reached by complete enclosure of engine and gearbox. In this paper, we present a capsule mounted on the chassis, adapted to the cramped space conditions in a European truck. The design has the advantage of ease of maintenance, since it is possible to attatch the upper capsule parts to the tipping-cab. The results of the noise and temperature measurements are also reported. The great reduction of the surface noise by the capsule requires the installation of a radiator-fan-system, which is designed to reduce noise considerably.

THE HIGH NOISE LEVEL OF HEAVY TRUCKS presents a serious social problem in our environment. At present, one truck produces the same amount of noise as fifteen cars. Nearly all states wish to reduce the noise level and to set the same limit for all motor vehicles by means of legislation, which poses particularly difficult problems for the truck manufacturers.

Middle and long term forecasts in Europe, based on the drive-by test conducted by ISO, suggest a reduction of up to 80 dB(A) for all vehicles.

According to a Swedish study at the Royal Academy for Engineering Science about the development of motor vehicles between 1980 and the year 2000, the noise limit will have to be as low as 80 dB(A) for trucks by 1985, if there is a steady growth of the annual gross national product. If, after 1980, the annual rate of increase is only slight or even decreasing, then the limit of 80 dB(A) will not be expected until 1990.

This means that in the future the noise level of heavy trucks must be reduced from 8 to 10 dB(A). The decision of ISO and ECE to measure the noise level of trucks during the accelerated drive-by in every gear - not only in 3. gear - also heightens the problem.

An analysis of the noise sources shows that the noise emitted by the surface of the engine and gearbox and the aerodynamic noise of the fan greatly affect the total noise of the truck. The noise generated by the intake and exhaust systems of our trucks is responsible for between 5 and 10 o/o of the total noise level. A reduction of these noise sources is technically possible without too great an expense. The other sources of truck noise, such as tyre-noise, noise emitted by the surface of the axles and power transmission proved to be below 80 dB(A) under the drive-by test-conditions of ISO 362 and therefore create no further problems. This paper is concerned with the ways of reducing the noise emitted by the surface of engine and gearbox and the aero-dynamic noise of the radiator fan system.

WAYS OF DECREASING THE NOISE MADE BY THE ENGINE SURFACE

The origin of this noise source lies in the combustion process of the diesel engine and in the mechanical impact of the moving parts of the engine. The impact sound which results from this, is emitted, on the one hand directly by the engine surface and, on the other, by the gearbox surface because of the rigid connection between the two. The noise of the gearbox itself is generally of little importance. First of all the main aim of the intensive research, however, is to reduce the noise emission of conventionally built diesel engines by optimization of the combustion process e. g. (1,2)*.

*Numbers in parentheses designate References at end of paper

SAE/P-79/80/$02.50
Copyright © 1979 Society of Automotive Engineers, Inc.

The success of these activities has so far been small and the noise reduction is far from fullfilling future requirements. In addition, these measures have often been in opposition to high fuel economy and to the attempts to reduce air pollution. Many and varied tests to attain a considerable amount of noise reduction by changes in design of the crankcase, oil pan and other engine parts have not been successful enough either.

According to the present day standard of engineering, the noise emission level required in the long term is only possible by passive measures. In this way the expansion of the air borne noise emitted by the engine and gearbox is prevented by means of a capsule (3, 4, 5, 6).

With conventional truck engines the capsule may either be fastened onto the engine or fixed on the chassis by means of the existing vehicle parts. Newly designed engines may have particular parts of the capsule incorporated in the engine. Such possibilities are more difficult to realise with high performance engines, because of the problem of strength.

If the effectiveness of the capsule should be between 10 and 15 dB(A), then the sound insulation of the capsule walls must be at least 10 dB higher, as the sound pressure level inside the capsule increases by this amount, because of the reflection of the sound waves inside the capsule. This increase could be reduced by the attatchment of absorbing material, but this solution presents us with two difficulties: firstly it takes up more room and secondly there is no suitable absorbing material, which is reliable enough in the environmental conditions inside the capsule.

When building every type of capsule, special care must be taken that the maintenance and supervision of the engine do not become too difficult and that small or medium repairs may be conducted without removal of the engine.

DESIGN OF STEYR-AVL ENGINE-CAPSULE

The problem was to design a capsule for the engine and gearbox for existing trucks, produced on the assembly line. There should be as few changes as possible to the engine and vehicle.

Despite the lack of room between the engine, driver's cab and chassis, Steyr decided, working in cooperation with the Anstalt für Verbrennungsmotoren, Prof. List (AVL), Austria, to produce a capsule fixed to the frame rails, because of the many advantages of this type of construction. The straight parallel design of our truck frame rails is ideal for this (Fig. 1). The capsule encloses the engine and gearbox completely. Except for openings for the intake and escape of the cooling air to and from the interior of the capsule, it is almost air-tight. Soft rubber seals, which are found between all the capsule and frame parts, provide a good seal. Steel sheets 1 mm thick are used for the capsule, but no sound absorbing material is used inside.

The water-cooling system for the engine must be placed outside the capsule, if this completely enclosed capsule system is used. The realisation of this design therefore depends on the development of a low noise radiator fan system. The test capsule was constructed for a 16 ton cab-over-engine truck. This vehicle is provided with a water-cooled 6 cyl-diesel engine with a turbo-charger. The engine has 190 kW power at 2600 rpm. A gearbox with 10 gears is directly and rigidly mounted on the engine, so that the engine and gearbox are in one unit.

THE COOLING OF THE INTERIOR OF THE CAPSULE

To prevent over-heating of the capsule, a ventilation system is installed (Fig. 2). A radial fan, which is fixed to the belt-pulley of the water pump, sucks cool air through pipes placed at the front of the radiator and blows it into the capsule. The warmed air passes through a silencer concentric to the exhaust pipe and through a second pipe concentric to the cardan-shaft. The inlet pipes in front of the fan are also equipped with sound absorbers. To keep the cooling power of the system as low as possible and to prevent local over-heating by radiation, exhaust manifolds and turbo-chargers are insulated with asbestos.

DESIGN OF THE CAPSULE (Fig. 3 and Fig. 4)

Basically the capsule is made of several firmly fixed parts and a number of removable covers. All the necessary outlets between the inside of the capsule and the outside are on the fixed walls. The removable maintenance covers are fixed to the frames and to each other by locks, which are quick and easy to use. When designing a chassis-mounted capsule, the torsion of the frame rails of the chassis, when driving the vehicle cross-country, should be taken into consideration. A wall is built between the frame rails to form a front end, which stretches from the cooling water outlet to the rear end, forming a flat end with the under-side of the frames. There are openings in this wall, not only for the cooling water outlet, but also for the cooling water inlet and for

the fan-driving shaft.

The rear part of the capsule consists of a bowl, which is U-shaped in the horizontal projection and which surrounds the rear part of the engine and rests on the upper side of the frames. This bowl contains the through-pipes for the air intake and exhaust.

To avoid conduction of impact sound by the exhaust pipe, a compensator of thin heat-resistant steel, with a plaited-steel casing, is welded into the pipe-line. The exhaust pipe leads freely through a silencer, which is needed to reduce the noise of the air escaping from the capsule. The silencer is divided length ways and consists of an outer steel cover, heat-resistant absorbent material and an inner cover of perforated plate.

Between the front wall and the U-shaped bowl are 2 side walls, which have no outlets and so can easily be removed, so access to the sides of the engine is hardly more difficult than without a capsule. The front wall, the U-shaped bowl and the 2 side covers form a flat flange facing, on which the upper cover rests and between which there is a soft seal. Attempts were made to place this flange facing as low as possible, so that the upper cover could be built large and deep. So, with the top cover removed, the engine can be maintained and there is easy access to the cylinder heads, injection nozzles, valves etc.

At the back, the upper cover of the gearbox is fastened to the U-shaped bowl. In this, there is a box with a collar for the gear selector rod. This cover rests lengthwise on the upper side of the frame rails of the chassis, diagonally towards the back on a wall between the frames. The wall forms the end of the capsule. On this wall rests the sound absorber for the cooling air of the capsule, which is divided lengthwise and lies concentric to the cardan-shaft.

The capsule under the frames forms a trough divided into 3 parts, from the front to the rear wall. By dividing it into 3 parts, each part is easier to handle, so that it is possible to strip it by the front axle and to maintain a certain amount of movement during torsion of the frames. The middle part of the trough rests on the other two parts and is therefore the easiest to dismantle. On the front part of the trough, there is a cover on one side for changing the oil filter. The rear part of the trough stretches from the fly wheel casing to the rear wall. The weight of the whole capsule is 90 kg.

ADVANTAGES OF THE CAPSULE SUPPORTED BY THE CHASSIS

As far as the vehicle manufacturer is concerned, this model of anti-noise capsule has several advantages for the engine in connection with the Steyr-truck:

1. By using the frames as part of the capsule, the difficulties of sealing the outlets of the engine suspension are overcome, as everything is inside the capsule.

2. The chassis-supported capsule is much simpler in construction because of the omission of the capsule support on the engine (no impact sound proofing is necessary).

3. After the cover has been removed, maintenance of the engine is much easier than with an engine-supported capsule. With the usual construction of a cab-over-engine truck with a binacle, it is possible, with adaptions, to lift off the upper cover of the capsule and, if necessary, the side cover above the frames, when the cab is tipped forward. The upper and side parts will then be accessible for maintenance without further difficulties. It is not advisable to use the cab floor as part of the upper part of the capsule for the following reasons: The noise level in the capsule increases by about 10 dB(A). The air borne sound insulation between the engine and the cab must be increased, by this amount, if no noise increase is desired in the cab. If the upper part of the capsule is separate, then there is a noticeable decrease in noise level compared with an engine with no capsule. If the driver's cab floor is used as the upper cover of the capsule, there are additional severe problems of heat insulation of the cab. The existing gap between the upper part of the capsule and the floor of the cab is of great importance for the out flow of the air from the engine cooling system, which lies outside the capsule. If this air flow is stopped by the connection of the two parts, then this creates a great difficulty in the design of a low noise cooling system.

4. The design of different PTO's for special vehicles is more feasible with a chassis mounted capsule.

The disadvantage is that the distance between the engine and the frame cannot be altered. The engine position of a cross-country four-wheel drive vehicle is generally higher than that of the usual rear-wheel drive road vehicle. Therefore a different design of the capsule is needed for each type of vehicle.

TEST RESULTS

On a test bench the acoustic efficiency of the capsule is checked. The overall effectiveness of the capsule is also tested by measuring the temperature inside the capsule and by twisting the frame. For all readings, the engine and gearbox unit and the capsule parts are built onto a vehicle frame, which is cut off behind the capsule, using the original engine mounting. A propeller shaft connects the engine to a fluid friction dynamometer with negligible noise emission. The testing room is built as an echo chamber. The sound power of the gearbox unit can be measured with a rotating microphone.

Fig. 5 shows the sound pressure level in dB(A) versus engine speed, at maximum power, both with and without a capsule. Fig. 6 shows a one-third octave level analysis with the engine running at rated speed. The noise reduction of between 13 and 14 dB(A) is attained by use of a capsule, right through the full speed range, as shown in Fig. 5. From the one-third octave level analysis it can be seen that the capsule begins to take effect at .2 kHz. Whereas with an engine not in a capsule the estimated "A"-weighted total noise level is determined exclusively by a frequency band of about 2 kHz, the predominant noise emission with the capsule mounted is in the one-third octave bands between .2 kHz and 2 kHz, showing an increase at about .3 kHz.

Thereby, as well as attaining a great reduction of"A"weighted noise level, a more acceptable frequency distribution is achieved by the suppression of the typical noise created by the diesel engine. As a noise source analysis shows, the contribution of the noise of the propeller shaft to the total noise level with the capsule mounted is so large, that a reduction of the total noise level at higher revs than 2000 rpm, would only be possible by the reduction of the noise of the propeller shaft. The propeller shaft runs about 1.5 m outside the capsule.

To prove that the engine capsule is air-tight, the frame rails are subjected to a test simulating the torsional stress of the frame during a cross-country drive. The noise level reading shows no deterioration of the effectiveness of the capsule.

The efficiency of the cooling fan inside the capsule is checked by measuring the temperature of the air and the temperature on the surface of engine and gearbox. Because of the high flow rate of the cooling air of 750 kg/h, there is no increase as far as the temperature inside the capsule and the temperature of the engine's lubrication oil are concerned. However, the oil in the gearbox reaches a temperature about 10 o/o higher with the installation of a capsule, because of the high ambient temperature of the air around the gearbox, which is only cooled by surface convection. The temperature of the cooling air of the capsule, escaping around the exhaust pipe, reaches 250°C. The flow resistance in the outlet pipes for the cooling air is so designed, that, when the pressure in the capsule is 100 N/m^2 during rated engine speed, 87 o/o of the cooling air blows through the cardan-shaft and 13 o/o through the pipe concentric to the exhaust pipe.

The change of temperature after the shut-off of the engine over a period of time is shown in Fig. 7: Before the shut-off, the engine runs for 45 minutes at full engine speed. The maximum temperature is reached within 5 to 15 minutes after the shut-off. After 20 minutes there is a noticeable drop in the temperature of all readings. The highest temperature occurs in the area around the exhaust pipe and the turbo-charger. Because the temperature rises around 30°C in relation to the running engine, the maximum temperatures in this case are just over 130°C. The greatest rise in temperature, of 50°C, occurs at the middle of the cylinder head, because of the heat accumulation in the upper part of the capsule. If the exhaust pipe and therefore the escape for the cooling air lead directly upwards, then a good through-current is possible by the resulting stack effect, to avoid a heat accumulation after the shut-off of the engine. Because it is then necessary to place the silencer behind the driver's cab, and so to shorten the floor of the truck considerably, this is not always an acceptable solution.

COOLING SYSTEM NOISE

The engine's cooling system must be placed outside the capsule, as it is not possible to develop sound absorbers of a practical size for the large amount of cooling air. Therefore the fan is not affected by the sound insulating effect of the capsule and great efforts are needed to reduce the fan noise. Whereas the fan noise of a high powered engine without a capsule with a cooling system of customary design is equal to the noise emitted by the surface of the engine, it is necessary, when dealing with an engine with a capsule, to reduce, by any means, fan noise by at least 10 dB(A). In addition, the outflow rate of the air is considerably worse with an engine with a capsule: the front wall of the capsule hinders the air flow much more than is usual with an engine without a capsule.

Therefore extensive research into reduction of the fan noise is necessary. The tests are conducted without keeping the engine running, in order to be able to measure just the fan noise. The fan is driven by a low noise electric motor. The radiator is supplied with hot water from a hot-water tank using an external water pump. To determine the cooling power, the temperature difference between the water which enters and that which leaves the radiator, is measured and so is the water flow-rate.

The existing direct input shaft for the fan leading from the water pump cannot be retained, because of the high revs. In order to allow a free choice of fan speed and of the height of the fan shaft, the drive is taken from the crank shaft over an intermediate bearing by a V-belt (Fig. 8). Four tubes run in a star-shape from the fan bearing to the fan cowl. Through this rigid connection between the fan bearing and the cowl, it is possible to have a tip clearence of just 2 mm between the fan wheel and the cowl. The diameter of the fan is designed as large as possible (640 mm). By this means, the fan speed and therefore the noise emission can be reduced whilst still maintaining the same cooling power, as tests have shown. A large diameter of fan also has the advantage of a more constant distribution of the air velocity through the radiator. A fan, designed with eight wide blades, proved to be the best.

The shifting of the fan plane in the space between the radiator and the front wall of the capsule into the best position is also necessary. Because of the high static pressure, which exists in the space between the fan outlet, the front wall of the capsule and the floor of the driver's cab, the clearence between the radiator and the cab floor must be completely sealed. If it is not sealed, back-streaming of the warmed air into the area in front of the radiator will occur, which decreases the cooling power of the radiator considerably. Fig. 9 shows a one-third octave sound pressure analysis just of the noise of the radiator system, measured in free field to the side at a distance of 7,5 m from the fan shaft. The "A"-weighted level is 74 dB(A). In our design it is at a difference of $\Delta T = 60^{\circ}C$ between the intake temperatures of the water and the air into the radiator, that the heat generated by the engine at maximum power is dissipated. The speed of the fan is 1600 rpm.

The conversion of the sound power level of the engine measured in the echo chamber at maximum power to the sound intensity level at 7.5 m from the engine axis is calculated to be 71 dB(A). Therefore the total maximum noise emission of engine and gearbox plus radiator and fan system is 76 dB(A). Together with the noise of the air intake and the exhaust, as well as the tyre noise, which is about 73 dB(A) on our vehicles, it must therefore be possible to reduce the total level to under 80 dB(A), according to ISO 362.

CONCLUSIONS

Despite the European custom of building the trucks with very cramped space in the area between the engine and the cab, it is possible to desgin an anti-noise capsule, which encloses a 6 cylinder engine and gearbox completely and is mounted on the chassis. As results show, the surface noise of the engine and gearbox can be reduced by 13 to 14 dB(A). The version of a capsule, mounted on the chassis, has advantages as regards accessibility for maintenance work and repairs. It is also possible by re-design to fix the upper capsule cover to the driver's cab. With a tipping-cab, these covers are automatically raised, which means, that accessibility to the upper part of the engine is scarcely more difficult than with a vehicle without a capsule.

The fan of the water-cooled engine is placed outside the capsule. Despite the difficult air-flow conditions, due to the front wall of the capsule, a cooling system was designed, whose noise is of the same level as that of the enclosed engine.

ACKNOWLEDGEMENT

This research was supported financially in part by the Forschungsförderungsfond der Gewerblichen Wirtschaft, Austria.

REFERENCES

1. G. E. Thien "Möglichkeiten zur Senkung des Geräuschpegels von Dieselmotoren". ("Possibilities of Reducing the Noise Level of Diesel Engines"), ATZ, 74. Jg., No. 7 (Juli 1972) S. 261 - 269.

2. E. W. Huber and E. Wodiczka "Bestimmung des Verbrennungsgeräusches von Dieselmotoren mit verschiedenen Verbrennungsverfahren". ("Combustion Noise Analysis of Diesel Engines with Different Combustion Systems"), MTZ, 31. Jg., No. 4 (1970) S. 153 - 156.

3. G. E. Thien and H. A. Fachbach "Design Concepts of Diesel Engines with Low Noise Emission". SAE-Paper 750838, 1975.

4. H. A. Fachbach and G. E. Thien "Musterausführungen geräuscharmer Dieselmotoren." ("Design Concepts of Diesel Engines with Low Noise Emission"), MTZ, 36. Jg., Nr. 10 (1975) pp. 261 - 266.

5. G. E. Thien and H. A. Fachbach "Quiet Automobiles - A Realistic Objective." FISITA 1976, Tokyo.

6. H. A. Fachbach and G. E. Thien "Ein neuer Weg zum geräuscharmen Fahrzeugmotor." FISITA 1978, Budapest. ("A New Way to a Vehicle-Engine with Low Noise Emission")

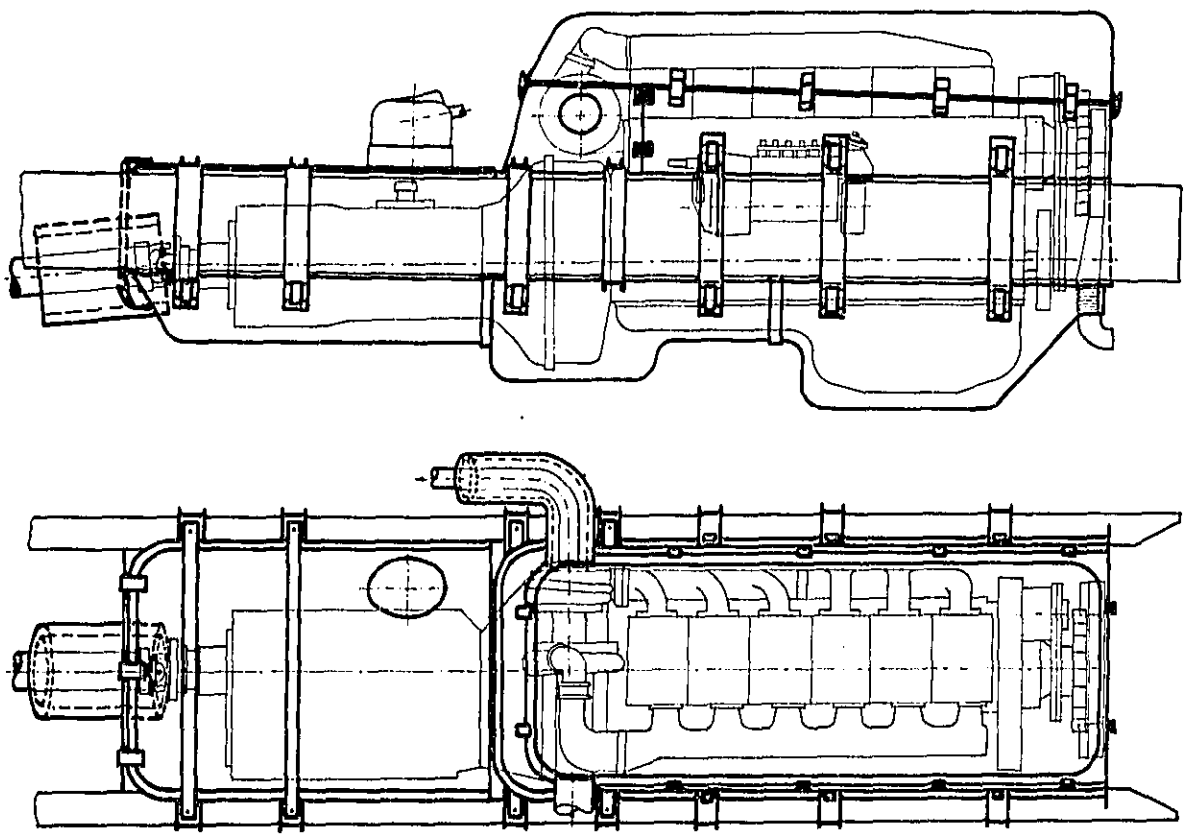

Fig. 1 - Design of a chassis mounted noise - reducing capsule of engine and gearbox

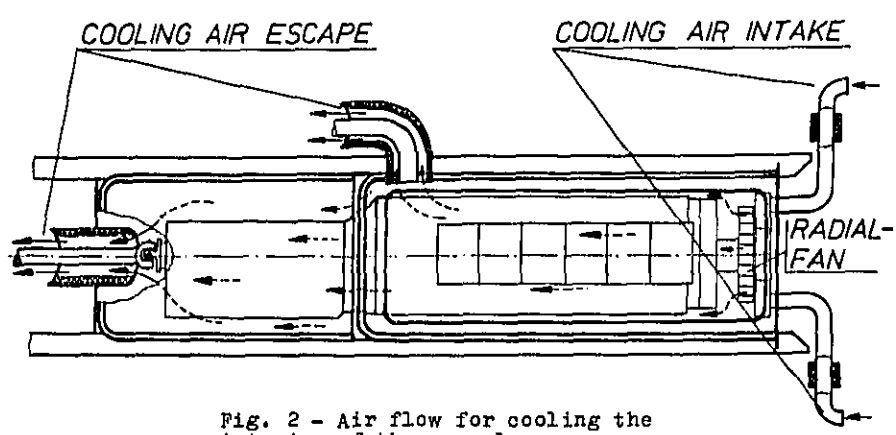

Fig. 2 - Air flow for cooling the interior of the capsule

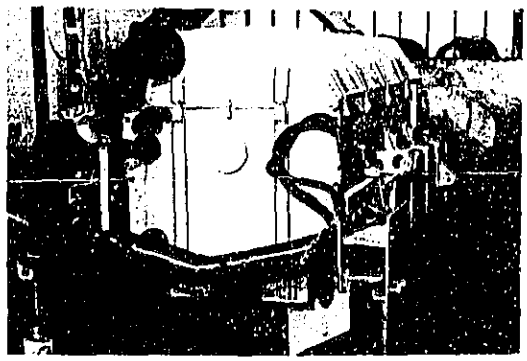

Fig. 3 - Front view of the engine with the capsule

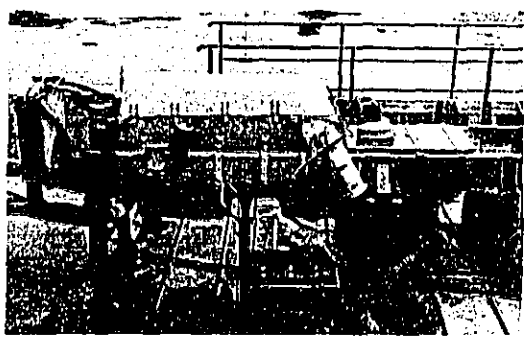

Fig. 4 - Side view of the engine with the capsule on free-field test bench

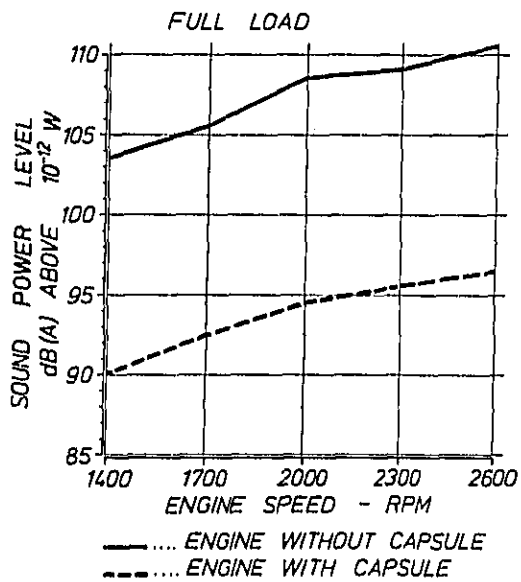

Fig. 5 - Noise of engine and gearbox (191 kW)

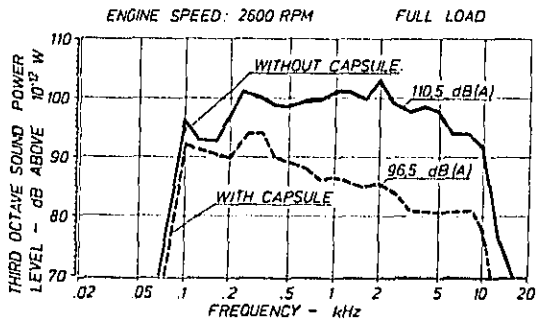

Fig. 6 - Noise of water-cooled 6-cyl. diesel engine for heavy truck

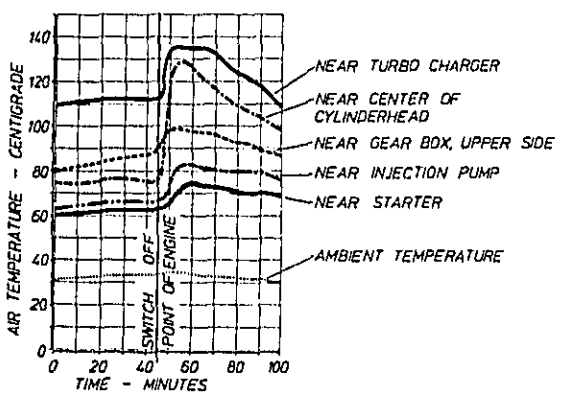

Fig. 7 - Temperature rise inside the capsule after shut off of the engine running at maximum power

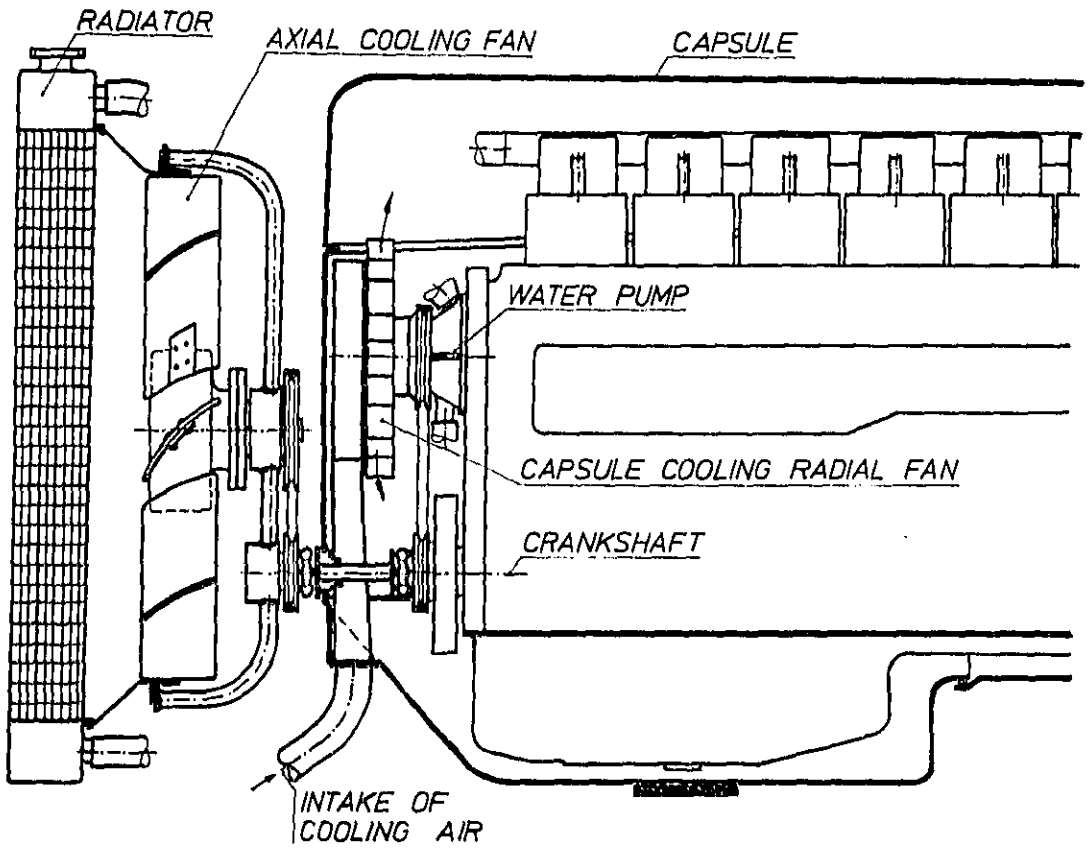

Fig. 8 - Water-cooling system of a diesel engine with sound reducing capsule

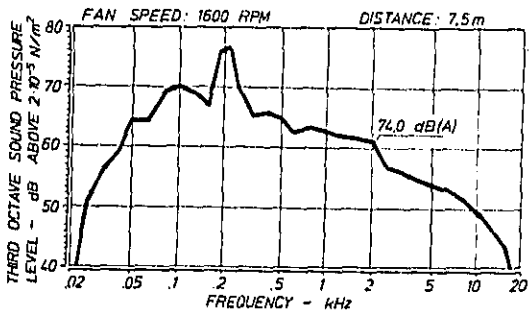

Fig. 9 - Water-cooled 6-cyl. diesel engine, noise of cooling system

790450

RESEARCH PROJECT FOR REDUCING THE NOISE OF TRUCK DIESEL ENGINES

Dipl. Ing. Karl F. Feitzelmayer
Prof. Dr. Ing. W. Schröder

Maschinenfabrik Augsburg Nürnberg (M.A.N.)
Aktiengesellschaft
(Germany)

ABSTRACT

The first efforts to attenuate noise from motor vehicles go back to the 1930s. Significant developments in noise attenuation research culminating in 1974 with the presentation (FVV-AVL) of a water-cooled and an air-cooled research engine enclosed in a close-fitting capsule are addressed.

Two basic studies are described as representative of individual research carried out by commercial vehicle manufacturers: body-mounted capsules for diesel truck engines and tests on close-fitting capsules performed on the test stand.

The enclosed water-cooled engine and a basic engine without a capsule were each mounted on a truck chassis in order to test the effectiveness of the capsule and to compare measurements taken with the enclosed engine on the test stand with those taken with the engine in the vehicle. Despite the discrepancies between the two sets of data, the results of the vehicle tests were satisfactory.

RESEARCH PROJECT FOR REDUCING THE NOISE OF TRUCK DIESEL ENGINES

THE NOISE SITUATION IN TRAFFIC - Noise has reached such intolerable proportions in densely populated, highly developed areas that corrective measures are imperative. Noise protection is justifiably of vital concern to our society (1)*

Any effort that could result in a reduction of noise in densely populated areas is therefore deserving of special attention.

The principle applied in other fields of environmental pollution of prosecuting the party at fault does not lend itself to the problem of traffic noise in densely settled areas since the manufacturers of motor vehicles, drivers, and traffic planners must all be implicated in the development of traffic and therefore of traffic noise.

In the early days of motoring emphasis was placed on the transport aspect, and lack of comfort was something taken for granted.

PROGRESS IN NOISE RESEARCH - As early as 1937 German legislation set upper limits on noise levels (2). Even before noise abatement moved into the focus of public attention, science and industry were pursuing approaches to the problem of reducing noise.

1960 witnessed one of the first systematic study projects (3) with the objective of determining the noise levels of internal combustion engines. This was carried out under the auspices of the FVV (4) (Research Association for Internal Combustion Engines).

In 1965 Priede (5) published work on a steel-skeleton engine, and in the same year the FVV commissioned an investigation on preliminary measures to be taken for reducing noise emission.

In 1966 work of a commercial vehicle manufacturer (6) was published with a body-mounted capsule around the engine compartment (see text).

Finally, in 1967 the research project of the FVV, "Future Designs for Low-Noise Diesel Engines" (7) was initiated. Based on the research engines to be built (one water-cooled and one air-cooled), a design concept was to be worked out for a low-noise engine suitable for production.

In 1974 the FVV research product (7) was terminated with the presentation of a water-cooled and an air-cooled research engine. The test results (8) were based on engine performance on the test stand.

RESULTS OF SEVERAL BASIC TESTS (6) - The development tendencies in the automotive industry in the 60s such as light-weight construction, high-speed engines, higher compression ratios, and lower costs all contributed towards a steady increase in vehicle noise. The tests conducted dealt with a full enclosure of a diesel engine, representing an indirect solution to the problem.

The projects had the following objectives:

1. Maximum noise attenuation at minimum expense.
2. Effectiveness in reducing both exterior and interior noise.
3. All problems pertaining to encasing the engine and to cooling.

Preliminary tests performed on a 4-

*Numbers in parentheses designate References at end of paper.

SAE/P-79/80/$02.50
Copyright © 1979 Society of Automotive Engineers, Inc.

cylinder in-line diesel engine with a displacement of 4.68 l and a rated output of 86 kW at 2500 rpm were intended to demonstrate to what extent an enclosure would be effective. The test arrangement is depicted in fig. 1.

The engine was mounted on a drivable tubular frame by means of vibration-damping rubber-metal mounts. The capsule consisted of an upper section and a lower section attached to the frame with rubber buffers to reduce vibration. In order to obtain only that portion of noise arising from moving engine components and from the improvements made, the induction and exhaust openings were removed, i.e. they were placed where they would be acoustically neutral. The engine was cooled by a supply of fresh water. All test measurements of the outside noise level were taken 1.5 m from the capsule wall with the engine operating at its rated speed under no load.

Fig. 2 shows the 3 capsule wall designs tested. Stage 1 consisted of 1.5 mm sheet metal and about 3 mm sound-absorbing material. The graph in fig. 2 demonstrates that even this simple capsule design resulted in a noise reduction of up to 14 dB in some frequency ranges.

In stage III 50 mm of rock wool behind perforated sheet metal was mounted on stage I. With this design a noise reduction of more than 12 dB was achieved in the frequency range 300 - 10,000 Hz in the preliminary tests (fig. 2, stage III curve).

The main test: after these successful results the main test was performed on a commercial vehicle. Fig. 3 displays the installation of the capsule in a forward-control vehicle. The objective was to reduce all noise emitted by the engine, including inlet, exhaust, fan, mechanical, and combustion noises. Noise transfer from the engine to the vehicle frame and from there to the cab was also to be cut down. The standard 6-cylinder, in-line engine of the front-control vehicle was replaced with a shorter 4-cylinder engine in order to make more room for the capsule. The capsule was made in accordance with the stage III design and consisted of 12 bolted parts. The transmission, air compressor, and generator were enclosed with the engine. Holes provided for the shifting rod, universal joint, fan drive, and all the lines were sealed with foam rubber. The capsule was attached to the frame with rubber buffers. Exhaust pipes and induction tubes within the capsule were insulated with asbestos. Fig. 4 illustrates the sound level directivity pattern for the engine with and without the capsule (measurements taken without fan). The measurements performed on a non-reflective concrete floor at 8 points yielded an arithmetical mean value of 12.5 dB(A) for the noise level reduction with the enclosed engine.

The road test was performed at various speeds at full load and while coasting on an asphalt street. Fig. 5 plots the noise level of the vehicles with and without the enclosed engine as a function of speed as well as the tire noise of both vehicles. The noise level drop at 55 km/hr. results from shifting the vehicle from fourth into fifth gear.

Tests with a close-fitting full capsule were performed on the test stand parallel to the tests carried out on the vehicle. (117 kW at 2500 rpm, 7.03 l displacement).

The tests were designed to provide answers to the following questions:

1. What improvements can be achieved by employing close-fitting capsuling of the loudest engine components ?

2. How does full and partial shrouding of the engine affect the heat balance of the engine ?

Both basic tests (vehicle and test stand) were intended to provide selection criteria for establishing beyond which reduction in noise level a total enclosure or only a partial enclosure of the engine is indicated. In accordance with test objectives no consideration was to be made of the fact that the solution could form the basis of results for a later test series. For this reason, to take an example, the rubber buffers (65 Shore) were cemented to the engine surface. Fig. 6 shows the construction of the lead capsule. A frame of 2 x 25 mm flat iron covering the individual buffers forms the supporting framework for the capsule of 2 mm sheet lead which is fastened to it. A surface density of 22 kg/m^2 would theoretically result in a noise level reduction of 30 dB. The cavity between the lead shell and the engine surface was filled with rock wool in order to reduce sound pressure between the walls. The engine weighed 650 kg, the capsule 160 kg. At full load and at a rated engine speed of 2500 rpm a noise attenuation of 15 dB(A) was achieved on the test stand.

Fig. 7 shows the course of the mean noise intensity in db(A) for the engine on the test stand measured at a distance of 1 m (microphone moved around vehicle) with and without the capsule. The engine speed was varied at full load between 1500 and 2700 rpm. The graph of rotational speed over the range of 1500-1700 rpm as a function of frequency with noise reduction represented by the band demonstrates the beginning of the capsule effect at 160 Hz. The measurements with the enclosure partly removed were well suited to determine contributing noise of the individual engine components, since the signal-to-noise ratio for most of the measuring points was sufficiently high due to the remaining capsule parts.

The tests yielded the following results:

1. Full enclosure. A noise reduction of 15 dB(A) can be achieved on the test stand.
2. Partial enclosure
   a) Front side
      Cylinder heads, valve covers, intake system, and induction line together 4.5 - 5 dB(A) noise intensity reduction
   b) A total of 13 separate sections were examined. To determine the noise portion of each section the capsule section in front of the section in question was removed.

It was confirmed that even with an enclosure of nearly all 13 sections a noise reduction of less than 10 db(A) was achieved. A comparison of this value of 10 dB(A) with the result of 15 dB(A) for the total enclosure clearly indicates future design objectives: a full enclosure of the engine.

THE AVL-FVV DESIGN OF A CLOSE-FITTING ENCLOSURE (8, 10). The development was based on a standard engine (Henschel D 562), adapted by modifying and adding components.

Fig. 8, which is a sectional view through the water-cooled engine, illustrates the constructional features.

Legend to fig. 8
1 = Soundproof supporting frame
2 = Cooling-air intake
3 = Cooling-air outlet, hot-gas side
4 = Cooling-air outlet, engine surface
5 = Oil-soaked lower part of capsule
6 = Lower part of highly stiffened crankcase
7 = Outer contour of engine capsule
8 = Impeller for capsule ventilation
9 = Flywheel housing

Other features worthy of mention include:

a) The main bearing mount (6) of the crankshaft is integral with a bearing support in the lower portion.

b) The design separates the lower oil-soaked cavity (5) from the dry upper cavity, in which all accessory components must be accommodated.

c) This partitioning of the upper from the lower cavities makes it possible to dispense with the side walls of the engine in order to save weight. The functions of the side walls are assumed by a sheet-metal skin (7) only 1 mm thick.

Capsule construction (fig. 8). A supporting frame (1) is provided, which is attached to the engine in such a way that vibrations are damped. A rubber membrane seals the upper dry cavity from the lower one. Cooling air is inducted at the front through mufflers by a radial-flow fan. It then flows in two separate streams into the cavity formed by the engine surface and the inner surface of the capsule. One of the streams is directed onto the hot-gas conducting parts (exhaust manifold) and emerges on the flywheel side through a passage (3) lined with absorbant material. Within the capsule, which is manufactured of ordinary automotive sheet metal, the exhaust pipe is separated from the engine by means of a corrugated tubing compensator. The other stream of air cools the rest of the engine surface and also emerges on the flywheel side through another absorbant surface (4). A drive for the cooling fan, generator, compressor, and servo steering pump was not provided for in the initial test design. The test stand arrangement for the enclosed research engine can be seen in figs. 9 and 10. Fig. 10 shows the upper and side covers provided as installation and maintenance aids.

The road tests of the research engine in a truck chassis were performed in order to ascertain whether a noise intensity reduction of 18-20 dB(A) as measured on the test stand could be achieved in actual operation. Two truck chassis truck A(11) and truck B(12) of the same model and size were employed in these tests. One vehicle was equipped with the low-noise research motor (vehicle A) while the other was equipped with a standard engine without capsule to serve as a control vehicle (vehicle B). On both vehicles only the noise portion emitted by the engine was to be measured. For this reason, the intake and exhaust system noises were eliminated by using additional noise attenuators with a total reduction of 35 dB (fig. 11 and 12). In truck A the fan driven directly by the engine was replaced by 4 electric truck fans (with cut-out switch). In truck B the fan was removed for the tests. Because of the low engine noise level the intake and exhaust lines of vehicle A had to be wrapped with soft lead; the interfering noise would otherwise have been too great. The transmission of vehicle A demonstrated such a high noise level during the first test run that it too had to be fully enclosed in a capsule. The generator, compressor, and servo steering pump were then driven by a power take-off unit mounted on the enclosed transmission. This unit was also fully enclosed and can be seen in fig. 11 as a box behind the engine.

Noise pattern at 7 m distance from the outer contour of the vehicle. Comparative values between enclosed and open engine.

Fig. 13 gives the values measured at a distance of 7 m on a stationary vehicle with the engine operating at the cut-off speed (2750 rpm) without load. The two outer curves plot the values of vehicle B with the unenclosed engine. Curve IV differs from curve III in that noise sources from muffler, intake system, and

exhaust system were eliminated in curve III. The innermost curve (I) represents the best operating state attained with a mean value of 72.3 dB(A) calculated from 8 measuring points. This represents only about 16 % of the sound intensity of the open control-engine as shown by curve III (mean value of III = 80.25 dB(A). An impressive feature is the uniform distribution of the noise level (curve 1) about vehicle A.

Acceleration drive-by tests in accordance with ISO R 362 (13) were carried out on a test track complying with test specifications (fig. 14). A measuring microphone was located 7.5 m from the center of the lane (ISO R 362); a second was set up at a distance of 15 m. The position of the vehicle was assigned to the corresponding sound level LA dB(A) (14) on the recording paper. The positional data always refer to the bumper of the vehicle. In this way every test run yielded a noise intensity curve through the whole track length of 20 m for the two microphones positioned at a distance of 7.5 and 15 m as well as the corresponding engine speed. We will now examine the measured values for the right side of the vehicle.

Fig. 14 plots the noise level curve LA 7.5 ISO (15), corresponding to the acceleration drive-by test in accordance with ISO R 362 specifications with a microphone distance of 7.5 m. The sound intensity is expressed in the following terms:

LA 7.5 ISO
| | Test procedure
| Microphone distance
Sound level

Curve LA 15 ISO shows the corresponding sound level at a distance of 15 m. Converting the sound level LA 7.5 ISO along the vehicle path to the corrected (standardized) distance of 7.5 m yields the noise level LN 7.5 ISO (or LN 15 ISO by converting to 15 m). The transition from LA to LN is indicated by arrows at the measuring points LA in fig. 14. The correction factors are dependent on distance and are given for the conversion of curve LA 7.5 ISO to LN 7.5 ISO. The distance marks along the vehicle path (A-O m, 10 m = microphone location) refer to the respective positions of the vehicle bumper at the time the measurement was taken at the microphone location. Vehicle A was at a point 12 m along the vehicle path when the maximum sound level was recorded at the microphone location (10 m).

Fig. 15 plots the distance-corrected noise levels LN dB(A) (16) as a function of distance along the vehicle path. The test procedure used is described in ISO R 362. A variation of this procedure is presently the topic of discussion and is called "ECE R-9 Revised" (17). (LN 7.5 ISO - noise level LN corrected to microphone distance 7.5 m, ISO R 362).

Test specifications ISO R 362 applied to vehicle A prescribe that the test be carried out in third gear. The cutoff engine speed may be attained in the course of the test. Owing to the low engine power of 117.6 kW, however, the engine of the empty vehicle A did not reach the cutoff speed along the test track from line A-A to line B-B (only 0.93 n max). Nevertheless, testing procedure ECE R-9 Revised was applied to vehicle A on an experimental basis. In accordance with test specification ECE R-9 Revised, as soon as the cutoff speed of the engine is attained within the testing distance, the vehicle should be shifted into the next higher gear until the cutoff speed can no longer be reached. These corrected sound levels LN 7.5 ISO, LN 15 ISO, as well as LN 7.5 ECE, LN 15 ECE (fig. 15) clearly demonstrate the dependency on engine speed even if the influence of the test procedure and therefore of the operational state of the engine is not clearly shown.

Fig. 16 illustrates the relation of the corrected noise level LN measured along the vehicle path to the corrected engine speed. This is the ratio of the momentary engine speed to the engine speed (n max) at maximum power output (2600 rpm). The engine speed ratio determined ranged from 0.73 to 0.94 n max (ISO) and from 0.74 to 0.796 n max. (ECE). This means that in the case of the ECE R-9 Revised test procedure the vehicle passes the microphone with a lower engine speed than in the case of the ISO procedure. As a result of the smaller rotational speed gradient, resonances are able to develop more readily and with less interference. A regression line through the individual noise level curves (fig. 16) displays a characteristic rise which is dependent on the test procedure. The ECE R-9 Revised procedure results in a steeper line and higher noise levels.

Increase per 100 rpm
LN 7.5 ECE = 4.36 dB(A)
LN 15 ECE = 3.97 "
LN 7.5 ISO = 1.90 "
LN 15 ISO = 0.60 "

The vehicle attains the first peak after 12 m with an engine speed of 2190 rpm corresponding to 0.84 n max.
In order to obtain only the engine noise in a subsequent test the rear axle of the vehicle was placed on jack stands on the test track. The noise level of the stationary vehicle was then determined throughout the engine speed range, once for the engine noise (in neutral) (LM) and once in third gear with the rear axle "free-wheeling" (LM+G). At the measuring point for the maximum noise level as determined by ISO R 362 (12 m vehicle path) and with the known engine speed for

this maximum (n max = 0.84), a noise level of 72 dB(A) (LM) and 72.8 dB(A) (LM+G) for engine and transmission and rear axle can be measured at constant engine speed, i.e. without acceleration influences. The curves for LM and LM+G appear at the bottom of fig. 16. In the ISO drive-by test the vehicle reached a speed of 29.88 km/hr at the measuring point 12 m along the vehicle path, corresponding to a measured engine speed of 0.84 n max.

Finally, fig. 17 shows the tire noise level LR 30 = 3 km/hr and the drive-by test at constant speed LV 30 = 30 km/hr. In addition the points above the 12 m measuring point indicate the various operational states of the vehicle at 0.84 max., that is the engine speed at the highest noise level in accordance with ISO:

α = vehicle raised on jack stands, engine noise n = 0.84 n max = LM

β = as in α, transmission, drive shaft and wheels in rotation = LG+M

γ = as in α, engine accelerated from 0.75 n max. to n max. (ISO static) = LN 7.5 ISO

δ = measured value at measuring point 12 m as in ISO R 362 road test = LN 7.5 ISO

If we assign a value of 100 % to the measured value of δ (fig. 17) = 82.45 dB(A), we obtain the following relative values for the sound energy distribution:

δ = 82.45 dB(A) = 100 % sound energy

α = 72 " = 8.91 " "

β = 72.8 " = 10.00 " "

γ = 76.45 " = 25.12 " "

LR30=66.5 " = 2.51 " " +

LV30=74.5 " = 15.90 " " ++

\+ tire noise v = 30 km/h

++ noise level in drive-by test at constant speed v = 30 km/h

The relation between the measured value δ (acceleration drive-by test ISO R 362) and the measured value γ (vehicle supported on stands) with the addition of the tire noise portion can be expressed as

$$L\delta - (L\gamma + L_R) = 72.37\ \%$$

72.37 % of the sound energy measured in the acceleration drive-by test must be accounted for by processes which depend, among other factors, on the acceleration. Further tests will be necessary to clarify these measured values.

Comparison of ISO drive-by test, truck A/truck B - Comparison of noise levels in the acceleration drive-by test in accordance with ISO R 362.
Vehicle A - with low-noise research engine
Vehicle B - with basic open engine
Both vehicles were tested without fan, intake, and exhaust noises. In its initial condition vehicle B had a noise level of 90 dB(A). This level was reduced to 87.5 dB(A) as soon as fan, intake, and exhaust noises were eliminated. The comparative value for vehicle A was 82.45 dB(A) or 68.4 % of the initial sound intensity of vehicle B.

A summary of the composite results demonstrates the difference in behavior of the water-cooled enclosed research engine with respect to noise emission on the test stand and in the vehicle.

1. A mean noise intensity reduction of 18-20 dB(A) was measured on the test stand, thus meeting the initial test objectives.

2. The test stand measurements are not fully reproducible with the engine mounted on a truck chassis. The following diagram compares values either measured at a distance of 1 m corrected to 7 m or measured directly at 7 m:
Noise level reduction 1 m to 7 m = 17 dB (A) (calculated)

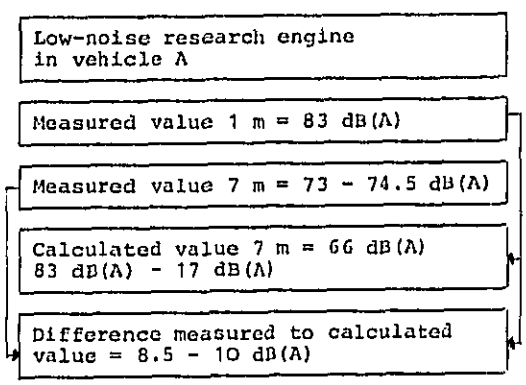

The total effect of the low-noise research engine is 8.5 - 10 dB(A) lower in the vehicle than on the test stand.

3. Part of this relatively poorer performance in the practical test can be seen in the frequency analysis of the loudest point in the ISO drive-by test. The total effect here collapses almost completely in the 500 Hz range (test stand attenuation approx. 10 dB). It is suspected that this is due to resonance of the body sheet metal and of the power plant. A further contributing factor could be the fact that the rubber engine

and capsule mounts were not designed for road operation.

4. The subjective appraisal of the drive-by noise by a large number of test persons did not correlate with the measured levels. THE VEHICLE IS PHYSIOLOGICALLY QUIETER THAN THE MEASURED VALUES WOULD INDICATE. The reason for this is a less sustained pulsation of the noise.

5. All other noise sources such as mufflers, induction system, transmission, drive shaft with intermediate bearing, rear axle transmission, tire noise, influence of the road surface (e.g. stones in the tire treads), radiator, and fan immediately become conspicuous in measurements of this nature and complicate the tests, as there are no ready solutions to make them quieter (tires, axles, radiator, fan).

6. Scattering of measured results: In the course of the tests the engine had to be removed several times from the vehicle. This resulted, among other things, in a difference in measured noise level of up to + 2 dB(A) (ISO R 362). This means that in addition to the measured values of 82.45 dB(A) discussed here, corresponding to one mounted state of the engine, there were other noise levels correspondingly higher.

7. A comparison of the measurements at distances 7.5 m and 15 m does not permit the application of the law of distances. Levels both too high and too low are registered. This is due to the frequency distribution and to emission conditions determined by the vehicle geometry which are constantly changing with distance to the recording microphones. Another reason might be the designation of the bumper as the reference point (ISO R 362).

The objective of this test series on vehicles, which covered a period of 3 years, was to compare test stand results with results achieved with the engine in the vehicle. With regard to the measured sound level reduction in the vehicle as well as the subjective impression of noise production, the results can be regarded as being very positive. The low-noise, water-cooled research engine was not designed to be used in a vehicle. For this reason this paper treats only of the acoustics, and not of the other problems involved in mounting and operating the engine in a vehicle. It remains the task of the engine designer who wishes to employ the results of the foregoing FVV-AVL project to take into account the characteristics of the vehicle itself.

REFERENCES

1. Verband der Automobilindustrie e.V. (VDA) (Ass. of Automobile Manuf.) "Stadtverkehr und Lärm", ("Urban traffic and noise"), Feb. 1978

2. StVZO = Highway code of the German Federal Republic

3. FVV, Physical Technical Bureau, Tech. Univ. of Berlin "Bestimmung der Lautheit von Verbrennungskraftmaschinen" ("Determination of sound levels of internal combustion engines") 1960

4. FVV = Research Ass. for Internal Combustion Engines

5. T. Priede, a) "Noise of Automotive Diesel Engines: its cause and reduction", SAE Detroit 1965
b) "Some studies into engines of automotive diesel engine noise and its control", Fisita, 1966

6. F. Juhász, "Geräuschminderung an einem MAN Lastwagen durch vollkommene Einkapselung", ("Noise reduction on an MAN truck by fully enclosing the engine"), Automobile-Technische Zeitung, no. 11, 1965.

7. FVV-AVL, "Zukunftskonstruktion geräuscharmer Dieselmotoren ("Future designs of low-noise diesel engines"), 1967

8. G.E. Thien and H.A. Fachbach, "Geräuscharme Dieselmotoren in neuartiger Bauweise" ("A new design concept of low-noise diesel engines"), Motortechnische Zeitung, vol. 35, no. 8 (1974).

9. MAN, "Hautenge Kapselung des MAN-Motors D 0836 HM 91 U" ("Close fitting capsule on the MAN engine D 0836 HM 91 U"), internal research report, 1968.

10. AVL = Anstalt für Verbrennungskraftmaschinen (Institute for Internal Combustion Engines), Prof. List, Graz, Austria.

11. Vehicle A - With low-noise research engine

12. Vehicle B - Standard engine without capsule

13. ISO R 362 - Acceleration drive-by noise test

14. LA dB(A) - Sound level dB(A)

15. LA 7.5 ISO
| | Test procedure
| Microphone distance
Sound level

16. LN dB(A) Distance-corrected sound level

17. ECE R-9 Revised - Sound level test in acc. with ISO R 362, but using highest gear in which the cutoff speed is not reached within the test range (line A-A to B-B).

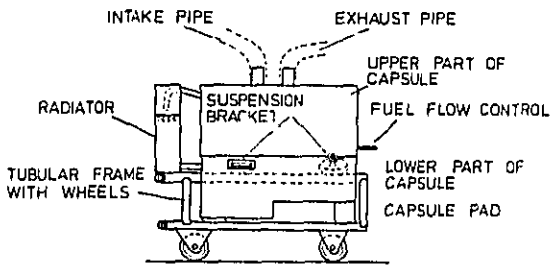

ENCAPSULED ENGINE ON DOLLY FOR PRELIMINARY TESTS

Fig. 1 - Encapsuled engine on dolly for preliminary tests

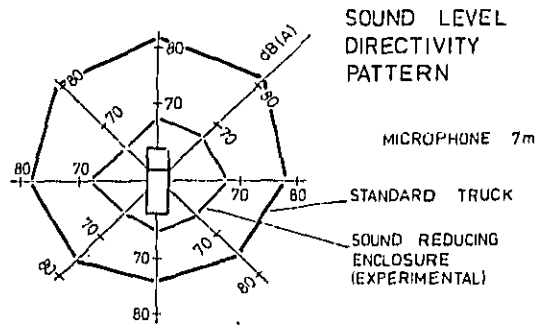

Fig. 4 - Sound level directivity pattern

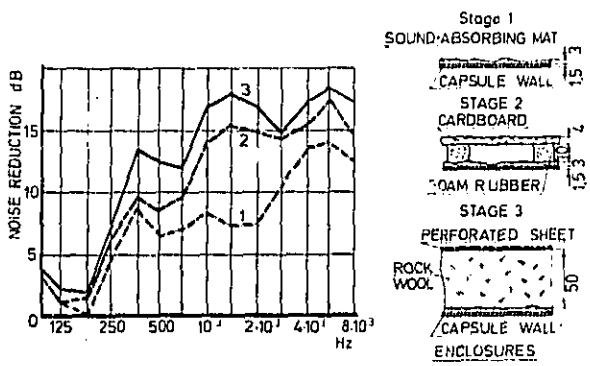

Fig. 2 - Noise intensity through capsule at n = 2500 rpm. Microphone distance 1.5 m, injection-pump side of engine; capsule construction

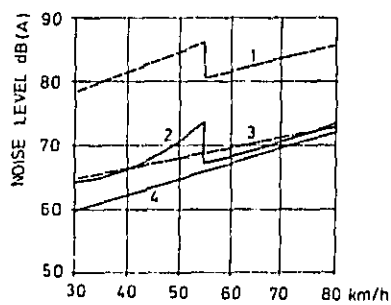

Fig. 5 - Sound level as a function of vehicle speed at full load in 4th and 5th gears
Curve 1 = Truck without capsule
2 = Truck with capsule
3 = Truck without capsule) tire
4 = Truck with capsule) noise

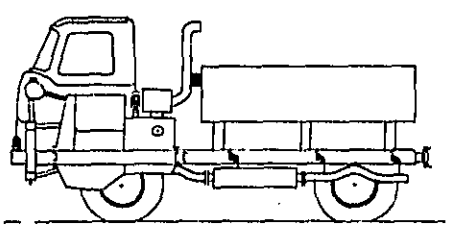

DIAGRAM DISPLAYING INSTALLATION OF CAPSULE IN FORWARD CONTROL VEHICLE WITHOUT FAN

Fig. 3 - Diagram displaying installation of capsule in forward-control vehicle without fan

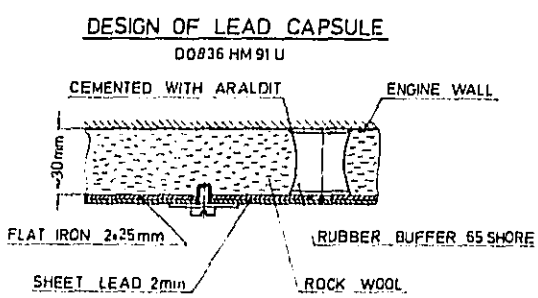

Fig. 6 - Design of lead capsule

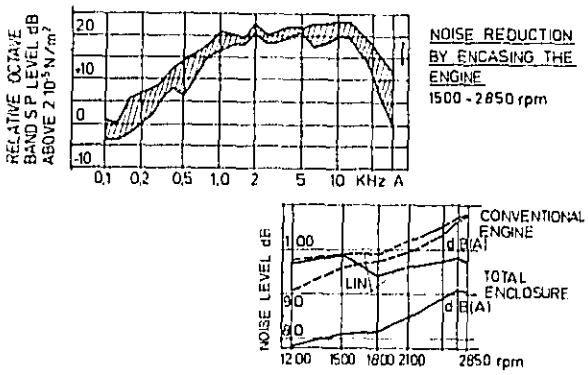

Fig. 7 - Noise reduction by encasing the engine for rotational speed range 1500 - 2700 rpm

Mean noise level in dB(A) with and without engine capsule

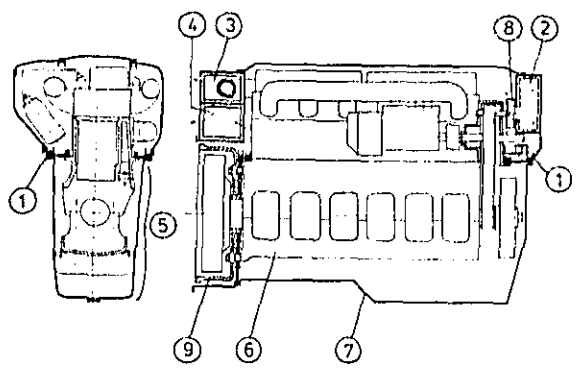

Fig. 8 - Schematic diagram of an enclosed diesel engine for commercial vehicles

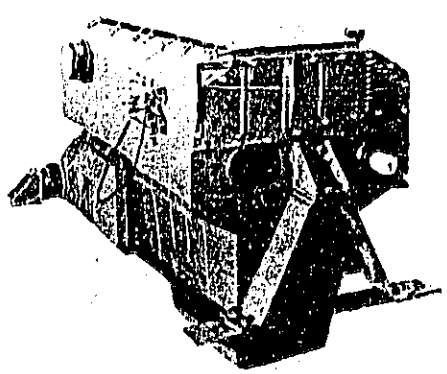

Fig. 9 - Engine with total enclosure, front view on test stand

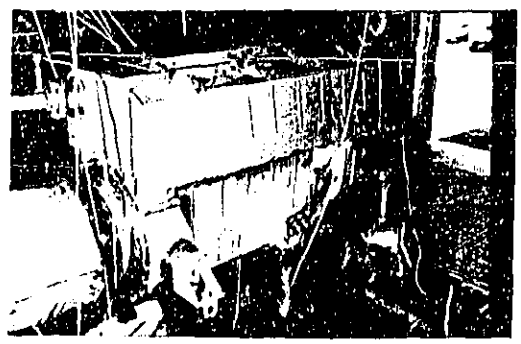

Fig. 10 - Engine with total enclosure, view from right rear, test stand

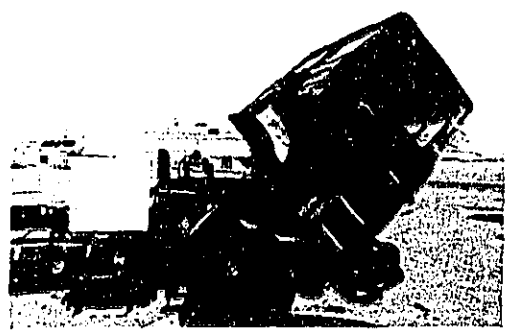

Fig. 11 - Truck A with low-noise research engine, view from right

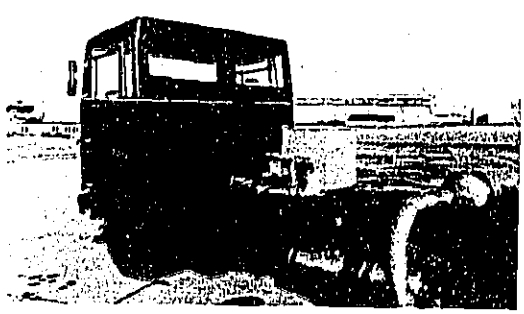

Fig. 12 - Truck A with low-noise research engine, view from left

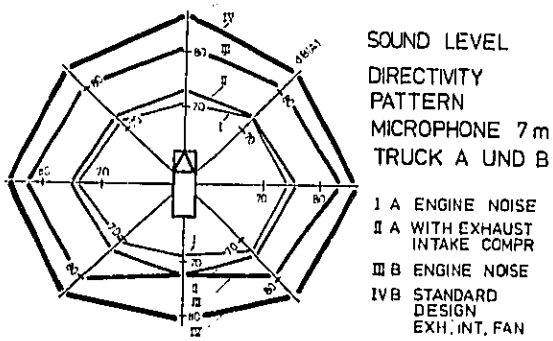

Fig. 13 - Trucks A and B, sound level directivity pattern

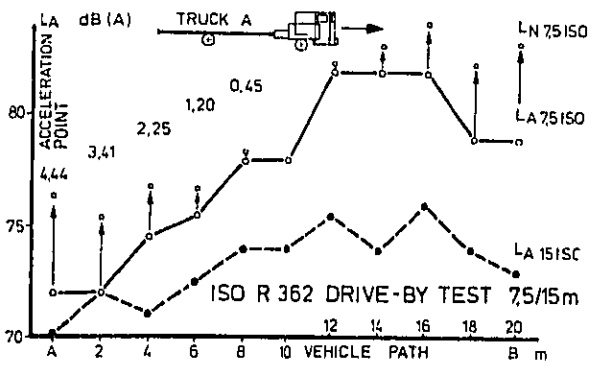

Fig. 14 - ISO R 362 drive-by test

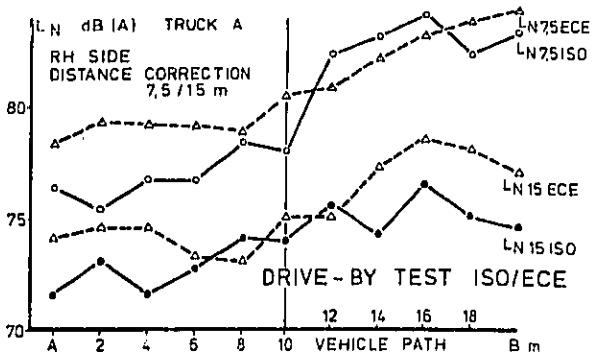

Fig. 15 - Comparison of test procedures ISO R 362 and ECE R-9 Revised

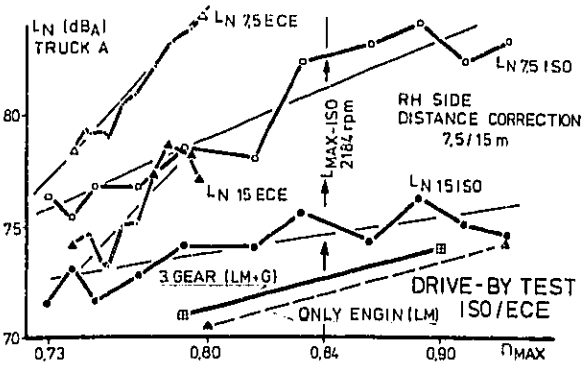

Fig. 16 - Comparison of test procedures ISO R 362 and ECE R-9 Revised relative to engine speed at max. output

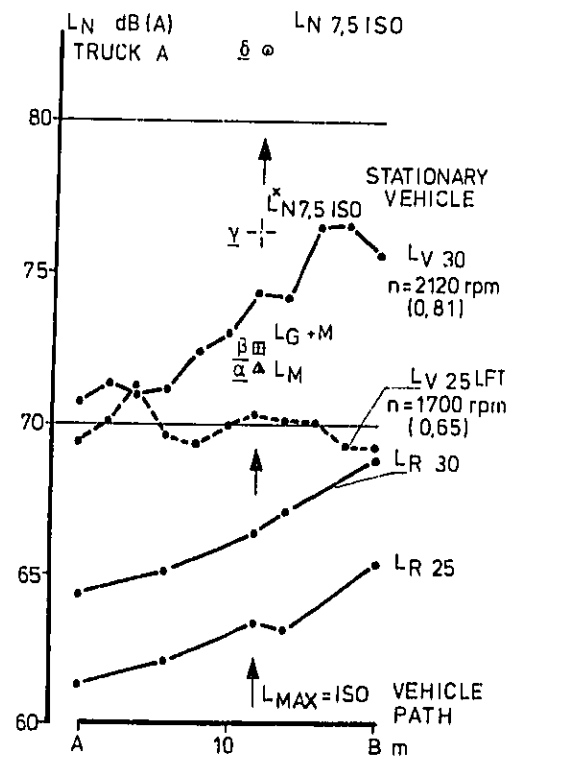

Fig. 17 - Sound level in acceleration drive-by test - dynamic portion

790451

NOISE EMISSION OF AIR-COOLED AUTOMOTIVE DIESEL ENGINES AND TRUCKS

Dr.-Ing. H.-A. Kochanowski
Dr.-Ing. W. Kaiser
Dipl.-Ing. D. Esche

Klöckner-Humboldt-Deutz AG
Cologne, G.F.R.

ABSTRACT

Examples of the development of two engine series of KHD company are given to illustrate the noise improvements achieved in the past. Moreover, the present development work for further noise reduction is reported.

Of special importance is an adequate combination of the various noise reduction measures to achieve low noise levels in acceleration tests of vehicles. In this connection, emphasis is given to measures on the combustion system, cooling blower, measures for the reduction of engine sound radiation and measures on the truck.

INITIAL DEVELOPMENT ACTIVITIES on air-cooled diesel engines were started by KHD some 4o years ago. First series production started in 1944. Since then KHD air-cooled engines have been continuously advancing with particular emphasis being given to an enviro-conscious design since the early sixties.

The current programme includes 4 air-cooled diesel engine families (1)+, two of which are mainly used for automotive applications, the other two are employed in the construction machinery sector. As the requirements laid down in the anti-noise legislation for construction machinery have become more and more stringent in Germany since 1965 substantial efforts have been made in the field of noise reduction.

In addition to the aim of achieving a noise reduction on the engine itself, development activities have also been performed to reduce the noise by the vehicle, since we are convinced that only a combination of suitable measures on both engine and on the vehicle will yield an optimized economical solution to the problem of attaining improved noise levels. Purpose of this paper is to outline some of the aspects of these development activities.

VEHICLES POWERED BY ENGINES OVER 200 HP, FL 413 SERIES

In this category, 6, 8, 1o and 12 cylinder engines of the 413-series are employed. The individual development stages can be demonstrated by the example of the 8-cylinder V-engine.

The F8L 413 has a bore of 12o mm, a stroke of 125 mm and develops an output of 169 kW (23o HP) at 265o/min, which corresponds to a brake mean effective pressure of 6.7 bar. A view of the engine is given on Fig. 1, showing the characteristical engine configuration with cooling air being supplied into the vee-space via the front mounted cooling blower. The cooling air then passes to both sides through the cylinder heads and around the cylinders outward.

In Fig. 2, the air-borne sound levels measured at 1 m from the engine side surface are shown versus engine speed (dotted line). The noise ppoduced by the cooling blower is included in these values. For comparison purposes the noise level spectrum of 1o different water-cooled engines, published in 1975 (2), has been included in this figure. Note that the noise levels recorded for the water-cooled engines do not include fan noise and that the noise of the air-cooled engine including fan noise even remains below that of the water-cooled engines.

This can mainly be attributed to the combustion principle employed for the naturally aspirated engines of this series which is basically retained for its successor, the FL 413 F series. The combustion chamber and the position of the injection jets are shown in Fig. 3. This system of direct injection with mixing taking place near the wall of the piston bowl is very favourable with

+Numbers in parentheses designate References at end of paper

SAE/P-79/80/$02.50
Copyright © 1979 Society of Automotive Engineers, Inc.

regard to acoustics due to combustion with a slow rate of pressure rise. The frequency analysis of the cylinder pressure of this combustion principle brings about a decay rate of approx. 5o dB per decade, a rate nearly equaling that of the Otto engine (3).

DEVELOPMENT OF THE FL 413 TO THE FL 413F

In the course of the further development of the FL 413 bore and stroke were enlarged by 5 mm each, these engines being designated FL 413F. Togehter with a revision of injection system, combustion chamber and timing it was possible to attain considerably higher brake mean effective pressures resulting in a rated power of 188 kW (256 HP) at a reduced speed of 25oo/min. This corresponds to a brake mean effective pressure of 7.o8 bar. The engine characteristics (5) are shown in Fig. 4. Design changes which affected the noise pattern of the engine include a reinforced crankcase, an enlarged main bearing diameter, a cast aluminium valve cover and an exhaust manifold which was changed from a sheet-metal version to a combination of castings and sheet-metal parts.

The noise values of this automotive engine incorporating the above improvements are also shown in Fig. 2 (drawn line). At the rated speed of 25oo/min the total noise level is only lol dB(A), measured laterally at 1 m distance from the engine. This low total noise level already indicates that further noise improvements can only be realized with difficulty.

NOISE REDUCTION ON THE TEST ENGINE, FL 413 F SERIES

To further reduce the noise level of this engine, it was first necessary to determine the noise produced by the individual engine components. For this purpose, the well-known covering technique was employed. With this technique the engine is totally enclosed so as to minimize the exterior noise. The noise level increases by exposing the surface sections of the components to be examined. Then, the noise level of these components can be calculated from the difference in the noise levels. Examples of costly and complicated covering techniques are given in the relevant literature. The technique employed by us was simplified to the greatest possible extent while still ensuring sufficient accuracy of the test results. The experimental enclosure became effective only above 2oo Hz. In the frequency range of interest with regard to acoustics the effect produced by the enclosure was between 15 and 25 dB(Figures 5 and 6). Therefore this technique permitted statements on those component noises falling below the total noise level by 15 dB(A) maximum.

Figure 7 indicates the noise levels of the components determined on the 8-cylinder 413 F engine with the aid of this covering technique. The two noisiest individual components are the exhaust gas pipe and the oil pan both at a level of 93 dB(A). The sum of the noise levels of cylinder liners and cylinder heads is 94 dB(A). When considering the substantially larger surfaces of cylinder heads and liners compared to the exhaust manifold this value is surprisingly low.

These results were obtained on the left-hand side of the engine and differ only slightly from those recorded on the right-hand side where the noise level is somewhat lower. Different values were of course recorded with the microphone position at 1 m in front of the engine since there the blower noise - which is practically unnoticeable on the side - is of greater influence.

As the noise levels of the individual components were now known, it was possible to determine on which components corrective measures had to be carried out so as to reduce the total noise level of the engine.

The noise occurring in the area of the cylinder and the cylinder head could be reduced by two measures. First, injection at rated speed was retarded by restricting the range of the advance unit by 2 degrees. By this measure the noise level could be reduced on the average of 0.8 dB(A) determined during measurements performed on several engines.

The effect of this retard on the other engine parameters was of course also taken into consideration. The exhaust gas emissions were substantially improved by the retarded injection and since the rise in the fuel consumption and the rise in smoke involved were so small, this could be fully accepted.

The second measure entailing a reduction of the noise, which according to the results of the component noise analysis seems to be produced by the cylinder liners and cylinder heads, can only be applied to air-cooled engines.

This engine has a space below the vee-space cover (see Fig. 7) which has a relatively high noise level caused by several sources, such as the blower, injection pump, cylinders, cylinder heads, ect. This noise can reach the outside of the engine by passing through the cooling fins of the cylinder

liners and heads. Therefore, a reduction of the noise level within the vee-space also entails a reduction of the noise level outside the engine. Such reduction in the vee-space was realized by providing the underside of the vee-space cover with absorption material. This material has a surface area of only 0.26 m^2 but was responsible for reducing the noise level of the engine by 0.8 dB(A) at 1 m distance.

Another component which largely influences the total noise level of the engine is the oil pan, in this case an aluminium casting (see Fig. 7). Here, it was attempted first to reduce the structure-borne sound level in the oil pan by stiffening the crankcase and thus improving the sound radiation effect. There was good reason for hoping that this method which showed excellent results in the case of serveral water-cooled engines, would be functional also for the air-cooled engine. We assumed that the crankcase of the air-cooled engine featuring a low overall height would be particularly responsive to additional stiffening. During the test it was noticed, however, that the use of a 23 mm thick stiffening plate between crankcase and oil pan had only a minor effect. It was also noted that this effect was dependent on the engine speed. Whereas at n = 2400/min a slight noise reduction was noted, the noise level increased at n = 2500/min on account of this stiffening plate.

Promising results were however obtained by coating the oil pan. A 6 mm mat of high density damping material which was glued to the oil pan proved to be the optimum coating material with regard to acoustics. By this coating, the noise level could be reduced on both engine sides by approx. 0.5 dB(A). We are continuing however to search for other coating materials and methods since gluing is, in our opinion, not an optimum solution with regard to costs and series production.

Coating also has a good acoustical effect on the sheet steel intake manifold. Here a 3 mm coating of dampening material brought about a reduction of the noise level of approx. 0.5 dB(A) at 1 m distance from the engine.

The results abtained on the test engine which, contrary to the series engine, included the aforementioned four noise silencing measures are given in Fig. 2 (dashed line). The noise reduction abtained extends over the entire speed range.

COOLING FAN

At the measuring point in front of the engine, the former cooling fan is influential in the overall noise level but only in case of high engine speed and high load since the blower of the 413-series engine is thermostatically controlled. A blower drive is shown in Fig. 8. The Fan is driven via a flexible coupling, protecting it against torsional vibrations, and by means of an hydrodynamic coupling. Control of this coupling is effected as a function of the load via an exhaust gas thermostat. Especially in the case of accelerated drive-by of vehicles powered by this engine, no effect of the blower on the vehicle noise can be determined.

Nevertheless, great effort has been made to reduce the objectional quality of the noise without the obligation of observing legally specified limits (6,7).

All of the blowers for the various engine types were revised successivley. The results of the fan development are demonstrated by the example of the 10 and 12 cylinder engine blowers (Fig. 9). At the same operating point these new fans feature reduced speed and improved efficiencies. However, the noise reduction obtained with these new fans is not only to be attributed to the higher efficiency. Decisive progress has been made using unequal spacing of the blades.

Figure 10 indicates the noise spectrum of the fan of the 12 cylinder vee-engine. The fan which is presently in production (upper curve) still features equal spacing of the blades and the peaks produced by the harmonics of the blade number are clearly visible. These peaks have largely been eliminated by providing unequal blade spacing. Therefore the noise produced by this new blower is considered as having a much lower annoyance factor. The broad-band noise is now fully covered by the engine noise. These new fans are currently beeing introduced into series production.

MEASURES ON THE VEHICLE WITH F8L 413 F ENGINE

About 50 p.c. of the engines of the 413 F series are installed in trucks.

In drive-by tests according to ECE R 9, noise values of 88 - 89 dB(A) were recorded for these vehicles equipped with standard FL 413 F engine. The measurement point under this code is at 7.5 m from the vehicle center line. Values recorded at a distance of 50 feet (in accordance with SAE J 366a) are about 6 dB(A) lower than those determined at a distance of 7.5 m.

Present European laws specify for these vehicles with engines over 200 HP a limit of 91 dB(A). In 1980, this limit will be reduced to 88 dB(A).

Thus, the vehicles which are now in production nearly meet the acoustical limit specified for 1980.

The more stringent regulation can be fully complied with by only minor acoustical improvements such as to the intake and exhaust gas systems. Improving the intake system meant optimizing the intake pipe lengths before the air cleaner; the costs involved are only negligible. Improvement on the exhaust gas side was attained by increasing the silencer volume by approx. 25 %. The noise levels which were then recorded during the accelerated drive-by fell below 87 dB(A). The next step was to fasten sound shields to the vehicle. Several versions which were tested are shown in Fig. 11. Shields marked number 1 were fastened to the cab and are tilted upwards together with it thus ensuring good access for maintenance purposes. Shields shown as number 2 are a necessary acoustical supplementation to shields No. 1 and were fastened to the vehicle frame. Both shields prevent propagation of noise sideways.

The cooling air coming from the cylinder liner and cylinder head sections is ducted downwards by these shields. Since the flow cross-sectional area required for the cooling air outlet must be maintained, the amount of noise propagating downwards can only be reduced by providing suitable absorption material on these shields.

Side shield No. 1 could not be coated due to the proximity of the hot exhaust pipe but this was carried out on No. 2. Together these shields brought about an improvement of the drive-by noise of 1.5 to 2 dB(A).

By fastening a further shield (No.3) which fully covers the lower engine as viewed from the side, the noise reduction was only 0.5 dB(A).

However drive-by noise was largely influenced by a further shield installation (No. 4) arranged horizontally and extending from the bumper of the vehicle to the front edge of the engine. This shield prevented the noise existing at the front end of the engine from expanding to the sides. The noise attenuation achieved by this shield was 1 dB(A).

The shields, together with the improvements made on the intake and exhaust gas systems resulted in a total noise reduction of approx. 5 dB(A), i.e. in accelerated drive-by, the noise level of this vehicle equipped with the standard engine is 84 dB(A).

It goes without saying that, examinations were made with regard to the effect of these shields in engine temperatures. When installing an air-cooled engine particular attention must be paid to the blower obtaining fresh and not recirculated cooling air. This was considered in the case of the tested vehicle and even under adverse conditions (high ambient temperature, high engine loading and low driving speed) there were no inadmissibly high temperatures noted. Accordingly, the engine can be operated without any reservation with the described shielding measures being incorporated.

For the vehicle powered by an engine of the 413 F series, the catalogue of acoustical measures is summarized in Fig. 12. The individual measures are quite unproblematic and can be easily introduced in series production. It is observed that the combination of all measures described entails a noise level which falls below the noise level of the current series-vehicle by 7 dB(A) and below the current limit value binding for Europe by 9 dB(A).

When adding the noise reductions resulting from the individual measures it is observed that the total noise reduction is greater than that which was actually measured on the vehicle. This, among other things, is attributed to the fact that some measures performed on the vehicle and on the engine affect the same noise sources, e.g. a noise reduction of 0.5 dB(A) measured on the vehicle may be caused by shield No. 3 as well as by the coating of the oil pan. The combination of both measures, however, does not bring about any further noticeable improvement.

The decision whether to use a coated oil pan or an additional side shield may be based either on the mere cost factor or on the aspect of simpler maintenance. The catalogue of measures described will be a basis for determining the cost optimized measures which would ensure compliance with certain future limit values. The costs for all noise reduction measures described are estimated by us to amount to a range of 1 - 2 % of the vehicle price.

VEHICLES POWERED BY ENGINES UNDER 200 HP, FL 912/913 SERIES

An investigation similar to that performed for the FL 413 F series engine is presently carried out for the second series of air-cooled engines which is applied in the automotive sector as 4 to 6 cylinder in-line engines. A 4 cylinder engine of this 912 series is depicted in Fig. 13. These engines, too, have been further developed into a 913 series featuring an enlarged bore of 102 mm and

a stroke of 125 mm. The 6 cylinder version of the 913 series developes 96 kW at 2800 rev/min.

The analysis of the noise produced by the individual components and the resulting measures for reducing the noise on engines of the 913 series are comparable to the work described for the 413 F engine. The fan noises, for example, were substantially reduced. In our opinion, it is therefore not necessary to go once again into details. What has to be mentioned, however, is the different combustion system of these two engines.

COMBUSTION NOISE

In comparison with the low noise combustion system of the FL 413 F series NA engines the FL 913 engine features a more rugged combustion system with central injection. As a first measure the combustion noise was reduced by employing slight turbocharging. In this case since the maximum engine rating was not to be increased by turbocharging the maximum engine speed could be reduced from n = 2800 rev/min to n = 2500 rev/min. The noise levels thus obtained are shown in Fig. 14 versus the brake mean effective pressure. The lower noise level (4) of approx. 4 dB(A) owing to the combustion with a lower pressure rise and the speed reduction is clearly noticeable. Another point of interest is that in the case of the slightly turbocharged engine the noise at full load is below the noise at low load. The noise occurring with the motored engine is shown in the left-hand side of the figure.

NOISE DURING ACCELERATION

In addition to reducing the noise under steady state conditions, the introduction of a smoother combustion system offered the advantage of lower noise during acceleration of the engine.

Figure 15 shows the noise increase during acceleration of the engine compared to the noise level determined under steady state conditions. It is obvious that the temperature of the engine is a decisive parameter affecting the noise during acceleration. As an example, the noises are shown in this figure as a function of the cylinder liner temperature. In the course of these tests other engine temperatures changed similar to the cylinder liner temperature. Only the oil temperature remained constant.

It is obvious that at a temperature which corresponds to the full load point the noise increase due to acceleration is somewhat above 1 dB(A). At lower cylinder temperatures, this value rises considerably. Thus it was an aim to achieve high temperatures to minimize the noise increase during acceleration. With the air-cooled engines this can be realized by appropriate regulation of the cooling blower.

MEASURES ON THE VEHICLE WITH F6L 913 ENGINE

A truck having a GVW of 7.5 t used for these tests was powered by a 6 cylinder of the 913 series. The acoustical limit value for this vehicle as specified in the European regulation ECE R 9 is 89 dB(A). This value is just met by the truck equipped with NA engine of standard design. Therefore, substantial efforts will have to be made so as to meet the limit value of 86 dB(A) which will be applicable as from 1980.

By installing the slightly turbo-charged engine described above, the noise level was already reduced by 4 dB(A) on left-hand side an 5.5 dB(A) on the right-hand side. So the noise in a distance of 7.5 m was 83.5 and 85 r respectively.

Further noise reductions were attained by adopting measures on the vehicle similar to those mentioned before with the F8L 413 F engine [+]. The work on the vehicle and the engine is still continued. The details and final results will be published later, but we are shure that noise levels will be even lower than those we reached with the bigger truck. In the case of the small truck the costs for all acoustical measures will amount to approx. 3 % of the vehicle price.

For this engine, the major noise reduction could be achieved by adopting slight turbocharging and reducing the speed. In the case of the vehicle equipped with an engine of the 413 F series, however - when taking the noise values of the 413 series as basis - the total noise reduction obtained was nearly identical with measures on the vehicle or on the engine.

[+]The work on the vehicle was performed by Magirus Deutz AG (a companyy of the IVECO) and the Institute for Motor Vehicles and Automotive Engines of the University of Stuttgart. Financial support is given by the Federal Environmental Agency of the Federal Republic of Germany

SUMMARY

The measures to reduce the noise must first be based on an analysis of the noise sources. Then appropriate actions for achieving a lower noise level can be determined for the individual engine type.

Evidence was given that, in the case of the two vehicular engine series presented, noise levels of 82 dB(A) at a distance of 7.5 m during accelerated drive-by are achievable. The corresponding level at a distance of 5o feet is 76 dB(A).

The expenditure for achieving such values is relatively low: the costs amount to approx. 2 to 3 % of the vehicle price. The air-cooled engines presented in this paper are well suited for obtaining the reduced noise level described.

Until now we do not see any way to further reduce the noise levels of the test vehicles beyound that achieved 82 dB(A) which would be reasonable in economical and technical aspects. In the future other vehicular noise sources (e.g. gearbox, tires) would be of growing importance. Independent of the good results obtained, we continue to find good technical and economic solutions to diminish the noise of internal combustion engines.

REFERENCES

1) O. Herschmann
"4o Jahre luftgekühlte Deutz-Dieselmotoren - eine technisch - wirtschaftliche Bilanz" MTZ 37, 1976, April - S. 117 - 124

2) T. Priede
"The Problem of Noise of Engines in Different Vehicle Groups" S.A.E. Paper 75 o7 95

3) H. Groß
"Noiseemission of Aircooled Diesel engines"
Tenth Annual Noise Control in Internal Combustion Engines 1978, University of Wisconsin, Madison

4) H. Groß
"Einfluß der Verbrennung auf das Motorgeräusch"
ATZ Automobiltechnische Zeitschrift 79 (1977) 4

5) E. Lichtner, J. Wahnschaffe
"Advancement of the Aircooled Deutz FL 413 Diesel Series"
Diesel + Gas Turbine Worldwide June 1977, Page 33 - 36

6) I. Killmann
"Progress in Fan Noise Reduction"
Diesel + Gas Turbine Progress Worldwide Nov/Dez. 1972 S. 3o - 31

7) D. Escke
"Beitrag zur Entwicklung von Kühlgebläsen für Verbrennungsmotoren"
MTZ 37, Okt. 1976, S. 399 - 4o3

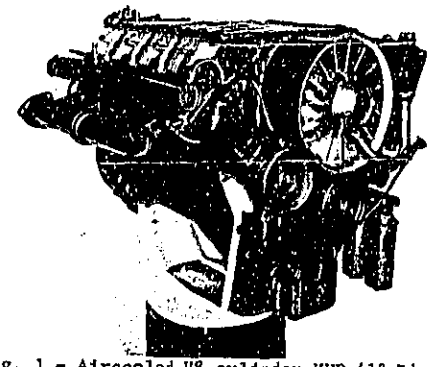

Fig. 1 - Aircooled V8 cylinder KHD 413 Diesel engine

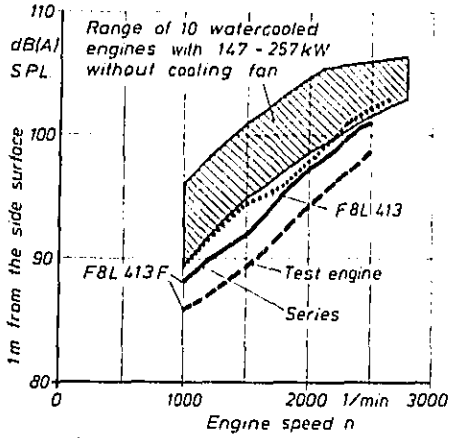

Fig. 2 - 413 Diesel engine at full load, with cooling fan

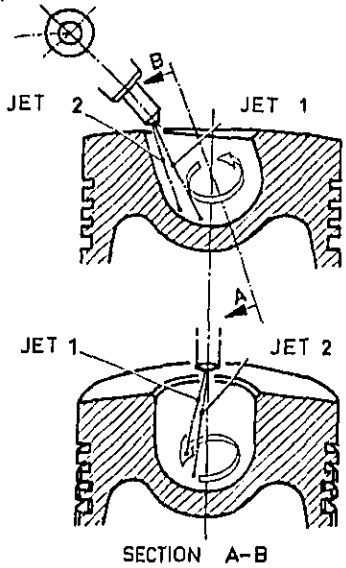

Fig. 3 - FL 413 F combustion chamber and position of the injection jets

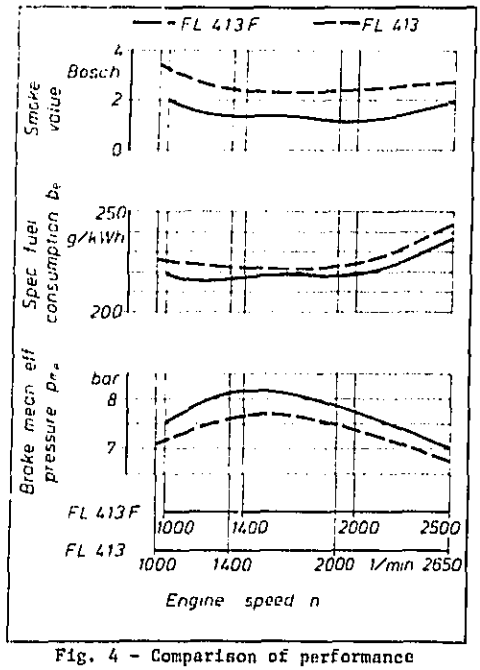

Fig. 4 - Comparison of performance

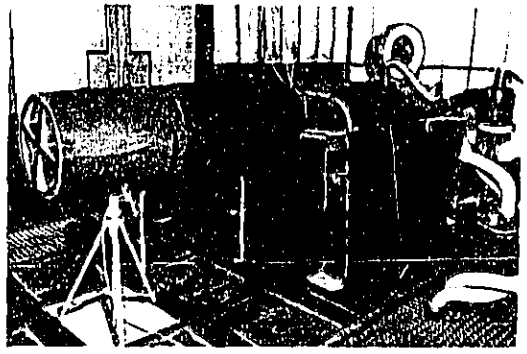

Fig. 5 - Experimental enclosure of the engine

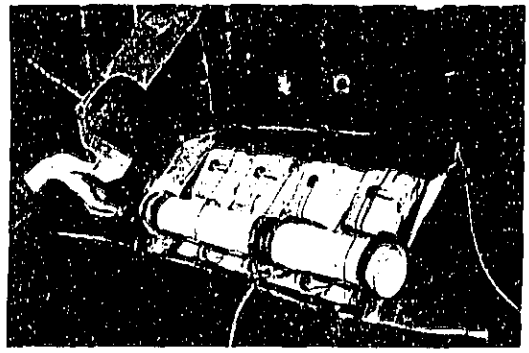

Fig. 6 - Covering technique-exposed components - valve cover and intake manifold

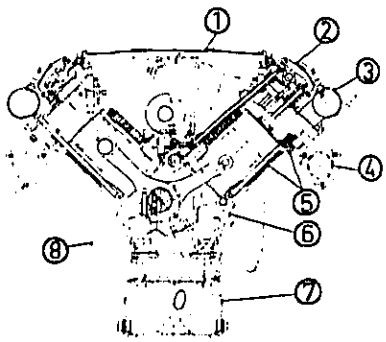

1	service cover	83
2	valve cover	92
3	intake manifold	90
4	exhaust manifold	93
5	cylinder + - head	94
6	crankcase	87
7	oil pan	93
8	flywheel housing	88
	oil cooler outlet	87
	fan	88
	fan housing and oil cooler surface	84
	vibration damper	84
	total noise	101 dBA

All measurements in dB (A), 1m from the left side surface, full load, 2500 RPM.

Fig. 7 - Engine noise analysis F8L 413F

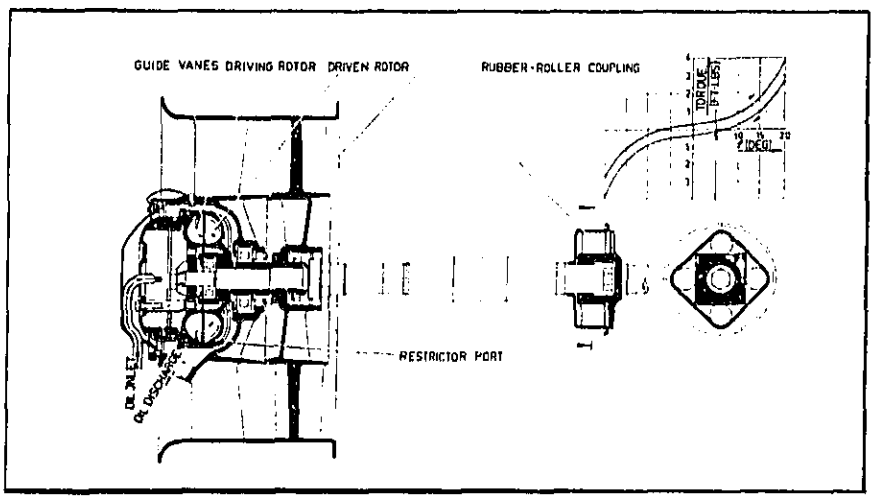

Fig. 8 - Fan drive with flexible and hydraulic couplings

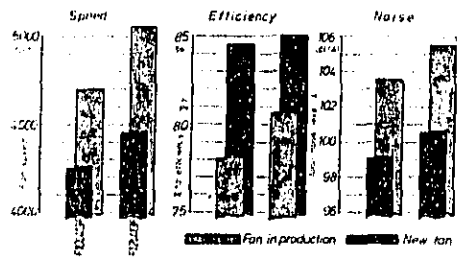

Fig. 9 - Comparison of cooling fans of Flo, 12 L 413 F engines at engine speed 2500 rpm

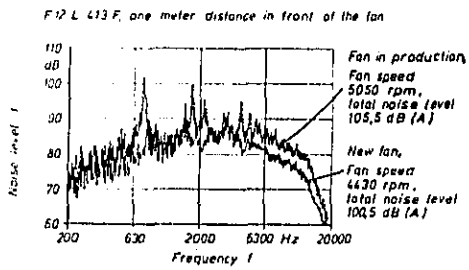

Fig. 10 - Comparison of fan frequency spectra at a cooling air mass flow of 4,3 kg/s

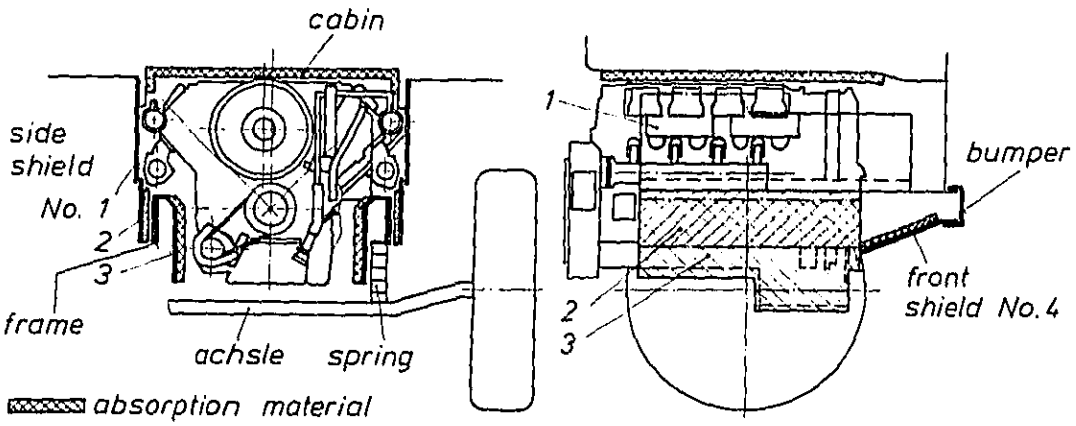

Fig. 11 - Shields and absorption material on vehicles equipped with F8L 413 F

Noise Reduction Measures	Sound Attenuation dB(A)
Exhaust and air intake system improved	-2
Truck: Side shields No. 1-4	3 - 3,5
Engine: Retarded injection Service cover foam coated Oil pan and intake manifold treated with damping material, new blower	2,5

	ECE R9 dB(A)	SAE J366a dB(A)
Todays Standard	89	83
Optimum Result	82	76

Fig. 12 - Results of noise reduction measures performed on the truck equipped with F8L 413 F

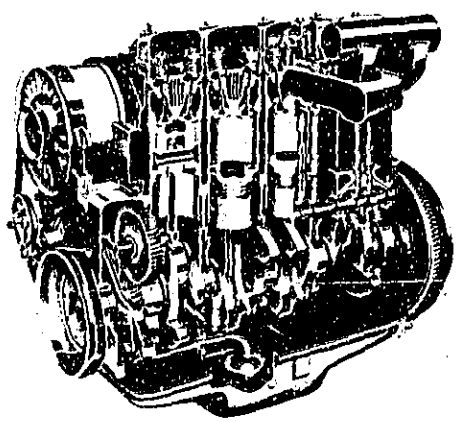

Fig. 13 - Aircooled 4 cylinder KHD 912 Diesel engine

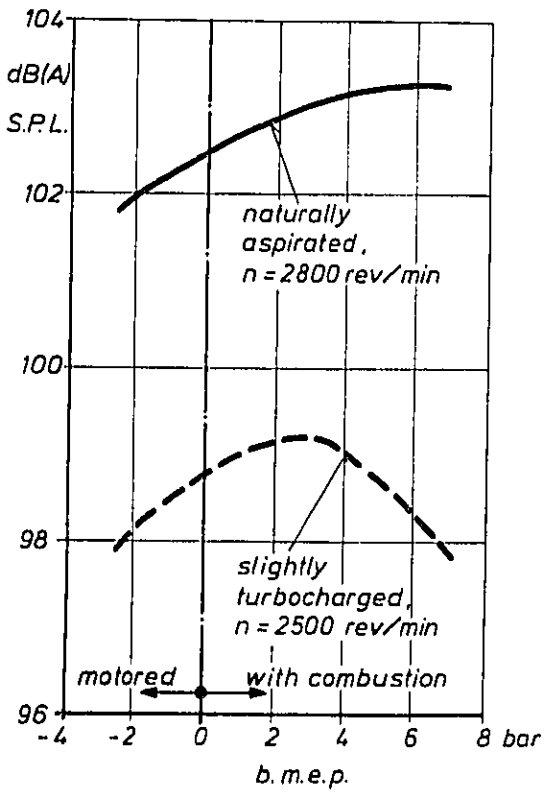

Fig. 14 - F6L 913, naturally aspirated and turbocharged both 96 kW (130 PS)

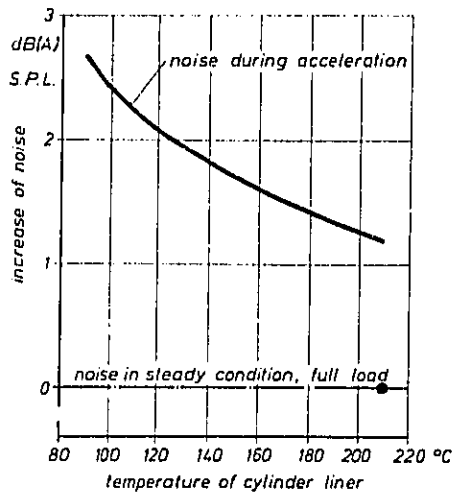

Fig. 15 - Noise during acceleration, F6L 913

790452

THE TRANSPORT AND ROAD RESEARCH LABORATORY QUIET HEAVY VEHICLE PROJECT

A.R. Cawthorne B.Sc. C.Eng. M.R.Ae.S.
J.W.Tyler Dip. Stats. F.Inst.H.E.

Transport and Road Research Laboratory
Crowthorne, England

ABSTRACT

Research into means of reducing noise from diesel-engined goods vehicles of 30-40 tonnes gross vehicle weight has shown that engine redesign can reduce noise from this component by 5-10 dB(A) within reasonable production, performance and cost constraints. Attention to the exhaust system, cooling package, engine covers and chassis design has resulted in a 10 dB(A) reduction in noise in the cab. Results are quoted from a number of experimental vehicle builds and the basis for a demonstration vehicle built to production standards which should meet a target drive-past noise level of 80 dB(A) is described.

AS A RESULT of a review of road traffic noise (Ref. 1) a programme of research and development was instigated in 1971 to produce demonstration quiet heavy diesel-engined commercial vehicles with external noise levels some 10 dB(A) lower than the existing values. Heavy articulated lorry tractors were chosen for the study since these were likely to be the most difficult to quieten, especially when fitted with engines capable of powering combinations of up to 44 tonnes gross vehicle weight which was then the proposed upper end of the normal UK design range.

The broad aim of the project was to assist the British vehicle industry to meet future requirements and demonstrate the levels which it was reasonable to set in future U.K. legislation without incurring severe economic penalties. With the cooperation of the manufacturers the project aimed to produce demonstration articulated vehicle tractors. The first was based upon the Leyland Buffalo with a gross vehicle weight limit of 32 tonnes and an engine of 212 bhp. The second was a Foden vehicle designed for a maximum gross vehicle weight of 44 tonnes and fitted with a Rolls Royce engine of 350 bhp. A target drive past noise level of 80 dB(A) was set. This level is based upon the standard BS 3425:1966 test and it should be noted that the microphones in this test are set at 7.5 m from the path of the vehicle and thus give higher noise readings than in the normal American test with microphones at 50 ft. The resulting target noise levels for components of the vehicle are shown in Table 1; the target noise level inside the driver's cab was set at 75 dB(A). Research on particular components of the system was carried out at the Institute of Sound and Vibration Research and the Motor Industry Research Association as well as at TRRL who also undertook the overall management of the project and coordination of the various activities. A vital aspect of the research proposals was that they should be suitable for incorporation in production, and the effect on operating costs evaluated. In its original concept the programme planned as the research phase would lead to custom built versions of the two vehicles which would then be used in a development phase leading to demonstration vehicles built to production standards. In the event, the experimental vehicles were produced but the development of a demonstration vehicle was pursued only on the Foden/Rolls Royce vehicle whilst the lessons learnt on the Leyland Buffalo are to be used in future product designs.

THE FODEN VEHICLE

The original Foden vehicle was a 6 x 2 tractor unit as shown in Fig. 1 powered by a 13 litre Rolls Royce engine, details of which are shown in Table 2. Transmission was via a Foden 9 speed gearbox with a worm drive rear axle with double reduction hubs. Initial work on the exhaust, cooling system and cab noise was carried out on this vehicle until a later model became available; this was a 4 x 2 chassis with a design gross vehicle weight of 38 tonnes as shown in Fig. 2. The engine was mounted further back in the chassis than normal to provide space for the special cooling package and the engine was modified to accept a different turbo-charger and camshaft which gave a useful reduction in noise emission. The Foden rear axle case was fitted with a hypoid head. The Foden glass reinforced plastic cab was mounted on pivot pins fitted with rubber bushes at the front and supported by steel coil springs with hydraulic dampers at the rear. The interior was lined with 1.5 inch thick sound absorbent polyurethane foam covered with decorative trim, an engine bonnet quilt was fitted, and the floor was covered with a loaded PVC and chip foam laminate. Successive stages in the build of this vehicle are shown in Table 3.

NOISE RESEARCH

ENGINE - Baseline noise measurements were made with the engine installed in the anechoic cell at ISVR with the dynamometer effectively isolated. The resulting spectrum for the standard engine is shown in Fig. 3. Figure 4 shows the contribution from the front end of the engine as revealed by partial acoustic covering. Figure 5 shows the effect of engine speed on overall noise and is typified by a change in slope at about 1700 rpm. (See also ref. 2). This meant that a reduction in maximum speed from 2100 rpm to 1900 rpm gave 3 dB(A) and the lower speed was used in the final demonstration vehicle. To check the effect of timing gears on front end noise these were replaced by a triplex roller chain drive resulting in an average reduction of 7 db(A). Evidence from cylinder pressure spectra, the effects of load boost and speed on noise and the influence of timing gear noise all pointed towards overall noise being mainly determined by combustion noise at low speeds and by mechanical noise at higher speeds. Accelerometer readings were taken over a grid on the engine surface resulting in vibration patterns as shown in Fig 6 for 200 Hertz where one of the major bending modes occurred. Note that the amplitudes in Fig. 6 represent rms vibration levels and not phase information which would give mode shape. The result of noise and vibration studies on the engine structure can be summarised as major modes at around 200, 350 and 500 Hertz. There were also several peaks controlled by the response of the sump at 620, 730 and 1100 Hertz and resonances of the structure occurred at 1.45, 1.6 and 1.9 kHz, the tappet cover being important at 2.8 kHz. Static deflection tests showed that the cylinder block was rigid compared with the crankcase. Under combustion loads the main bearings moved downwards dragging the sidewalls of the crankcase in at the bottom deck level and out at sump rail level. The basic structure was a major noise radiator mainly due to the large area rather than the the particularly high vibration levels. The sump was the second most important noise radiator having high vibration levels in the frequency range 2.5 to 4 kHz.

REVISED STRUCTURE - A research engine was designed by ISVR using the standard running gear in a strengthened cylinder block/crankcase structure. Figure 7 shows cross sections of the original engine and the revised structure, the latter incorporating a ladder type bed plate containing the lower halves of the main bearings thus providing greater stiffness in the crankcase. The bottom deck of the cylinder block was moved to the lower end of the cylinders to form a rigid section to reduce flexing of the cylinder block walls caused by distortion of the crankcase. The outer faces of the crankcase were flat to enable close fitting damped panels to be attached. To reduce the noise from timing gears which was apparent in the standard engine, these gears were removed to the rear of the engine though the oil pump remained at the front. The fuel injection pump used had a low noise specification. Tests showed that there was little advantage to be obtained from changing injection timing and the standard 26° btdc was used. A thick U-section rubber moulding was fitted to the flange of the aluminium sump to effect some isolation. Laminated panels consisting of a central sheet of perforate and outer sheets of mild steel sandwiched together with layers of neoprene were fitted to the side and front surfaces of the engine.

NOISE CHARACTERISTICS OF RESEARCH ENGINE - Test bed measurements of engine noise for the research and the standard engines are compared in Table 4 and the spectra are shown in Fig. 3. Subsequent tests have suggested that the reductions in noise indicated in Table 4 are conservative and a reduction of 10 dBA has been shown to be obtained in many conditions. The modified structure still retained the main bending mode at about 200 Hz but the second bending mode at 490 Hz was largely eliminated. Vibration levels on the sump of the research engine were reduced by up to 20 dB compared with the original engine above 2.5 kHz and by about 10 dB in the 500 to 2000 Hz range, this was attributed to the effect of the bed plate up to 2 kHz and above that frequency sump isolation was the main contributor. The laminated panels attached to the revised structure attenuated the transmitted vibration levels by up to 20 dB at frequences between 2.5 and 10 kHz. Thus the ISVR re-design of the Rolls Royce engine had made a valuable contribution to the reduction in vehicle noise levels and Rolls Royce were sufficiently impressed to start work on production drawings following the basic principles laid down.

EXHAUST SYSTEM - Basic silencer designs were produced using the ISVR computer-aided design package and MIRA then produced practical versions of these designs and tested them in a special noise test facility. The original engine gave an open-pipe exhaust noise level of 109 dB(A) at 2,100 rpm with the microphone 7.5 m from the end of the pipe and 60° off the axis. A slightly revised camshaft and modified valve clearances resulted in a reduction in noise of 6 - 8½ dB(A) over the upper speed range. The fitting of a different turbo-charger gave a further reduction of 3 dB(A) at higher speeds with some increase at lower speeds; a useful increase in engine torque was also obtained. Silencer development was carried out with this standard of engine modification. A number of commercially available silencers were tested as well as the experimental versions. Some of the proprietary silencers achieved the required attenuation above 200 Hz but none was sufficiently effective at lower frequencies. An additional requirement of 90 dB(C) at 7.5 m was used as a target for the low frequency test, it was also found that back pressures from the more effective proprietary silencers were too high for the engine requirements. In all, 22 versions of the experimental silencers were built and tested before the final design was achieved. This consisted of twin cylindrical boxes of 254 mm diameter with a total volume 186 litres, and gave a back pressure of 3.9 cm of mercury. It is important to note that these silencers were entirely reactive in design, thus disposing of absorption sections containing material which might clog or be blown out of the system. The size of holes and

percentage open area in the perforated sections of the silencers proved to be critical factors. Hole sizes of less than 1.5 mm dia gave the best acoustic performance but clogging with exhaust products occurred during running and holes of about 3 mm were shown to be necessary; with holes of this size the percentage open area had to be between 5 and 10 per cent for adequate performance. On the basis of a spatial average the final silencers met the target noise level requirement of 69 dB(A) at 7.5 metres although somewhat short of the 90 dB(C) target at lower engine speeds due to difficulty in silencing the engine firing components. The silencers were of comparatively simple construction and should prove reliable in use, the ratio of the volume of the final silencers to the swept volume of the engine was approximately 16, this ratio depending principally upon the back pressure specified.

COOLING SYSTEM - The cooling system fitted to the original vehicle used an 8 bladed axial fan and measurements of cooling system noise made at fan speeds up to 2400 rev/min indicated that a reduction of up to 25 db would be necessary in order to meet the target. A variety of alternative fan types was considered and a double inlet forward curved multi-vane centrifugal type was chosen as available at the time and likely to meet both the required cooling and noise levels. This fan was driven by a hydraulic motor with an engine-driven hydraulic pump and the resulting cooling package is shown in Fig. 8. Test bed readings with this system indicated that its cooling and noise performance should be considerably better than target but when installed in the vehicle it was found that cooling performance was well below that required; this was attributed to loss in fan performance due to unfavourable location and loss of radiator performance due to unequal distribution of air flow owing to the close proximity to the fan. Various modifications were tried to overcome this difficulty but the eventual solution was the adoption of a mixed flow fan designed by the National Engineering Laboratory. The centrifugal cooling package was used in the testing of the experimental vehicle from which the noise values are quoted below, it was adequate for normal U.K. summer weather but the cooling performance would not be sufficient for extreme European summer temperatures.

COMPLETE VEHICLE NOISE RESULTS

STANDARD VEHICLE BASELINE NOISE - Table 5 shows the overall emitted noise when the vehicle was tested according to BS 3425:1966. Examples of the resulting noise spectra are shown in Fig. 9; the spectra shown in Fig. 10 were obtained with the vehicle stationary and engine running. This demonstrates how the low frequency content of exhaust noise dropped when the engine governor came into operation. Fan noise, with blade passing frequency of about 350 Hz remained at a significant level.

Passing noise measurements were obtained with an unladed tractor unit operating at a range of speeds between 32 and 96 km/h, when coasting with engine stopped and gears disengaged, when cruising with engine maintaining constant speed in top gear and when accelerating at full throttle in top gear. The results are illustrated in Fig. 11 for the original Foden vehicle. Figure 12 shows the importance of fan noise, even on this comparatively noisy vehicle. The fan also affected the noise levels within the cab which rose to 91-92 dB(A) in the noisiest conditions. On this vehicle the fitting of softer engine mountings and the improvement in cab trim, together with the enclosure of the engine within a tunnel made of 22 gauge aluminium resulted in a reduction in noise in the cab of 6 dB(A). The Foden F3 vehicle with the glass reinforced plastic cab showed an overall internal noise level of 78 dB(A) maximum in gears 1-7 during acceleration and values of 81-83 dB(A) were measured in gears 8 and 9, where wind noise was becoming predominant at the higher road speeds. The spectra for the noise in the cab of the F2 and F3 vehicles are shown in Fig. 13. This difference is mainly due to the improved engine mounts, engine enclosure and adequately sealed and trimmed cab. A test with the tunnel enclosure removed showed a 3 dB(A) increase in the maximum internal noise level. The effectiveness of the acoustic treatment of the cab was tested in stages with the results shown in Table 6.

EXTERNAL NOISE WITH THE F3 VEHICLE - The noise level obtained on the BS test with the F3 vehicle was 86 dB(A). The effect of removing the tunnel enclosure from the standard Rolls Royce engine is shown in Fig. 14, where it may be seen that most attenuation due to the enclosure occurred above 500 Hz. At this point in the tests a tonal effect was identified as coming from the tyres. Changing to tyres with a pattern of five circumferential ribs without a pronounced edge pattern removed this effect and reduced drive pass noise levels by 2 dB(A). A test on this vehicle to show the exhaust brake effect upon noise during deceleration showed that an increase of 3.5 dB(A) occurred with this in operation.

TESTS WITH FINAL EXPERIMENTAL VEHICLE (F4) -

External Noise - A comparison of the noise levels achieved by the F4 vehicle and the F1 vehicle is shown in Table 5. The highest noise level emitted by the F4 was almost 10 dB(A) lower than that produced by the F1. In both cases the maximum noise was recorded in fifth gear.

Figure 15 shows a comparison of the spectra of the noise emitted by the two vehicles. The noise levels recorded for the F4 tractor with laden trailer in passing noise tests are shown in Fig. 16.

Cab Noise - The noise levels measured inside the cab of the original F1 vehicle and the final F4 vehicle showed reductions of from 8.5 to 14 dB(A) with an average level of 78 dB(A) in the F4 vehicle. The noise in the F4 contained a peak at about 200 Hz, which was identified as associated with the fan drive hydraulic motor and this was later removed. It was also noted that noise in the F4 cab increased with speed, particularly in higher gears, in contrast with the F1 where levels remained the same in each gear regardless of speed. This effect was undoubtedly due to the fact that wind noise could be more readily heard in the quieter F4 cab.

COMPARISON OF F4 WITH OTHER CURRENT VEHICLES - Table 7 shows a comparison of maximum external noise on a range of vehicles including the final results obtained with the F4 experimental vehicle.

SUMMARY OF RESEARCH ON THE FODEN/ROLLS ROYCE VEHICLE

The ISVR/Rolls Royce research engine emitted noise levels of 9-10 dB(A) lower than the standard engine. A prototype of this engine to production standards has been built by Rolls Royce Motors Ltd. The final silencer design which was entirely reactive, i.e. without any absorption elements, came within 2 dB(A) of the target. At high engine speeds it came within 2 dB(C) of the target but at low engine speeds this target was exceeded by a larger margin. A production version of this silencer is now being tested. The cooling package in the experimental vehicle met the noise targets but provided insufficient cooling to meet maximum European summer temperatures. A new cooling pack with a mixed flow fan has now been built and is being tested. Initial indications are that this will meet both noise and cooling targets.

The maximum external noise of the final research vehicle was 83.5 dB(A). With modifications incorporated in the demonstration vehicle the target level of 80 dB(A) has been obtained.

THE LEYLAND VEHICLE

The standard Leyland Buffalo was a 4 x 2 tractor unit as shown in Fig. 17 powered by a Leyland 8 litre turbo-charged diesel engine, details of which are given in Table 2. The engine was coupled via a range-change 10 speed gearbox to a hub reduction rear axle. A pressed steel cab was fitted which was trimmed with rubber mats in the footwells and a resin bonded glass fibre headlining. The engine cover and the walls of the engine compartment were of a double steel skinned construction with mineral wool packing.

NOISE RESEARCH

ENGINE AND TRANSMISSION - Baseline noise measurements were made at ISVR on a specially constructed outside test facility giving a close approximation to free field conditions.

The effect of engine speed on noise is shown in Fig. 18 for the left hand side of the engine. The overall level of about 100 dB(A) at 1 metre at rated speed and load made this one of the quietest diesel engines in its class tested by ISVR.

The spectrum of noise from this engine is given in Fig. 19 and shows that the predominant noise is around 1250 Hz and a low frequency peak occurs at 200 Hz. The results of accelerometer readings taken over a grid of points on the engine surface confirmed the presence of a 200 Hz vibration in the horizontal direction as can be seen in Fig.20. At higher frequencies the engine walls vibrated in the form of panel modes, the levels being high at the unsupported walls and at a minimum at rigid cast sections. In the vertical direction up to 1250 Hz (Fig. 21) 'flapping' modes occurred where the vibration level increased from a minimum at the cylinder block/crankcase junction to a maximum at the crankcase skirt. As there is no phase cancellation from flapping modes, acoustic radiation was high. The major source of noise was the cylinder block and crankcase, the sump having an important effect at the front. Front noise was also markedly affected by timing gear noise. Rocker cover and exhaust manifold were significant but less important sources.

REVISED STRUCTURE - The experimental ISVR/Leyland quiet engine was reached in two main stages. The first stage used the standard cylinder block with the crankcase modified by attaching a 1 inch thick bearing beam integral with the bearing caps (Fig. 22). The final stage employed a revised crankcase design (ladder frame) used with a modified cylinder block. Standard running parts were used and the completed design included front chain drive in place of gear drive for the timing system, laminated damping panels on the crankcase and cylinder block walls, a sump decoupled by a U-section neoprene gasket, an additional damped cover over the standard rocker cover and a quieter injection pump.

A generalised view of the ladder frame crankcase is given in Fig. 23 where it can be seen to consist of two parts split at the crankshaft centre line. The upper part had thicker web and wall sections while the lower half comprised a ladder frame construction designed for high stiffness against longitudinal bending. The whole was dimensioned to take standard components. The modified cylinder block retained the normal cylinder liner and injector housings but the external walls and top deck were thickened.

NOISE CHARACTERISTICS OF RESEARCH ENGINES - The integral bearing plate design was noisier than the standard engine by $\frac{1}{2}$ to $2\frac{1}{2}$ dB(A) under full load although at light loads the engines were similar. The spectra of the two engines given in Fig. 19 show that the noise increase occurred mainly at frequencies above 1 kHz. The vibration levels of the modified engine were lower at low frequencies, and higher at frequencies above 250 Hz because the integral bearing plate was excited close to its natural frequency and in turn excited the crankcase walls. Development therefore moved on to the ladder frame design.

The ladder frame research engine nearly reached the project target, giving 92/94 dB(A) at 1 m, a reduction of 6 dB(A). Not all the modifications were regarded by the manufacturers as commercially acceptable in the form developed by ISVR. This engine demonstrated principles but needed design changes for commercial production purposes. The spectra of the standard and research engines are compared in Fig. 24.

On the left hand (injection pump) side of the engine the overall contribution of the modified crankcase at rated speed and load, was to reduce noise radiation by 2 dB(A) at a metre. There was a reduction in noise level at frequencies around 200 and 250 Hz corresponding to the reduction in the lower vibrational modes of the revised crankcase. However significant peaks remained at 1000 Hz, 2500 Hz and 8000 Hz. Vibration levels over the crankcase surface were reduced by up to 50 per cent over the lower part of the crankcase

skirts at frequencies up to 630 Hz. At frequencies between 800 Hz and 1250 Hz the acceleration levels were reduced by about 30 per cent at the crankcase skirt.

The laminated damped covers reduced noise levels by 1-3 dB(A) and the results correlated well with the reduction in vibration levels, showing little reduction below 800 Hz and an increasing improvement with frequency above 1000 Hz.

Replacement of the fuel pump by the low noise specification version reduced the engine noise by 0.5 dB(A) at 1000 rev/m at full load to 4 dB(A) at rated speed and load. The isolated sump reduced noise level by 2 dB(A) on the left hand side of the engine. This effect was fairly constant at full load through the speed range and was concentrated in the frequency band 800-2500 Hz.

EXHAUST SYSTEM - The work on the quieter exhaust system for the Leyland vehicle preceded that on the Foden and so the techniques available were not so advanced and problems were experienced with the high gas flow of these large engines. However designs were produced which approached the exhaust noise target although these included sections containing absorbent material.

The open pipe exhaust noise of the original Leyland diesel engine was 96 dB(A) at 2200 rev/min at 7.5 metres and 60° off axis. A total of 25 versions of the experimental silencers were designed by ISVR and MIRA and tested on the noise test facility. It was during the tests on the silencers for the Leyland engine that the use of perforated tube sections in the extended inlet/outlet expansion chambers was developed in an attempt to reduce back pressure. A design incorporating perforate bridges in an expansion chamber was finally produced by ISVR which, when used with an absorbent section, gave a noise level of 73 dB(A) at below the maximum back pressure.

With the success of the subsequent work on silencers for the Rolls Royce engine there is no doubt that a silencer for the Leyland engine which met the target noise and back pressure values without absorbent material could have been produced.

COOLING SYSTEM - The original cooling system in the vehicle used on 8 bladed axial fan. Measurements of cooling system noise, made at a fan speed of 2850 rev/min showed that a reduction of 17 dB(A) was required to meet the project target of 84 dB(A) at 1 metre.

A cab roof cooling system, illustrated in Fig. 25, was designed for this vehicle to avoid the problem of having to increase the fan duty to maintain the airflow through an engine enclosure. This position also had the advantage of allowing maximum use of ram air. An axial flow fan, driven by a hydraulic motor, discharged the cooling air vertically above the cab. The engine enclosure was ventilated by a bleed from the cooling system plenum chamber. Measurements on this system showed that it met the noise target at a fan speed of 1500 rev/min and at this speed achieved the cooling performance required for temperate climates.

COMPLETE VEHICLE NOISE RESULTS

BASELINE NOISE DATA ON STANDARD VEHICLE - Table 8 shows the overall noise levels emitted when the vehicle was accelerated past the microphone in three gears in accordance with BS 3425: 1966. Operation in 7th gear gave the highest noise levels and the spectra produced in this gear can be seen in Fig. 26. When tested unladen, driven at constant speed, and then coasted with the engine switched off, results were as shown in Fig. 27. The noise level was 6 dB(A) lower when coasting than when the engine provided enough power to maintain constant speed.

Cab noise in the standard vehicle was about 88 dB(A) when the vehicle was accelerated through the gears.

MODIFICATIONS TO THE STANDARD VEHICLE - In addition to the experimental silencer and cooling system the engine and gearbox were fully shielded by a sheet steel enclosure lined with protected polyurethane foam. The enclosure was ventilated by an air inlet at the front and a duct from the rear of the enclosure to the cooling system plenum chamber on the cab roof. The cab trim was improved by using thicker insulating material, improving the barrier between the power unit and the cab and improving the gear lever gaiter and its seal to the floor of the cab. The standard Leyland engine was used in the research vehicle at this stage.

NOISE MEASUREMENTS ON THE FINAL RESEARCH VEHICLE - The external noise levels (at 7.5 metres) emitted during acceleration tests compared with the original vehicle are given in Table 8; levels had been reduced by 10 dB(A) to 79.5 dB(A). The spectra shown in Fig. 28 demonstrate that significant attenuations had been achieved at all frequencies. At these lower general noise levels rear axle gear meshing noise at about 500-1000 Hz became noticeable and the pronounced peaks in the spectra at 250 Hz were due to tyre tread pattern effects. Cab noise was reduced to 78 dB(A), and the spectra in Fig. 29 show that this result was achieved with reductions at both high and low frequencies.

With the engine and gearbox enclosure removed the noise external level increased to 85 dB(A).

The Leyland research vehicle is compared with a range of current vehicles in Table 7.

SUMMARY OF RESEARCH ON THE LEYLAND VEHICLE

The Leyland research engine emitted noise levels of 6 dB(A) lower than the standard engine. This engine demonstrated principles but needed design changes to make it commercially viable. The cab roof mounted cooling system met noise and temperate climate cooling requirements and together with the quieter exhaust system enabled the research vehicle to meet the target noise level of 80 dB(A).

TYRE NOISE

The main conclusions of the work on tyre noise at TRRL as applied to the QHV project are:-

(1) Radial-ply tyres are some 3-4 dB(A) quieter than cross-ply tyres.
(2) Quietest tread patterns are those with 5 or

more circumferential grooves with no pronounced shoulder patterns.

(3) Traction tyres with pronounced edge serrations are noisier than the tyres described in (2) by up to 5 dB(A) in the dry. On wet surfaces the difference between tread pattern tends to reduce.

(4) A typical radial ply tyre with 5 circumferential grooves emitted a noise level of 79-82 dB(A). When the surfaces were wet these noise levels were increased by 8-9 dB(A). A pervious macadam surface can help to reduce noise when wet, measurements indicating some 4-6 dB(A) reduction compared with a smooth macadam surface. (Ref. 3).

CONCLUSIONS

The TRRL Quiet Heavy Vehicle Project succeeded in producing two research vehicles, having greatly reduced external and internal noise levels. The larger of the two, the Foden/Rolls Royce tractor has been developed to production standards and will enable the costs of production and operation to be evaluated. This final demonstration vehicle has recorded 80 dB(A) in BS acceleration tests and satisfies all the objectives of the QHV project.

The work has involved developments in engine noise control, cooling package, engine enclosure and exhaust system. These have been drawn together into a practical vehicle design which we hope will point the way for future heavy road transport.

ACKNOWLEDGEMENTS

This report was prepared in the Transport Engineering Division of the Transport Systems Department.

The authors would like to thank Director TRRL for permission to publish this paper and the following people whose particular efforts, together with those of their staff, have ensured satisfactory progress and outcome of the research phase of the QHV Project.

Fodens Ltd: Mr R P Lewis - Project Manager for Fodens. Mr J F Collins - Deputy Project Manager.

Rolls Royce Motors Ltd: Mr G Collin - Project Manager for Rolls Royce (Engine).

Leyland: Mr R J Price - Project Manager, Mr J Varley and Mr A M Porkess.

MIRA: Mr C H G Mills - Project Supervisor, Mr J West - Project Leader (Cooling, Exhaust, Vehicles Structures)

ISVR: Professor T Priede - Project Supervisor, Mr E C Grover - Project Leader (Engine) and Professor P Davies - Project Leader (Exhaust Silencers).

REFERENCES

1. The working group on research into traffic noise. TRRL LR 357, 1970.

2. D. Anderton, E. C. Grover, N. Laylor, T. Priede. The Automotive Diesel Engine - it's Combustion, Noise and Design. Inst. Mech. Eng. Conference on Land Transport Engines, January 1977.

3. J. R. Brown. "Pervious bitumen-macadam surfacings laid to reduce splash and spray at Stonebridge, Warwickshire". Department of the Environment TRRL Report LR 563, Crowthorne 1973 (Transport and Road Research Laboratory).

Table 1 - Upper Limits of Sound Levels to be emitted by Vehicle components

Research* Organisation	Source	Maximum level dB(A) at 1 m	at 7.5 m
ISVR	Engine including gearbox	92	77
	Air intake, exhaust system (computer modelling)	84	69
MIRA*	Cab noise	- 75 dB(A)	-
	Cooling system	84	69
	Exhaust system (development of practical systems)	84	69 (Additional target of 90 dB(C)

*MIRA were to design the vehicle cab to provide 3 dB(A) attenuation of the sound level emitted to the roadside by the power unit

TRRL	Tyre road surface noise	-	75 - 77

Table 2 - Details of Engines

Engine Details	Leyland	Rolls Royce
Cycle/Aspiration	4. Turbocharged	4. Turbocharged
Cylinders No.	6	6
Arrangement	In line	In line
Inclination	Vertical	Vertical
Bore	118 mm	130.5 mm
Stroke	125 mm	152.4 mm
Capacity	8.2 L	13.09 L
Max. Power	158 kw (212 bhp)	262 kw (352 bhp) [320 bhp]
Max. Power Speed	2200 rev/min	2100 rev/min [1950 rev/min]
Max. BMEP	* 158 lbf/in^2	182 lbf/in^2 [186 lbf/in^2]
Boost pressure at max. power	* 17 lbf/in^2	18 lbf/in^2 [21 lbf/in^2 gauge]
Exhaust Back Pressure (max.)	37 mm Hg	51 mm Hg
Cylinder Head	1 fixed head	2 bolted

* modifications shown in square brackets

Table 3 - Identification of the Four Builds of the Foden Tractor

Vehicle reference	Vehicle type and condition
F1	Foden 3-axled tractor (44 ton capability) with 350 b.h.p. Rolls Royce turbocharged diesel engine. All components standard; vehicle as delivered to MIRA.
F2	Foden 3-axled tractor with experimental silencers and cooling system (centrifugal fan), improved cab insulation, engine and gearbox remote enclosure, and standard Rolls Royce engine (as in F1). The Vehicle was returned to Fodens in this condition for replacement with the later 2-axled chassis.
F3	Foden 2-axled tractor with new g.r.p. cab and hypoid rear axle. The exhaust system was as removed from F2. The cooling system was the same experimental design as in F2 but was 'packaged' to allow easy fitting and removal. The engine was the standard Rolls Royce but with revised camshaft design and later type turbocharger.

Table 3 - continued

Vehicle reference	Vehicle type and condition
F4	Foden 2-axled tractor as F3 with final experimental exhaust and cooling systems and fitted with quietened ISVR/RR 'research' engine. In this condition the vehicle was evaluated and returned to Fodens for the development phase of the Project.

Table 4 - Overall noise levels of standard Rolls Royce engine and 'research' engine

	1000		1500		2100 rev/min	
1. Standard (with front gears)	FL	NL	FL	NL	FL	NL
Offside	95	90	98	94	105	100
Front	98	93	100	97	107	102
Nearside	96	91	99	95	105	100
2. 'Research'						
Offside	88	83	91	89	97	94
Front	87	84	90	89	97	96
Nearside	89	85	92	90	99	97

FL = full load
NL = no load

Table 5 - Comparison of the noise emitted by the original Foden F1 vehicle and the final 'research' vehicle F4 (Modified BS 3425 Test)

Original vehicle F1			Final 'research' vehicle F4		
	Noise emitted, dB(A)			Noise emitted	
Gear	Right hand side	Left hand side	Gear	Right hand side	Left hand side
5	93.0	92.0	4	82.0	81.5
6	92.5	91.0	5	83.5	83.5
7	90.5	90.0	6	80.0	80.5

Table 6 - Trim conditions selected for the assessment of the acoustic treatment fitted in the cab

	Cab trim condition	Maximum dB(A) levels in 7th Gear
A	Cab fully treated	78.0
B	With bonnet cover removed	79.0
C	With bonnet cover and floor mats removed	80.0
D	With all acoustic treatment removed	85.0
E	With absorbent material only removed (bonnet cover and floor mats in place)	84.0

Table 7 - Some 'in use' noise levels of current heavy vehicles

Vehicle	Engine power kW	Max. gvw tonnes	External noise dB(A)	Internal cab noise dB(A) (at max. power speed)
1	150	35	91	82½
2	-	32.5	93	-
3	-	42	87	77
4	-	35	93½	82
5	160	32.5	89	82
6	143	32.5	86½	83
7	230	38	88	82
Foden F4 research vehicle	260	38	83½	78
Leyland research vehicle	158	32	79½	78

Table 8 - Comparison of the noise emitted by the original Leyland vehicle and the final 'research' vehicle (Modified BS 3425 Test)

Original vehicle			Final 'research' vehicle		
	Noise emitted dB(A)			Noise emitted dB(A)	
Gear	Right hand side	Left hand side	Gear	Right hand side	Left hand side
5	87.0	86.0	5	79.0	78.0
6	89.0	87.5	6	79.5	79.0
7	89.5	87.0	7	79.0	78.0

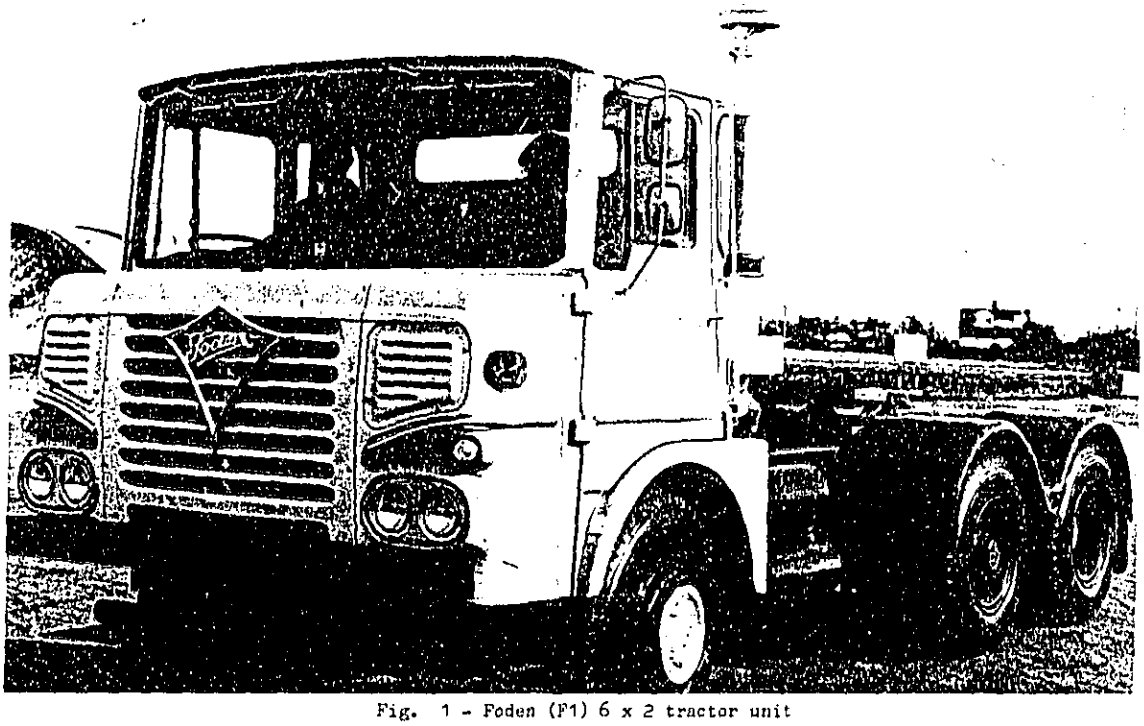

Fig. 1 - Foden (F1) 6 x 2 tractor unit

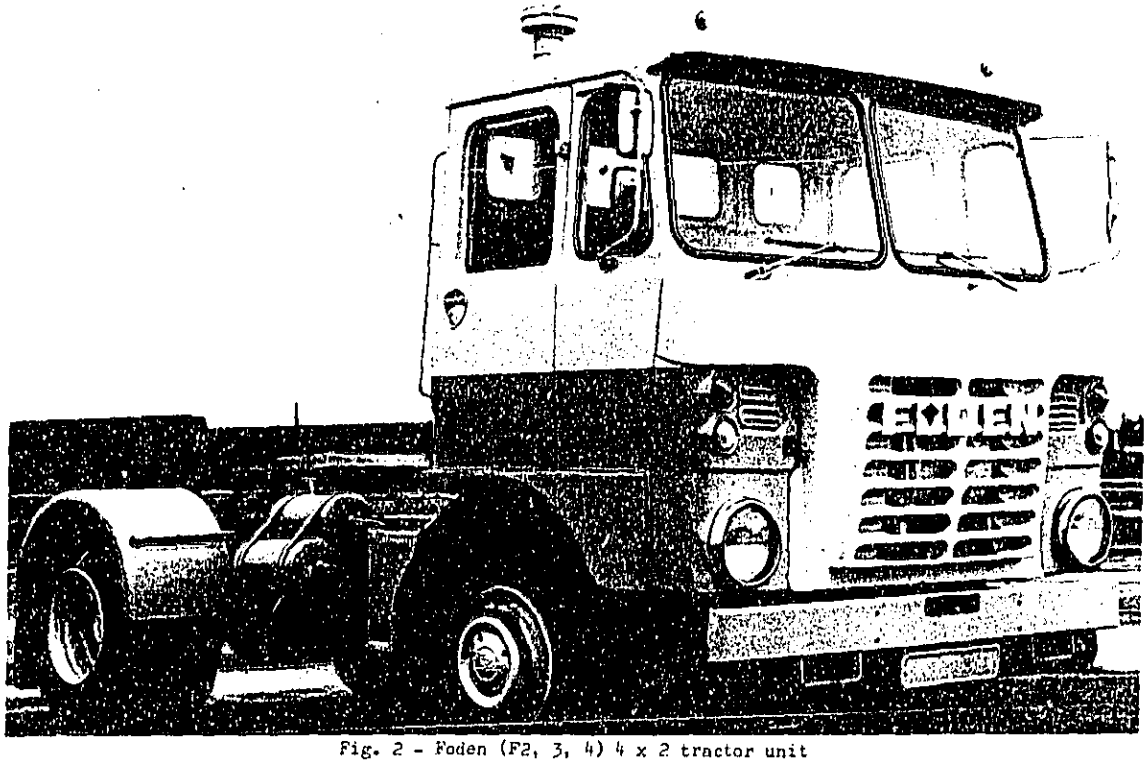

Fig. 2 - Foden (F2, 3, 4) 4 x 2 tractor unit

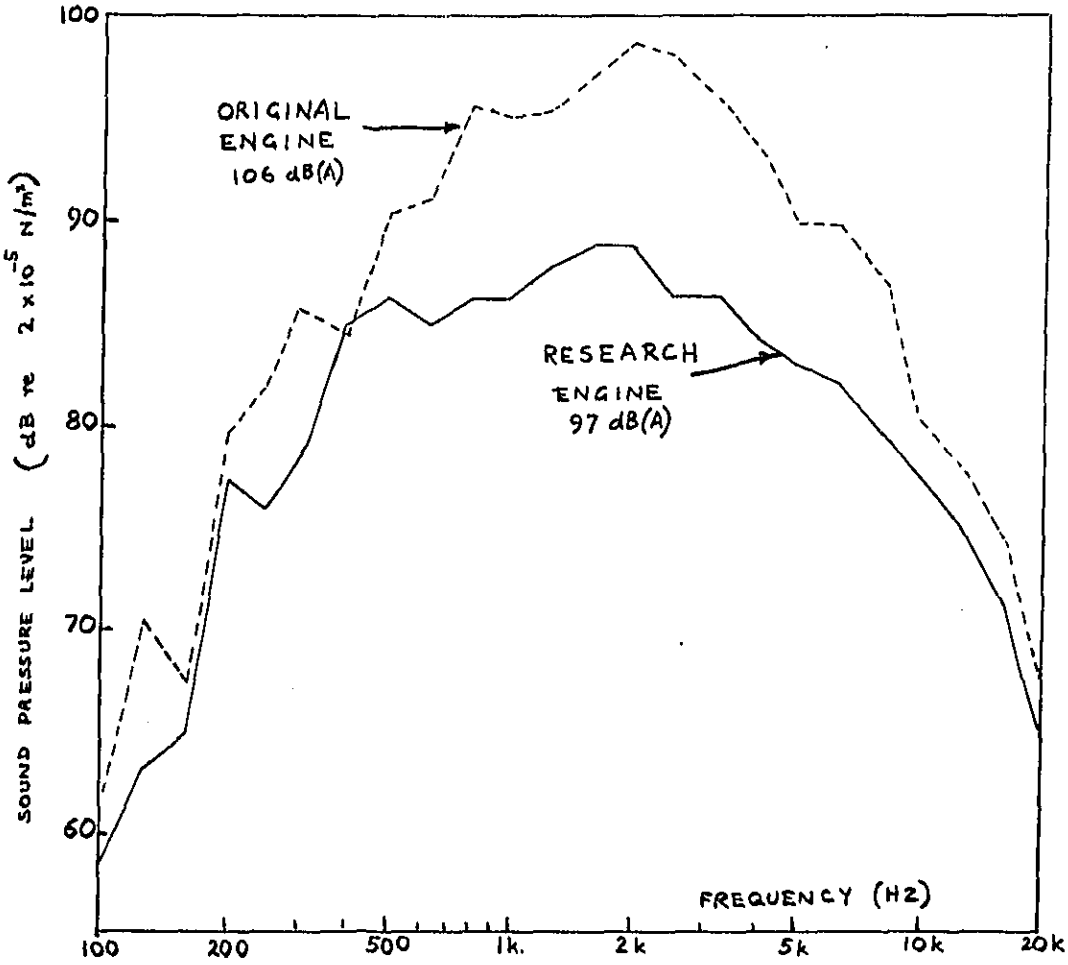

Fig. 3 - Test cell comparison of A-weighted noise spectra on nearside of standard and research engines at rated condition (2100 rpm, full load)

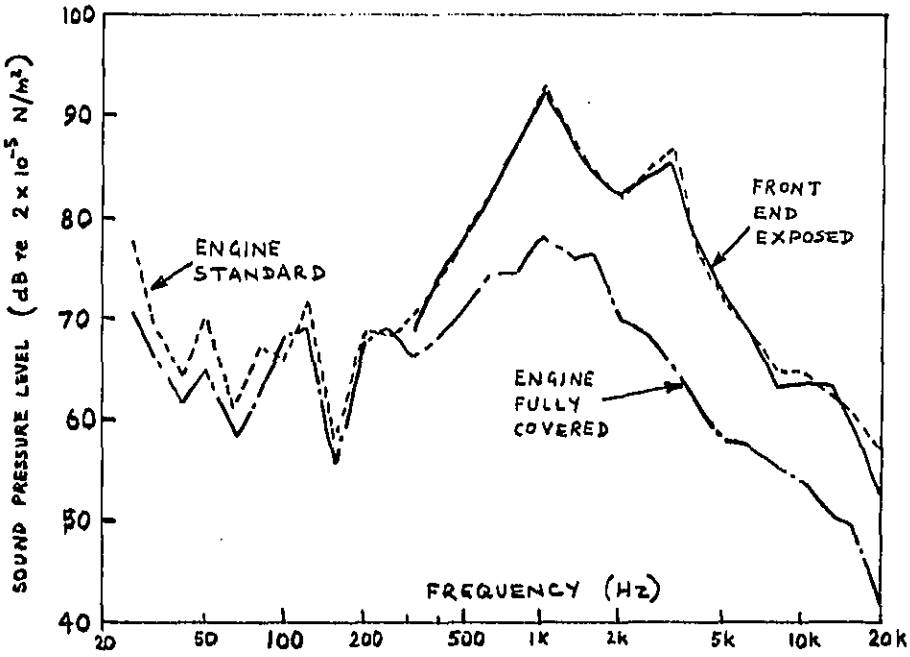

Fig. 4 - Measurements showing noise contribution from front of standard Eagle engine at 1000 rpm

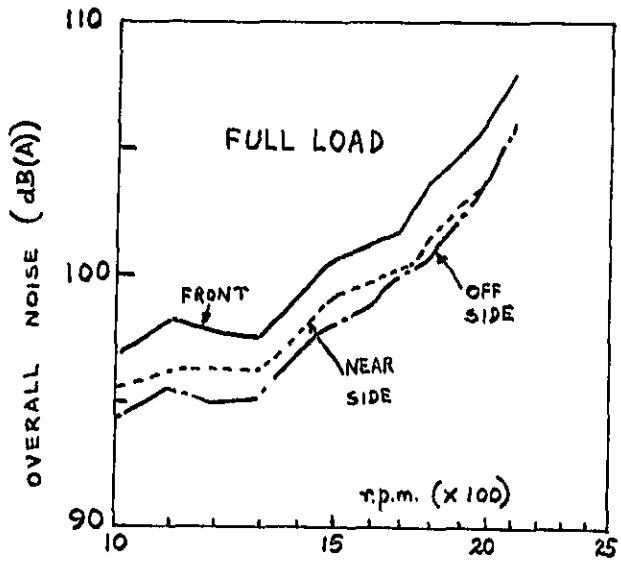

Fig. 5 - Variation of overall noise with speed for standard Eagle engine

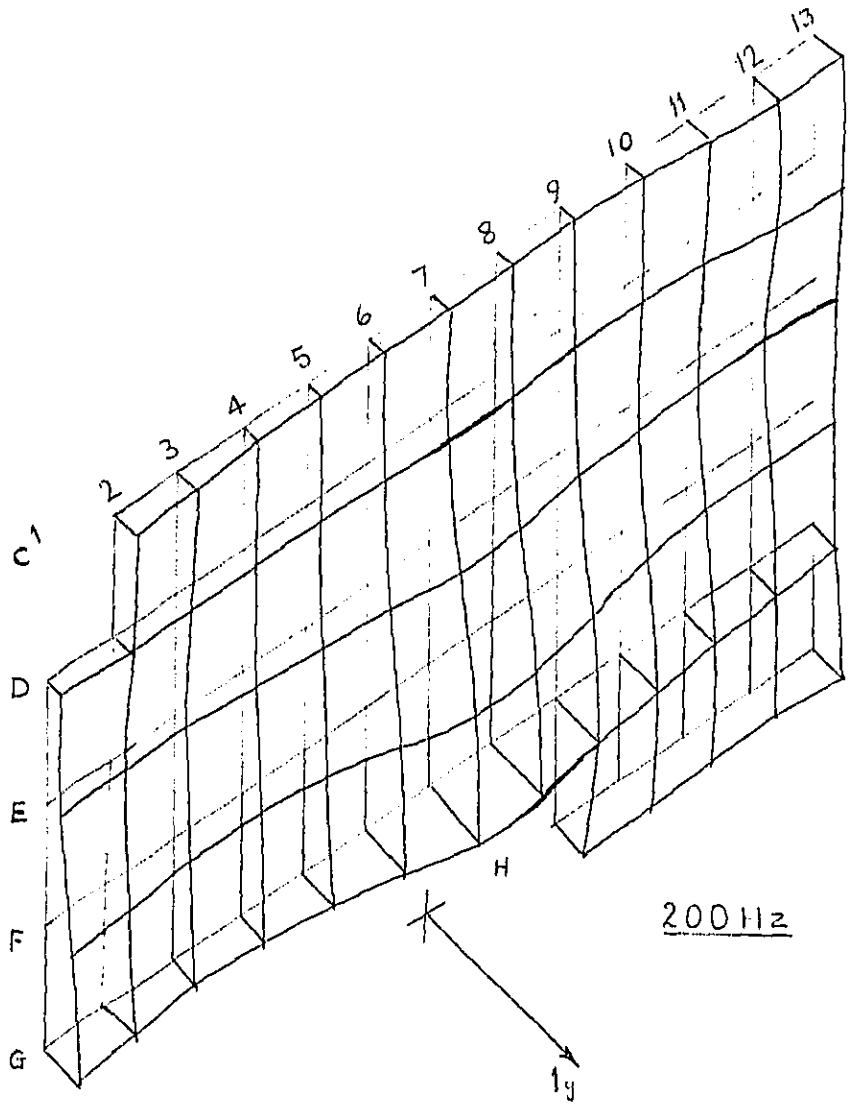

Fig. 6 - Typical engine surface vibration pattern

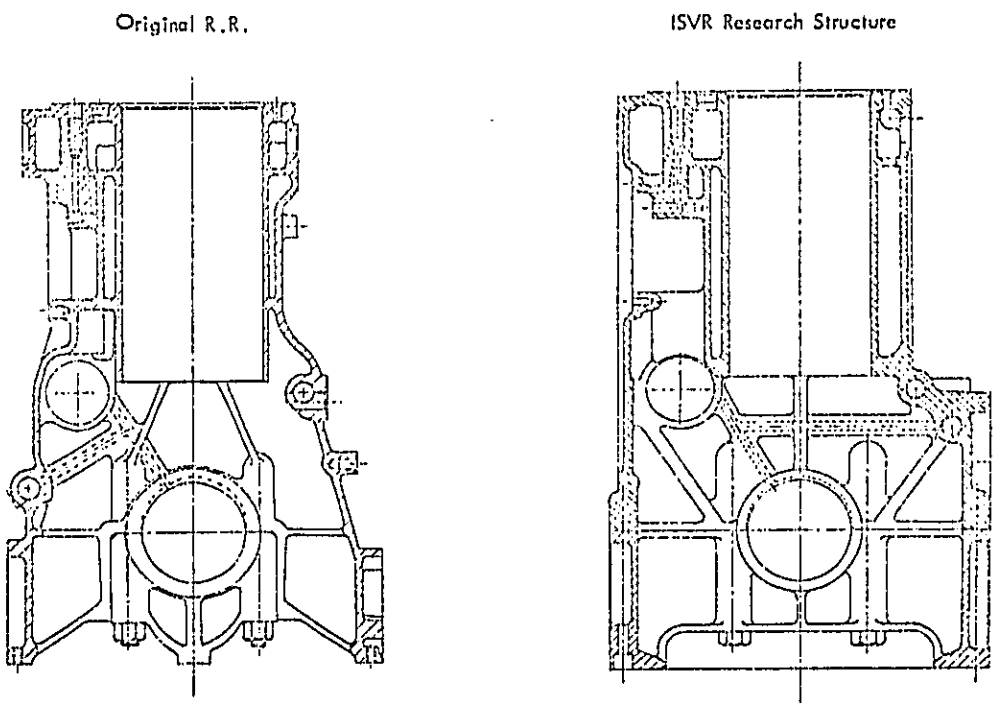

Fig. 7 - Rolls Royce engine structures

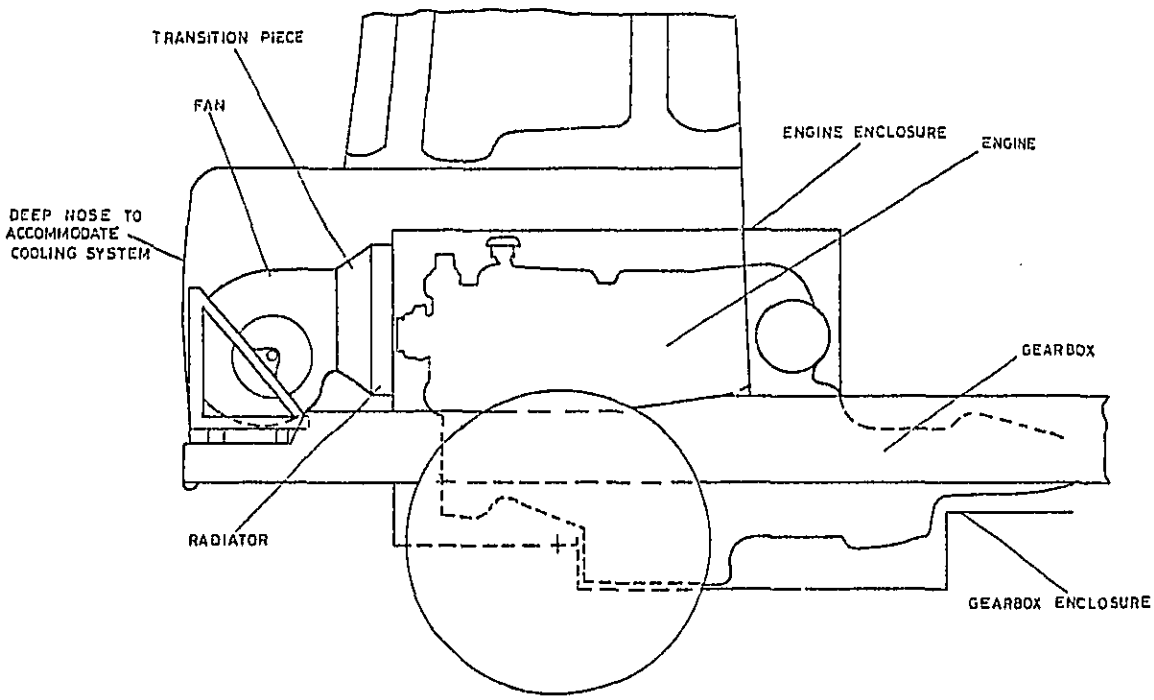

Fig. 8 - Cooling system in F2 tractor unit

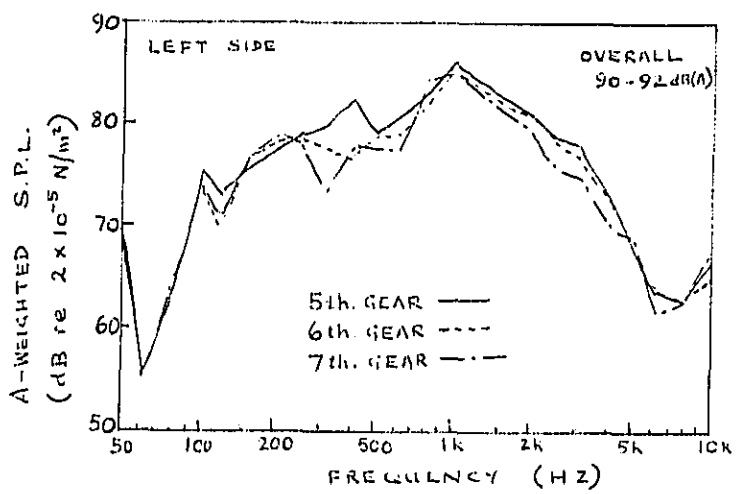

Fig. 9 - External noise spectra for Foden F1 as supplied (LHS)

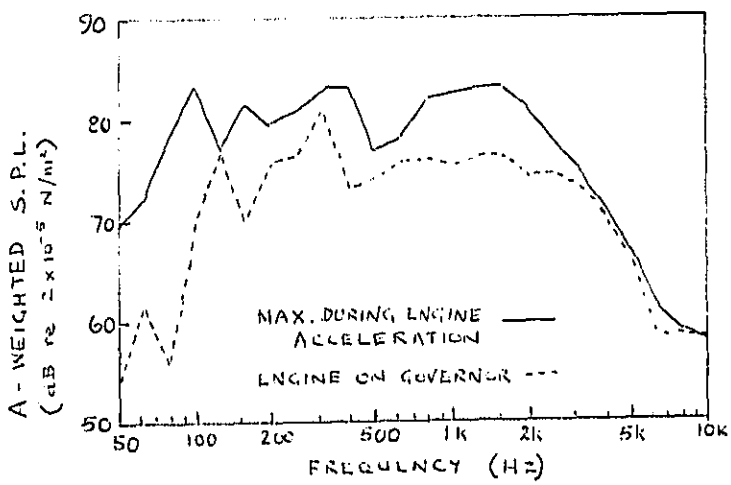

Fig. 10 - Spectra of F1 vehicle noise during a stationary test (RHS)

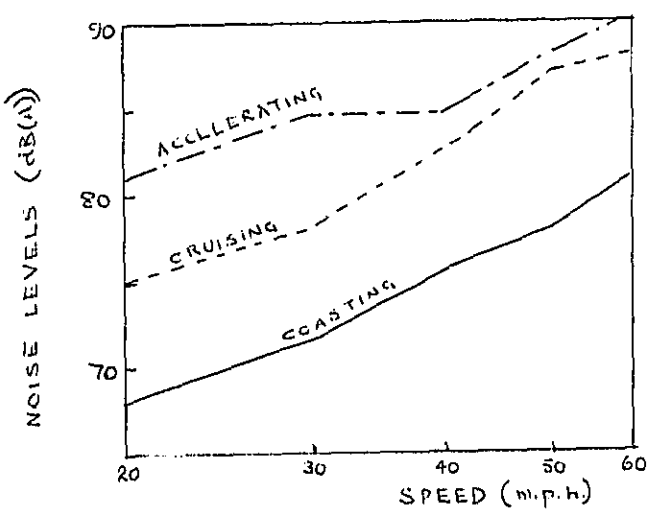

Fig. 11 - Passing noise versus speed for the F1 Foden vehicle

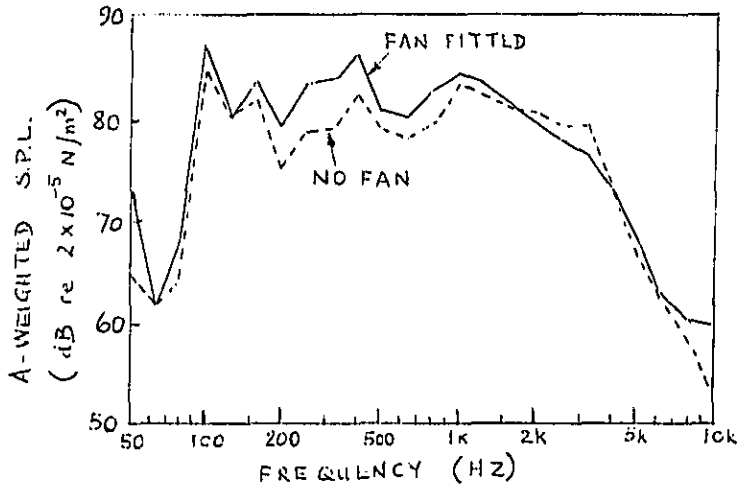

Fig. 12(a) - The effect of standard cooling fan on the noise emitted by Foden F1 vehicle

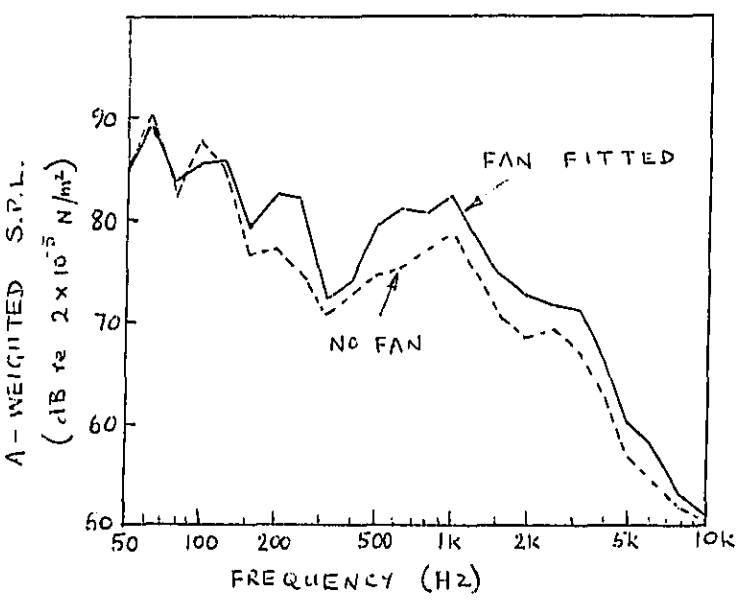

Fig. 12(b) - The effect of standard cooling fan on the noise in the cab of Foden F1 vehicle

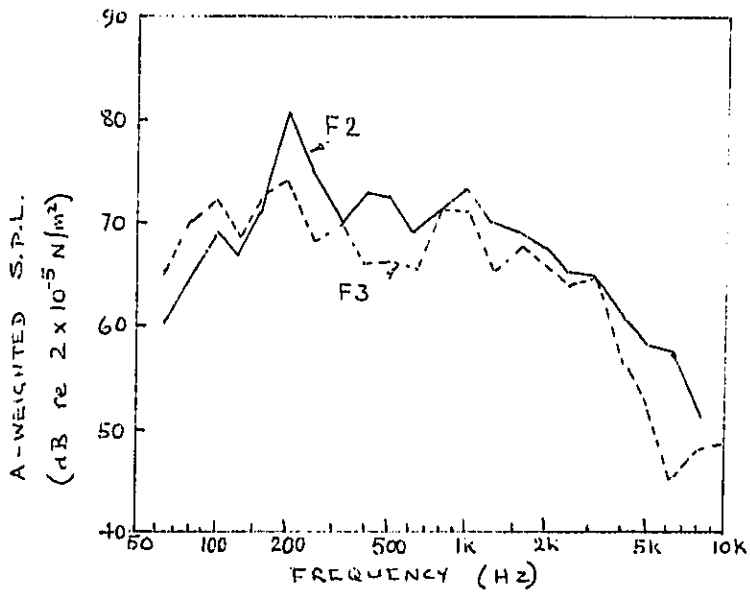

Fig 13. - Comparison of noise spectra measured in Foden test vehicle cabs

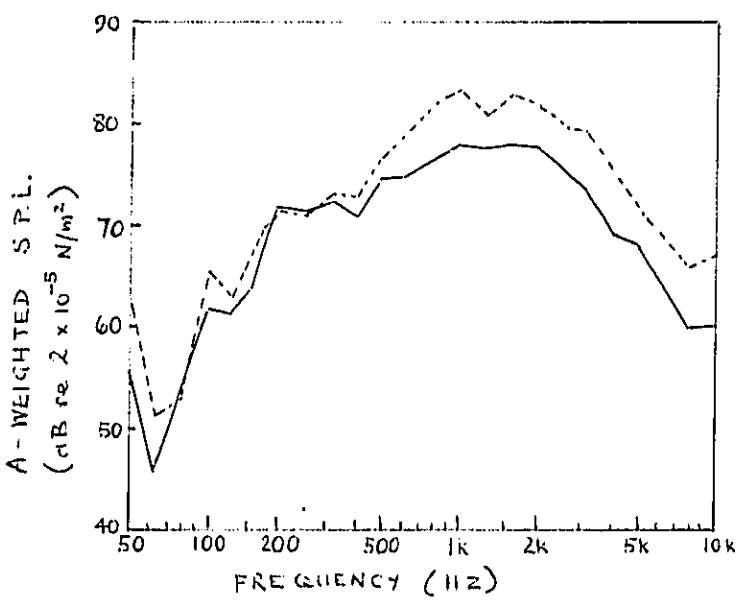

Fig. 14 - The effect of the tunnel enclosure on the noise emitted by the F3 vehicle

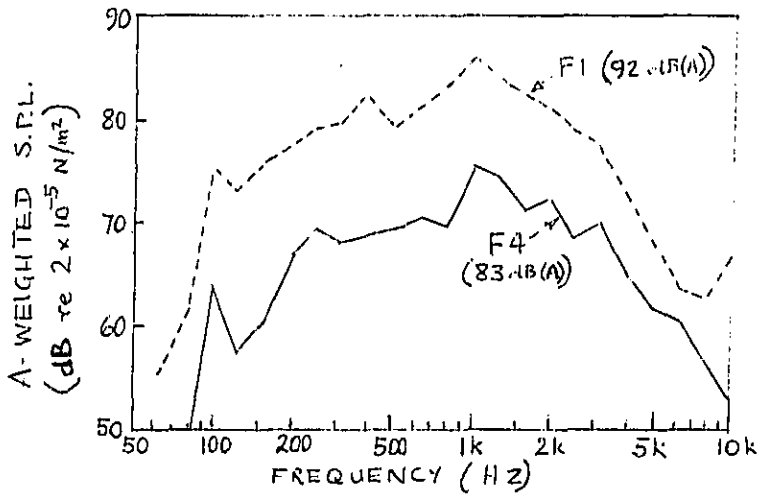

Fig. 15 - Noise emitted by final F4 research vehicle compared with that of early F1 standard (LH side)

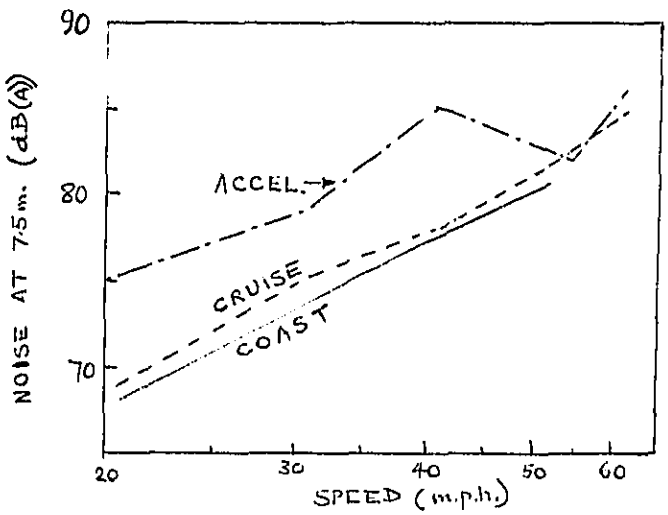

Fig. 16 - Passing noise of Foden F4 with loaded trailer

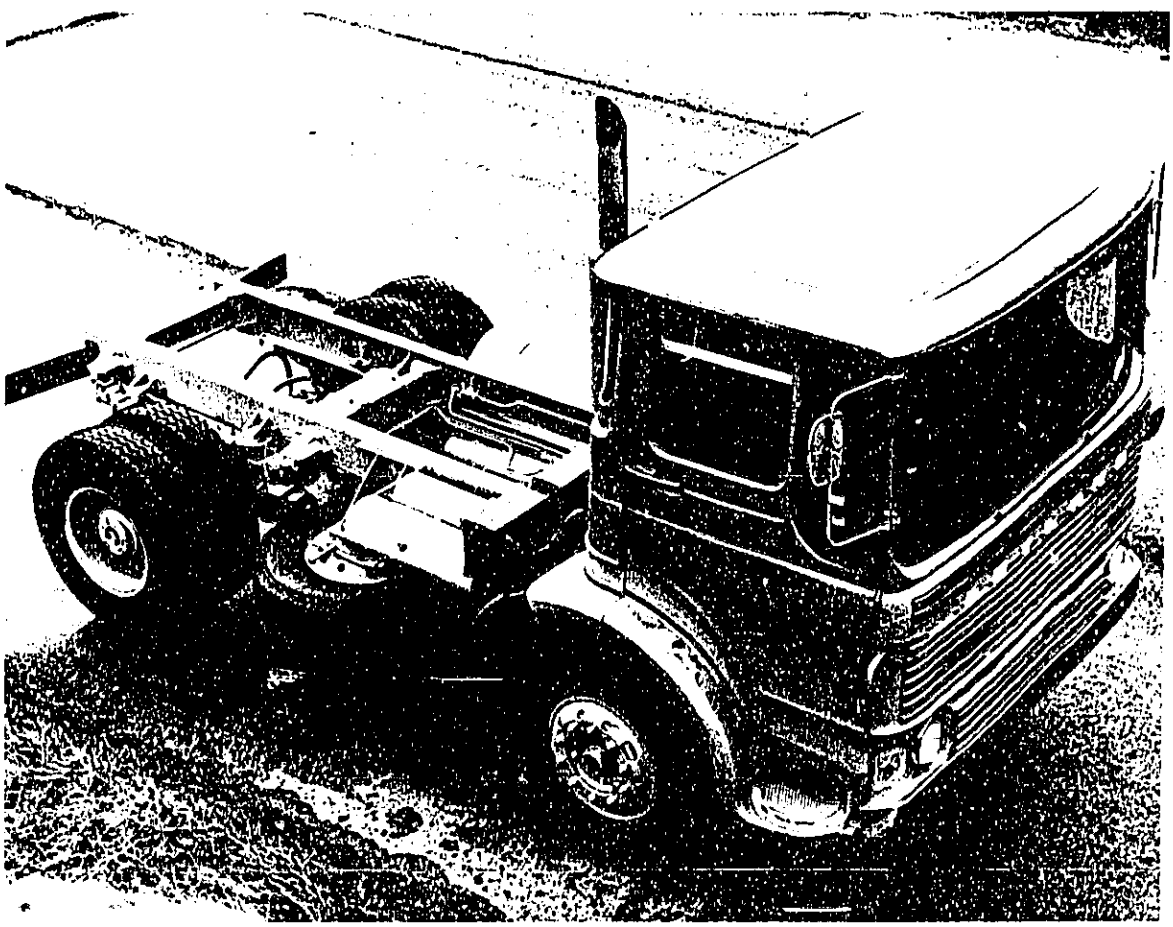

Fig. 17 - Leyland Buffalo - original vehicle

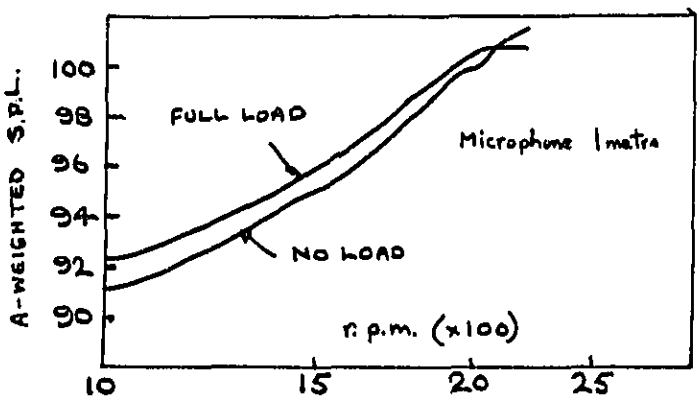

Fig. 18 - Noise levels on left hand side of Leyland engine at full and no load conditions

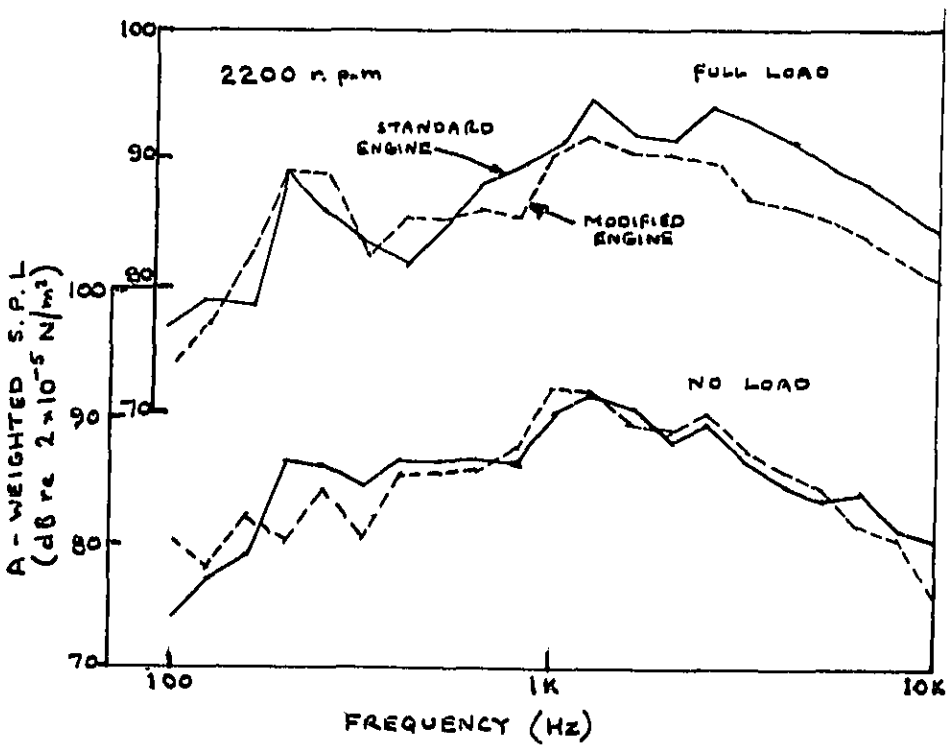

Fig. 19 - Spectra of noise from right hand side of standard and integral bearing plate engines

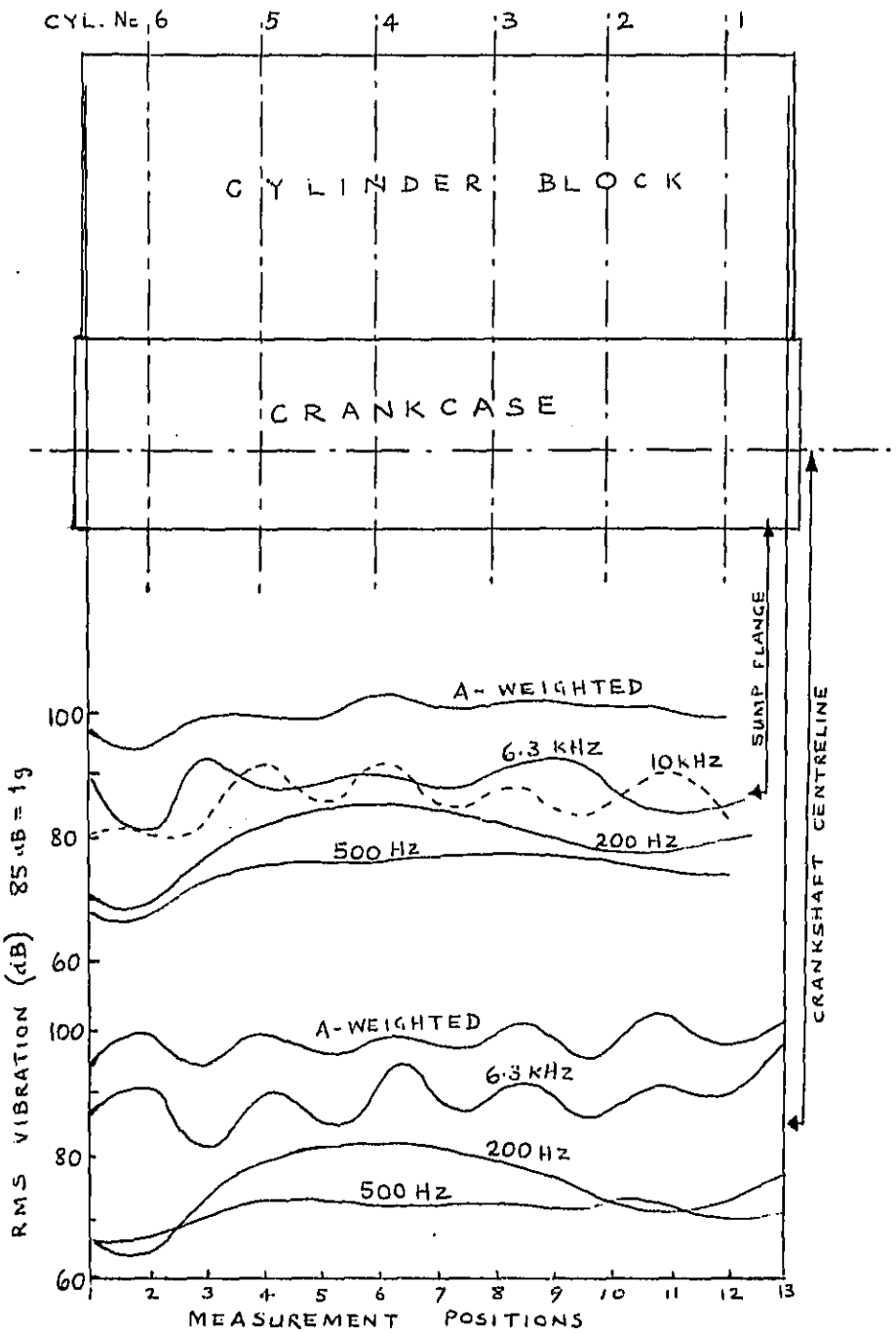

Fig. 20 - Vibration patterns along two horizontal planes on Leyland engine

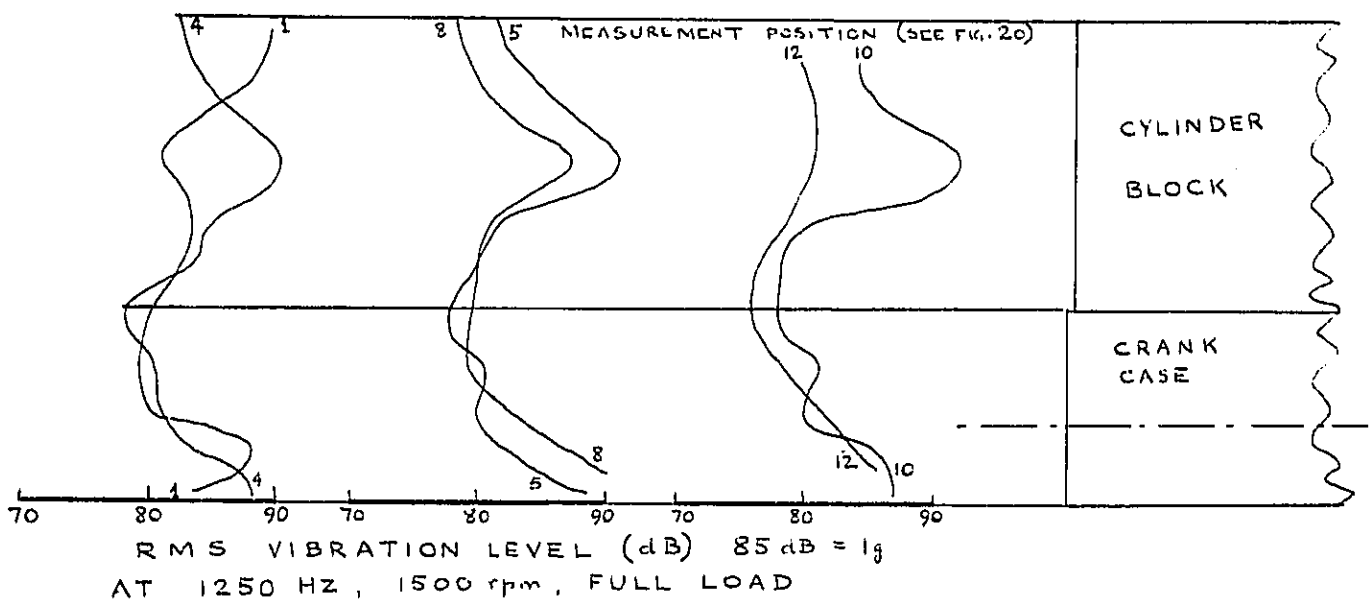

Fig. 21 - Vibration patterns along vertical planes on Leyland engine

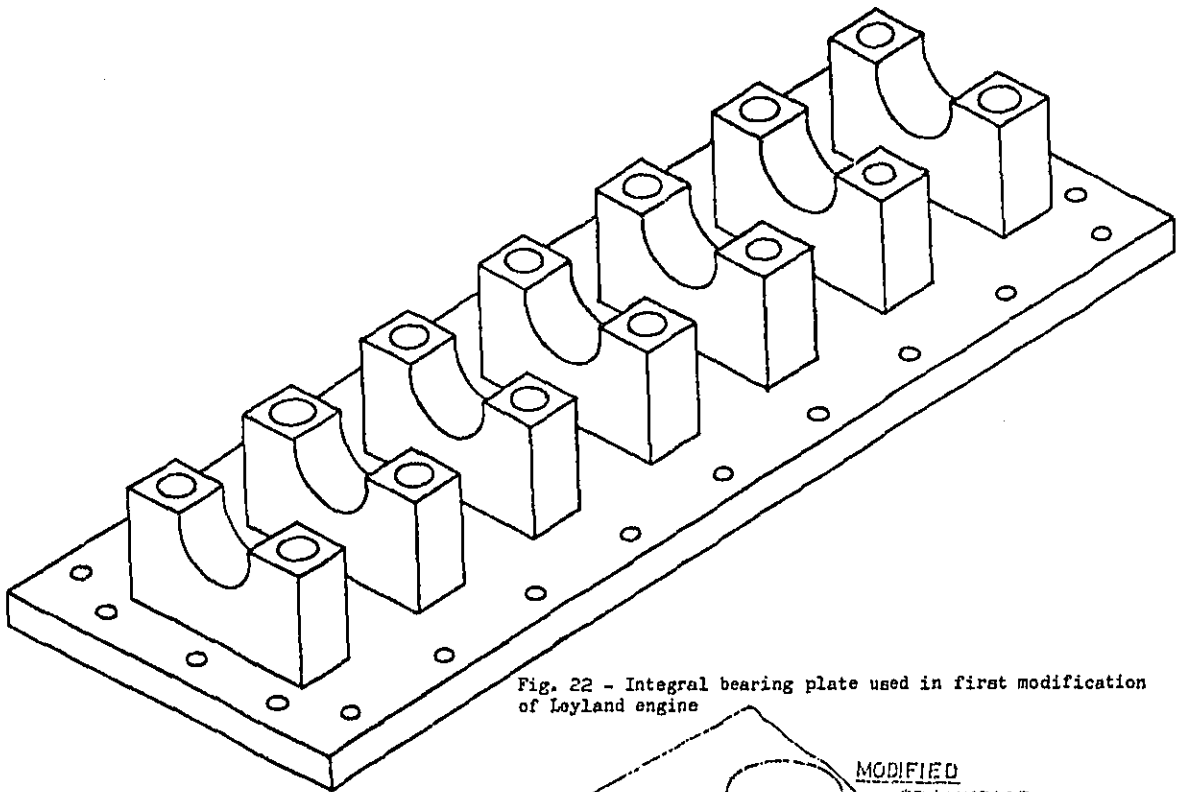

Fig. 22 - Integral bearing plate used in first modification of Leyland engine

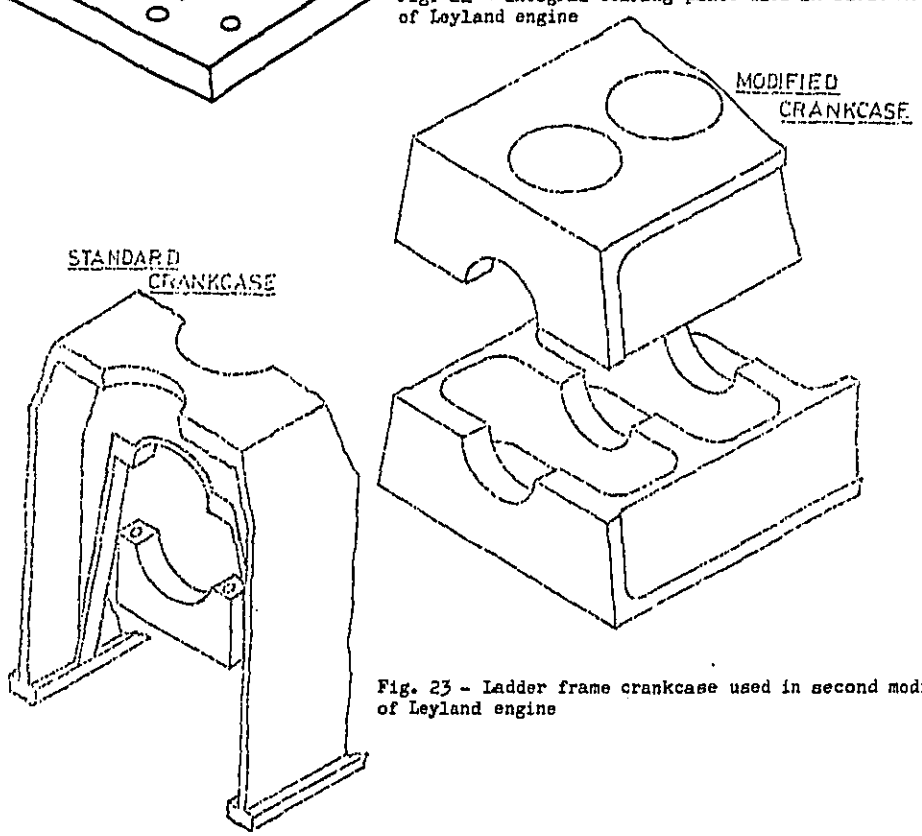

Fig. 23 - Ladder frame crankcase used in second modification of Leyland engine

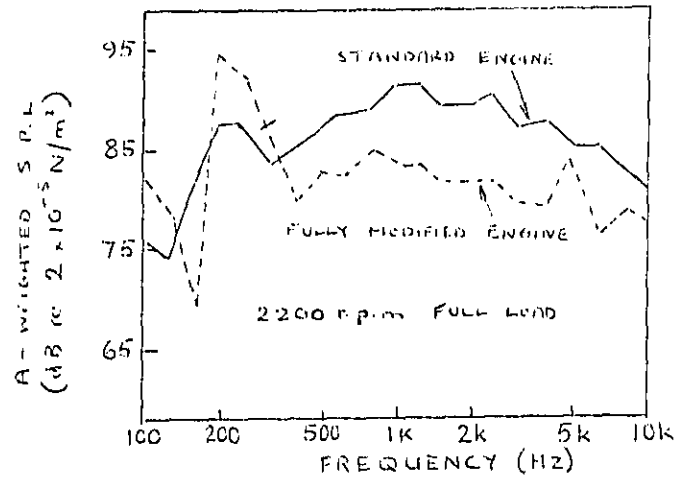

Fig. 24 - Spectra of noise from the standard and fully modified Leyland engine

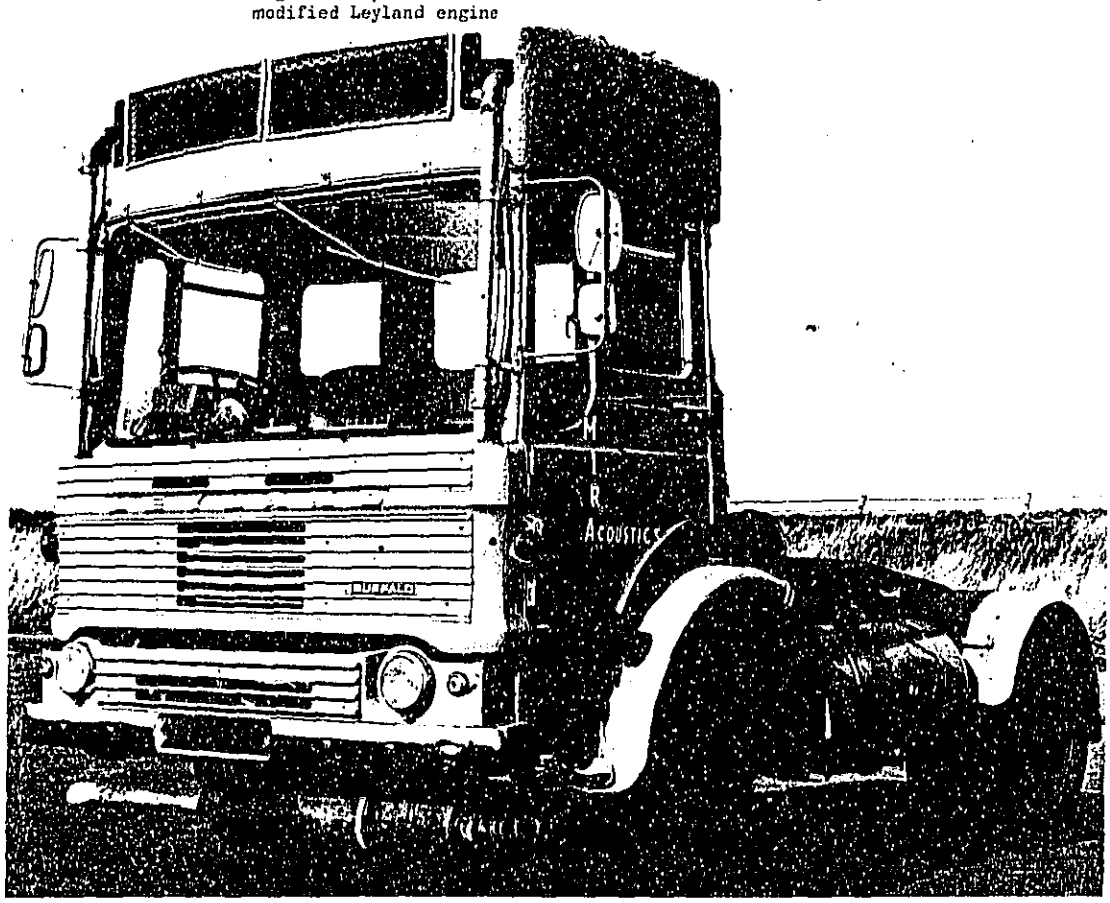

Fig. 25 - Leyland tractor unit with roof mounted cooling system

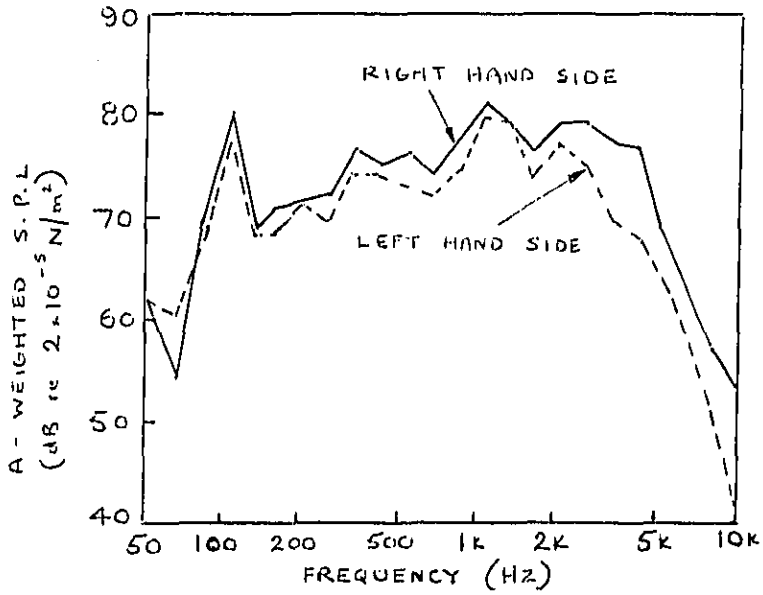

Fig. 26 - Spectra of the noise emitted from the original Leyland vehicle (acceleration in 7th gear)

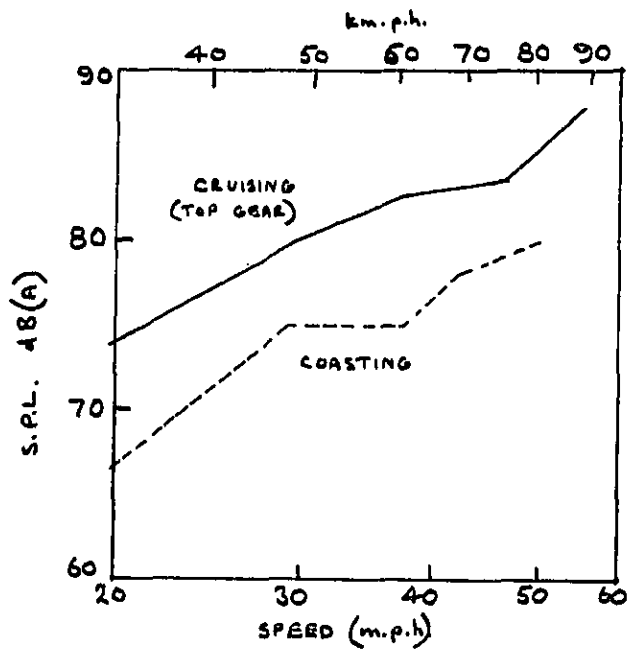

Fig. 27 - Passing noise of the standard Leyland vehicle (unladen)

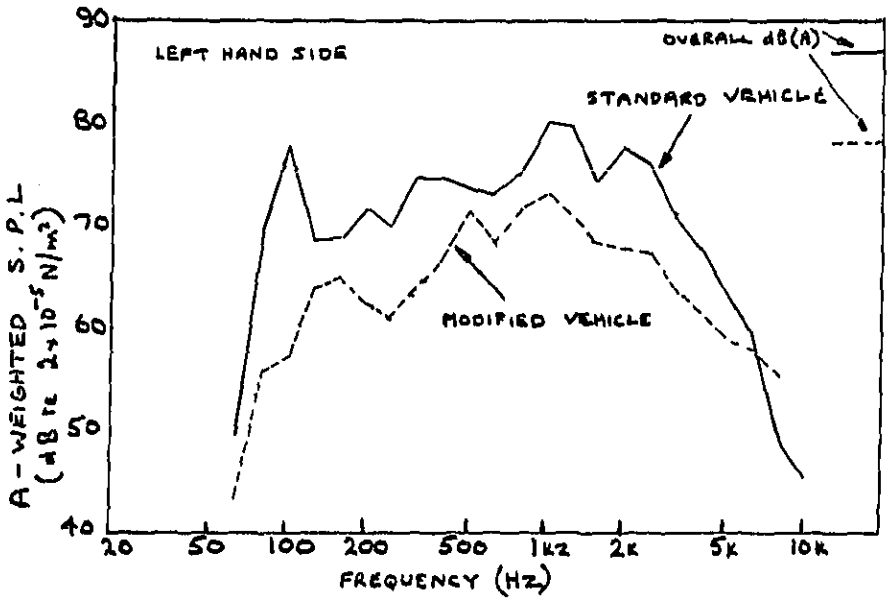

Fig. 28 - Comparison of the spectra of the noise emitted by the standard and modified Leyland vehicle (acceleration in 7th gear)

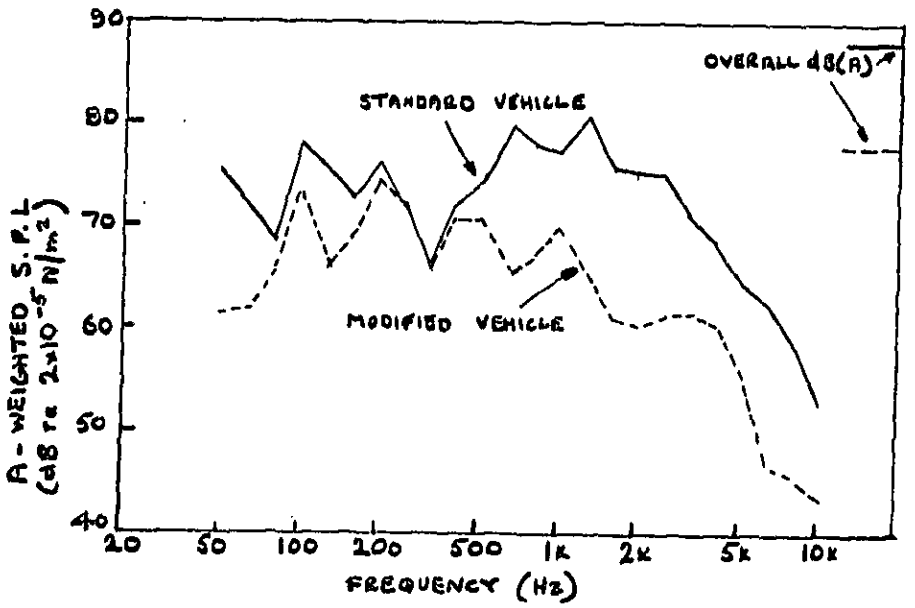

Fig. 29 - Comparison of the spectra of the noise in the cab of the standard and modified Leyland vehicle (acceleration in 7th gear)

790454

STATISTICAL APPROACH FOR DIESEL ENGINE NOISE ANALYSIS

R. PADOAN AND M. JOCTEUR MONROZIER

RENAULT VEHICULES INDUSTRIELS

(FRANCE)

ABSTRACT

In urban traffic vehicle use leads to running conditions which vary essentially according to torque and speed . An experimental multiparametric analysis has been carried out on this subject . The results of the experiment confirm the main noise causing parameters . Noise prediction formulae can also be drawn up for any engine running conditions . As a result of this analysis the noise of one of the engines could be reduced by 7 dB(A) by acting on combustion and mechanical parts, as well as on sound radiation .

A FEW YEARS AGO, noise was the concern of specialized laboratories, and road vehicle manufacturors only dealt with the problem as a matter of secondary importance . Now the recent and rapid evolution of regulations in this area has lead to a drastic change in this situation . Noise will in the near future become one of the important technical parameters intervening in the design of vehicles, particularly that of commercial vehicles . The latter in Europe are essentially fitted with diesel engines which constitute the major source of noise and present the most important technical problems . In point of fact, noise abatement research carried out on vehicles shows that the applicable solutions fall into two large categories :

- -noise reduction at source by action on the engine itself
- - noise reduction by using screens hung either on the engine or on the vehicle .

Use of screens or encapsulation in different forms appears to be worthy of consideration .·It is much less obvious that inherently less noisy engines can be developed within the framework of reasonable industrial and economical considerations . Quite clearly such engines would be of interest . They would greatly simplify the task of the vehicle layout designer, therby avoiding problems in vehicle maintenance as well as in accessibility, which result from the use of screens . But, from another point of view a radical change in engine design and production procedures could lead to changes in the related levels of investment . These changes are of major concern to the motor industry .

Under these conditions, it appears advisable to analyse the different aspects of this subject in detail, and in particular to return to the source of the problem, i.e. the noise regulations. Roughly speaking, these regulations, in Europe, impose a maximum noise limit level for commercial vehicles . However, when dealing with noise, the conditions under which the vehicles are used, are very different, depending on whether they are used in town or on the highway. For town driving, the noise level is not only the result of the highest level of noise emitted when the engine is operating at peak power or peak speed conditions (conditions very seldom used) but the result of noise emitted at all the intermediate conditionsused, whether transitory or stabilized . Hence, within the perspective of the drastic regulations foreseen around the year 1985, it is quite probable that these circumstances will be taken into account . The end result could be a parallel set of regulations relating the required lowering of the noise level in urban areas to the most suitable cost factor .

In the face of such a situation, the vehicle manufacturor, especially if he builds engines, must attempt to adapt his research in the field of acoustics to the different points of view which have been referred to above . This is

SAE/P-79/80/$02.50
Copyright © 1979 Society of Automotive Engineers, Inc.

why we have analysed in depth and detail the acoustical behavior of all the engines we manufacture .

This research programme was conducted to cover the following four aspects of which the latter two are of greater importance :

1. The general situation of our engines as compared with engines produced throughout the world, for which the I.S.V.R. supplied very interesting data .
2. Behavior of our engines as related to general trends which are now well defined .
3. Characterisation of acoustical emissions in all possible conditions of operation .
4. Drafting of formulae so as to allow an estimation of the noise level within all these conditions of operation .

In order to obtain these objectives, we organised a data bank, and used a statistical approach with the help of corresponding modern analytical techniques.

METHODOLOGY

Noise measurements are delicate and hence, considerable precautions were taken during the research programme in order to keep the measurement errors within 1 dB(A) in absolute terms and 0.25 dB(A) in relative terms .

Noise level measurements were carried out in a semi-anechoic cell which had the following characteristics :

- Total volume = 380 m3 (wide = 5.8 m, long = 11.7 m, high = 5.6 m) .
- Reflective flooring = steel slabs and tiling .
- Sound absorbant walls (the limiting frequency is 250 Hz, the cell is anechoic above 250 Hz and sound-reflecting below) .

The advantages of obtaining measurements in a cell, as compared to measurements obtained on a parked vehicle with, say, a brake on the transmission shaft, and on which the inlet exhaust, and cooling fan noises have been deleted, are the following :

- A higher degree of precision in measurements, and stability in the conditions of operation of the engine (torque, engine speed, temperature levels, fuel consumption, smoke) .
- Insensitivity to weather conditions (ambient temperature, temperature of inlet tract, fuel temperature : all stable within $\pm$ 1° C) .

Disadvantages also exist :

- Obtaining measurements in an enclosed space reduces the frequential spectrum, or alternately requires considerable investments (for a very large anechoic space) .
- The contribution of different parts of an engine to the overall noise level of a vehicle are related to the location of the engine in the vehicle . In a cell, all these different contributions have an equal importance .

The noise was characterized by the following measurements :

- "A" weighted one third octave and overall sound pressure level measured at a distance of 1 metre from the engine and in 8 directions .
- "A" weighted one third octave and overall acoustic power level (obtained from sound pressure measurements in free and far field over an area surrounding the engine) .

Engines have essentially variable conditions of operation, preliminary measurements showed the influence of engine speed gradients as opposed to corresponding stabilized engine speed (Fig. 1) .

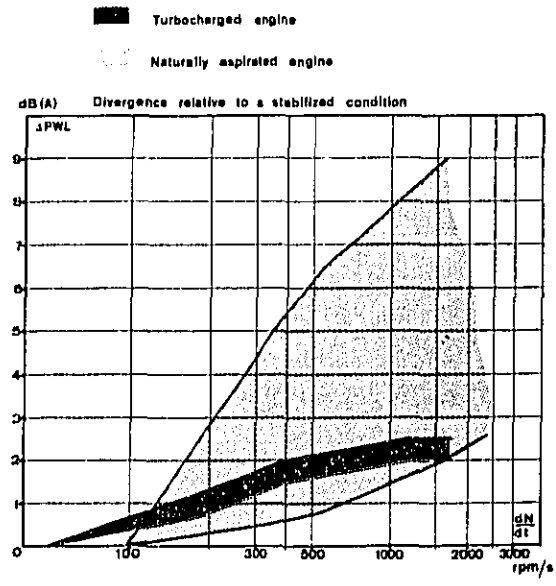

Fig. 1 - Effect of transient conditions

These effects are comparatively small for natirally aspirated engines ; they are more important for supercharged

engines, especially at low engine speeds. In order to simplify the study in a first period, this parameter was not studied . It should however be kept in mind when determining the noise level emitted by vehicles in the course of acceleration .

The measurements were carried out under various stabilized conditions :

- 4 to 5 engine speeds between 1000 RPM and the shut-off speed .
- 6 torque ratings between maximum torque and negative torque .

In order to account for differences in injection point settings, 3 different settings were applied : nominal advance N, N + 4°, N - 4° . Thus 90 different conditions of operation are represented for each engine . The operational parameters were characterized by engine speed torque, injection advance, the maximum pressure gradient and the highest pressure within the combustion chamber, as well as by the one third octave spectrum of pressure in the combustion chamber . These data are automatically stored in a computer .

A certain number of supplementary data elements related to engine design features (weight, number of cylinders, bore, stroke ...) are recorded manually.

METHODS OF ANALYSIS AND RESULTS

16 engines have been analysed in the course of the research, the power range varies from 117 to 356 ch, all the engines operate with two different combustion systems : the MAN type - ID"M" - and the RVI - ID "B" - ; the latter is akin to the conventional direct injection combustion system with intake induced air swirl .

The total amount of data elements stored is in the region of 200,000 .

Table 1 - Engine data

Speed rpm	Displacement (l)	Power (ch)	Aspiration	Type	No of cylinders	Injection M = MAN B = Classical
2400	8.8	185	NA	L	6	B
2400	8.82	187	NA	L	6	B
2300	14.8	280	NA	V	8	B
2800	8.4	182	NA	V	8	B
2200	8.8	225	TC	L	6	B
2200	12	312	TC	L	6	B
2300	14.8	350	TC	V	8	B
2100	12.5	330	TC	L	6	B
2200	9.6	250	TC	L	6	B
2600	5.9	127	NA	L	4	M
2200	6.33	117	NA	L	4	M
2200	7.92	147	NA	L	5	M
2200	9.5	176	NA	L	6	M
2200	12	217	NA	L	6	M
2200	12	230	TC	L	6	M
2900	5.5	157	TC	L	6	M

CLASSICAL ANALYSIS - The noise data (averages and variation or dispersion fromaverages) are presented as two dimensional plots (noise versus one choosen parameter) and in a torque-speed space diagram covering all the engine operating conditions .

This method of data representation allows the abnormally noisy engines to be recognized as well as showing the relative importance of the parameters studied . It also anables engines to be classified in different families with respect to their behaviour .

An example of comparison between the acoustic power levels of different engines is graphically illustrated in Fig. 2 . It will be noted that if the dispersion band is wide at low engines speeds (11 dB(A) . But, at the maximum power condition, once the two engines which are " foreign " to the population have been eliminated, the band is only 6 dB (A) wide . The shaded area in Fig. 2 represents the outline of measurements obtained by I.S.V.R. on 24 engines in the 80 to 350 ch range .

Hence the results presented in this paper are in good agreement with the I.S.V.R. results showing that the results of this paper are a representative sample .

The search for an explanation of noise emitted against one single operational or structural parameter : B.M.E.P. mean piston speed, power, power to weight ratio, engine speed, does not provide (with the exception of the two last mentioned parameters) an opportunity to derive any significant correlation (Fig. 3) . The evolution of noise emitted in relation with the ratio between the weight of the engine block casting and the indicated power rating shows a fairly neat trend : a decrease of 6 dB (A) when the ratio is doubled, which can be explained by the " mass effect " .

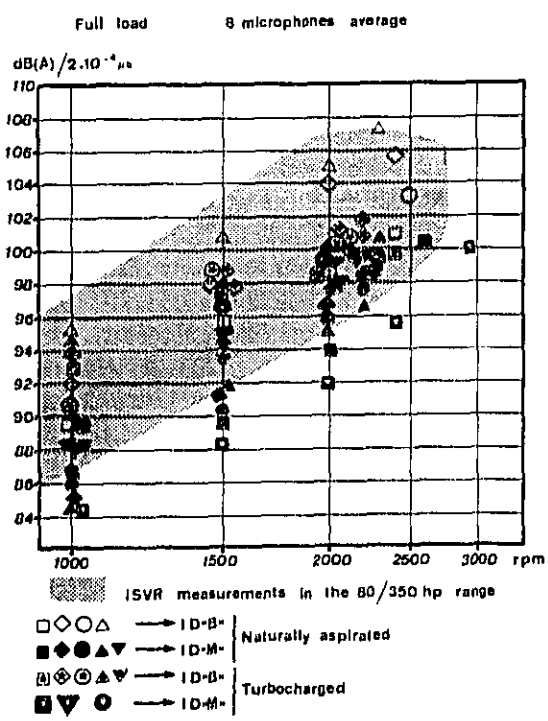

Fig. 2 - Noise versus speed at full load

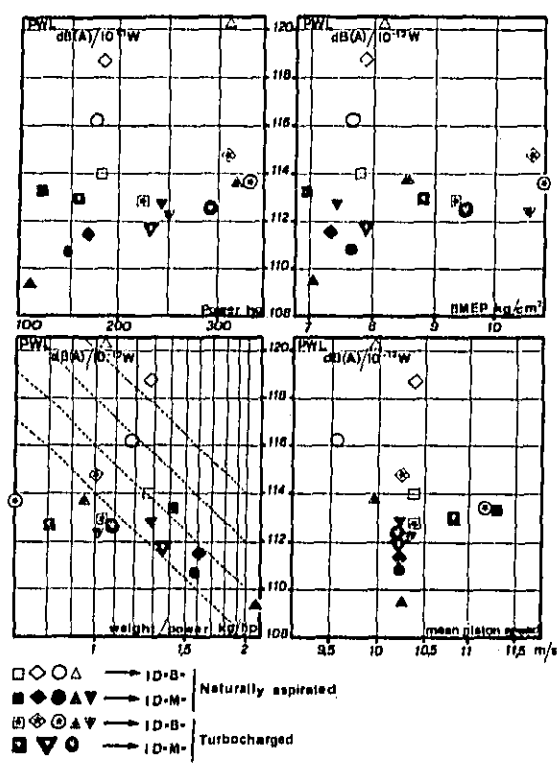

Fig 3 - Noise versus different parameters

The evolution of the level of acoustic intensity in relation to the torque and engine speed ratings allows a form of insight into the influence of different combustion systems and of the effect of automatic injection advance devices (Fig. 4) . Engines with direct injection of the MAN type both supercharged and naturally aspirated have a very regular behaviour pattern, the isobars run parallel . All direct injection engines produce conditions (the effect of the lack of an automatic injection advance system on supercharged engines is also apparent in that the spacing between curves is irregular) .
The evolution of noise as a function of injection - advance at various points in the torque engine speed space diagram enables the importance of this parameter to be reckoned (Fig 5) .

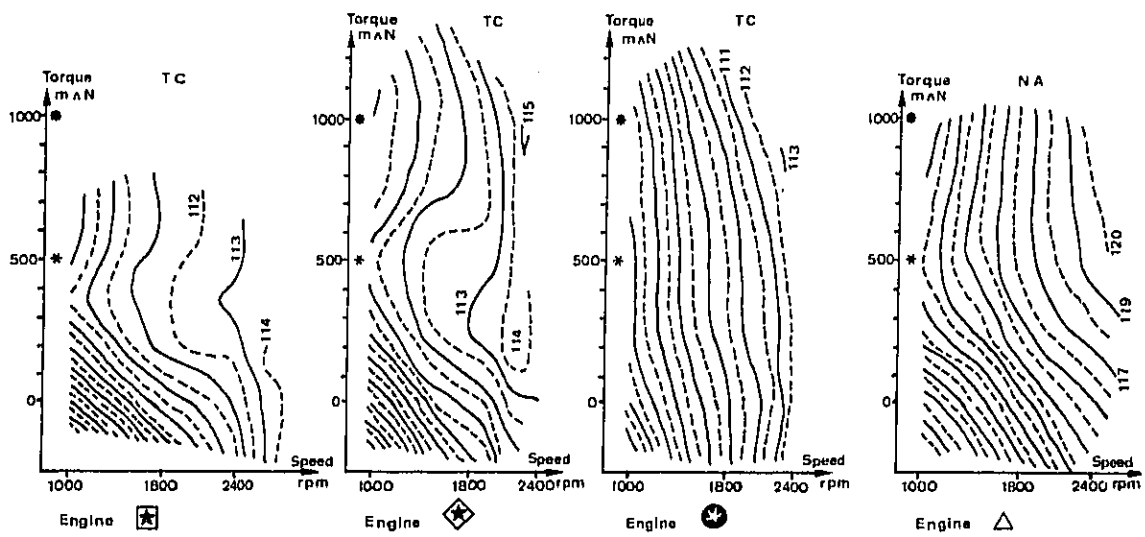

Fig 4 - Isobars in torque V.S. speed diagram

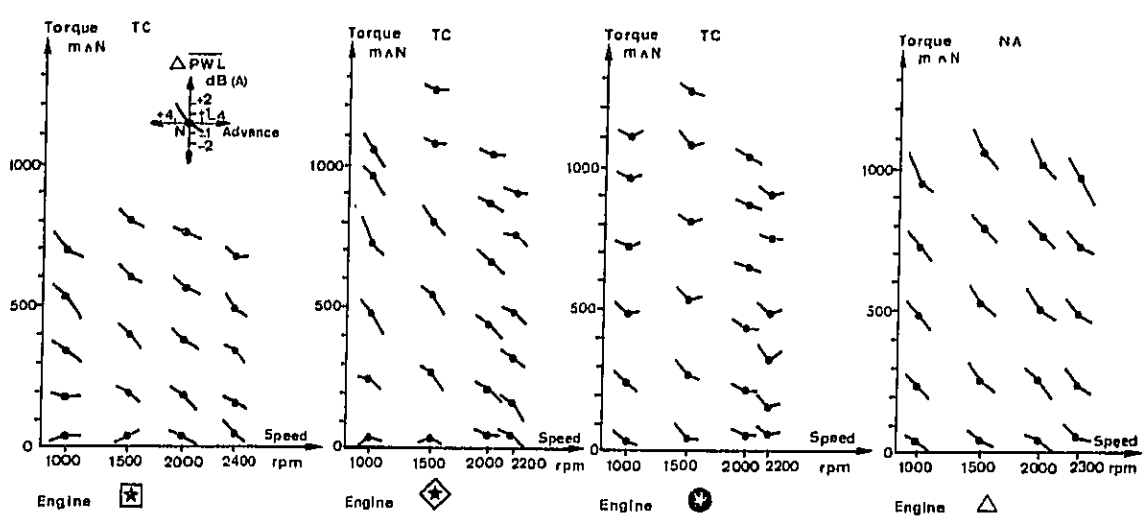

Fig. 5 - Effect of advance in torque V.S. speed diagram

It is apparent that all engines do not react in the same way when given different settings, and that, for some engines, this parameter exercises a strong influence on the noise level (up to 2.5 dB(A) for 4°) .

It is therefore apparent that the number of variables which exercise an influence on the noise level is very large . It is therefore not enough to try to explain the noise level within a 2 or 3 dimensional space diagram, and we were led to the use of more elaborate methodes of visualisation .

MAIN COMPONENT ANALYSIS (see Appendix) . The capacity of the computer on hand limited the scope of the tables to approximately 6,000 values (out of 200,000), analytical operations were therefore fractioned .

A first analysis (Fig. 6) using 11 engines, 12 variables and 264 observations afforded the visualisation of the close relations which exist between noise, engine speed, power, load and structural parameters (cylinder displacement, bore, weight ...) . The plane Δ_1 Δ_2 shows the best correlation : 88 % of the noise is explained. The importance of engine speed is of course confirmed . Also observed, but to a lesser level, is the importance of the cylinder displacement and cylinder bore . But, in this analysis, the engine speed variable overshadows the influence of all other parameters . Hence, in order to eliminate this effect, an analysis was carried out on the residual part of the linear regression on engine speed . Having also noted the difference in behaviour of the MAN type engines compared to other direct injection systems, these families of engines were separated and a separate analysis was drawn up for each family . The most apparent conclusion for these two analysis, albeit with different degrees of magnitude, is the influence of load and cylinder capacity . The other variables all have a lower rate of incidence on the noise level (Fig. 7 and 8)

This type of analysis, which is of interest when one has access to a large and homogenous data bank, nevertheless remains very global in character . Although, it does allow the investigation of those correlations which exist between different variables, it does not allow them to be quantified .

Five variables, those most closely related to noise, having been chosen through main component analysis, a series of regressions was carried out so as to determine the best possible adjustments using the smallest number of variables and formulae .

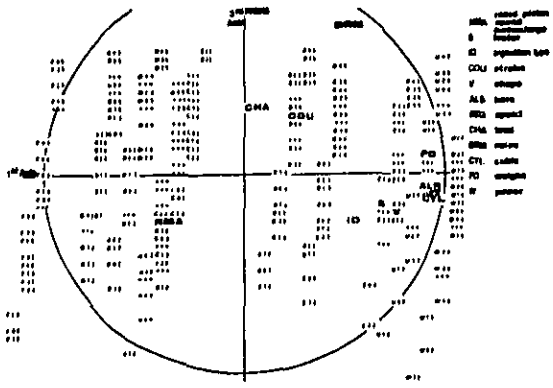

Fig. 6 - Main component analysis (all the engines)

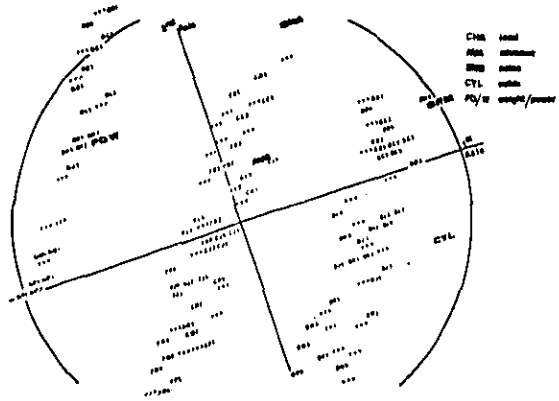

Fig. 7 - Main component analysis (without speed - MAN injection

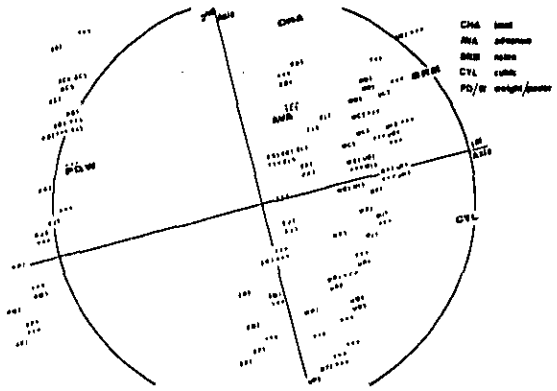

Fig. 8 - Main component analysis (without speed - classical injection

The best results were obtained when these engines were divided into three families :

1 - Direct injection (MAN), naturally aspirated and supercharged engines :

$$PWL = 92,3 + 34,5 \text{ Log. } \frac{N}{1000} + 2,8 \frac{ch}{100} + 0,49 \text{ cyl.} \quad (1)$$

where :
PWL is the level of acoustic power/10^{12} W
N is the engine speed in RPM
Ch is the percentage of torque developped over maximum torque rating .
This formula determines the level of acoustic power within the whole torque engine speed operational space diagram (from 1000 RPM) . Typical difference between sound calculated against sound measured is of ± 1 dB (A) .

2 - Conventional direct injection and naturally aspirated engines :

$$PWL = 91,1 + 28,8 \text{ Log. } \frac{N}{1000} + 6 \frac{ch}{100} + 0,86 \text{ cyl.} \quad (2)$$
$$(\sigma = 1,4 \text{ dB (A)})$$

3 - Conventional direct injection supercharged engines :

$$PWL = 103,7 + 21,2 \text{ Log. } \frac{N}{1000} + 4,8 \frac{ch}{100} \quad (3)$$
$$(\sigma = 2,3 \text{ dB (A)})$$

The result in this last case is not so satisfactory, which is understandable when the shape of the equi-noise level curves in the torque-engine speed space diagram for this family of engines (Fig. 4) is examined . Because they are valid within the whole operational space diagram for these engines, these formulae can be used to calculate the mean acoustic intensity level emitted by engines fitted to vehicles operating in any kind of use, or on typical urban operating cycles .

EXAMPLE OF APPLICATION

One of the engines previously investigated had a noise level which stood clearly outside the "cloud" of readings obtained from other engines (6 in line cylinders, atmospheric induction, direct injection, 180 ch) .

The objective which was determined and achieved, was to reduce its noise level to that of the average peak noise level of the other engines, without any loss in its other performance ratings (smoke, fuel consumption, weight, power ...) in other words a reduction of 7 dB(A) in the acoustic intensity level (from 121 to 114 dB(A) / 10^{-12} W) .

Six remedial solutions were retained : three in the field of structural response, two in the field of mechanical excitation, one in the field of combustion generated excitation .

It is always a rewarding method, when one is attempting to reduce the level of noise radiating from a structure, to make this radiation as homogenous as possible by working on the outstanding parts . The classical method consisting in masking off different parts of the engine and measuring the acoustic power level radiated by the walls of these components, completed by measurements taken from pressure and velocity on their surface,

$$P_{ac}(\vec{r}) = \int_{S \text{ (engine)}} \langle P(\vec{r}).v(\vec{r}) \rangle \, dS \quad (4)$$

has allowed the quantification of the most outstanding components which are the inlet mainfold, the oil sump and the timing case cover (Fig. 9) .

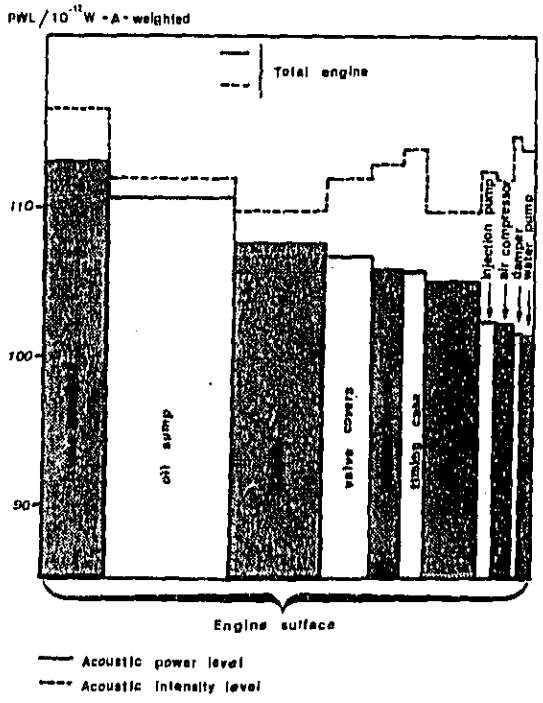

Fig. 9 - Relative weight of the different engine components (at full power) .

Taking their response and the method of acoustic excitement which is theirs, into account, remedial actions engaged into were the following :

- Stiffening the timing case cover .
- Decoupling the inlet manifold from the rest of the engine .
- Applying an oil sump with a discontinuous structure .

The level of mechanical noise being comparatively high, two lines of action were followed :

- Reducing the engine speed from 2600 RPM to 2400 RPM (compensated for by an increased load) .
- Increasing the helix angle on the ten timing gears (20° instead of 6°) .

The pressure gradient and the peak pressure in the combustion chamber were found to be relatively high in comparison with MAN type direct injection engines so that means to reduce them were investigated . This line of research consisted in modifying the main injection setting parameters (diameter of injection pump pistons, of injector discharge orifices, the ineffective part of the piston stroke and injection advance) so as to profoundly modify the pressure curve, or gradient, and the peak pressure rating (without any loss in power) and to analyse the consequences inflicted on other parameters such as smoke, specific fuel consumption, noise .

Fig. 10 shows the evolution of the noise level for this engine as a function of the pressure gradient and of peak combustion chamber pressure . It is apparent that the reduction in noise emitted covers a wide margin (6 dB(A)) . There is therefore a rewarding field of possible noise abatement available in modifying these parameters .

The investigation, by means of a main component analysis (Fig. 11) of correlations existing between injection parameters, performance and the cylinder pressure diagram, supplies the following indications :

- Pressure and the peak pressure gradient are strongly correlated .
- The parameter which most strongly influences the $dp/d\alpha$ is the injector needle-closing angle .
- Increasing the late closing timing of the injector needle increases the amount of smoke produced .
- The smoke can be reduced by increasing the rate of injection .

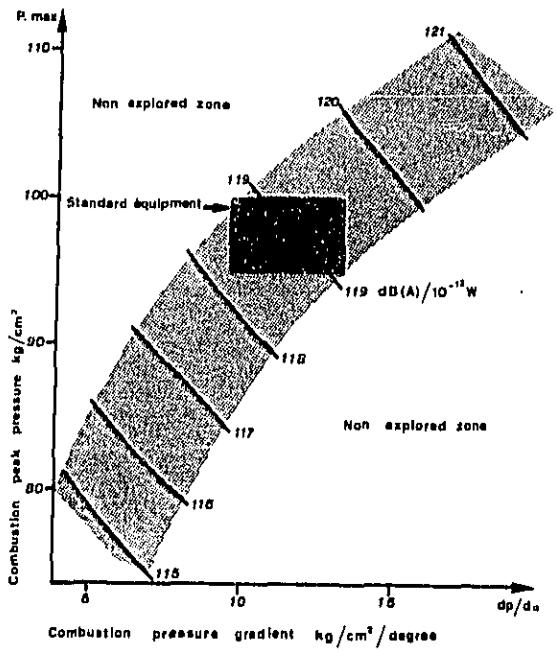

Fig. 10 - Correlation between noise, pressure and pressure gradient .

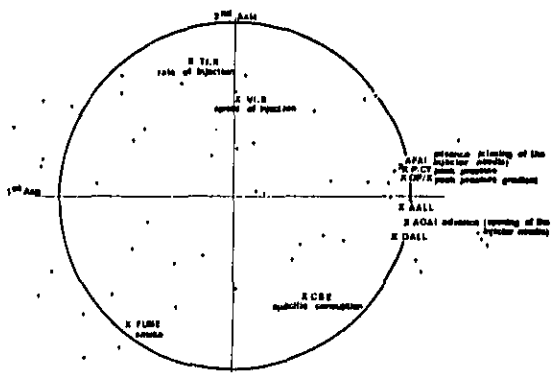

Fig. 11 - Main component analysis with injection parameters, performances and cylinder pressure diagram .

This analytical work supplied the information enabling a combustion setting to be obtained which allows a perceptible reduction in noise.

The various attenuation in the overall level of engine noise obtained in the course of these different lines of action are listed below :

Modifications	At 1500 RPM Full load	At max. speed full load
Timing casing cover	- 0.5 dB(A)	- 1 dB(A)
Inlet manifold	- 2.5 dB(A)	- 2 dB(A)
Oil sump	- 0.5 dB(A)	- 1 dB(A)
Reducing speed 2600 - 2400	0 dB(A)	- 1 dB(A)
Timing gears	- 2.5 dB(A)	- 0.5 dB(A)
Combustion	- 1 dB(A)	- 1.5 dB(A)
Total	- 7 dB(A)	- 7 dB(A)

CONCLUSIONS

The first conclusion derived from the work presented in the paper is that the level of knowledge, in this field, is still too low to be able to envisage the design of an engine which will be both a performing and a quiet engine, whilst remaining within the framework of traditional concepts.

The possibility of reducing the noise level of traditionally designed engine is, in fact, limited.

At design office level, measures are taken so as to render the noise emissions over the whole of the outer surface as uniform as possible. Under these conditions only combustion offers the possibility of obtaining improvements. These are, however, relatively small if the engine performance (power to weight ratio, specific fuel consumption, exhaust gas emissions) have to be left unaltered.

Under these conditions, at vehicle level (before going over to encapsulation) there remains little to be done except to design motive-power lines affording a reduction in time spent within conditions of high noise emission, this, especially in urban use, would result in a noticeable reduction in noise pollution.

Finally, within the scope of the new regulations, engines destined for use without sound-screens should not exceed

$$103 \text{ to } 106 \text{ dB (A)} / 10^{-12} W$$

and this will inevitably, in our opinion, lead to new type of concepts which will require a very large research effort.

ACKNOWLEDGEMENT

We would like to acknowledge the financial assistance of Institut de Recherches des Transports (IRT) in France which enabled us to carry out the greater part of work reported in this paper.

APPENDIX

Main component analysis method allows to visualize data in a higher order space ($\mathbb{R}^n$) in a preferential two order space ($\mathbb{R}^2$) permetting to minimise and to measure the information lose.

In the case of a normalised and centred n lines and p column matrix of n observations for p variables, the analysis consists in determining :

- the main inertia axis Δq of the p vector variable bundle in the n order observation space,

and to project on the plane formed by the first main axes ($\Delta 1$, $\Delta 2$ or $\Delta 1$, $\Delta 3$ or $\Delta 2$, $\Delta 3$...) on the other hand the observations.

Finally, if the information provided by any one plane is sufficient :

- a vicinity of "observation-points" away from the origin means that these observations wholly behave in the same way in relation to the variables ;
- a colinearity between "variable-vectors" whose end is near the unit circle means that the variables are well correlated. If the variables are not correlated, the corresponding "vector-variables" are perpendicular ;
- the "vector-variables" whose end is near from the origin are not accounted for in this plane.

790502

APPLICATION OF ACOUSTIC INTENSITY MEASUREMENT TO ENGINE NOISE EVALUATION

J. Y. Chung, J. Pope and D. A. Feldmaier
Fluid Dynamics Research Department
General Motors Research Laboratories
Warren, Michigan 48090

ABSTRACT

This paper is concerned with the application to engine noise analysis of a cross-spectral method of measuring acoustic intensity recently developed at the General Motors Research Laboratories. The effectiveness and practicality of the approach is demonstrated in a series of tests conducted with a naturally-aspirated, two-stroke V-8 diesel engine. A rapid space-time averaging technique for determining the sound power radiated by sections of different engine components is demonstrated, as well as detailed mappings of noise emission by the engine surface. Noise-source ranking of engine components is performed based on intensity measurements made at the engine surface, and the total engine sound power is determined by summing these individual contributions. The sound power determined at the engine surface in this way is compared with estimates of engine sound power based on acoustic intensity measurements made both over a spherical surface and a set of planar surfaces enclosing the engine. Agreement to within 0.1 dB and 0.5 dB respectively is obtained. This close agreement is a good indication of the overall accuracy and effectiveness of the acoustic intensity method.

THE STRUCTURAL VIBRATION of diesel engines has long been recognized as a major noise source. The topic was previously discussed at an SAE diesel engine noise conference in 1975 (1).* The present conference is concerned with reviewing subsequent developments. One factor that has become more significant since the previous conference is the increased use of digital analysis in engine noise studies. This has been evidenced in various ways in recent work (2-6). Of particular significance has been the increased availability of digital FFT (Fast Fourier Transform) equipment for laboratory and test-cell use. It is this latter development, coupled with the development of a practical procedure for the measurement of acoustic intensity (7,8) that has made possible the techniques described in this paper.

*Numbers in parentheses designate References at end of paper.

Acoustic intensity is the net rate of flow of acoustic energy per unit area and can be defined in a general way for still air by means of the relationship

$$I_r = \overline{pu_r} \quad , \qquad (1)$$

where I_r is the component of intensity in the r direction, p is the acoustical pressure, u_r is the acoustical velocity component in the r direction, and the superscript bar denotes time averaging. The total radiated sound power of a noise source such as an engine can be determined by integrating the normal component of acoustic intensity over a surface enclosing the source as in the following relationship,

$$\text{Sound Power} = \int_S I_n dS \quad . \qquad (2)$$

If the general expression for acoustic intensity given in Equation (1) is used to evaluate the sound power, the measurement surface enclosing the source can be located at any distance from the source, in particular it can be at the surface of the source itself. Conventionally the sound power of an engine is determined by making sound pressure level (SPL) measurements remotely from the engine either in a reverberation room or in an anechoic room. The anechoic room approach has been used in the Calspan studies (2). In the anechoic room approach the sound power of an engine is determined using the far-field approximation for the acoustic intensity where it is assumed that the acoustical velocity is in the direction of wave propagation. In the far-field approximation

$$I_r = \frac{\overline{p^2}}{\rho c} \qquad (3)$$

where the subscript r denotes the direction of wave propagation and ρ and c are respectively the air density and speed of sound in air. To measure acoustic intensity in the far-field, therefore it is necessary only to measure the mean-square acoustic pressure. This approach cannot be used however in the acoustic near-field close to the engine. In this latter case both the pressure and the acoustic velocity have to be measured simultaneously and combined as indicated in the general defini-

SAE/P-79/80/$02.50
Copyright © 1979 Society of Automotive Engineers, Inc.

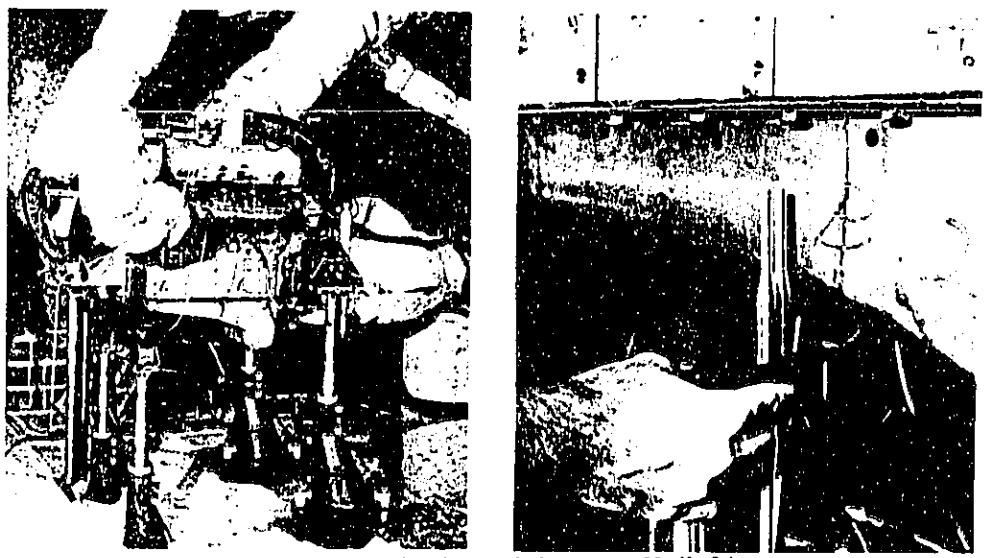

Fig. 1 - Engine in anechoic test cell (left), and two-microphone intensity probe (right)

tion of acoustic intensity in Equation (1).

The advantage of being able to make acoustic intensity measurements in the acoustic near-field of an engine is obvious, for it is then possible to go right up to the surface of the engine and find out where the noise is coming from. With the conventional remote SPL measurements, noise-source ranking of different parts of the engine requires elaborate experimental tests. One method is the so-called lead-cladding technique in which some parts of the engine are covered with lead sheet to prevent sound radiation while noise is measured from the remaining exposed portions of the engine. As well as being tedious and time-consuming, the lead-cladding method assumes that all the component noise sources of an engine are uncorrelated. This assumption is generally incorrect. Another advantage of a near-field method of measuring acoustic intensity would therefore be that it avoids the problems associated with the use of the lead-cladding technique.

The present paper describes the use of a near-field method of measuring acoustic intensity developed at the General Motors Research Laboratories and demonstrates its effectiveness in measurements made on a diesel engine as an example. This method of measurement of acoustic intensity involves the use of a two-microphone probe and is inherently different from the single-microphone SPL measurements. A description of the measurement technique and its experimental verification have been presented in other publications (7,8). A brief review of the method is presented here prior to the presentation of the results for the engine.

In the experimental results for the engine, use of a rapid space-time averaging technique for determining the sound power radiated by sections of different engine components is demonstrated, as well as detailed mappings of noise emission by the engine surface. Noise-source ranking of engine components is performed based on intensity measurements made at the engine surface and the total engine sound power is determined by summing these individual contributions. The sound power determined at the engine surface in this way is compared with estimates of engine sound power based on acoustic intensity measurements made both over a spherical surface and a set of planar surfaces enclosing the engine. The close agreement that was obtained is an indication of the accuracy and effectiveness of the acoustic intensity method.

The work reported here was done with a naturally-aspirated, two-stroke, V-8 diesel engine. This engine was mounted on a dynamometer test stand in an anechoic test cell as shown in Figure 1. For all measurements, the engine was run at a mid-range, half-load condition (540 N-m at 1500 r/min). To minimize possible sources of extraneous noise, the air intake pipe, exhaust pipe downstream of the manifolds, and the transmission were wrapped with lead sheathing and fiberglass (see Figure 1).

DESCRIPTION OF CROSS-SPECTRAL METHOD OF MEASURING ACOUSTIC INTENSITY

The need to make acoustic intensity measurements has been recognized since the early 1930's (9-21). In the reported measurement procedures, generally two or more pressure sensors are used, and a precise knowledge is required of the phase and gain factors of the sensor systems. This makes the measurement procedures impractical for routine measurements. Recently,

a cross-spectral method has been developed (7,8) which is free from any requirement in instrument calibration other than a standard calibration of the microphone gain factors.* Laboratory tests of the method have shown it to be practical and accurate (7,8).

The method uses a finite difference approximation of the pressure and the velocity on the right side of equation (1) using the pressures measured at two closely spaced microphones, i.e.

$$p \approx \frac{1}{2}(p_1 + p_2) \quad , \tag{4}$$

$$u_r \approx \frac{i}{\rho \Delta r \omega}(p_2 - p_1) \quad , \tag{5}$$

where complex values of the pressure and velocity are used in the expressions, and where

ρ = density of air

Δr = microphone spacing

ω = angular frequency

$i = \sqrt{-1}$

p_1 and p_2 = pressures measured at microphones 1 and 2 respectively.

Substituting Equations (4) and (5) into Equation (1) it can be shown that the acoustic intensity can be expressed in terms of the imaginary part of the cross-spectrum (8), or

$$I_r = \mathrm{Im}\left\{[G_{12} \cdot G_{12}^S]^{1/2}\right\} / \rho \Delta r \omega |H_1||H_2| \quad , \tag{6}$$

where Im denotes the imaginary part of a complex number and $|H_1|$ and $|H_2|$ are gain factors of microphones 1 and 2 respectively, also

G_{12} = cross-spectrum between p_1 and p_2

G_{12}^S = cross-spectrum between p_1 and p_2 measured under a "switched condition" i.e. two microphones are interchanged with respect to their sensing locations.

The purpose of this switching procedure is to eliminate automatically the measurement error caused by phase mismatch between the two microphone channels. It is the cross-spectral formulation combined with this switching procedure which makes the intensity measurement practical.

This measurement procedure is valid in any region of the acoustic field of a sound source. In particular it can be used to measure the acoustic intensity very close to an engine surface so that the sound power radiated by the surface can be determined. This engine "surface intensity" cannot be determined by sound pressure level measurements. In fact, the near-field sound pressure level has been shown to over-estimate the engine component sound power radiation by as much as 20 dB(A) (2).

The intensity measurements, reported here were made with a probe consisting of two 6.35 mm (1/4") Brüel and Kjaer condenser microphones spaced 16 mm apart (Figure 1). The associated signal analysis which included the algebraic manipulation shown in Equation (6) was performed by a Hewlett-Packard 5451B Fourier analyzer.

The cross-spectrum calculations were performed "on-line" by the Fourier analyzer using a block size of 512 points. The analog-to-digital converter sampling rate was locked to engine rotation speed with 512 samples per engine revolution. For the engine speed of 1500 r/min, it provided a data sampling rate of 12.8 kHz, thus yielding a Nyquist frequency of 6.4 kHz and a frequency resolution of 25 Hz. To prevent aliasing the signals were low-pass filtered before analog-to-digital conversion using -96 dB/octave filters with the 6 dB point at 5.0 kHz. No data sampling trigger was used, so the beginning of each block was free to vary with respect to engine rotation phase. The time domain blocks were weighted with a Hanning window prior to computation of their Fourier transforms. The signals were further conditioned by A-weighting before analog-to-digital conversion.

Typically, 128 ensemble averages were performed in each of the "switched" and "unswitched" configurations during the intensity determinations. Data acquisition time for each intensity measurement was approximately 60 seconds.

SPACE-AVERAGING TECHNIQUE - Early investigations of the spatial variation of intensity over the surface of the engine (see below) indicated that in order to adequately characterize the noise radiation from the engine surface a measuring station would be required for each 150 mm^2 of surface area. With the available equipment, intensity measurements at the resulting 30,000 stations required for a complete engine survey would be quite tedious and would require many weeks. In order to make complete-engine measurements practical, and because it was recognized that 150 mm^2 resolution would be much finer than usually necessary for noise control purposes, a space-averaging procedure was developed.

The averaging technique consists of moving the two-microphone probe by hand over the area being surveyed during the course of the ensemble averaging in the cross-spectrum computation. In this way time and space averaging are performed simultaneously. During the averaging, every effort is made to cover the area in question uniformly--and hence obtain a true spatial average. The accuracy of the averaging technique was verified by means of a simple comparison experiment which will be described later in this paper. Use of this averaging technique allows adequate characterization of the sound radiation from the various engine surfaces using many fewer measurements (typically one per 0.05 m^2 of engine surface).

MEASUREMENT ACCURACY - As discussed previously (7), the absolute accuracy of the inten-

*A similar cross-spectral formulation without the procedure for eliminating error due to instrument phase mismatch was reported in Reference 21.

sity measurement is limited by the microphone spacing chosen for the intensity probe. With the 16 mm spacing used in this study, the measured intensity can be expected to be highly accurate at frequencies up to about 3.5 kHz. Above this frequency, the measured intensity will deviate from the actual intensity, the measured value being systematically too low. This deviation depends on several factors, including frequency, direction of sound propagation, and the nature of the sound field. Initially, the deviation increases with frequency. A sample calculation for the case of a plane wave showed that at 4.0 kHz the measured intensity is, at most, 1.0 dB below its true value.

The microphone cartridges and preamplifiers used in this study were carefully phase matched by the supplier. This meant that only the instrumentation downstream of the microphone preamplifiers needed to be exchanged. An electric switch at this point in the measurement system was used in place of the mechanical rotation of the intensity probe which generally would be required. Experience in using this particular switching scheme with the 16 mm microphone spacing suggests that the measured intensities should be considered highly accurate only at frequencies above about 300 Hz. Accuracy is still quite acceptable (±0.5dB) at frequencies as low as 200 Hz.*

It should be noted that intensity and sound power levels in this report referred to as "A-weighted levels" actually represent A-weighted levels within the frequency range 250 Hz to 3.5 kHz, only. Since this is the dominant range of engine noise, it is believed that for noise-control purposes these levels are essentially equivalent to the true A-weighted levels.

TEMPORAL AND SPATIAL CHARACTERISTICS OF INTENSITY FIELD CLOSE TO THE ENGINE SURFACE

Before undertaking a survey of the noise radiated by the complete engine and all of its various components, a pilot investigation of the characteristics and properties of the acoustic intensity field at several points on the engine was undertaken. Results from this initial investigation provide a basis for confidence in the accuracy of the work which is described in the later sections of this report.

STATIONARITY IN TIME OF SINGLE-POINT MEASUREMENTS - Acoustic intensity was measured at several locations close to the surface of the engine, and was monitored as a function of time. It was found that trends of variation with time can occur at some points on the engine. For these measurements, the intensity probe was mounted on a tripod and oriented so as to measure the component of intensity normal to the engine surface at a point approximately 20 mm from the surface.** One test was performed without moving the probe between measurements, but it soon was found that the probe could be moved between individual measurements and subsequently replaced in its original position with sufficient accuracy so as not to affect the measurements.* Thus it was possible to use just one probe to monitor several engine locations during the same engine run.

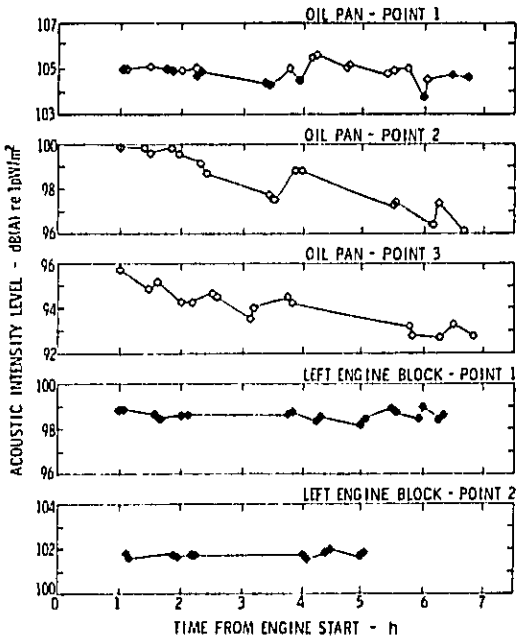

Fig. 2 - Intensity variability with time for single-point measurements. (◆ indicates tests done on one day; ◇ indicates test done on next day, see text for explanation on trends for oil pan points 2 and 3)

Both the stationarity of intensity measurements during a single engine run, and run-to-run consistency were investigated. Figure 2 shows the results of this investigation. During two engine runs, a total of five locations on two different components were studied in detail.** The intensity at the re-measured location, "oil pan point 1" (given in Figure 2), shows good run-to-run consistency. The intensity at this point, as well as the two points on the block which were studied, show very little long term variation. Two of the points on the oil pan do show significant intensity changes with time, however. Note that at "oil pan point 2" the intensity decreases 4 dB(A) over a 6 hour period.

Despite appearances, it should not be assumed that the oil pan is emitting less sound

*To work at lower frequencies, the microphone spacing should be increased and/or the circuit-switching procedure extended to encompass all instrumentation including the microphone cartridges.

**The measuring point is defined to be the point midway between the two microphones of the intensity probe.

*See discussion of spatial variations below.

**Additional "spot checks" were performed over several months at these and other measuring points.

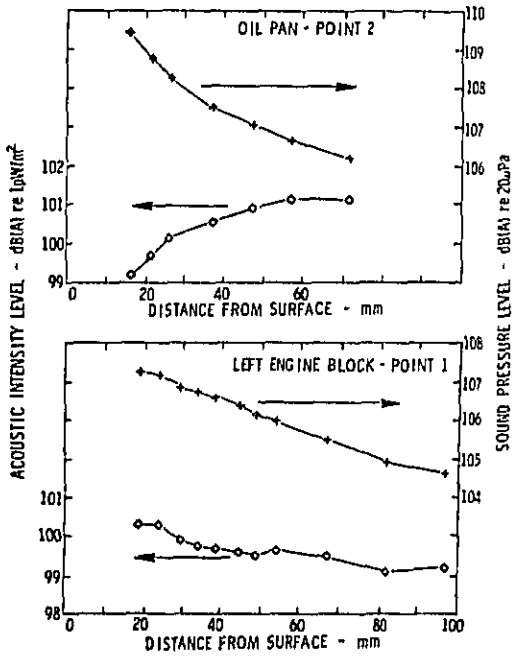

Fig. 3 - Intensity and sound level variability with distance for two points on the engine

with time. The points measured were not a random sample, but were chosen because initially they appeared to be locations of relatively intense radiation. Evidence from space-averaged intensity measurements (see below) suggests that the near-field radiation pattern simply shifts with time, and that when an "intense" region becomes "quiet", a previously "quiet" region becomes "intense". Specifically, despite the intensity variations at fixed measuring stations, when space-averaged over engine surface regions on the order of 0.05 m^2 the intensity is essentially constant in time.

Lastly, it can be mentioned that the sound pressure level (SPL) was monitored simultaneously with the intensity. At all locations measured, changes in SPL usually corresponded to changes in intensity level. There were several occasions, however, when SPL and intensity level changes appeared to be independent.

SPATIAL VARIATIONS - Figure 3 shows the variation in intensity level and in SPL as a function of distance from the engine surface at locations on the oil pan and the block. In order to avoid bias due to time-dependent variations, measurements were made at measuring stations first as the probe was drawn away from the engine surface and again while the probe was moved back toward the surface. The plots presented represent the average of the two measurements.

Notice that for the location on the engine block both intensity and SPL decrease as the distance from the surface increases, as might normally be expected for a simple sound source. For the location on the oil pan, the SPL decreases as expected, but the intensity increases as the distance from the surface increases. Presumably, the intensity increase with distance represents a combination of two phenomena. As distance from the noise source increases, wave divergence causes the intensity levels to decrease. Simultaneously, however, the probe "sees" more of the surface and hence other sources. Thus, if the measurement point is less intense than the surrounding areas, the intensity, which is a vector quantity, would increase as the distance from the surface increased. Presumably, this latter effect is dominant in the case of the oil pan measurement point.

Table 1 - Verification of Space-Averaging Technique

Acoustic intensity and sound pressure levels measured at discrete points:

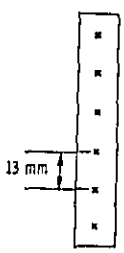

	Sound pressure level dB(A) re 20μPa	Acoustic intensity level dB(A) re 1pW/m²
	105.7	91.7(-)
	105.5	83.3(-)
	105.7	86.6
	105.6	93.2
	105.4	96.0
	105.6	97.4
Average:	105.6	92.4

Space averages over same area:

Test No.	Sound pressure level dB(A) re 20μPa	Acoustic intensity level dB(A) re 1pW/m²
1	105.6	93.3
2	105.5	92.6
3	105.5	91.1
4	105.6	92.7
Average:	105.6	92.5

In fact, close to the surface of the engine, the intensity distribution can show large variation over a relatively small spatial interval. Table 1 shows the intensity measured over six points on the engine block. Notice the reversal from radiation to absorption as well as the 10.8 dB(A) variation in radiation magnitude over a distance of just 39 mm, despite the nearly constant SPL over this same distance.

VERIFICATION OF ACCURACY OF SPACE-AVERAGING TECHNIQUE - In order to verify the accuracy of the previously described space-averaging technique, a simple comparison test was performed. Space-averaged intensity was measured over the area defined by the six points of Table 1. Four measurements were performed (Table 1), yielding

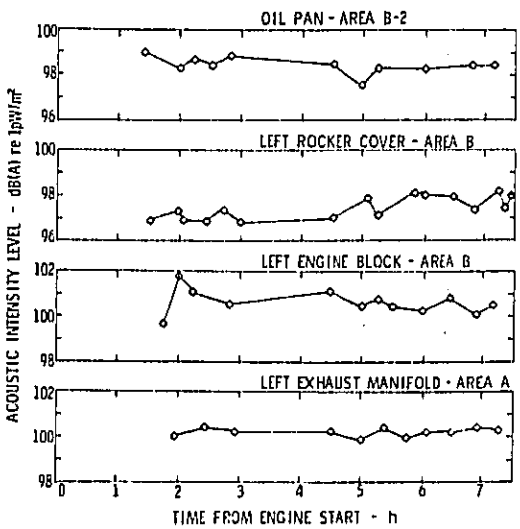

Fig. 4 - Intensity variability with time for space-averaged measurements over several regions

a mean value of 92.5 dB(A) which may be compared with the mean of the six single point measurements, 92.4 dB(A). This very close [0.1 dB(A)] agreement gives credence to the accuracy of the technique.

When used for measurements over larger regions of the engine, space-averaged intensity measured successively by the same operator was typically quite repeatable [±0.5 dB(A)]. Often, however, initial measurements by different operators would show differences up to ±2 dB(A). In all cases the differences were identified as being a result of the operators surveying slightly different areas. Thus in order to prevent problems due to operator bias it is important that all operators understand the exact boundaries of the region which is to be surveyed.

STATIONARITY IN TIME OF SPACE-AVERAGED MEASUREMENTS - Previously it was observed that single-point intensity measurements could show considerable variation with time. Figure 4 shows comparable data for space-averaged intensity measurements, and it is evident that these data show much less variation with time. Unfortunately, this improved stationarity in time is accompanied by somewhat increased random variability in some cases (see the engine block data, in particular), but this does not appear to be much of a problem. Presumably this random error could be reduced by improved time and space averaging, i.e. increasing the number of ensemble averages in the cross-spectrum determination.

MEASUREMENTS OVER THE ENGINE SURFACE

SOURCE RANKING - Two kinds of source ranking are of interest: average intensity ranking and sound power ranking. Sound power ranking

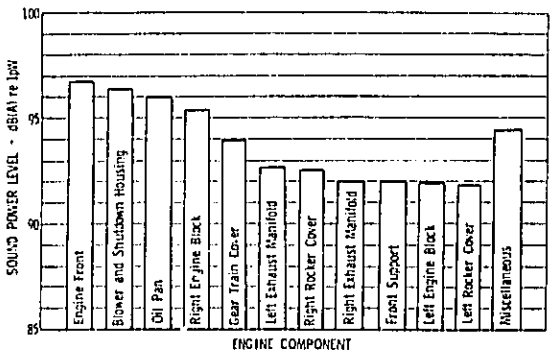

Fig. 5 - A-weighted sound power level radiated by the principal engine components

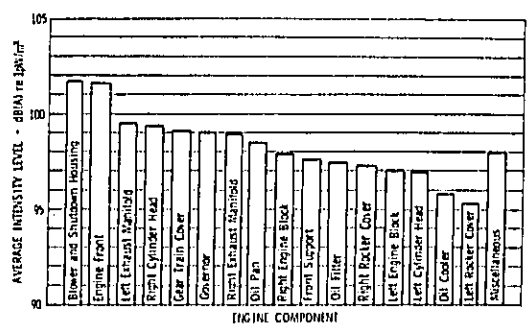

Fig. 6 - Average A-weighted acoustic intensity level for the principal engine components

accounts for total sound radiation by a particular component regardless of size. Average intensity ranking normalizes the sound power in terms of the surface area of the part in question.

Figures 5 and 6 show sound power and average intensity rankings obtained for the engine, and Figure 7 shows the spectrum of the sound power radiated by each component. Space-averaged intensity was measured over 98 regions into which the engine surface was subdivided. For these measurements, the probe was hand-held approximately 20 mm from the surface being surveyed, in an orientation to measure the component of intensity normal to the surface. No surveyed area was larger than 0.13 m^2, while typical areas were about half this size. The measured intensity was multiplied by the area of the control surface over each region surveyed, yielding the sound power radiated through the surface. Since the control surface was located just 20 mm from the actual engine surface, it is assumed that all sound power passing through it is radiated by the engine surface directly beneath it. Summing such sound powers for all portions of a particular component then gives the total sound power radiated by that component. This quantity is used in the sound power ranking. Dividing by the total control surface area of the component gives the average

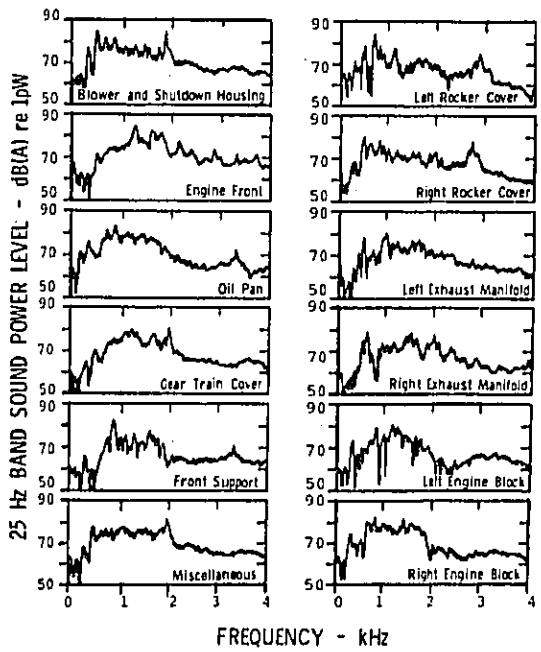

Fig. 7 - A-weighted frequency spectra (25 Hz bandwidth) of sound power radiated by components ranked in Figure 5

intensity over the component, and it is this quantity which is used in the average intensity ranking.

In both rankings the engine front and the blower and shutdown housing assembly emerge as the largest, and essentially equal, sources. In the sound power ranking, the oil pan and right engine block rank slightly below the engine front and top. The gear train cover is 1.5 dB(A) below the right engine block and the left exhaust manifold is 1.2 dB(A) below the gear train cover. The remaining "principal sources" all radiate within 1 dB(A) of each other and the left exhaust manifold. Note the similarities and differences shown in the frequency content of the sound radiation.

Two separate sound power source rankings were performed. With the exception of the engine front and the two rocker covers, the sound power radiated by each component differs by less than 1 dB(A) in the two tests. The levels and spectra referred to above come from the second, more recent measurement. The points of disagreement are of particular interest because they are most likely due to differences in engine configuration for the two tests, and illustrate the importance of such differences in engine noise testing.

The disagreement between measurements for the engine front stem from the fact that during the first set of tests, a rotation encoder assembly used in data acquisition was attached to the crankshaft at the front of the engine. Intensity measurements and aural observations during this run indicated that this encoder assembly and/or its housing were radiating a substantial amount of noise. For the second set of tests, the encoder assembly was removed. The sound power radiated by the front of the engine was 3.3 dB(A) lower in the second set of tests than in the first set. This suggests that the first measurements were contaminated by extraneous noise, and that the second measurements are more accurate measure of engine noise radiation.*

The sound power of the left rocker cover was found to be 2.5 dB(A) less in the second set of measurements than in the first set. For the right rocker cover, the second sound power measurement was 1.9 dB(A) lower than the first. Examination of the data showed that these differences were due almost completely to differences in the radiation from the inboard sides facing the blower and shutdown housing where radiating regions in the first measurements became absorptive regions in the second measurements. The reason for this is not known, but one reasonable explanation is that removal of the rocker covers (a service procedure performed regularly in the laboratory) and subsequent replacement in a slightly different location, or with different contact pressure, results in different vibration inputs to the rocker cover thus yielding a change in the sound radiation characteristics. It should also be noted that the frequencies of the absorbed energy correspond to the primary frequencies radiated by the blower and shutdown housing.

Concerning the average intensity ranking, it is interesting to observe that after the blower and shutdown housing assembly and engine front are accounted for, the next six sources rank within 1 dB(A) of each other, averaging 2.5 dB(A) below the top sources. The average intensity for the remaining "principal sources" declines very gradually, the 16th ranked source being only 6 dB(A) below the 1st ranked source.

It should be noted that the complete component-source sound power radiation and ranking evaluation described above was completed in less than one working day. This is a very significant reduction over the several weeks typically required for a source-ranking evaluation by a conventional technique such as the lead cladding method. Moreover, as suggested earlier, this near-field intensity method for source ranking is inherently more accurate.

RADIATION FROM THE ENGINE FRONT - In order to illustrate the kind of detail which is available from acoustic intensity measurements, it is instructive to examine the intensity pattern measured on the engine front -- one of the principal noise source regions. Figure 8 shows this pattern. Note the strongly radiating region (labelled "D") between the water pump and the pulley, and the strong radiation from the pulley (region "A") itself.** Radiation from these

*Notice that the front engine support is a non-negligible source in the component rankings.

**For these measurements, there was no belt on the pulley. Presumably, different results would be found in an application with a belt mounted.

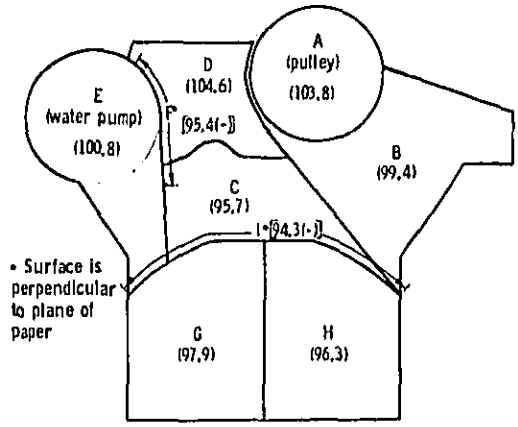

Fig. 8 - A-weighted sound intensity levels for various regions at the front of the engine

regions is in contrast to the absorption exhibited by the "side" surface of the water pump (region "F") and the region labeled "I".

Radiation "maps" of this type can be constructed for any desired area of the engine, in as much detail is desired.

SUMMATION OF COMPONENT SOUND POWERS TO OBTAIN TOTAL ENGINE-RADIATED SOUND POWER - The total sound power radiated by the engine can be determined by summing the sound powers of each of the various components.* When this calculation was done, the sound power radiated by the engine was found to be 104.9 dB(A) re 1pW, a result which will be compared to other sound power level estimates in a later section. This estimate of the engine radiated sound power should be considered a lower bound. Due to the size of the probe there were regions of the engine surface which were inaccessible (e.g., between the rocker cover and the blower). The sound radiated by these areas was neither measured nor included in the total. However, because the area of these omitted regions was quite small compared with the total surface area of the engine, the effect of omission on the measured total of engine noise radiation is negligible (less than 0.2 dB). In any event, if this were a problem, it could be overcome by measuring over a hypothetical surface which does not follow the contour of each component precisely.

SEMI-FAR FIELD INTENSITY MEASUREMENTS OVER A SPHERICAL SURFACE SURROUNDING THE ENGINE TO DETERMINE TOTAL ENGINE-RADIATED SOUND POWER

Measurements of acoustic intensity were made at points on the surface of an imaginary sphere surrounding the engine. The purpose of these measurements was to determine the total sound power radiated by the engine. This sound power can then be compared to the value obtained by summing the sound power of the various components as described in the previous section.

In the far field of a source, the intensity in the direction of sound propagation is proportional to the mean-square acoustic pressure. (In fact, using the conventional reference quantities for sound pressure and intensity levels, 20 μPa and 1 pW/m^2 respectively, the corresponding decibel levels are almost exactly equal numerically.) The far-field sound power radiated by a source in a free field is usually evaluated using SPL-derived "intensity" levels integrated over a sphere* centered on the source. The configuration of the test stand within our laboratory did not permit a conventional measurement to be performed accurately. Instead, the radial intensity was measured directly (i.e., using the GMR cross-spectral method) on a sphere of 1.1 m radius with its origin at the center of the engine.

For this purpose, the center of the engine was defined to be in the plane of the tops of the airbox covers, midway between cylinders 2 and 3, and over the crankshaft centerline. Measurements were made on the sphere at 20 points chosen so each point represented equal surface areas on the sphere. These points are the midpoints of the faces of an icosahedron which fits around the sphere. The intensity was measured at each point by positioning the two-microphone probe on a tripod so the intensity was measured normal to the surface of the sphere, i.e., in the radial direction. The coordinates of the measurement points are shown in Figure 9.

Since each point represents an equal surface area, the average radial intensity over the sphere, $\bar{I}_R$, is simply the arithmetic mean of the measured intensities. The sound power, W, radiated through the sphere of surface area A_s can then be determined by the relation:

$$W = A_s \cdot \bar{I}_R \quad . \qquad (7)$$

*It should be mentioned that the control surface areas used for the total sound power determination sometimes differed slightly from the areas used for the source-ranking component sound power determination, because of differently defined control surfaces. The difference occurs only when there is an acute ("inside") angle formed by two components. For the source-ranking, the control surface over one component was considered to extend to the surface of the adjoining component. For the total sound power calculation, however, the control surface over one component extended only to within 20 mm of the surface of the other component thus giving a continuous, closed control surface over the whole engine.

*If a semi-anechoic room is available, i.e. a room with all surfaces anechoic except a single reflecting plane, a hemisphere is substituted for the sphere.

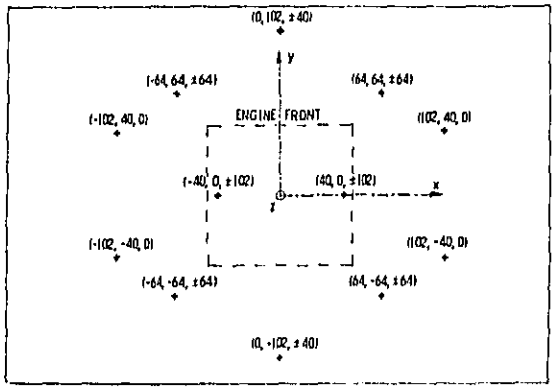

Fig. 9 - Top view of engine showing intensity probe coordinates for spherical measurements [(x,y,z) coordinates in centimeters relative to center of engine]

Actually, the surface area of the sphere in this relationship is understood to be the effective area, i.e., the surface area after account is taken of blockage by the transmission, intake and exhaust pipes, and the engine supports where the control surface passes through them. Thus a better form of Equation (7) is:

$$W = (A_s - A_b)\ \bar{I}_R \quad , \qquad (8)$$

where A_b is the blocked area, and now A_s is the total surface area of the sphere.

The results of the measurements for the engine operating at 1500 r/min and 540 N-m load are shown in Table 2, which lists A-weighted acoustic intensity level and sound pressure level at the points given in Figure 9. The range for the intensity level is 4.6 dB(A) and for the pressure level it is 4.4 dB(A), excluding points 3 and 12. Presumably, the reason the levels at these points are so low is that the intensity probe was very close to a fiberglass surface in the vicinity of the engine (see below). It should be noted that the pressure levels are generally about 1 dB(A) above the intensity levels which indicates that the measurements are not quite in the far field. One exception to the 1 dB(A) difference is at point 11, where the intensity level is 2.2 dB below the pressure level. This measurement point was about 30 cm from a fiberglass blanket covering the transmission. Substituting the appropriate values into Equation (8) yields 105.0 dB(A) re 1pW as the level of sound power radiated through the spherical control surface.

Applying the principle of conservation of energy to the control volume, the engine-radiated sound power, W_e, is obtained from the sound power radiated through the spherical control surface, W, by the relation:

$$W_e = W - W_r + W_a \quad , \qquad (9)$$

Table 2 - Acoustic Intensity and Sound Pressure Levels Measured Over a Sphere Surrounding the Engine

Point No.	Measurement location coordinates (cm from center of engine) x	y	z	Acoustic Intensity Level [dB(A) re $1pW/m^2$]	Sound Pressure Level [dB(A) re $20\mu Pa$]
1	0	102	40	92.2	91.2
2	0	102	-40	93.7	94.3
3	64	64	64	80.7	84.7
4	64	64	-64	91.8	92.9
5	102	40	0	92.5	93.1
6	40	0	102	96.4	97.5
7	40	0	-102	94.5	95.8
8	102	-40	0	93.3	94.1
9	64	-64	64	93.9	94.8
10	64	-64	-64	92.1	93.3
11	0	-102	40	94.9	97.1
12	0	-102	-40	87.6	90.5
13	-64	-64	64	93.7	94.4
14	-64	-64	-64	92.7	94.1
15	102	-40	0	93.1	94.0
16	-40	0	102	96.1	96.7
17	-40	0	-102	94.1	95.5
18	-102	40	0	92.5	93.1
19	-64	64	64	92.7	93.2
20	-64	64	-64	92.9	93.6

where W_r and W_a are extraneous sound radiation and absorption within the control volume respectively. These latter factors are needed to account for effects due to surfaces within the control volume which are not usually considered to be a part of the engine for noise measurement purposes. For the spherical control volume, these surfaces are the parts of the air intake pipe upstream of the shutdown housing, the exhaust pipes downstream of the manifolds, the transmission, and the engine supports. With the exception of the latter, these surfaces were lead and fiberglass wrapped to minimize sound radiation, and covered with 15 cm of fiberglass. The engine support stands are isolated from the engine by rubber mounts.*

The quantity W_r-W_a was measured by integrating the measured intensity over the surfaces in question, and was found to be 81.4 dB(A). Substitution into Equation (9) yields the result that W_e is essentially equal to W.

INTENSITY MEASUREMENTS OVER PLANAR AREAS SURROUNDING ENGINE

The surface intensity measurements described in the previous section were made by

*This analysis of the effect of extraneous surfaces is, of course, equivalent to simply redefining the control volume such that the control surface is no longer a true sphere, but becomes sphere-like while excluding the extraneous surfaces.

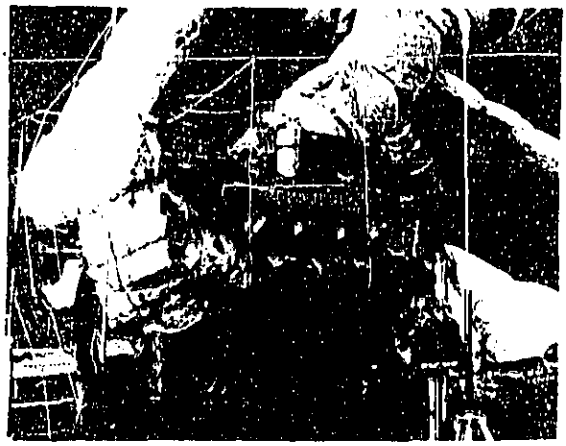

Fig. 10 - String "box" surrounding engine with planar areas

manually moving the two-microphone probe over the surface of the engine. For some tests however, it may be unsafe or it may be too difficult to move the probe over the surface by hand. Tests were therefore conducted to determine if an automated scanning mechanism could use the space-averaging technique to measure the intensity over various areas of an object. For an automatic scan to be feasible, the probe would probably need to be moved over planar areas. It was hoped that this scan could be used to locate regions of high intensity which would be further investigated. However, because of the distance of the probe from the engine surface for these tests, the differences in intensity were not as great as those measured near the surface.

An imaginary "box" consisting of seven planar areas was constructed to totally enclose the engine. The areas were marked by a grid of strings attached to tripods, as shown in Figure 10. The "box" was made to measure as close to the engine as possible while still maintaining a small number of planar areas. Ideally, the sides of the "box" would be within several centimeters of the engine surfaces, but the fiberglass wrapping on the exhaust pipe increased the size of the "box" so some measurements were as far as 35 cm from the surface. Since the engine was a "V" type, the box consisted of a lower triangular section and an upper rectangular section to follow the shape of the engine. The intensity measurements were made by manually moving the two-microphone probe over each area indicated by the strings; however, if a mechanism had been available to traverse the area it could have been used.

Figure 11 shows the measurement "box" unfolded into two dimensions along with measured A-weighted intensity levels. It will be noted that because the "box" could not follow the exact shape of the engine, there were many regions where only a portion of the box area was directly above the engine surface. To facilitate comparisons among these regions, the

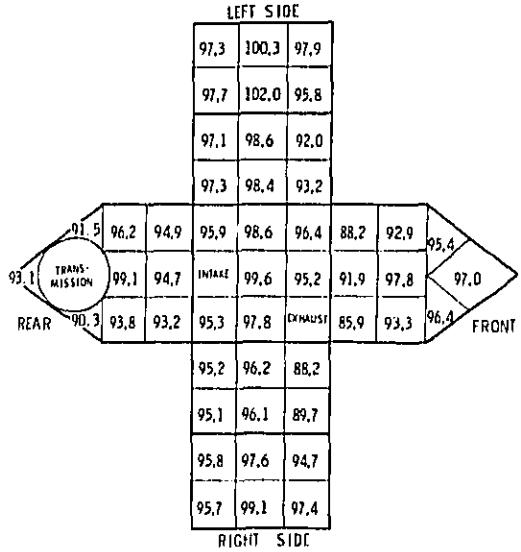

Fig. 11 - Sound intensity level [dB(A) re $1pW/m^2$] for each of the sections in the planar areas surrounding the engine

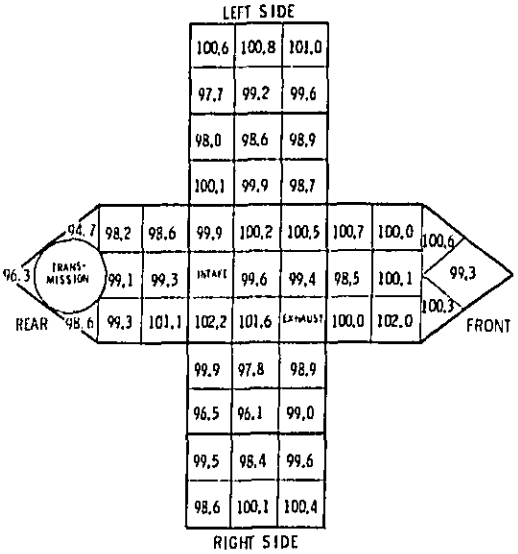

Fig. 12 - Normalized sound intensity level [dB(A) re $1pW/m^2$] for each of the sections in the planar areas surrounding the engine

data were normalized by dividing the measured intensities by the ratio of engine surface beneath the region to the area of the region. These normalized data are shown in Figure 12.

The total range of the intensity levels shown in this figure is only 6.1 dB(A), excluding the areas around the transmission. This indicates that the large local variations in intensity at the engine surface are averaged together due to the distance of the "box" from

the engine. It appears that the areas at the front and top of the engine have slightly greater intensities, but the differences are insignificant. While these measurements over the planar surfaces do not appear promising for locating regions of high acoustic intensity, the technique may still be useful if the planar areas can be constructed closer to the engine surface.

Since these measurements form a closed surface around the engine, the sound power over the areas can be summed to determine the total sound power output of the engine. The sound power level of the engine using this method was found to be 105.4 dB(A), which will be compared to other estimates in the next section.

As explained in the previous section, the sound power radiated or absorbed by extraneous surfaces within the control volume needs to be considered. The only such surfaces contained within the box were the intake and exhaust pipes, which were lead-wrapped and covered with 15 cm of fiberglass. The net sound power radiation (i.e., radiation minus absorption) of these surfaces was found to be 69.8 dB(A), which is negligible compared to the sound power level of the engine of 105.4 dB(A).

COMPARISON OF TOTAL SOUND POWER LEVELS

The tests described so far presented three different estimates of the total sound power output of the engine operating at 1500 r/min with 540 N-m load. The surface intensity method presented in this paper determined the sound power of each component by measuring the intensity near the surface. The total sound power level of the engine of 104.9 dB(A) re 1pW was determined by adding the sound power of the individual components. In the second method described previously, the intensity was measured at 20 points on an imaginary sphere surrounding the engine such that each measurement point represented an equal area. The total sound power level determined in this manner was 105.0 dB(A). The third method of measuring sound power, discussed in the last section, uses measurements of intensity over a set of planar areas forming a closed surface around the engine. The total sound power level was found to be 105.4 dB(A). These results are summarized in Table 3.

Although additional examples of this type would be desirable, the close agreement between the sound power obtained in the three determinations appears to effectively demonstrate the accuracy of the intensity method. The observation that the sum of the sound powers radiated by component sources is equal to the total engine-radiated sound power [0.5 dB(A) (12%) difference at most], in particular, appears to enhance confidence in the findings. This agreement is particularly significant when contrasted with about 2 dB(A) (60%) difference in the corresponding quantities which is consistently obtained when the conventional lead-cladding method of component source evaluation is used (2).

Table 3 - Total Sound Power Level of the Engine

Measurement Method	Sound Power Level [dB(A) re 1pW]
Intensity measurement near engine surface and sound power of individual components summed	104.9
Intensity measurement at points on sphere in pseudo far field	105.0
Intensity measurement over planar areas	105.4

ACKNOWLEDGMENTS

The authors would like to thank M. C. Mills and S. J. Doggett for their assistance during the measurements. We would also like to acknowledge the encouragement of R. Hickling and D. L. Smith during the project.

REFERENCES

1. "Diesel Engine Noise Conference," SAE Special Publication SP-397, August, 1975.

2. T. Trella, R. Mason and R. Karsick, "External Surface Noise Radiation Characteristics of Truck Diesel Engines -- Their Far-Field Signatures and Factors Controlling Abatement" SAE paper 780174, presented at SAE Congress and Exposition, Cobo Hall, Detroit, MI, February - March, 1978.

3. J. Y. Chung, "The Use of Digital Fourier Transform Methods in Engine Noise Research", SAE paper 770010, SAE Transactions, 1977.

4. M. E. Wang and M. J. Crocker, "Recent Application of Coherence Techniques for Noise Source Identification", Proceedings of 1978 International Conference on Noise Control Engineering, San Francisco, CA, May, 1978.

5. R. H. Lyon and R. G. DeJong, "Designing Diesel Engines for Reduced Noise", paper presented at EPA-University Seminar, Purdue University, West Lafayette, IN, October, 1976.

6. R. J. Alfredson, "A New Technique for Noise Source Identification on a Multi-cylinder Automotive Engine", Proceedings of Noise-Con 77, NASA Langley Research Center, Hampton, VA, October, 1977.

7. J. Y. Chung and J. Pope, "Practical Measurement of Acoustic Intensity -- The Two-Microphone Cross-Spectral Method", Proceedings of 1978 International Conference on Noise Control Engineering San Francisco, CA, May, 1978.

8. J. Y. Chung, "Cross-Spectral Method of Measuring Acoustic Intensity Without Error Caused by Instrument Phase Mismatch", J. Acoust. Co. A., Vol. 64, pp. 1613-1616, 1978.

9. H. F. Olsen, "System Responsive to the Energy Flow of Sound Waves", U.S. Patent No. 1892644, December 1932.

10. C. W. Clapp, F. A. Firestone, "The Acoustic Wattmeter -- An Instrument for Measuring Sound Energy Flow," J. Acoust. Soc. Am., Vol. 13, pp. 124-136, 1941.

11. S. Baker, "An Acoustic Intensity Meter," J. Acoust. Soc. Am., Vol. 27, No. 2, pp. 269-273, 1955.

12. T. J. Schultz, "Acoustic Wattmeter," J. Acoust. Soc. Am., Vol. 28, No. 4, pp. 693-699, 1956.

13. T. J. Schultz, "Outlook for In-situ Measurement of Noise from Machines," J. Acoust. Soc. Am., Vol. 54, No. 4, pp. 982-984, 1973.

14. T. J. Schultz, P. W. Smith, C. I. Malme, "Measurement of Acoustic Intensity in a Reactive Sound Field," J. Acoust. Soc. Am., Vol. 57, No. 6, Part 1, pp. 1263-1268, 1973.

15. G. Huber, "Analysis of Errors in Measuring Machine Noise Under Free Field Conditions," J. Acoust. Soc. Am., Vol. 54, No. 4, pp. 965-975, 1973.

16. J. F. Burger, C. J. J. Van Der Merwe, B. G. Van Zyl, L. Joffe, "Measurement of Sound Intensity Applied to the Determination of Radiated Sound Power," J. Acoust. Soc. Am., Vol. 53, No. 4, pp. 1167-1168, 1973.

17. B. G. Van Zyl, F. Anderson, "Evaluation of the Intensity Method of Sound Power Determination," J. Acoust. Soc. Am., Vol. 57, No. 3, pp. 682-686, 1974.

18. T. H. Hodgson, "Investigation of the Surface Acoustical Intensity Method for Determining the Noise Sound Power of a Large Machine In-situ," J. Acoust. Soc. Am. 61, No. 2, 487-492, 1977.

19. W. Stahel, H. P. Lambrich, "Development of an Instrument for the Measurement of Sound Intensity and Its Application in Car Acoustics," external publication, INTERKELLER AG, Zurich, Switzerland, 1977.

20. F. Friundi, "The Utilization of the Intensity Meter for the Investigation of the Sound Radiation of Surfaces," external publication, INTERKELLER AG, Zurich, Switzerland, 1977.

21 F. J. Fahy, "Measurement of Acoustic Intensity Using the Cross-Spectral Density of Two Microphone Signals," J. Acoust. Soc. A., (L), Vol. 62, No. 4, pp. 1057-1059, October, 1977.